ADVANCED GASIFIER AND WATER GAS SHIFT TECHNOLOGIES FOR LOW COST COAL CONVERSION TO HIGH HYDROGEN SYNGAS

FINAL TECHNICAL REPORT

Reporting Period

Start Date: October 1, 2014

End Date: September 30, 2016

Principal Author

Andrew Kramer Principal Investigator/Program Manager

September 30, 2016

DOE Award Number

DE-FE0023577 (DOE NETL)

Gas Technology Institute
1700 South Mount Prospect Road
Des Plaines, IL 60018

DISCLAIMER

ABSTRACT

The Gas Technology Institute (GTI) and team members RTI International (RTI), Coanda Research and Development, and Nexant, are developing and maturing a portfolio of technologies to meet the United States Department of Energy (DOE) goals for lowering the cost of producing high hydrogen syngas from coal for use in carbon capture power and coal-to-liquids/chemicals. This project matured an advanced pilot-scale gasifier, with scalable and commercially traceable components, to readiness for use in a first-of-a-kind commercially-relevant demonstration plant on the scale of 500-1,000 tons per day (TPD). This was accomplished through cold flow simulation of the gasifier quench zone transition region at Coanda and through an extensive hot-fire gasifier test program on highly reactive coal and high ash/high ash fusion temperature coals at GTI. RTI matured an advanced water gas shift process and catalyst to readiness for testing at pilot plant scale through catalyst development and testing, and development of a preliminary design basis for a pilot scale reactor demonstrating the catalyst. A techno-economic analysis was performed by Nexant to assess the potential benefits of the gasifier and catalyst technologies in the context of power production and methanol production. This analysis showed an 18% reduction in cost of power and a 19% reduction in cost of methanol relative to DOE reference baseline cases.

TABLE OF CONTENTS

Appendix

LIST OF FIGURES

Figure **Page**

LIST OF TABLES

Table **Page**

EXECUTIVE SUMMARY

The Gas Technology Institute (GTI) and RTI International (RTI) are developing and maturing technologies to meet the United States Department of Energy (DOE) goals for lowering the cost of producing high hydrogen syngas from coal for use in carbon capture power and coal-to-liquids/chemicals. The objective of this project was to mature GTI's entrained flow gasifier technology to readiness for use in a first-of-a-kind commercially-relevant demonstration plant on the scale of 500-1,000 tons per day (TPD) by 2020, and to advance the RTI advanced Water Gas Shift (WGS) catalyst technology on a path towards demonstration at similar scale and schedule.

Clean coal conversion processes with acceptable carbon emissions, whether to power via Integrated Gasification Combined Cycle (IGCC) plants or to liquids/chemicals, are typically characterized by high capital costs for the plants and high cost of product relative to carbon-equivalent alternatives. The gasifier and catalyst technologies being advanced under this effort showed promise to significantly improve these areas, potentially offering 15%-25% reduction in both plant capital cost and cost of product.

This effort addressed the principal technical risks for the gasifier and catalyst technologies in support of validating the anticipated benefits, which were subsequently evaluated in a techno-economic analysis to quantitatively assess the benefits in the context of both coal-to-power and coal-to-methanol. For the gasifier, this effort addressed risks in the areas of quench zone design, processing of highly reactive coals, processing of high ash + high ash fusion temperature (AFT) coals, and structural characteristics of residual carbon at high conversion operations. For the WGS catalyst, this effort identified optimal catalyst formulation and processing parameters to establish a high conversion and attrition resistant catalyst for testing in a subsequent pilot scale test rig.

Gasifier quench zone cold flow simulations (Task 2 in this effort) provided valuable design guidance for gasifier design scale-up, both through validation of the efficacy of the current pilot plant outlet design and in identifying critical gas/liquid momentum ratios for reliable quench zone operations. A follow on effort (Task 6) was performed to more fully characterize the physics driving jet-jet interactions in the quench zone, leading to definition of a modified test apparatus to provide appropriate similitude of quench zone hydrodynamics for a demonstration scale gasifier.

Gasifier pilot plant testing (Task 3 in this effort) established the feasibility for this gasifier technology to meet performance and life goals on highly reactive feedstocks and on feedstocks with high ash and high ash fluid temperatures (> 1500°C). Residual carbon surface area and porosity data were obtained for carbon conversion ranging from 85%-97%, providing detailed data for use in anchoring performance models for use in predicting commercial gasifier performance. It also demonstrated the ability to operate the gasifier in hybrid mode with natural gas comprising up to 35% of the feed on a higher heating value (HHV) basis, which offers plant optimization options.

RTI successfully developed a catalyst optimized to provide reactivity and stability comparable to commercial sweet WGS catalysts that was suitable for use in the transport reactor design, with attrition resistance superior to that of fluidized catalytic cracking (FCC) catalysts. A novel catalyst preparation approach that eliminates hazardous hexavalent chromium from the manufacturing

process was demonstrated as well. A preliminary Basic Engineering Package (BEP) and cost estimate was prepared for a 5,000 scfh pilot-scale Advanced Transport Water Gas Shift (ATWGS) reactor skid. Techno-economic analyses were prepared to estimate the impact of the ATWGS in commercial plants for power and methanol production.

The Nexant-led techno-economic analysis provided a basis for assessing the combined portfolio of GTI and RTI technologies in the context of commercial-scale IGCC and Coal-To-Methanol plants, as well as the ability to identify specific impacts of the gasifier and ATWGS. The combined technologies (including RTI's Warm Desulfurization Process and Direct Reduction of Sulfur Process) yields a 20% reduction in plant capital cost and 18% reduction in cost of electricity (COE) relative to a state-of-the-art reference case. For Coal-To-Methanol plants, the benefit is a 22% reduction in plant capital cost and 19% reduction in methanol Required Selling Price (RSP).

Completion of the quench zone simulation and the pilot plant gasifier testing were successful in establishing technical readiness of the gasifier technology for scale-up to the 500-1,000 TPD range. GTI is working with prospective partners to prove out gasifier performance and economic benefits prior to 2020. Findings from the current program substantiated the basis for gasifier inputs used in the techno-economic analysis, which indicates that the gasifier by itself offers a 13% reduction in capex and 12% reduction in cost of product for IGCC, and an 18% reduction in capex and 15% reduction in cost of product for Coal-To-Methanol.

Completion of the bench-scale optimization of the ATWGS catalyst combined with preliminary basic engineering package (BEP) and cost estimate for a pilot-scale skid offers the potential for RTI's advanced WGS technology to be advanced to readiness for commercial-scale demonstration in the 2020 time-frame, as well. Findings from Task 4 substantiated the basis for ATWGS inputs used in the techno-economic analysis, which indicates that the ATWGS by itself offers a 2.5% reduction in capex and 2.3% reduction in cost of product for IGCC, and a 0.9% reduction in capex and 1.2% reduction in cost of product for Coal-To-Methanol.

In conclusion, this project successfully positioned the combined portfolio of GTI and RTI technologies on a path for readiness to support demonstration at commercially-relevant scale by 2020, offering >15% reduction in the cost of coal conversion to power and chemicals.

1.0 INTRODUCTION

1.1 DOCUMENT SCOPE

The purpose of this document is to describe the effort performed under the "Advanced Gasifier and Water Gas Shift Technologies" contract, DE-FE0023577, awarded to Aerojet Rocketdyne (AR) by the United States Department of Energy (DOE) – National Energy Technology Laboratory (NETL), and subsequently novated to the Gas Technology Institute (GTI) by NETL after GTI acquired rights to the technology from AR.

1.2 PROJECT SUMMARY

The Gas Technology Institute (GTI) and RTI International (RTI) are developing and maturing technologies to meet the United States Department of Energy (DOE) goals for lowering the cost of producing high hydrogen syngas from coal for use in carbon capture power and coal-to-liquids/chemicals. The objective of this project was to mature GTI's entrained flow gasifier technology to readiness for use in a first-of-a-kind commercially-relevant demonstration plant on the scale of 500-1,000 tons per day (TPD) by 2020, and to advance the RTI advanced Water Gas Shift (WGS) catalyst technology on a path towards demonstration at similar scale and schedule.

Clean coal conversion processes with acceptable carbon emissions, whether to power via Integrated Gasification Combined Cycle (IGCC) plants or to liquids/chemicals, are typically characterized by high capital costs for the plants and high cost of product relative to carbon-equivalent alternatives. The gasifier and catalyst technologies being advanced under this effort showed promise to significantly improve these areas, potentially offering 15%-25% reduction in both plant capital cost and cost of product.

This effort addressed the principal technical risks for the gasifier and catalyst technologies in support of validating the anticipated benefits, which were subsequently evaluated in a techno-economic analysis to quantitatively assess the benefits in the context of both coal-to-power and coal-to-methanol. For the gasifier, this effort addressed risks in the areas of quench zone design, processing of highly reactive coals, processing of high ash + high ash fusion temperature (AFT) coals, and structural characteristics of residual carbon at high conversion operations. For the WGS catalyst, this effort identified optimal catalyst formulation and processing parameters to establish a high conversion and attrition resistant catalyst for testing in a subsequent pilot scale test rig.

The Statement of Project Objectives (SOPO) is defined in the award document, and also in the Program Management Plan (PMP), the latest version being document number RD14-228, Rev 2, issued October 28, 2015. The SOPO was updated subsequent to novation of the contract to GTI in May 2016. Summary description of the objectives for each of the tasks are as follows:

Task 2 – Quench Zone Simulation: Coanda used the existing GTI quench zone simulator to characterize quench zone flow fields for pilot plant and scaled-down demonstration gasifier configuration using cold flow simulation. The objective was to establish a suitable degree of geometric, kinematic and dynamic similitude for the gasifier outlet/quench zone transition region

and a cold flow model, with the results serving as the basis for guiding scale-up decisions to a demonstration scale (500-1000 TPD capacity) gasifier design.

Task 3 – Pilot Plant Gasifier Testing: Previous pilot plant testing and gasifier design effort identified a number of technical aspects to address prior to advancing into a demonstration-scale gasifier design. These were to:

(1) Assess the thermal environments associated with highly reactive coals (such as lignite and sub-bituminous) to confirm feasibility of gasifier component designs

(2) Establish the ability to operate the gasifier on high ash content, high ash fusion temperature (AFT) coals, demonstrating continuous slag discharge capability and component feasibility in the challenging thermal environments posed by high AFT coals.

(3) Characterize the properties of residual carbon at high conversion to provide a basis for improved performance prediction as carbon conversion approaches 99%.

The primary objective of this effort was to address these technical challenges in support of demonstration scale gasifier design. A secondary objective was to assess the feasibility of operating the compact gasifier in a hybrid mode, with simultaneous feeding of coal and natural gas.

Task 4 – Advanced Water Gas Shift Technology Development: This task accumulated sufficient lab-scale data on catalyst development and testing to complete a techno-economic evaluation for an integrated system consisting of GTI's gasification and RTI's Advanced Water Gas Shift (AWGS) processes. A preliminary engineering definition study was performed on a pilot skid apparatus.

Task 5 – Techno-Economic Analysis: A systems analysis was performed to show the commercial potential for the portfolio of technologies being advanced under the project in the context of IGCC and Coal-To-Methanol (CTM) applications.

Task 6 – Quench Zone Simulation Follow-on Work: Coanda performed a detailed assessment of jet-jet interactions to guide scale up of the quench zone, where quench water is sprayed into the gasifier syngas product. Study results were used to guide definition of a test apparatus to evaluate jet-jet interactions on hydrodynamics and mixing with good similitude to a demonstration-scale gasifier.

1.3 ABBREVIATIONS

µm	Micrometer
AACRP	Activated Amine Carbon dioxide Recovery Process
AFT	Ash Fluid Temperature
AFWGS	Advanced Fixed-bed Water Gas Shift
AGTF	Advanced Gasification Test Facility
AGWGST	Advanced Gasifier & Water Gas Shift Technologies
AR	Aerojet Rocketdyne
ASME	American Society of Mechanical Engineers
ASTM	American Society for Testing and Materials
ATWGS	Advanced Transport Water Gas Shift
AWGS	Advanced Water Gas Shift
BEP	Basic Engineering Package
BET	Brunauer, Emmett and Teller
Bo	Bond Number
BTU	British Thermal Unit
Ca	Capillary Number
CAPEX	Capital Expenditure
cc	Cubic Centimeter
Cm	Centimeter
COE	Cost of Electricity
CTM	Coal-To-Methanol
DAP	Data Attainment Period
DOE	Department of Energy
DSP	Dry Solids Pump
DSRP	Direct Sulfur Recovery Process
FBR	Fixed Bed Reactor
FCC	Fluidized Catalytic Cracking
FFTF	Flex Fuel Test Facility
g	Gram
GC	Gas Chromatograph
GHG	Greenhouse Gas
gpm	Gallons Per Minute
GTI	Gas Technology Institute
h	Hour
HHV	Higher Heating Value
HT	High Temperature
ICP	Inductively Coupled Plasma
IGCC	Integrated Gasification Combined Cycle
IR	Infrared
kg	Kilogram
kWh	Kilowatt Hour
LT	Low Temperature

m	Meter
MAF	Moisture and Ash Free
mL	Milliliter
MM	Million
NETL	National Energy Technology Laboratory
PDI	Phase-Doppler Interferometry
PFD	Process Flow Diagram
PIV	Particle Image Velocimetry
PMP	Project Management Plan
ppmv	Parts Per Million - Volume
Pr	Prandtl Number
PRB	Powder River Basin
psia	Pounds per Square Inch - Absolute
psig	Pounds per Square Inch - Gauge
Re	Reynolds Number
RSP	Required Selling Price
RTI	RTI International
s	Second
SA	Surface Area
scfh	Standard Cubic Feet per Hour
Sk	Stokes Number
SOPO	Statement of Project Objectives
STP	Standard Temperature and Pressure
TAP	Technology Analysis Plan
TEA	Techno-Economic Analysis
TEB	Triethyl Borane
TOC	Total Overnight Cost
TOS	Time On Stream
TPC	Total Plant Cost
TPD	Tons Per Day
vol%	Volume %
WDP	Warm Desulfurization Process
We	Weber Number
WGS	Water Gas Shift
wt%	Weight Percent
XRD	X-Ray Diffraction

2.0 TASK 2: QUENCH ZONE SIMULATION

The quench zone is where raw syngas exiting the gasifier at temperatures greater than the ash fusion temperature interact with pressure-atomized water jets, with the syngas cooled to suitable process temperatures (~400°C) via vaporization of the water droplets. It is a highly turbulent zone due to the injection of the water droplet jets at relatively high velocity into the raw syngas stream from the perimeter of the quench vessel. Early pilot plant gasifier testing showed a propensity for blockage of the gasifier outlet with frozen slag, leading to misdirected syngas flow within the quench zone and subsequent shutdown of the process. A modified pilot plant gasifier outlet was tested, providing 100's of hours of reliable operation. Given the impact of the quench zone on reliable gasifier operation, there was a need to perform detailed cold flow modelling at a suitable level of similitude relative to hot fire conditions to inform demonstration scale gasifier design. The objectives of Task 2 in this project were to: (1) Systematically test the existing cold flow model with both pilot plant gasifier outlet designs at a high level of similitude to validate suitability of model approach; (2) Perform testing of a scaled demonstration gasifier outlet over a range of operating conditions to assess impact of design options on quench zone behavior. The section below describes the approach and results for this effort at a summary level. Details of experimental approach and results are presented in the Task 2 Topical Report, RD15-223.

2.1 EXPERIMENTAL METHODS

A detailed similitude analysis was carried out for the pilot plant and scaled demonstration outlet configurations to achieve the best possible correspondence between the cold flow model and actual gasifier conditions. Similitude is the degree to which the actual system and physical model are equivalent, and is characterized by three types of similitude – geometric, kinematic and dynamic.

Similitude is established through the process of dimensional analysis, a method for reducing the number and complexity of experimental variables. A phenomenon depending on n dimensional variables x_1, x_2, ... x_n can be reduced to $n - k$ dimensionless variables, where k is the number of fundamental dimensions (mass, length, temperature, time).

For the quench zone depicted in Figure 1, there are 22 key properties and 7 fundamental dimensions (mass, length, time, and temperature), resulting in $n - k = 15$ non-dimensional parameters. This includes consideration of slag parameters.

There are five hydrodynamic parameters: Gas flow Reynolds number, droplet Reynolds number, droplet Weber number, liquid/gas velocity ratio and liquid/gas momentum (inertia) ratio. In addition to these parameters, the similitude analysis also considers the droplet Stokes number to assess the extent to which droplet entrainment within the quench zone happens over the characteristics length scale.

There are eight thermodynamic parameters: Gas and liquid Prandtl numbers, gas and liquid kinetic energy/enthalpy ratios, vapor/liquid density ratio, liquid/gas heat capacity ratio, and two Jakob numbers – one on a heat of vaporization basis, the other on the basis of subcooling. Droplet vaporization time is also included in the similitude analysis, which is looked at in the context of other relevant time scales within the quench zone.

Slag flow is characterized by the Bond number (relative influence of gravitational and surface tension forces) and a form of the Capillary number (relative importance of viscous and surface tension forces).

Similitude for the pilot scale gasifier is summarized in Table 1 for a non-vaporizing flow case using water as the quench spray fluid. There were also tests using HA-134a as a vaporizing fluid, which provided improved visibility into the relative impact of vaporization on quench zone flow fields.

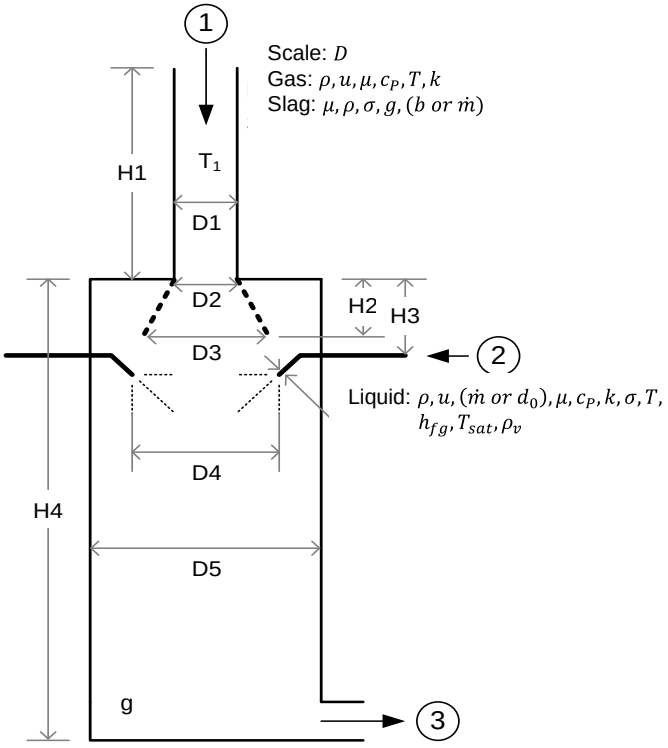

Figure 1: Illustration of key properties for the quench zone, including slag.

Table 1: Similitude assessment for pilot plant gasifier model using non-vaporizing water as the quench spray fluid.

Parameter	*Pilot*	*Model (Air/Water)*	*Ratio (Pilot/Model)*	*Notes*
Gas flow	Baseline	Baseline	3.3	Velocity in model same as pilot.
Liquid flow	Baseline	Baseline	4.9	Model flow rate determined by other similitude requirements.
Re_D	57,000	59,000	1.0	Regime match required ($Re > 10^4$)
We_{d50}	0.4	0.05	7	Based on gas velocity. Regime match required (droplets approx. spherical for $We_d < \sim 1$ and no secondary break up for $We_d < \sim 10$).
Re_{d50}	55	26	2.1	Close match not required. More important to find value that provides Stokes number similitude.
$\frac{u_L}{u_G}$	1.8	3.0	0.6	Stokes number match prioritized in pilot model testing.
$\frac{\dot{m}_L u_L}{\dot{m}_G u_G}$	1.42	1.58	0.9	Stokes number match prioritized in pilot model testing.
Sk_{d50}	0.17	0.17	1.0	$f(We,\ Re_{D_{50}})$ Close match desired to match droplet trajectory for values O(1).
Sk_{d90}	0.25	0.31	0.8	Similitude of larger drops also important (values closer to 1, longer evaporation time).
Bo	2.6	7.4	0.4	Length scale assumed to be drip-lip width, b. Gravitational forces dominate surface tension (Bo > 1) for model and pilot.
Ca^*	71	5.5	13	Velocity scale assumed to be ($\propto \sqrt{gb}$). Viscous forces dominate surface tension (Ca > 1) for model and pilot.

A schematic and picture of the cold flow quench zone model are shown in Figure 2. The apparatus was constructed at a 1:1 scale relative to the 18 TPD pilot plant gasifier, providing a high degree of geometric similitude. The model was built, commissioned and initially tested in late 2013 under an AR-funded project. The gasifier section, outlet cone and the upper section of the quench vessel were fabricated from formed clear acrylic sheets, permitting optical access for instrumentation and video recording equipment. Detailed definition of the experimental apparatus and operating approach is presented in the Task 2 Topical Report, RD15-223.

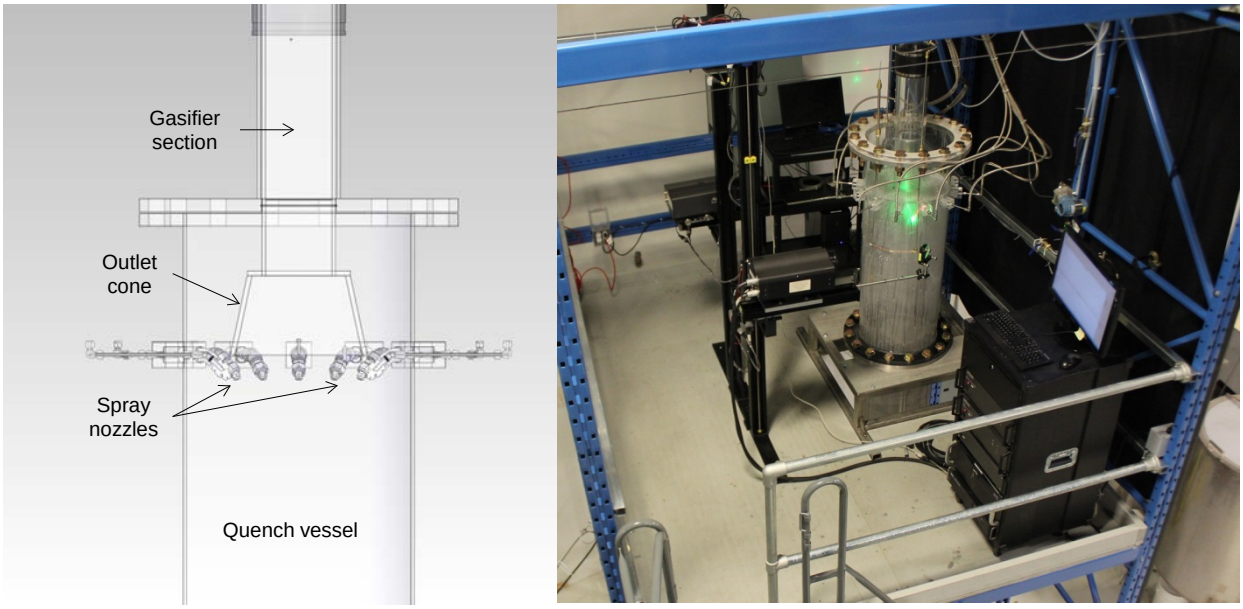

Figure 2: Schematic and picture of the cold flow quench zone model, configured to match pilot plant scale outlet design.

Flow visualization and phase-Doppler velocimetry were the primary forms of data obtained in testing, with the techniques further described below:

Flow visualization: Flow visualization was the primary means of evaluating flow patterns in the quench zone. A Phantom v7.3 high speed digital camera was used in this test program, providing 800 x 600 maximum resolution and a maximum speed of 6888 frames-per-second. The quench zone was illuminated with a 10W laser sheet. High speed video, combined with seeded flow, also provided a basis to perform Particle Image Velocimetry (PIV) to ascertain localized velocity and trajectory.

Phase-Doppler Velocimetry: Localized measurements of liquid droplet velocity field and droplet size were obtained using an Artium Inc. PDI200 MD phase-Doppler interferometer (PDI). PDI is a non-intrusive laser-based measurement technique, based on laser-Doppler anemometry, in which the diameter, velocity and volume flux of individual droplets are measured simultaneously. The instrument consists of separate transmitter and receiver units, positioned such that they focus at the same point. A laser beam from the transmitter unit is split into two beams of equal intensity. The two beams are focused using a transmitter lens and made to intersect at a shallow angle,

forming the measurement volume. Light scattered by objects passing through the measurement volume is collected by a receiver lens and focused onto a photodetector. The component of the object's velocity in the plane of the two laser beams and perpendicular to their axis can be determined from the frequency shift of scattered light intensity (Doppler effect). The object's size can be determined from the phase-shift between signals received at photodetectors separated by a known distance (most systems use three photodetectors – two pairs – to provide adequate range and resolution). By focusing two pairs of different colored beams on the same point, but oriented in different planes (see Figure 3), the velocity can be resolved in the two dimensions perpendicular to the common beam axis. For practical reasons, measurement of the droplet size is based only on the pair of beams having the shorter wavelength. The PDI transmitter and receiver units are mounted on traverses that can be traversed in two dimensions in the quench zone, in a grid measuring approximately 12 in. x 48 in.

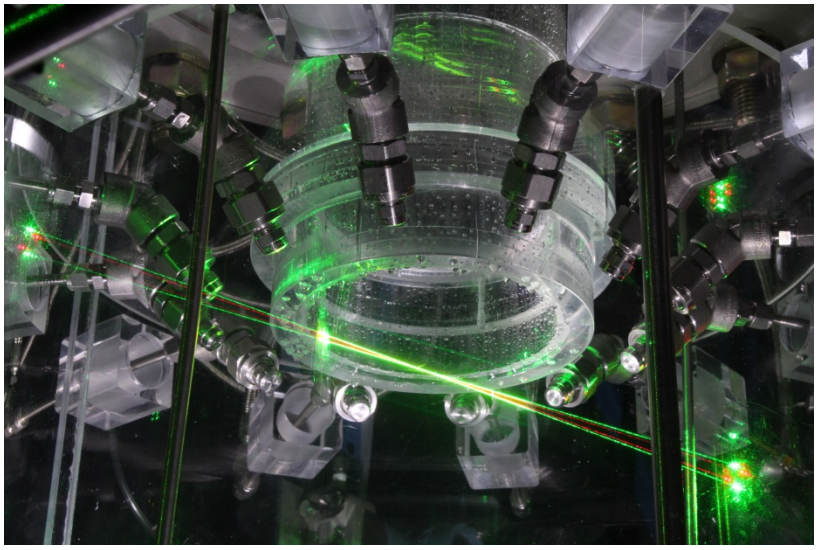

Figure 3: PDI beams traversing the outlet of the pilot plant gasifier model configured with cylindrical outlet. In the set-up shown, the green lasers are measuring the droplet size and vertical component of velocity. The red lasers (less visible) measure the horizontal velocity perpendicular to the common beam axis.

2.2 RESULTS AND DISCUSSION

Pilot scale testing evaluated the influence of nozzle angle, nozzle axial position relative to gasifier outlet, and outlet geometry using the air/water system to evaluate the influence on flow patterns. In summary, it was established that increasing the downward orientation of the nozzle decreased the tendency for recirculation of flow back towards the outlet. However, this comes at the expense of water spray penetration to the core of the syngas. It was also observed that increasing the axial distance between the outlet and the nozzles decreased the tendency for recirculation of flow towards the outlet.

The most pronounced difference among outlet configurations was observed with the introduction of slag simulant for tests with the cylindrical outlet and the conical outlet, with screen capture images shown in Figure 4 for the original cylindrical design and Figure 5 for the conical design, below. Changing the outlet geometry from the original cylindrical design to the modified conical design had the following impacts on slag behavior at the outlet:

(1) The original cylindrical outlet showed significant interaction between the quench liquid emanating from the nozzles and the slag before it could disengage from the gasifier outlet. The slag would often be displaced towards the axis of the outlet, which would account for the frequent observation of slag blockages at the outlet of the original design.

(2) Shearing of the slag streams due to interaction with nozzle jets, along with natural instabilities of vertical liquid columns, lead to formation of irregular droplet geometries, referred to colloquially as “barbells”, “fishhooks”, and “teardrops”. These were very similar to actual slag droplets recovered from pilot plant testing with the original outlet (see bottom of Figure 4). Presumably, the slag froze into these shapes shortly after being distorted by the impinging jets.

(3) The conical outlet provides a drip lip that is isolated from the nozzles, allowing the slag stream to break up prior to exiting the outlet and producing small, well-formed droplets. There was very little apparent interaction between the nozzle jets and falling slag droplets. Again, this is largely consistent with experimental observations from testing of the conical outlet, where most of the coarse slag droplets are spherical in nature.

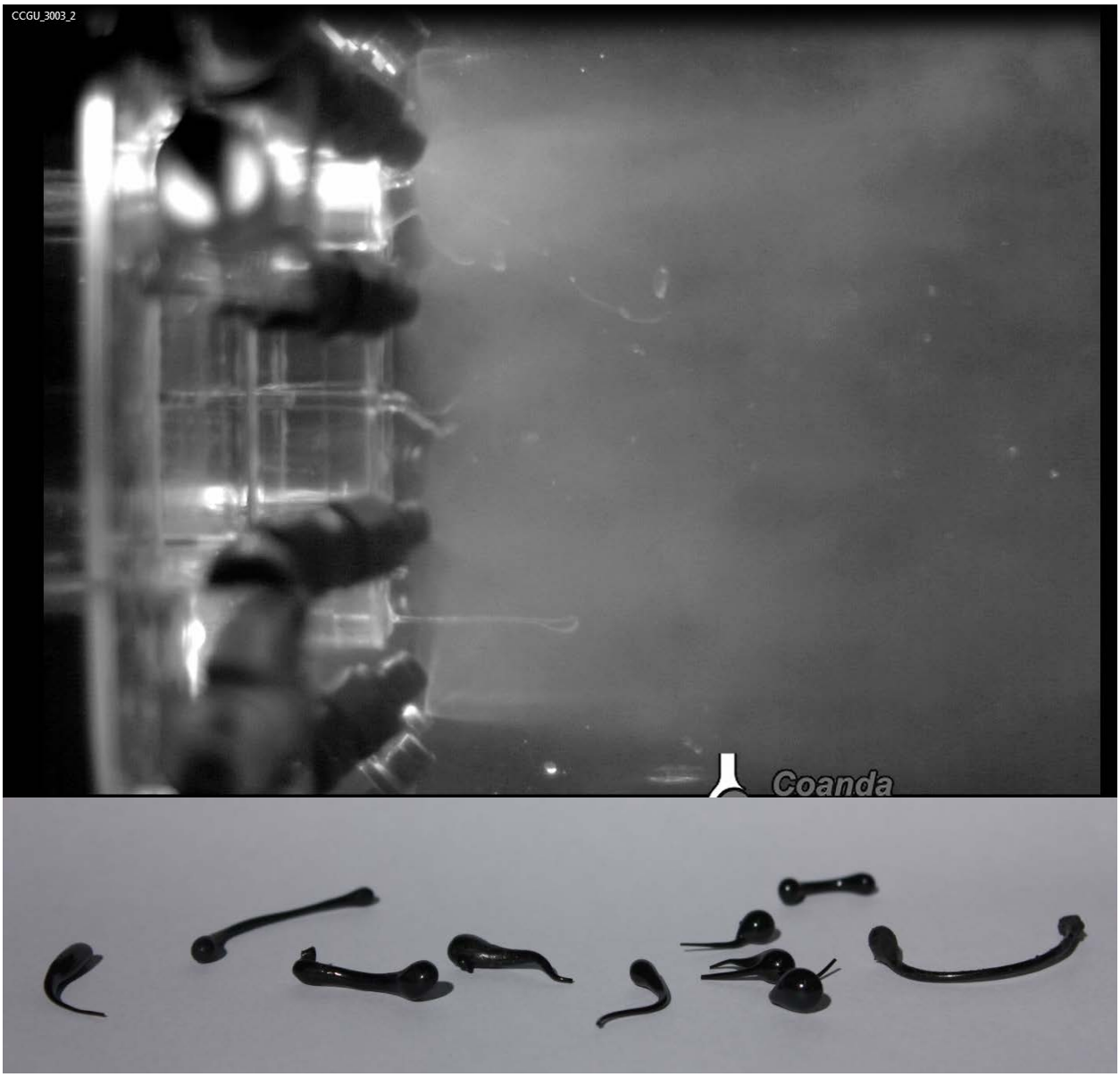

Figure 4: Testing with the original cylindrical outlet design, showing interaction between quench liquid emanating from jets and simulated slag (upper picture). Actual slag droplets corresponding to shapes seen in the simulated testing are shown in the lower picture.

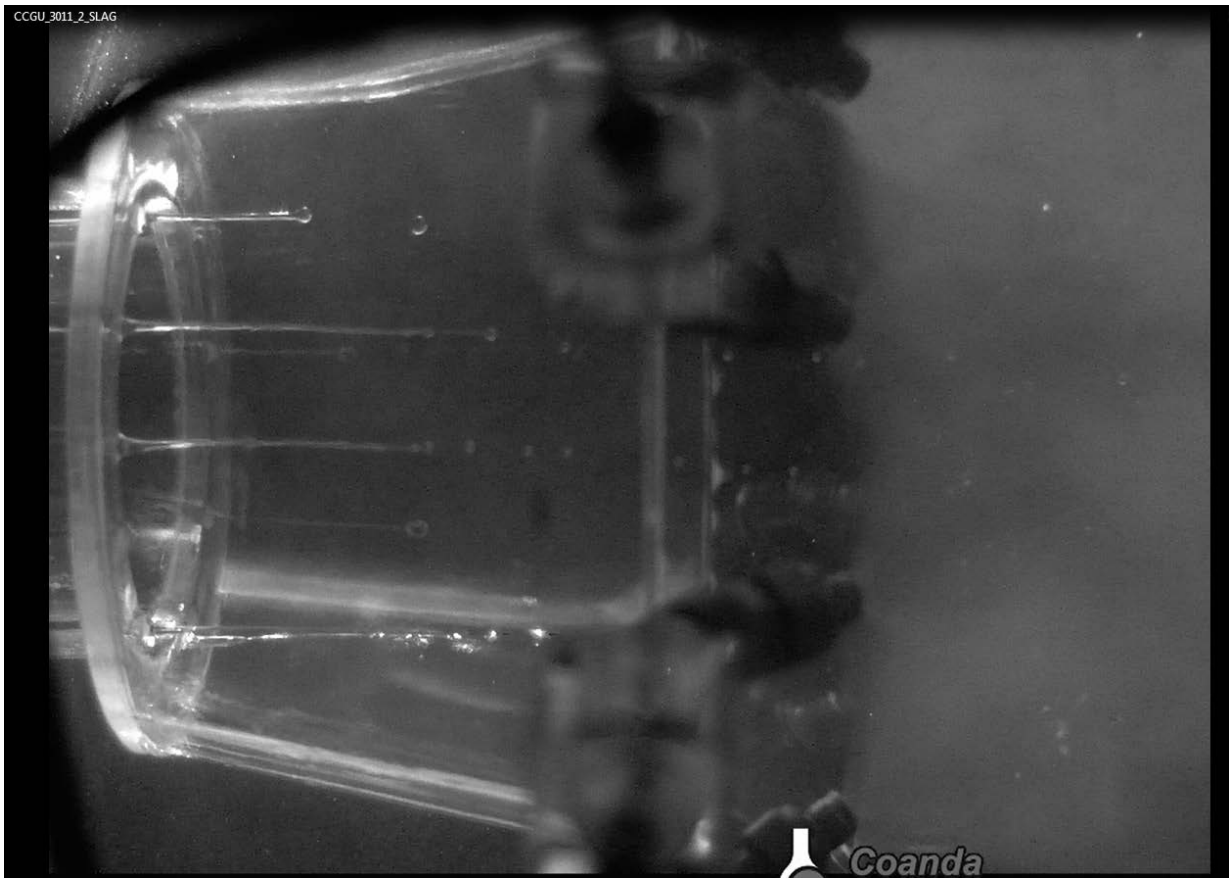

Figure 5: Testing with the modified concical outlet design, showing slag disengagement and formation of spherical drops prior to exiting the gasifier outlet.

In summary, pilot scale testing provided good validation of similitude to actual pilot plant gasifier testing, establishing the suitability of using this physical model to gain insight into demonstration scale gasifier outlet design.

Testing for the demonstration plant gasifier evaluated impacts of: (1) Axial location of nozzles relative to outlet, (2) influence on slag flow for axial location of nozzles relative to outlet; (3) Outlet cone length; (4) Influence of liquid/gas momentum ratio on propensity for recirculation of spray towards outlet; (5) Evaporating flow influence on quench zone hydrodynamics; and (6) PDI evaluation of water droplet hold-up in cone to assess potential cooling effect.

Scaled demonstration quench zone testing indicated that axial location of nozzles had no significant impact on flow patterns or slag discharge. A shorter outlet cone length appeared to be less susceptible to water spray intrusion into the outlet, however there was still some intrusion, and the shorter cone length allows spray to penetrate more closely to the slag drip lip within the outlet.

The observation of recirculation of quench spray back up the axis and into the cone outlet triggered an interest in better understanding the underlying causes. To that effect, a series of tests varying liquid/gas momentum ratio over a range of flow rates were run. A typical overall flow pattern is

depicted in Figure 6. While most of the quench spray continues downward, some fraction of the spray travels against the direction of gas flow up into the outlet. Decreasing the ratio of liquid/gas momentum eventually resulted in suppression of recirculation along the axis, and provided insights into desired momentum ratio values for use in demonstration plant design. Subsequent testing with HA-134a as the quench fluid showed no recirculation under any circumstances, which indicates that designing on the basis of air/water test data should provide a conservative outlet design with regards to quench spray intrusion into the outlet cone.

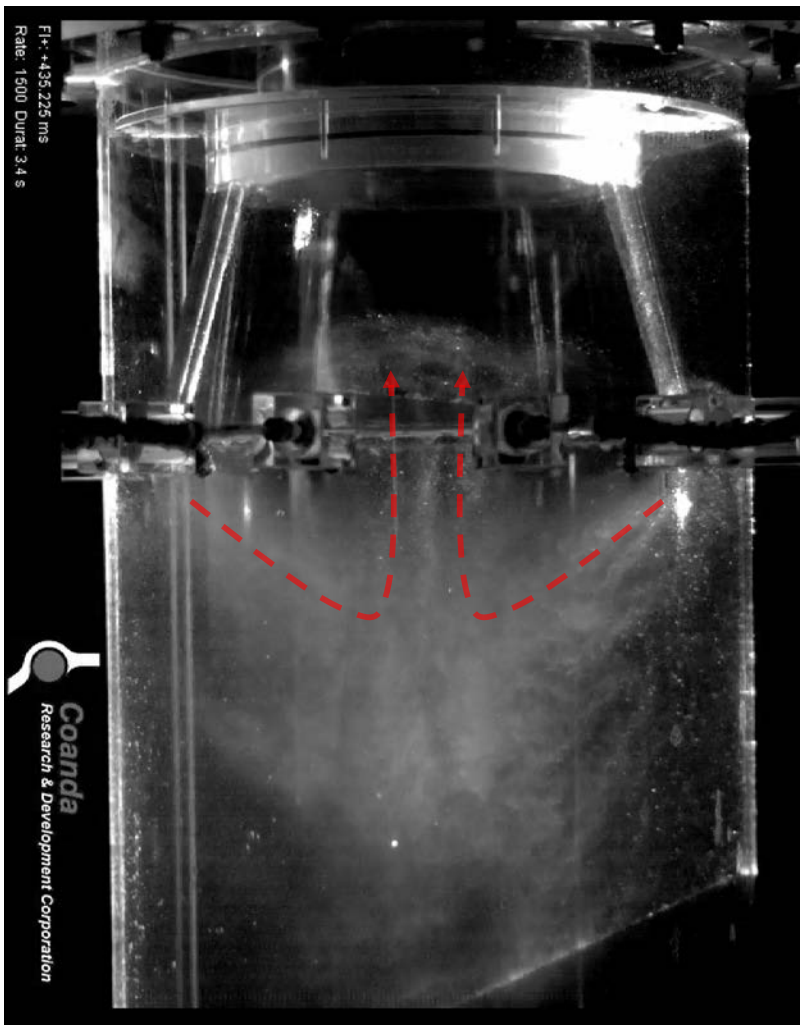

Figure 6: Quench spray shown recirculating to the center of the outlet. Extent of recirculation is dependent upon the ratio of downward gas momentum relative to quench spray jet momentum.

PDI data was obtained at the reference air/water flow condition for the scaled demonstration outlet to more fully characterize water droplet intrusion into the quench zone. The results are shown in Figure 7, with a contour plot of water hold-up (or liquid water content, LWC, in g/m^3). In the bulk of the zone, holdup values are less than 100 g/m^3 (similar to pilot plant results shown in Figure 7). Close to the cone wall, holdup values range from 100-1000 g/m^3. Values > 1000 closest to the wall are suspected to be due to interference from droplet accumulation on the internal surface of the cone. Where measurements indicate backflow into the cone, values of axial velocity were less than 0.5 m/s, typically about 0.1 m/s in the areas with greatest hold-up. Mean droplet diameters ranging from 200-300 µm indicate some possible coalescence by finer droplets within the cone. This PDI data, combined with estimated thermal environments within the cone, provides a basis for assessing persistence of droplets within the quench cone.

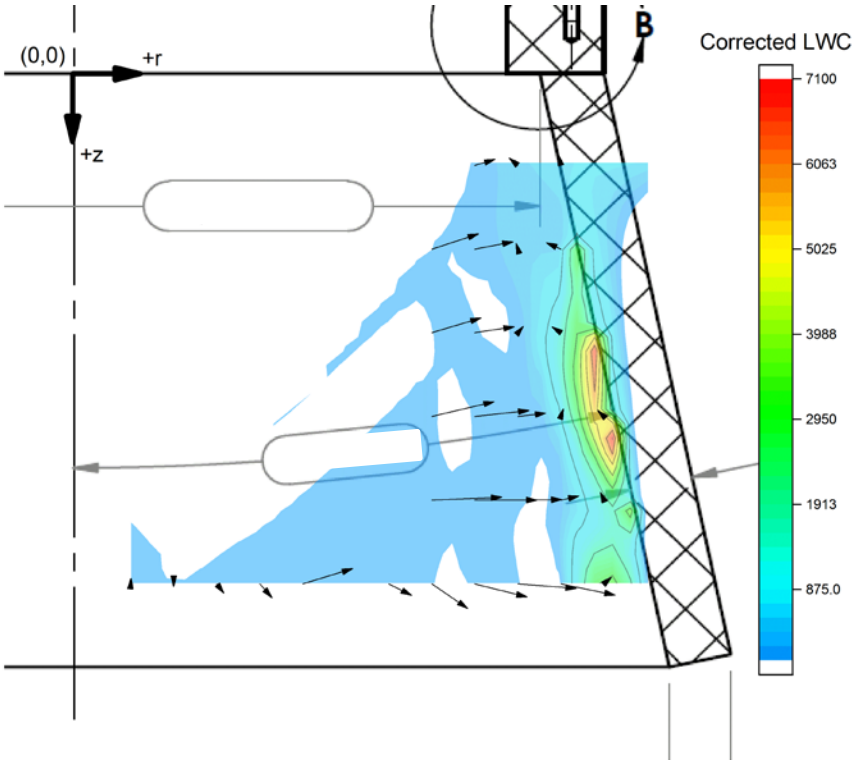

Figure 7: Liquid hold-up contours (in g/m^3) measured by PDI in the scaled demonstration gasifier cone outlet at reference air/water flow conditions.

2.3 CONCLUSIONS

The cold flow modelling approach employed in Task 2 showed excellent consistency with observable pilot plant gasifier results, provides excellent hydrodynamic similitude, and offers acceptable thermodynamic similitude. On that basis, it was concluded that the modelling approach was suitable for use in the scaled demonstration outlet test effort.

Air/water tests and air/HA134a tests show similar flow patterns in the recirculation zones near the vessel perimeter and in the mixing zone downstream of the quench nozzles. However, the air/water system tends to overstate the propensity for quench spray recirculation to the outlet relative to an evaporating quench system. Therefore, the air/water system provides a conservative assessment of quench zone performance with respect to assessing flow patterns and water ingress at the gasifier outlet.

The influences of quench spray nozzle angle, axial distance between cone outlet and spray nozzles, and cone length were evaluated to assess impact on quench zone performance.

- Directing the spray nozzle angle further away from the outlet decreased recirculation backwards towards the outlet. However, this reduces quench spray penetration of the hot syngas, so it should not be the primary design variable manipulated to achieve suitable quench zone flow patterns.
- Increasing axial distance between the gasifier outlet and quench nozzles did slightly reduce the extent of quench spray backflow reaching the outlet. This design variable is of limited utility, as the quench nozzle jets and recirculating spray serve to shield the surrounding vessel from radiant heating by the exiting syngas.
- A shorter cone tends to suppress quench spray recirculation into the outlet. A longer cone provides greater separation between the relatively cool quench zone and the slag drip lip at the top of the cone outlet. Evaluation of water flux into the outlet relative to available heat load in the outlet to vaporize the water before it can impact the slag drip lip indicates a preference for use of the longer cone in the demonstration plant design.

For the nozzle angle tested, a liquid/gas momentum ratio < 1.0 is low enough to avoid recirculation of quench spray back into the cone outlet. Since this is for the air/water system, this would be a conservative ratio. This conclusion should be considered preliminary until a more thorough assessment of the physics and scaling relationships for interaction between these jets is performed.

The project successfully accomplished the objectives set out in Task 2 of the contractual Statement of Project Objectives, in verifying the ability to establish acceptable similitude and providing design guidance for the gasifier outlet to avoid build-up of slag. The test program also indicated other considerations for quench system design that should be considered for a follow-on study. Specifically, recommended follow-on actions are:

- A detailed assessment of jet-jet interactions relevant to an atomized liquid jet and down-flowing gas column. The purpose is to clearly define the physics governing the scale-up of this specific type of jet-jet interaction.
- Using the results from the above assessment, design and fabricate a full scale demonstration gasifier quench zone that is also full length. The purpose of this is twofold – (1) Verify jet-jet interaction dependencies on operating parameters and (2) assess mixing of quench spray within the gas stream to ensure adequate cooling of the syngas before it exits the quench vessel.

3.0 TASK 3: PILOT PLANT GASIFIER TESTING

The GTI compact gasifier is an entrained flow design that achieves rapid conversion of coal to synthesis gas through GTI's proprietary rapid mix injector and plug flow reactor design approach. Commercial application of this technology is expected to offer a highly efficient, low cost and high availability gasifier.

Design, fabrication and initial testing of the pilot plant compact gasifier were completed in 2011. Findings from this initial test program, as well as subsequent gasifier design and pilot plant testing, identified a number of technical aspects to address prior to advancing into a demonstration-scale gasifier design. These were as follows:

(1) Assess the thermal environments associated with highly reactive coals (such as lignite and sub-bituminous) to confirm feasibility of gasifier component designs

(2) Establish the ability to operate the gasifier on high ash content, high ash fusion temperature (AFT) coals, demonstrating continuous slag discharge capability and component feasibility in the challenging thermal environments posed by high AFT coals.

(3) Characterize the properties of residual carbon at high conversion to provide a basis for improved performance prediction as carbon conversion approaches 99%.

The primary objective of this effort was to address these technical challenges in support of demonstration scale gasifier design. A secondary objective was to assess the feasibility of operating the compact gasifier in a hybrid mode, with simultaneous feeding of coal and natural gas.

The overarching goal of this effort is to mature the advanced pilot-scale gasifier design with scalable and commercially traceable components to readiness for use in a first-of-a-kind commercially-relevant demonstration plant on the scale of 500-1,000 tons per day (TPD) by 2020.

The section below describes the approach and results for this effort at a summary level. Details of experimental approach and results are presented in the Task 3 Topical Report, RD15-229.

3.1 EXPERIMENTAL METHODS

Pilot Plant Description:

Testing of the 18 TPD pilot plant gasifier was performed at the Gas Technology Institute in Des Plaines, Illinois. The facility is shown in Figure 8. The control room, feed system, gasifier, coarse slag discharge and gasifier ancillary systems are housed in the Advanced Gasification Test Facility (AGTF). The cyclone, candle filter, ZnO sulfur removal bed, fine particulate lock hoppers, syngas flare, and on-line gas analysis are housed in the Flex Fuel Test Facility (FFTF). The facility and the pilot plant gasifier were designed, fabricated and initially tested under previous programs.

Figure 8. The pilot plant gasifier test program used existing equipment and infrastructure located in the Advanced Gasification Test Facility (left) and Flex Fuel Test Facility (center) at the Gas Technology Institute.

An overall schematic for the pilot plant gasifier is shown in Figure 9. Fuel (coal and/or natural gas) enter the gasifier via the top of the injector. The process flow diagram for coal transport, dense phase feed, gasifier, and gasifier ancillary systems is shown in Figure 10. Detailed description of the facility is provided in Task 3 Topical Report RD15-229.

Testing with the high ash/high ash fusion temperature (AFT) coal in August 2014 revealed significant challenges to continuous removal of slag from the gasifier quench vessel and slag lock hopper. GTI discussed this issue with the DOE/NETL project manager, and received concurrence to implement modifications to the slag discharge system as part of this project. The key elements of this modification are shown in Figure 11, and are described as follows:

(1) Relocation of syngas line from T-315 quench cross to G-302C quench vessel. This allowed modification of T-315 from a dry slag discharge to a slag bath, enabling back-pulsing of the outlet cone on T-315 to disrupt accumulations of solids there.

(2) Modification to T-315 for slag bath water flow. Sufficient slag bath water was required to cool the product slag to < 150°F prior to discharge. For the high ash coal, a flow rate of 2 gpm was estimated to be sufficient.

(3) Installation of a new (smaller) slag discharge vessel, T-306, to support discharge of the coarse slag/water mixture.

(4) Installation of a slag bath water lock hopper system, T-317 and T-319, providing batch let-down of slag bath water received from T-315 and T-305.

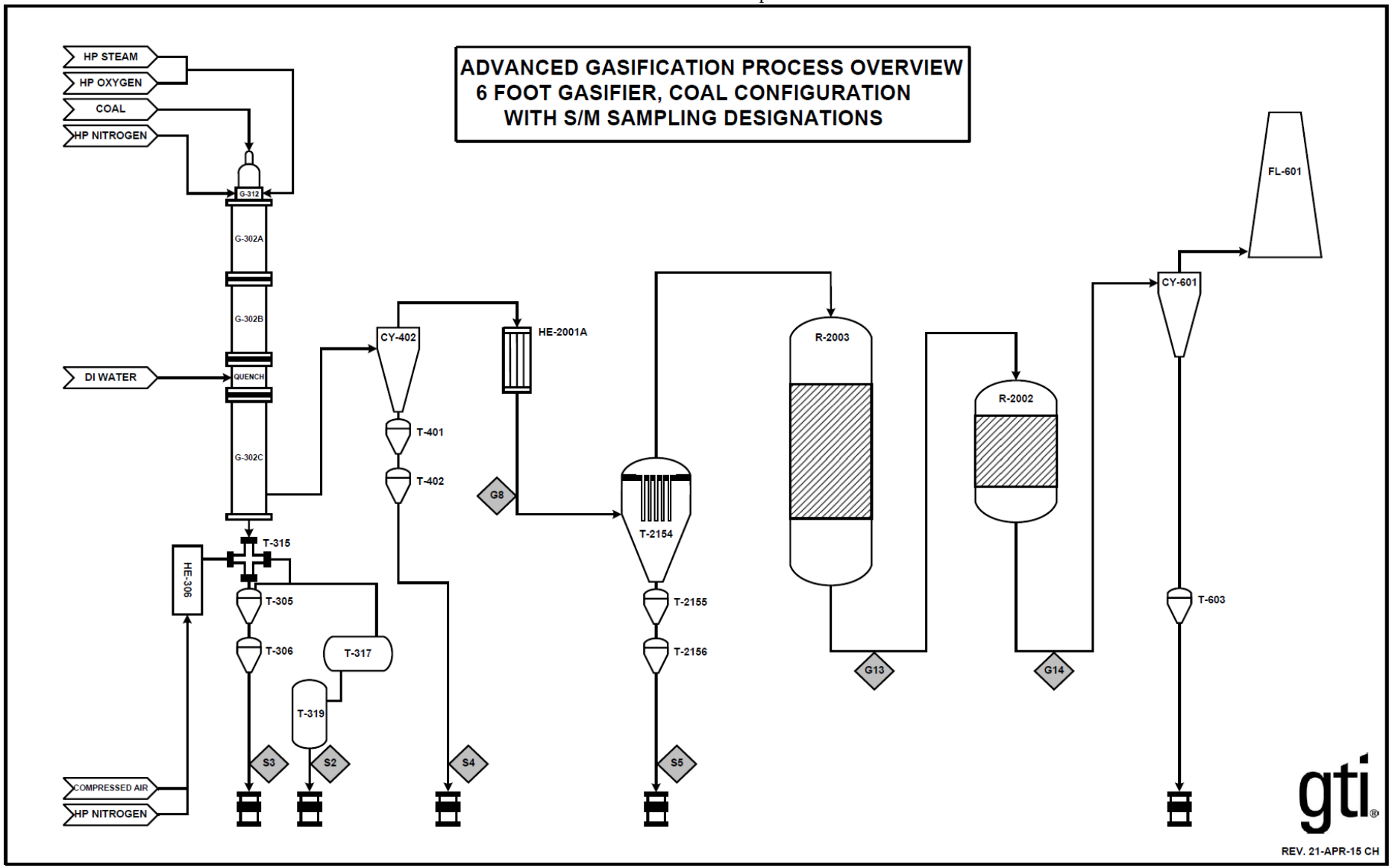

Figure 9. Process flow schematic for the pilot plant gasifier test facility.

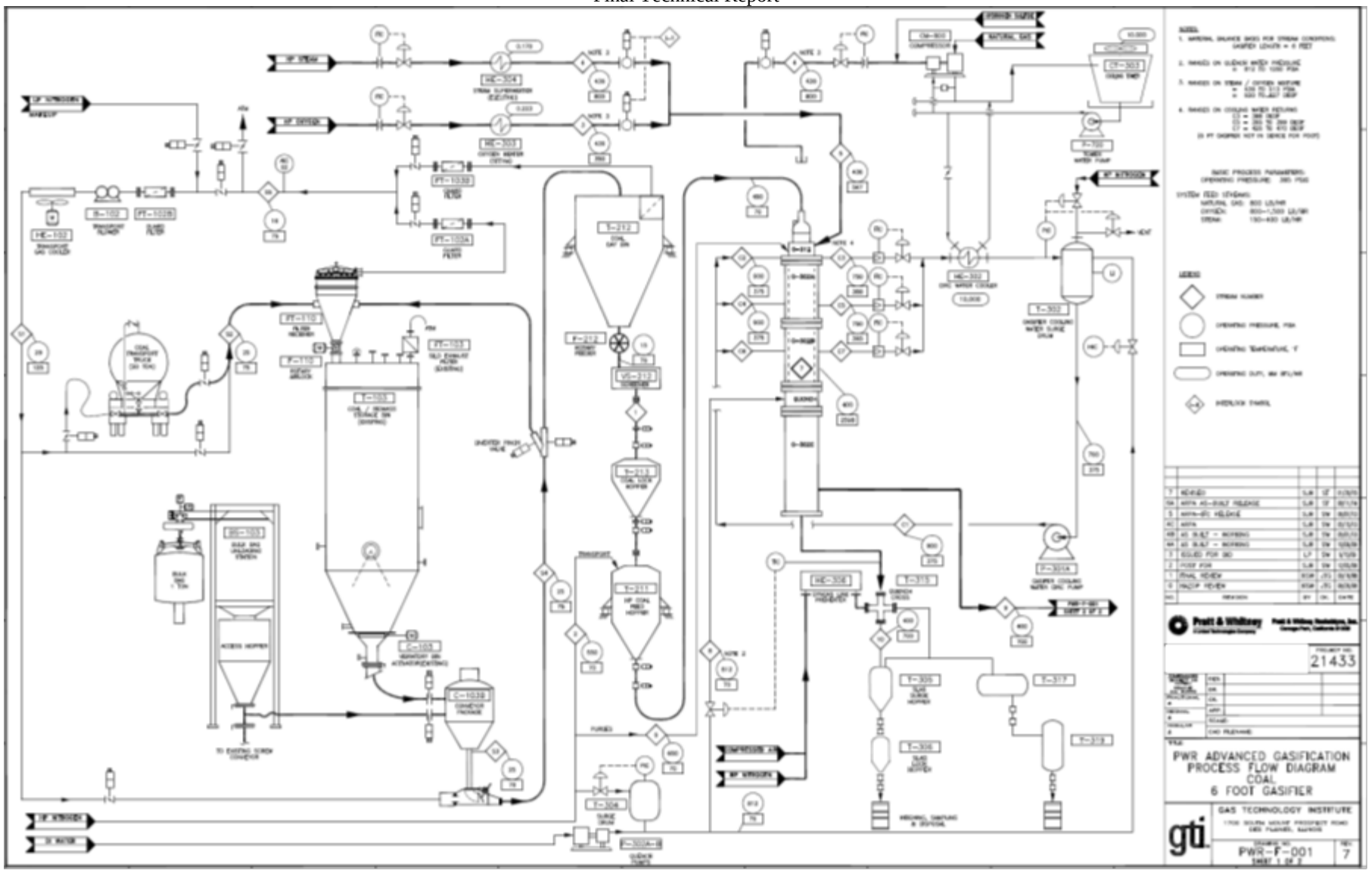

Figure 10. Process flow diagram for pilot plant coal supply, dense phase feed system, gasifier, and slag discharge.

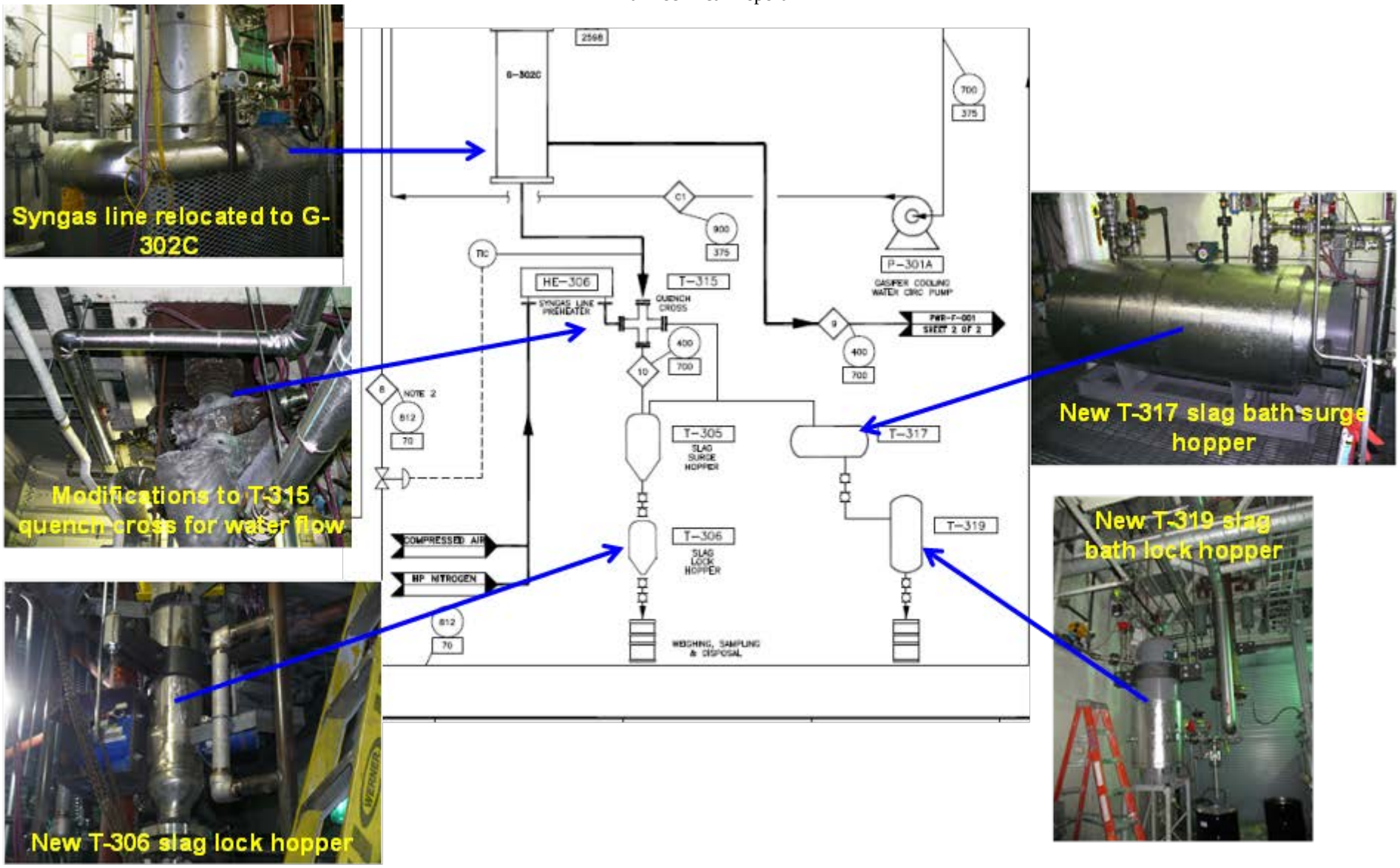

Figure 11. Slag discharge system modifications overview.

Pilot plant gasifier hardware is shown in Figure 12. The gasifier injector and liner are installed in an ASME-stamped steel pressure vessel. Testing for this project used the 3' liner configuration, corresponding to a residence time of ~0.10-0.15 seconds, depending upon operating flow rates. Installation of the liner is shown in Figure 13. A pentad-style injector was used for all tests, with injector installation shown in Figure 14.

Please refer to the Task 3 Topical Report for details on process measurements and operations for the pilot plant.

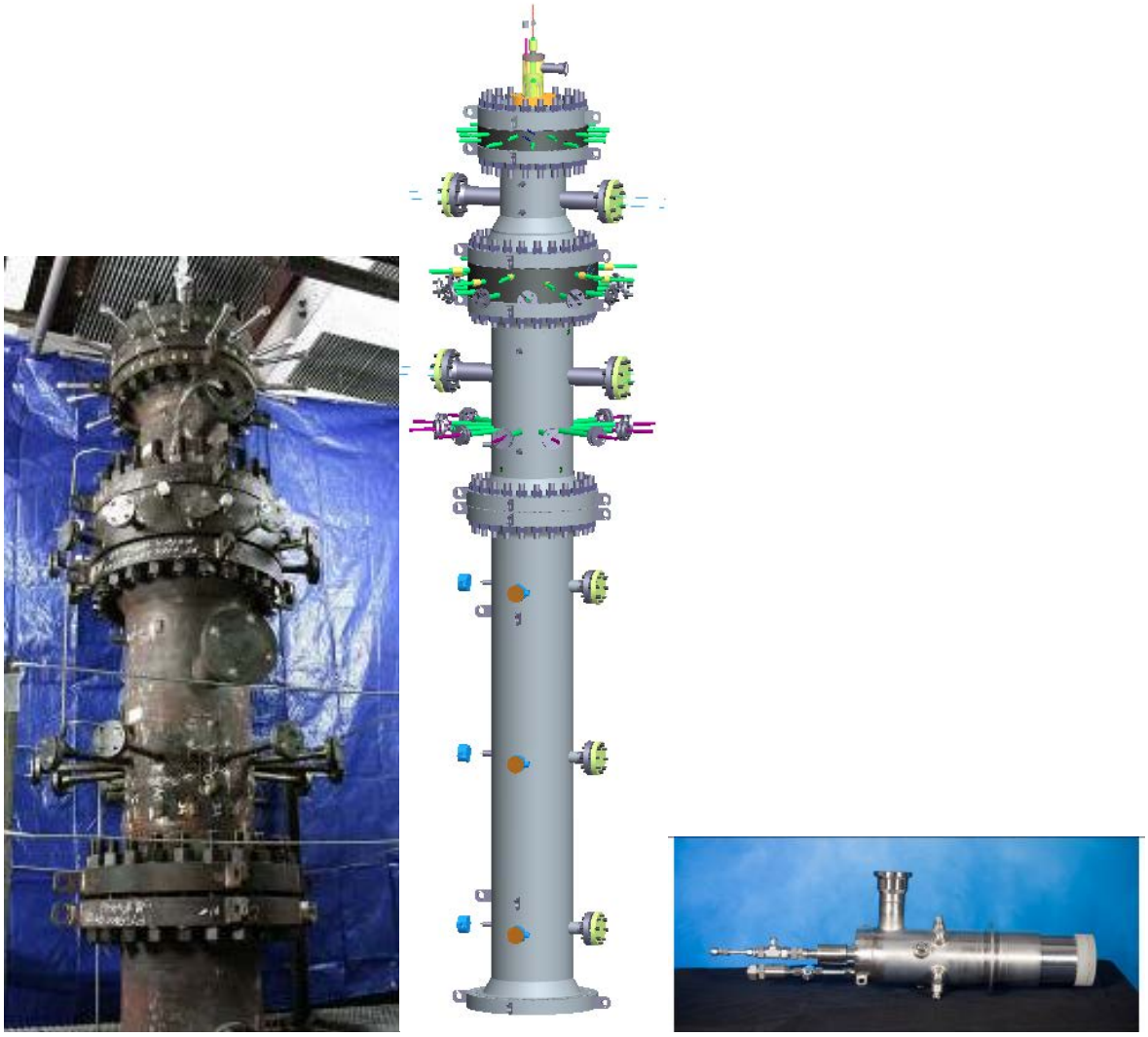

Figure 12. Pilot plant gasifier pressure vessel (left), overall assembly (center), and pentad injector (right).

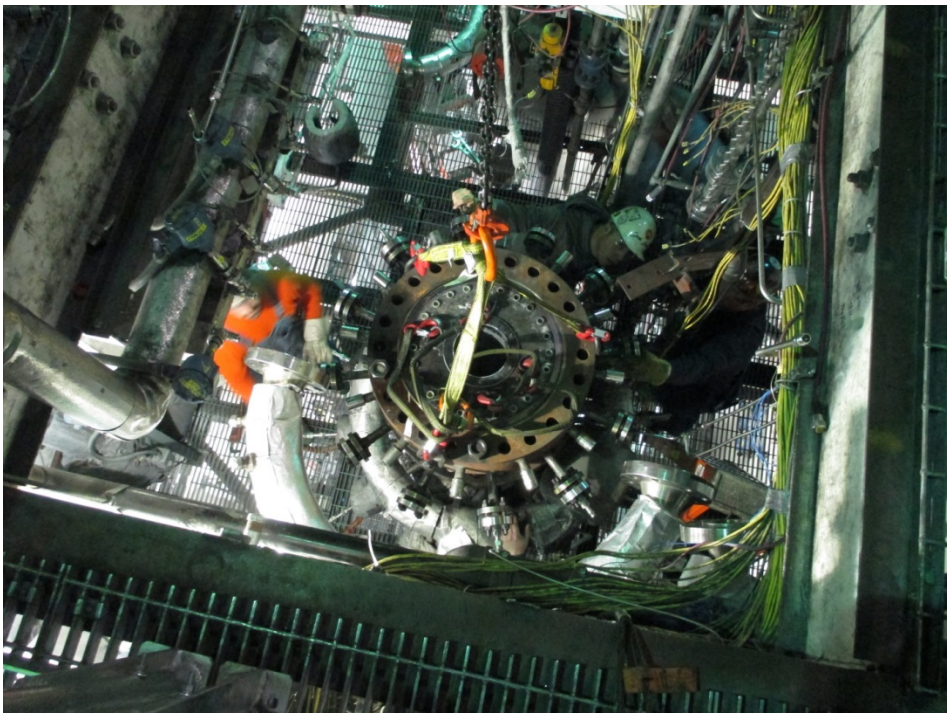

Figure 13. View looking at top of gasifier vessel, with liner installed.

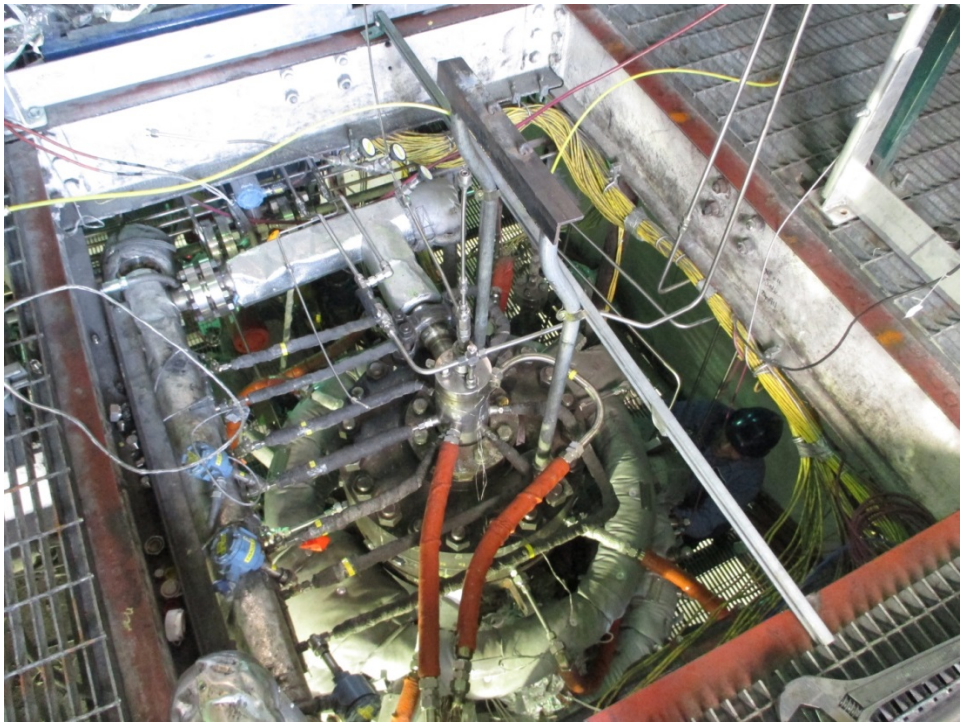

Figure 14. View looking at top of gasifier vessel, with injector installed. Coal is fed into the injector via the line coming down through the top center of the injector. The oxygen/steam mixture is fed via the 2" line coming into the side of the injector from the top of the picture.

Two modifications were made to the gasifier to support testing of the high ash/high AFT coals:

(1) Installation of a Vega Americas (formerly Ohmart/Vega) gamma source and MiniTrac detector (see Figure 15) to detect buildup of solids within the quench vessel.

(2) Design, fabrication and installation of wall wash spray lances to disrupt build-up of material in the upper section of the quench vessel, and incorporating view ports to provide a view at the gasifier outlet in support of flame confirmation.

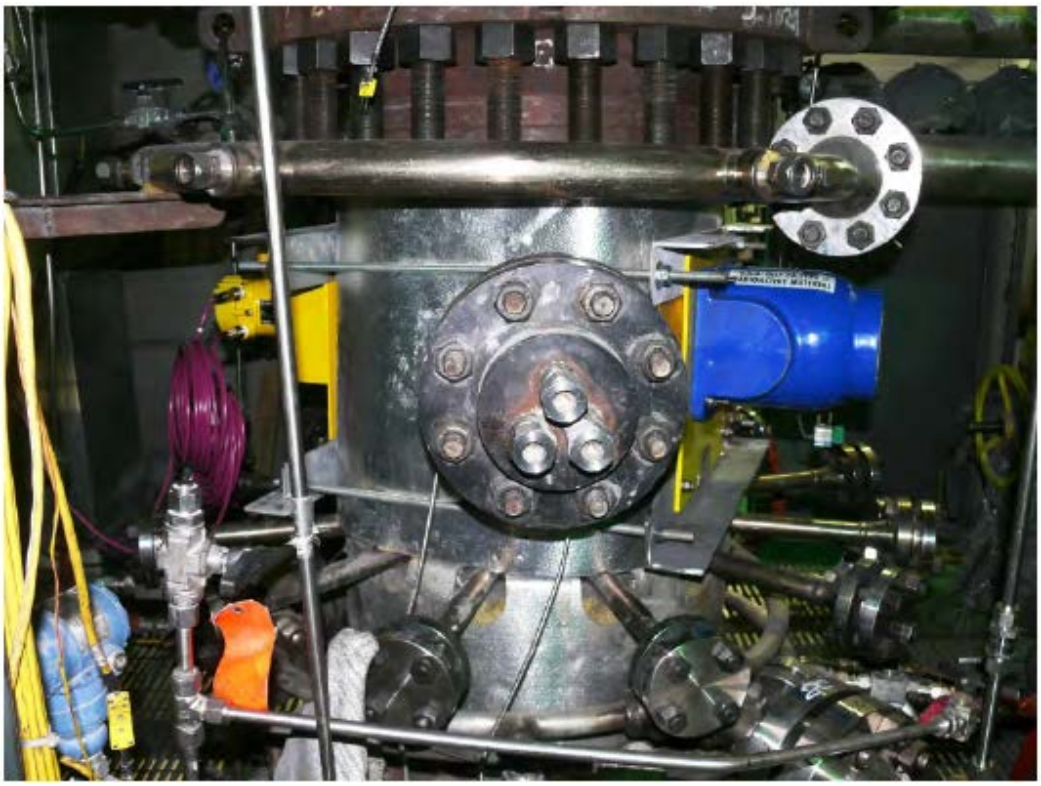

Figure 15. View of gasifier quench vessel just downstream of gasifier outlet, showing installation of Vega Americas gamma source (blue device on the right) and MiniTrac detector (yellow device on the left). This system provided real-time detection of solids build-up within the quench vessel.

Three coals were tested as part of this program. Proximate, ultimate and HHV analysis was performed for each of the Data Attainment Periods (DAP's). Table 2 below summarizes averaged coal properties for these feedstocks.

Table 2. Averaged coal properties for highly reactive (Powder River Basin) and high ash/high AFT (Xinyuan, Xinjing) coals tested on this project.

Coal Name	Powder River Basin	Xinyuan	Xinjing
Coal Type	Sub-bituminous	Anthracite	Anthracite
Moisture (As fed, wt%)	10.88	0.73	0.58
Ash (As fed, wt%)	6.80	25.02	23.96
Carbon (MAF, wt%)	82.32	74.25	75.45
Hydrogen (MAF, wt%)	5.05	3.93	3.57
Nitrogen (MAF, wt%)	1.01	1.31	1.30
Sulfur (MAF, wt%)	0.53	1.33	2.54
Oxygen (MAF, wt%, by difference)	19.51	4.66	4.16
HHV (MAF, BTU/lb)	12,577	14,814	14,731

Profilometry Measurements:

The injector faceplate was subjected to measurement post-test on a Coordinate Measuring Machine, which generates a contour across the faceplate with precision of +/- 0.001". Profiles obtained before and after this test program are compared to assess potential loss of material from the injector faceplate.

Residual Carbon Characterization:

Samples from the solids product streams (coarse slag, T-306 slag water solids, T-319 slag bath solids, cyclone fines and filter fines) were assessed for carbon content. Those specimens that represented the greater fraction of residual carbon in gasifier products were analyzed to determine surface area and porosity of the residual char. Since these solids samples tended to be predominantly slag (carbon content ranging from 5%-40%), surface area and porosity for the residual carbon was determined by difference between the original sample and an "ashed" sample, from which the residual carbon was oxidized. The assumption here is that the difference corresponds to surface area and porosity associated with the carbon that was removed.

Full mercury-intrusion-porosimetry analyses were performed with the Micromeritics AutoPore IV instrument. This analysis covers the range of pore diameters between 0.0030 μm and 180 μm. Besides a tabulation of the intrusion-versus-pressure data, and plots of those data, also included in a typical report are one particle-density value (labeled "Bulk Density" by the Micromeritics software), normally taken at 25 psia applied pressure, and the "Apparent (Skeletal) Density" measured at the highest applied pressure, which is ≈60,000 psia.

Nitrogen surface-area analyses were performed with the Micromeritics ASAP-2010 instrument. This employs the BET (Brunauer, Emmett, and Teller) method to determine the surface area of a sample, by use of nitrogen adsorption onto the sample's surface at liquid-nitrogen temperatures.

The lower limit of measurement is primarily determined by the quantity of sample which can be introduced into the instrument's sample holders (20cc of bulk volume, maximum). Surface-area measurements in the 5 - 10 m^2/g range are possible, given a large-enough volume/mass of sample.

Porosity attributed specifically to the residual carbon within the samples is obtained by comparing porosimetry data obtained on the original and "ashed" samples. Residual carbon porosity, $\boldsymbol{\varepsilon_C}$, is calculated as follows:

$$\boldsymbol{\varepsilon_C} = \frac{\boldsymbol{V_C}/\boldsymbol{m_C}}{\boldsymbol{V_C}/\boldsymbol{m_C} + \mathbf{1}/\boldsymbol{\rho_C}}$$

where the pore volume attributed to carbon, $\frac{\boldsymbol{V_C}}{\boldsymbol{m_C}}$, is calculated from

$$\frac{\boldsymbol{V_C}}{\boldsymbol{m_C}} = \frac{\left(\frac{\boldsymbol{V_T}}{\boldsymbol{m_T}} - (\mathbf{1} - \boldsymbol{X_C})\frac{\boldsymbol{V_A}}{\boldsymbol{m_A}}\right)}{\boldsymbol{X_C}}$$

Other parameters are defined as follows:

$\frac{\boldsymbol{V_T}}{\boldsymbol{m_T}}$ = Total pore volume of original sample per unit mass

$\frac{\boldsymbol{V_A}}{\boldsymbol{m_A}}$ = Total pore volume of ashed sample per unit mass

$\boldsymbol{X_C}$ = Weight fraction of carbon in the original sample

$\boldsymbol{\rho_C}$ = Skeletal density of carbon, assumed to be 1.2 g/cm^3 for these calculations

Surface area per unit mass attributed specifically to the residual carbon, $\boldsymbol{S_C}$, within the samples is obtained by comparing surface area data obtained on the original and "ashed" samples, and is calculated as follows:

$$\boldsymbol{S_C} = \frac{\boldsymbol{S_T} - \boldsymbol{S_A}}{\boldsymbol{X_C}}$$

where

$\boldsymbol{S_T}$ = Surface area of original sample per unit mass

$\boldsymbol{S_A}$ = Surface area of ashed sample per unit mass

$\boldsymbol{X_C}$ = Weight fraction of carbon in the original sample

3.2 RESULTS AND DISCUSSION

Highly Reactive Coal Testing:

The objective of the highly reactive coal testing task was to establish the feasibility of gasifier operations on these coals, particularly with regards to the ability of gasifier internal components (injector, liner) to withstand the thermal environments generated from the conversion of these feeds. This was to be established by operating the pilot plant gasifier on PRB coal at representative conditions, with assessment of measured thermal environments relative to design conditions and inspection of the injector and liner post-test.

Test conditions and results (carbon conversion, mass/energy/elemental balances) are summarized in Table 3. Data quality was acceptable, with all four data points within 10% on overall mass and energy balance. Carbon balance was within 6%.

Table 3. Test conditions and summary results for pilot plant gasifier testing on highly reactive (PRB) coal

	Highly Reactive Coal			
	DAP 240	**DAP 241**	**DAP 242**	**DAP 243**
Coal (lb/hr)	1329	1355	1302	1310
Oxygen (lb/hr)	1000	1050	1100	1050
Steam (lb/hr)	76	76	75	80
Nitrogen (lb/hr)	174.4	175.2	173.9	175.6
Conversion (%)	97.39%	98.11%	98.66%	97.40%
Mass Balance (%)	102.8%	100.8%	106.3%	108.9%
Enthalpy Balance (%)	95.4%	96.0%	99.3%	98.0%
Carbon Balance (%)	94.2%	94.0%	102.6%	97.4%
Hydrogen Balance (%)	105.0%	101.2%	105.2%	112.1%
Nitrogen Balance (%)	112.8%	114.8%	129.6%	118.3%
Sulfur Balance (%)	84.5%	84.6%	91.2%	91.7%
Oxygen Balance (%)	103.6%	100.5%	105.6%	110.5%
Moisture (As fed)	11.81	10.65	11.66	11.10
Ash (As fed)	6.66	6.51	7.14	7.97
Coal (MAF, as fed)	81.53	82.84	81.20	80.93

Carbon conversion ranged from 97% to almost 99% for this highly reactive coal, even though residence time was < 0.15 seconds and outlet temperatures were approximately those expected for commercial operations. Therefore, no performance issues are expected with PRB coal.

The thermal environments measured at the injector faceplate and along the liner were found to be well within the design basis for both components. Post-test inspection showed no visible impact to hardware condition.

The partial quench system in the compact gasifier does lead to some Water Gas Shift (WGS) reaction occurring as the raw synthesis gas is cooled from the gasifier outlet temperature. While there is a significant increase in the hydrogen content relative to the predicted equilibrium syngas composition, it is still far from the equilibrium value of the final quenched gas mixture. This is because the WGS reaction kinetics slow rapidly with decreasing temperature. The relationship between the actual and predicted ratios of H_2/CO and CO_2/CO relative to predicted gasifier outlet temperature is shown in Figure 16.

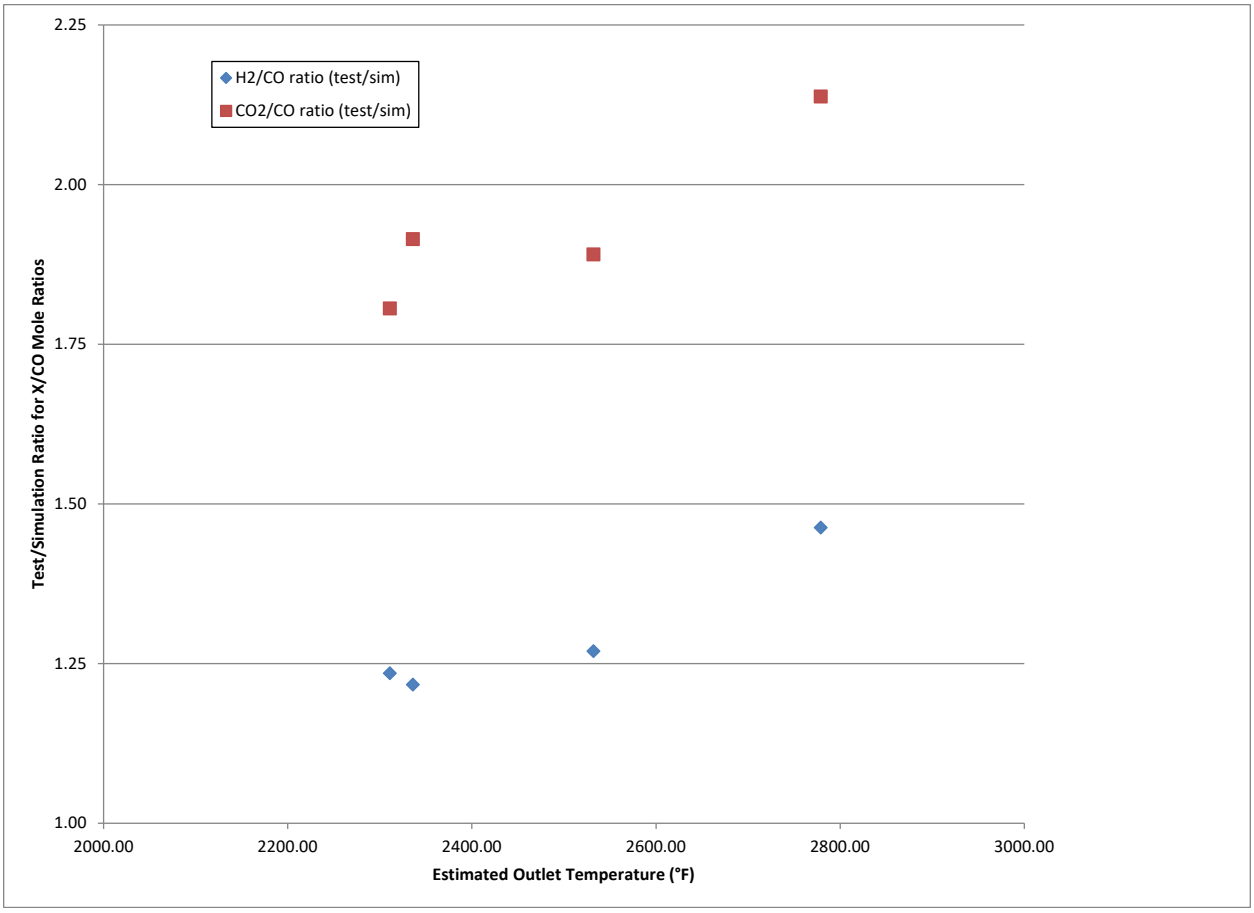

Figure 16. Ratio of test data versus predicted data for H_2/CO and CO_2/CO ratios increases with increasing estimated gasifier outlet temperature on PRB coal.

<u>High Ash Fusion Temperature Coal Testing:</u>

Conventional entrained flow gasifier technologies are severely constrained in their ability to process high ash fusion temperature (AFT) coals. For low to moderate ash levels, flux (such as

limestone) may be added to reduce AFT to more manageable temperatures, preferably < 1300°C. However, for feedstocks with >20% ash by weight, the incremental penalty of introducing additional inerts has a significant negative impact on process performance and economics.

The objectives of this effort were to test two high ash/high AFT (~25% ash, >1500°C AFT) anthracite coals to assess the ability of the compact gasifier to manage the associated thermal environments, to exhibit reliable slag discharge from the system, and to obtain data on the dependency of residual carbon surface area and porosimetry for the purpose of anchoring gasifier performance models at high carbon conversion.

Test conditions and results (carbon conversion, mass/energy/elemental balances) are summarized in Table 4. Data quality was acceptable, with all eight data points within 10% on overall mass and energy balance. Carbon balance was within 7%. However, for DAP 230, the spread between overall mass balance and carbon balance was >10%, so this point was not used in subsequent data analysis.

Table 4. Test conditions and summary results for pilot plant gasifier testing on high ash/high AFT coals.

	Xinyuan Coal					Xinjing Coal		
	DAP 230	**DAP 231**	**DAP 233**	**DAP 248**	**DAP 249**	**DAP 234**	**DAP 235**	**DAP 237**
Coal (lb/hr)	1035	1096	1039	1062	1079	1070	1064	1018
Natural Gas (lb/hr)								
Oxygen (lb/hr)	1040	960	1120	1080	1040	1040	980	1120
Steam (lb/hr)	200	200	200	200	200	200	200	200
Nitrogen (lb/hr)	113.3	168.4	169.9	164	164.8	169.4	172.8	129.2
Conversion (%)	95.78%	89.28%	97.02%	96.36%	94.04%	90.08%	85.25%	96.02%
Mass Balance (%)	108.1%	104.0%	101.3%	100.0%	97.7%	104.4%	104.1%	102.6%
Enthalpy Balance (%)	92.7%	100.6%	94.9%	103.1%	96.6%	103.3%	103.9%	99.6%
Carbon Balance (%)	95.3%	99.2%	99.0%	107.0%	98.0%	105.8%	105.6%	101.8%
Hydrogen Balance (%)	117.2%	98.5%	105.2%	94.2%	94.8%	104.5%	102.7%	103.5%
Nitrogen Balance (%)	135.1%	131.3%	121.3%	131.8%	122.2%	127.5%	134.5%	126.9%
Sulfur Balance (%)	73.8%	98.5%	87.5%	102.0%	97.8%	92.7%	93.5%	85.3%
Oxygen Balance (%)	111.2%	99.0%	103.5%	96.2%	94.9%	103.0%	101.6%	102.2%
Ash Balance (%)	100.0%	100.0%	100.0%	100.0%	100.0%	100.0%	100.0%	100.0%
Heat Loss (MMBTU/hr)	0.94	0.59	0.80	0.67	0.79	0.76	0.41	1.03
Moisture (As fed)	0.53	0.64	0.53	0.89	1.05	0.65	0.52	0.58
Ash (As fed)	26.43	24.36	25.33	24.59	24.41	24.34	22.95	24.60
Coal (MAF, as fed)	73.04	75.00	74.14	74.52	74.54	75.01	76.53	74.82

The thermal environments posed by these coals were well within the design capabilities of the injector and liner designs. Outlet temperatures (shown in Table 5, inferred based on process simulation using actual feed streams and measured heat losses) ranged from 3400°F to 4200°F, well above the ~3000°F target outlet temperature expected for commercial operation on these coals.

Carbon conversion ranged from 89% to 97% on the Xinyuan coal, and 85% to 96% on the Xinjing coal, providing a good span of carbon conversion from which to assess trends of surface area and porosity associated with the remaining carbon.

Surface area per unit residual carbon relative to carbon conversion is shown for each of the samples in Figure 17. In general, values are consistent among the various sample streams for a given DAP. A similar plot, this one showing weighted surface area data for the overall DAP sample streams, is shown in Figure 18. Both coals had similar surface area values and showed similar decrease in surface area per unit residual carbon with increasing carbon conversion, with a linear trend corresponding to approximately 62 m^2/g at 85% carbon conversion, decreasing to 36 m^2/g at 97%. This significant decrease confirms the importance of incorporating treatment of surface area as a function of carbon conversion into calculation of the Thiele modulus in support of coal gasifier modelling.

Residual carbon porosity data showed much less of a trend relative to carbon conversion, as seen in Figure 19. The Xinyuan coal porosity tended to range between 50%-60%. Xinjing coal tended to range between 70% and 80%, with one of the four points at about 50%. In the absence of a clear trend, and in the interest of forming a conservative assessment of carbon conversion in gasifier modelling, it is recommended that a constant porosity value of 50% be used in model calculations.

Table 5. Actual syngas composition measured downstream of gasifier and simulation predictions for gasifier outlet composition for pilot plant gasifier testing on high ash/high AFT coals.

	Xinyuan Coal					Xinjing Coal		
	DAP 230	**DAP 231**	**DAP 233**	**DAP 248**	**DAP 249**	**DAP 234**	**DAP 235**	**DAP 237**
Coal (lb/hr)	1035	1096	1039	1062	1079	1070	1064	1018
Natural Gas (lb/hr)								
Oxygen (lb/hr)	1040	960	1120	1080	1040	1040	980	1120
Steam (lb/hr)	200	200	200	200	200	200	200	200
Nitrogen (lb/hr)	113.3	168.4	169.9	164	164.8	169.4	172.8	129.2
Conversion (%)	95.78%	89.28%	97.02%	96.36%	94.04%	90.08%	85.25%	96.02%
Actual Syngas Composition								
Carbon Dioxide	23.5%	17.9%	25.1%	23.1%	20.3%	19.9%	19.2%	26.3%
Carbon Monoxide	50.2%	54.0%	49.2%	49.2%	51.0%	53.2%	52.8%	48.4%
Carbonyl Sulfide	0.0%	0.0%	0.0%	0.0%	0.0%	0.1%	0.1%	0.1%
Hydrogen	26.0%	27.6%	25.2%	27.3%	28.2%	26.1%	27.2%	24.5%
Hydrogen Sulfide	0.3%	0.4%	0.4%	0.4%	0.4%	0.7%	0.7%	0.7%
Methane	0.0%	0.0%	0.0%	0.0%	0.0%	0.0%	0.0%	0.0%
Simulation Results								
Temp (F)	3744.00	3423.00	4181.00	3967.00	3613.00	3925.00	4108.00	4197.00
Carbon Dioxide	15.4%	14.9%	17.2%	14.4%	14.3%	18.4%	20.5%	19.8%
Carbon Monoxide	67.0%	59.1%	68.0%	67.7%	65.0%	61.2%	55.0%	66.7%
Carbonyl Sulfide	0.2%	0.1%	0.3%	0.2%	0.1%	0.3%	0.4%	0.7%
Hydrogen	17.1%	25.6%	14.3%	17.4%	20.3%	19.5%	23.6%	12.5%
Hydrogen Sulfide	0.3%	0.4%	0.2%	0.3%	0.4%	0.6%	0.6%	0.3%
Methane	0.0%	0.0%	0.0%	0.0%	0.0%	0.0%	0.0%	0.0%

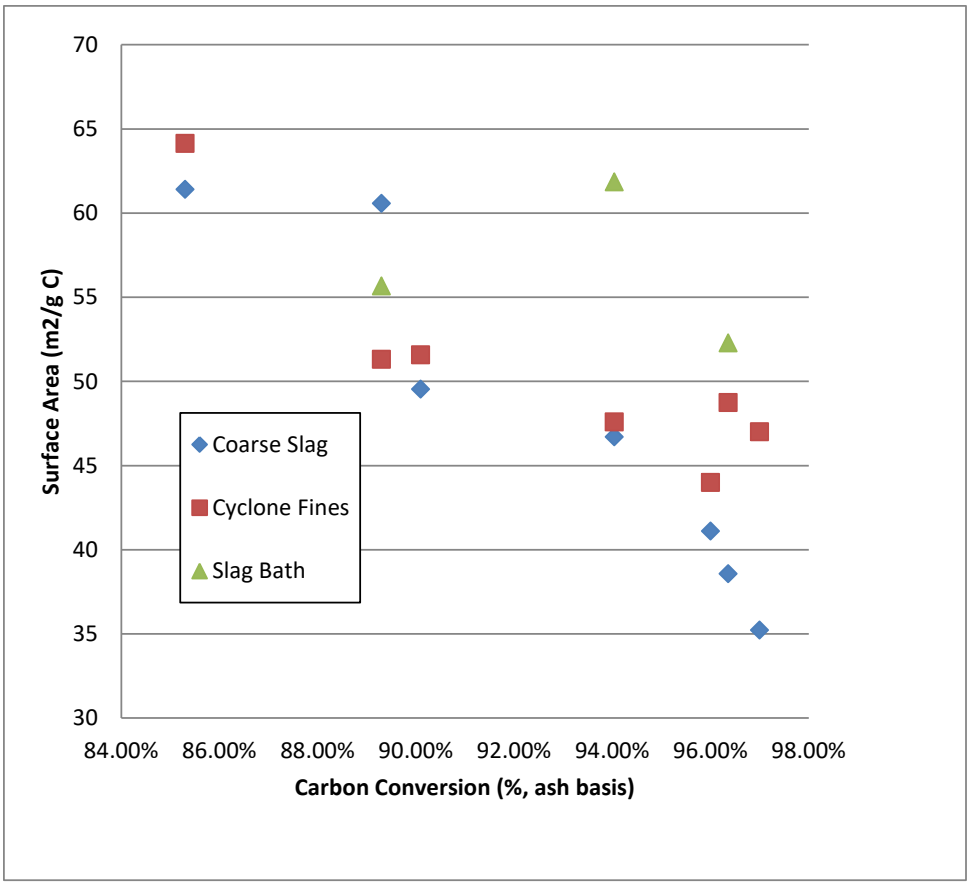

Figure 17. Surface area per unit of residual carbon plotted against carbon conversion for the high ash/high AFT coal data points.

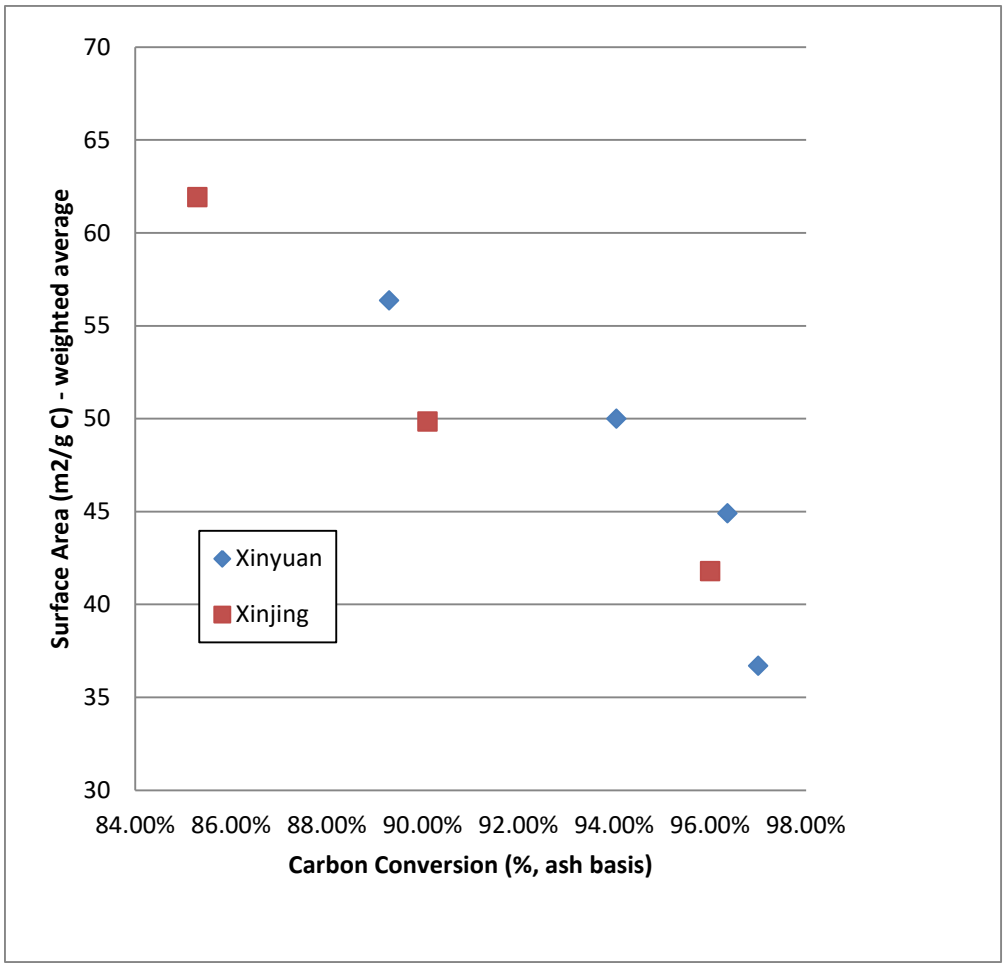

Figure 18. Surface area per unit of residual carbon for each of the high ash/high AFT DAP's, weighted corresponding to carbon content in each of the sample streams.

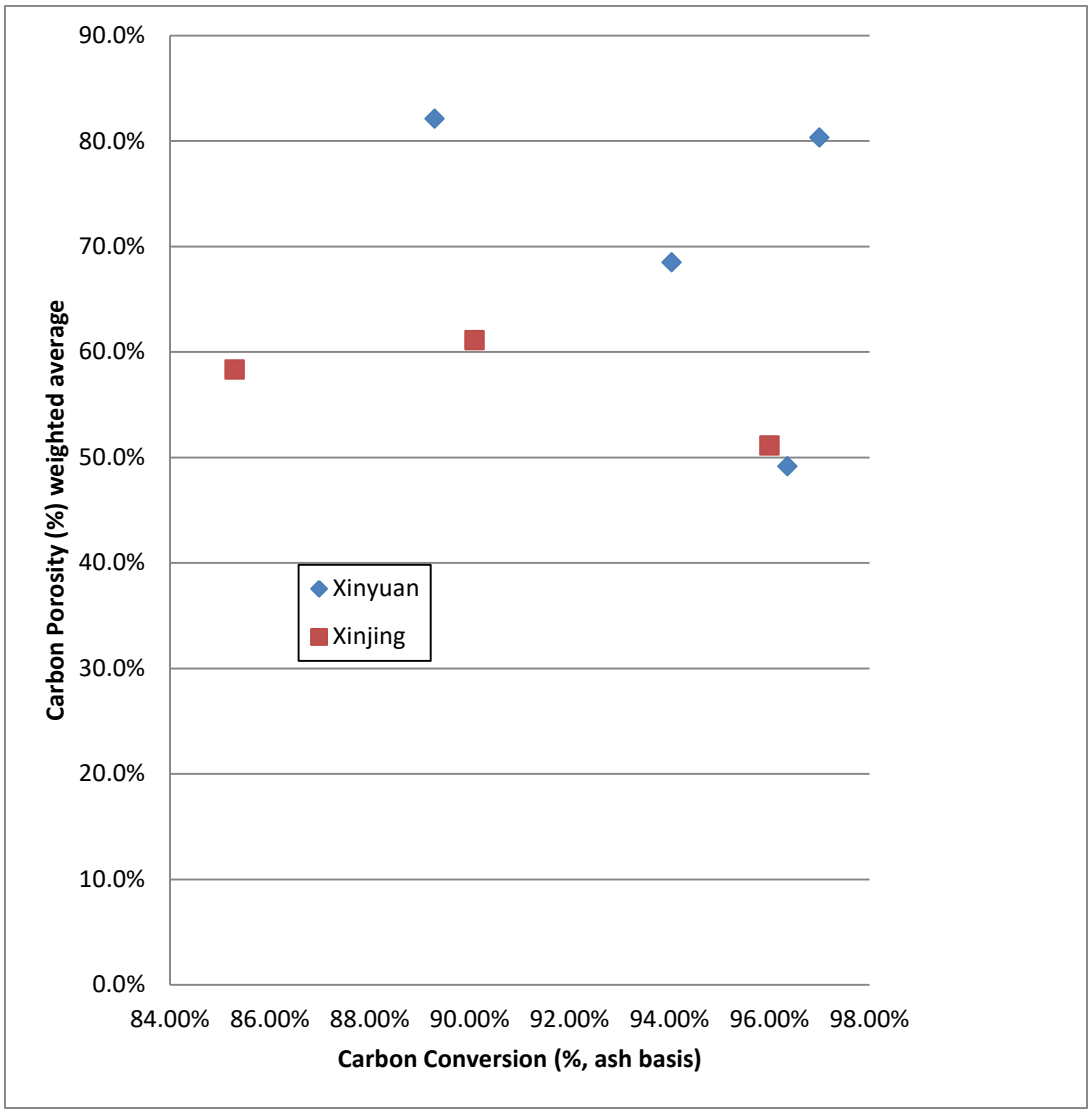

Figure 19. Porosity of residual carbon for each of the high ash/high AFT DAP's, weighted corresponding to carbon content in each of the sample streams.

The injector and liner were inspected after testing was completed. The liner was completely covered with slag which conformed to the contours of the liner in the zone with the most severe thermal environment, and a thicker layer of slag deposited in the cooler zone. Profilometry results for the injector are shown in Figure 20. This evaluation showed that no greater than 0.001" of material was lost over the course of 160 hours of additional testing. For cumulative hot fire test time of >900 hours, this injector has shown no measurable loss of parent material. Delamination of the ~ 0.005" thick erosion barrier was observed in the zone with most severe thermal environment (corresponding to the "dips" in the plots), but it appears that cooling is sufficient to prevent any corrosion or erosion of the parent material.

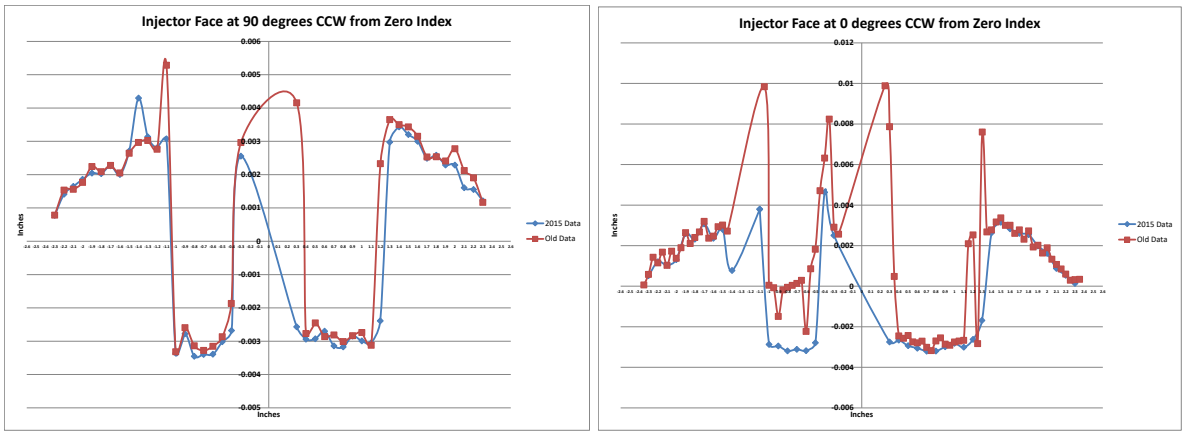

Figure 20. Profilometer traverses of the injector faceplate, showing loss of ~ 0.005" erosion resistant layer but no loss of parent material.

Hybrid Gasification Testing:

The recent emergence of large volumes of relatively inexpensive natural gas reserves via shale hydraulic fracturing (fracking) in North America, coupled with interest in reducing the carbon emissions associated with coal conversion to power and chemicals, led to an interest in assessing the feasibility and impact of co-firing natural gas with coal in entrained flow gasifiers. Such a capability over a meaningful range (up to 50% natural gas by HHV) could provide significant flexibility for power and chemical plants to achieve GHG emissions targets with reduced need for Water Gas Shift reactors and lower CO_2 removal requirements.

The objectives for this effort were to demonstrate the feasibility of hybrid coal/natural gas operations up to a maximum natural gas content of 49% (HHV basis), and to use these data as the basis for predicting commercial-scale gasifier syngas composition with hybrid operations.

Test conditions and results (carbon conversion, mass/energy/elemental balances) are summarized in Table 6. Data quality was good, with all four data points within 10% on overall mass and energy balance. Carbon balances were also within 10%. Within the constraints imposed by facility natural gas supply capabilities, testing was run at data points ranging from 17% to 34% natural gas on an HHV basis.

Table 6. Test conditions and summary results for pilot plant gasifier testing in hybrid mode with natural gas and PRB coal.

	Hybrid Testing			
	DAP 244	**DAP 245**	**DAP 246**	**DAP 247**
Coal (lb/hr)	1164	1126	1048	1077
Natural Gas (lb/hr)	125	225	275	150
Oxygen (lb/hr)	1050	1150	1160	1035
Steam (lb/hr)	75	74	73	74
Nitrogen (lb/hr)	171.6	170.1	160.2	162.3
Conversion (%)	95.51%	95.36%	93.86%	94.34%
Mass Balance (%)	97.6%	98.3%	100.2%	106.8%
Enthalpy Balance (%)	93.9%	95.7%	95.9%	101.4%
Carbon Balance (%)	90.3%	91.8%	93.7%	98.6%
Hydrogen Balance (%)	97.0%	97.6%	98.8%	107.8%
Nitrogen Balance (%)	119.7%	113.4%	129.8%	129.8%
Sulfur Balance (%)	79.9%	84.3%	80.8%	89.0%
Oxygen Balance (%)	97.1%	97.3%	98.9%	107.0%
Ash Balance (%)	100.0%	100.0%	100.0%	100.0%
Heat Loss (MMBTU/hr)	1.08	1.25	1.25	1.25
Moisture (Aa fed)	9.83	10.62	9.84	11.52
Ash (As fed)	6.65	6.56	6.53	6.38
Coal (MAF, as fed)	83.52	82.82	83.63	82.10
NG HHV/ Total HHV (%)	17.2%	27.9%	33.6%	21.2%

Actual and predicted syngas compositions are shown in Table 7. The general intent was to maintain outlet temperatures close to 2300°F to minimize variation of outlet gas composition due to change in outlet temperature. Changes due to WGS reaction in the quench zone were small compared to other testing, perhaps due to the increased presence of H_2 in the syngas to begin with, in addition to the relatively low temperature at the outlet.

The measured impact of natural gas input on syngas composition is shown in Figure 21. There is a significant increase in H_2/CO ratio with increasing fraction of natural gas in the feed. At 50% natural gas on an HHV basis, predicted H_2/CO ratio is 0.93 as compared to 0.52 for PRB without any natural gas. This corresponds approximately to 0.78 moles of ($CO+CO_2$) for every mole of ($CO+H_2$) for operations on 100% PRB, versus 0.63 for hybrid operation at 50% natural gas. For

an IGCC operation, hybrid operations could result in 20% reduction in CO_2 emissions for the same power output.

Table 7. Actual syngas composition measured downstream of gasifier and simulation predictions for gasifier outlet composition for pilot plant gasifier testing in hybrid mode with natural gas and PRB coal.

	Hybrid Testing			
	DAP 244	**DAP 245**	**DAP 246**	**DAP 247**
Coal (lb/hr)	1164	1126	1048	1077
Natural Gas (lb/hr)	125	225	275	150
Oxygen (lb/hr)	1050	1150	1160	1035
Steam (lb/hr)	75	74	73	74
Nitrogen (lb/hr)	171.6	170.1	160.2	162.3
Conversion (%)	95.51%	95.36%	93.86%	94.34%
Actual Syngas Composition				
Carbon Dioxide	13.2%	10.8%	10.8%	12.6%
Carbon Monoxide	51.6%	50.8%	49.2%	51.4%
Carbonyl Sulfide	0.0%	0.0%	0.0%	0.0%
Hydrogen	34.7%	37.8%	39.1%	35.5%
Hydrogen Sulfide	0.1%	0.1%	0.1%	0.1%
Methane	0.3%	0.5%	0.7%	0.3%
Simulation Results				
Temp (F)	2360.00	2226.00	2267.00	2291.00
Carbon Dioxide	9.3%	8.3%	8.9%	10.1%
Carbon Monoxide	56.0%	53.0%	50.0%	54.0%
Carbonyl Sulfide	0.0%	0.0%	0.0%	0.0%
Hydrogen	34.5%	38.5%	40.9%	35.7%
Hydrogen Sulfide	0.2%	0.1%	0.1%	0.1%
Methane	0.0%	0.0%	0.0%	0.0%

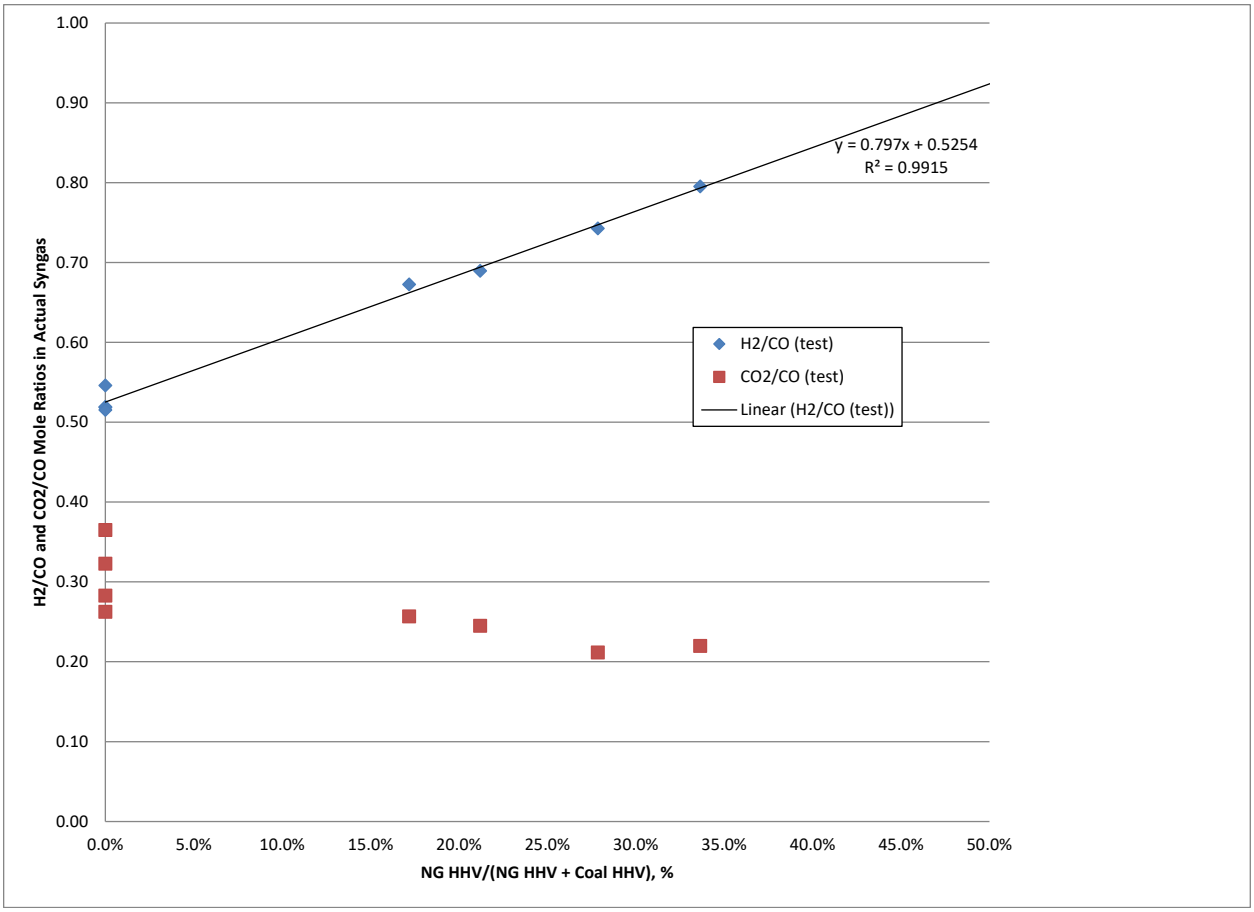

Figure 21. Impact of natural gas content in hybrid gasifier operations on the ratio of hydrogen to carbon monoxide in the syngas product.

Hybrid operation is predicted to have a significant impact on H_2/CO ratio in the product syngas, carbon content per unit syngas produced, and consumption of oxygen per unit syngas produced. Commercial scale performance predictions on PRB, Illinois #6, and Xinyuan coal are presented in Table 8. Product gas H_2/CO ratio increases by ~0.5 for all three cases. The amount of carbon per unit useful syngas, $(CO + CO_2)/(CO + H_2)$, decreases by approximately 25% for hybrid operations. And oxygen consumption per unit syngas decreases by 5%-10%, depending upon coal type. Clearly, hybrid operation presents interesting options for decreasing the carbon intensity of coal conversion, as well as for debottlenecking of a gasification plant constrained by Air Separation Unit capacity.

Table 8. Comparison of predicted commercial-scale coal-based and hybrid coal/natural gas operations for PRB, Illinois #6, and Xinyuan coals. Cases are based on 49% natural gas feed on an HHV basis.

	PRB		Illinois #6		Xinyuan	
	Coal	Hybrid	Coal	Hybrid	Coal	Hybrid
Coal (lb/hr)	234920	118890	187300	96030	227210	114000
Nitrogen (lb/hr)	12216	6182	9740	5100	11815	5900
Oxygen (lb/hr)	148660	140000	143650	136460	176850	162230
Steam (lb/hr)	0	0	40000	0	40000	0
NG (CH4), (lb/hr)	0	49521	0	49255	0	52123
Temp (F)	2301	2302	2501	2501	3000	3000
H2/CO	0.47	0.92	0.74	1.15	0.72	1.23
(CO+CO2)/(H2+CO)	0.71	0.55	0.67	0.52	0.76	0.57
O2/(CO+H2), (lb/lb mol)	8.99	8.46	8.67	8.24	10.70	9.75

3.3 CONCLUSIONS

- Thermal environments were more challenging for the highly reactive sub-bituminous coal as compared to other feedstocks, but were well within design capabilities of gasifier components.

- High ash + high AFT coals can be processed, with continuous slag discharge successfully demonstrated. The gasifier was operated at outlet temperatures as high as 2350°C, which was still well within thermal margins of gasifier design.

- The trend of surface area and porosity in residual carbon as a function of carbon conversion was established for the anthracitic high ash, high AFT coals, and can be used to enhance performance models in support of more accurate gasifier sizing to achieve target carbon conversion.

- No measurable loss of parent material greater than 0.001" was observed for the injector faceplate over a cumulative total of >900 hours of operation. The injector faceplate design appears to be feasible for providing long injector life. The gasifier liner was completely covered with slag, which is expected to provide good protection of the underlying parent material in support of achieving liner life goals.

- Hybrid operations demonstrated up to 34% natural gas on a HHV basis. Operations at 50% or more natural gas content appears feasible, with significant improvement in H_2/CO ratio, reduction in carbon emissions per unit syngas, and reduced oxygen consumption per unit syngas the expected benefits.

4.0 TASK 4: ADVANCED WATER GAS SHIFT TECHNOLOGY DEVELOPMENT

RTI is developing an advanced transport reactor-based water gas shift (ATWGS) process that has lower costs and higher thermal efficiency than conventional fixed-bed water gas shift (WGS) processes. A key requirement for RTI's ATWGS process is a fluidizable and attrition resistant WGS catalyst. Based on a promising fluidizable iron-based (Fe-based) catalyst formulation identified in DOE/NETL Cooperative Agreement DE-FE0012066, the primary objective in this project was development of this promising catalyst formulation to optimize its performance and attrition resistance for RTI's ATWGS process. The optimization success criteria included catalyst activity equal to or better than commercial fixed-bed WGS catalyst, stable activity for 200 hours of continuous operation, and an attrition value equal to or better than commercial fluid catalytic cracking (FCC) catalyst.

Based on the selected catalyst, RTI developed a preliminary basic engineering package (BEP) for an ATWGS pilot plant supporting future development efforts, based on a process flow diagram, a heat and mass balance, and a preliminary equipment design for a pilot scale ATWGS process. This design basis was then used to develop budgetary estimates for detailed design, construction and one calendar-year of operation for a pilot-scale ATWGS system.

Task 4 was divided into three subtasks: Subtask 4.1 – Catalyst Development; Subtask 4.2 – Catalyst Testing; and Subtask 4.4 – Preliminary Design of AWGS System. A detailed Topical Report was prepared for Subtasks 4.1 and 4.2 in Subtask 4.1/4.2 Topical Report: Catalyst Development and Performance Testing for Advanced Water Gas Shift Process", submitted in September 2016. Details on the BEP are presented in "Subtask 4.4 Topical Report: Basic Engineering Package for the Advanced Transport Water Gas Shift Process", also submitted in September 2016.

4.1 EXPERIMENTAL METHODS

In the U.S. Department of Energy National Energy Technology Laboratory (DOE/NETL) Cooperative Agreement DE-FE-0012066, RTI completed a technical feasibility analysis of a novel concept for enriching the hydrogen concentration in a syngas mixture based on a process consisting of fluidized-bed water gas shift (WGS) catalysts and a transport reactor coupled with a solids cooler. As one of the key components of this novel process was the fluid-bed WGS catalyst, RTI tested one or two candidate fluidized-bed catalyst formulations for typical low temperature sweet WGS (LT-WGS), high temperature sweet WGS (HT-WGS), and sour WGS commercial applications.

The three fundamental criteria for suitable fluidized-bed formulations were:

- Attrition resistance comparable to catalysts used in commercial fluid catalytic crackers (FCCs)
- Catalyst activity similar to commercial fixed-bed catalysts
- Stable conversion performance for about 200 hours

Only an iron-based (Fe-based) catalyst that had originally been developed for an alternative application met all three of these criteria. This Fe-based HT-WGS catalyst achieved approximately 72% CO conversion compared to 78% CO conversion for a commercial HT-WGS catalyst at similar operating conditions for 500 hours. Based on the success of this technical feasibility evaluation, DOE funded a task under Cooperative Agreement DE-FE0023577 to continue development of this Fe-based HT-WGS catalyst specifically for this advanced transport-based water gas shift process (ATWGS).

Using the same three criteria to evaluate catalyst performance for ATWGS, RTI's approach was to use available knowledge about existing commercial Fe-based catalysts to generate new formulations that would improve or lead to improvements of the baseline catalyst formulation. Currently commercial Fe-based WGS catalysts are available from major catalyst suppliers such as BASF, Haldor-Topsøe, Synetix, Clariant, etc. The typical as-received composition for these Fe-based catalysts is 74–89% Fe_2O_3, 6–14% Cr_2O_3 and miscellaneous other components, such as CuO, Co_2O_3 and/or MgO. The as-received catalyst must be partially reduced before it becomes catalytically active for the WGS reaction. During this partial reduction, the Fe_2O_3 is reduced into the catalytically active Fe_3O_4 phase, but should not be reduced further into FeO or metallic Fe.

The life time of commercial Fe-based HT-WGS catalysts is an average of 3 to 5 years. The activity decrease is mostly due to the thermal sintering of the Fe_3O_4 magnetite phase. Until equipment design constraints for maximum temperature are exceeded, the deactivation can be compensated for by increasing the reaction temperature. Additionally, the Fe-based catalysts can tolerate minor sulfur concentrations (<50 parts-per-million by volume of H_2S) with essentially no deactivation, unlike copper-based (Cu-based) catalysts.

The primary reason these commercial catalysts are not suitable for the ATWGS is that they are only available in shapes/geometries that are suitable for fixed-bed applications. Although a practical solution would be to convert available commercial catalysts into particles with a size distribution suitable for a transport reactor, by processing the green catalyst formulation into particles rather than pellets, tablets, or extrudates, this approach will not work. The particles formed in this manner fail the attrition resistance criterion. For this reason, RTI's plan was to start with the baseline Fe-based catalyst formulation and modify or use alternative precursors, preparation steps, and reduction procedures to improve catalyst performance leveraging available knowledge about commercial Fe-based catalysts.

Catalyst Development Methodology:

RTI's expertise and knowledge on fluidizable material design was combined with a literature survey on Fe-based HT-WGS catalysts to identify the key parametric factors for improving catalyst performance of our baseline Fe-based catalyst. Table 9 summarizes these factors.

Table 9. Key Parameters for Catalyst Development

Catalyst Activity	Structural	Preparation
Iron content	Adapting spinel materials	Calcination
Promoters	Structural promoters	Starting materials
Reduction/Activation processes		Washing process

More specifically, the following catalyst components were identified as the key components to investigate for optimizing catalyst performance:

1. Iron component: Fe_2O_3 forms the active component of the Fe-based WGS catalyst. The amount of this oxide in the conventional Fe-based WGS catalyst is typically in the range of 74-89%. The iron oxide content of this baseline catalyst formulation was about 46%. Thus, increasing the iron content in our fluidized-bed catalyst formulations could be anticipated to help improve the catalyst activity. To this end, catalyst formulations with iron contents ranging from 45 to 65% were investigated to study the influence of iron oxide content on the catalyst activity and the particle attrition.

2. Promoter type and content: Promoters play multiple roles in commercial Fe-based WGS catalysts. First, they can improve the catalyst activity thereby increasing CO conversion during WGS reaction. Next, they can minimize hydrocarbon formation, especially methane formation. Finally, they can potentially lower the amount of steam necessary to inhibit competing reactions catalyzed by the active Fe phase. The two key promoters that were considered for the current catalyst formulation were:

    a. Copper component: A recent survey suggests that addition of a small amount of active components such as Cu, cobalt, ruthenium, nickel, platinum, osmium, gold, palladium, rhenium lead, silver, etc., can improve catalyst activity. Cu was found to be the most effective one in the list. The presence of Cu not only increases the catalyst activity but also potentially lowers steam requirements typically expressed as the steam to CO ratio. The ability to effectively operate at lower steam to CO ratios can significantly lower the parasitic steam/power requirements for the WGS process for CO-rich syngas.

    b. Base oxide component: The presence of base oxide (alkali or alkali metal group oxides) in the catalyst can suppress the formation of by-product methane.

3. Stabilizer/support: Chromium oxide acts as a stabilizer in conventional Fe-based HT-WGS catalysts. However, it is a toxic component, especially in the form of Cr^{6+}.

Based on RTI's expertise associated with the preparation of attrition-resistant materials, a support material was identified that would provide both surface area to improve the dispersion of the iron oxide and adequately anchor it to this surface, which should slow down deactivation caused by sintering of the iron oxide crystallites. An added benefit of this approach was the potential to eliminate the need for any chromium in the catalyst making both the catalyst and its preparation more environmentally friendly.

Catalyst attrition resistance is controlled through a combination of composition and processing procedures. For a given catalyst composition, the synthesis conditions such as precipitation conditions, washing conditions, cake reslurry conditions, spray drying conditions and the post processing conditions all play important roles in determining the physical properties of the resultant catalyst formulation. Because of their impact on catalyst attrition resistance, the effect of the aforementioned parameters on catalyst performance and physical stability were investigated as part of this catalyst development task.

Catalyst Synthesis:

The fluid-bed Fe-based HT-WGS catalyst formulations prepared in this project were made using a co-precipitation procedure shown in Figure 22. Details on the procedure are discussed in the Topical Report for Subtasks 4.1/4.2.

Figure 22. Schematic representation of the catalyst synthesis process.

Summary of Catalyst Formulations Prepared:

Different catalyst formulations were prepared to parametrically test different compositions and preparation procedures with the goal of optimizing the performance and attrition resistance of the baseline Fe-based HT-WGS catalyst formulation. To effectively identify trends which could be used for optimization, the approach involved manipulating one specific parameter at a time while maintaining the other parameters constant.

Preparation of baseline Fe-based HT-WGS catalyst formulation:

As previously mentioned, the baseline catalyst for this project was developed for another application under a different project. Furthermore, the specific formulation tested during the selection process was from an optimized pilot plant production batch from DOE/NETL Cooperative Agreement DE-FC26-06NT42758. To ensure the team working on the current project was both familiar and had actual hands-on experience with the preparation procedures for making the baseline Fe-based HT-WGS catalyst formulation, one of the first formulations made was to duplicate the baseline catalyst formulation. Preparation of this baseline formulation also ensured

that a fresh baseline catalyst formulation was being used for comparison eliminating the potential that the age of the baseline catalyst formulation was adversely impacting its performance.

Preparation of Fluidized-bed Fe-based HT-WGS catalysts with different iron content:

A series of catalysts were prepared to investigate the impact of iron oxide content on catalyst performance and attrition resistance. The target range for the iron concentration was from 0 to 90 wt% with the upper limit being defined by commercial Fe-based HT-WGS catalysts. During preparation of these catalyst formulations, it was found that the attrition resistance for formulations with iron content ≥ 60 wt% would be unacceptable for ATWGS. Thus, the upper practical limit for the iron content of the catalyst formulations prepared was 60 wt%. Table 10 shows the specific iron content of the catalyst formulations prepared. The support content was adjusted to compensate for the large changes being made in the iron content. The content of the promoters was maintained constant.

Table 10. Catalyst Formulations with varying Iron Content

Sample ID	13838-38	13838-9	13838-24	13838-14A	13838-34
Fe_2O_3	0	49.17	54.97	60.56	65.01

Preparation of Fluidized-bed Fe-based HT-WGS catalysts with different promoters:

A number of different catalyst formulations were made to evaluate the effects of various promoters on catalyst performance and attrition. Because of the importance of Cu as a promoter in commercial Fe-based HT-WGS catalysts, two series of catalyst formulations were made to investigate the effects of copper. In the first series, three catalyst formulations were made in which only the Cu content was varied. The specific copper content for these catalyst formulations is provided in Table 11. In the second series of catalyst formulations, a high Cu content (10 wt%) was selected and the iron content was varied to evaluate if the relative ratio of Cu to Fe affected catalyst activity. The specific Cu and iron contents for this second series of catalyst formulations is shown in Table 12.

Table 11. Catalyst Formulations with varying Copper Content

Sample ID	13838-9	13838-46	13838-33B
CuO	6.01	0.00	10.01

Table 12. Catalyst Formulations with varying Copper Content

Sample ID	13838-33A	13838-33B
CuO	10.01	10.01
Fe_2O_3	45.17	50.20

Improvement of Fluidized-bed Fe-based HT-WGS catalyst attrition:

During the performance testing, it was discovered that higher iron content positively impacted the catalyst activity. It was also clearly demonstrated that the higher iron content resulted in poorer catalyst attrition resistance than the original preparation procedure. Modifications were explored to two of the key preparation procedures that influence attrition resistance. Table 13 shows the catalyst formulations made at different conditions for proprietary preparation procedure A. The target iron content for these formulation was 60 wt%. Table 14 shows the catalyst formulations made at different conditions for proprietary preparation procedure B. Two sets of catalyst formulations were made, one with an iron content of about 60 wt% and one with an iron content of about 55 wt%.

Table 13. Fe-Based HT-WGS Catalyst Formulations prepared with different conditions for Preparation Procedure A

Sample ID	13838-16A	13838-16B	13838-10
Preparation Procedure A	Baseline	2	3

Table 14. Fe-Based HT-WGS Catalyst Formulations prepared with different conditions for Preparation Procedure B

Sample ID	**13838-14A**	**13838-14B**	**13838-24**	**13838-62**
Preparation Procedure B	Baseline	2	Baseline	2
Iron content	60.56	60.56	54.97	54.60

As the optimization of the catalyst preparation procedure made to accommodate less expensive replacements for the support precursor and precipitating agent also resulted in an improvement in attrition resistance, a final preparation using the optimized new preparation procedure was also made with an iron content of about 60 wt%. The identification for this catalyst formulation was 13838-96.

Modifications for Reducing Production Cost of the ATWGS catalysts:

RTI explored modifications to the original baseline production process which could reduce production cost for the ATWGS catalyst formulations. These modifications included:

- Replacement of the support precursor with a less costly alternative.
- Use of an alternative precipitating agent.

By starting with these alternative precursors, the preparation procedure needed multiple adjustments to ensure that the final catalyst formulation would have the same properties as our

optimal catalyst formulation. Because RTI's key objectives were to optimize catalyst performance and attrition resistance, these criteria were used to sequentially optimize each adjustment to the preparation procedure. The sequential series of catalyst formulations made to optimize the catalyst performance and attrition resistance is provided in Table 15.

Table 15. Optimization matrix for lower cost route ATWGS Catalyst Samples

Sample ID	13838-75	13838-79	13838-83	13838-87	13838-92	13838-33B
Precursors	New (cheaper)	New	New	New	New	Optimized
Preparation Procedure A	Baseline	4	5	6	6	Baseline
Washing	Baseline	Baseline	Baseline	Baseline	7	Baseline

Catalyst Characterization and Performance Testing:

Catalyst Characterization:

The prepared catalyst formulations were analyzed by a series of tools including ICP, XRD, BET surface area, tap density and attrition measurement.

Microreactor System and Product Analysis:

HT-WGS catalyst performance was evaluated in a packed-bed microreactor system with simulated syngas mixtures. The process flow diagram for the microreactor system is shown in Figure 23. Further details on the apparatus are provided in the Topical Report for Subtasks 4.1/4.2.

Dry gas samples from the systems are analyzed by an Agilent 3000 gas analyzer (Micro GC). The Micro GC was calibrated for Argon (Ar), H_2, CO, CO_2 and C_1 to C_6 hydrocarbons (namely n-alkanes and 1-alkenes). An Ar tracer was used in the feed gas to quantify product gas flow rates.

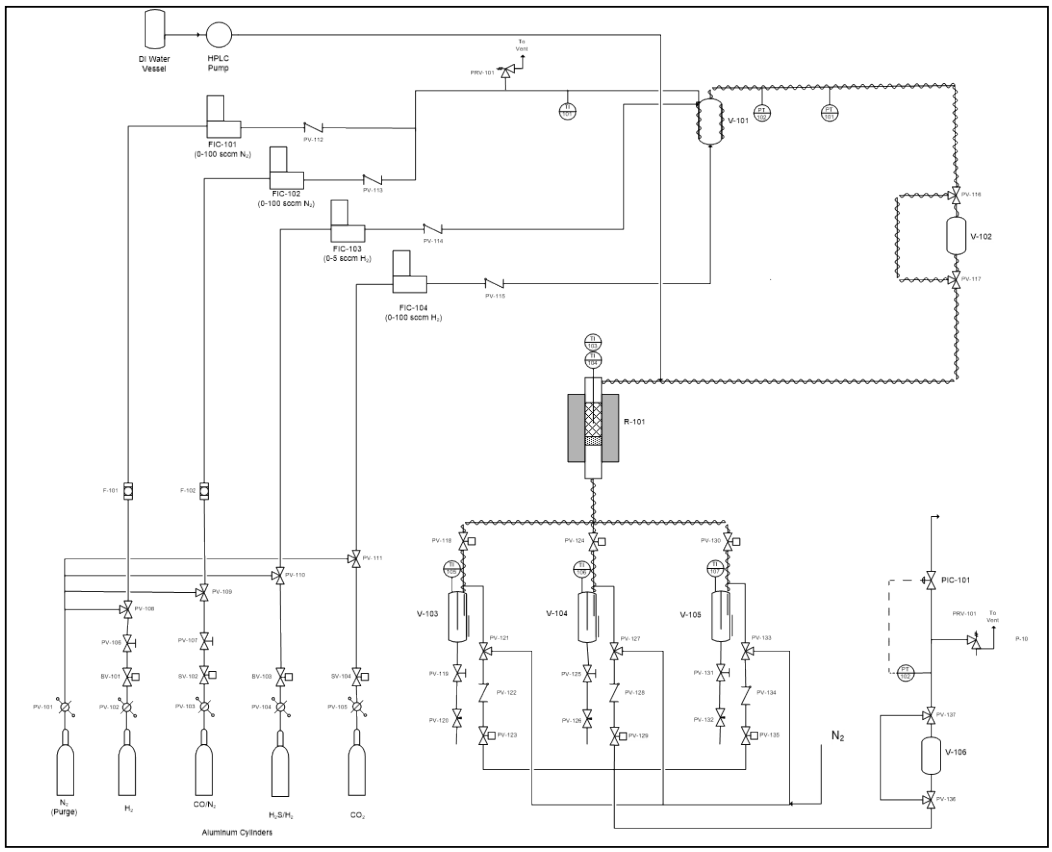

Figure 23. Process Flow Diagram of the Microreactor System

Test Matrix:

The active catalyst bed in the reactor tube was comprised of a 3:1 alumina:catalyst ratio on a volume basis that was sandwiched between the two inert layers of alumina. The catalyst loading in the reactor tube was about 3g. The catalyst was reduced in-situ under the syngas environment. Two types of catalyst performance tests were conducted. One was used to evaluate catalyst activity. The other was used to test catalyst stability. In the activity test, the effluent composition was measured at a series of four temperatures between 300ºC and 400°C. For the stability test, all the operating conditions were maintained constant for > 150 hours of operation during which changes in the effluent composition were monitored to identify changes in CO conversion and selectivity for competing reactions, namely methanation. Table 16 lists the specific operation conditions for the catalyst activity and stability tests.

Table 16. Reaction Conditions for Catalyst Performance tests

Reaction Condition	Activity Test	Stability Test
Temperature [°C]	300-450	375
Pressure [psig]	500	500
Space velocity at STP [h^{-1}]	5,000	5,000
Component [vol%]		
H_2	17.7	17.7
CO	23.0	23.0
CO_2	10.6	10.6
CH_4	2.8	2.8
H_2O	45.9	45.9

4.2 RESULTS AND DISCUSSION

Subtask 4.1/4.2 – Catalyst Development/Catalyst Testing

Benchmarking the Catalyst Performance for Commercial and Baseline Catalysts:

Shiftmax 120, a commercial HT-WGS catalyst produced by Clariant, was used to establish the numerical targets for representative catalyst activity and stability for conventional commercial catalysts. Testing showed it provided approximately 78% conversion and was stable for over 300 hours.

The results from the standard activity and stability testing for RTI's baseline ATWGS catalyst formulation achieved a slightly lower stable CO conversion (72% vs. 78%) than the commercial catalyst, stable over 140 hours of operation.

Attrition testing of standard equilibrium fluid catalytic cracking (FCC) catalyst resulted in an attrition loss of about 6.0 wt% and was utilized to establish a comparative performance standard for our ATWGS attrition testing. Attrition testing of the baseline catalyst formulation resulted in an attrition loss of 1.7 wt%, showing greater attrition resistance than conventional equilibrium FCC catalyst.

Effect of iron content on catalyst activity and attrition resistance:

Iron oxide is the active component in commercial HT-WGS catalyst. The iron content of the commercial catalyst is as high as 74-89%. In the baseline formulation, iron oxide content is around 46%, which is much lower than the commercial catalyst. An immediate opportunity to increase activity was to increase the iron content of the catalyst formulations. A series of catalyst formulations were made with higher iron content. The results from characterization of the catalyst formulations are provided in Table 17.

Table 17. Characterization results for Catalyst Formulations with varying Iron content

Sample ID	13838-38	13838-9	13838-24	13838-14A
Fe_2O_3	0	49.17	54.97	60.56
BET SA m^2/g	74.68	66.97	64.47	69.75
Attrition (DI% 21/42 μm)	0.97/3.45	1.57/4.42	65/78	72.40/57.00
Density (g/cm^3)	1.75	1.46	0.92	0.42

Characterization results for catalyst formulations prepared to evaluate the effects of iron content revealed that the formulations with up to 50% iron content exhibited a decent attrition resistance (13838-38 and 13838-9), which was better than FCC catalyst. However, for the catalyst formulations with iron content > 50%, the attrition numbers had increased to >65%, and density

dropped significantly. BET surface area, on the other hand, stayed relatively steady (60~70 m^2/g) over all the catalyst formulations across the entire range of iron content.

XRD patterns of catalysts with 50%, 55% and 60% iron oxide content are shown in Figure 24. When the iron content is around 50%, three distinct crystalline phases can be clearly identified with iron oxide as the dominating phase. For catalyst formulations with iron content above 50%, the only clearly crystalline phase is the iron oxide. The crystalline phases associated with the support material are not present. The loss of a strong crystalline support phase would lead to a significant reduction in the mechanical strength of the catalyst formulation. For the XRD peaks associated with iron oxide, this iron oxide phase seems to suggest that even the iron oxide phase is more amorphous and less crystalline than for the baseline formulation.

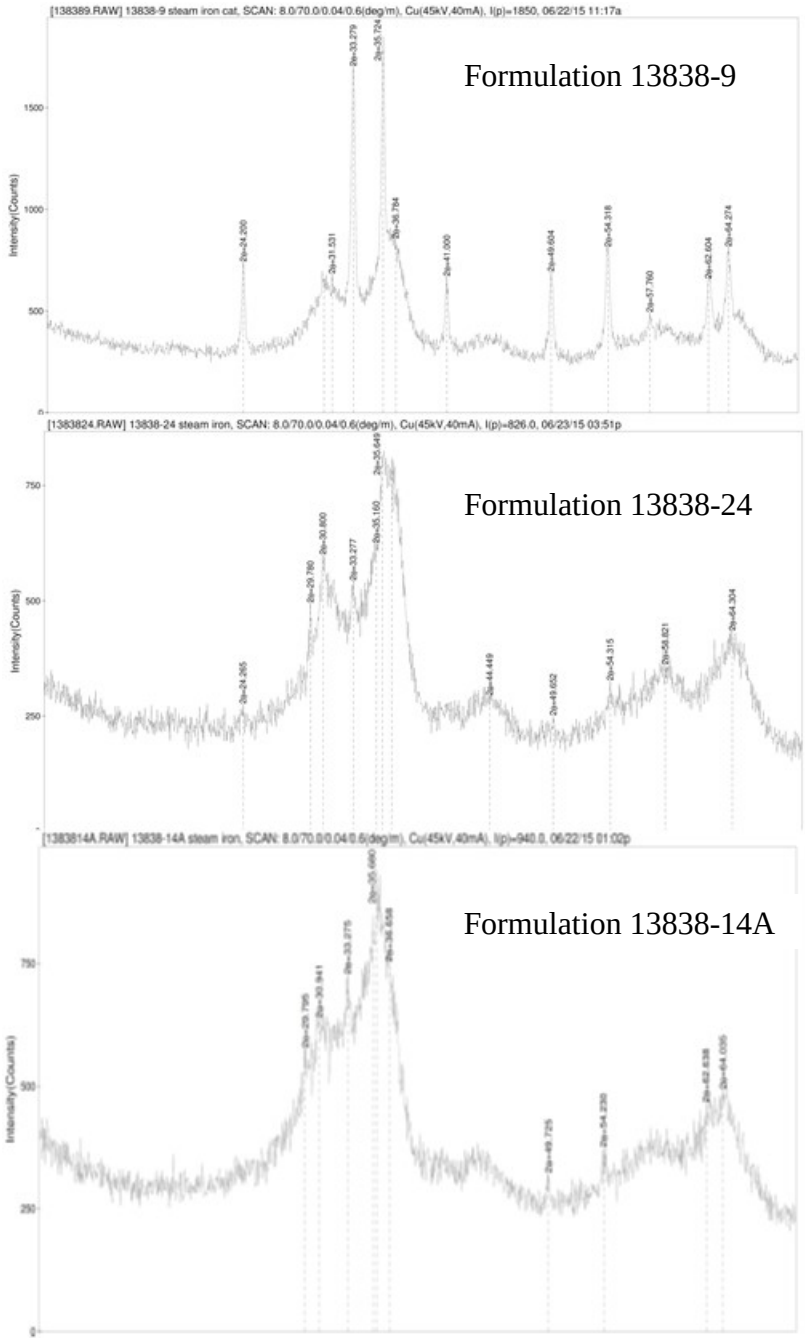

Figure 24. XRD patterns of HT-WGS catalyst with varying Iron contents

Figure 25 presents the results from catalyst activity tests for these different iron content formulations. CO conversion increases with increasing iron content in the catalyst formulation. Catalyst formulations with iron contents of 55 and 60 wt% were able to achieve equilibrium CO conversion values at reaction temperatures ≥ 400°C. It can also be seen that these catalysts with higher iron content also had better activity at lower temperatures (<350°C). The catalyst

formulations demonstrated that iron was essential to increasing catalyst activity at temperatures below 450°C.

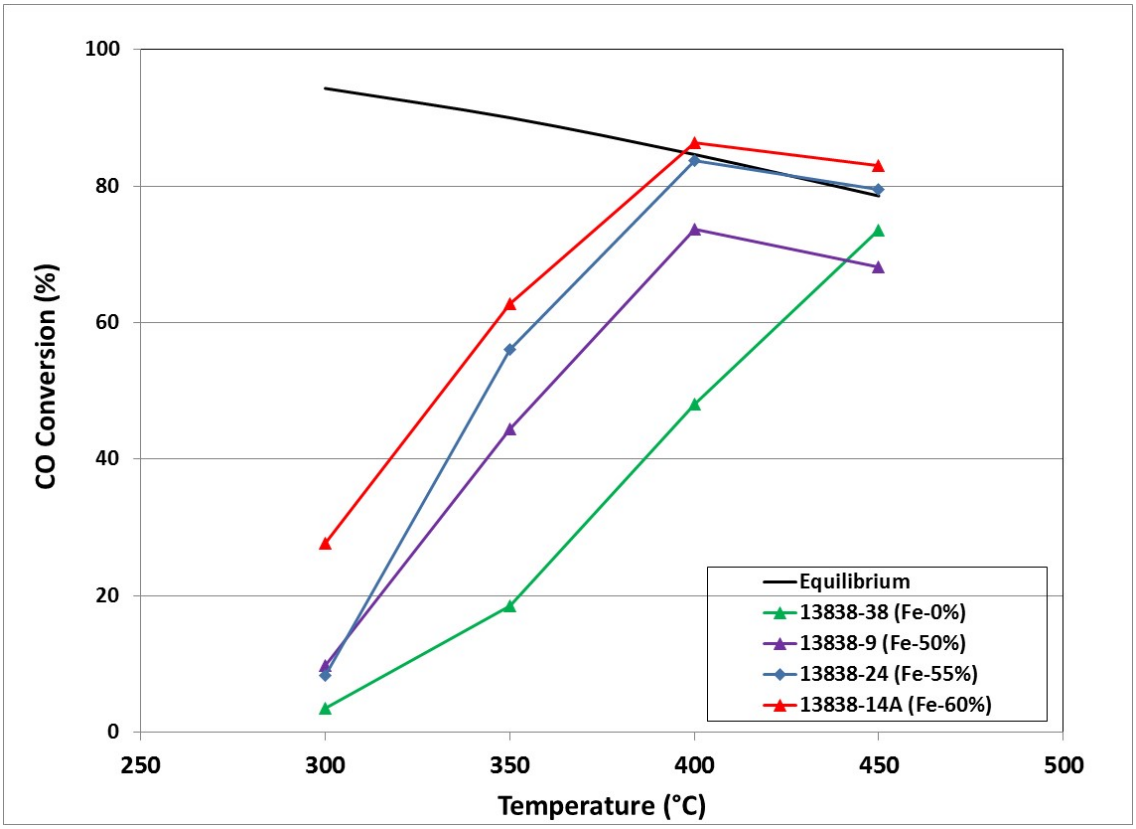

Figure 25. Catalyst Performance as a function of Iron Content

Efforts on improving attrition for catalysts with higher iron content:

Catalyst activity results indicated that there is a trade-off with increasing iron content, which helps boost the catalyst activity, but adversely affects the attrition resistance. When iron content is >50%, the catalyst attrition resistance falls below the accepted target value. Therefore, there is significant potential benefit for improving the attrition resistance of catalyst formulations with iron contents > 50 wt%. RTI explored two key preparation procedures that could significantly improve attrition resistance. However, neither of these paths yielded catalysts that satisfied goals for catalyst attrition values. Further exploration of these preparation procedures has the potential to offer suitable attrition resistance, but was beyond the scope of the current effort. Further details of the preparation procedure effort is presented in the Topical Report for Subtasks 4.1/4.2.

Improvement of Catalyst Performance through Promoters:

The impact of promoters was explored, with the objectives being to improve catalyst activity for the HT-WGS reaction, to depress hydrocarbon formation (especially methane), and to enhance

catalyst stability under more constrained operation conditions such as lower steam/carbon ratio and the presence of H_2S.

Effect of Copper Content on Catalyst Activity and Attrition:

A series of Fe-based HT-WGS catalyst formulations were prepared with different Cu content. Table 18 and Table 19 present the catalyst characterization results for these different formulations. Table 18 shows that for a Cu content of < 5wt%, there is little or no impact on BET surface area, density or attrition resistance. At a Cu content of 10 wt%, the BET surface area and attrition resistance decreased and density increased. Although the attrition resistance decreased, it still meets our target value. Because increasing Cu content does result in lower attrition resistance, an upper limit for Cu content in the optimized catalyst formulation was set at 10 wt%.

Table 18. Characterization results for Fe-based Catalyst Formulations with different Cu Content but same Fe content

Sample ID	13838-9	13838-46	13838-33A
CuO	6.01	0.00	10.01
BET SA m^2/g	66.97	67.80	53.49
Attrition (DI% 21/42 μm)	1.57/4.42	1.47/5.32	6.39/10.48
Density (g/cm^3)	1.46	1.42	1.71

Table 19. Characterization results for Fe-based Catalyst Formulations with same Cu Content but different Fe content

Sample ID	13838-33A	13838-33B
CuO	10.01	10.01
Fe_2O_3	45.17	50.20
BET SA m^2/g	65.03	53.49
Attrition (DI% 21/42 μm)	6.06/15.46	6.39/10.48
Density (g/cm^3)	1.61	1.71

The results from catalyst activity testing for the catalyst formulations with the high Cu content are shown in Figure 26, including comparison to the baseline catalyst formulation. The catalyst formulations with 10 wt% Cu content exhibited higher CO conversion compared to the baseline catalyst, while still meeting the attrition resistance target.

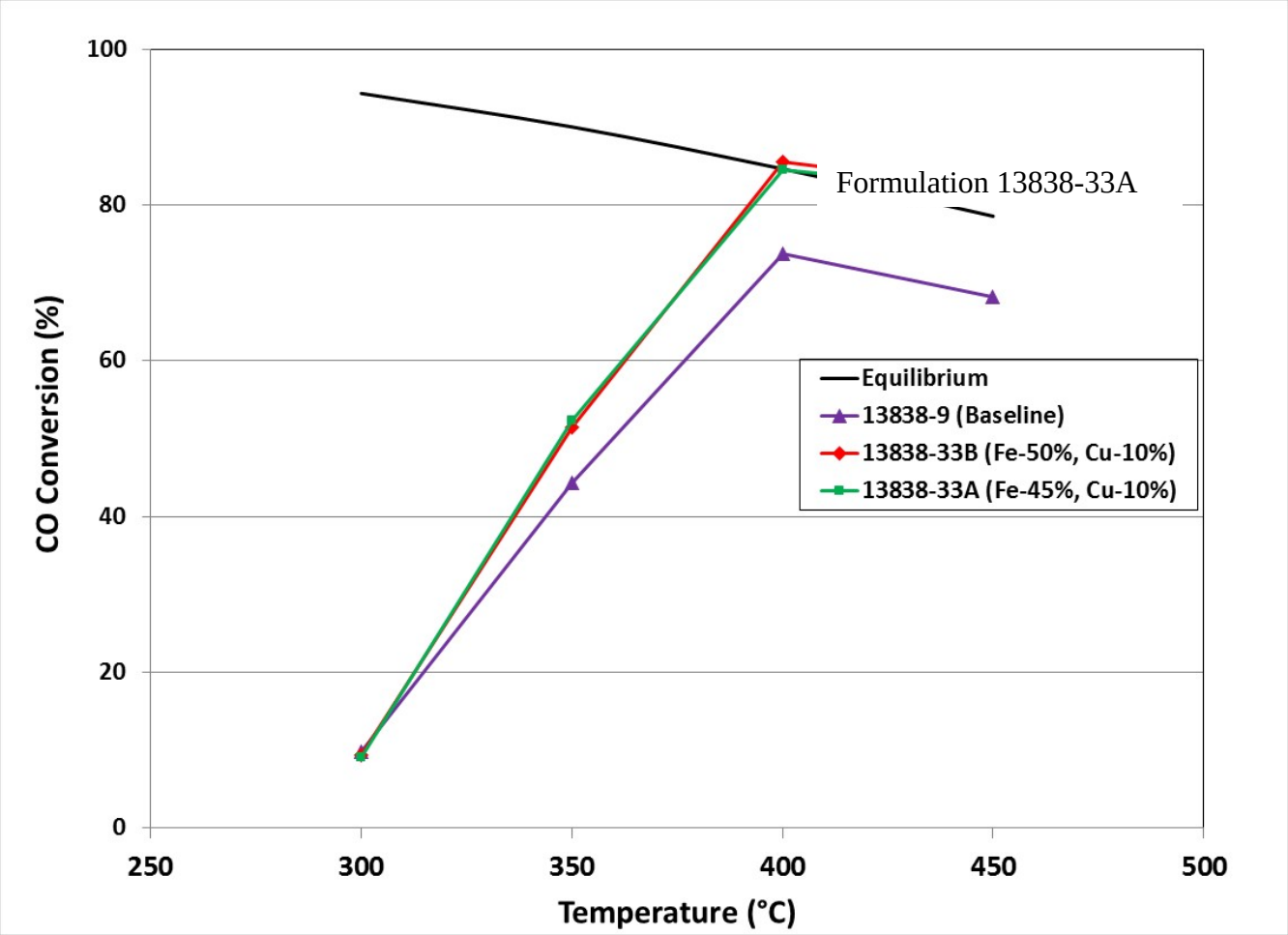

Figure 26. Catalyst Performance as a function of copper content

Long-term stability of the optimized Fe-based HT-WGS catalyst:

Test results discussed earlier indicated that the only modification that resulted in improved catalyst activity that still met the attrition resistance target was increasing the Cu content to 10 wt%. A stability test was conducted for this optimized catalyst formulation (13838-33B). Figure 27 presents the results of this catalyst stability test. It can be seen that the catalyst exhibited a stable CO conversion for a duration of about 200 hours, with negligible selectivity towards methane formation. The stable CO conversion was found to be about 75%, which is more favorably comparable to that exhibited by the commercial HT-WGS catalyst (78%) than the baseline formulation (72%).

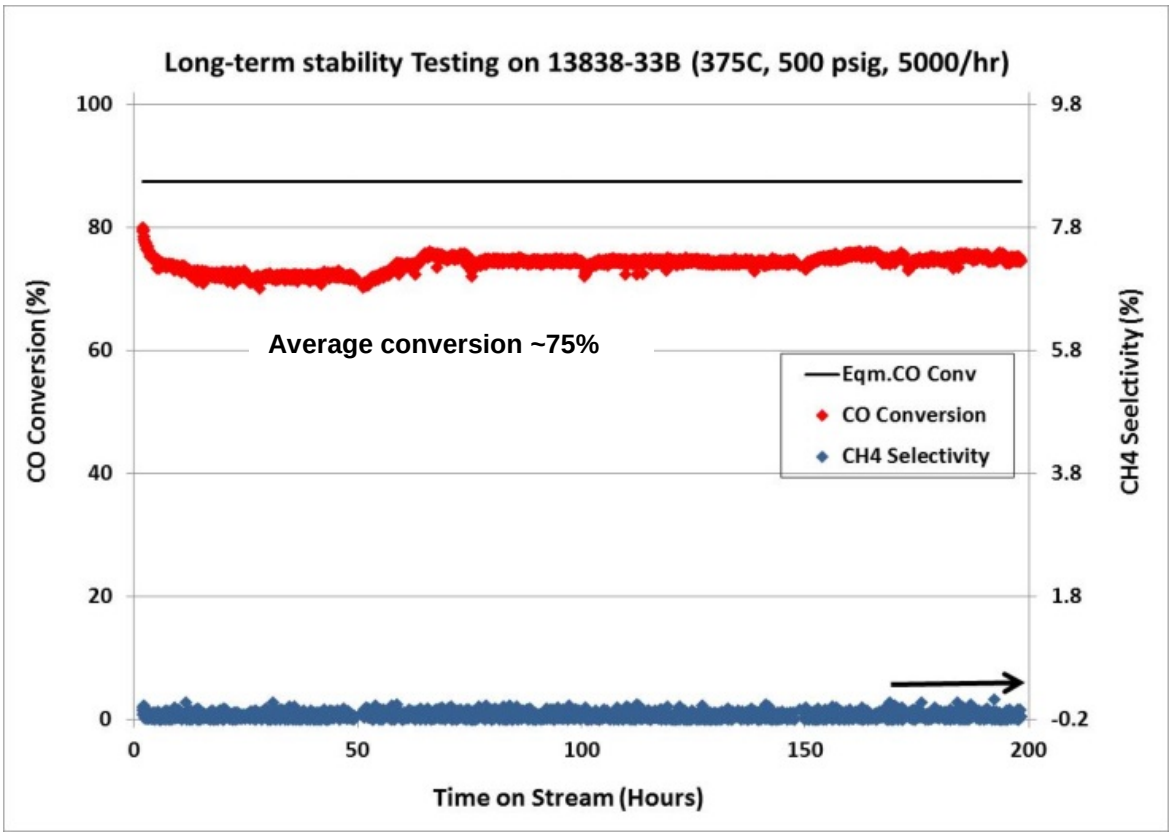

Figure 27. Catalyst Performance of HT-WGS sample (13838-33B) as a function of TOS

Modifications for Reducing Production Cost:

An alternative support precursor and precipitating agent were identified that could significantly reduce the production cost for the fluidized-bed Fe-based HT-WGS catalyst formulation and potentially reduce emissions generated during catalyst production. Because of the potential cost benefits, an effort was made to use the alternative support precursor and precipitating agent along with sequential adjustments to preparation procedure A to optimize the catalyst formulation for this production process. Table 20 summarizes the catalyst characterization results for the formulations prepared in this optimization effort and provides comparison values for the new optimized catalyst formulation. Figure 28 presents a graphical representation of the catalyst characterization results for this series.

Table 20. Optimization Matrix for Reducing Catalyst Production Cost

Sample ID	13838-75	13838-79	13838-83	13838-87	13838-33B
Precursors	New	New	New	New	Optimized
Preparation procedure A	Baseline	4	5	6	Baseline
BET SA m^2/g	79.4	62.7	62.3	57.2	53.5
Attrition (DI% 21/42 μm)	10.9/18.80	8.14/19.70	8.48/19.5	5.75/15.58	6.39/10.48
Density (g/cc)	1.11	1.32	1.42	1.57	1.71

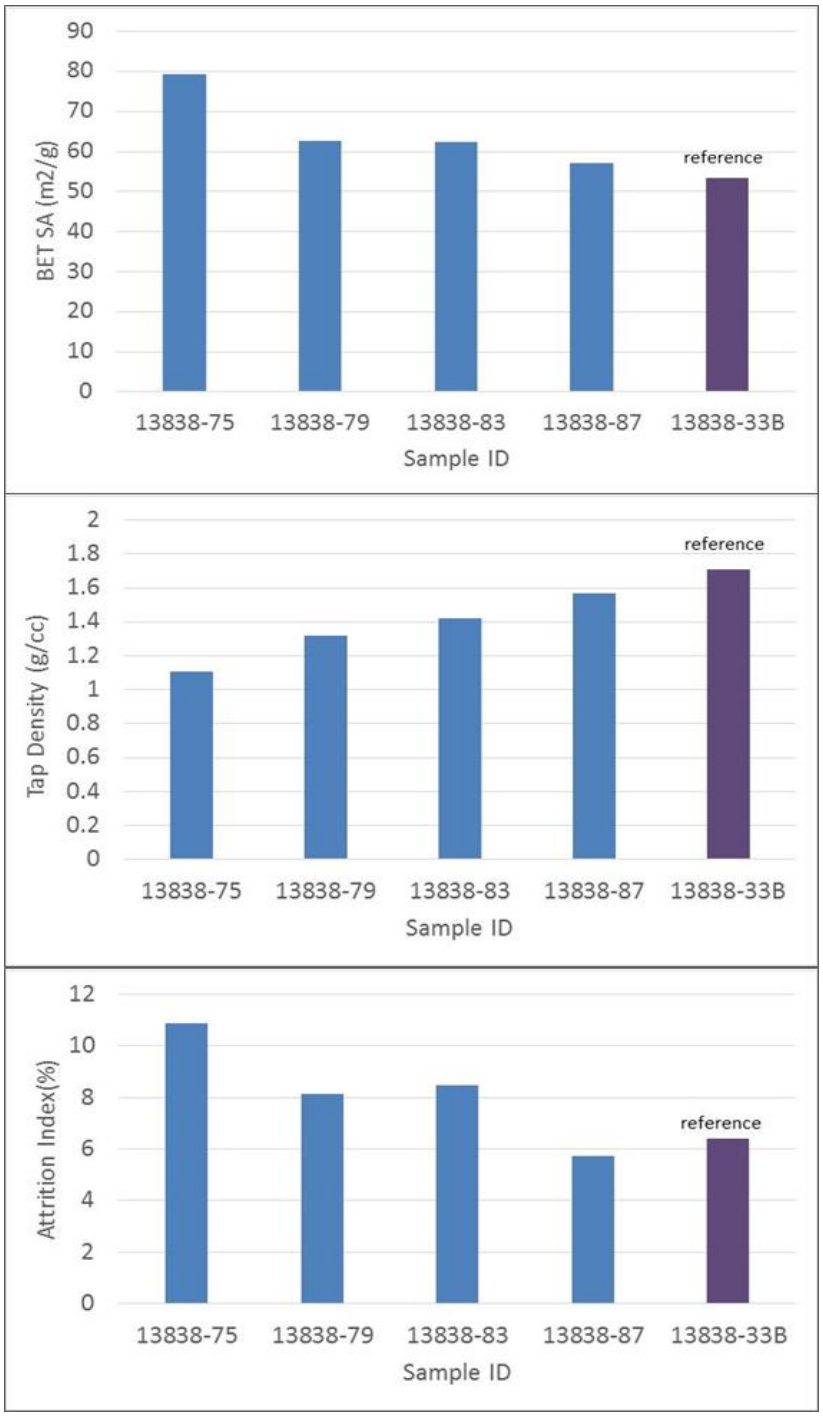

Figure 28. A comparison of BET surface area, tap density and attrition index of the catalysts prepared using the Reduced Cost Production Process

The alternative support precursor and precipitating agent resulted in a catalyst formulation that was similar to the new optimized catalyst formulation but could be optimized further. Through sequential adjustments in preparation procedure A, the attrition resistance of the catalyst formulation from the new reduced cost production process was optimized. For the final optimized catalyst formulation using the reduced cost production process, the attrition test value was about 5.8% which is slightly lower (i.e., better) than for the optimized catalyst formulation made with the baseline production process.

ICP analysis indicated relatively high concentrations of residual ion content in the catalyst formulations with the new precursors and optimization for preparation procedure A (Formulations 13838-75 to 13838-87). As the presence of this residual ion might have an adverse effect on catalyst performance, in particular catalyst stability, a final optimization formulation was prepared with different washing conditions. This new formulation with improved washing conditions successfully reduced the residual ion concentration by over 90%.

Figure 29 presents the results for activity testing of the catalyst formulations prepared with these new alternative precursors. Catalyst formulation 13838-87, which had an attrition resistance value better than the target value, also demonstrated the highest CO conversion especially for temperatures between 300°C and 400°C.

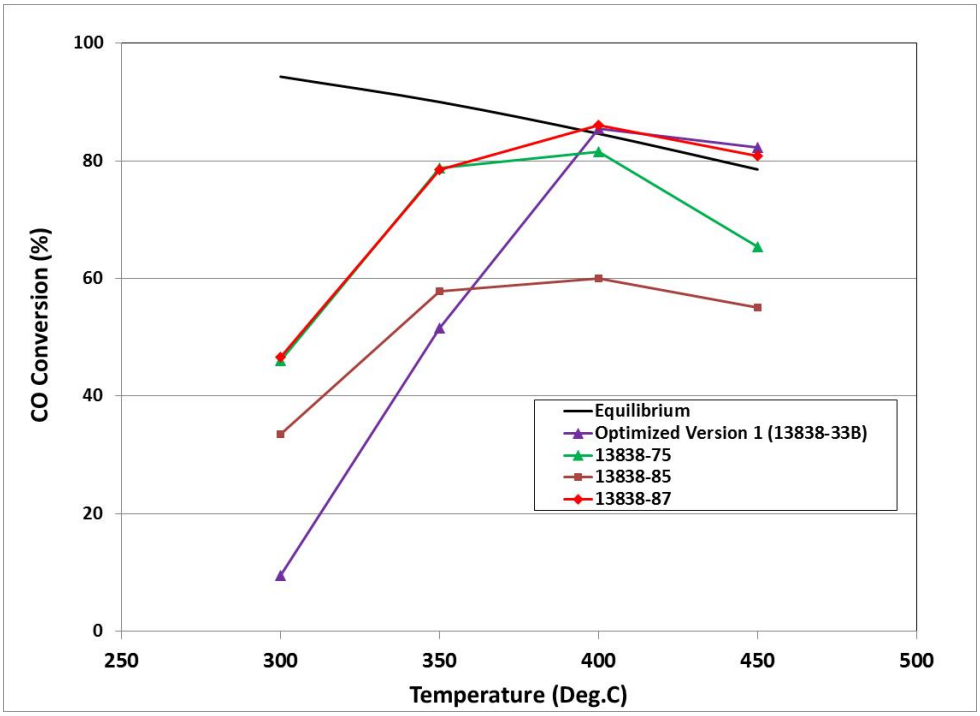

Figure 29. Catalyst Performance of the catalysts with reduced cost production process

Because this catalyst formulation 13838-87 should have additional benefits from a lower production cost, RTI conducted a standard catalyst stability test with this formulation. The results

of the stability test are shown in Figure 30, showing that this catalyst formulation demonstrated a long term stable CO conversion of about 77%. Because this catalyst formulation 13838-87 best fulfilled the catalyst selection criteria and was made with the lowest cost commercial production process, this catalyst formulation represents the final optimized and recommended ATWGS catalyst formulation for this project.

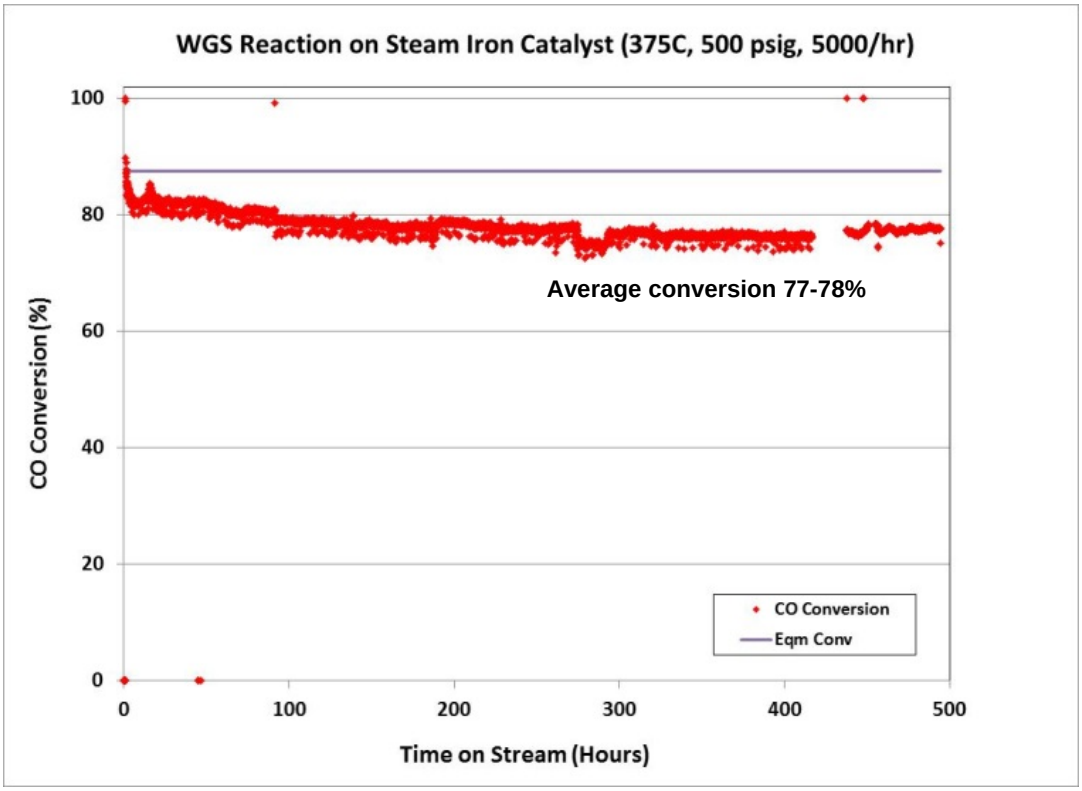

Figure 30. Catalyst Performance of HT-WGS sample (13838-87) as a function of Time On Stream (TOS)

Subtask 4.4 – Preliminary Design of ATWGS System

Pilot Scale ATWGS Description:

The process flow diagram (PFD) for the ATWGS process is shown in Figure 31. The primary components of the ATWGS process are the transport reactor, solids cooler and a fluidized-bed WGS catalyst. In the proposed pilot-scale system, some pre-conditioning equipment for the syngas has been included. The three functions to be performed by this pre-conditioning equipment are to heat up the syngas to a suitable inlet temperature, reduce the sulfur concentration of the syngas feed to < 50 parts-per-million by volume (ppmv), and enable adding steam to the syngas feed. The post-conditioning equipment consists of several heat exchangers to remove the sensible heat for the product syngas, a filter to capture catalyst fines entrained out of the reactor, and a knock out pot for collection of condensed water.

A transport reactor system is proposed, composed of a mixing zone and a riser. In the mixing zone, the syngas feed is intimately mixed with the catalyst particles returning from the solids cooler. Incorporating a mixing zone ensures that the syngas and catalyst are adequately mixed to promote fast heat and mass transfer between the syngas and catalyst particles. Because of the mixing in this zone, the WGS reaction will begin to occur.

At the top of the mixing zone, the diameter of the reactor decreases, which increases the superficial velocity and results in the entrainment of the catalyst particles by the gas. The syngas continues to undergo more WGS as it is entrained through the riser.

After being entrained by the syngas through the riser, the gas-solid mixture enters a cyclone that effectively separates the product gas from the catalyst particles. The product gas with some fines that are too small to be captured by the cyclone are sent on to the post-condition system which cools the product gas, captures the catalyst fines in a filter, and separates any condensate from the syngas prior to sending it on to a flare. The catalyst particles separated by the cyclone fall into the solids cooler, where some of their sensible heat is extracted as steam before being returned to the mixing zone.

Host Site Specifications/Assumptions:

One of the first steps in finalization of the BEP would be selection of a potential host site for this pilot-scale demonstration. The selection of a host site is important, because the host site will provide a large amount of the information that is required to establish a design basis document. Further details on host site assumptions are provided in the Topical Report for Subtask 4.4.

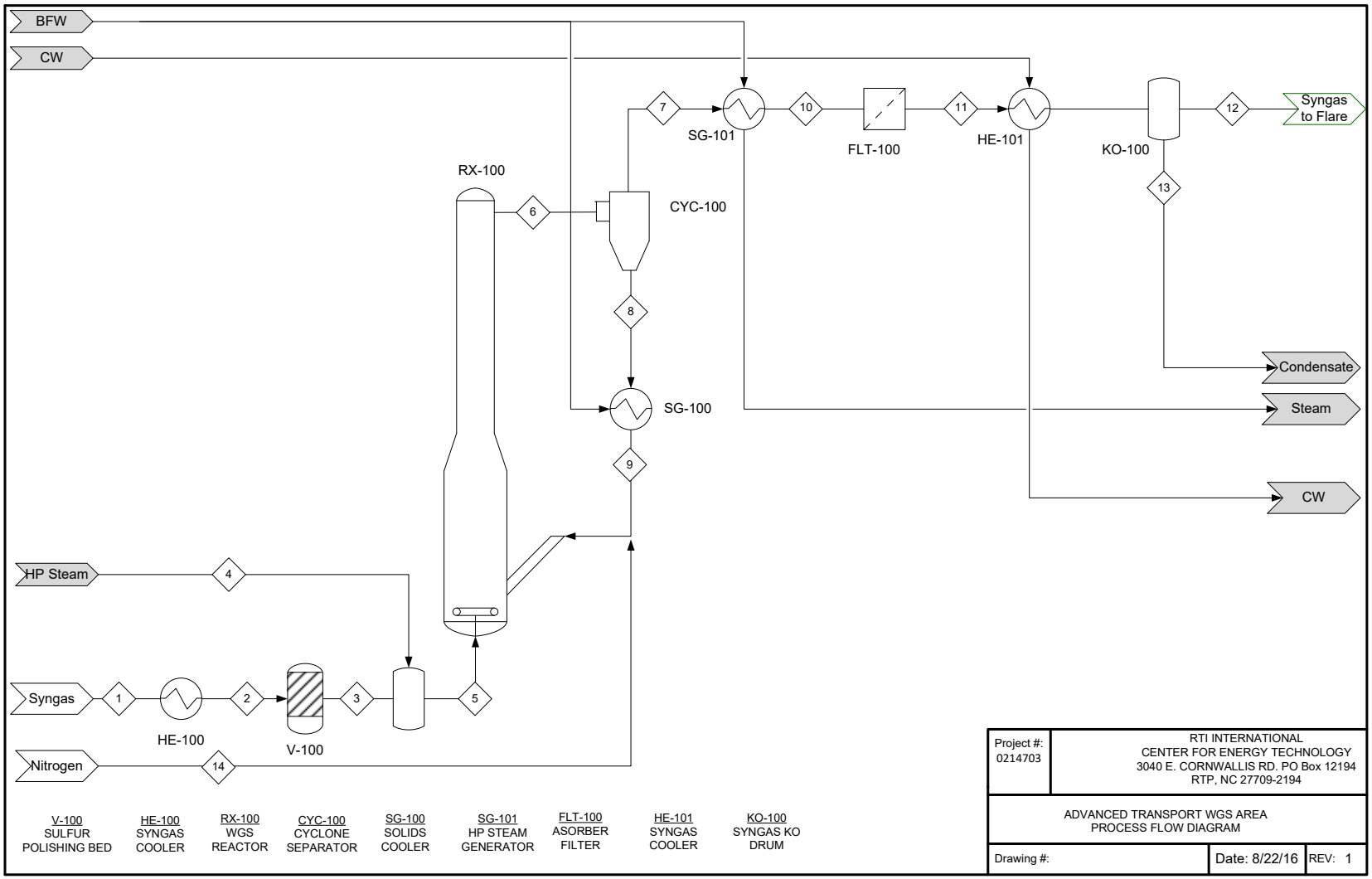

Figure 31. Process Flow Diagram for Advanced Transport Water Gas Shift Process

Major Equipment:

A heat and mass balance was performed on the PFD using ASPEN Plus V8.8, based on a target CO conversion of 90%, and was used as the basis for sizing major equipment.

The specific equipment for which design estimations were completed for the ATWGS pilot-scale system are listed in Table 4. Heat and mass balances provided the basis from which the equipment was sized. ASPEN Plus V8.8 was used for estimating design parameters for all of the ancillary equipment including the Start-up Heater (HE-101), Sulfur Polishing Bed (V-100), Cyclone (CYC-100), Syngas Cooler (SG-101), Syngas Filter (FLT-100), and Syngas Cooler (HE-101). For the key components of the transport reactor system, the specific dimensions were calculated based on RTI's knowledge and expertise in fluidized/transport systems and input from external expert consultants. Further details on equipment design are provided in the Topical Report for Subtask 4.4, as are considerations for instrumentation/control and for safety/environmental.

Table 21. Equipment List for Pilot –Scale ATWGS System

TAG ID	DESCRIPTION
HE-100	Start-up Heater
V-100	Sulfur Polishing Bed
RX-100	WGS Transport Reactor with Refractory Lining
CYC-100	Cyclone Separator
SG-100	Solids Cooler (Steam Generator)
SG-101	Syngas Cooler (Steam Generator)
FLT-100	Syngas Filter
HE-101	Syngas Cooler

Capital Cost Estimate:

Based on the preliminary equipment design, ASPEN Process Economic Analyzer (APEA) and vendor quotes (where available from historical data) were used to develop the bare erected cost (BEC) of each piece of major equipment, which is provided in Table 22 along with information and tag identification numbers. Additional details are provided in the Subtask 4.4 Topical Report.

Table 22. Capital cost of the major equipment in the Advanced Transport Water Gas Shift process

TAG ID	DESCRIPTION	TYPE	BEC ($)
HE-100	Start-up Heater	Furnace	135,600
V-100	Sulfur Polishing Bed	ZnO Bed	126,800
RX-100	WGS Transport Reactor with Refractory Lining	Transport Reactor	1,558,708
CYC-100	Cyclone Separator	Cyclone Separator	10,800
SG-100	Solids Cooler (Steam Generator)	Shell and Tube Heat Exchanger	35,769
SG-101	Syngas Cooler (Steam Generator)	Shell and Tube Heat Exchanger	64,800
FLT-100	Syngas Filter	Sintered Metal Filter	19,605
HE-101	Syngas Cooler	Shell and Tube Heat Exchanger	51,400
Total Capex			**2,003,530**

Since facility integration costs are highly specific to a given facility, they were not included in this cost estimate. When an actual host site is identified, this estimated BEC will need to be revised to account for facility integration and for any differences between the assumptions made and the actual conditions that exist at the host site.

Operation and Maintenance Cost Estimate:

In addition to the cost of construction of the ATWGS pilot-scale system, there will be costs associated with the operations. The key components of this operating cost will be labor, utilities, and supplies. Details are presented in the Topical Report for Subtask 4.4. In summary, operation and maintenance costs for a one calendar-year operating period were estimated to total $1,653,594.

4.3 CONCLUSIONS

Subtasks 4.1/4.2 – Catalyst Development/Catalyst Testing

Multiple versions of potential ATWGS catalyst formulations were synthesized and tested under this project task with the objective of optimizing the catalyst performance and attrition resistance of the baseline ATWGS catalyst formulation identified under DOE/NETL Cooperative Agreement DE-FE0012066. Through these catalyst formulations we were able to show that increasing iron content did result in more WGS activity, but at Fe concentrations > 50 wt% the resulting attrition values for these samples did not meet our target value. Several attempts to alter the preparation procedures to improve the attrition resistance of catalyst formulations did improve the attrition value, but they still did not meet our target attrition value. The main activity benefits at the higher Fe concentrations seem to be linked with an amorphous Fe phase which does not easily lend itself to preparing mechanically strong attrition-resistant catalyst formulations.

Evaluation of potential promoter materials did result in the demonstration that increasing Cu content to about 10 wt% did increase WGS activity. However, the catalyst formulations with 10 wt% Cu also had slightly higher attrition values, but these values were still within our target value. Our optimized catalyst formulation (13838-33B) with 10 wt% Cu demonstrated a long term stable CO conversion of about 75%. This became our first version of an optimized ATWGS catalyst.

Based on RTI's previous proprietary experience with commercial catalyst production, we were also able to identify an alternative support precursor and precipitating agent that could lower production cost and potentially eliminate emissions during the production process. Although introduction of these new precursor components did require some additional optimization of the preparation procedures, we did successfully identify a catalyst formulation that had higher WGS activity and acceptable attrition resistance. In long-term stability testing, the stable CO conversion for this catalyst formulation was close to 77% (almost identical to commercial HT-WGS catalyst). Because of its excellent overall performance (WGS activity, attrition resistance, and catalyst stability) that met all of our fundamental criteria and the utilization of a reduced cost production process, we selected this formulation (13838-87) as our final optimized and recommended ATWGS catalyst formulation for this project.

Based on the catalyst development efforts completed on this project, we have thus been able to identify two optimized catalyst formulations (13838-33B and 13838-87) having combined performance (WGS activity, long-term stability, and attrition resistance) that represent an improvement over the original baseline catalyst formulation. The best of these optimized formulations (13838-87) meets all of our key criteria with the added advantage that its production process is commercially viable, employs low cost precursors, and eliminates the need for any special emission control equipment in the production process.

One specific advantage of all the catalyst formulations prepared under this project has been the absence of chromium. This is a key component in commercial HT-WGS catalysts. The presence of hexavalent chromium ion in the production process and in the eventual disposal of the spent catalysts increases the potential for human exposure to this toxic chromium ion. Because none of the catalyst formulations developed in this project contain any chromium, these catalyst formulations are more environmentally friendly than standard commercial HT-WGS catalysts.

Subtask 4.4 – Preliminary Design of ATWGS System

A preliminary BEP for a pilot-scale ATWGS system has been prepared to develop a preliminary budgetary estimate with which to seek funding to design, build, and operate a pilot-scale ATWGS system at a host site. Because a specific host site has not yet been identified, assumptions were made about the host site. The key assumptions were that the host site should have the ability to provide a suitable syngas stream at about 400 psig. We have also assumed that the host site will have sufficient space to install the pilot-scale system and the necessary utilities. The specific utilities that have been assumed in the preparation of this BEP include electric power, 400 psig nitrogen, 400 psig steam, cooling water and instrument air. In terms of support equipment/facilities, we have assumed that the product syngas will be flared and water treatment facilities exist for the process condensate.

Heat and mass balances, sized equipment and estimated bare erected equipment costs were developed based on these assumptions. Operation and maintenance were estimated for one calendar year of 24/7 operation. For this pilot-scale system, approximately 4,000 hours of operation during this year was assumed. Included in the budget is production of two reactor fills for the fluidized-bed WGS catalyst and a reasonable estimate for utilities.

Based on the cost estimation completed, the cost for construction and installation of the pilot-scale ATWGS system would be about $2.0 million with an estimated operating budget of approximately $1.65 million for one calendar year of operation.

The path forward for the current technology would involve the following steps:

- Identification of a funding opportunity that will support this pilot-scale project,
- Identification and negotiation of a host site agreement,
- Completion of a detailed engineering package for the pilot-scale ATWGS system for the specific host site,
- Construction and installation of the ATWGS pilot plant,
- Preparation of a limited commercial production batch for sufficient fluidized-bed WGS catalyst for at least two system fills,
- Development of commissioning, startup, operating and shut down procedures, and
- Implementation of the operational plan.

5.0 TASK 5: TECHNO-ECONOMIC ANALYSIS

5.1 ANALYTICAL METHODOLOGY

A detailed description of the analytical methodology for this study was defined in a Technology Analysis Plan submitted to NETL in September 2015. The overall objective of Task 5 was to (1) assess how best to integrate the ATWGS technology into the combined R-GAS™ and RTI advanced syngas desulfurization process, and (2) evaluate the techno-economic benefits of such an integrated process.

The Techno-Economic Analysis submitted as the Topical Report for Task 5 documents the detailed study completed for both IGCC power production and CTL applications, specifically, methanol production from a coal-to-methanol (CTM) plant.

The specific case studies completed provide a comparison of an integrated plant utilizing GTI's R-GAS™, RTI's advanced syngas desulfurization process and ATWGS technologies with a reference plant using commercially available technologies, and a case from the previous DE-FE0012066 study that also utilizes GTI's R-GAS™ gasification and RTI's advanced syngas desulfurization process, which includes RTI's warm gas desulfurization process (WDP), RTI's direct sulfur recovery process (DSRP), RTI's advanced fixed-bed water-gas shift process (AFWGS), and an activated amine CO_2 recovery process (AACRP). All comparison studies conducted for this report capture 90% CO_2 for storage.

To identify and determine any synergistic advantages of integrating the RTI ATWGS technology into an IGCC, an additional design case was developed, on top of the four cases previously completed in the DE-FE0012066 study. These are shown in Table 23. One of these cases is the Reference Case, which is Nexant's model of Case S1B selected from NETL Report 1399. The most promising case from the previous study is Case 1b, the IGCC plant with CO_2 capture that integrates GTI's R-GAS™ gasification technology with RTI's advanced syngas cleanup process (WDP + AFWGS + AACRP + DSRP). Case 1e, which adds RTI's ATWGS technology to the two advanced technologies of Case 1b (RTI's ATWGS replaces RTI's AFWGS), is the case of interest for the current study. It is anticipated to provide additional synergistic benefits above and beyond that of Case 1b.

To identify and determine any synergistic advantages of integrating the RTI ATWGS reactor technology, an additional design case is developed, on top of the four CTM cases previously completed in the DE-FE0012066 study. These are shown in Table 24. One of these cases is the Reference Case, which is Nexant's model of the reference Case 2 selected from the DOE Crude Methanol Study. The most promising case from the previous study is Case 2b, the CTM plant with CO_2 capture that integrates GTI's R-GAS™ gasification technology with RTI's advanced syngas cleanup process. Case 2e, which adds RTI's ATWGS technology to the two advanced technologies in Case 2b, is the case of interest for the current study. It is anticipated to provide additional synergistic benefits above and beyond that of Case 2b.

The specific technologies included in each of the five CTM plant configurations are identified in the CTM case study matrix shown in Table 24.

Table 23. Case Study Matrix for IGCC with CO_2 Capture

Case Name for Current Study	Case 1a[1]	Case 1b	Case 1c	Case 1d	Case 1e
Case Name in Previous Study[2]	Case 2a	Case 2b	Case 2c	Case 2d	N/A
Gasification Technology					
Shell Gasification with Lockhopper-Based Feed System	✓			✓	
GTI R-GAS™ Gasifier with Dry Solids Pump (DSP) Feed System		✓	✓		✓
Gas Cleanup[3]					
Two-Stage Selexol™ for CO_2 and Sulfur Removal	✓		✓		
RTI WDP with AACRP		✓		✓	✓
Water-Gas Shift					
Sour Shift	✓		✓		
RTI AFWGS		✓		✓	
RTI ATWGS					✓
GE 7FB Advanced Gas Turbine	✓	✓	✓	✓	✓
CO_2 Drying and Compression (to 2,200 psig)	✓	✓	✓	✓	✓

[1] Reference Case based on Nexant's benchmark simulation of the NETL Report 1399 Case S1B

[2] Previous study cases used "2" as a prefix e.g Case 2a, 2b, 2c and 2d because these were addressing Task 2 of the study.

[3] Selexol™ removes H_2S and CO_2. Additional trace contaminant cleanup technologies will be included as defined by DOE/NETL baseline studies

Reference case from previous DE-FE0012066 study

Best performing case from previous DE-FE0012066 study

Other DE-FE0012066 study cases

Case of interest in this study

Table 24. Case Study Matrix for CTM Plants with CO_2 Capture

Case Name for Current Study	Case 2a[1]	Case 2b	Case 2c	Case 2d	Case 2e
Case Name in Previous Study[2]	Case 3a	Case 3b	Case 3c	Case 3d	N/A
Gasification Technology					
Shell Gasification with Lockhopper-Based Feed System	✓			✓	
GTI R-GAS™ Gasifier with DSP Feed System		✓	✓		✓
Gas Cleanup[3]					
Rectisol® for CO_2 and Sulfur Removal	✓		✓		
RTI WDP with AACRP		✓		✓	✓
Water-Gas Shift					
Sour Shift	✓		✓		
RTI AFWGS		✓		✓	
RTI ATWGS					✓
Methanol Production	✓	✓	✓	✓	✓
NGCC Power Generation with Fluor Econamine CO_2 Capture	✓	✓	✓	✓	✓
CO_2 Drying and Compression (to 2,200 psig)	✓	✓	✓	✓	✓

[1] Reference Case based on Nexant's benchmark simulation of the DOE Crude Methanol Study Case 2

[2] Previous study cases used "3" as a prefix e.g Case 3a, 3b, 3c and 3d because these were addressing Task 3 of the study.

[3] Rectisol® removes H_2S and CO_2. Additional trace contaminant cleanup technologies will be included as defined by DOE/NETL baseline studies

Reference case from previous DE-FE0012066 study

Best performing case from previous DE-FE0012066 study

Other DE-FE0012066 study cases

Case of interest in this study

5.2 RESULTS AND DISCUSSION

IGCC Results

The GTI gasifier technology offers favorable impacts on all plant parameters relative to the DOE Reference design configuration of Case 1a (i.e., comparing Case 1c with 1a): with 1.38 percentage point increase in plant efficiency, a 12.8% reduction in TOC, and an 11.7% reduction in COE. With respect to comparing the two water-gas shift technologies that RTI offers (ATWGS in Case 1e versus AFWGS in Case 1b), the ATWGS in Case 1e has a slight advantage over that of Case 1b, with an incremental increase in efficiency of 0.31 percentage points and an extra 4.2 MWe from the stream turbine while reducing the capital cost and cost of electricity by 2.5% and 2.3% respectively. Table 25 confirms the improved thermal efficiency of RTI's advanced WGS processes, as seen from the increases in steam turbine output between cases with conventional WGS processes and AFWGS/ATWGS (i.e., Case 1b vs. Case 1c, Case 1a vs. Case 1d, and Case 1e vs. Case 1b).

Sensitivity analyses were carried out to determine the effects of various parameters of the GTI R-GAS™ system and RTI advanced syngas cleanup, including WDP, DSRP, AFWGS/ATWGS and AACRP on the overall IGCC COE, with the results of these sensitivities summarized below. Other parameters investigated, and included in the Task 5 Topical Report are: feedstock cost, IGCC plant capacity factor, CO_2 sales price, and cost of CO_2 emissions.

Table 25. Impact of GTI R-GAS™ and RTI ATWGS Technologies on IGCC

Case	Case 1a	Case 1b	Case 1c	Case 1d	Case 1e
IGCC Configuration					
Gasifier	Shell	GTI	GTI	Shell	GTI
Sulfur and CO_2 Removal	Selexol™	RTI WDP	Selexol™	RTI WDP	RTI WDP
Shift Reactors	Sour FBR	AFWGS	Sour FBR	AFWGS	ATWGS
Plant Parameters					
Steam Turbine output (MWe)	224.1	211.3	209.3	226.4	215.5
Efficiency, % HHV	31.32%	32.75%	32.70%	31.53%	33.06%
Capital Cost (TOC), $/kW	5,400	4,428	4,709	5,054	4,316
COE, mills/kWh	145.3	122.0	128.3	137.3	119.2
Relative Impact					
Case comparison basis		**1b vs. 1c**	**1c vs. 1a**	**1d vs. 1a**	**1e vs. 1b**
Steam Turbine output (MWe)		+2.0 (1.0%)	-14.8 (-6.6%)	+2.3 (1.0%)	+4.2 (+2.0%)
Efficiency, % HHV			+1.38% pt		+0.31% pt
Capital Cost (TOC), $/kW			-691 (12.8%)		-112 (2.5%)
COE, mills/kWh			-17.0 (11.7%)		-2.8 (2.3%)

Figure 32 shows how the Case 1b and 1e IGCC COEs change as the GTI DSP and R-GAS™ gasifier TPC varies from -30% to +30%. Also shown in figure is the reference Case 1a IGCC COE at 145.3 mills/kWh.

For both the Case 1b and Case 1e IGCC cases, roughly every 5% increase in the R-GAS™ gasification system (including DSP and gasifier) TPC, or the equivalent of $16MM in TPC, increases the IGCC COE by 1 mill/kWh.

Figure 33 shows how the Case 1b and 1e IGCC COEs change as the RTI WDP system TPC varies from -30% to +30%. The RTI WDP system TPC includes the costs for the RTI WDP, DSRP and AACRP processes. It also includes the AFWGS TPC for Case 1b and ATWGS TPC for Case 1e. For reference purposes, the Case 1a IGCC COE of 145.3 mills/kWh is shown in Figure 33 as well.

For both cases, roughly every 9% increase in RTI WDP TPC, equivalent to about $16MM, increases the IGCC COE by 1 mill/kWh.

Figure 34 shows how the Case 1e COE changes with respect to just the ATWGS TPC as it varies from -30% to +30%. For reference purposes, the Case 1a IGCC COE of 145.3 mills/kWh and Case 1b IGCC COE of 122.0 mills/kWh are shown in Figure 34 as well.

Figure 34 shows that at the high-end (+30% of baseline) of the ATWGS TPC, its COE, at 120.6 mills/kWh varies little from the baseline and is still less than the Case 1a and Case 1b IGCC. This is because the ATWGS TPC makes up only a small fraction of the total CAPEX and variation to the TPC does not affect the COE to a large extent.

Figure 35 shows how the Case 1e COE changes with respect to the ATWGS catalyst cost as it varies from -50% to +50%. The Case 1a IGCC COE and Case 1b IGCC COE of 145.3 mills/kWh and 122.0 mills/kWh respectively are shown in Figure 34 as well.

Figure 35 shows that at the high-end (+50% of baseline) of the ATWGS catalyst cost, its COE, at 120.5 mills/kWh, varies little from the baseline and is still lower than the Case 1a and Case 1b IGCC.

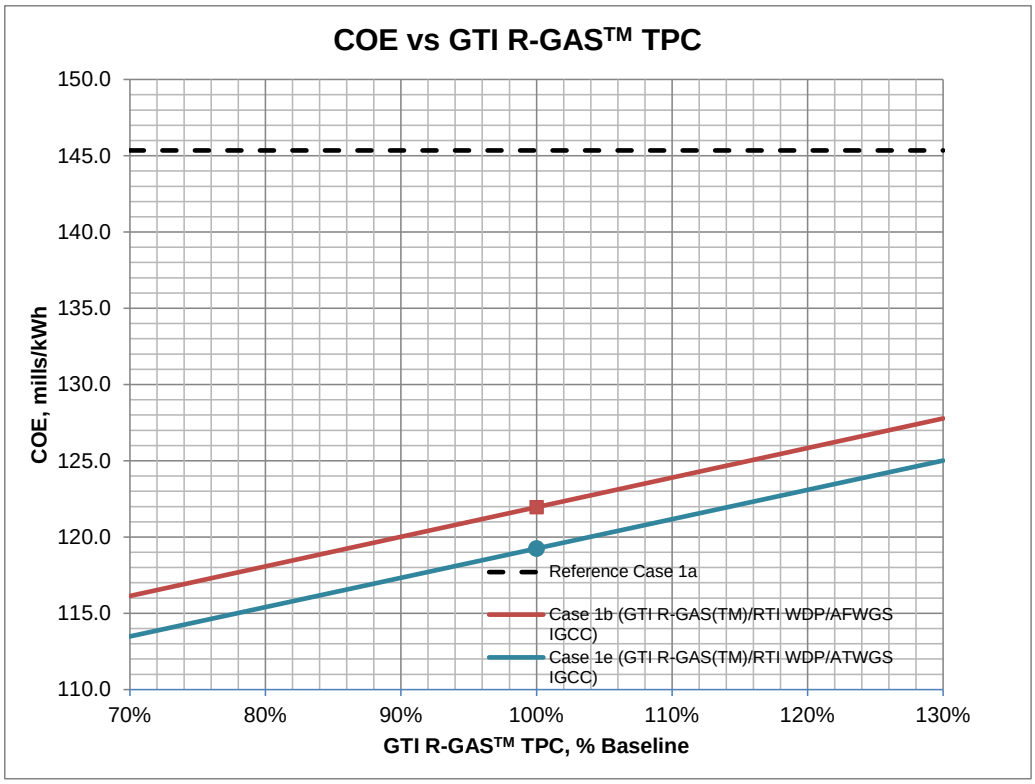

Figure 32. Sensitivity Analysis – COE vs GTI R-GAS™ TPC

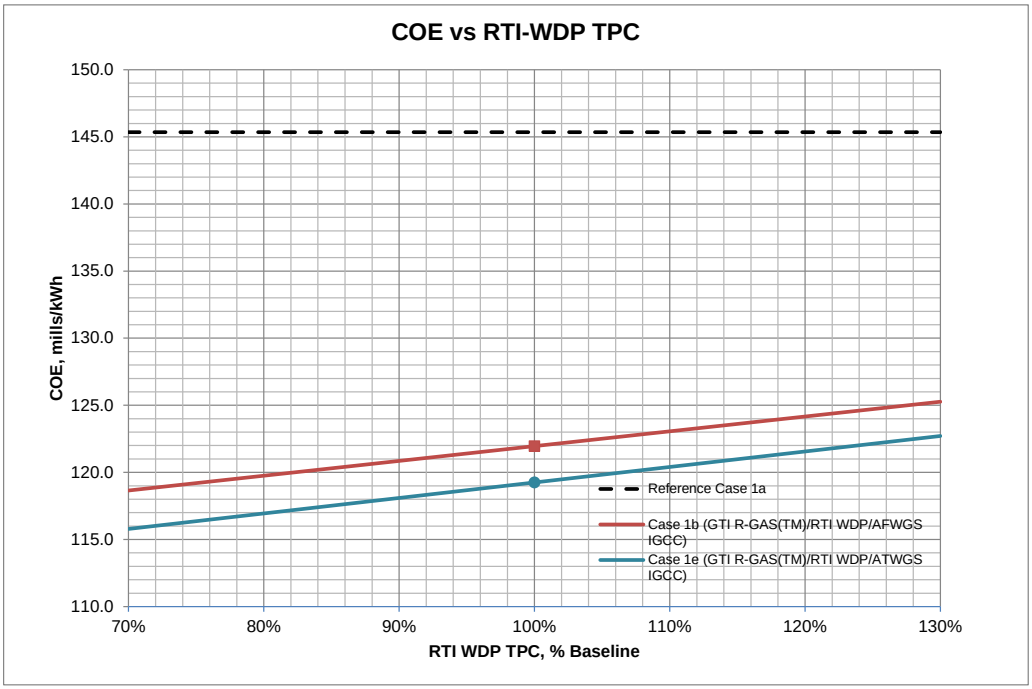

Figure 33. Sensitivity Analysis – COE vs RTI WDP System Cost

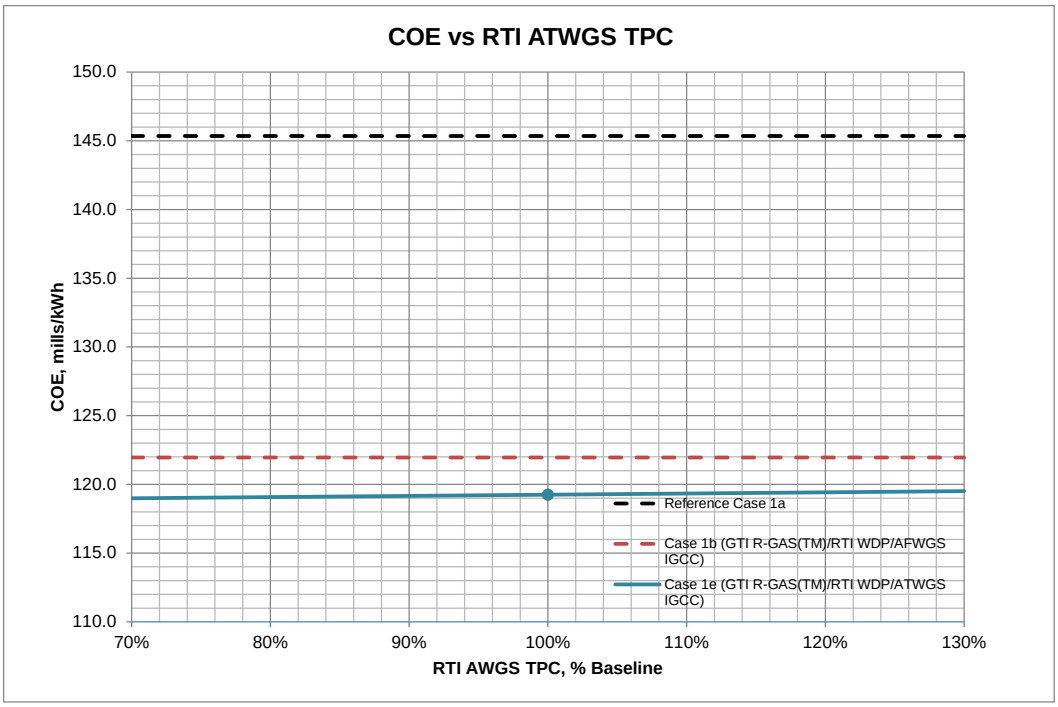

Figure 34. Sensitivity Analysis – COE vs RTI ATWGS System Cost

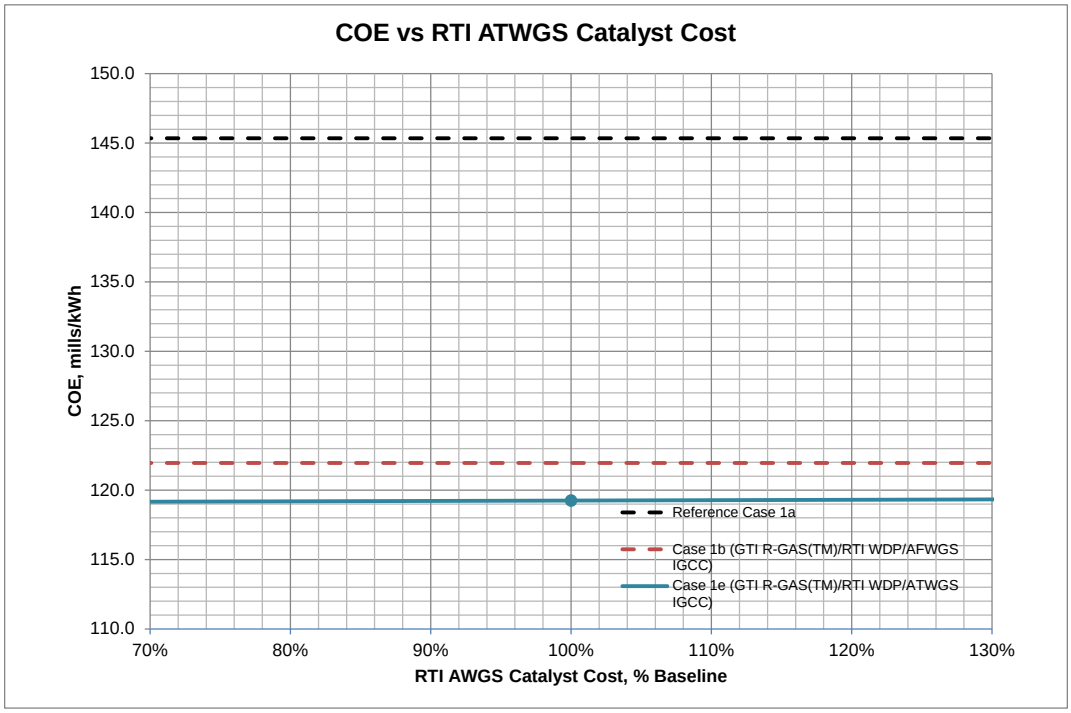

Figure 35. Sensitivity Analysis – COE vs RTI ATWGS Catalyst Cost

Coal To Methanol Results

Table 26 summarizes the results of all the CTM cases studied, which includes Case 2a through 2d from the prior DE-FE0012066 study, and Case 2e from this study, and provides some insight into the relative impacts of the GTI and RTI technologies on CTM production.

Table 26. Impact of GTI R-GAS™ and RTI AWGS Technologies on CTM

Case	Case 2a	Case 2b	Case 2c	Case 2d	Case 2e
CTM Configuration					
Gasifier	Shell	GTI	GTI	Shell	GTI
Sulfur and CO_2 Removal	Rectisol®	RTI WDP	Rectisol®	RTI WDP	RTI WDP
Shift Reactors	Sour FBR	AFWGS	Sour FBR	AFWGS	ATWGS
Plant Parameters					
Steam Turbine output (MWe)	264.7	239.2	199.1	292.8	248.7
Thermal Efficiency, % LHV	53.1%	56.3%	56.5%	52.9%	56.6%
Capital Cost (TOC), $1,000/mtpd	577.1	453.1	476.3	549.3	449.0
Loan Guarantee RSP, $/ton	424.1	347.3	359.5	408.9	343.3
Relative Impact					
Case comparison basis		**2b vs. 2c**	**2c vs. 2a**	**2d vs. 2a**	**2e vs. 2b**
Steam Turbine output (MWe)		+40.1 (20.1%)	-65.6 (-24.8%)	+28.1 (10.6%)	+9.5(4.0%)
Thermal Efficiency, % LHV			+3.4% pt		+0.3% pt
Capital Cost (TOC), $1,000/mtpd			-100.8 (17.5%)		-4.1 (0.9%)
Loan Guarantee RSP, $/ton			-64.6 (15.2%)		-4.0 (1.2%)

The GTI gasifier technology offers favorable impacts on all plant parameters relative to the Case 2a DOE Reference CTM plant configuration (i.e., comparing Case 2c with 2a): with a 3.4 percentage point increase in thermal efficiency, a 17.5% reduction in TOC, and a 15.2% reduction in RSP. When comparing the two water-gas shift technologies offered by RTI (AWGS in Case 2e versus two fixed-bed sweet WGS reactors in Case 2b), the AWGS in Case 2e increases thermal efficiency by 0.3 percentage points while reducing the capital cost and RSP by 0.9% and 1.2% respectively.

The GTI gasifier technology offers favorable impacts on all plant parameters relative to the Case 2a DOE Reference CTM plant configuration (i.e., comparing Case 2c with 2a): with a 3.4 percentage point increase in thermal efficiency, a 17.5% reduction in TOC, and a 15.2% reduction in RSP. When comparing the two RTI advanced WGS processes (ATWGS in Case 2e versus AFWGS in Case 2b), ATWGS in Case 2e increases thermal efficiency by 0.3 percentage points and steam turbine output by 9.5 MWe while reducing the capital cost and RSP by 0.9% and 1.2%, respectively.

As with the IGCC scenario, RTI considers both AFWGS (Case 1b and 2b) and ATWGS (Case 1e and 2e) processes as advanced water-gas shift technologies that can offer significant techno-economic advantages over a conventional WGS process. RTI's claim of improved thermal efficiency can be seen in Table 26 based on increases in steam turbine output between cases with conventional WGS processes and AFWGS/ATWGS (i.e., Case 2b vs. Case 2c, Case 2d vs. Case 2a, and Case 2e vs. Case 2b). It is recommended that a follow-up study to be conducted to investigate it in more detail.

Sensitivity analyses were carried out to determine the effects of various parameters of the GTI R-GAS™ system and RTI advanced syngas cleanup, including WDP, DSRP, AFWGS/ATWGS and

AACRP on the overall methanol product RSP, with the results of these sensitivities summarized below. Other parameters investigated, and included in the Task 5 Topical Report, include: CTM plant CF, feedstock (coal and natural gas) cost, electric selling price, CO_2 sales price, cost of CO_2 emissions and CCF.

Figure 36 shows how the methanol RSPs for Case 2a and 2e change as the GTI DSP and R-GAS™ gasifier TPC vary from -30% to +30%. Also shown in Figure 36 are the methanol RSPs for the reference Case 2a at $517.8/ton and $441.3/ton for the commercial fuels and loan guarantee finance structures respectively. Figure 36 also shows that at the high end of the GTI R-GAS™ TPC (+30%), the methanol RSPs for Cases 2b and 2e are still less than the methanol RSP for the Case 2a reference plant.

Under the commercial fuels financing structure, every 1.6% increase in DSP and gasifier TPC, equivalent to about $12MM, increases the methanol RSP by $1/ton. Under the loan guarantee financing structure, every 1.9% increase in DSP and gasifier TPC, equivalent to about $14.5MM, increases the methanol RSP by $1/ton.

Figure 37 shows how methanol RSPs for Case 2b and 2e change as the RTI WDP system TPC varies from -30% to +30%. The RTI WDP system TPC includes the costs for the RTI WDP process, DSRP, AFWGS/ATWGS and AACRP process. For reference purposes, the Case 2a reference plant methanol RSPs at $517.8/ton for the commercial fuels and $441.3/ton for the loan guarantee finance structures are shown in Figure 37 as well. From Figure 37, it can be seen that at the high end of the RTI WDP TPC (+30%), the methanol RSPs for Cases 2b and 2e are still less than the RSP for the reference Case 2a CTM plant.

Under the commercial fuels financing structure, every 3.5% increase in RTI WDP TPC, equivalent to about $12MM, increases the methanol RSP by $1/ton. Under the loan guarantee financing structure, every 4.3% increase in RTI WDP TPC, equivalent to about $14.5MM, increases the methanol RSP by $1/ton.

Figure 38 shows how the Case 2e methanol RSP changes with respect to just the ATWGS TPC as it varies from -30% to +30%. For reference purposes, the Case 2a and 2b methanol RSPs at ($517.8/ton and $423.7/ton respectively) for the commercial fuels and ($441.3/ton and $363.6 respectively) for the loan guarantee finance structures are shown in Figure 38.

Figure 38 shows that at the high-end (+30% of baseline) of the ATWGS TPC, its RSP ($419.9/ton and $360.3/ton for the commercial fuels and loan guarantee finance structures respectively) varies little from the baseline and is still less than the Case 2a and Case 2b methanol RSPs. This is because the ATWGS TPC makes up only a small fraction of the total CAPEX and variation to its cost does not affect the RSP to a large extent.

Figure 39 shows how the Case 2e methanol RSP changes with respect to the ATWGS catalyst cost as it varies from -50% to +50%. Also shown in Figure 39 are the Case 2a and 2b methanol RSPs for reference. Like the ATWGS TPC, Figure 39 shows that at the high-end (+50% of baseline) of the ATWGS catalyst cost, its methanol RSP is little changed from the baseline and still lower than the Case 2a and Case 2b RSPs.

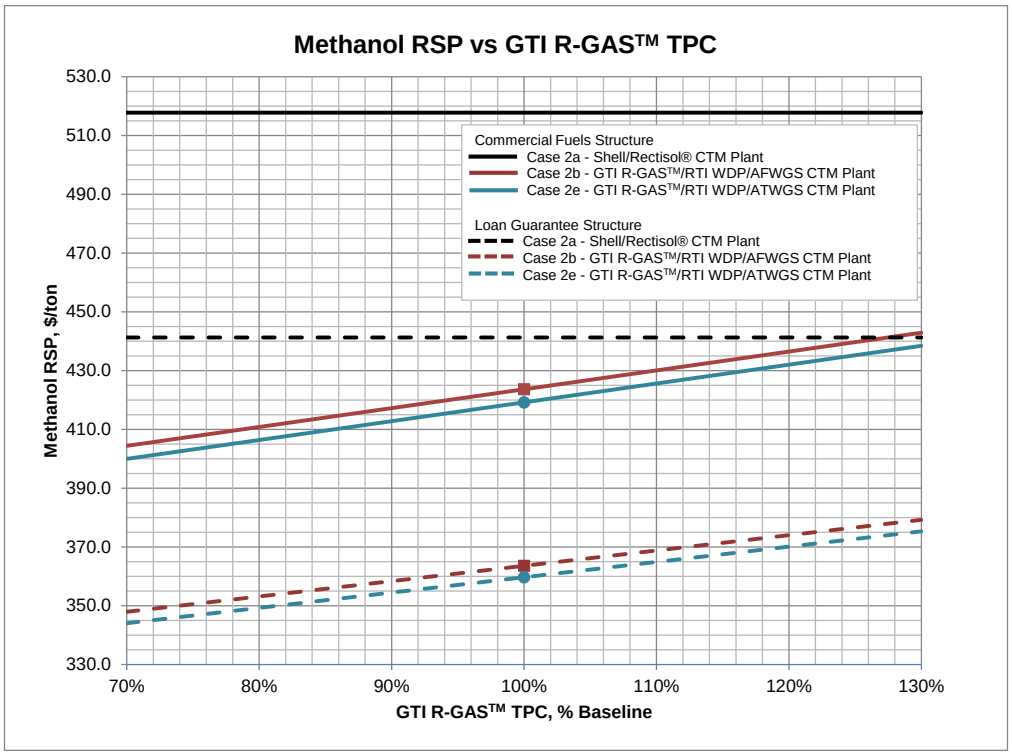

Figure 36. Sensitivity Analysis – RSP vs GTI R-GAS™ TPC

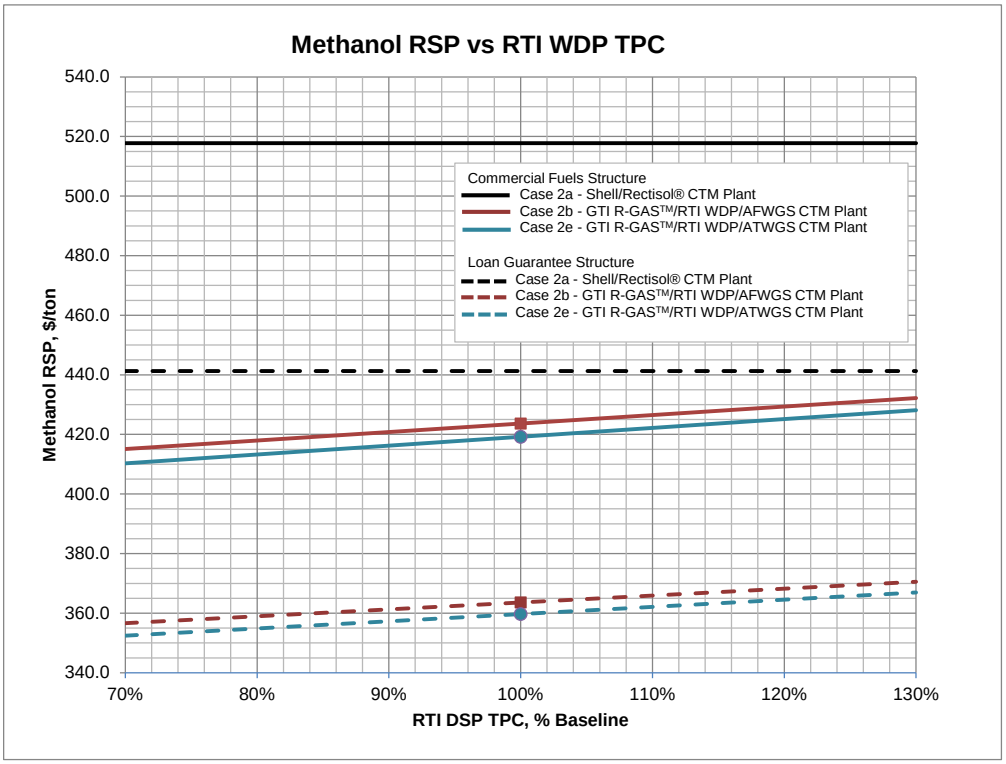

Figure 37. Sensitivity Analysis – RSP vs RTI WDP TPC

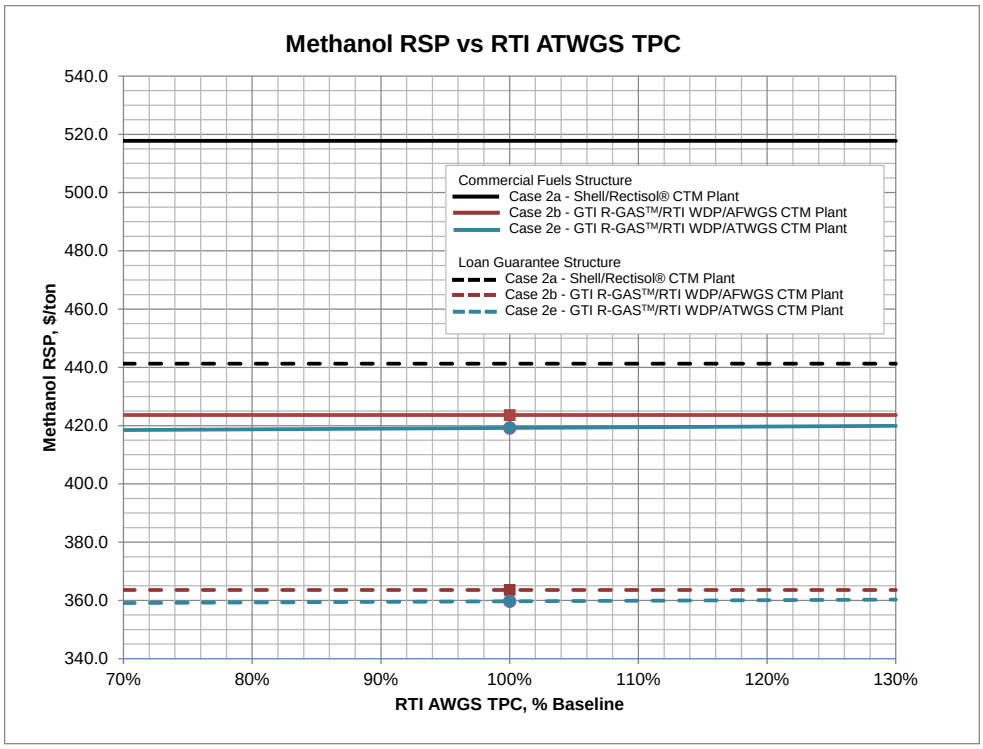

Figure 38. Sensitivity Analysis – COE vs RTI ATWGS System Cost

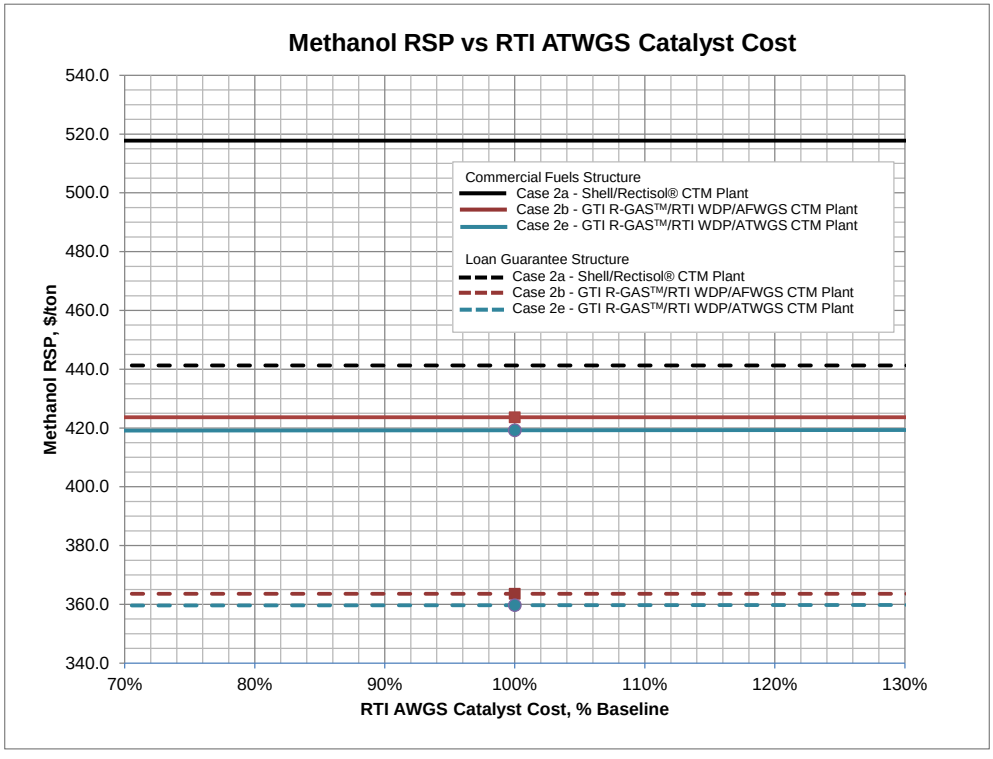

Figure 39. Sensitivity Analysis – COE vs RTI ATWGS Catalyst Cost

5.3 CONCLUSIONS

This study evaluated the techno-economic benefits of integrating RTI's novel Advanced Transport Water-Gas Shift (ATWGS) reactor technology into a combined GTI R-GAS™ gasification and RTI advanced syngas desulfurization process for integrated gasification combined cycle (IGCC) and coal-to-liquids (CTL) production applications. These integrated technologies offer significant benefits relative to the best performing state-of-the-art reference case. For IGCC, the combined technologies yield 1.7 percentage points IGCC efficiency improvement with 20% lower capital cost and 18% lower cost of electricity. For Coal To Methanol these technologies yield 3.5 percentage points higher plant thermal efficiency with a 22% reduction in capital cost and 19% lower methanol Required Selling Price. Sensitivity studies showed that the benefits were robust over +/-30% variations in Total Plant Cost for each of the plant sections incorporating these advanced technologies.

6.0 TASK 6: QUENCH ZONE SIMULATION FOLLOW-ON WORK

This follow-on study to Task 2 was motivated by concerns regarding the ability to adequately model quench zone hydrodynamics in the demonstration unit at reduced scale. In particular, the parameters governing similitude with respect to penetration of the spray into the syngas jet, mixing behavior, and liquid and syngas kinematics in the demonstration unit are difficult to simultaneously match in the current apparatus. This follow-on work was intended to improve understanding of momentum exchange between raw syngas and quench spray, prior to proceeding with further cold-flow testing with the demonstration gasifier geometry.

The goal of this follow-on study is to determine an approach for improving similitude of quench zone hydrodynamics of the demonstration gasifier in a cold-flow apparatus, for implementation in a future phase of study. This is achieved through satisfying the following objectives:

1. Re-evaluate quench-zone hydraulic similitude with focus on spray penetration and mixing behavior.
2. Evaluate alternative options for modelling the demonstration gasifier hydrodynamics in cold-flow.
3. Provide a detailed engineering cost estimate of the recommended option from (2).
4. Provide a proposal for a demonstration apparatus test program using the apparatus in (3).

The options in (2) are evaluated based primarily on their scientific merit. However, a preliminary cost estimate of each option is also provided to inform future decisions.

6.1 ANALYTICAL METHODOLOGY

The overall approach for establishing similitude is discussed in the section on Task 2, with a comprehensive discussion in the Topical Report for Task 2 and Task 6. The focus of this effort is on modelling spray penetration and mixing hydrodynamics in cold-flow, with the results serving as the basis for guiding scale-up decisions to a demonstration scale gasifier design. In particular, the effort focused on studying factors affecting i) mixing behavior, ii) spray penetration, and iii) disruption of syngas flow. Research into these factors is based on a survey of the literature, theoretical analysis, and a review of data from previous phases of the current study.

Syngas Jet Mixing:

Cooling of the hot syngas from the reactor depends on contact between the hot gas phase and coolant. Thus, in addition to atomization performance of the nozzles, the quench process is also dependent on mixing performance. Satisfactory heat transfer performance can be demonstrated in cold-flow through i) droplet size measurement, and ii) verification of adequate uniformity of the liquid distribution in a plane that is safely upstream of the syngas take-off.

The flow of syngas through the quench zone resembles that of a jet discharging axially into a pipe. It therefore shares similarities with jet flows and pipe flows. Profiles of mean concentration (and mean velocity) in jet mixing and pipe flows are self-similar for fully-turbulent flows. However, concentration fluctuations decrease with increasing Reynolds number of the jet or pipe flow, as the fluctuating component of velocity increases. We may conclude from this that the large-scale mixing behavior is similar across a wide range of Reynolds number, while the smaller-scale mixing

is dependent on Re. For the gasifier quench zone, operating at a lower syngas Reynolds number in the model than in the plant therefore captures the largest scales of mixing, in terms of mean concentration, while providing conservative estimates of concentration fluctuations.

Mixing of Gas Jets and Liquid Sprays:

The flow in the gasifier is further complicated by the quench spray, which mixes with the gas and evaporates. In addition, then, to requiring approximate similitude of the syngas Reynolds number to capture large-scale mixing behavior, we also require adequate similitude in terms of the jet-spray interaction. This means, as a first criterion, the ratio of velocity between the liquid and gas phases should be maintained as closely as is reasonably possible. In addition, however, there are other characteristics of the spray to consider, as described in the following sections.

Penetration of a Single Droplet into a Gas:

Based on conservation of momentum for the droplet, and taking the drag coefficient, C_d, as a function of droplet Reynolds number, Re_d, the penetration distance x for a single droplet of diameter d through surrounding gas where the density ratio of liquid/gas is given by $\frac{\rho_l}{\rho_g}$ is approximated by the equation

$$\frac{x}{d} = \frac{10}{3} \times \frac{\rho_l}{\rho_g} \times \frac{1}{C_d(0.4Re_{d0})}$$

where $C_d(0.4Re_{d0})$ indicates a drag coefficient evaluated at a value of 0.4 of the initial Reynolds number.

Scaling this equation relative to reactor diameter, D, instead of droplet diameter, and given that the ratio between $C_d(0.4Re_{d0})$ and $C_d(Re_{do})$ is in the range of 1.5 to 2.5 over the range of Re of greatest interest allows a simplified approximation yielding the following relationship:

$$\frac{x}{D} \simeq \frac{5}{3} \times \left(\frac{\rho_l}{\rho_g} \times \frac{d}{D} \times \frac{1}{C_d}\right) = \frac{5}{3} \times Sk$$

Thus, penetration of individual droplets is shown to be governed by similitude of Stokes number.

Spray and Jet Penetration

In studies of sprays and jets in cross-flow the spray penetration has been measured as a function of axial distance from the nozzle tip. Similitude is often correlated using expressions of the form:

$$\frac{y}{d} = Aq^n \left(\frac{z}{d}\right)^m \quad (1)$$

where y is the penetration depth, z is distance downstream of the injection point, d is the jet or orifice diameter, and A and n are empirical constants. q is the momentum flux ratio:

$$q = \frac{\rho_l u_l^2}{\rho_g u_g^2}$$

Thus, for single spray nozzles, penetration is seen to be governed by the momentum flux ratio $\rho_l u_l^2/\rho_g u_g^2$ and jet or drop diameter d. From further analysis, it is observed that this is nearly identically equivalent to using momentum ratio used in previous phases of the current study. Combining this observation with approximate values of 0.375 for n and 0.25 for m, and substitution of reactor diameter for droplet diameter, allows a simplified scaling expression to be derived in the form of:

$$\frac{y}{D} = A\left(\frac{\dot{m}_l u_l}{\dot{m}_g u_g}\right)^{\frac{3}{8}}\left(\frac{z}{D}\right)^{\frac{1}{4}}$$

Thus, similitude of spray penetration with downstream distance from the nozzles is primarily a function of the momentum ratio.

Spray Data Analysis:

An understanding of spray nozzle performance is required to properly prescribe the design and operating conditions of a physical cold-flow model. Droplet size and velocity are equally important, as they affect both Stokes number and the liquid-to-gas momentum flux ratio, which have been identified as important criteria of similarity with respect to the quench zone hydrodynamics.

Spray Characterization:

The performance of the reference quench spray nozzle was characterized with phase-Doppler interferometry (PDI), as well as photographs of spray patterns.

PDI measurements in still air indicate that the liquid volume fraction farther than 1 inch from the spray is consistently less than 1%, which supports the assumption that the spray is well-dispersed, and that droplet interactions are rare.

The majority of liquid is to be found near the edge of the spray. The proportion is estimated at roughly 85-90%, however there is no clear demarcation between the inner and outer regions of the spray. The flux decays exponentially with distance from the nozzle tip for both nozzles studies, as shown by the close agreement between the data points and exponential curve-fits.

Velocity and Size Distribution:

Trends in droplet sizes and velocities are summarized below:

Close to the nozzle tip (distances of 3 inches or less), droplet velocities exhibited strong increasing trends with nozzle pressure. Additionally, the measured liquid droplet velocities were highest in this region, with values close to the theoretical nozzle orifice liquid velocities calculated using continuity.

Droplet sizes decreased with increasing nozzle pressure. However, the decreases were modest at pressures above 500 psig. For example, at 2-3 inches away from the tip, a reference nozzle

exhibited a decrease of only 15 μm in droplet size over a pressure range 500 psig $< \Delta P <$ 1500 psig.

The liquid near the spray axis consists primarily of droplets less than 50 microns in diameter. Average downward velocities are generally less than 10 m/s, and the droplet size and velocity appear randomly distributed. It appears that droplets produced in this size range are preferentially entrained into the core along with gas, due to their low Stokes number.

Larger droplets, which form the bulk of the size distribution ($D_{V_{50}} \approx d_{32} \approx 100$ μm), are rarely found in the core area of the spray. However, they make up the majority of the liquid at the edge of the spray. There is a strong correlation between size and velocity, with velocity increasing with drop size. The largest drops typically have axial velocity of about 20 m/s or more, which increases with injection pressure.

Analysis Conclusions:

Spray momentum and penetration are key factors in the gasifier quench performance. However, the optimum condition is not clearly evident: shallow or weak penetration of coolant into the syngas jet leaves a jet of unquenched syngas along the centerline. Although entrained liquid will eventually reach the core through turbulent mixing, this may require use of an excessively long quench tube. Conversely, excessive penetration may overly disrupt the syngas flow, causing unquenched gas to either be accelerated along the centerline, or deflected radially. A major focus of future testing should be to further examine effects of momentum ratio in the demonstration model.

Analysis in previous phases had been based primarily on velocity along the centerline, and comparisons with Spraying Systems measurements. We should, however, focus greater attention to analysis of the edge of the spray in future phases. The trends in spray characterization data generally remain consistent with prior dimensional analysis. Since understanding of the spray distribution and pattern is crucial to the scaling process, further nozzle characterization of the spray nozzle selected for the demonstration unit (#26 capacity), both as a single nozzle and in a cluster, is recommended.

The PDI analysis supports a conclusion that the majority of the spray in the quench zone has significant slip velocity relative to the gas in the immediate vicinity of the quench zone, rather than consisting of a gas jet with suspended droplets. It therefore appears that hydraulic nozzles are appropriate for continued testing.

6.2 RESULTS AND DISCUSSION

Scaling Evaluation:

For the purposes of evaluating jet-jet interactions and overall mixing, the preceding analysis indicates that the jet momentum and velocity ratios are the most important criteria of similarity, and that if necessary, similitude of the Stokes number may be relaxed somewhat.

Calculations for a full-scale demonstration cold-flow apparatus indicate that there is not a substantial advantage in terms of similitude by increasing the size of apparatus to the demonstration scale. This is primarily because scaling the experiment at atmospheric pressure while maintaining kinematic similitude affects Stokes number and momentum ratio in a similar way. This is because of the mathematical forms of Π_5 and Sk:

$$\Pi_5 = \frac{\dot{m}_l u_l}{\dot{m}_g u_g} = \frac{\rho_l N u_l^2 d_0^2}{\rho_g u_g D^2}$$

$$Sk = \frac{\rho_l}{\rho_g}\frac{d_{V50}}{D}\frac{1}{C_d} \approx \frac{\rho_l}{\rho_g}\frac{d_{V50}}{D}\frac{\rho_g u d_{V50}}{\mu_g} \approx \frac{\rho_l u d_{V50}^2}{\mu_g D}$$

Considering these scaling equations in the context of the dimensional parameters which can be controlled with relative ease:

1. Nozzle size: this is the parameter modified using our current scaling strategy.
2. Apparatus scale: this strategy was the original focus of the present work.
3. Gas density: Pressurized gas is already supplied to the apparatus.
4. Number of nozzles: Increasing the number of nozzles increases liquid mass flow and momentum ratio without affecting velocity or Stokes number.

Table 27 shows a comparison of first-order effects of modifying each of these parameters independently. It is noted that increasing the scale of the apparatus has a similar effect as the current strategy, which is to decrease Stokes number and momentum ratio by selecting a smaller-orifice nozzle. An alternative to increasing the geometric scale that provides slightly more of an advantage in terms of similitude is to increase the pressure (and therefore gas density) at the existing scale. As shown in Table 28, pressurizing the vessel to approximately 2.5 bar (abs) results in further reduction of Stokes number, with approximately the same quality of similitude of the momentum ratio. The other method for varying momentum ratio and Stokes number independently is by changing the number of nozzles. There are, however, practical limitations to the number of nozzles that can be physically mounted inside the vessel.

Table 27: First-order effects of modifying operating parameters in a cold-flow model. $\boldsymbol{d}$ *= nozzle or droplet diameter,* $\boldsymbol{D}$ *= scale;* $\boldsymbol{\rho_g}$ *= gas density (operating pressure);* $\boldsymbol{N}$ *= number of nozzles;* $\boldsymbol{\Delta P}$ *= nozzle injection pressure.*

Parameter	$\boldsymbol{\frac{\rho_l N u_l^2 d_0^2}{\rho_g u_g^2 D^2}}$	$\boldsymbol{Sk \approx \frac{\rho_l u d^2}{\mu_g D}}$	**Notes**
$d \downarrow$	$\downarrow\downarrow$	$\downarrow\downarrow$	Current strategy
$D \uparrow$	$\downarrow\downarrow$	$\downarrow$	Similar effects as current strategy
$\rho_g \uparrow$	$\downarrow$	-	Weak effect on Sk
$N \uparrow$	$\uparrow$	-	Possible coalescence for closely spaced nozzles

Estimated Cost:

A preliminary cost estimate of implementing each of the apparatus options discussed in the previous study is presented in Table 28. The following is noted about the table:

- These estimates convey only an approximate level of cost commitment required, and are not intended for detailed budget planning.
- Continuing to use the current apparatus in its present state entails only the minimum recommissioning costs.
- Because a larger-diameter vessel does not fit within the current apparatus frame this option involves constructing an entirely new apparatus.
- Increasing the pressure in the existing apparatus requires some components, including the test section, to be replaced.

Table 28: Comparison of scaling options. In each scenario, the nozzle offering optimum similitude is selected.

Apparatus	Momentum	Drag	Cost
Demo Gasifier (reference)	1.0	1.0	
Current Scale	1.12	6.4	$20,000
Full Scale	1.19	2.6	$250,000
Pressurized Current Scale	0.88	2.0	$125,000

6.3 CONCLUSIONS

Analysis of jet-jet interactions and mixing leads to the conclusion that the momentum ratio of quench spray to gasifier syngas product is the key scaling relationship, with droplet penetration being the other key consideration.

Similitude analysis indicates that a pressurized cold flow apparatus at the same scale as the current one would provide equivalent or superior similitude to one corresponding to the dimensions of the demonstration-scale gasifier, at significantly less cost.

TASK 2: QUENCH ZONE SIMULATION

TOPICAL REPORT

Reporting Period

Start Date: October 1, 2014

End Date: September 30, 2015

Principal Author

Steve Fusselman Principal Investigator/Program Manager

September 30, 2015

DOE Award Number

DE-FE0023577 (DOE NETL)

Aerojet Rocketdyne of DE, Inc.

8900 DeSoto Avenue

Chatsworth, CA 91311

DISCLAIMER

ABSTRACT

Aerojet Rocketdyne (AR) has developed an innovative gasifier concept incorporating advanced technologies in ultra-dense phase dry feed system, rapid mix injector, and advanced component cooling to significantly improve gasifier performance, life, and cost compared to commercially available state-of-the-art systems. A key feature of the AR gasifier design is the transition from the gasifier outlet into the quench zone, where the raw syngas is cooled to ~ 400°C by injection and vaporization of atomized water. Earlier pilot plant testing revealed a propensity for the original gasifier outlet design to accumulate slag in the outlet, leading to erratic syngas flow from the outlet. Subsequent design modifications successfully resolved this issue in the pilot plant gasifier. In order to gain greater insight into the physical phenomena occurring within this zone, AR developed a cold flow simulation apparatus with Coanda Research & Development with a high degree of similitude to hot fire conditions with the pilot scale gasifier design, and capable of accommodating a scaled-down quench zone for a demonstration-scale gasifier. The objective of this task was to validate similitude of the cold flow simulation model by comparison of pilot-scale outlet design performance, and to assess demonstration scale gasifier design feasibility from testing of a scaled-down outlet design. Test results did exhibit a strong correspondence with the two pilot scale outlet designs, indicating credible similitude for the cold flow simulation device. Testing of the scaled-down outlet revealed important considerations in the design and operation of the demonstration scale gasifier, in particular pertaining to the relative momentum between the downcoming raw syngas and the sprayed quench water and associated impacts on flow patterns within the quench zone. This report describes key findings from the test program, including assessment of pilot plant configuration simulations relative to actual results on the pilot plant gasifier and demonstration plant design recommendations, based on cold flow simulation results.

TABLE OF CONTENTS

EXECUTIVE SUMMARY

Aerojet Rocketdyne (AR) has developed an innovative gasifier concept incorporating advanced technologies in ultra-dense phase dry feed system, rapid mix injector, and advanced component cooling to significantly improve gasifier performance, life, and cost compared to commercially available state-of-the-art systems. A key feature of the AR gasifier design is the transition from the gasifier outlet into the quench zone, where the raw syngas is cooled to ~ 400°C by injection and vaporization of atomized water. Earlier pilot plant testing revealed a propensity for the original outlet design to accumulate slag in the outlet, leading to erratic syngas flow from the outlet. Subsequent design modifications successfully resolved this issue in the pilot plant gasifier. In order to gain greater insight into the physical phenomena occurring within this zone, AR developed a cold flow simulation apparatus with Coanda Research & Development with a high degree of similitude to hot fire conditions in the pilot scale gasifier design, and capable of accommodating a scaled-down quench zone for a demonstration-scale gasifier.

The objective of the current effort is to establish a suitable degree of similitude for the gasifier outlet/quench zone transition region and a cold flow model, with the results serving as the basis for guiding scale-up decisions to a demonstration scale (~800 TPD capacity) gasifier design. The significantly different results from the two different pilot plant outlet designs provide a unique opportunity to validate the cold flow model for the pilot scale design. The initial testing of the cold flow apparatus constructed in 2013 under AR funding showed clear differences between these two configurations in cold flow. On that basis, AR defined a program to assess quench zone hydrodynamics over a range of operating parameters and geometries for both pilot plant configurations and a scaled 800 TPD gasifier outlet configuration using the existing facility and gasifier designs. This test program was incorporated into the current effort, DE-FE0023577, as Task 2.

In the current work, physical modeling is used to simulate the gasifier system, by using another system exhibiting similar flow characteristics. The degree to which the model reflects the plant behavior is determined by similitude, the degree to which the two systems are equivalent. There are three types of similitude:

(1) Geometric – where the model and actual systems have the same shape

(2) Kinematic – where the model and actual systems have the same flow patterns

(3) Dynamic – where the model and actual systems have the same ratio of forces

Similitude is established through the process of dimensional analysis, a method for reducing the number and complexity of experimental variables. The theorem states that a phenomenon depending on n dimensional variables x_1, x_2, ... x_n can be reduced to $n - k$ dimensionless variables, where k is the number of fundamental dimensions (mass, length, temperature, time). For independent modeling of the quench zone and slag flows, there are a total of 17 key properties and 4 fundamental dimensions in the former, and 5 key properties comprising 3 fundamental dimensions in the latter, thus resulting in a total of 15 non-dimensional parameters. Based on these parameters, a high degree of similitude was established for quench zone hydrodynamic parameters, with a limited degree of similitude established for thermodynamic parameters associated with evaporating flow.

The test apparatus was constructed at the same dimensions as the pilot plant gasifier. For the scaled demonstration gasifier outlet, the gasifier and outlet components were sized to be installed in the existing pilot-scale quench vessel and provide geometric similitude with the demonstration plant. Most tests were conducted using an air/water system, which provided good visualization of flow fields but was not able to replicate the impact of vaporizing quench spray on flow patterns. Evaporating flow impacts were assessed using an air/HA134a (1,1,1,2-tetrafluoroethane) system. High speed video was used in flow visualization tests. Phase-Doppler interferometry was used to characterize localized droplet density, size and velocities (axial and radial) in selected locations.

Pilot scale testing was performed over a range of geometries and operating variables, with and without slag simulant (glycerine), using an air/water system. The pilot scale model demonstrated excellent consistency with observable pilot plant gasifier results, provides excellent hydrodynamic similitude, and offers acceptable thermodynamic similitude. On that basis, it was concluded that the modelling approach was suitable for use in the scaled demonstration outlet test effort.

Demonstration scale testing focused on the conical outlet, assessing the impact of key parameters on hydrodynamics. Experiments also offered insight into the rate of water ingress into the outlet, confirmed the absence of quench spray/slag interactions in the scaled unit, and assessed the impact of evaporating quench spray on overall flow patterns. Test results indicated that cone length and axial location of nozzles relative to outlet had a small impact on flow patterns. The longer cone was determined to be preferable as a means to provide superior isolation of the slag drip lip from any recirculating quench spray. Testing with HA134a as the quench liquid revealed more benign recirculation patterns with recirculating flow, so the air/water test results are considered to be conservative with respect to adverse flow patterns near the outlet. The liquid/gas momentum ratio was varied, and it was determined that a momentum ratio < 1.0 avoided quench spray recirculation into the outlet cone.

The project successfully accomplished the objectives set out in Task 2 of the contractual Statement of Project Objectives, in verifying the ability to establish acceptable similitude and providing design guidance for the gasifier outlet to avoid build-up of slag. The test program also indicated other considerations for quench system design that should be considered for a follow-on study. Specifically, recommended follow-on actions are:

- A detailed assessment of jet-jet interactions relevant to an atomized liquid jet and down-flowing gas column. The purpose is to clearly define the physics governing the scale-up of this specific type of jet-jet interaction.
- Using the results from the above assessment, design and fabricate a full scale demonstration gasifier quench zone that is also full length. The purpose of this is twofold – (1) Verify jet-jet interaction dependencies on operating parameters and (2) assess mixing of quench spray within the gas stream to ensure adequate cooling of the syngas before it exits the quench vessel.

1.0 INTRODUCTION

1.1 DOCUMENT SCOPE

The purpose of this document is to describe key findings from the quench zone simulation test program, including assessment of pilot plant configuration simulations relative to actual results on the pilot plant gasifier and demonstration plant design recommendations, based on cold flow simulation results.

This Topical Report summarizes the effort performed under Task 2: Quench Zone Simulation as part of contract DE-FE0023577 awarded to Aerojet Rocketdyne by the United States Department of Energy (DOE) – National Energy Technology Laboratory (NETL).

1.2 OBJECTIVES

The objective of the current effort is to establish a suitable degree of geometric, kinematic and dynamic similitude for the gasifier outlet/quench zone transition region and a cold flow model, with the results serving as the basis for guiding scale-up decisions to a demonstration scale (~800 TPD capacity) gasifier design.

The desired functions of the gasifier quench zone are as follows:

(1) Cool raw syngas exiting the gasifier to suitable temperature for downstream processes

(2) Avoid accumulation of slag at the gasifier outlet that may lead to blockage and shutdown

(3) Avoid development of misdirected syngas flow patterns

(4) Achieve “reasonably uniform” temperature of syngas exiting the quench vessel

(5) Avoid operationally challenging build-ups within the quench vessel

The raw syngas is cooled by spraying atomized water into the syngas exiting the gasifier just beneath the gasifier outlet. Early testing of the 18 TPD pilot scale gasifier in 2010 revealed significant issues for the original gasifier outlet design with respect to items (2) and (3), above, with frequent accumulation of solidified slag at the gasifier outlet creating an asymmetric opening that directed very hot syngas against the walls of the quench vessel. This original design had a cylindrical outlet with water spray nozzles directly underneath the cylinder. Analysis of the test results led to a conical outlet design, with a slag “drip lip” recessed back into the gasifier to thermally and hydrodynamically isolate the slag discharge point from the turbulent flow and cooling of the quench zone. This conical design was successfully tested in late 2010, and has been incorporated into subsequent pilot plant component designs and the demonstration scale gasifier conceptual design.

Although the current design has been successfully demonstrated over 100’s of hours and multiple feedstocks, there remained uncertainty as to how to scale the design from 18 TPD to ~800 TPD. In 2012, Aerojet Rocketdyne (AR) funded Coanda Research & Development

Corporation to perform a scoping study assessing quench zone hydrodynamics and defining an affordable cold flow model achieving a suitable level of similitude to inform gasifier design scale-up. In 2013, AR funded the design, fabrication and initial testing of this cold flow model.

The significantly different results from the two different outlet designs provided a unique opportunity to validate the cold flow model for the pilot scale design. The initial testing in 2013 showed clear differences between these two configurations with the cold flow model. On that basis, AR defined a program to assess quench zone hydrodynamics over a range of operating parameters and geometries for both pilot plant outlet configurations and a scaled 800 TPD gasifier outlet configuration using the existing facility and gasifier designs. This test program was proposed to DOE-NETL as Task 2 under DE-FE0023577, which NETL funded in late 2014.

The effort defined under the contractual Statement of Project Objectives (SOPO) is as follows:

> **TASK 2 – Quench Zone Simulation**: Coanda will use the existing AR quench zone simulator to characterize quench zone flow fields for pilot plant and scaled-down demonstration gasifier configuration using cold flow simulation.
>
> Subtask 2.1 – Pilot Scale Quench Zone Optimization: Scale models of the original and modified pilot plant quench zone designs will be evaluated to assess qualitative differences in flow patterns relative to observed performance in hot fire testing to validate simulation fidelity. Systematic variations in quench zone geometry will be performed to characterize quench spray coverage in the quench zone and to assess the propensity for quench spray intrusion into the gasifier outlet. Spray nozzle geometry (two axial locations and two spray angles) and cone geometry (two cone lengths) will be tested. A technical review will be held to validate test program readiness prior to moving forward with Subtask 2.2.
>
> Subtask 2.2 – Demonstration Scale Model: The model reactor vessel will be exchanged with one of the appropriate diameter to maintain geometric similitude with the demonstration scale gasifier. Characterization of flow field and spray distribution will be performed for a sub-set of geometries selected based on findings from pilot scale testing.
>
> Subtask 2.3 – Analysis and Reporting of Results: Key findings from the test program will be summarized in a topical report. This will include assessment of pilot plant configuration simulations relative to actual results on the gasifier and demonstration plant design recommendations, based on cold flow simulation results.

This Topical Report discusses the results accomplished under Task 2 of DE-FE0023577.

1.3 ABBREVIATIONS

AGWGST	Advanced Gasifier & Water Gas Shift Technologies
TPD	Tons Per Day
PDI	Phased Doppler Interferometry
PIV	Particle Image Velocimetry

2.0 EXPERIMENTAL METHODS

2.1 SIMILITUDE ANALYSIS

Physical modeling is a means to simulate a given system using another system exhibiting similar flow characteristics. The degree to which the model reflects reality is determined by similitude, the degree to which the two systems are equivalent. There are three types of similitude:

(1) Geometric – where the model and actual systems have the same shape

(2) Kinematic – where the model and actual systems have the same flow patterns

(3) Dynamic – where the model and actual systems have the same ratio of forces

In many instances, a high degree of similitude can be established for specific phenomena of interest. For example, Figure 1 shows good similitude is established between a simple inclined flat plate measuring a few inches in length and the plume of oil dispersing from a grounded tanker several hundred feet long.

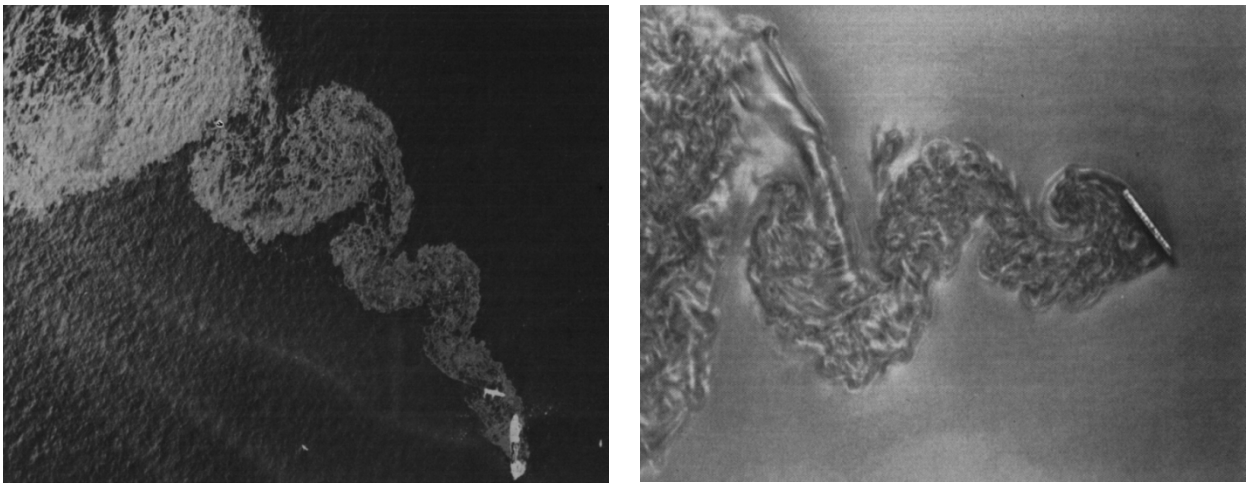

Figure 1: An example of similitude achieved between oil dispersal plume characteristics for a grounded tanker (left) and a model using an inclined flat plate (right)

Similitude is established through the process of dimensional analysis, a method for reducing the number and complexity of experimental variables. A phenomenon depending on n dimensional variables x_1, x_2, ... x_n can be reduced to $n - k$ dimensionless variables, where k is the number of fundamental dimensions (mass, length, temperature, time).

For the quench zone depicted in Figure 2, there are 17 key properties (summarized in Table 1) and 4 fundamental dimensions (mass, length, time, and temperature), resulting in $n - k = 13$ non-dimensional parameters. Of these, 5 are hydrodynamic, and the remaining 8 describe the system's thermodynamics.

Table 1: Dimensional parameters of the quench-zone problem.

Symbol	*Units*	*Description*	*Reference location (where applicable)*	*Comments*
D	m	Reference scale	Tube liner (diameter)	
ρ_G	kg/m^3	Gas density	Tube liner	Calculated from measured pressure and temperature in cold-flow model
u_G	m/s	Gas velocity	Tube liner	Calculated from measured gas mass-flow and continuity in cold-flow model
μ_G	Ns/m^2	Gas viscosity	Tube liner	
c_{P_G}	J/kgK	Gas specific heat at constant pressure	Tube liner	
T_G	K	Gas temperature	Tube liner	Measured directly in cold-flow model.
k_G	W/mK	Gas thermal conductivity	Tube liner	
ρ_L	kg/m^3	Liquid density	N/A	Assumed constant everywhere
$\dot{m}_L$	kg/s	Liquid mass flow	Nozzle orifice	Measured directly in cold-flow model.
u_L	m/s	Liquid velocity	Nozzle orifice	Calculated from measured liquid mass flow and continuity in cold-flow model.
d_{50}	μm	Liquid droplet diameter	Near nozzle orifice	Mean diameter based on volume, measured approx. 1 in. from nozzle tip.
c_{P_L}	J/kgK	Liquid specific heat at constant pressure	N/A	Constant everywhere
h_{fg}	J/kgK	Liquid heat of vaporization	N/A	Constant everywhere
T_G	K	Liquid temperature	Upstream of nozzles	Measured directly in cold-flow model.
T_{sat}	K	Liquid saturation temperature	Near nozzle orifice	At quench zone pressure.
k_L	W/mK	Liquid thermal conductivity	N/A	Constant everywhere
σ	N/m	Liquid surface tension	N/A	Constant everywhere.

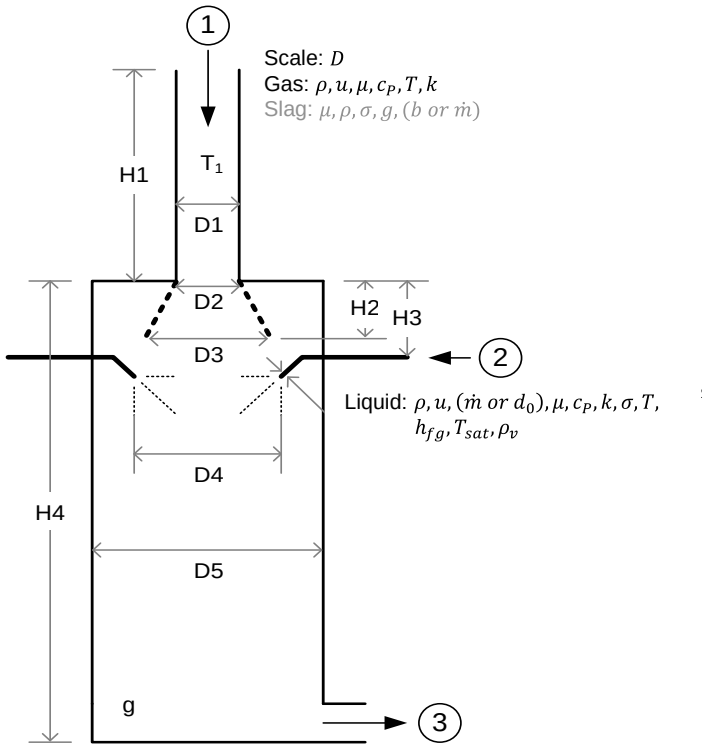

Figure 2: Illustration of key properties for the quench zone, not including slag.

The parameters selected for similitude analysis of the quench zone, excluding slag, are as follows:

Hydrodynamic parameters:

Gas flow Reynolds number: $Re_D = \frac{\rho_G u_G D}{\mu_G}$

Droplet Reynolds number: $Re_{d_{50}} = \frac{\rho_G u_L d_{50}}{\mu_G}$

Droplet Weber number: $We_{d_{50}} = \frac{\rho_L u_L^2 d_{50}}{\sigma_L}$

Liquid/gas velocity ratio: $\frac{u_L}{u_G}$

Liquid/gas momentum (inertia) ratio: $\frac{\dot{m}_L u_L}{\dot{m}_G u_G}$

Note that the mass flow of the gas $\dot{m}_G$ can be obtained from other quantities listed in Table 1, and is therefore not a separate independent parameter (i.e., we could have written the definition of momentum ratio as $\dot{m}_L\, u_L/(\rho_G\, u_G^2 \times \frac{\pi}{4} D^2\,)$.

In addition to the above dimensionless hydrodynamic parameters, the similitude assessment also includes droplet Stokes number ($Sk_{d_{50}}$) to assess the extent to which droplet entrainment within the quench zone happens over the characteristic length scale (in this case, gasifier diameter).

$$Sk_{d_{50}} = \frac{u_G \tau}{D} = \frac{\rho_L}{\rho_G} \times \frac{d_{50}}{D} \times \frac{1}{C_d}$$

where τ is the droplet's aerodynamic relaxation time – the time-constant of decay of relative velocity between the droplet and a constant free-stream – and C_d is the droplet's drag coefficient, a function of $Re_{d_{50}}$.

Thermodynamic parameters:

Prandtl number (gas and liquid): $Pr = \frac{c_P \mu}{k}$

Kinetic energy/enthalpy ratio (liquid and gas): $\frac{u^2}{c_P T}$

Vapor/liquid density ratio: $\frac{\rho_v}{\rho_L}$

Liquid/gas heat capacity ratio: $\frac{c_{P_L}}{c_{P_G}}$

Jakob number (heat of vaporization basis): $Jm_1 = \frac{\dot{m}_G}{\dot{m}_L} \times Ja_1 = \frac{\dot{m}_G}{\dot{m}_L} \times \frac{c_{P_G}(T_G - T_{sat})}{h_{fg}}$

Jakob number (degree of subcooling basis): $Ja_2 = \frac{c_{P_G}(T_L - T_{sat})}{h_{fg}}$

In addition to the dimensionless thermodynamic parameters, the similitude assessment also considers droplet evaporation time (t_e), which is looked at in the context of other relevant time scales within the quench zone.

$$\frac{t_e}{D/u_L} \approx \frac{\mathrm{Pr}_G^{\frac{2}{3}} Re_{d_{50}}^{\frac{1}{2}}}{3.6\, Jm_1} \times \frac{\dot{m}_G}{\dot{m}_L} \times \frac{d_{50}}{D} \times \frac{\rho_L}{\rho_G}$$

Considering the slag, as shown in Figure *3*, there are 5 slag properties, and 3 fundamental dimensions, so 2 additional non-dimensional parameters are introduced. These are the Bond number and a form of Capillary number.

Table 2: Key dimensional parameters of the slag flow.

Symbol	*Units*	*Description*	*Reference location (where applicable)*	*Comments*
μ_S	Ns/m^2	Slag viscosity	Drip lip	Wide range of estimated values, depending on materials and location.
ρ_S	kg/m^3	Slag density	Drip lip	
σ_S	N/m	Slag surface tension	Drip lip	Estimated value
g	m/s^2	Gravitational constant	N/A	
b	m	Width/diameter of slag column	Drip lip	Assumed to be approx. the drip-lip width

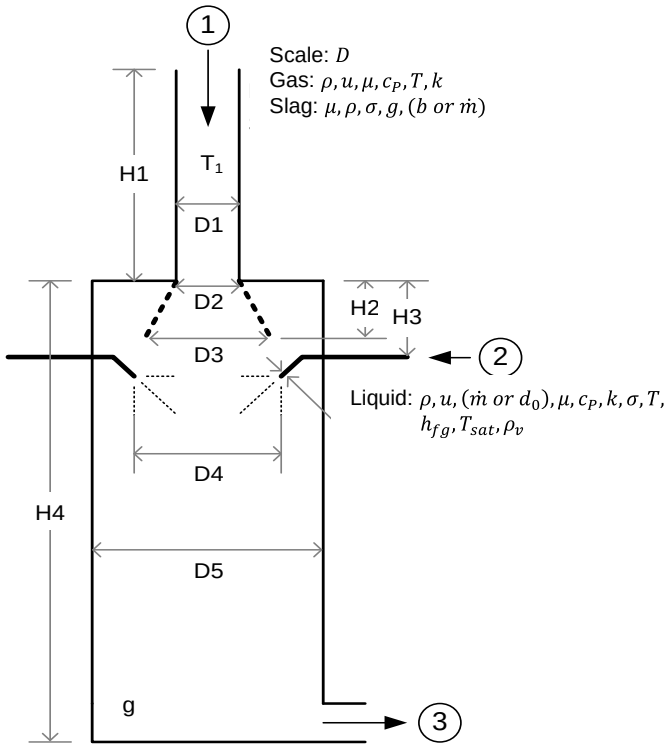

Figure 3: Illustration of key properties for the quench zone, including slag.

The Bond number, Bo, reflects the relative influence of gravitational and surface tension forces on slag behavior .

$$Bo = \frac{\rho_S g b^2}{\sigma_S}$$

In the current context, Bond number is the primary factor determining the break-off length of slag columns attached to the drip-lip.

The modified capillary number, Ca^*, is a measure of the relative importance of viscous and surface tension forces on slag behavior.

$$Ca^* = \frac{\mu_S \sqrt{gb}}{\sigma_S}$$

Similitude for the pilot scale gasifier is summarized in the tables below for non-vaporizing flow using water (Table 3) and for vaporizing flow (Table 4) using the halocarbon HA134a. Glycerine was used as the slag simulant. Similitude for the scaled demonstration gasifier outlet is summarized for non-vaporizing flow using water in Table *5*. In general, excellent similitude was established for hydrodynamic parameters in all cases. While Jakob number similitude (see Table 4) was not as good due to practical limitations for a cold flow apparatus (the accessible sensible heat from the gas phase is very limited relative to that required to evaporate the liquid phase), the droplet evaporation time to transit time ratio was in a comparable range, which

provides a reasonable indication of overall impact of evaporating flow on quench zone hydrodynamics.

Achieving a high degree of similitude for Bond and Capillary numbers is challenging in a number of ways. Slag properties are highly dependent upon composition and temperature, so are only approximately known in the region of interest. Also, it was not readily apparent as to the proper length and velocity scales to employ. Therefore, the similitude achieved for these parameters is established on a "best efforts" basis, with the model values in the same regime (gravity dominates surface tension in the Bond number, viscous forces dominate surface tension in the Capillary number) as for the pilot and demo cases.

Table 3: Similitude assessment for pilot plant gasifier model using non-vaporizing water as the quench spray fluid.

Parameter	*Pilot*	*Model (Air/Water)*	*Ratio (Pilot/Model)*	*Notes*
Gas flow	Baseline	Baseline	3.3	Velocity in model same as pilot.
Liquid flow	Baseline	Baseline	4.9	Model flow rate determined by other similitude requirements.
Re_D	57,000	59,000	1.0	Regime match required ($Re > 10^4$)
We_{d50}	0.4	0.05	7	Based on gas velocity. Regime match required (droplets approx. spherical for $We_d < \sim 1$ and no secondary break up for $We_d < \sim 10$).
Re_{d50}	55	26	2.1	Close match not required. More important to find value that provides Stokes number similitude.
$\frac{u_L}{u_G}$	1.8	3.0	0.6	Stokes number match prioritized in pilot model testing.
$\frac{\dot{m}_L u_L}{\dot{m}_G u_G}$	1.42	1.58	0.9	Stokes number match prioritized in pilot model testing.
Sk_{d50}	0.17	0.17	1.0	$f(We,\ Re_{D_{50}})$ Close match desired to match droplet trajectory for values O(1).
Sk_{d90}	0.25	0.31	0.8	Similitude of larger drops also important (values closer to 1, longer evaporation time).
Bo	2.6	7.4	0.4	Length scale assumed to be drip-lip width, b. Gravitational forces dominate surface tension (Bo > 1) for model and pilot.
Ca^*	71	5.5	13	Velocity scale assumed to be ($\propto \sqrt{gb}$) . Viscous forces dominate surface tension (Ca > 1) for model and pilot.

Table 4: Similitude assessment for pilot plant gasifier model using evaporating HA134a as the quench spray fluid.

Parameter	*Pilot*	*Model (Air/HA134a)*	*Ratio (Pilot/Model)*	*Notes*
Re_D	57,000	58,000	1.0	Regime match required ($Re > 10^4$)
We_{d50}	0.4	0.2	1.7	Based on gas velocity. No droplet deformation expected in this range.
Re_{d50}	55	12	4.5	Close match not required.
$\frac{u_L}{u_G}$	1.8	3.0	0.6	Heat/mass transfer characteristics prioritized in HA134a testing.
$\frac{\dot{m}_L u_L}{\dot{m}_G u_G}$	1.42	1.91	0.7	Heat/mass transfer characteristics prioritized in HA134a testing.
Sk_{d50}	0.17	0.058	3.0	Conservative mis-match. Droplets more fluid-following in model.
Sk_{d90}	0.25	0.112	2.2	
Bo	2.6	7.4	0.4	Rough estimate. Slag properties highly variable. Length scale not well known (assumed to be drip-lip width, b).
Ca^*	71	5.5	13	Velocity scale unknown – assumed to be ($\propto \sqrt{gb}$).
Jm_1	1.99	0.41	4.8	Limited in cold-flow by operating temperatures
Ja_2	-0.31	0.19	-1.6	HA134a superheated. Cooling required to prevent flashing.
$\frac{t_e}{D/u_L}$	0.25	0.69	0.4	Longer evaporation time than plant provides conservative estimate.
ρ_v/ρ_L	13.8×10^{-3}	4.4×10^{-3}	3.2	Greater expansion of HA134a deemed conservative (more pronounced effect on flow field).
Pr_L	6.985	3.530	2.0	Not considered important in dispersed phase.
Pr_G	0.673	0.82	0.8	Not considered a critical parameter.
$\frac{u^2}{c_P T}$	~0	~0	N/A	Kinetic energy negligible compared with thermal energy

Table 5*: Similitude assessment for scaled demonstration plant gasifier model using non-vaporizing water as the quench spray fluid.*

Parameter	*Pilot*	*Model (Air/Water)*	*Ratio (Pilot/Model)*	*Notes*
Re_D	571,700	34,400	17	Regime match required ($Re > 10^4$)
We_{d50}	0.8	0.01	123	Regime match only required in this range ($We < 1$)
Re_{d50}	96	10	10	Close match not required.
$\frac{u_L}{u_G}$	3.6	6.8	0.5	Momentum ratio match prioritized in pilot model testing.
$\frac{\dot{m}_L u_L}{\dot{m}_G u_G}$	2.5	2.5	1.0	Pilot similitude optimized around this parameter
Sk_{d50}	0.03	0.06	0.4	Exact match not required for values below approx. 0.1 (fluid-following drops)
Sk_{d90}	0.05	0.12	0.4	Fluid-following assumption slightly less valid for largest drops.
Bo	150	68	2.2	Slag properties highly variable. Mis-match is conservative if assumptions regarding length scale and slag properties are valid. For both model and pilot, gravitational forces dominate surface tension (Bo > 1).
Ca^*	197	10	20	Velocity scale unknown – assumed to be ($\propto \sqrt{gb}$). For both model and pilot, viscous forces dominate surface tension (Ca > 1).

Table 6: Similitude assessment for scaled demonstration plant gasifier model using evaporating HA134a as the quench spray fluid.

Parameter	*Pilot*	*Model (Air/HA134a)*	*Ratio (Pilot/Model)*	*Notes*
Re_D	571,700	27,700	20.6	Regime match required ($Re > 10^4$)
We_{d50}	0.8	0.02	51.6	Regime match only required in this range ($We < 1$)
Re_{d50}	96	3	29.9	Close match not required.
$\frac{u_L}{u_G}$	3.6	6.7	0.5	Heat/mass transfer characteristics prioritized in HA134a testing.
$\frac{\dot{m}_L u_L}{\dot{m}_G u_G}$	2.5	2.9	0.9	Good match in spite of lower priority given to this parameter.
Sk_{d50}	0.03	0.01	2.2	Stokes numbers approaching zero for entire distribution (fluid-following).
Sk_{d90}	0.05	0.02	1.9	
Bo	150	68	2.2	Slag properties highly variable. Mis-match deemed conservative.
Ca^*	197	10	20.3	Velocity scale unknown – assumed to be ($\propto \sqrt{gb}$).
Jm_1	2.17	0.60	3.6	Limited in cold-flow by operating temperatures
Ja_2	-0.34	0.31	-1.1	HA134a superheated. Cooling required to prevent flashing (approx. 5°C).
$\frac{t_e}{D/u_L}$	2.49	2.92	0.9	Non-dimensional evaporation time prioritized.
ρ_v/ρ_L	14.1×10^{-3}	4.4×10^{-3}	3.2	Greater expansion of HA134a deemed conservative (more pronounced effect on flow field).
Pr_L	4.258	3.530	1.2	Not considered important in dispersed phase.
Pr_G	0.572	0.825	0.7	Not considered a critical parameter.
$\frac{u^2}{c_P T}$	~0	~0	N/A	Kinetic energy negligible compared with thermal energy

2.2 EXPERIMENTAL APPARATUS

A schematic and picture of the cold flow quench zone model are shown in Figure 4. The apparatus was constructed at a 1:1 scale relative to the 18 TPD pilot plant gasifier, providing a high degree of geometric similitude. The model was built, commissioned and initially tested in late 2013 under an AR-funded project. The gasifier section, outlet cone and the upper section of the quench vessel were fabricated from formed clear acrylic sheets, permitting optical access for instrumentation and video recording equipment.

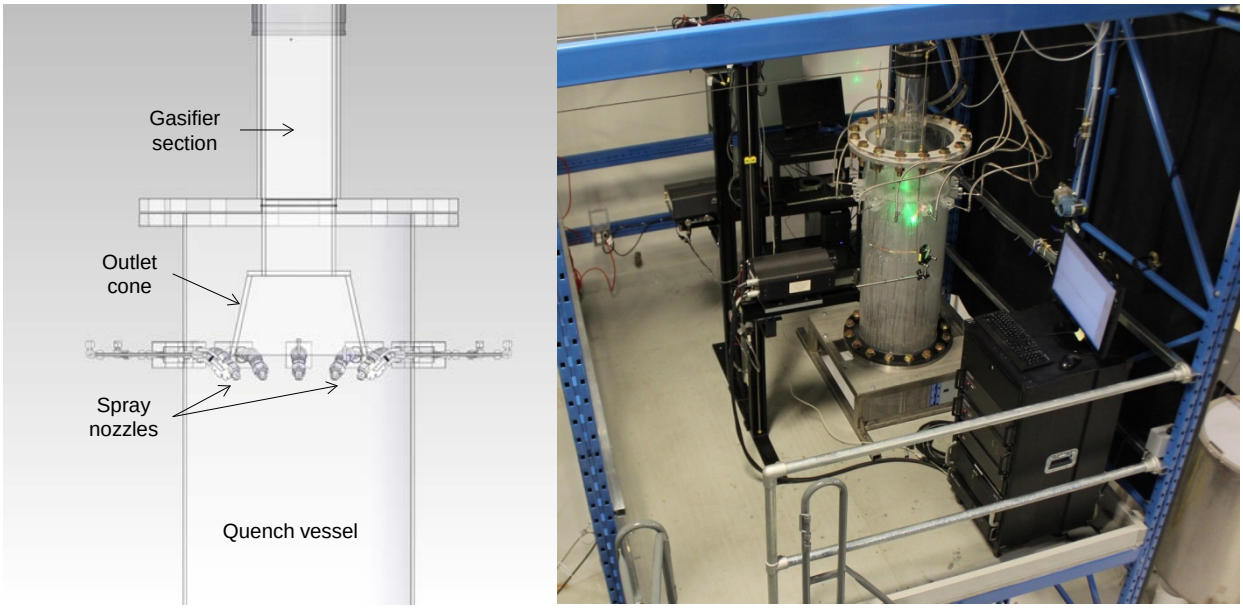

Figure 4: Schematic and picture of the cold flow quench zone model, configured to match pilot plant scale outlet design.

Process flow is shown schematically in Figure 5. Air discharged from the blower (E-10) is optionally fed through an air dryer (E-11) and pre-heater (E-12) before entering the reactor through a PVC tee (not shown). Due to height restrictions on the apparatus, the tee is used to reduce the flow development length upstream of the reactor and help deliver a more uniform inlet flow than would exist if an elbow were used. For demonstration-scale gasifier model testing, a perforated-plate flow distributor was installed downstream of the transition to the larger-diameter gasifier tube, thus ensuring a fully-developed flow condition well upstream of the tube-liner exit.

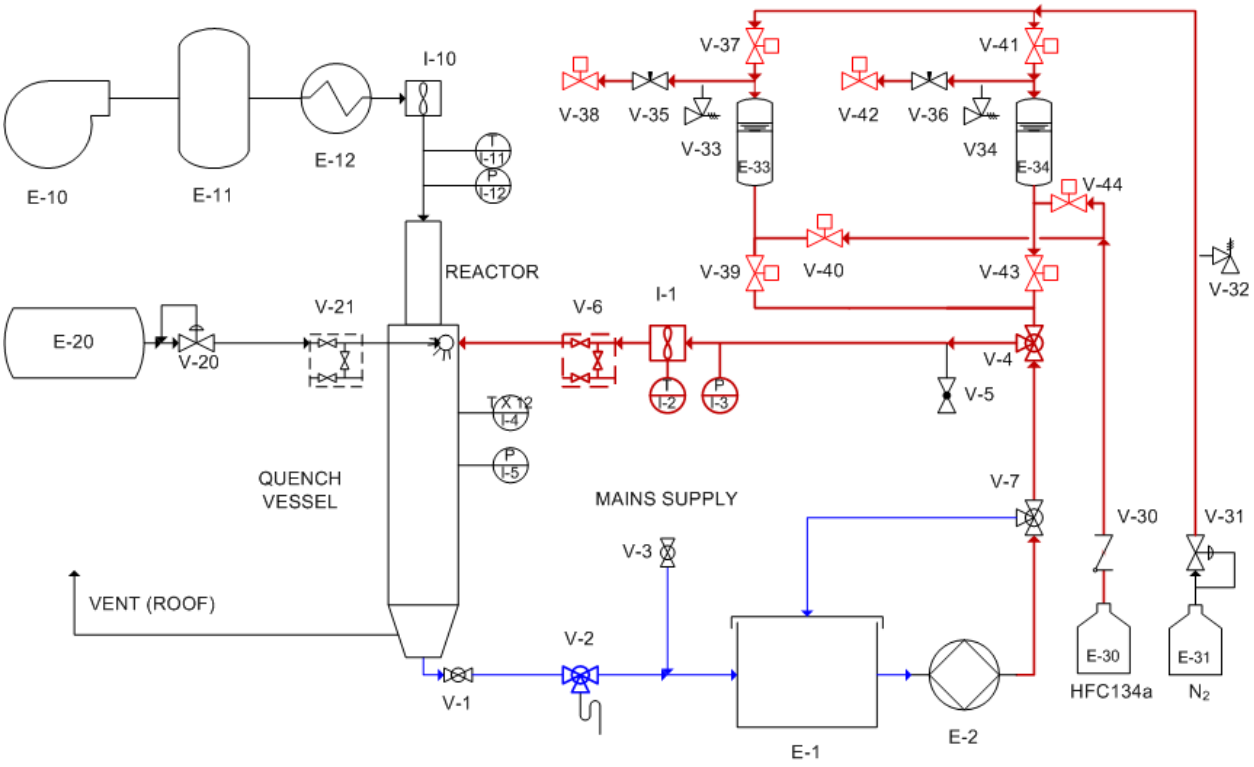

Figure 5: Process schematic for the overall quench zone simulation system.

Upon exiting the reactor section (representing the gasifier liner), the air flow encounters the quench spray, which, depending on the configuration, may be water or HA134a.

The air, quench liquid, and (when applicable) quench vapor flow downwards through the quench vessel, subsequently entering a simple air-liquid separator. Liquid is drained out the bottom of the separator, which may either be returned to the reservoir (E-1) or simply discarded through a floor-drain. The air, along with any evaporated quench liquid or entrained droplets, is vented to atmosphere through the roof of the laboratory building.

The apparatus is designed such that different reactor sections can be substituted into the model relatively easily. Specifically, the apparatus allowed change-out of gasifier outlet types (cylindrical vs. conical for the pilot scale tests, long vs. short cone for demonstration scale tests), spray nozzle angle relative to the outlet, and distance between gasifier outlet and spray nozzle plane.

Nozzles are mounted in twelve acrylic blocks equally spaced circumferentially around the upper part of the quench vessel. The nozzle position can be adjusted relative to the quench vessel centerline to replicate the actual pilot plant geometries. Each nozzle is mounted on a swivel joint providing ±22.5° angular movement. The swivel joint is attached to a 45° elbow, so that the nozzle orientation relative to the plane of the gasifier outlet can be varied from 22.5° to 67.5°.

A series of nozzles was characterized in water-spray using phase-Doppler interferometry, to determine the combination of nozzle type and manifold pressure that would provide the best similarity with respect to flow kinematics and Stokes number. It is noted that a similar nozzle characterization was not practical in an evaporating flow. Although this was primarily due to

cost considerations and long delivery times for obtaining sufficient HA134a for such testing, such testing was also deemed to be of limited value due to technical challenges in obtaining these measurements.

The model liquid circuit contains two inlet branches, selectable with a 3-way valve (V-4), depending on the fluid used. In tests using water as the quench liquid, water is supplied continuously to the valve manifolds (V-6) from a reservoir (E-1) by a 3-stage piston pump (E-2). The pump is generally operated near maximum speed, which minimizes pressure pulsations in the liquid circuit, and also prevents the motor coils from overheating. Primary adjustment to the manifold pressure is performed by manually adjusting a bypass valve (V-7). Fine adjustments are then achieved by manually adjusting the motor speed, or by engaging automatic control using the liquid pressure (I-3) or flow rate (I-1) as a feedback signal to the motor variable-frequency drive. The flow loop is also configured to function using an air-atomizing nozzle. In this case, air from a receiver (E-20) is regulated to the desired pressure with a regulating valve (V-20), and distributed to the nozzles through an air manifold (V-21). Liquid recovered in the separator can be either returned to the reservoir (E-1) or disposed of through a floor drain.

For testing using 1,1,1,2-tetrafluoroethane (HA134a), tests must be run in batches by providing quench liquid from one of two pressurized ½-gallon sample bottles (E-33 and E-34). Prior to a test, one or both sample bottles is filled by siphoning liquid HA134a from a supply bottle (E-30). The vapor pressure of HA134a at ambient temperature is not sufficient to drive the required flow, nor to sufficiently atomize droplets in the quench zone. The sample bottle is therefore pressurized prior to and during the test, using compressed dry nitrogen gas (E-31) supplied through a pressure regulator (V-31). Operation of the HA134a system, including liquid injection, filling, vapor and air bleed, and purging, is accomplished by a system of computer-controlled solenoid valves (V-34 – V-37), the nitrogen pressure-regulator (V-31), and bleed valves (V-35 and V-36). To prevent overpressure and/or back-flow, pressure relief valves (V-32 – V-34) and a check-valve (V-30) are provided. Two parallel identical HA134a circuits are used to permit quasi-continuous operation by filling one bottle while the other is being discharged.

2.3 INSTRUMENTATION AND MEASUREMENTS

Flow visualization: Flow visualization was the primary means of evaluating flow patterns in the quench zone. A Phantom v7.3 high speed digital camera was used in this test program, providing 800 x 600 maximum resolution and a maximum speed of 6888 frames-per-second. The quench zone was illuminated with a 10W laser sheet. High speed video, combined with seeded flow, also provided a basis to perform Particle Image Velocimetry (PIV) to ascertain localized velocity and trajectory.

Phase-Doppler Velocimetry: Localized measurements of liquid droplet velocity field and droplet size were obtained using an Artium Inc. PDI200 MD phase-Doppler interferometer (PDI). PDI is a non-intrusive laser-based measurement technique, based on laser-Doppler anemometry, in which the diameter, velocity and volume flux of individual droplets are measured simultaneously. The instrument consists of separate transmitter and receiver units, positioned such that they focus at the same point. A laser beam from the transmitter unit is split into two beams of equal intensity. The two beams are focused using a transmitter lens and made to intersect at a shallow angle, forming the measurement volume. Light scattered by objects passing through the measurement volume is collected by a receiver lens and focused onto a

photodetector. The component of the object's velocity in the plane of the two laser beams and perpendicular to their axis can be determined from the frequency shift of scattered light intensity (Doppler effect). The object's size can be determined from the phase-shift between signals received at photodetectors separated by a known distance (most systems use three photodetectors – two pairs – to provide adequate range and resolution). By focusing two pairs of different colored beams on the same point, but oriented in different planes (see Figure 5), the velocity can be resolved in the two dimensions perpendicular to the common beam axis. For practical reasons, measurement of the droplet size is based only on the pair of beams having the shorter wavelength. The PDI transmitter and receiver units are mounted on traverses that can be traversed in two dimensions in the quench zone, in a grid measuring approximately 12 in. x 48 in.

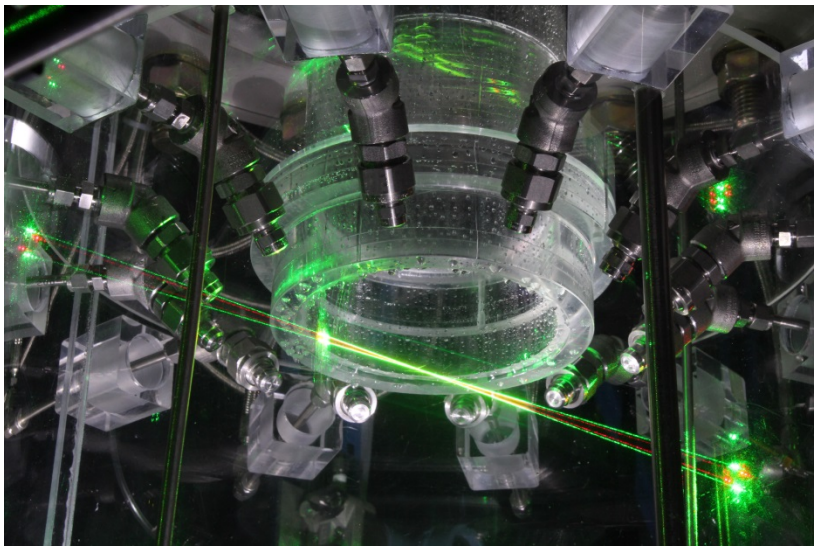

Figure 5: PDI beams traversing the outlet of the pilot plant gasifier model configured with cylindrical outlet. In the set-up shown, the green lasers are measuring the droplet size and vertical component of velocity. The red lasers (less visible) measure the horizontal velocity perpendicular to the common beam axis.

3.0 RESULTS AND DISCUSSIONS

3.1 PILOT SCALE TESTING

3.1.1 Test matrix

The test matrix for pilot plant gasifier configurations of the quench zone model is listed in Table 7. The following impacts were evaluated:

(1) Impact of nozzle angle on flow patterns (Test 3001 vs. Test 3002)

(2) Axial location of nozzles relative to outlet (Test 3004 vs. Test 3002 for cylindrical outlet, and Test 3006/3012 vs. Test 3005 for cone). This is the difference between H2 and H3 shown in Figure 2.

(3) Outlet geometry (Test 3002 for original cylindrical design vs. Test 3005 for cone without slag simulant, and Test 3003 vs. Test 3011 with slag simulant)

(4) Impact of Reynolds number on flow behavior in outlet cone (Tests 3006 through 3010).

(5) Impact of evaporating quench liquid (HA134a) on quench zone flow patterns (Tests 3014 through 3016).

Table 7: Test matrix for quench zone testing of pilot plant scale outlet configurations.

Test #	Outlet	Axial Location	Nozzle Spray Angle	Air Flow (CFM)	Quench Spray Fluid	Quench Spray Flow	Slag Simulant ?	Test Objectives
3001	Straight	Baseline	Baseline + 50%	Baseline	Water	Baseline		Assess impact of spray nozzle angle on quench zone flow patterns.
3002	Straight	Baseline	Baseline	Baseline	Water	Baseline		Baseline case for original pilot plant gasifier with cylindrical outlet.
3003	Straight	Baseline	Baseline	Baseline	Water	Baseline	Yes	Characterize slag interaction with quench spray in baseline case for original pilot plant gasifier with cylindrical outlet.
3004	Straight	Baseline + 2"	Baseline	Baseline	Water	Baseline		Assess impact of increased separation between gasifier outlet and spray nozzles.
3005	Cone	Baseline	Baseline	Baseline	Water	Baseline		Baseline case for modified pilot plant gasifier with conical outlet.
3006	Cone	2 x Baseline	Baseline	Baseline	Water	Baseline		Assess impact of increased separation between gasifier outlet and spray nozzles.
3007	Cone	2 x Baseline	Baseline	0.3 x Baseline	Water	Baseline		Assess impact of reduced syngas flow on flow fields within gasifier outlet cone. 30% of baseline flow.
3008	Cone	2 x Baseline	Baseline	0.7 x Baseline	Water	Baseline		Assess impact of reduced syngas flow on flow fields within gasifier outlet cone. 30% of baseline flow.
3009	Cone	2 x Baseline	Baseline	2 x Baseline	Water	Baseline		Assess impact of inacreased syngas flow on flow fields within gasifier outlet cone. 200% of baseline flow.
3010	Cone	2 x Baseline	Baseline	3 x Baseline	Water	Baseline		Assess impact of inacreased syngas flow on flow fields within gasifier outlet cone. 300% of baseline flow.
3011	Cone	Baseline	Baseline	Baseline	Water	Baseline	Yes	Characterize slag interaction with quench spray in baseline case for original pilot plant gasifier with conical outlet.
3012	Cone	2 x Baseline	Baseline	Baseline	Water	Baseline		Repeat of Test 3006 to get improved image quality.
3014	Cone	Baseline	Baseline	Baseline	HA134a	Baseline		Baseline configuration with conical outlet using evaporating flow (HA134a)
3015	Cone	Baseline	Baseline	Baseline	HA134a	Baseline		Assess impact of evaporating flow on flow fields in the quench zone area, using the baseline conical outlet.
3016	Cone	Baseline	Baseline	Baseline	HA134a	Baseline	Yes	Assess impact of evaporating flow on slag behavior in the quench zone area, using the baseline conical outlet.

3.1.2 Flow visualization

The influence of nozzle angle on flow patterns was evaluated in Tests 3001 and 3002, with screen capture images shown in Figure 6, below. The large nozzle angle (nozzle positioned in a more downstream orientation) test video differed from the baseline configuration (Test 3002) in the following ways:

(1) Notable decrease in water recirculating onto the back of the cylindrical outlet, with fewer water drops falling off the lip of the gasifier outlet.

(2) Significant shortening of the recirculation zone behind the nozzles, with earlier flow reattachment to the quench vessel walls.

(3) Eliminated incidence of large water droplets impacting on the quench vessel walls. The 45° angle nozzles were much more likely to propel droplets coming off of the gasifier outlet across the quench vessel and impact the wall.

(4) The rate of small droplets impacting the opposite quench vessel wall was greatly diminished.

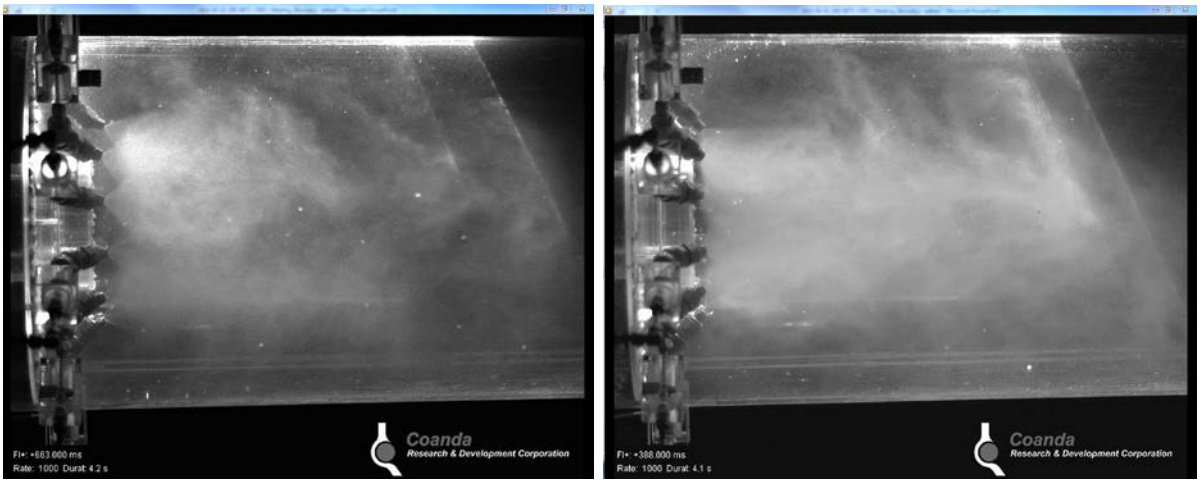

Figure 6: Screen capture of video from Test 3001 (left) with spray nozzles at a 67.5° angle relative to the horizontal plane at the gasifier outlet and Test 3002 (right) at a 45° angle.

The influence of nozzle axial position relative to gasifier outlet on flow patterns was evaluated in Tests 3004 and 3002 for the cylindrical outlet, with screen capture images shown in Figure 7, below. Increasing the distance between the outlet and nozzles impacted flow in the following ways:

(1) Notable decrease in water recirculating onto the back of the cylindrical outlet, with fewer water drops falling off the lip of the gasifier outlet.

(2) No apparent change in the rate of small droplets impacting the opposite quench vessel wall.

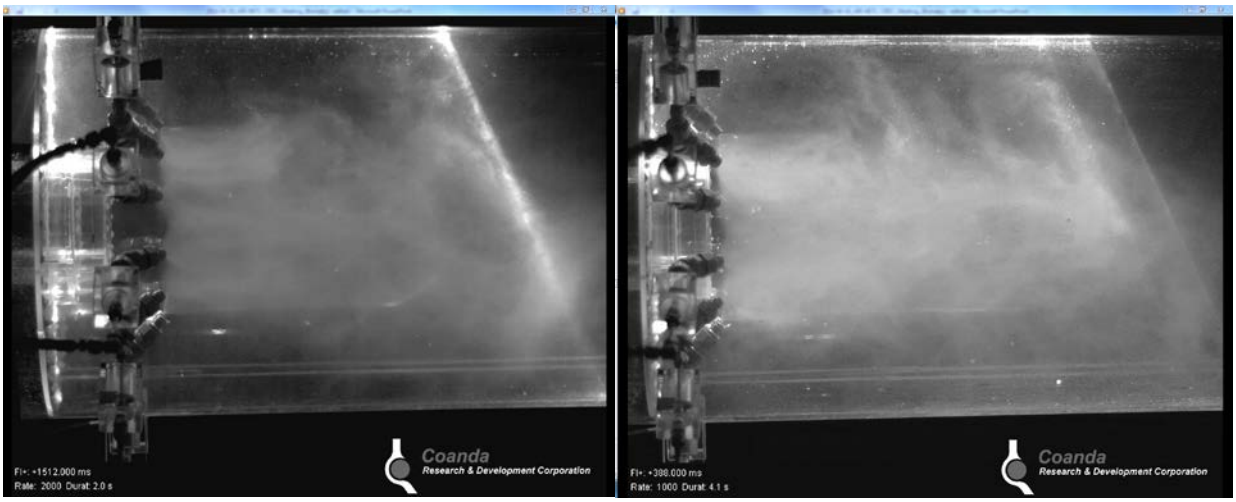

Figure 7: Screen capture of video from Test 3004 (left) with spray nozzles 2" farther from the outlet compared to baseline configuration in Test 3002 (right).

The influence of nozzle axial position relative to gasifier outlet on flow patterns was evaluated in Tests 3012 and 3005 for the conical outlet, with screen capture images shown in Figure 8, below. Increasing the distance between the outlet and nozzles impacted flow in the following ways:

(1) Some decrease in water recirculating onto the back of the conical outlet, with fewer water drops falling off the lip of the gasifier outlet.

(2) No incidence of large water droplets impacting on the quench vessel walls in either case.

(3) No apparent change in the rate of small droplets impacting the opposite quench vessel wall.

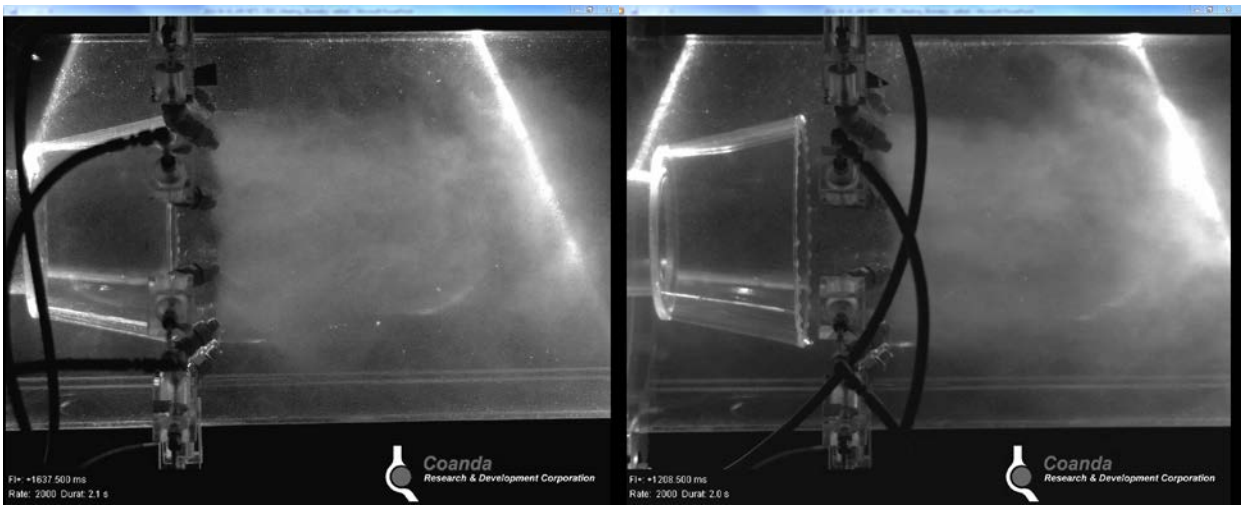

Figure 8: Screen capture of video from Test 3005 (left) with spray nozzles 2" farther from the outlet compared to baseline cone outlet configuration in Test 3012 (right).

The influence of outlet geometry on flow patterns was evaluated in Tests 3002 for a cylindrical outlet and 3005 for the conical outlet, with screen capture images shown in Figure 9, below. It is noted that because of the different diameter of the gasifier outlet between these two geometries there is a corresponding change in the nozzle tip location to maintain similar radial position relative to the outlet. Changing the outlet geometry from the original cylindrical design to the modified conical design had the following impacts:

(1) Large decrease in water recirculating onto the back of the conical outlet, with fewer water drops falling off the lip of the gasifier outlet.

(2) Large decrease in rate of large water droplets impacting on the quench vessel walls. This is possibly due to a lower density spray field caused by the increased nozzle tip diameter.

(3) No apparent change in the rate of small droplets impacting the opposite quench vessel wall.

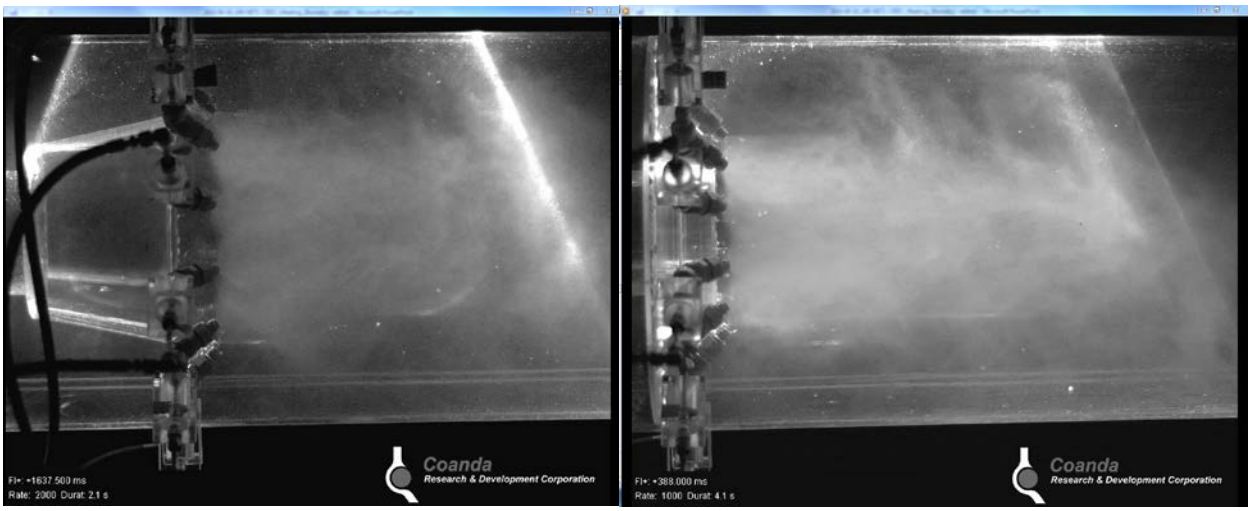

Figure 9: Screen capture of video from Test 3005 (left) with cone outlet in baseline configuration compared to baseline cylindrical outlet configuration in Test 3002 (right).

The most pronounced difference among outlet configurations was observed with the introduction of slag simulant in Tests 3003 for a cylindrical outlet and 3011 for the conical outlet, with screen capture images shown in Figure 10 for the original cylindrical design and Figure 11 for the concial design, below. Changing the outlet geometry from the original cylindrical design to the modified conical design had the following impacts on slag behavior at the outlet:

(1) The original cylindrical outlet showed significant interaction between the quench liquid emanating from the nozzles and the slag before it could disengage from the gasifier outlet. The slag would often be displaced towards the axis of the outlet,

which would account for the frequent observation of slag blockages at the outlet of the original design.

(2) Shearing of the slag streams due to interaction with nozzle jets, along with natural instabilities of vertical liquid columns, lead to formation of irregular droplet geometries, referred to colloquially as “barbells”, “fishhooks”, and “teardrops”. These were very similar to actual slag droplets recovered from pilot plant testing with the original outlet (see bottom of Figure 10). Presumably, the slag froze into these shapes shortly after being distorted by the impinging jets.

(3) The conical outlet provides a drip lip that is isolated from the nozzles, allowing the slag stream to break up prior to exiting the outlet and producing small, well-formed droplets. There was very little apparent interaction between the nozzle jets and falling slag droplets. Again, this is largely consistent with experimental observations from testing of the conical outlet, where most of the coarse slag droplets are spherical in nature.

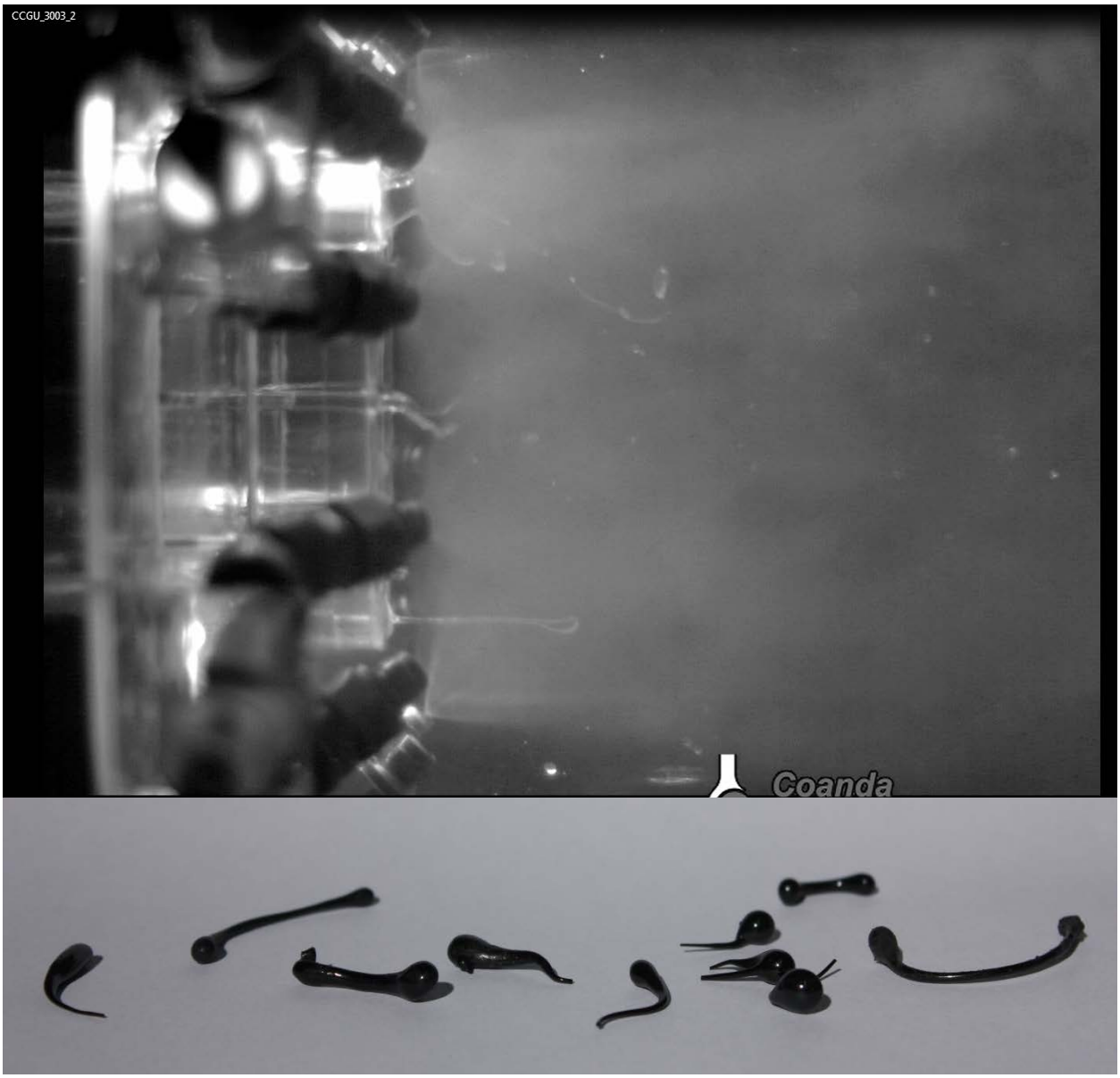

Figure 10: Testing with the original cylindrical outlet design, showing interaction between quench liquid emanating from jets and simulated slag (upper picture). Actual slag droplets corresponding to shapes seen in the simulated testing are shown in the lower picture.

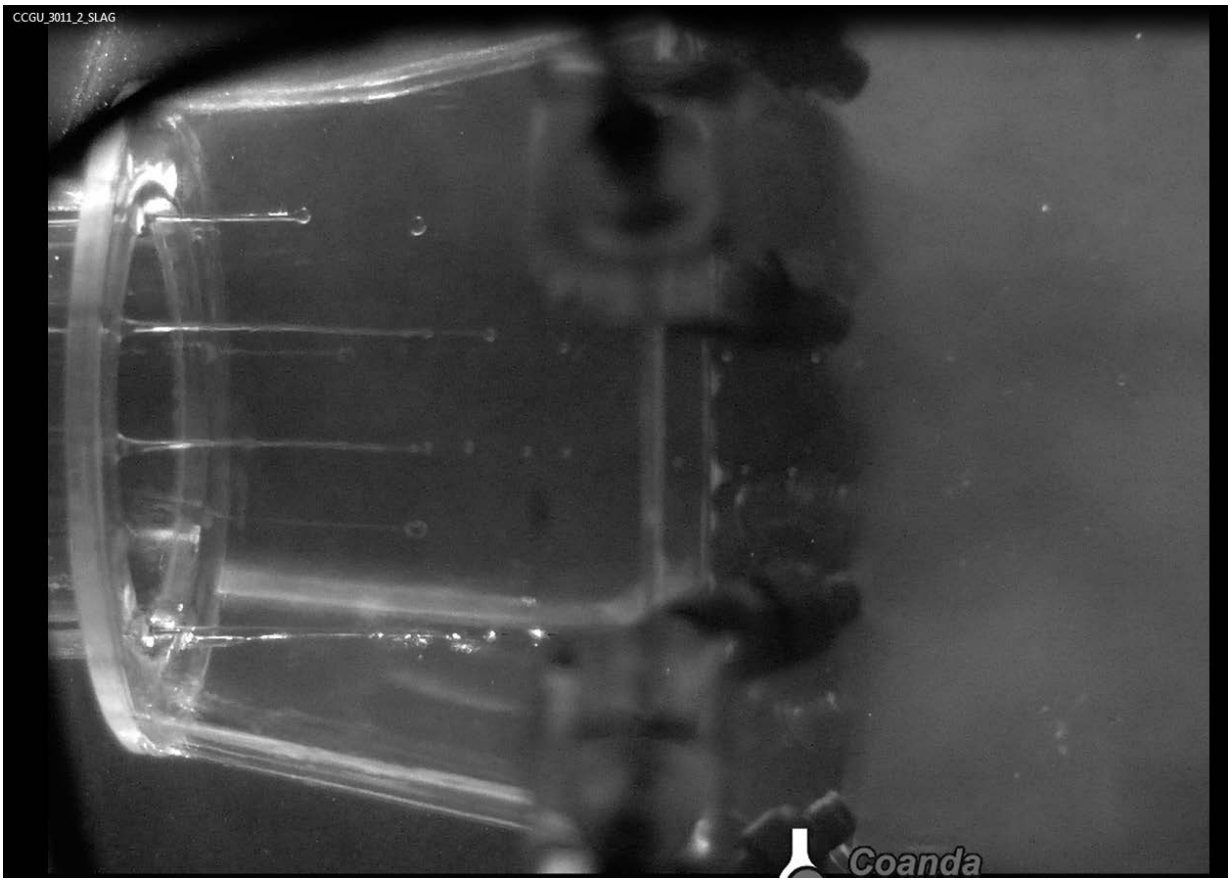

Figure 11: Testing with the modified concical outlet design, showing slag disengagement and formation of spherical drops prior to exiting the gasifier outlet.

There was also interest in characterizing the impact of Reynolds number on flow patterns within the cone, to assess whether or not hot syngas with molten fine slag droplets might tend to circulate out to the surface of the cone and deposit slag on the cooled surfaces. This would eventually lead to slag build-up in the cone, potentially leading to blockage. This was evaluated at Reynolds numbers ranging from 30% to 300% of the baseline value, in order to capture the full range of potential design space. Best visibility was obtained at lowest Reynolds numbers, as these had the highest density of water mist seeding. Visual assessment of results from Test 3006 through 3010 showed similar flow characteristics for all, with no apparent patterns of direct impingement of gas flow onto the outlet surface. The general behavior appears similar for all of these cases: the mixing zone of the gas jet expands in a way that is consistent with expectations based on numerous investigations of round turbulent jets penetrating a fluid at rest (e.g. List, EJ, 1982. *Turbulent Jets and Plumes*, Ann. Rev. Fluid Mech., vol. 14 189-212.). The jet diffusion angle appears approximately parallel to the conical outlet wall in Figure 12. The turbulent mixing zone between the jet core and the recirculating flow is populated by a series of vortex structures which are also characteristic of free jets.

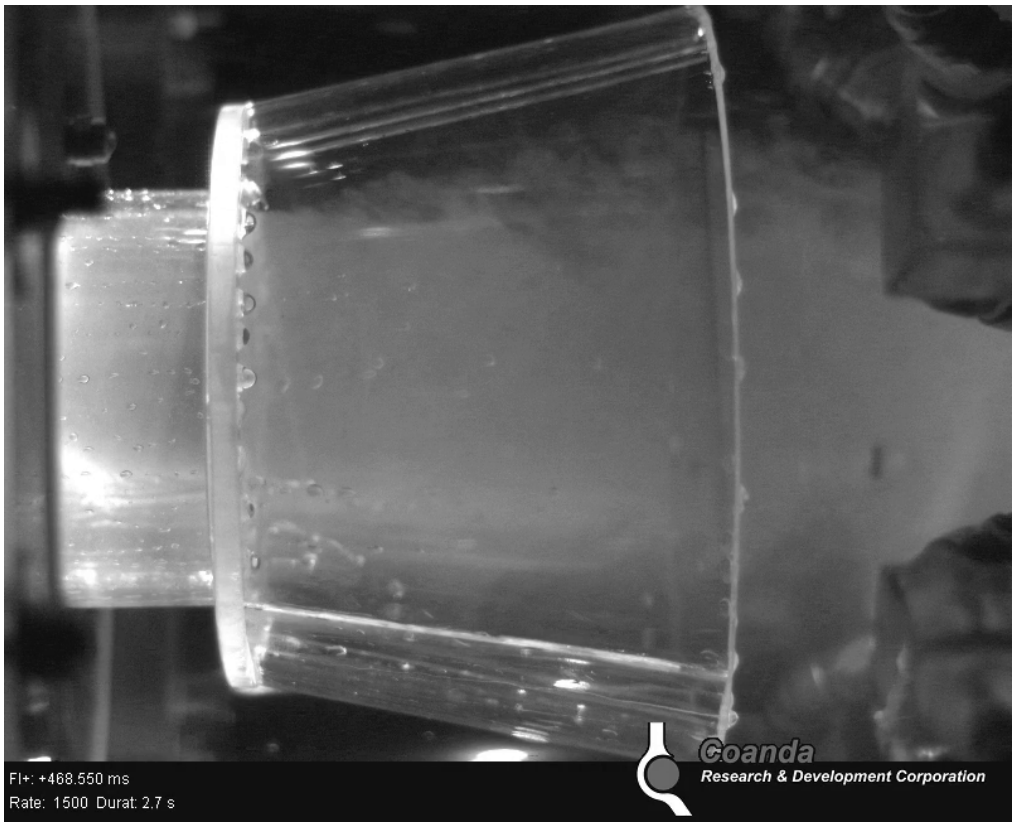

Figure 12: Screen capture of seeded flow behavior in conical outlet at 30% of normal gas flow condition. .

Achieving similitude for vaporizing flow is challenging in several ways. The actual gasifier quench zone environment has a ~2000 F drop in gas temperature as the loss of sensible heat from the gas causes vaporization of the quench water. There are significant gradients in temperature and gas density throughout the quench zone, in particular right at the gasifier outlet. The challenge is reflected in the Jakob numbers in Table 2, where a mismatch in Jm_1 of 4.8 reflects the deficit in sensible heat available to vaporize the quench liquid. The ratio of vaporization time to droplet flight time of 1.9 is closer, but still indicates that the model will be much less likely to offer full vaporization than the actual pilot plant gasifier environment, leading the model to err on the side of understating the full impact of evaporating quench liquid on quench zone flow patterns.

The diminished capacity to cause evaporation notwithstanding, the image from Test 3015 for non-seeded flow with HA134a quench liquid shows a pronounced decrease in the amount of liquid circulating around the quench zone outside of the immediate vicinity of the nozzle jets, as compared to Test 3005 with the same geometry and with water as the quench liquid. This is shown in Figure 13, where it is clear that the nozzle jets with liquid HA134a are narrower and penetrate less deeply into the quench vessel.

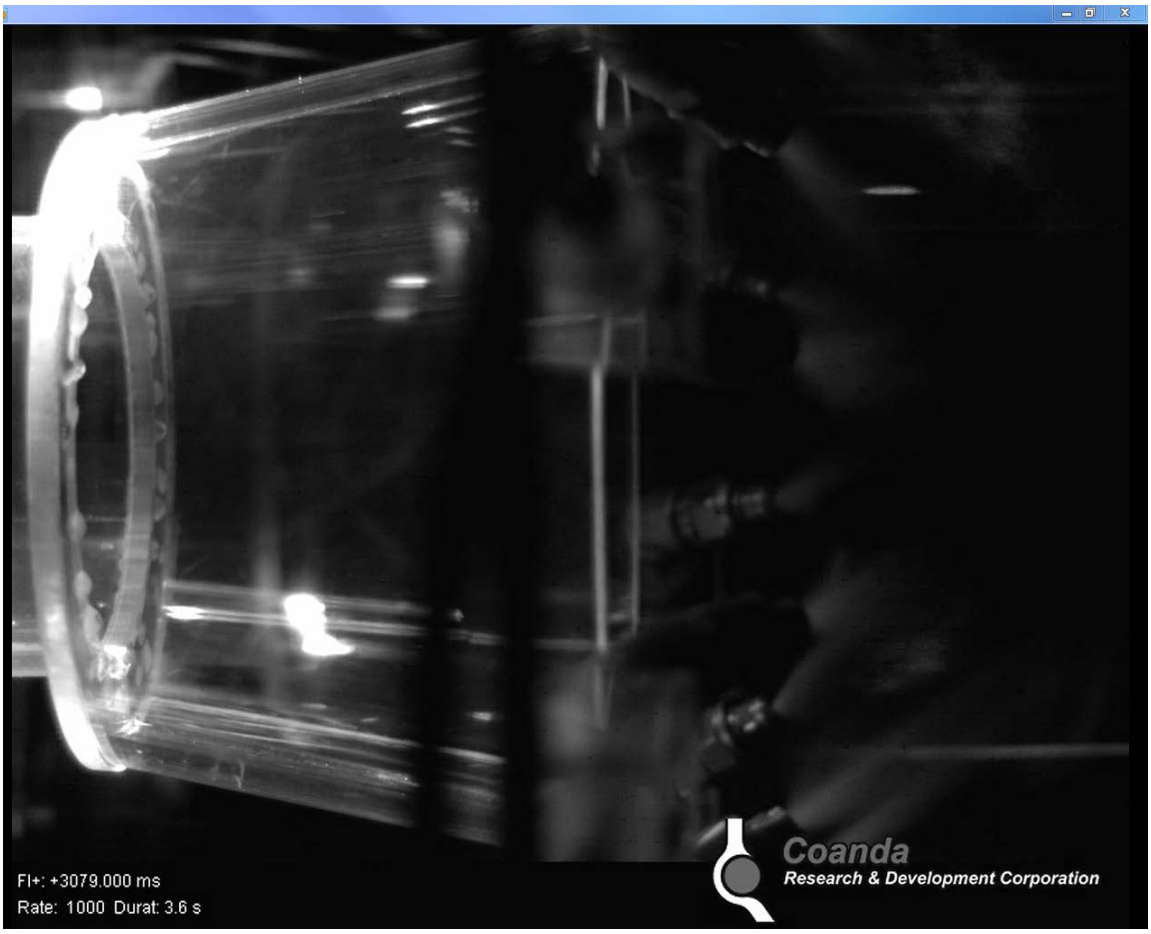

Figure 13: Testing with HA134a as quench liquid in Test 3015, using the same geometry and hydrodynamic parameters as Test 3005 using water as the quench liquid .

Addition of water vapor to the gas jet results in seeded flow. The water vapor condenses/freezes on contact with the HA134a stream, creating a visible fog that is roughly analogous to the quenched syngas, with the frozen water particles that cause the opacity of the fog corresponding to frozen fine slag particles entrained in the quenched syngas. Video for seeded flow from Test 3015, shown in Figure 14, illustrates how quenched syngas recirculates back into the outlet area along the inner surface of the cone, penetrating all the way back to the drip lip. This raises questions regarding impact of recirculation flow on the thermal environment within the cone. What is the liquid water hold-up in the gas recirculating back into the cone, what is the velocity of the recirculating flow, and how big are the water droplets? Also, how much total gas is recirculating into the cone, and is it sufficient to cool the liner drip lip such that slag accumulation could occur? These questions will be discussed further in Section 3.1.3 using PDI measurements from Test 3006 as the basis for quantifying impacts.

Test 3016 assessed the impact of evaporating flow on slag discharge. Testing showed no change in slag flow characteristics with HA134a as the quench liquid (see Figure 15), exhibiting characteristics identical to that seen in Test 3011.

Figure 14: Testing with HA134a as quench liquid in Test 3015, using gas seeded with water vapor to highlight flow patterns of cooled gas. The water vapor condenses/freezes upon contact with HA134a, creating a cloudy gas roughly analogous to quenched syngas.

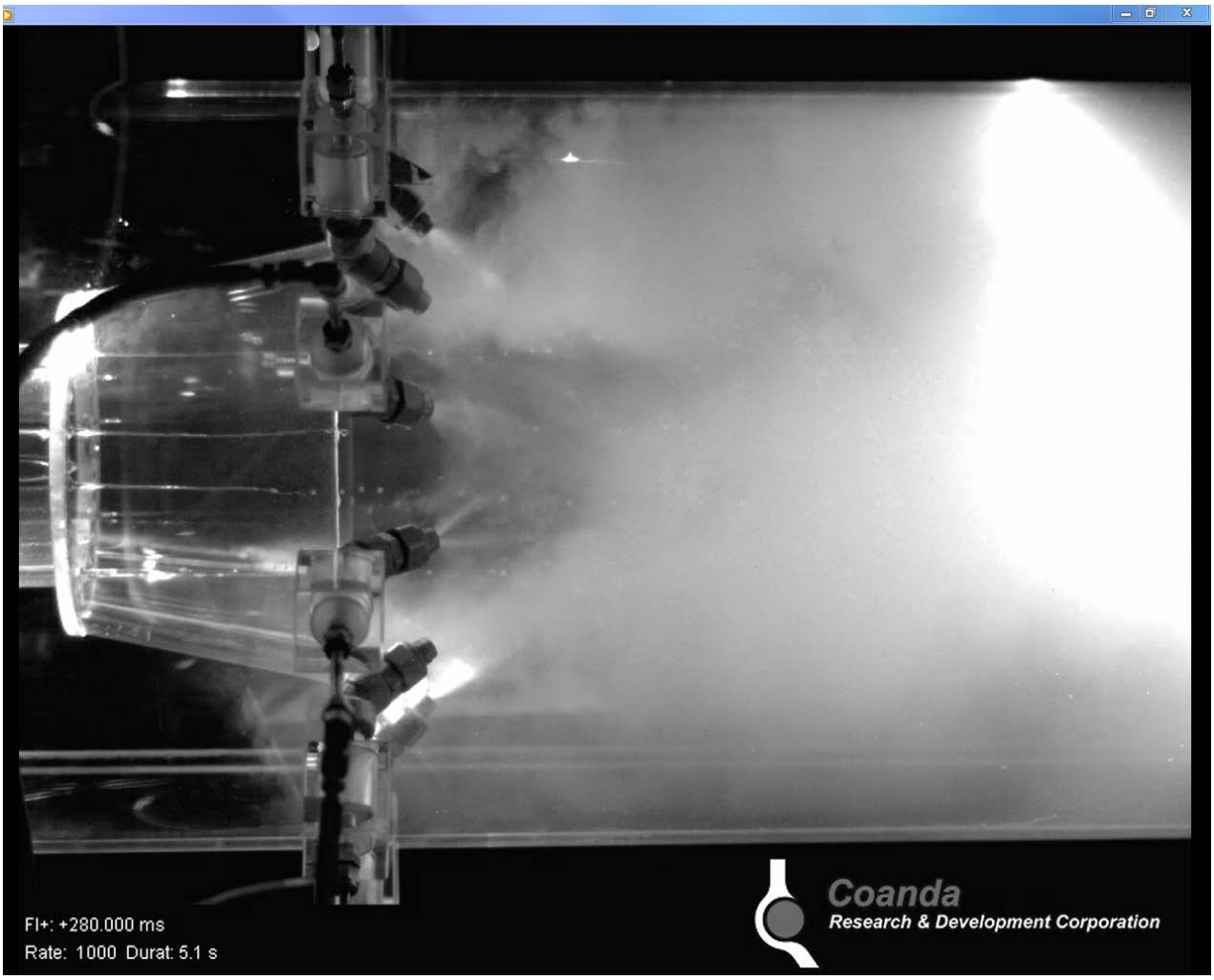

Figure 15: Testing with HA134a as quench liquid in Test 3016, with simulated slag flow.

3.1.3 Evaluation of Pilot Scale Test Results

Pilot scale test results are evaluated in the context of the following questions:

(1) Do results indicate satisfactory similitude between the cold flow model and actual pilot plant test observations?

(2) Is the experimental methodology adequate for obtaining relevant data for the scaled demonstration gasifier outlet design?

(3) Do the experimental results support feasibility of the conical outlet architecture?

(4) What experimental effort is recommended for the scaled demonstration gasifier outlet design?

Similitude:

From an analytical perspective, a high degree of geometric, kinematic and dynamic similitude was achieved, at least on a hydrodynamic basis. From a thermodynamic basis, similitude was less than ideal, even with the evaporating flow cases, due to the significant difference in sensible heat available from the model gas compared to the actual syngas. However, the bias in the similitude approach is conservative in the sense that the flow is less vaporized in the model than in the actual gasifier, so that the model will tend to overstate the effect of droplet penetration and recirculation, which is of greatest concern for reliable gasifier outlet operation. While the approach used here understates the impact of evaporating quench liquid on flow patterns, there was no indication that evaporating flow causes additional challenges to actual gasifier operations. On that basis, it is anticipated that full similitude of thermodynamic parameters would not reveal any substantial additional insights into quench zone behavior.

From the perspective of comparability of model observations to test results, we are limited by the ability to observe the internals of the pilot plant gasifier. However, the stark contrast between slag/nozzle jet interactions for the model using the original cylindrical outlet design and the modified conical outlet design aligns exceptionally well with test results.

The model showed extensive slag/nozzle jet interaction prior to slag disengagement from the outlet lip, with slag being displaced towards the centerline of the outlet by force of the nozzle jets. This was consistent with observed slag accumulations at the gasifier outlet for this design, observed on multiple test runs. Furthermore, the distortion of slag droplets due to hydrodynamic effects of nozzle jet impingement observed in the model was very similar to the actual shape of coarse slag droplets observed in testing.

For the conical model, observation of slag disengagement before entering the quench zone, formation of spherical slag droplets, and the absence of significant slag/nozzle jet interaction was entirely consistent with the trouble-free long duration operation of the conical outlet and the properties of the coarse slag produced from those tests.

In summary, the pilot scale model demonstrated excellent consistency with observable pilot plant gasifier results, provides excellent hydrodynamic similitude, and offers acceptable thermodynamic similitude. On that basis, it was concluded that the modelling approach was suitable for use in the scaled demonstration outlet test effort.

Experimental Methodology:

High speed videography provided good qualitative assessment of flow patterns within the quench zone. Phase-Doppler interferometry provided good quantitative, localized data on droplet trajectories, hold-up, and diameter. Particle Image Velocimetry was not as useful, as it was a challenge to obtain sufficient seed density at suitable frame rates to get good resolution.

In aggregate, the experimental methodology implemented on the pilot scale model was demonstrated to provide the needed information.

Design Feasibility:

The data support an assessment that the conical outlet architecture provides a feasible design space offering reliable slag discharge from the gasifier. However, flow visualization tests with HA134a indicated some level of quenched gas recirculation into the outlet. PDI results for Test 3006 are shown in Figure 16. Based on a rough estimate of total liquid water intake rate at the

outlet (based on holdup and velocity), droplet vaporization time (based on droplet velocity and a conservative estimate of localized gas temperature), and local thermal environments, any water entering the recirculation zone is predicted to have evaporated long before it can reach the outlet of the gasifier. Therefore, water ingress at the gasifier outlet does not appear to present an operational challenge for the outlet design, at least at the pilot scale.

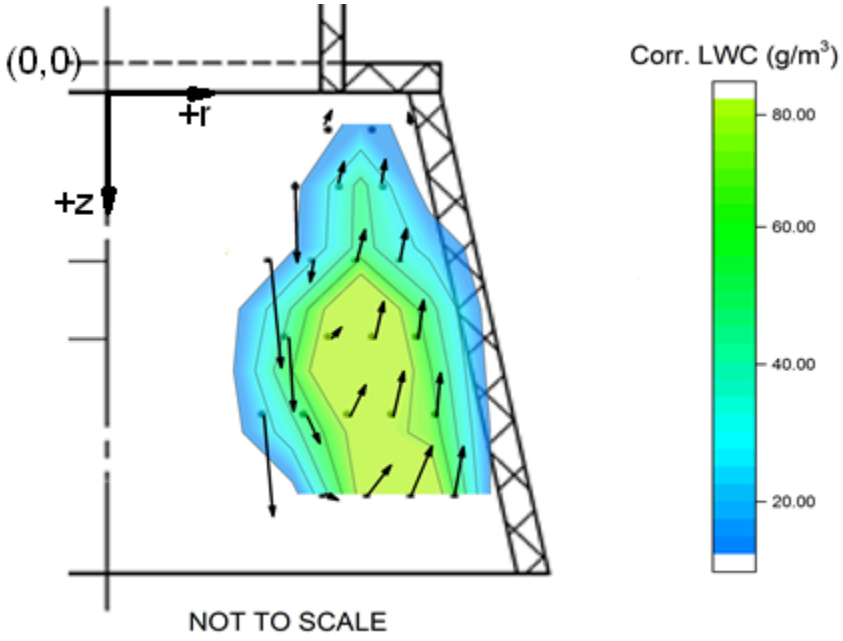

Figure 16: PDI data from Test 3006 showing velocity vectors and water hold-up in the recirculation zone along the inner surface of the outlet cone.

Recommended Scaled Demonstration Gasifier Model Effort:

In consideration of the pilot scale results, the recommended scaled demonstration gasifier model test effort is as follows:

(1) Limit testing to conical outlet architecture.

(2) Focus testing on hydrodynamics, with variation on key parameters:

   a. Cone length

   b. Distance between gasifier outlet and nozzles

   c. Liquid/gas momentum (inertia) ratios

   d. Impact of turndown (decreased flow rates)

(3) Perform PDI analysis for baseline configuration and operating conditions to assess potential ingress of water into outlet cone.

(4) Perform slag simulation to verify continued absence of interference by nozzle jets.

(5) Assess selected conditions with evaporating flow to verify absence of impact.

3.2 DEMONSTRATION SCALE TESTING

3.2.1 Test matrix

The test matrix for demonstration plant gasifier configurations of the quench zone model is listed in Table 8. The following impacts were evaluated:

(1) Axial location of nozzles relative to outlet (Test 3017 vs. Test 3021 at 100% flows, and Test 3019 vs. Test 3023 for 50% flows, and Test 3051 vs. Test 3053 at modified baseline flows, and Test 3052 vs. Test 3054 for modified turndown flows).

(2) Influence on slag flow for axial location of nozzles relative to outlet (Test 3018 vs. Test 3022 at 100% flows, and Test 3020 vs. Test 3024 for 50% flows).

(3) Outlet cone length (Tests 3027 and 3029 for shortened cone vs. Tests 3051 and 3052 for long cones).

(4) Influence on liquid/gas momentum ratio on propensity for recirculation of spray along axis into cone (Tests 3035-3050).

(5) Evaporating flow influences on quench zone hydrodynamics (Test 3025).

(6) PDI evaluation of water droplet hold-up in cone to assess potential cooling effect.

Table 8: Test matrix for quench zone testing of scaled 800 TPD demonstration plant gasifier outlet configurations.

Test #	Reactor height above nozzles	Cone Type	Nozzle Type	Liquid	Seeding?	Gas Flow	Liquid Flow	Slag Sim.	Liquid/Gas Momentrum Ratio
3017	Baseline	Long	Baseline	Water	N/A	Baseline	Baseline		1.25
3018	Baseline	Long	Baseline	Water	N/A	Baseline	Baseline	•	1.25
3019	Baseline	Long	Baseline	Water	N/A	0.5 x Baseline	0.5 x Baseline		1.27
3020	Baseline	Long	Baseline	Water	N/A	0.5 x Baseline	0.5 x Baseline	•	1.27
3021	2 x Baseline	Long	Baseline	Water	N/A	Baseline	Baseline		1.25
3022	2 x Baseline	Long	Baseline	Water	N/A	Baseline	Baseline	•	1.25
3023	2 x Baseline	Long	Baseline	Water	N/A	0.5 x Baseline	0.5 x Baseline		1.20
3024	2 x Baseline	Long	Baseline	Water	N/A	0.5 x Baseline	0.5 x Baseline	•	1.20
3025	Baseline	Long	Baseline	HA134a	With and without	0.6 x Baseline	0.8 x Baseline		2.90
3027	Baseline	Short	Baseline	Water	N/A	0.7 x Baseline	Baseline		2.45
3029	Baseline	Short	Baseline	Water	N/A	0.35 x Baseline	0.5 x Baseline		2.50
3035	Baseline	Long	Baseline	Water	N/A	Baseline	Baseline		1.25
3036	Baseline	Long	Baseline	Water	N/A	0.75 x Baseline	Baseline		2.24
3037	Baseline	Long	Baseline	Water	N/A	0.9 x Baseline	Baseline		1.35
3038	Baseline	Long	Baseline	Water	N/A	1.2 x Baseline	Baseline		0.84
3039	Baseline	Long	Baseline	Water	N/A	0.8 x Baseline	1.1 x Baseline		2.00
3040	Baseline	Long	Baseline	Water	N/A	1.1 x Baseline	1.1 x Baseline		1.19
3041	Baseline	Long	Baseline	Water	N/A	1.3 x Baseline	1.1 x Baseline		0.92
3042	Baseline	Long	Baseline	Water	N/A	0.6 x Baseline	0.8 x Baseline		2.18
3043	Baseline	Long	Baseline	Water	N/A	0.7 x Baseline	0.8 x Baseline		1.52
3044	Baseline	Long	Baseline	Water	N/A	Baseline	0.8 x Baseline		0.85
3045	Baseline	Long	Baseline	Water	N/A	0.55 x Baseline	0.6 x Baseline		1.65
3046	Baseline	Long	Baseline	Water	N/A	0.6 x Baseline	0.6 x Baseline		1.12
3047	Baseline	Long	Baseline	Water	N/A	0.7 x Baseline	0.6 x Baseline		0.85
3048	Baseline	Long	Baseline	Water	N/A	0.35 x Baseline	0.4 x Baseline		1.40
3049	Baseline	Long	Baseline	Water	N/A	0.4 x Baseline	0.4 x Baseline		1.09
3050	Baseline	Long	Baseline	Water	N/A	0.5 x Baseline	0.4 x Baseline		0.80
3051	Baseline	Long	Baseline	Water	N/A	0.7 x Baseline	Baseline		2.45
3052	Baseline	Long	Baseline	Water	N/A	0.35 x Baseline	0.5 x Baseline		2.25
3053	2 x Baseline	Long	Baseline	Water	N/A	0.7 x Baseline	Baseline		2.45
3054	2 x Baseline	Long	Baseline	Water	N/A	0.35 x Baseline	0.5 x Baseline		2.25

3.2.2 Flow visualization

The influence of distance between outlet and nozzles was assessed for overall flow patterns, propensity for backflow into the outlet cone, and influence on slag flow from the outlet. The general observations from these tests were as follows:

(1) Some backflow of quench spray into the center of the cone outlet, along the axis, was observed. This had not been seen in pilot scale testing.

(2) Outlet-nozzle distance had no significant impact on flow patterns. The additional distance did lead to a slight decrease in the amount of spray recirculating into the cone outlet, as would be expected.

(3) Turndown (to 50% from 100%) at constant momentum ratio had no apparent impact on flow patterns or the tendency for spray to recirculate into the outlet.

(4) As with pilot scale testing, there was no influence of the quench zone parameters on simulated slag (glycerine) behavior for this cone outlet.

Cone depth was also evaluated. Test 3027 with a shorter cone (Figure 17) showed a significantly decreased propensity for quench spray intrusion into the cone outlet, both in magnitude and frequency, relative to the longer cone testing in Test 3051 (Figure 18) at the same conditions. A possible explanation for this is the reduced extent of spreading of the turbulent mixing layer with the shorter cone prior to contacting the quench zone, which would give a somewhat greater momentum flux for the gas at the outlet, tending to suppress spray intrusion. However, spray intrusion still occurs with the shorter cone, and the droplets that do make it into the quench zone are in much closer proximity to the drip lip for the shorter cone.

Figure 17: View of recirculation into short outlet cone from Test 3027.

Figure 18: View of recirculation into baseline (long) outlet cone from Test 3051.

The observation of recirculation of quench spray back up the axis and into the cone outlet triggered an interest in better understanding the underlying causes. To that effect, a series of tests varying liquid/gas momentum ratio over a range of flow rates (Tests 3035-3050) was run. A typical overall flow pattern is depicted in Figure 19. While most of the quench spray continues downward, some fraction of the spray travels against the direction of gas flow up into the outlet. The influence of increasing gas flow rate (and momentum) in the recirculation pattern is illustrated with screen captures from Tests 3036, 3037 and 3038 in Figure 20. As the liquid/gas momentum ratio decreases (from left to right in the photos), the quench spray is increasingly displaced out of and away from the cone outlet.

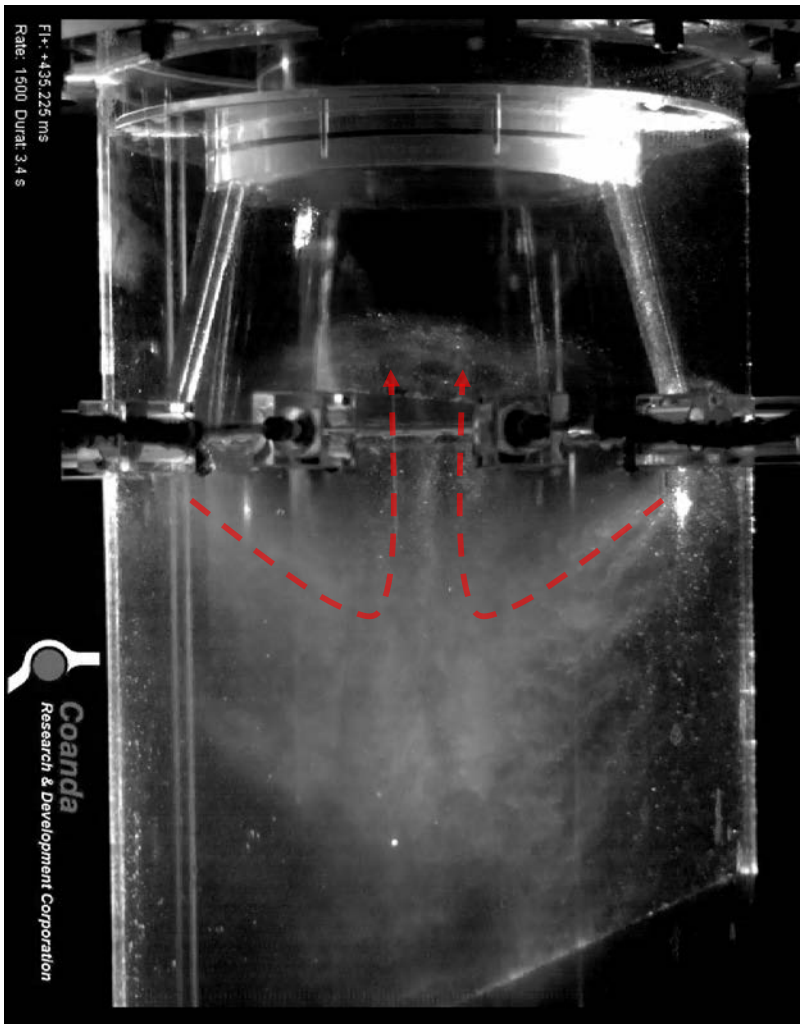

Figure 19: Quench spray shown recirculating to the center of the outlet. Extent of recirculation is dependent upon the ratio of downward gas momentum relative to quench spray jet momentum.

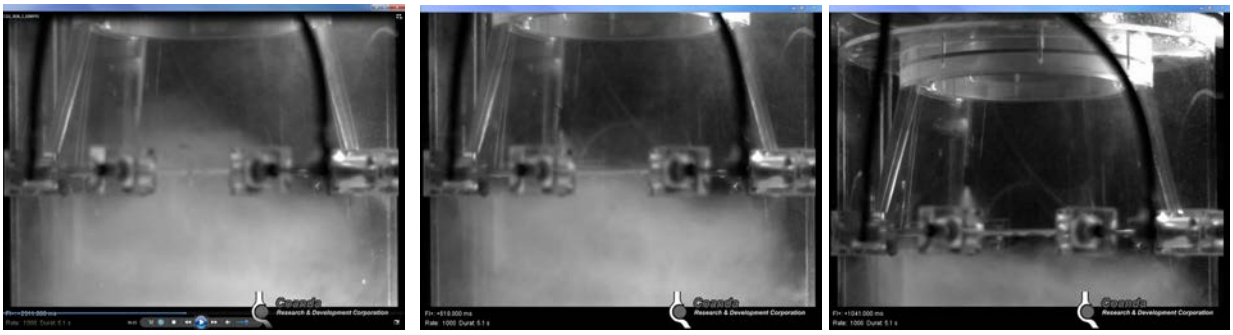

Figure 20: Impact of decreasing liquid/gas momentum ratio on quench spray intrusion into cone. Momentum ratios of 2.24 (left, Test 3036), 1.35 (center, Test 3037) and 0.84 (right, Test 3038).

Since quench spray recirculation was observed in air/water tests corresponding to a high degree of similitude at conditions scaled directly to the demonstration scale gasifier outlet design, there was interest in assessing whether or not testing with evaporating quench spray (HA134a) would show similar results.

Test 3025 was run with air and HA134a, with a liquid/gas momentum ratio considerably greater than any of the points run with the air water mixtures. The test was run without seeded flow (dry air) and seeded flow (air with water vapor) to offer improved visualization. Flow visualization screen shots are shown in Figure 21.

The upper left hand picture in Figure 21 shows dry air interacting with the HA134a jets. In contrast to the non-vaporizing water jets, the HA134a jets create a a much narrower plume of spray. As the jet interacts with the gas stream, flow of the jet is visibly disrupted, creating vortices in the flow that are of comparable length scale to jet diameter. However, there are no free droplets remaining to render visible any recirculation zones, either at the perimeter of the quench vessel or along the axis of the cone. Nor is there a visible plume of spray mixed with gas exiting the quench zone area.

The upper right hand picture captures the moment as the water vapor-seeded air just begins to contact the HA134a jets. The turbulent parts of the plumes become much more visible, but the overall visible flow features remain largely unchanged. The lower left hand picture shows flow after water vapor fully contacts the quench zone, with a much more visible mixing zone and a pronounced plume of gas/vapor/HA134a flowing out of the mixing zone. Recirculation at the perimeter and at the axis are not observed.

The lower right hand picture shows the steady state behavior of the air/HA134a system with water vapor-seeded flow. The mixing zone is fully obscured by the frozen water vapor droplets generated by contact between the wet air and the cold HA134a. The portions of the HA134a jets outside of the cone appear much like they do without seeded flow. At steady state, some recirculation of flow is observed around the outside of the cone, illustrating the presence of back-flow at the quench zone perimeter. However, there is a complete absence of recirculation of quench spray into the cone outlet. This is especially noteworthy given the much greater liquid/gas momentum ratio in this test relative to the comparable air/water case. Apparently, the evaporation process has a significant impact on the propensity for quench spray, or even cooled quench gas, to recirculate along the axis in the direction of the outlet.

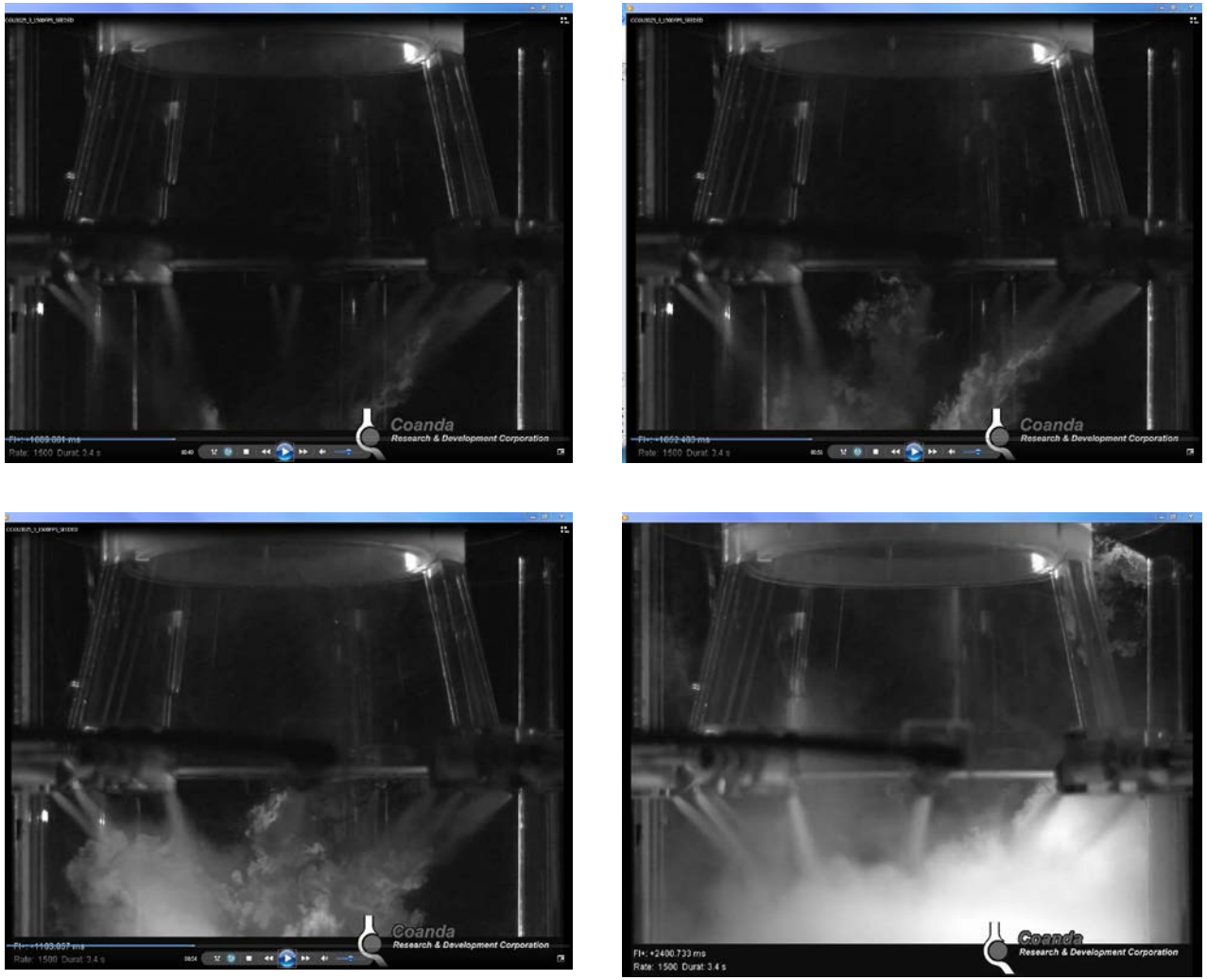

Figure 21: T-3025, with dry air (upper left), as water vapor-seeded air just begins to contact HA134a (upper right), after water vapor fully contacts just (lower left), and at steady state with seeded flow (lower right).

PDI data was obtained at the reference air/water flow condition for the scaled demonstration outlet to more fully characterize water droplet intrusion into the quench zone. The results are shown in Figure 22, with a contour plot of water hold-up (or liquid water content, LWC, in g/m^3). In the bulk of the zone, holdup values are less than 100 g/m^3 (similar to pilot plant results shown in Figure 16). Close to the cone wall, holdup values range from 100-1000 g/m^3. Values > 1000 closest to the wall are suspected to be due to interference from droplet accumulation on the internal surface of the cone. Where measurements indicate backflow into the cone, values of axial velocity were less than 0.5 m/s, typically about 0.1 m/s in the areas with greatest hold-up. Mean droplet diameters ranging from 200-300 µm indicate some possible coalescence by finer droplets within the cone. This PDI data, combined with estimated thermal environments within the cone, provides a basis for assessing persistence of droplets within the quench cone.

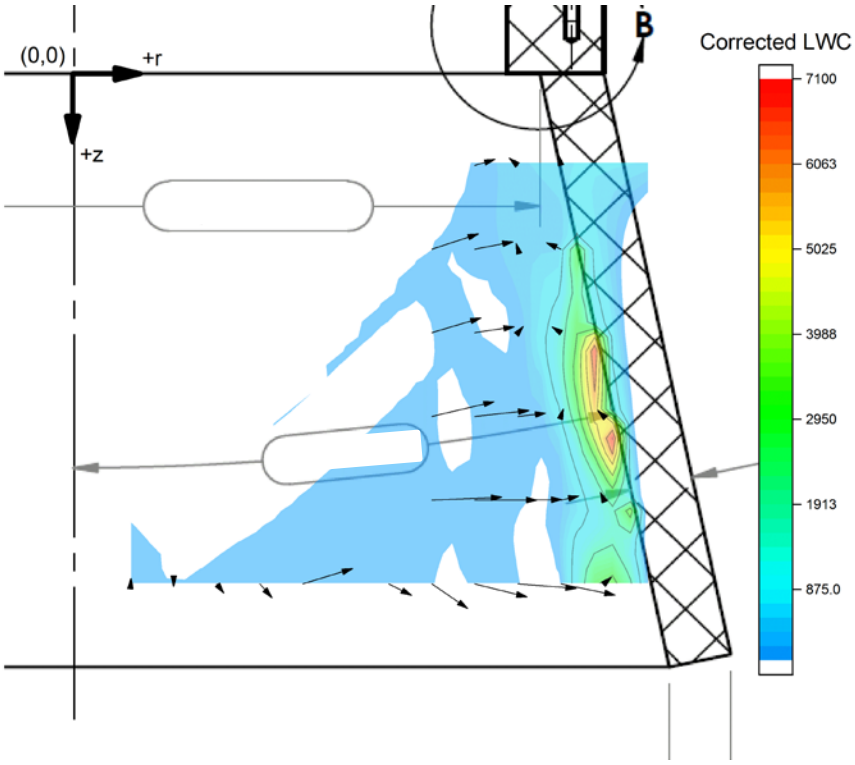

Figure 22: Liquid hold-up contours (in g/m^3) measured by PDI in the scaled demonstration gasifier cone outlet at reference air/water flow conditions.

3.2.3 Evaluations of Demonstration Scale Test Results

Test results from the demonstration scale outlet test were evaluated in the context of the following questions:

(1) Does axial location of quench nozzles relative to gasifier outlet have a significant impact on quench zone flow patterns or slag discharge behavior?

(2) Does outlet cone length impact quench zone flow patterns?

(3) Is there a significant impact of liquid/gas momentum ratio on flow behavior and, if so, is there a range in which any adverse flow patterns are avoided?

(4) Does modelling the system with an evaporating quench spray (HA134a) show any significant difference relative to air/water testing?

(5) Is the presence of water ingress large enough to potentially impact slag discharge?

Impact of Axial Location of Quench Nozzles:

No significant impact was observed with regards to either quench zone flow patterns or slag discharge. While the propensity for quench spray backflow into the outlet does diminish with distance between outlet and nozzles, this appears to be merely a result of increased distance between the nozzles and outlet, and does not appear to be a sensitive design parameter. Therefore, the baseline design appears reasonable in this respect.

Impact of Outlet Cone Length:

The two outlet designs corresponded to a length equivalent to that used in the pilot plant and a length that maintained gasifier diameter/cone outlet diameter ratio from the pilot plant. The shorter cone appeared to suppress backflow of quench spray into the outlet, possibly due to the greater momentum flux at the outlet as a result of a lesser degree of free-jet expansion in the shorter cone. However, this effect was not sufficient to eliminate backflow, so selection of cone length should be based on other considerations.

Impact of Liquid/Gas Momentum Ratio:

This parameter had a large effect on the extent of quench spray ingress into the outlet cone along the axis. Based on a series of tests using a laser sheet to illuminate the plane at the exit of the outlet cone, the liquid/gas momentum ratio corresponding to the onset of spray entering the outlet cone at varying gas Reynolds numbers was identified, referred to as the critical momentum ratio. These results are shown in Figure 23. It appears that operating at momentum ratios less than 1.0 is sufficient to prevent backflow. However, there is some uncertainty as to the extent to which the scaling characteristics of gas/quench jet interactions are understood. A literature review was initiated, but the findings from that review as of the date of this report were not conclusive. Upon developing a more satisfactory understanding of these scaling relationships, further testing of the cold flow apparatus should be strongly considered.

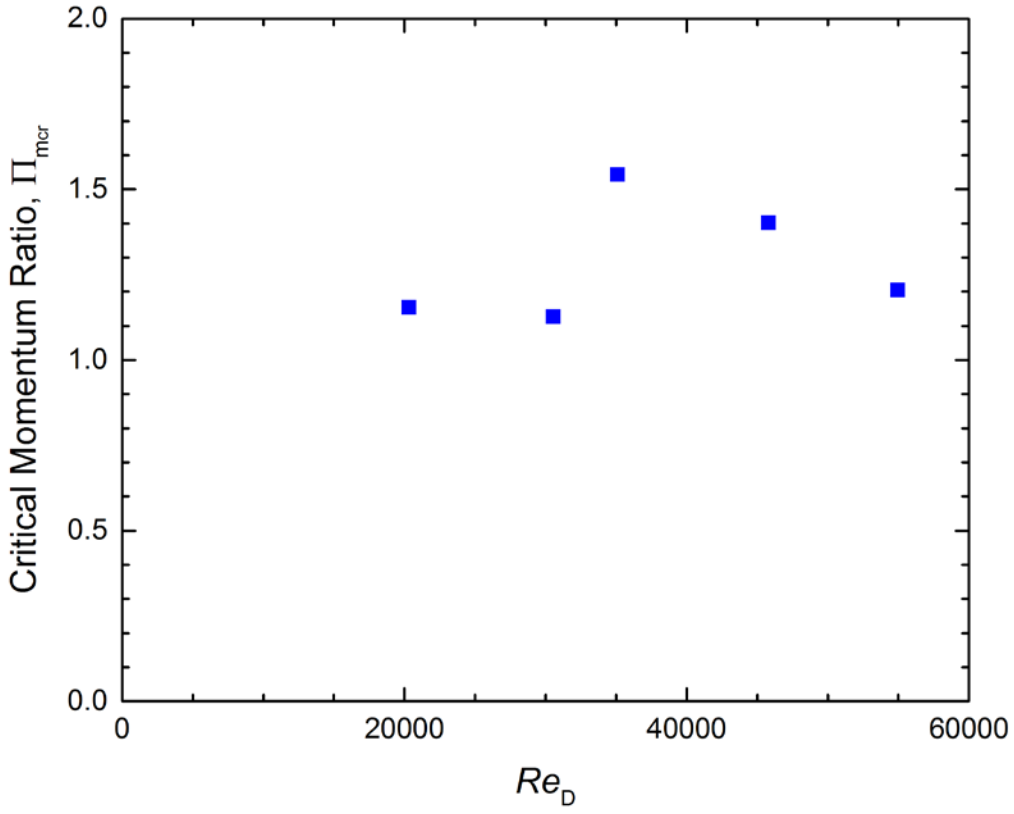

Figure 23: Data from Tests 3035-3050, indicating liquid/gas momentum ratios at which spray recirculating along the axis is observed to just enter the cone, plotted relative to Reynolds number of exiting gas flow. At momentum ratios lower than 1, there appears to be little backflow of spray into the cone along the axis.

Impact of Evaporating Flow:

Use of HA134a in place of water showed a significant change in outlet flow patterns, where backflow along the axis was not observed. Other flow patterns, such as the turbulent zone where the quench spray and gas interact, as well as the large scale recirculation patterns around the perimeter of the upper quench zone, appear similar. This indicates that testing with the air/water system provides a reasonable representation of gas/liquid mixing as well as the outer recirculation zones, and provides a conservative assessment of propensity for backflow along the axis.

Assessment of Water Ingress:

The potential presence of water droplets recirculating into the outlet zone poses the risk of causing slag accumulation within the outlet due to cooling effects. This assessment was divided into two questions:

(1) How long does it take to vaporize water droplets entering the outlet cone? Will the droplets vaporize before they impact the slag drip lip?

(2) Is the thermal environment in the cone sufficient to vaporize the flux of water entering the cone before it reaches the outlet?

These two questions were assessed using "worst case" values that would overstate the potential for non-vaporized water to reach the gasifier drip lip. It was determined that the time-scale for droplet vaporization was about an order of magnitude less than the time scale required for overall water vaporization (which balances radial heat flux to the cone wall against water ingress flux at the outlet cone). The magnitude of the vaporization time combined with typical velocity results in a length scale comparable to the longer quench cone. Therefore, the longer cone is preferable in support of thermal isolation of the slag drip lip.

4.0 CONCLUSIONS

The cold flow modelling approach employed in this effort showed excellent consistency with observable pilot plant gasifier results, provides excellent hydrodynamic similitude, and offers acceptable thermodynamic similitude. On that basis, it was concluded that the modelling approach was suitable for use in the scaled demonstration outlet test effort.

Air/water tests and air/HA134a tests show similar flow patterns in the recirculation zones near the vessel perimeter and in the mixing zone downstream of the quench nozzles. However, the air/water system tends to overstate the propensity for quench spray recirculation to the outlet relative to an evaporating quench system. Therefore, the air/water system provides a conservative assessment of quench zone performance with respect to assessing flow patterns and water ingress at the gasifier outlet.

The influences of quench spray nozzle angle, axial distance between cone outlet and spray nozzles, and cone length were evaluated to assess impact on quench zone performance.

- Directing the spray nozzle angle further away from the outlet decreased recirculation backwards towards the outlet. However, this reduces quench spray penetration of the hot syngas, so it should not be the primary design variable manipulated to achieve suitable quench zone flow patterns.
- Increasing axial distance between the gasifier outlet and quench nozzles did slightly reduce the extent of quench spray backflow reaching the outlet. This design variable is of limited utility, as the quench nozzle jets and recirculating spray serve to shield the surrounding vessel from radiant heating by the exiting syngas.
- A shorter cone tends to suppress quench spray recirculation into the outlet. A longer cone provides greater separation between the relatively cool quench zone and the slag drip lip at the top of the cone outlet. Evaluation of water flux into the outlet relative to available heat load in the outlet to vaporize the water before it can impact the slag drip lip indicates a preference for use of the longer cone in the demonstration plant design.

For the nozzle angle tested, a liquid/gas momentum ratio < 1.0 is low enough to avoid recirculation of quench spray back into the cone outlet. Since this is for the air/water system, this would be a conservative ratio. This conclusion should be considered preliminary until a more thorough assessment of the physics and scaling relationships for interaction between these jets is performed.

The project successfully accomplished the objectives set out in Task 2 of the contractual Statement of Project Objectives, in verifying the ability to establish acceptable similitude and providing design guidance for the gasifier outlet to avoid build-up of slag. The test program also indicated other considerations for quench system design that should be considered for a follow-on study. Specifically, recommended follow-on actions are:

- A detailed assessment of jet-jet interactions relevant to an atomized liquid jet and down-flowing gas column. The purpose is to clearly define the physics governing the scale-up of this specific type of jet-jet interaction.
- Using the results from the above assessment, design and fabricate a full scale demonstration gasifier quench zone that is also full length. The purpose of this is

twofold – (1) Verify jet-jet interaction dependencies on operating parameters and (2) assess mixing of quench spray within the gas stream to ensure adequate cooling of the syngas before it exits the quench vessel.

TASK 3: PILOT PLANT GASIFIER TESTING

TOPICAL REPORT

Reporting Period

Start Date: October 1, 2014

End Date: October 30, 2015

Principal Author

Steve Fusselman Principal Investigator/Program Manager

October 30, 2015

DOE Award Number

DE-FE0023577 (DOE NETL)

Aerojet Rocketdyne of DE, Inc.
8900 DeSoto Avenue
Canoga Park, CA 91309

DISCLAIMER

ABSTRACT

Aerojet Rocketdyne (AR) has developed an innovative gasifier concept incorporating advanced technologies in ultra-dense phase dry feed system, rapid mix injector, and advanced component cooling to significantly improve gasifier performance, life, and cost compared to commercially available state-of-the-art systems. Design, fabrication and initial testing of the pilot plant compact gasifier was completed in 2011 by a development team led by AR. Findings from this initial test program, as well as subsequent gasifier design and pilot plant testing by AR, identified a number of technical aspects to address prior to advancing into a demonstration-scale gasifier design. Key among these were an evaluation of gasifier ability to handle thermal environments with highly reactive coals; ability to handle high ash content, high ash fusion temperature coals with reliable slag discharge; and to develop an understanding of residual properties pertaining to gasification kinetics as carbon conversion approaches 99%. The gasifier did demonstrate the ability to withstand the thermal environments of highly reactive Powder River Basin coal, while achieving high carbon conversion in < 0.15 seconds residence time. Continuous operation with the high ash fusion temperature Xinyuan coal was demonstrated in long duration testing, validating suitability of outlet design as well as downstream slag discharge systems. Surface area and porosity data were obtained for the Xinyuan and Xinjing coals for carbon conversion ranging from 85% to 97%, and showed a pronounced downward trend in surface area per unit mass carbon as conversion increased. Injector faceplate measurements showed no incremental loss of material over the course of these experiments, validating the commercially traceable design approach and supportive of long injector life goals. Hybrid testing of PRB and natural gas was successfully completed over a wide range of natural gas feed content, providing test data to anchor predictions for commercial operation of hybrid coal/natural gas gasification plants.

TABLE OF CONTENTS

LIST OF FIGURES

Figure **Page**

LIST OF TABLES

Table **Page**

EXECUTIVE SUMMARY

Aerojet Rocketdyne (AR) and the Gas Technology Institute (GTI) are developing and maturing entrained flow gasifier technologies to meet the United States Department of Energy (DOE) goals for lowering the cost of producing high hydrogen syngas from coal for use in carbon capture power and coal-to-liquids/chemicals. The project will mature an advanced pilot-scale gasifier with scalable and commercially traceable components to readiness for use in a first-of-a-kind commercially-relevant demonstration plant on the scale of 500-1,000 tons per day (TPD) by 2020.

Design, fabrication and initial testing of the pilot plant compact gasifier were completed in 2011 by a development team led by AR. Findings from this initial test program, as well as subsequent gasifier design and pilot plant testing by AR, identified a number of technical aspects to address prior to advancing into a demonstration-scale gasifier design. These were as follows:

(1) Assess the thermal environments associated with highly reactive coals (such as lignite and sub-bituminous) to confirm feasibility of gasifier component designs

(2) Establish the ability to operate the gasifier on high ash content, high ash fusion temperature (AFT) coals, demonstrating continuous slag discharge capability and component feasibility in the challenging thermal environments posed by high AFT coals.

(3) Characterize the properties of residual carbon at high conversion to provide a basis for improved performance prediction as carbon conversion approaches 99%.

The primary objective of this effort was to address these technical challenges in support of demonstration scale gasifier design. A secondary objective was to assess the feasibility of operating the compact gasifier in a hybrid mode, with simultaneous feeding of coal and natural gas.

Testing with the high ash/high ash fusion temperature (AFT) coal in August 2014 revealed significant challenges to continuous removal of slag from the gasifier quench vessel and slag lock hopper. Under this project, the slag discharge system was modified to a slag bath approach, and the syngas line was re-routed to a location above a converging section of the quench section outlet to place it above potential blockage points. The slag bath system provided reliable, continuous operation during long duration testing.

Two modifications were made to the gasifier to support testing of the high ash/high AFT coals. Wall wash lances were incorporated into the upper section of the quench zone to displace buildup of fine slag material, which in earlier testing had led to misdirection of syngas flow. Also, flame detector ports were installed at the gasifier outlet to provide redundancy of flame confirmation. This approach proved to be very useful in sustaining long duration test operations.

Highly reactive coal testing was performed on Powder River Basin sub-bituminous coal. Thermal environments measured at the injector faceplate and along the liner were found to be well within the design basis for both components. Carbon conversion ranged from 97% to almost 99% in a

residence time of <0.15 seconds, at gasifier outlet temperatures in the same range as intended for commercial operations.

Testing of high ash/high AFT coals demonstrated that the gasifier could manage the thermal environments associated with these feedstocks. Gasifier outlet temperatures were estimated to range from 3400°F to 4200°F for these tests, well above the 3000°F outlet temperature required to maintain slagging conditions at the outlet of the gasifier. Carbon conversion ranged from 85% to 97%, providing several samples to serve as the basis for assessing dependency of residual carbon surface area and porosity as a function of carbon conversion. Surface area decreased from 62 m^2/g at 85% carbon conversion to 36 m^2/g at 97% conversion. Porosity showed no clear dependence on carbon conversion, ranging from 50% to 80%. A value of 50% is recommended for use in performance modelling to provide a conservative basis.

Hybrid testing of PRB coal with natural gas demonstrated the ability to run at mixtures up to 34% natural gas on an HHV basis. Operations at 50% or more natural gas content appears feasible, with significant improvement in H_2/CO ratio, reduction in carbon emissions per unit syngas, and reduced oxygen consumption per unit syngas the expected benefits.

No measurable loss of parent material greater than 0.001" was observed for the injector faceplate over a cumulative total of >900 hours of operation. The injector faceplate design appears to be feasible for providing long injector life. The gasifier liner was completely covered with slag, which is expected to provide good protection of the underlying parent material in support of achieving liner life goals.

1.0 INTRODUCTION

1.1 DOCUMENT SCOPE

The purpose of this document is to describe key findings from the pilot plant gasifier test program, specifically regarding testing on highly reactive coal, high ash/high ash fusion temperature coal, and hybrid gasifier operations on coal with natural gas.

This Topical Report summarizes the effort performed under Task 3: Pilot Plant Gasifier Testing as part of contract DE-FE0023577 awarded to Aerojet Rocketdyne (AR) by the United States Department of Energy (DOE) – National Energy Technology Laboratory (NETL).

1.2 OBJECTIVES

Aerojet Rocketdyne (AR) and the Gas Technology Institute (GTI) are developing and maturing entrained flow gasifier technologies to meet the United States Department of Energy (DOE) goals for lowering the cost of producing high hydrogen syngas from coal for use in carbon capture power and coal-to-liquids/chemicals. The project will mature an advanced pilot-scale gasifier with scalable and commercially traceable components to readiness for use in a first-of-a-kind commercially-relevant demonstration plant on the scale of 500-1,000 tons per day (TPD) by 2020.

Design, fabrication and initial testing of the pilot plant compact gasifier were completed in 2011 by a development team led by AR. Findings from this initial test program, as well as subsequent gasifier design and pilot plant testing by AR, identified a number of technical aspects to address prior to advancing into a demonstration-scale gasifier design. These were as follows:

(1) Assess the thermal environments associated with highly reactive coals (such as lignite and sub-bituminous) to confirm feasibility of gasifier component designs

(2) Establish the ability to operate the gasifier on high ash content, high ash fusion temperature (AFT) coals, demonstrating continuous slag discharge capability and component feasibility in the challenging thermal environments posed by high AFT coals.

(3) Characterize the properties of residual carbon at high conversion to provide a basis for improved performance prediction as carbon conversion approaches 99%.

The primary objective of this effort was to address these technical challenges in support of demonstration scale gasifier design. A secondary objective was to assess the feasibility of operating the compact gasifier in a hybrid mode, with simultaneous feeding of coal and natural gas.

The contract Statement of Project Objectives defines the effort as follows:

Task 3 – Pilot Plant Gasifier Testing: This effort will test pilot plant gasifier hardware in hybrid (coal + natural gas) mode and on highly reactive and high AFT coals.

Subtask 3.1 – Facility Review and Activation: The pilot plant facility will be reconfigured and reactivated for planned testing. Coal supplies that support test objectives (highly reactive and high AFT coals) will be secured. Pulverized coal and zinc oxide (for sulfur removal from syngas) will be procured. A literature review and analysis plan will be developed for the analysis of residual carbon obtained from gasifier slag samples. A safety review will be held for operation on highly reactive coal and for facility configuration and operations in hybrid mode. At the conclusion of facility activation, a test readiness review will be held by facility owner to authorize test operations. A technical review open to DOE and project team will be conducted, assessing overall technical readiness (for testing and data evaluation), which will be held prior to advancing into Subtasks 3.2 and 3.4.

Subtask 3.2 – Highly Reactive Coal Testing: The pilot plant gasifier will be operated on a highly reactive coal feedstock for approximately 50 hours cumulative test time, obtaining detailed mass and energy balance data at three or more operating points. Testing will establish the feasibility of gasifier operations on highly reactive coal.

Subtask 3.3 – High AFT Coal Testing: The pilot plant gasifier will be operated on two (or more) coals with high AFT (>1500°C) at conditions supporting reliable slag discharge and corresponding to carbon conversion ranging from 90-99%. Detailed mass and energy balance data at six or more operating points will be obtained, with porosimetry and surface area analysis performed on residual carbon in solids samples recovered from the entrained flow gasifier coarse and fine slag discharge streams. Feasibility of continuous gasifier operations on high AFT (and preferably coal with ash >25% as well) will be demonstrated. Testing will explore thermal margin of the gasifier design. Post-test evaluation of the injector (profilometry comparison before and after) and liner (visual inspection for pitting) will be performed to assess feasibility of commercial component life.

Testing of high AFT coal, either in whole or in part, may be performed at any time depending upon feedstock availability and if the plant is already properly configured for AR testing. Some portion of high AFT testing may also be performed in conjunction with testing under subtasks 3.2 and 3.4, provided that it offers cost effective realization of program objectives.

Subtask 3.4 – Hybrid Gasification Testing: The pilot plant gasifier will be operated on a mixture of coal and natural gas, with a minimum of 51% coal by HHV. Feasibility of hybrid mode operation will be established. Approximately 50 hours of cumulative testing will be performed, obtaining detailed mass and energy balance data at three or more operating points. Test data will establish the H_2:CO ratio attainable in hybrid operation with the given coal feedstock, and serve as the basis for predicting H_2:CO ratio for commercial scale operation on a low rank and bituminous coal.

Subtask 3.5 – Pilot Plant Test Results: Gasifier performance analysis from subtasks 3.2, 3.3 and 3.4 will be summarized in a topical report. Predicted H_2:CO ratio for hybrid gasifier operation, with multiple coals will be presented. Residual carbon analyses results at >90% conversion will be presented. Operational findings from testing on highly reactive and high AFT coals will be

summarized, and will be used to refine performance inputs to the Techno-Economic Analysis in Task 5.

1.3 ABBREVIATIONS

AFT	Ash Fusion Temperature
AGTF	Advanced Gasification Test Facility
AGWGST	Advanced Gasifier & Water Gas Shift Technologies
AR	Aerojet Rocketdyne
ASME	American Society of Mechanical Engineers
ASTM	American Society for Testing and Materials
BTU	British Thermal Unit
DAP	Data Attainment Period
DOE	Department of Energy
FFTF	Flex Fuel Test Facility
GC	Gas Chromatograph
GHG	Greenhouse Gas
gpm	Gallons Per Minute
GTI	Gas Technology Institute
HHV	Higher Heating Value
IR	Infrared
MAF	Moisture and Ash Free
mL	Milliliter
NETL	National Energy Technology Laboratory
PRB	Powder River Basin
TEB	Triethyl Borane
TPD	Tons Per Day
WGS	Water Gas Shift
µm	Micrometer

2.0 EXPERIMENTAL METHODS

2.1 GASIFIER PILOT PLANT FACILITY

Testing of the 18 TPD pilot plant gasifier was performed at the Gas Technology Institute in Des Plaines, Illinois. The facility is shown in Figure 1. The control room, feed system, gasifier, coarse slag discharge and gasifier ancillary systems are housed in the Advanced Gasification Test Facility (AGTF). The cyclone, candle filter, ZnO sulfur removal bed, fine particulate lock hoppers, syngas flare, and on-line gas analysis are housed in the Flex Fuel Test Facility (FFTF). The facility and the pilot plant gasifier were designed, fabricated and initially tested under previous programs.

Figure 1. The pilot plant gasifier test program used existing equipment and infrastructure located in the Advanced Gasification Test Facility (left) and Flex Fuel Test Facility (center) at the Gas Technology Institute.

An overall schematic for the pilot plant gasifier is shown in Figure 2. Fuel (coal and/or natural gas) enter the gasifier via the top of the injector. Oxygen and steam are fed into the side of the injector. Nitrogen purges are introduced at multiple points in the gasifier for the purpose of maintaining clean instrumentation ports and field of view through the flame detector ports. De-ionized water used to quench the raw syngas to ~ 400°C is injected at the gasifier outlet.

Syngas exits the quench vessel, G-302C, and is piped over to the cyclone, CY-402, in the FFTF for initial solids removal. The candle filters in T-2154 provides removal of fine solids > 1 micrometer (μm), with the clean syngas then processed through hot ZnO beds in R-2003 and R-2002 for H_2S and COS removal prior to flaring through FL-601.

Coarse slag and larger particles fall through G-302C into the slag bath in the quench cross, T-315. Coarse slag flows concurrently downward from T-315 into the slag surge drum, T-305. A dip tube inserted through a nozzle at the top of T-305 siphons off the bath water, along with some amount of fine slag entrained in the flow, and discharges it to the slag bath water system T-317 and T-

319). The coarse slag is discharged into the coarse slag lock hopper, T-306. S3, S2, S4 and S5 are the solids (and water) sampling points. G8, G13 and G14 are the gas sampling points.

The process flow diagram for coal transport, dense phase feed, gasifier, and gasifier ancillary systems is shown in Figure 3. "Super sacks" of pulverized coal weighing approximately 1500 lb each are discharged into the Cyclonaire conveyor system, C-103B, then pneumatically conveyed over to the T-212 day bin on the top (5^{th}) floor of Bay 2 in the AGTF. Load cells on T-212 record the weight of material dispensed to the T-213 dense phase feed system lock hopper, which cycles between atmospheric pressure to receive coal from T-212 and process pressure (~450-500 psig) to discharge coal into the T-211 high pressure coal feed hopper. A 3/8" line from the T-211 outlet at the ground floor of AGTF conveys coal up to the gasifier injector on the 5^{th} floor of the AGTF, with a line length of approximately 75 feet. Steam is supplied from a package boiler located in the FFTF, and is at, or close to, saturated conditions within the AGTF. Oxygen is supplied at ambient temperature from a liquid oxygen evaporator on the supply pad located outside of the FFTF. The oxygen is superheated to ~200°C using saturated steam from FFTF. The steam and oxygen are mixed in the feed line that enters the injector. Natural gas is brought up to process pressure using compressor CM-800, which is located within an enclosure nearby the AGTF building. All feed streams to the gasifier enter via the injector on the 5^{th} floor of the AGTF.

Testing with the high ash/high ash fusion temperature (AFT) coal in August 2014 revealed significant challenges to continuous removal of slag from the gasifier quench vessel and slag lock hopper. AR and GTI discussed this issue with the DOE/NETL project manager, and received concurrence to implement modifications to the slag discharge system as part of this project. The key elements of this modification are shown in Figure 4, and are described as follows:

(1) Relocation of syngas line from T-315 quench cross to G-302C quench vessel. This allowed modification of T-315 from a dry slag discharge to a slag bath, enabling back-pulsing of the outlet cone on T-315 to disrupt accumulations of solids there.

(2) Modification to T-315 for slag bath water flow. Sufficient slag bath water was required to cool the product slag to < 150°F prior to discharge. For the high ash coal, a flow rate of 2 gpm was estimated to be sufficient.

(3) Installation of a new (smaller) slag discharge vessel, T-306, to support discharge of the coarse slag/water mixture.

(4) Installation of a slag bath water lock hopper system, T-317 and T-319, providing batch let-down of slag bath water received from T-315 and T-305.

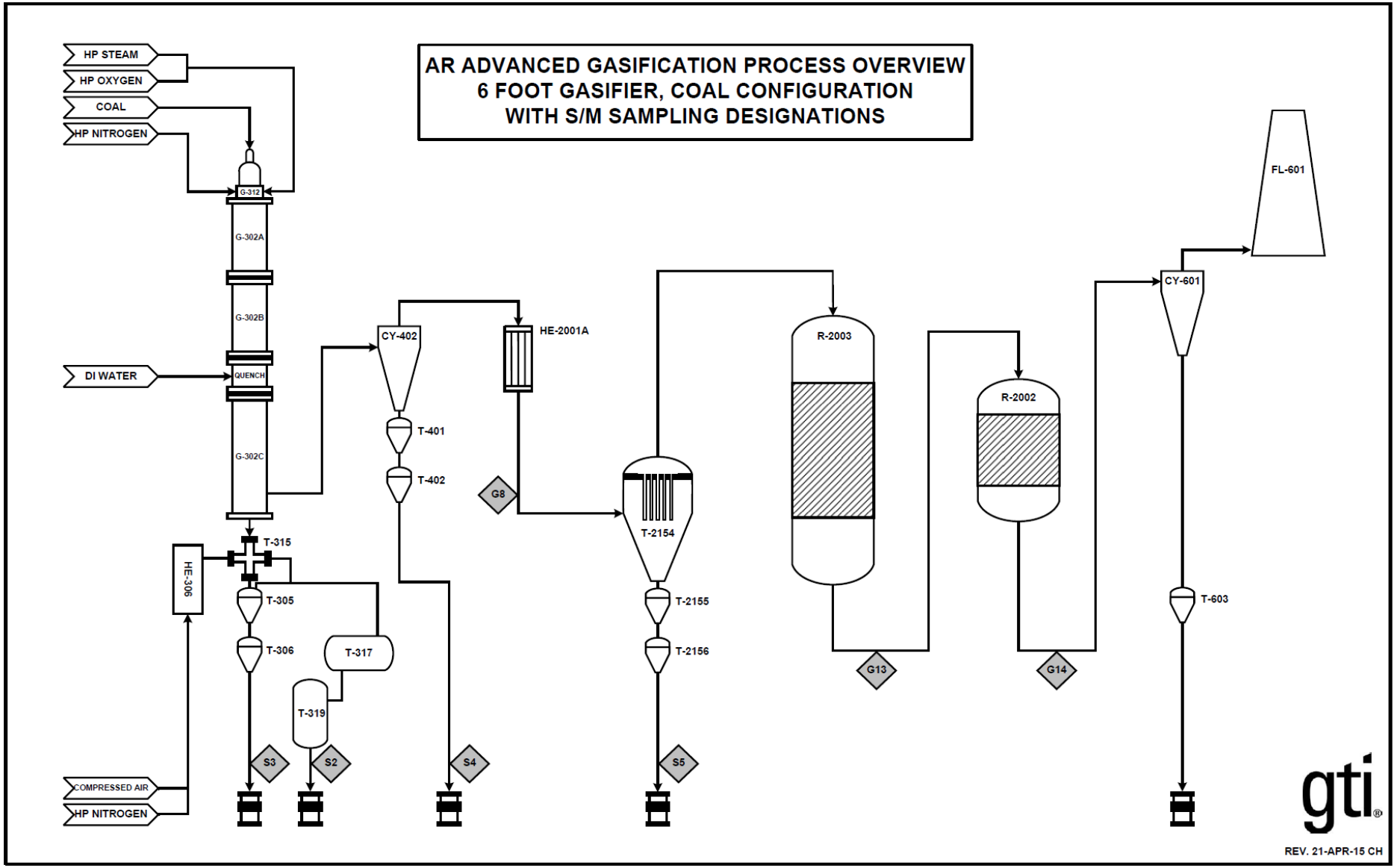

Figure 2. Process flow schematic for the pilot plant gasifier test facility.

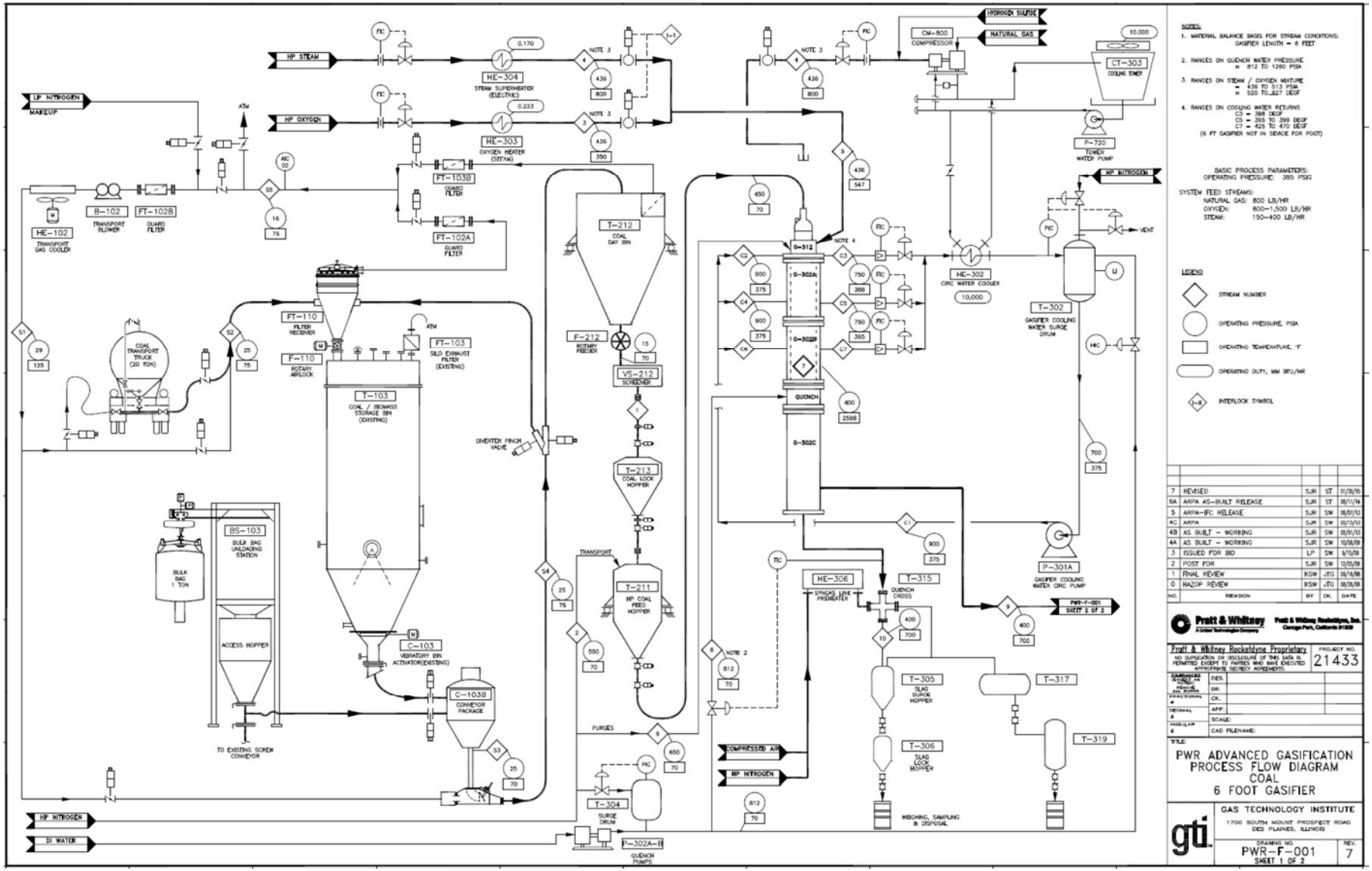

Figure 3. Process flow diagram for pilot plant coal supply, dense phase feed system, gasifier, and slag discharge.

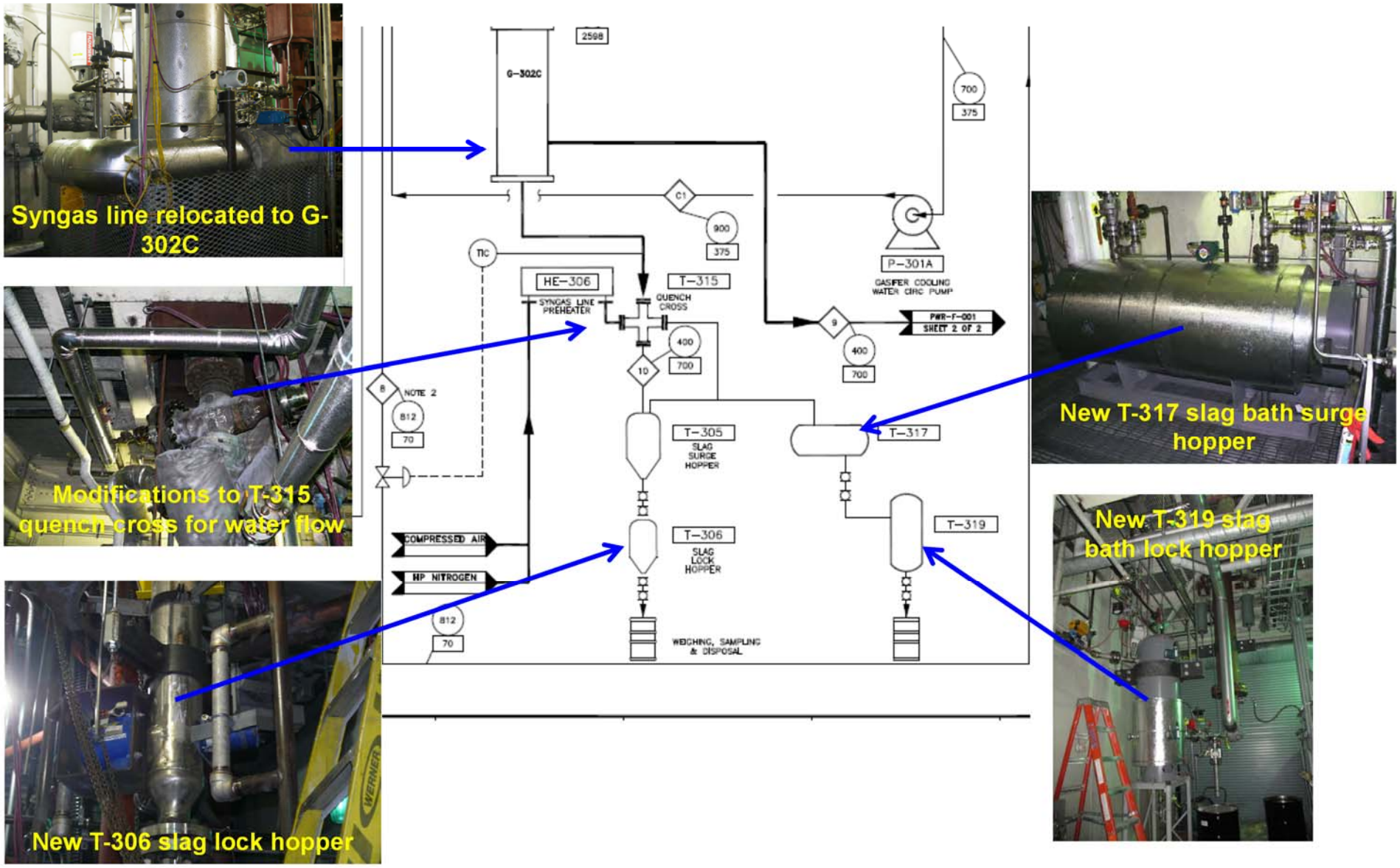

Figure 4. Slag discharge system modifications overview.

Pilot plant gasifier hardware is shown in Figure 5. The gasifier injector and liner are installed in an ASME-stamped steel pressure vessel. Testing for this project used the 3' liner configuration, corresponding to a residence time of ~0.10-0.15 seconds, depending upon operating flow rates. Installation of the liner is shown in Figure 6. A pentad-style injector was used for all tests, with injector installation shown in Figure 7.

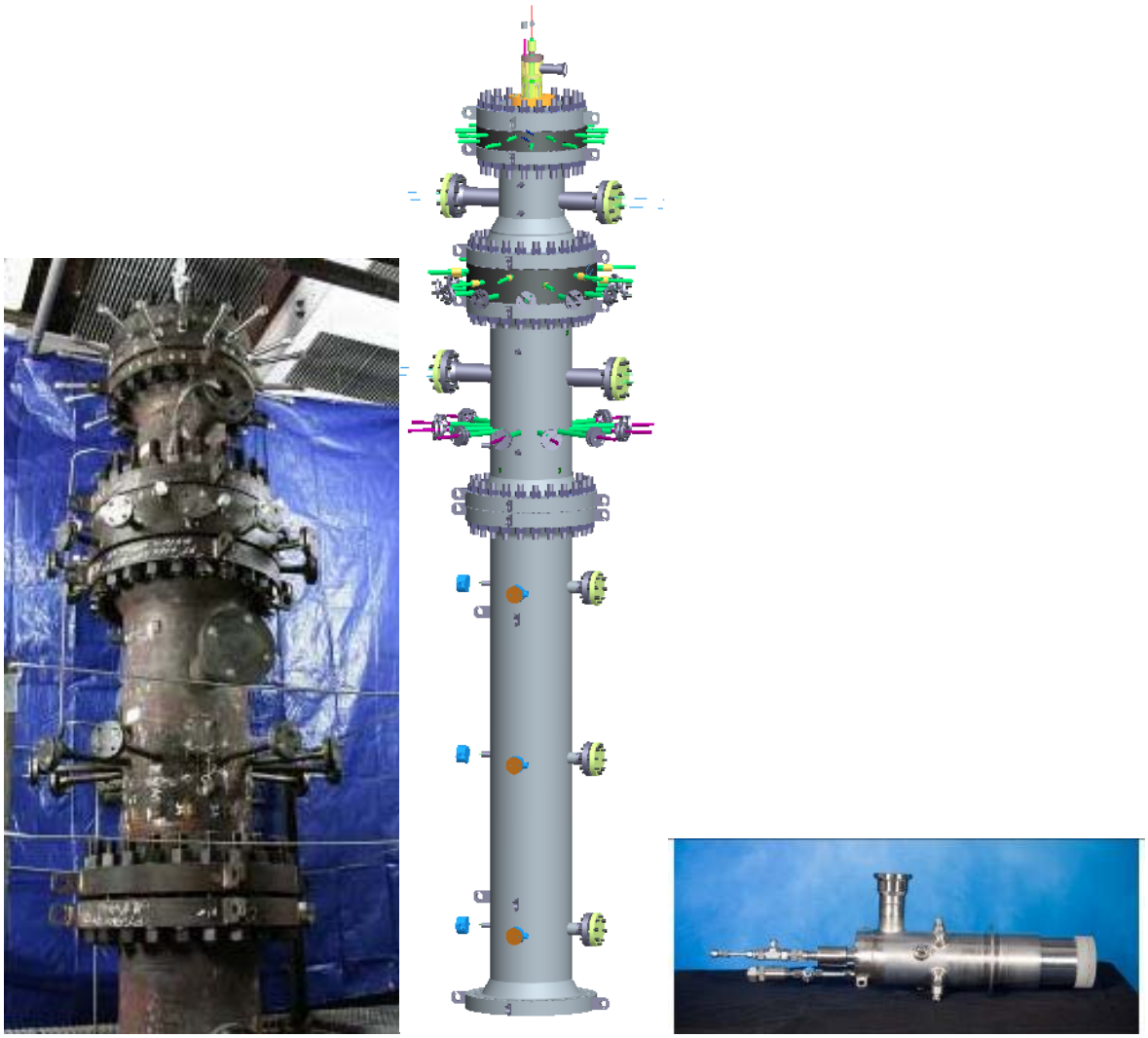

Figure 5. Pilot plant gasifier pressure vessel (left), overall assembly (center), and pentad injector (right).

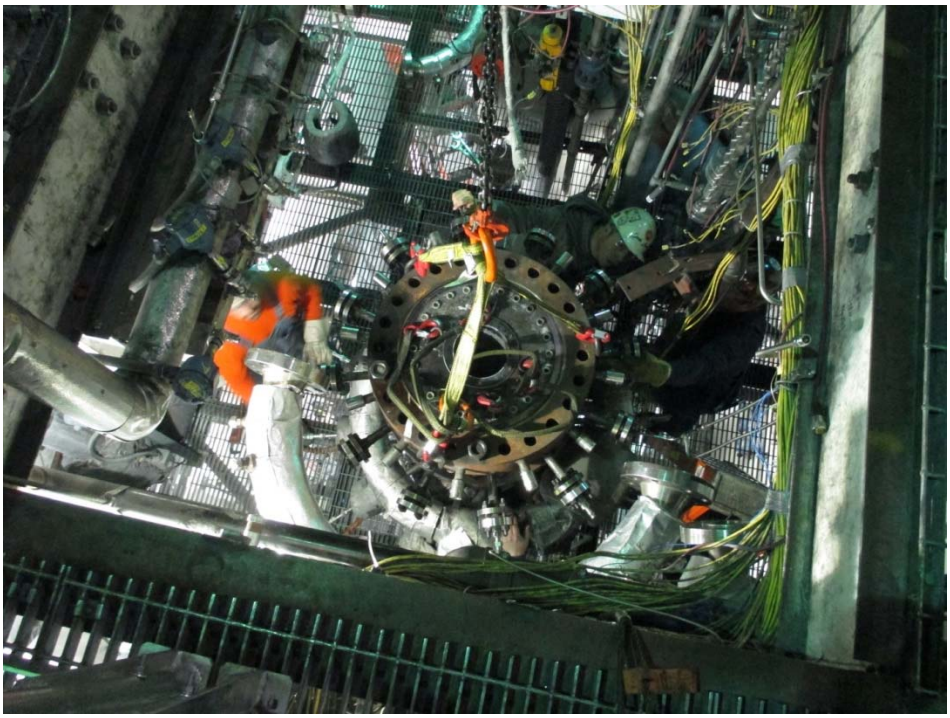

Figure 6. View looking at top of gasifier vessel, with liner installed.

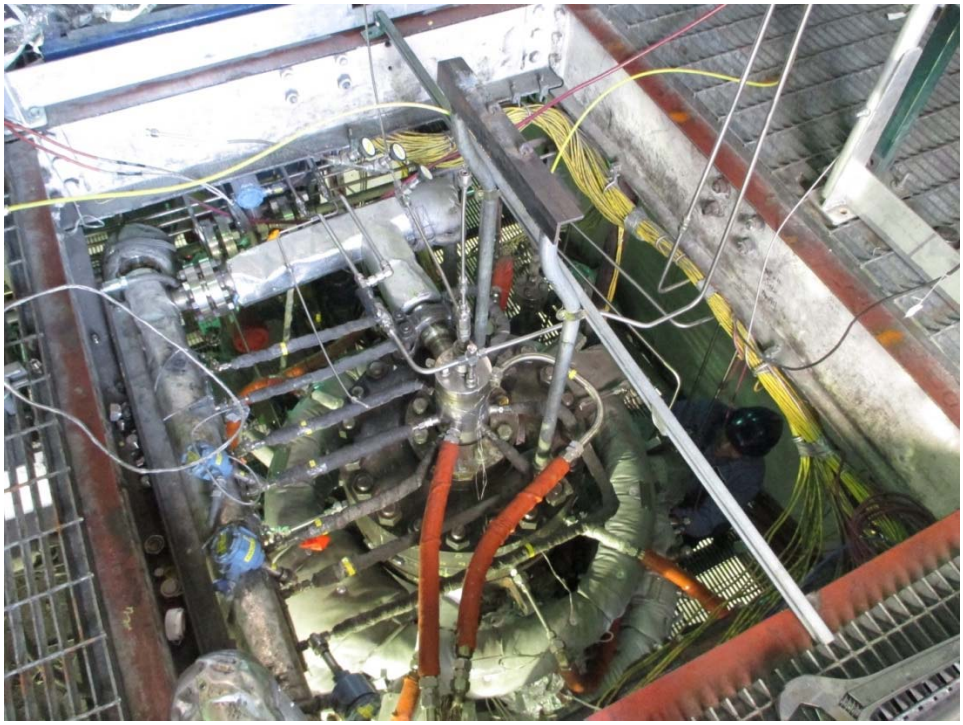

Figure 7. View looking at top of gasifier vessel, with injector installed. Coal is fed into the injector via the line coming down through the top center of the injector. The oxygen/steam mixture is fed via the 2" line coming into the side of the injector from the top of the picture.

Two modifications were made to the gasifier to support testing of the high ash/high AFT coals:

(1) Installation of a Vega Americas (formerly Ohmart/Vega) gamma source and MiniTrac detector (see Figure 8) to detect buildup of solids within the quench vessel (see Figure 9). Testing on high ash/high AFT coals in August 2014 revealed a strong tendency of fine slag from this coal to bridge within the upper quench zone, leading to misdirected flow of the hot syngas (> 2800°F) within the quench vessel. Attenuation of the signal reaching the MiniTrac detector corresponded to build-up of material within the quench vessel at that location, and also provided real-time visibility into the efficacy of the wall wash spray lances for material displacement.

(2) Design, fabrication and installation of wall wash spray lances to disrupt build-up of material in the upper section of the quench vessel, and incorporating view ports (see Figure 10) to provide a view at the gasifier outlet (see Figure 11) in support of flame confirmation. The lances have horizontal slits machined into the outer tube. The slits are positioned just within the inner diameter of the quench vessel, shooting a flat sheet of high pressure water (see Figure 12) along the wall to disrupt material build-up. An installed wall wash spray lance with Ametek flame detector is shown in Figure 13.

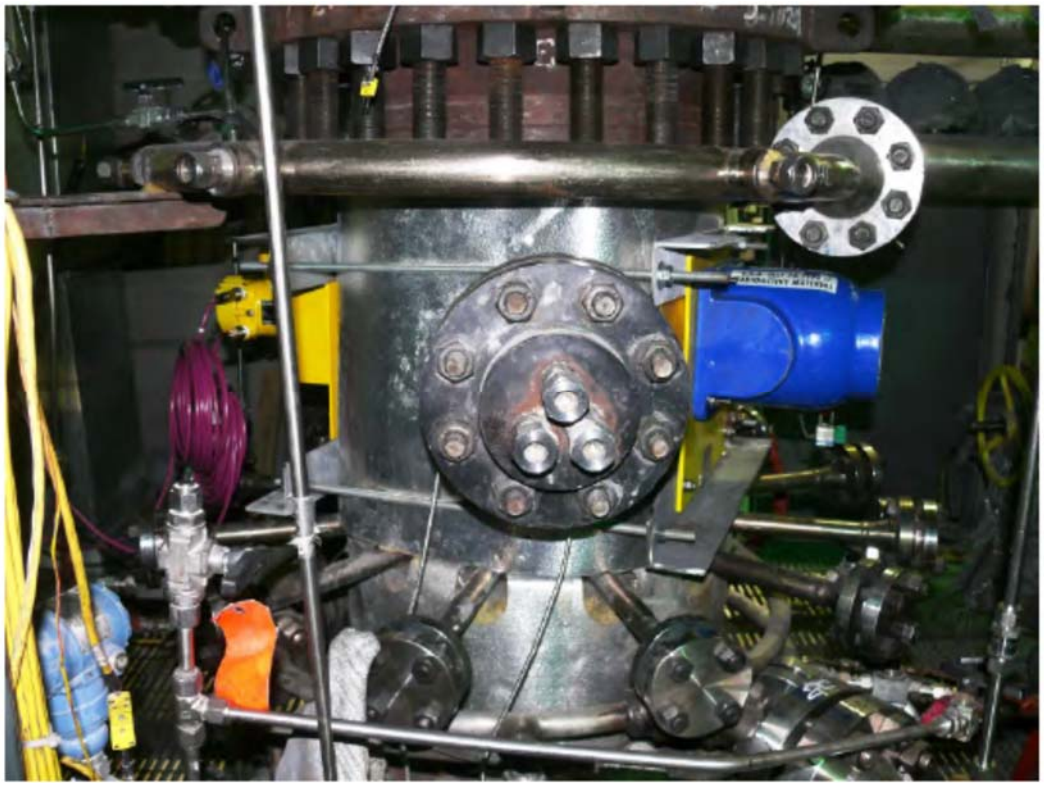

Figure 8. View of gasifier quench vessel just downstream of gasifier outlet, showing installation of Vega Americas gamma source (blue device on the right) and MiniTrac detector (yellow device on the left). This system provided real-time detection of solids build-up within the quench vessel.

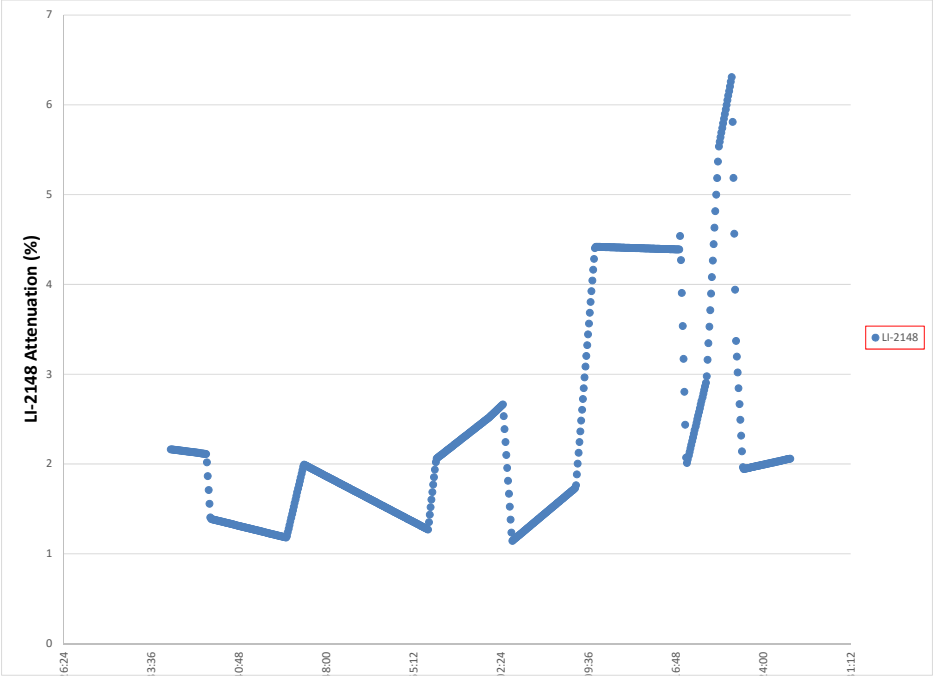

Figure 9. Example of results from LI-2148 Vega Americas detector for indication of solids build-up in quench vessel during testing. Data in the figure are from test operations, showing both accumulation of solids as well as removal of solids using the wall wash quench lances.

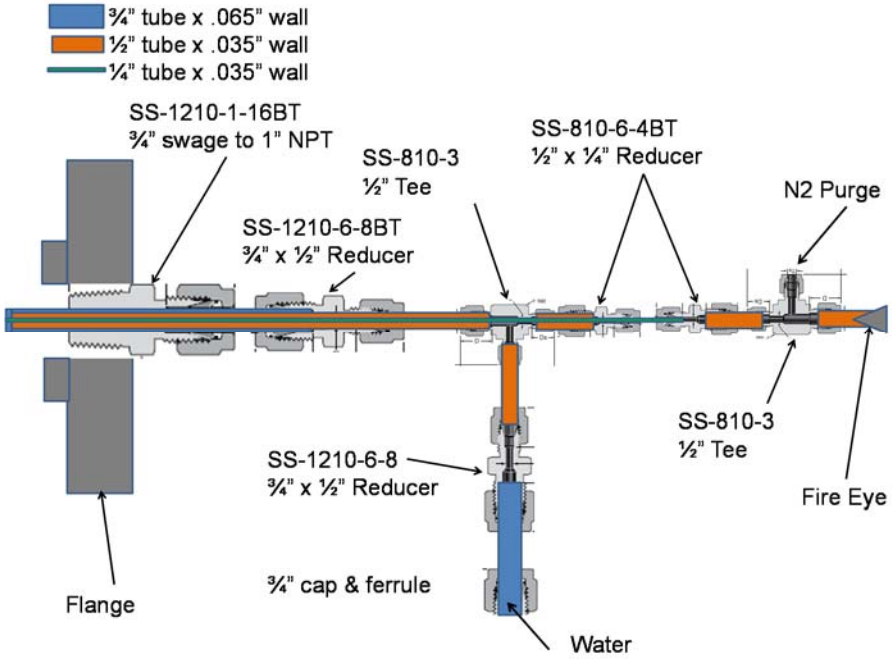

Figure 10. Cross sectional view of wall wash lance design with integral view port passageway (via ¼" tube) for "Fire Eye" (for Lumasense and Ametek flame detectors).

Figure 11. View of wall wash lance with integral view port, from the end installed in the gasifier. View port is via ¼" tube in the center. Wall wash spray is via the horizontal slit in the ¾" tube wall located about 2" from the end of the lance.

Figure 12. Atmospheric testing of the wall wash lance was used to evaluate spray pattern and to assess flow rate as a function of pressure drop.

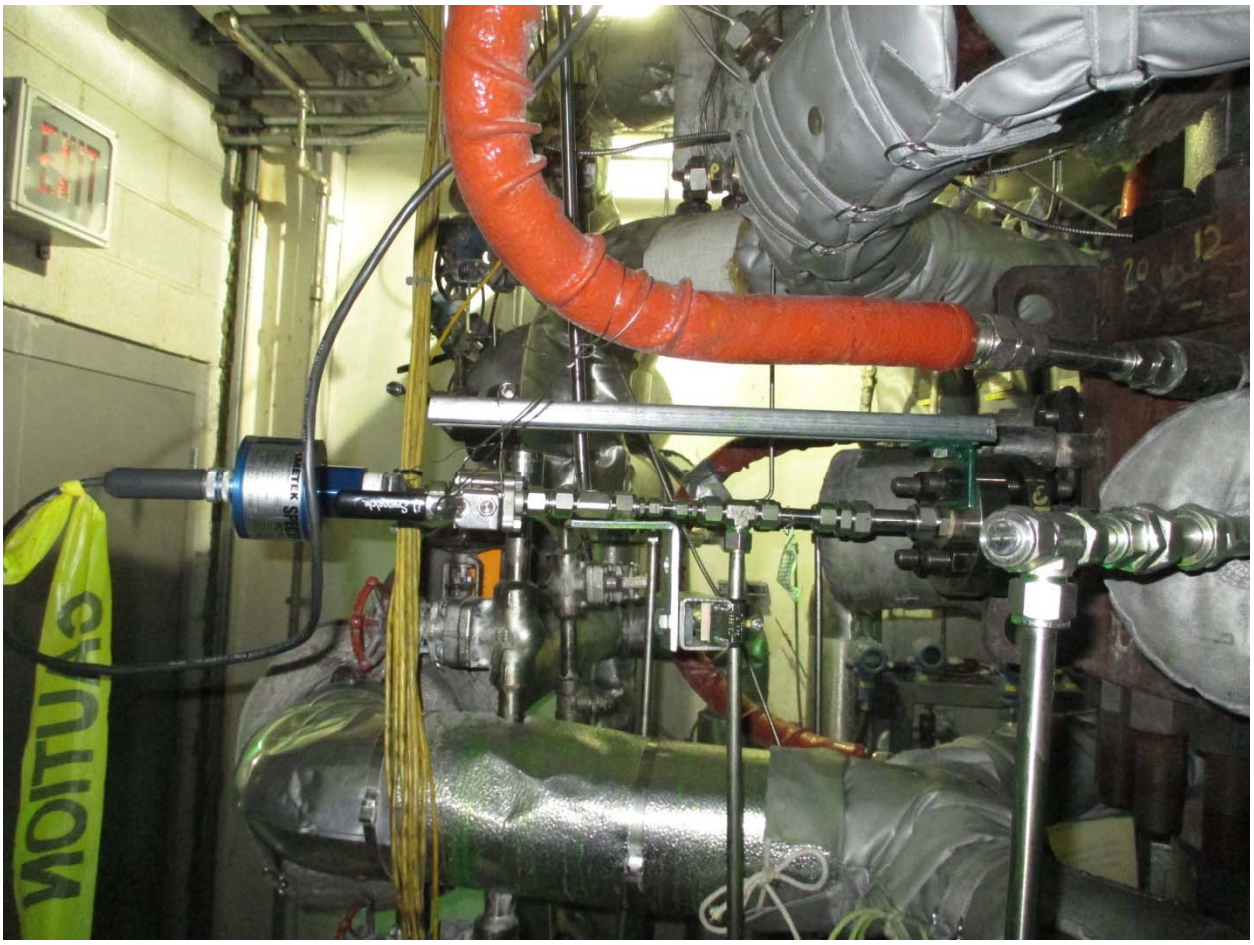

Figure 13. Wall wash lance design with integral view port passageway installed at gasifier outlet, in the same plane as the quench lances.

There are over 1,000 measured variables (inputs/outputs) in the pilot plant gasifier facility that are recorded throughout testing. Key process measurements and operational attributes are described below:

Input Streams:

Coal Preparation

Consol Energy Research & Development in South Park, PA, pulverized coal feedstocks to ~ 70% passing 200 mesh. In the process, some amount of moisture is removed from the coal as well. For all of the feedstocks, sufficient moisture was removed to allow for reliable ultra-dense phase feed transfer within the pilot plant gasifier feed line from the feed hopper to the gasifier.

Coal flow rate

Instantaneous coal flow rate is measured by a Granucor velocity meter on the feed line at the outlet from T-211, the high pressure coal feed tank. For accurate mass balance, a time-averaged flow rate is calculated from the rate of coal feed dispensed from the T-212 day bin into the T-213 lock hopper.

Oxygen flow rate

Oxygen mass flow rate is measured by in-line vortex and Coriolis flow meters just upstream of the gasifier injector.

Steam mass flow rate is measured by an in-line vortex flow meter just upstream of the gasifier injector.

N2 flow rates

There are multiple sources of nitrogen flow into the gasifier and the downstream facility. Flow of nitrogen accompanying the pulverized coal in the dense phase feed line is estimated from an orifice plate device measuring nitrogen flow into the T-211 high pressure coal feed tank, and corrected to account for the volume of coal being displaced by the nitrogen. Other purges are monitored on dedicated rotameters for each purge line. Overall on-line flow measurement of nitrogen flows to the gasifier, AGTF facility bay, and FFTF facility are used as a check against the aggregate nitrogen flows via individual measurements.

Quench water flow rate

Quench water flow rate is measured with an in-line vortex flow meter upstream of the quench spray lances.

Wall wash water flow rate

The amount of water used to displace build-up within the quench vessel is estimated from the drop in level of the T-302 cooling water surge drum, from which the wall wash water is drawn.

Slag bath flow rate

Water feed to the slag bath is measured with an in-line vortex flow meter.

Output Streams:

Syngas flow rate

Syngas flow rate is measured at two points downstream of the gasifier. The first flow measurement is at a venturi flow meter located downstream of the cyclone particulate removal device and upstream of the candle filters. This is also in close

proximity to the G8 sampling station for gas composition analysis, enabling good correction of flow meter readings for gas composition. The second measurement is taken via an orifice plate downstream of the candle filter system. This measurement is subjected to distortions due to periodic pulsing of the candle filters with nitrogen.

Coarse Slag Discharge

Coarse slag discharges from T-306 on a batch basis. The slag and water are dumped into a strainer, which allows most of the water and some fine slag/char to pass through. The wet coarse slag is dumped from the strainer into a barrel, where the weight is recorded for each dump. For DAP's 240-249, samples of the water passing through the strainer were obtained to assess solids content and composition.

Cyclone Fines Slag Discharge

Cyclone fines slag discharges from T-402 on a batch basis. The fines are dumped into a barrel, with the incremental weight of fines entering the barrel recorded.

Candle Filter Fines Slag Discharge

Candle filter fines slag discharges from T-2156 on a batch basis. The fines are dumped into a barrel, with the incremental weight of fines entering the barrel recorded.

Slag water

Slag water accompanying the T-306 discharge is estimated based on the number of discharges from T-306 during a DAP, the volume of T-306, and the estimated volume of slag discharged with the water during the DAP.

Bath water

The amount of bath water discharged from T-319 is estimated from an in-line magnetic flow element flow meter between the coarse slag surge drum T-305 and the slag bath/water surge hopper, T-317. All of the water from T-317 is discharged via T-319.

Composition:

Coal Composition

Proximate, ultimate and HHV analysis was performed for each of the Data Attainment Periods (DAP's). Table 1 below summarizes averaged coal properties for the three feedstocks tested in this project.

Table 1. Averaged coal properties for highly reactive (Powder River Basin) and high ash/high AFT (Xinyuan, Xinjing) coals tested on this project.

Coal Name	Powder River Basin	Xinyuan	Xinjing
Coal Type	Sub-bituminous	Anthracite	Anthracite
Moisture (As fed, wt%)	10.88	0.73	0.58
Ash (As fed, wt%)	6.80	25.02	23.96
Carbon (MAF, wt%)	82.32	74.25	75.45
Hydrogen (MAF, wt%)	5.05	3.93	3.57
Nitrogen (MAF, wt%)	1.01	1.31	1.30
Sulfur (MAF, wt%)	0.53	1.33	2.54
Oxygen (MAF, wt%, by difference)	19.51	4.66	4.16
HHV (MAF, BTU/lb)	12,577	14,814	14,731

Solids samples

A scoop of solids is obtained for each dump from T-306 during the course of a DAP, and accumulated in a plastic-lined 5 gallon bucket. The cumulative sample is then manually agitated with the intent of homogenizing the sample, from which a representative sample is withdrawn for analysis.

A sample thief is used to obtain fines from five separate locations in the cyclone fines slag drum and the candle filter fines slag drum for each DAP.

Slag water and bath water samples

Roughly 500 mL of T-306 slag water is obtained from each discharge of T-306 and accumulated in a carboy. The carboy is weighed, then the water decanted off through a filter to recover solids for analysis.

Roughly 500 mL of T-319 bath water is obtained at several points throughout a DAP and accumulated in a carboy for subsequent analysis. The carboy is weighed initially to obtain overall weight, then decanted and filtered to recover solids for analysis.

Gas analysis

An on-line gas chromatograph provides real-time analysis of syngas sampled upstream of the candle filters (sample location G8, shown in Figure 2). Dry syngas

composition is recorded every 2-3 minutes, providing H_2, O_2, CO, CO_2, N_2, H_2S, COS and CH_4. Additionally, for natural gas feed, the system analyzes for ethane, propane and butane.

Water content in the syngas is analyzed gravimetrically. Syngas is continuously drawn from G8, depressurized, filtered, and then cooled to condense out the moisture. Water content is determined based on the mass of water recovered relative to the amount of syngas drawn into the system during the sampling period.

Gasifier Operations

Prior to testing a pressure check is performed on the facility to ensure facility readiness for operation. Pre-heat of the ZnO beds (for H_2S and COS removal from syngas) commences after that. The test team cycles process valves and performs other process check-outs to ensure facility readiness. In general, this activity is accomplished in a 16-24 hour period preceding light-off.

The gasifier start sequence is an automated process, requiring that multiple instrumentation and manual interlocks be cleared/confirmed prior to initiation. In general, the start sequence begins with a series of inert gas purges of process lines, followed by initiation of coal flow. After confirmation of adequate coal flow rate, the start sequence enables discharge of ~0.5 lb quantity of triethyl borane (TEB) into the gasifier, followed shortly thereafter by the start of oxygen flow. TEB is hypergolic with oxygen, and provides a highly reliable start for the pilot plant gasifier. Dual IR detectors provide flame confirmation. After the start sequence completes, the Safety Instrumented System monitors the IR detectors, as well as other critical process measurements. In the event that there is an interruption in flame signal beyond a given amount of time, or indication of loss of coal flow, an emergency shutdown is triggered to place the system into a safe condition.

Only a few seconds elapse between TEB discharge and gasifier ignition. It then takes ~10 minutes for the facility to settle out at the operating system pressure and stable coal flow rate. After that, the team allows a 1-2 hour settling period to ensure stable operation prior to commencing a DAP.

Once gasifier operations are stable, the test team initiates a DAP. At that point, no changes are made to any of the gasifier operating parameters (coal, oxygen and steam flow rates) for the duration of the DAP. The team places empty barrels at each of the solids discharge points, and the barrels labeled with the specific DAP number. A DAP will typically last from 4-6 hours.

After all data points are obtained, the test team shuts down the gasifier, depressurizes the system, and begins post-test activities. Typically, the gasifier is cool enough after 4 hours to remove the injector, and after 8 hours to open the pressure vessel, enabling hardware inspections. Solid samples are obtained and consolidated for analysis. Residual coal, spent ZnO, and slag residues are consolidated for disposal. Post-test facility checks are performed (key valves, candle filters, leak checks), and any maintenance items are recorded.

Test operations run around the clock. The test crew is comprised of 8 GTI personnel (3 engineers in the Control Room – one for gasifier, one for coarse slag discharge, one for cyclone/filter slag discharge; 4 technicians in the field for solids handling, coal transfer, and general facility operations; and 1 analytical chemist for GC and sampling operations) and 1 AR engineer.

2.2 PROFILOMETRY MEASUREMENTS

The injector faceplate was subjected to measurement post-test on the Coordinate Measuring Machine at Aerojet Rocketdyne, which generates a contour across the faceplate with precision of +/- 0.001". Profiles obtained before and after this test program are compared to assess potential loss of material from the injector faceplate.

2.3 RESIDUAL CARBON CHARACTERIZATION

Samples from the solids product streams (coarse slag, T-306 slag water solids, T-319 slag bath solids, cyclone fines and filter fines) were assessed for carbon content. Those specimens that represented the greater fraction of residual carbon in gasifier products were analyzed to determine surface area and porosity of the residual char. Since these solids samples tended to be predominantly slag (carbon content ranging from 5%-40%), surface area and porosity for the residual carbon was determined by difference between the original sample and an "ashed" sample, from which the residual carbon was oxidized. The assumption here is that the difference corresponds to surface area and porosity associated with the carbon that was removed.

Full mercury-intrusion-porosimetry analyses were performed with the Micromeritics AutoPore IV instrument. This analysis covers the range of pore diameters between 0.0030 μm and 180 μm. Besides a tabulation of the intrusion-versus-pressure data, and plots of those data, also included in a typical report are one particle-density value (labeled "Bulk Density" by the Micromeritics software), normally taken at 25 psia applied pressure, and the "Apparent (Skeletal) Density" measured at the highest applied pressure, which is ≈60,000 psia.

Nitrogen surface-area analyses were performed with the Micromeritics ASAP-2010 instrument. This employs the BET (Brunauer, Emmett, and Teller) method to determine the surface area of a sample, by use of nitrogen adsorption onto the sample's surface at liquid-nitrogen temperatures. The lower limit of measurement is primarily determined by the quantity of sample which can be introduced into the instrument's sample holders (20cc of bulk volume, maximum). Surface-area measurements in the 5 - 10 m^2/g range are possible, given a large-enough volume/mass of sample.

Porosity attributed specifically to the residual carbon within the samples is obtained by comparing porosimetry data obtained on the original and "ashed" samples. Residual carbon porosity, $\boldsymbol{\varepsilon_C}$, is calculated as follows:

$$\varepsilon_C = \frac{V_C/m_C}{V_C/m_C + 1/\rho_C}$$

where the pore volume attributed to carbon, $\frac{V_C}{m_C}$, is calculated from

$$\frac{V_C}{m_C} = \frac{\left(\frac{V_T}{m_T} - (1 - X_C)\frac{V_A}{m_A}\right)}{X_C}$$

Other parameters are defined as follows:

$\frac{V_T}{m_T}$ = Total pore volume of original sample per unit mass

$\frac{V_A}{m_A}$ = Total pore volume of ashed sample per unit mass

X_C = Weight fraction of carbon in the original sample

ρ_C = Skeletal density of carbon, assumed to be 1.2 g/cm^3 for these calculations

Surface area per unit mass attributed specifically to the residual carbon, S_C, within the samples is obtained by comparing surface area data obtained on the original and "ashed" samples, and is calculated as follows:

$$S_C = \frac{S_T - S_A}{X_C}$$

where

S_T = Surface area of original sample per unit mass

S_A = Surface area of ashed sample per unit mass

X_C = Weight fraction of carbon in the original sample

3.0 RESULTS AND DISCUSSION

3.1 HIGHLY REACTIVE COAL TESTING

Low rank coals, such as lignites and sub-bituminous coals, have a tendency to be highly reactive. While this is favorable with regards to carbon conversion in a short residence time entrained flow gasifier, it raises the concern that excessive localized thermal environments may be generated in the zones where mixing and reaction of oxygen with coal occurs. This is a particular concern with the compact gasifier, where near-stoichiometric temperatures in the oxygen burn-out zone are generated due to the plug flow pattern suppressing back-mixing of relatively cool syngas.

The initial intent was to test a North Dakota lignite. However, Consol declined to process this feed due to safety concerns associated with lignite's reactivity. The University of Utah offered to pulverize the lignite, and they were successful in pulverizing the feedstock to approximately 70% passing 200 mesh. However, they did not have the facilities to dry the lignite beyond air drying, which left too much moisture (~23% by weight) in the pulverized lignite relative to the equilibrium moisture (18.5% per ASTM D1412) for it to flow suitably in a dense phase transport system.

In the absence of a viable lignite supply option, the team sought out sub-bituminous feedstocks. A Powder River Basin (PRB) coal was obtained courtesy of First Energy in Akron, Ohio, and transported to Consol for pulverization and drying. The PRB coal was dried to 10-11% moisture, which was sufficient for reliable feeding via the ultra-dense phase transport system at the pilot plant. This PRB feed was used for all of the highly reactive coal testing, as well as with natural gas in hybrid gasifier test operations.

3.1.1 Objectives

The objective of the highly reactive coal testing task was to establish the feasibility of gasifier operations on these coals, particularly with regards to the ability of gasifier internal components (injector, liner) to withstand the thermal environments generated from the conversion of these feeds. This was to be established by operating the pilot plant gasifier on PRB coal at representative conditions, with assessment of measured thermal environments relative to design conditions and inspection of the injector and liner post-test.

3.1.2 Test Results

Test conditions and results (carbon conversion, mass/energy/elemental balances) are summarized in Table 2. Data quality was acceptable, with all four data points within 10% on overall mass and energy balance. Carbon balance was within 6%.

Table 2. Test conditions and summary results for pilot plant gasifier testing on highly reactive (PRB) coal

	Highly Reactive Coal			
	DAP 240	**DAP 241**	**DAP 242**	**DAP 243**
Coal (lb/hr)	1329	1355	1302	1310
Oxygen (lb/hr)	1000	1050	1100	1050
Steam (lb/hr)	76	76	75	80
Nitrogen (lb/hr)	174.4	175.2	173.9	175.6
Conversion (%)	97.39%	98.11%	98.66%	97.40%
Mass Balance (%)	102.8%	100.8%	106.3%	108.9%
Enthalpy Balance (%)	95.4%	96.0%	99.3%	98.0%
Carbon Balance (%)	94.2%	94.0%	102.6%	97.4%
Hydrogen Balance (%)	105.0%	101.2%	105.2%	112.1%
Nitrogen Balance (%)	112.8%	114.8%	129.6%	118.3%
Sulfur Balance (%)	84.5%	84.6%	91.2%	91.7%
Oxygen Balance (%)	103.6%	100.5%	105.6%	110.5%
Moisture (As fed)	11.81	10.65	11.66	11.10
Ash (As fed)	6.66	6.51	7.14	7.97
Coal (MAF, as fed)	81.53	82.84	81.20	80.93

3.1.3 Discussion

Carbon conversion ranged from 97% to almost 99% for this highly reactive coal, even though residence time was < 0.15 seconds and outlet temperatures were approximately those expected for commercial operations. Therefore, no performance issues are expected with PRB coal.

The thermal environments measured at the injector faceplate and along the liner were found to be well within the design basis for both components. Post-test inspection showed no visible impact to hardware condition.

The partial quench system in the compact gasifier does lead to some Water Gas Shift (WGS) reaction occurring as the raw synthesis gas is cooled from the gasifier outlet temperature. While there is a significant increase in the hydrogen content relative to the predicted equilibrium syngas composition, it is still far from the equilibrium value of the final quenched gas mixture. This is because the WGS reaction kinetics slow rapidly with decreasing temperature. The relationship between the actual and predicted ratios of H_2/CO and CO_2/CO relative to predicted gasifier outlet temperature is shown in Figure 14. Actual syngas composition and predicted composition at gasifier outlet from a process simulator (ChemCAD) are shown in Table 3.

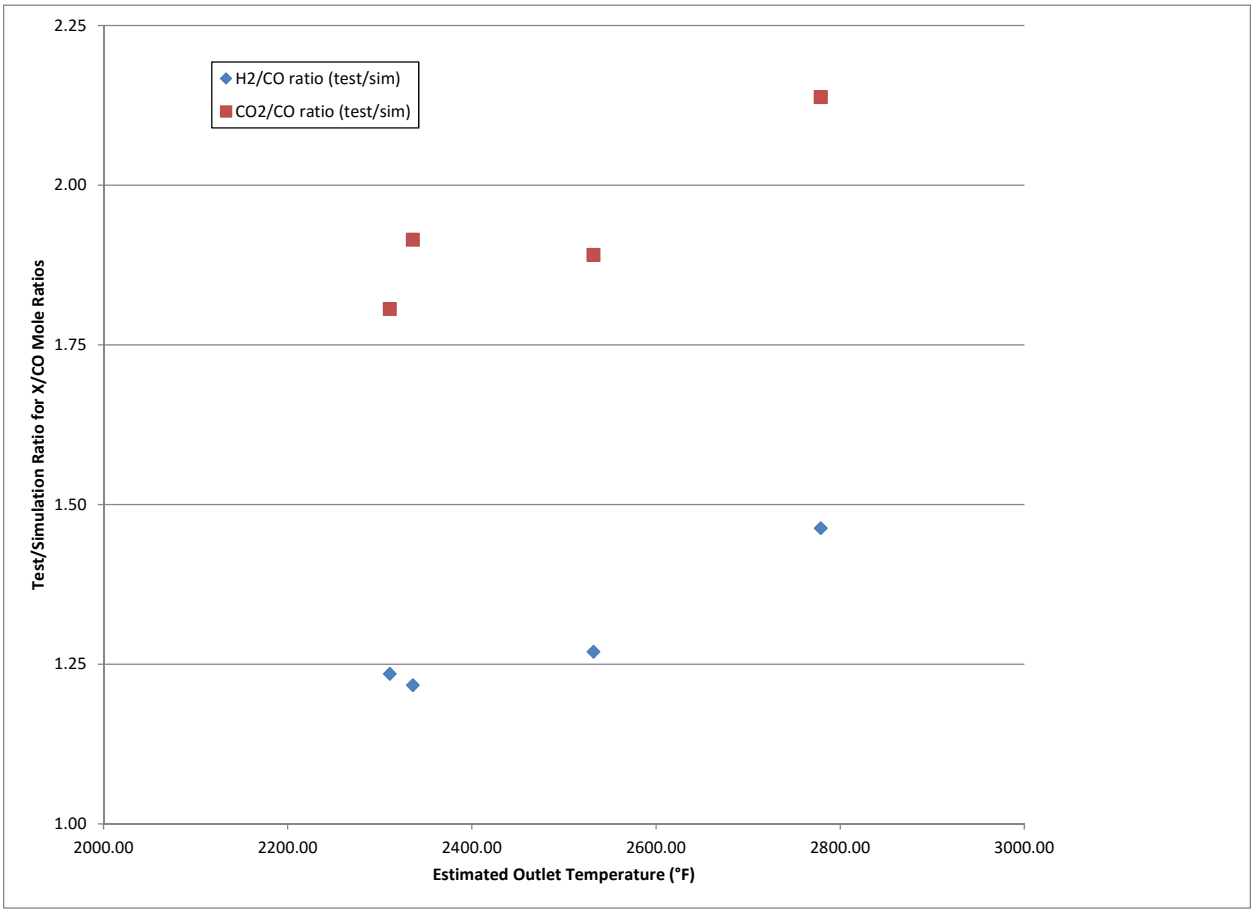

Figure 14. Ratio of test data versus predicted data for H_2/CO and CO_2/CO ratios increases with increasing estimated gasifier outlet temperature on PRB coal.

Table 3. Actual syngas composition measured downstream of gasifier and simulation predictions for gasifier outlet composition for pilot plant gasifier testing on highly reactive (PRB) coal

	Highly Reactive Coal			
	DAP 240	**DAP 241**	**DAP 242**	**DAP 243**
Coal (lb/hr)	1329	1355	1302	1310
Natural Gas (lb/hr)				
Oxygen (lb/hr)	1000	1050	1100	1050
Steam (lb/hr)	76	76	75	80
Nitrogen (lb/hr)	174.4	175.2	173.9	175.6
Conversion (%)	97.39%	98.11%	98.66%	97.40%
Actual Syngas Composition				
Carbon Dioxide	15.4%	14.7%	19.3%	17.5%
Carbon Monoxide	54.5%	56.0%	53.0%	54.3%
Carbonyl Sulfide	0.0%	0.0%	0.0%	0.0%
Hydrogen	29.8%	29.0%	27.5%	28.0%
Hydrogen Sulfide	0.2%	0.2%	0.2%	0.2%
Methane	0.2%	0.1%	0.0%	0.1%
Simulation Results				
Temp (F)	2336.00	2311.00	2779.00	2532.00
Carbon Dioxide	9.2%	9.3%	11.2%	10.8%
Carbon Monoxide	62.5%	63.7%	65.4%	63.3%
Carbonyl Sulfide	0.0%	0.0%	0.0%	0.0%
Hydrogen	28.0%	26.8%	23.2%	25.7%
Hydrogen Sulfide	0.2%	0.2%	0.2%	0.2%
Methane	0.0%	0.0%	0.0%	0.0%

3.2 HIGH ASH FUSION TEMPERATURE COAL TESTING

Conventional entrained flow gasifier technologies are severely constrained in their ability to process high ash fusion temperature (AFT) coals. For low to moderate ash levels, flux (such as limestone) may be added to reduce AFT to more manageable temperatures, preferably < 1300°C. However, for feedstocks with >20% ash by weight, the incremental penalty of introducing additional inerts has a significant negative impact on process performance and economics.

The challenges are exacerbated when the high ash, high AFT coal is also low reactivity, as these coals are insufficiently reactive for processing in lower temperature gasifier technologies that do not need to melt the ash (such as fluidized bed and fixed bed technologies). China possesses large

reserves of anthracite coals with high ash (~25%) and high AFT (>1500°C), and the coal companies that produce these reserves have stated that they have not as of yet seen a satisfactory coal gasification technology. The reactivity of residual carbon from these anthracite coals as the process approaches 100% conversion needs to be addressed. In earlier pilot plant testing on bituminous coals, it was established that performance modelling required consideration of the Thiele modulus on effective reaction rate for remaining carbon particles. Since the Thiele modulus is dependent upon residual carbon surface area and porosity, and these in turn tend to vary with carbon conversion, it would be very helpful to performance modelling at high conversion to have experimental data for these parameters in the 90%-99% carbon conversion range.

The compact gasifier provides a unique technology with much greater thermal margins to accommodate high AFT coals while providing the environments conducive to efficient gasification of low reactivity carbon. Given the extensive coal reserves of this type in China and India in search of a suitable technology, there is considerable interest in assessing performance of these coals in the pilot plant compact gasifier.

3.2.1 Objectives

The objectives of this effort were to test two high ash/high AFT (~25% ash, >1500°C AFT) anthracite coals to assess the ability of the compact gasifier to manage the associated thermal environments, to exhibit reliable slag discharge from the system, and to obtain data on the dependency of residual carbon surface area and porosimetry for the purpose of anchoring gasifier performance models at high carbon conversion.

3.2.2 Test Results

Test conditions and results (carbon conversion, mass/energy/elemental balances) are summarized in Table 4. Data quality was acceptable, with all eight data points within 10% on overall mass and energy balance. Carbon balance was within 7%. However, for DAP 230, the spread between overall mass balance and carbon balance was >10%, so this point was not used in subsequent data analysis.

Table 4. Test conditions and summary results for pilot plant gasifier testing on high ash/high AFT coals.

	Xinyuan Coal					Xinjing Coal		
	DAP 230	DAP 231	DAP 233	DAP 248	DAP 249	DAP 234	DAP 235	DAP 237
Coal (lb/hr)	1035	1096	1039	1062	1079	1070	1064	1018
Natural Gas (lb/hr)								
Oxygen (lb/hr)	1040	960	1120	1080	1040	1040	980	1120
Steam (lb/hr)	200	200	200	200	200	200	200	200
Nitrogen (lb/hr)	113.3	168.4	169.9	164	164.8	169.4	172.8	129.2
Conversion (%)	95.78%	89.28%	97.02%	96.36%	94.04%	90.08%	85.25%	96.02%
Mass Balance (%)	108.1%	104.0%	101.3%	100.0%	97.7%	104.4%	104.1%	102.6%
Enthalpy Balance (%)	92.7%	100.6%	94.9%	103.1%	96.6%	103.3%	103.9%	99.6%
Carbon Balance (%)	95.3%	99.2%	99.0%	107.0%	98.0%	105.8%	105.6%	101.8%
Hydrogen Balance (%)	117.2%	98.5%	105.2%	94.2%	94.8%	104.5%	102.7%	103.5%
Nitrogen Balance (%)	135.1%	131.3%	121.3%	131.8%	122.2%	127.5%	134.5%	126.9%
Sulfur Balance (%)	73.8%	98.5%	87.5%	102.0%	97.8%	92.7%	93.5%	85.3%
Oxygen Balance (%)	111.2%	99.0%	103.5%	96.2%	94.9%	103.0%	101.6%	102.2%
Ash Balance (%)	100.0%	100.0%	100.0%	100.0%	100.0%	100.0%	100.0%	100.0%
Heat Loss (MMBTU/hr)	0.94	0.59	0.80	0.67	0.79	0.76	0.41	1.03
Moisture (As fed)	0.53	0.64	0.53	0.89	1.05	0.65	0.52	0.58
Ash (As fed)	26.43	24.36	25.33	24.59	24.41	24.34	22.95	24.60
Coal (MAF, as fed)	73.04	75.00	74.14	74.52	74.54	75.01	76.53	74.82

3.2.3 Discussion

The thermal environments posed by these coals were well within the design capabilities of the injector and liner designs. Outlet temperatures (shown in Table 5, inferred based on process simulation using actual feed streams and measured heat losses) ranged from 3400°F to 4200°F, well above the ~3000°F target outlet temperature expected for commercial operation on these coals.

As was seen with the PRB coal, there is a significant WGS reaction in the quench zone, as indicated in Figure 15, showing actual/simulated ratios for H_2 and CO_2 relative to CO relative to inferred gasifier outlet temperature. As with PRB, higher outlet temperatures resulted in a greater apparent extent of CO conversion in the quench zone via the WGS reaction.

Carbon conversion ranged from 89% to 97% on the Xinyuan coal, and 85% to 96% on the Xinjing coal, providing a good span of carbon conversion from which to assess trends of surface area and porosity associated with the remaining carbon. Samples for analysis were taken from solid streams comprising 83%-100% of the unconverted carbon, with specific samples and carbon content shown in Table 6. Candle filter fines were typically only a small fraction of total carbon, so these were not analyzed. Carbon in T-319 bath water for later tests (after refinements in test operations) contained little of the residual carbon as well, so only the sample from DAP 231 was analyzed.

Surface area per unit residual carbon relative to carbon conversion is shown for each of the samples in Figure 16, with individual sample results summarized in Table 7. In general, values are consistent among the various sample streams for a given DAP. A similar plot, this one showing weighted surface area data for the overall DAP sample streams, is shown in Figure 17. Both coals had similar surface area values and showed similar decrease in surface area per unit residual carbon with increasing carbon conversion, with a linear trend corresponding to approximately 62 m^2/g at 85% carbon conversion, decreasing to 36 m^2/g at 97%. This significant decrease confirms the importance of incorporating treatment of surface area as a function of carbon conversion into calculation of the Thiele modulus in support of coal gasifier modelling.

Residual carbon porosity data showed much less of a trend relative to carbon conversion, as seen in Figure 18, with individual sample results summarized in Table 8. The Xinyuan coal porosity tended to range between 50%-60%. Xinjing coal tended to range between 70% and 80%, with one of the four points at about 50%. In the absence of a clear trend, and in the interest of forming a conservative assessment of carbon conversion in gasifier modelling, it is recommended that a constant porosity value of 50% be used in model calculations.

Table 5. Actual syngas composition measured downstream of gasifier and simulation predictions for gasifier outlet composition for pilot plant gasifier testing on high ash/high AFT coals.

	Xinyuan Coal					Xinjing Coal		
	DAP 230	**DAP 231**	**DAP 233**	**DAP 248**	**DAP 249**	**DAP 234**	**DAP 235**	**DAP 237**
Coal (lb/hr)	1035	1096	1039	1062	1079	1070	1064	1018
Natural Gas (lb/hr)								
Oxygen (lb/hr)	1040	960	1120	1080	1040	1040	980	1120
Steam (lb/hr)	200	200	200	200	200	200	200	200
Nitrogen (lb/hr)	113.3	168.4	169.9	164	164.8	169.4	172.8	129.2
Conversion (%)	95.78%	89.28%	97.02%	96.36%	94.04%	90.08%	85.25%	96.02%
Actual Syngas Composition								
Carbon Dioxide	23.5%	17.9%	25.1%	23.1%	20.3%	19.9%	19.2%	26.3%
Carbon Monoxide	50.2%	54.0%	49.2%	49.2%	51.0%	53.2%	52.8%	48.4%
Carbonyl Sulfide	0.0%	0.0%	0.0%	0.0%	0.0%	0.1%	0.1%	0.1%
Hydrogen	26.0%	27.6%	25.2%	27.3%	28.2%	26.1%	27.2%	24.5%
Hydrogen Sulfide	0.3%	0.4%	0.4%	0.4%	0.4%	0.7%	0.7%	0.7%
Methane	0.0%	0.0%	0.0%	0.0%	0.0%	0.0%	0.0%	0.0%
Simulation Results								
Temp (F)	3744.00	3423.00	4181.00	3967.00	3613.00	3925.00	4108.00	4197.00
Carbon Dioxide	15.4%	14.9%	17.2%	14.4%	14.3%	18.4%	20.5%	19.8%
Carbon Monoxide	67.0%	59.1%	68.0%	67.7%	65.0%	61.2%	55.0%	66.7%
Carbonyl Sulfide	0.2%	0.1%	0.3%	0.2%	0.1%	0.3%	0.4%	0.7%
Hydrogen	17.1%	25.6%	14.3%	17.4%	20.3%	19.5%	23.6%	12.5%
Hydrogen Sulfide	0.3%	0.4%	0.2%	0.3%	0.4%	0.6%	0.6%	0.3%
Methane	0.0%	0.0%	0.0%	0.0%	0.0%	0.0%	0.0%	0.0%

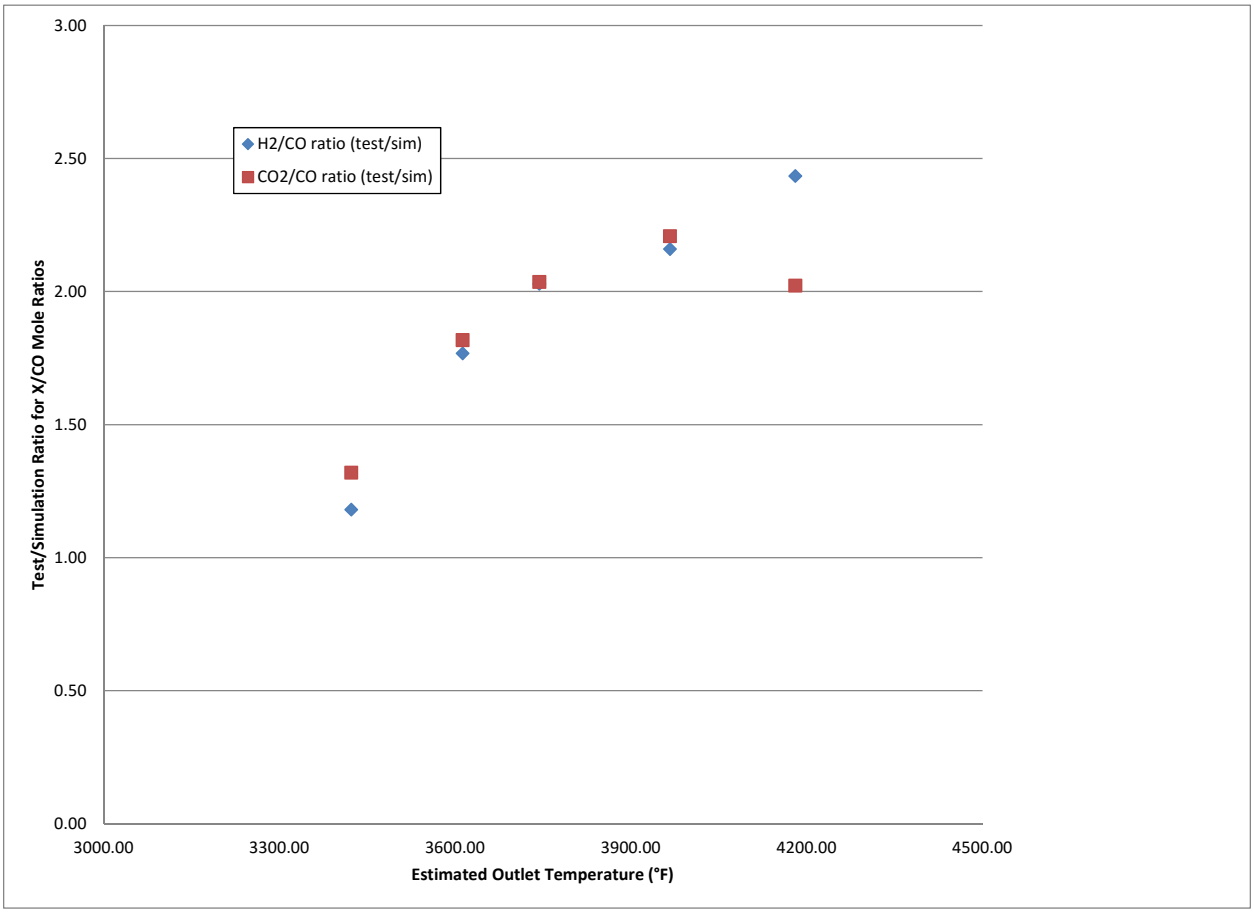

Figure 15. Ratio of test data versus predicted data for H_2/CO and CO_2/CO ratios increases with increasing estimated gasifier outlet temperature for Xinyuan coal.

Table 6. Residual carbon content in the solids streams from pilot plant gasifier testing on high ash/high AFT coals. Cells highlighted in green correspond to samples that were submitted for surface area and porosity analysis.

	Xinyuan Coal					Xinjing Coal		
	DAP 230	**DAP 231**	**DAP 233**	**DAP 248**	**DAP 249**	**DAP 234**	**DAP 235**	**DAP 237**
Coal (lb/hr)	1035	1096	1039	1062	1079	1070	1064	1018
Natural Gas (lb/hr)								
Oxygen (lb/hr)	1040	960	1120	1080	1040	1040	980	1120
Steam (lb/hr)	200	200	200	200	200	200	200	200
Nitrogen (lb/hr)	113.3	168.4	169.9	164	164.8	169.4	172.8	129.2
Conversion (%)	95.78%	89.28%	97.02%	96.36%	94.04%	90.08%	85.25%	96.02%
Unconverted C (lb atom/hr)								
Slag	1.2	2.6	1.4	1	1.5	4.9	6.9	1.6
T-306 Slag Water	N/A	N/A	N/A	0.7	0.6	N/A	N/A	N/A
Cyclone	0.5	1.9	0.2	0.3	0.9	0.8	1.6	0.5
Filter	0.1	0.1	0	0	0.4	0	0.1	0
T-319 Bath Water	0.6	1.9	0	0.1	0.2	0.1	0.2	0.1

Table 7. Surface area analyses results for solids samples.

	Raw Sample		Ashed Sample				
Description	BET surface area, m^2/g	%C	BET surface area, m^2/g	%C	Net Area	Net % C	**Carbon surface area, m^2/g**
DAP-231 Coarse slag solids	**9.16**	14.44	**0.45**	0.06	8.71	14.38	**60.57**
DAP-233 Coarse slag solids	**2.58**	6.52	**0.29**	0.02	2.29	6.5	**35.23**
DAP-234 Coarse slag solids	**12.47**	24.15	**0.51**	0.01	11.96	24.14	**49.54**
DAP-235 Coarse slag solids	**18.33**	28.9	**0.60**	0.03	17.73	28.87	**61.41**
DAP-237 Coarse slag solids	**3.84**	8.38	**0.40**	0.01	3.44	8.37	**41.10**
DAP-231 Cyclone Fines	**19.14**	35.39	**1.00**	0.03	18.14	35.36	**51.30**
DAP-233 Cyclone Fines	**5.03**	7.86	**1.34**	0.01	3.69	7.85	**47.01**
DAP-234 Cyclone Fines	**17.68**	32.1	**1.13**	0.01	16.55	32.09	**51.57**
DAP-235 Cyclone Fines	**30.32**	45.42	**1.21**	0.03	29.11	45.39	**64.13**
DAP-237 Cyclone Fines	**9.55**	19.06	**1.17**	0.01	8.38	19.05	**43.99**
DAP-231 Slag bath water solids	**23.69**	39.99	**1.44**	0.02	22.25	39.97	**55.67**
DAP-248 Coarse slag solids	**3.02**	6.88	**0.37**	0.01	2.65	6.87	**38.57**
DAP-249 Coarse slag solids	**5.03**	10.03	**0.35**	0.01	4.68	10.02	**46.71**
DAP-248 T-306 Slag Water Solids	**9.11**	15.73	**0.89**	0.01	8.22	15.72	**52.29**
DAP-249 T-306 Slag Water Solids	**12.08**	18.17	**0.85**	0.01	11.23	18.16	**61.84**
DAP-248 Cyclone Fines	**6.61**	11.05	**1.23**	0.01	5.38	11.04	**48.73**
DAP-249 Cyclone Fines	**12.00**	22.99	**1.08**	0.04	10.92	22.95	**47.58**

Table 8. Porosity analyses results for solids samples.

	Raw Sample			Ashed Sample				
Description	Total Intrusion Volume (mL/g)	Apparent Density (g/mL)	%C	Total Intrusion Volume (mL/g)	Apparent Density (g/mL)	%C	Intrusion Volume For Carbon (mL/g)	**Carbon Porosity (%)**
DAP-231 Coarse slag solids	0.7787	1.9562	14.44%	0.1562	2.2848	0.06%	4.4671	**84.28%**
DAP-233 Coarse slag solids	0.3858	2.2859	6.52%	0.1316	2.3270	0.02%	4.0304	**82.87%**
DAP-234 Coarse slag solids	0.4248	2.0681	24.15%	0.1296	2.3879	0.01%	1.3520	**61.87%**
DAP-235 Coarse slag solids	0.4846	1.9781	28.90%	0.2210	2.3080	0.03%	1.1331	**57.62%**
DAP-237 Coarse slag solids	0.2025	2.2662	8.38%	0.1197	2.4724	0.01%	1.1078	**57.07%**
DAP-231 Cyclone Fines	1.4642	1.8333	35.59%	0.4674	2.0372	0.03%	3.2682	**79.68%**
DAP-233 Cyclone Fines	0.6759	2.0771	7.86%	0.6148	2.1190	0.01%	1.3922	**62.56%**
DAP-234 Cyclone Fines	0.7054	1.6821	32.10%	0.5219	2.2577	0.01%	1.0936	**56.75%**
DAP-235 Cyclone Fines	0.8985	1.7641	45.42%	0.5449	2.3022	0.03%	1.3234	**61.36%**
DAP-237 Cyclone Fines	0.5113	2.0518	19.06%	0.5392	2.1659	0.01%	0.3928	**32.04%**
DAP-231 Slag bath water solids	1.7909	1.5360	39.99%	0.5359	2.0543	0.02%	3.6742	**81.51%**
DAP-248 Coarse slag solids	0.1724	2.3141	6.88%	0.1544	2.3679	0.01%	0.4160	**33.30%**
DAP-249 Coarse slag solids	0.3037	2.1538	10.03%	0.1709	2.2858	0.01%	1.4949	**64.21%**
DAP-248 T-306 Slag Water Solids	0.5512	2.0763	15.73%	0.2912	2.2387	0.01%	1.9441	**70.00%**
DAP-249 T-306 Slag Water Solids	0.6771	2.0827	18.17%	0.3225	2.2741	0.01%	2.2741	**73.18%**
DAP-248 Cyclone Fines	0.6234	1.9263	11.05%	0.5819	2.1913	0.01%	0.9575	**53.47%**
DAP-249 Cyclone Fines	0.8963	1.9590	22.99%	0.5088	1.9952	0.04%	2.1943	**72.48%**

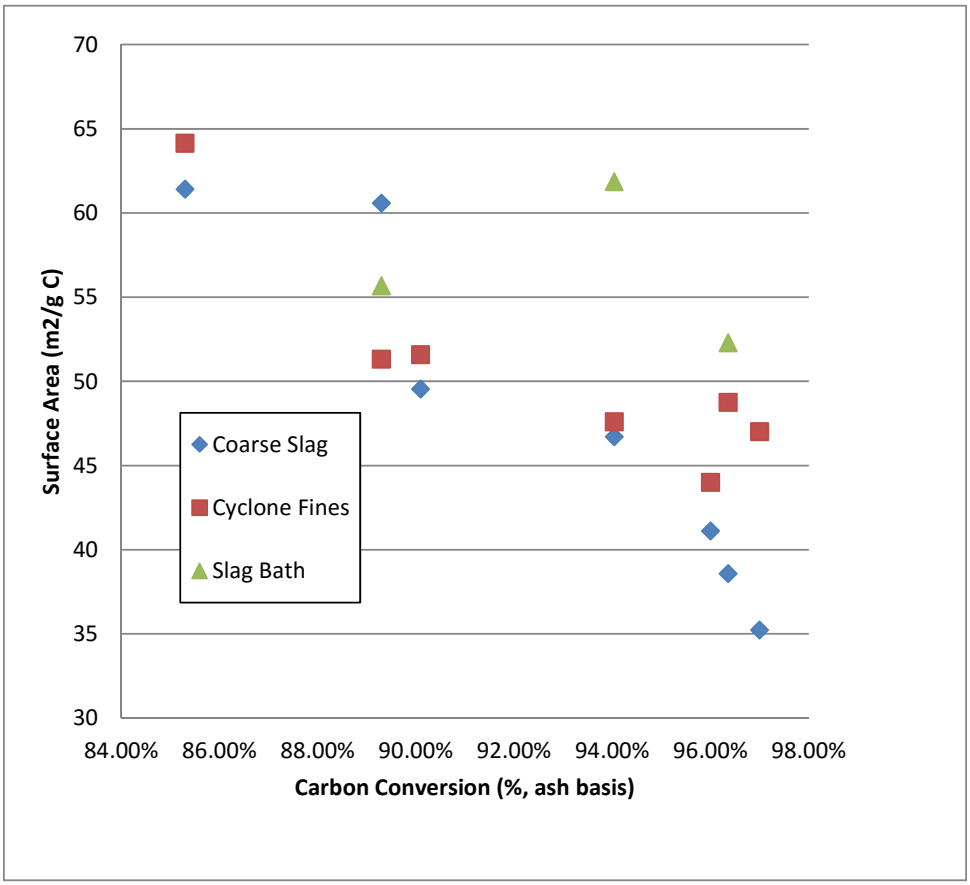

Figure 16. Surface area per unit of residual carbon plotted against carbon conversion for the high ash/high AFT coal data points.

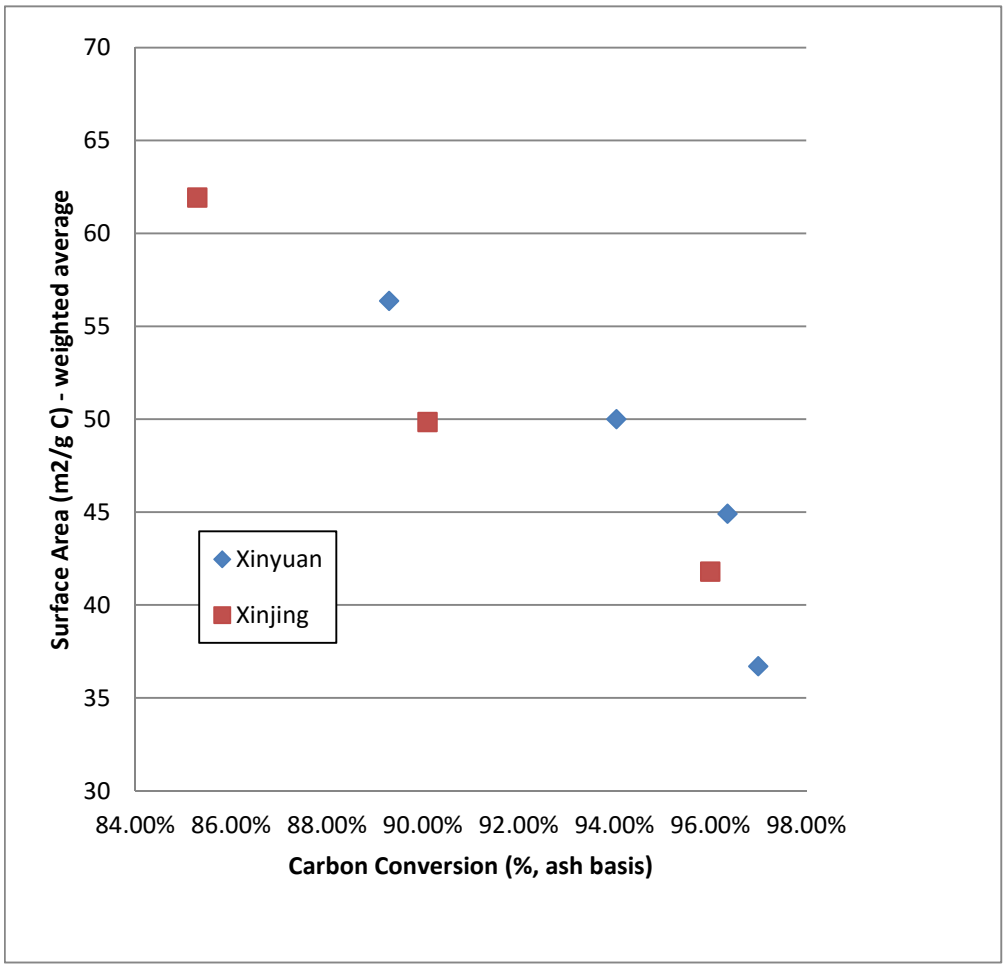

Figure 17. Surface area per unit of residual carbon for each of the high ash/high AFT DAP's, weighted corresponding to carbon content in each of the sample streams.

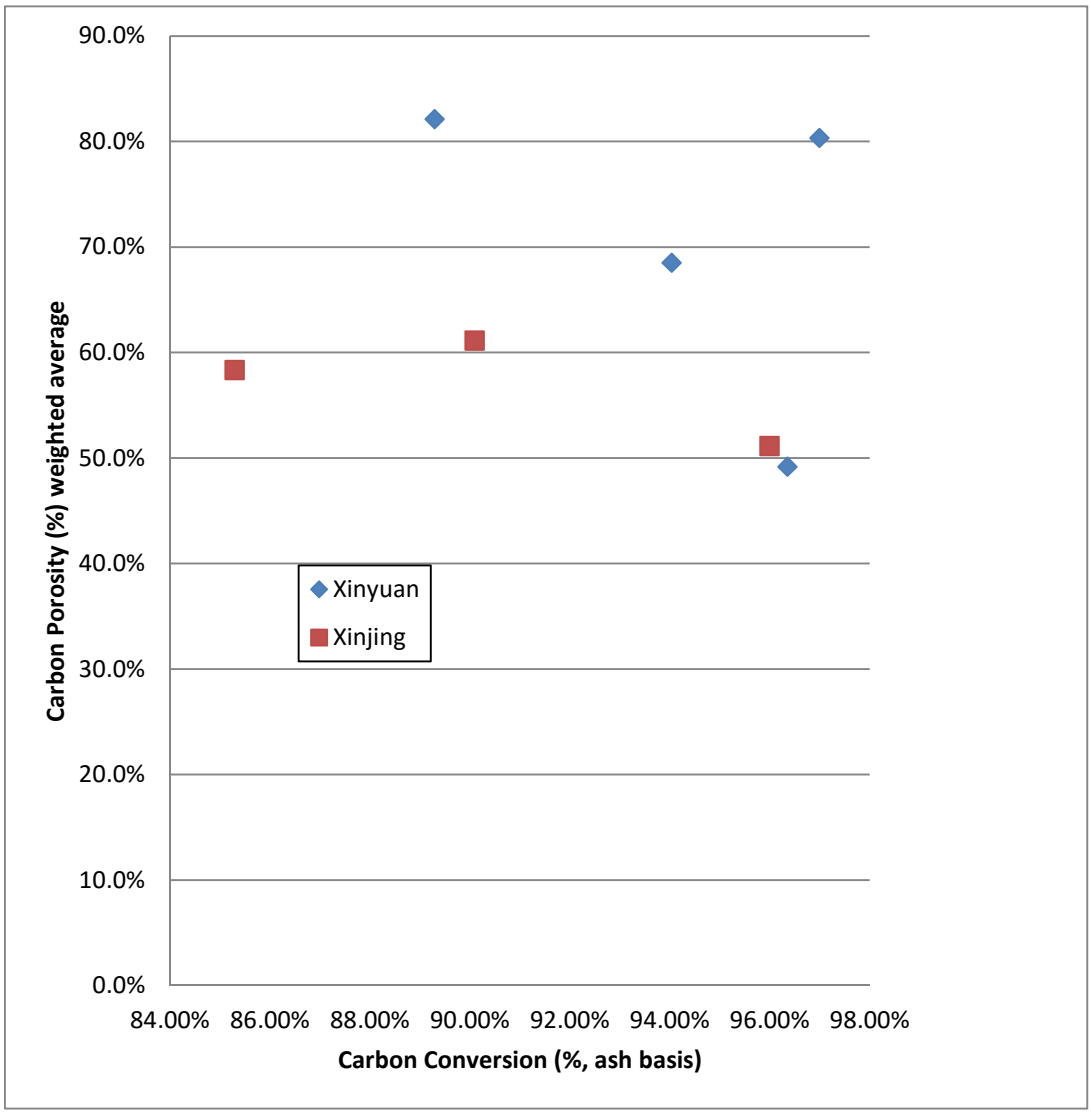

Figure 18. Porosity of residual carbon for each of the high ash/high AFT DAP's, weighted corresponding to carbon content in each of the sample streams.

The injector and liner were inspected after testing was completed. The liner was completely covered with slag which conformed to the contours of the liner in the zone with the most severe thermal environment, and a thicker layer of slag deposited in the cooler zone. The injector was removed and returned to AR for profilometry, with results shown in Figure 19. This evaluation showed that no greater than 0.001" of material was lost over the course of 160 hours of additional testing. For cumulative hot fire test time of >900 hours, this injector has shown no measurable loss of parent material. Delamination of the ~ 0.005" thick erosion barrier was observed in the zone with most severe thermal environment (corresponding to the "dips" in the plots), but it appears that cooling is sufficient to prevent any corrosion or erosion of the parent material.

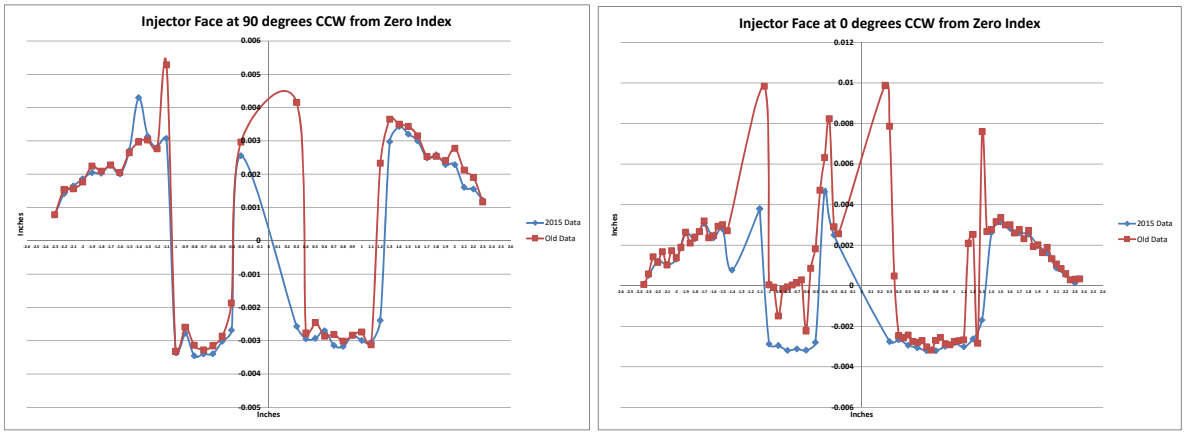

Figure 19. Profilometer traverses of the injector faceplate, showing loss of ~ 0.005" erosion resistant layer but no loss of parent material.

3.3 HYBRID GASIFICATION TESTING

The recent emergence of large volumes of relatively inexpensive natural gas reserves via shale hydraulic fracturing (fracking) in North America, coupled with interest in reducing the carbon emissions associated with coal conversion to power and chemicals, led to an interest in assessing the feasibility and impact of co-firing natural gas with coal in entrained flow gasifiers.

Such a capability over a meaningful range (up to 50% natural gas by HHV) could provide significant flexibility for power and chemical plants to achieve GHG emissions targets with reduced need for Water Gas Shift reactors and lower CO_2 removal requirements.

3.3.1 Objectives

The objectives for this effort were to demonstrate the feasibility of hybrid coal/natural gas operations up to a maximum natural gas content of 49% (HHV basis), and to use these data as the basis for predicting commercial-scale gasifier syngas composition with hybrid operations.

3.3.2 Test Results

Test conditions and results (carbon conversion, mass/energy/elemental balances) are summarized in Table 9. Data quality was good, with all four data points within 10% on overall mass and energy balance. Carbon balances were also within 10%. Within the constraints imposed by facility natural gas supply capabilities, testing was run at data points ranging from 17% to 34% natural gas on an HHV basis.

Table 9. Test conditions and summary results for pilot plant gasifier testing in hybrid mode with natural gas and PRB coal.

	Hybrid Testing			
	DAP 244	**DAP 245**	**DAP 246**	**DAP 247**
Coal (lb/hr)	1164	1126	1048	1077
Natural Gas (lb/hr)	125	225	275	150
Oxygen (lb/hr)	1050	1150	1160	1035
Steam (lb/hr)	75	74	73	74
Nitrogen (lb/hr)	171.6	170.1	160.2	162.3
Conversion (%)	95.51%	95.36%	93.86%	94.34%
Mass Balance (%)	97.6%	98.3%	100.2%	106.8%
Enthalpy Balance (%)	93.9%	95.7%	95.9%	101.4%
Carbon Balance (%)	90.3%	91.8%	93.7%	98.6%
Hydrogen Balance (%)	97.0%	97.6%	98.8%	107.8%
Nitrogen Balance (%)	119.7%	113.4%	129.8%	129.8%
Sulfur Balance (%)	79.9%	84.3%	80.8%	89.0%
Oxygen Balance (%)	97.1%	97.3%	98.9%	107.0%
Ash Balance (%)	100.0%	100.0%	100.0%	100.0%
Heat Loss (MMBTU/hr)	1.08	1.25	1.25	1.25
Moisture (Aa fed)	9.83	10.62	9.84	11.52
Ash (As fed)	6.65	6.56	6.53	6.38
Coal (MAF, as fed)	83.52	82.82	83.63	82.10
NG HHV/ Total HHV (%)	17.2%	27.9%	33.6%	21.2%

3.3.3 Discussion

Actual and predicted syngas compositions are shown in Table 10. The general intent was to maintain outlet temperatures close to 2300°F to minimize variation of outlet gas composition due to change in outlet temperature. Changes due to WGS reaction in the quench zone were small compared to other testing, perhaps due to the increased presence of H_2 in the syngas to begin with, in addition to the relatively low temperature at the outlet.

The measured impact of natural gas input on syngas composition is shown in Figure 20. There is a significant increase in H_2/CO ratio with increasing fraction of natural gas in the feed. At 50% natural gas on an HHV basis, predicted H_2/CO ratio is 0.93 as compared to 0.52 for PRB without any natural gas. This corresponds approximately to 0.78 moles of ($CO+CO_2$) for every mole of

($CO+H_2$) for operations on 100% PRB, versus 0.63 for hybrid operation at 50% natural gas. For an IGCC operation, hybrid operations could result in 20% reduction in CO_2 emissions for the same power output.

Table 10. Actual syngas composition measured downstream of gasifier and simulation predictions for gasifier outlet composition for pilot plant gasifier testing in hybrid mode with natural gas and PRB coal.

	Hybrid Testing			
	DAP 244	**DAP 245**	**DAP 246**	**DAP 247**
Coal (lb/hr)	1164	1126	1048	1077
Natural Gas (lb/hr)	125	225	275	150
Oxygen (lb/hr)	1050	1150	1160	1035
Steam (lb/hr)	75	74	73	74
Nitrogen (lb/hr)	171.6	170.1	160.2	162.3
Conversion (%)	95.51%	95.36%	93.86%	94.34%
Actual Syngas Composition				
Carbon Dioxide	13.2%	10.8%	10.8%	12.6%
Carbon Monoxide	51.6%	50.8%	49.2%	51.4%
Carbonyl Sulfide	0.0%	0.0%	0.0%	0.0%
Hydrogen	34.7%	37.8%	39.1%	35.5%
Hydrogen Sulfide	0.1%	0.1%	0.1%	0.1%
Methane	0.3%	0.5%	0.7%	0.3%
Simulation Results				
Temp (F)	2360.00	2226.00	2267.00	2291.00
Carbon Dioxide	9.3%	8.3%	8.9%	10.1%
Carbon Monoxide	56.0%	53.0%	50.0%	54.0%
Carbonyl Sulfide	0.0%	0.0%	0.0%	0.0%
Hydrogen	34.5%	38.5%	40.9%	35.7%
Hydrogen Sulfide	0.2%	0.1%	0.1%	0.1%
Methane	0.0%	0.0%	0.0%	0.0%

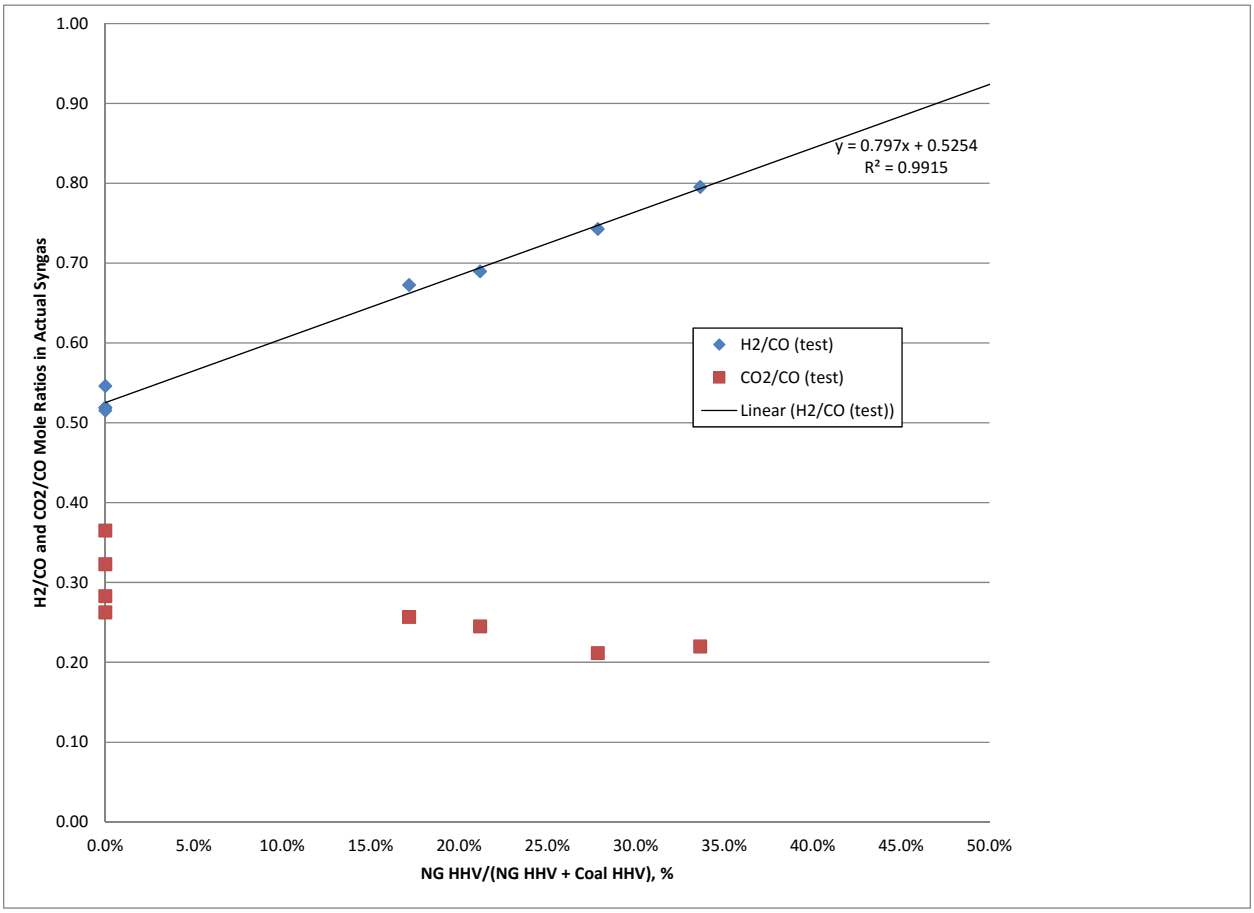

Figure 20. Impact of natural gas content in hybrid gasifier operations on the ratio of hydrogen to carbon monoxide in the syngas product.

Hybrid operation is predicted to have a significant impact on H2/CO ratio in the product syngas, carbon content per unit syngas produced, and consumption of oxygen per unit syngas produced. Commercial scale performance predictions on PRB, Illinois #6, and Xinyuan coal are presented in Table 11. Product gas H2/CO ratio increases by ~0.5 for all three cases. The amount of carbon per unit useful syngas, $(CO + CO_2)/(CO + H_2)$, decreases by approximately 25% for hybrid operations. And oxygen consumption per unit syngas decreases by 5%-10%, depending upon coal type. Clearly, hybrid operation presents interesting options for decreasing the carbon intensity of coal conversion, as well as for debottlenecking of a gasification plant constrained by Air Separation Unit capacity.

Table 11. Comparison of predicted commercial-scale coal-based and hybrid coal/natural gas operations for PRB, Illinois #6, and Xinyuan coals. Cases are based on 49% natural gas feed on an HHV basis.

	PRB		Illinois #6		Xinyuan	
	Coal	Hybrid	Coal	Hybrid	Coal	Hybrid
Coal (lb/hr)	234920	118890	187300	96030	227210	114000
Nitrogen (lb/hr)	12216	6182	9740	5100	11815	5900
Oxygen (lb/hr)	148660	140000	143650	136460	176850	162230
Steam (lb/hr)	0	0	40000	0	40000	0
NG (CH4), (lb/hr)	0	49521	0	49255	0	52123
Temp (F)	2301	2302	2501	2501	3000	3000
H2/CO	0.47	0.92	0.74	1.15	0.72	1.23
(CO+CO2)/(H2+CO)	0.71	0.55	0.67	0.52	0.76	0.57
O2/(CO+H2), (lb/lb mol)	8.99	8.46	8.67	8.24	10.70	9.75

4.0 CONCLUSIONS

- Thermal environments were more challenging for the highly reactive sub-bituminous coal as compared to other feedstocks, but were well within design capabilities of gasifier components.

- High ash + high AFT coals can be processed, with continuous slag discharge successfully demonstrated. The gasifier was operated at outlet temperatures as high as 2350°C, which was still well within thermal margins of gasifier design.

- The trend of surface area and porosity in residual carbon as a function of carbon conversion was established for the anthracitic high ash, high AFT coals, and can be used to enhance performance models in support of more accurate gasifier sizing to achieve target carbon conversion.

- No measurable loss of parent material greater than 0.001" was observed for the injector faceplate over a cumulative total of >900 hours of operation. The injector faceplate design appears to be feasible for providing long injector life. The gasifier liner was completely covered with slag, which is expected to provide good protection of the underlying parent material in support of achieving liner life goals.

- Hybrid operations demonstrated up to 34% natural gas on a HHV basis. Operations at 50% or more natural gas content appears feasible, with significant improvement in H_2/CO ratio, reduction in carbon emissions per unit syngas, and reduced oxygen consumption per unit syngas the expected benefits.

September 2016

Subtask 4.1/4.2 Topical Report: Catalyst Development and Performance Testing for Advanced Water Gas Shift Process

DOE/NETL Cooperative Agreement: DE-FE0023577
Reporting Period Start: February 1, 2015
Reporting Period End: September 30, 2015

Authors: J.P. Shen, P. Sharma, D. Denton, and B. Turk

Submitted By

RTI International
P.O. Box 12194
Research Triangle Park, NC
27709-2194
http://www.rti.org/

Disclaimer

This report was prepared as an account of work sponsored by an agency of the United States Government. Neither the United States Government nor any agency thereof, nor any of their employees, makes any warranty, express or implied, or assumes any legal liability or responsibility for the accuracy, completeness, or usefulness of any information, apparatus, product, or process disclosed, or represents that its use would not infringe privately owned rights. Reference herein to any specific commercial product, process, or service by trade name, trademark, manufacturer, or otherwise does not necessarily constitute or imply its endorsement, recommendation, or favoring by the United State Government or any agency thereof. The views and opinions of authors expressed therein do not necessarily state or reflect those of the United States Government or any agency thereof.

Abstract

RTI is developing an advanced transport reactor-based water gas shift (ATWGS) process that has lower costs and higher thermal efficiency than conventional fixed-bed water gas shift (WGS) processes. A key requirement for RTI's ATWGS process is a fluidizable and attrition resistant WGS catalyst. Based on a promising fluidizable iron-based (Fe-based) catalyst formulation identified in DOE/NETL Cooperative Agreement DE-FE0012066, the primary objective in this project was development of this promising catalyst formulation to optimize its performance and attrition resistance for RTI's ATWGS process. The optimization success criteria included catalyst activity equal to or better than commercial fixed-bed WGS catalyst, stable activity for 200 hours of continuous operation, and an attrition value equal to or better than commercial fluid catalytic cracking (FCC) catalyst.

Through the catalyst development conducted in this project, we examined the effects of varying the iron content, promoter type and content, support materials, and preparation procedures on performance and attrition resistance. Our efforts demonstrated that increasing iron content did result in increased catalytic activity, but also resulted in a relatively large drop in attrition resistance. Copper, which is one of the standard promoters used in commercial WGS catalysts, promoted increased catalytic activity, but also resulted in lower attrition resistance as the copper concentration increased. By optimizing the composition of the catalyst formulation for iron and copper content, we developed a catalyst formulation which had a stable CO conversion of about 75% for over 200 hours and an attrition value essentially identical to FCC catalyst. For our final optimization of our catalyst formulation, we expanded our success criteria to include optimizing the catalyst preparation for minimizing cost and environmental emissions during commercial production. The optimized formulation identified in the last round of our optimization efforts had a stable CO conversion of about 77%, essentially identical to commercial fixed-bed WGS catalysts, for 500 hours and an attrition value slightly better than FCC catalysts. With this optimized catalyst formulation, RTI is ready to move forward to making a limited commercial production batch for supporting a pilot-scale demonstration of RTI's ATWGS process.

One specific advantage of all the catalyst formulations prepared under this project has been the absence of chromium. Chromium is a key component in commercial high-temperature WGS catalysts. The toxic nature of hexavalent chromium ion increases the risk for human exposure in the production process and in the eventual disposal of the spent catalyst. Because none of the catalyst formulations developed in this project contain any chromium, our optimal catalyst formulation is more environmentally friendly than standard commercial high-temperature WGS catalysts.

Table of Contents

List of Tables

List of Figures

Number Page

Executive Summary

A technical feasibility evaluation of RTI's advanced transport reactor-based water gas shift (ATWGS) process completed under DOE/NETL cooperative agreement DE-FE0012066 demonstrated that:

- RTI's ATWGS process has significant economic benefits, with lower capital costs and lower parasitic load, over conventional fixed-bed water gas shift (WGS) processes.
- RTI had a viable candidate iron-based (Fe-based) catalyst formulation for the ATWGS process that had demonstrated a stable CO conversion similar to a commercial fixed-bed WGS catalyst (72% RTI vs. 78% commercial) for about 500 hours of continuous operation with an attrition value lower than equilibrium fluid cataltytic cracking (FCC) catalyst.

Although RTI's candidate formulation was extremely well suited for the ATWGS process, it was actually designed for a different application. As the objective for DOE/NETL cooperative agreement DE-FE0012066 was technical feasibility evaluation of the ATWGS concept, essentially no catalyst development/optimization was performed. In this project, the key objective was to optimize RTI's Fe-based catalyst formulation for RTI's ATWGS process. Defined optimizatiuon criteria were established, which included:

- Catalyst activity similar to or greater than commercial fioxed-bed catalyst,
- Demonstration of stable performance for 200 hours of operation, and
- An attriton value similar to or better that equilibrium FCC catalysts.

Using this set of criteria to evaluate catalyst formulations, series of catalyst formulations were synthesized, characterized and tested with varying iron content, promoter type and content, stabilizers/supports, and process conditions with the objective of preparing an optimized catalyst formulation for the ATWGS process. We attempted to effectively leverage the available expertise and knowledge that has been employed to optimize the commercial fixed-bed catalyst, by using this knowledge base as a yardstick to guide our selection of the most promising variations to test. From our catalyst development efforts were have discovered the following trends:

- Catalyst formulations with increasing the iron content (from 0 to 65%) demonstrated higher WGS catalyst activity; however, the attrition resistance of the higher iron content formulations was significantly lower when the iron oxide content was >50%. For catalyst formulations with iron oxide content ≤50%, catalyst attrition (0.97 to 1.57%) was found to be comparable or better than the targeted value (≤6.0%). When the iron oxide content was ≥50%, the resulting formulations did not meet our attrition criterion. The XRD patterns showed as the iron content was increased, that at ≥50%, the iron oxide and support phases both became significantly less crystalline and more amorphous. It is this decrease

in the the crystalline nature of the support that is believed to cause the significant change in attriton resistance.

- Catalyst formulations with varying Cu content (0 to 10%) showed that higher Cu content (10%) exhibited higher catalyst activity. The attrition resistance was also observed to decrease with increasing in Cu content. However, at the maximum Cu conent tested, the catalyst formulation's attriton value still met our attriton criterion (~6.0% attrition).
- All other promoters tested had no change or actually adversely affected catalyst performance or attrtition resistance.

From this work, we identified an optimized catalyst formulation (13838-33B) that we completed a long term stability test in which this formulation demonstrated a stable CO conversion of about 75% (78% for commercial) with an attrition value of about 6%.

Although this catalyst formulation met the objectives of this project, RTI used our expertise on commercial production of catalysts to complete an additional optimization study which added minimizing cost and environmental emissions to our set of optimization criteria. This optimized catalyst formulation (13838-87) from this second optimization study was based on lower cost precursors which also resulted in less environmental emissions during the preparation process. During long term stability testing, this catalyst formulation demonstrated a stable CO conversion of 77% (essentially equal to the 78% for commercial catalysts) with an attrition value of 5.8%. Based on its optimized performance and production benefits this optimized catalyst formulation was chosen as our final optimized and recommended ATWGS catalyst formulation for this project.

Based on the catalyst development efforts completed in this project, we have been able to identify two optimized catalyst formulations (13838-33B and 13838-87) that represent an improvement over the original baseline catalyst formulation and meet all the catalyst development criteria for WGS activity, long-term stability, and attrition resistance. Our recommended catalyst formulation also offers lower production costs and reduced emission during production. One specific advantage of all the catalyst formulations prepared under this project has been the absence of chromium. These catalyst formulations are more environmentally friendly than standard commercial high-temperature WGS catalysts, because the absence of chromium reduces the potential for human exposure or release of the toxic hexavalent chromium ion during production and handling and disposal of the spent catalyst.

1. Introduction

In the U.S. Department of Energy National Energy Technology Laboratory (DOE/NETL) Cooperative Agreement DE-FE-0012066, RTI completed a technical feasibility analysis of a novel concept for enriching the hydrogen concentration in a syngas mixture based on a process consisting of fluidized-bed water gas shift (WGS) catalysts and a transport reactor coupled with a solids cooler. The combination of a transport reactor and solids cooler upon which this novel concept was based was shown to provide an effective means of capturing a significant portion of the reaction heat generated in the reactor and transferring this heat to the solids cooler for steam generation. Because the catalyst was capturing a significant portion of the reaction heat, the reactor also operated at lower temperature promoting more favorable thermodynamic conditions and greater carbon monoxide (CO) conversion. The results from the technical feasibility evaluation indicated that the concept was technically sound and that there was a significant economic benefit over conventional fixed-bed WGS reactor systems. As one of the key components of this novel process was the fluid-bed WGS catalyst, RTI tested one or two candidate fluidized-bed catalyst formulations for typical low temperature sweet WGS (LT-WGS), high temperature sweet WGS (HT-WGS), and sour WGS commercial applications.

The three fundamental criteria for suitable fluidized-bed formulations were:

- Attrition resistance comparable to catalysts used in commercial fluid catalytic crackers (FCCs)
- Catalyst activity similar to commercial fixed-bed catalysts
- Stable conversion performance for about 200 hours

Only an iron-based (Fe-based) catalyst that had originally been developed for an alternative application met all three of these criteria. This Fe-based HT-WGS catalyst achieved approximately 72% CO conversion compared with 78% CO conversion for a commercial HT-WGS catalyst at similar operating conditions for 500 hours. Based on the success of this technical feasibility evaluation, DOE funded a task under Cooperative Agreement DE-FE0023577 to continue development of this Fe-based HT-WGS catalyst specifically for this advanced transport-based water gas shift process (ATWGS).

Using the same three criteria to evaluate catalyst performance for ATWGS, our approach was to use available knowledge about existing commercial Fe-based catalysts to generate new formulations that would improve or lead to improvements of our baseline catalyst formulation. Currently commercial Fe-based WGS catalysts are available from major catalyst suppliers such as BASF, Haldor-Topsøe, Synetix, Clariant, etc. The typical as-received composition for these Fe-

based catalysts is 74–89% Fe_2O_3, 6–14% Cr_2O_3 and miscellaneous other components, such as CuO, Co_2O_3 and/or MgO [1-3]. The as-received catalyst must be partially reduced before it becomes catalytically active for the WGS reaction. During this partial reduction, the Fe_2O_3 is reduced into the catalytically active Fe_3O_4 phase, but should not be reduced further into FeO or metallic Fe.

The reaction mechanism of Fe-based WGS catalysts is generally accepted to be a redox-type mechanism. The two most popular mechanisms are the regenerative (Rideal–Eley type) and the associative (Langmuir–Hinshelwood type) mechanisms shown schematically in Figure 1 [1-2]. The former is often perceived as more suitable for Fe/Cr catalysts [1]. The regenerative mechanism is usually facilitated by the exchange of electrons between Fe^{2+} and Fe^{3+} in the octahedral site of magnetite during WGS catalysis [4-5].

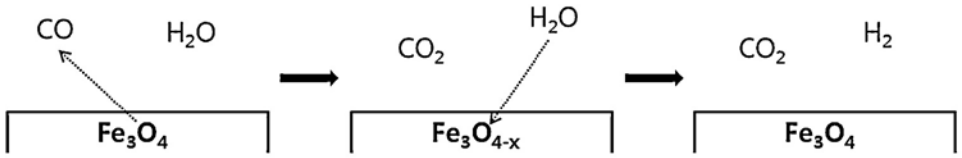

(a) Regenerative Mechanism (Rideal-Eley Type)

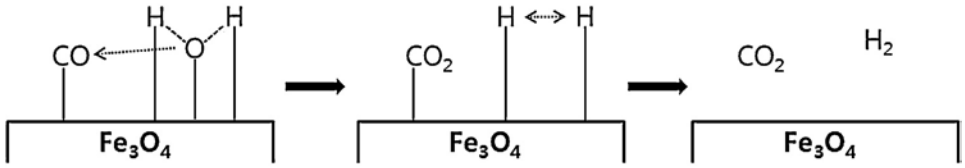

(b) Associative Mechanism (Langmuir-Hinshelwood Type)

Figure 1. The mechanisms of HT-WGS Fe-based catalysts

The life time of commercial Fe-based HT-WGS catalysts is an average of 3 to 5 years [1, 6]. The activity decrease is mostly due to the thermal sintering of the Fe_3O_4 magnetite phase. Until equipment design contraints for maxiumum temperature are exceeded, the deactivation can be compensated for by increasing the reaction temperature [7]. Additionally, the Fe-based catalysts can tolerate minor sulfur concentrations (<50 parts-per-million by volume of H_2S) with essentially no deactivation, unlike copper-based (Cu-based) catalysts [7].

The primary reason these commercial catalysts are not suitable for the ATWGS is that they are only available in shapes/geometries that are suitable for fixed-bed applications. Although a practical solution would be to convert available commercial catalysts into particles with a size

distribution suitable for a transport reactor, by processing the green catalyst formulation into particles rather than pellets, tablets, or extrudates, this approach will not work. The particles formed in this manner fail the attrition resistance criterion. For this reason, our plan was to start with our baseline Fe-based catalyst formulation and modify or use alternative precursors, preparation steps, and reduction procedures to improve catalyst performance leveraging available knowledge about commercial Fe-based catalysts.

2. Catalyst Development and Performance Testing

2.1 Catalyst Development Methodology

RTI's expertise and knowledge on fluidizable material design was combined with a literature survey on Fe-based HT-WGS catalysts to identify the key parametric factors for improving catalyst performance of our baseline Fe-based catalyst. Table 1 summarizes the factors identified and their anticipated beneficial impacts.

Table 1. Key Parameters for Catalyst Development

Catalyst Activity	Structural	Preparation
Iron content	Adapting spinel materials	Calcination
Promoters	Structural promoters	Starting materials
Reduction/Activation processes		Washing process

More specifically, the following catalyst components were identified as the key components to investigate for optimizing catalyst performance:

1. Iron component: Fe_2O_3 forms the active component of the Fe-based WGS catalyst. The amount of this oxide in the conventional Fe-based WGS catalyst is typically in the range of 74-89%. The iron oxide content of this baseline catalyst formulation was about 46%. Thus, increasing the iron content in our fluidized-bed catalyst formulations could be anticipated to help improve the catalyst activity. To this end, catalyst formulations with iron contents ranging from 45 to 65% were investigated to study the influence of iron oxide content on the catalyst activity and the particle attrition.

2. Promoter type and content: Promoters play multiple roles in commercial Fe-based WGS catalysts. First, they can improve the catalyst activity thereby increasing CO conversion during WGS reaction. Next, they can minimize hydrocarbon formation, especially methane formation. Finally, they can potentially lower the amount of steam necessary to inhibit competing reactions catalyzed by the active Fe phase. The two key promoters that were considered for the current catalyst formulation were:

    a. Copper component: A recent survey suggests that addition of a small amount of active components such as Cu, cobalt, ruthenium, nickel, platinum, osmium, gold, palladium, rhenium lead, silver, etc., can improve catalyst activity. Cu was found to

be the most effective one in the list. The presence of Cu not only increases the catalyst activity but also potentially lowers steam requirements typically expressed as the steam to CO ratio. The ability to effectively operate at lower steam to CO ratios can significantly lower the parasitic steam/power requirements for the WGS process for CO-rich syngas.

b. Base oxide component: The presence of base oxide (alkali or alkali metal group oxides) in the catalyst can suppress the formation of by-product methane.

3. Stabilizer/support: Chromium oxide acts as a stabilizer in conventional Fe-based HT-WGS catalysts. However, it is a toxic component, especially in the form of Cr^{6+}.

   Based on RTI's expertise associated with the preparation of attrition-resistant materials, we have a much better understanding of the interaction between active and support materials. We were confident that we could use this expertise to find a support material that would provide both surface area to improve the dispersion of the iron oxide and adequately anchor it to this surface, which should slow down deactivation caused by sintering of the iron oxide crystallites. An added benefit of this approach was the potential to eliminate the need for any chromium in the catalyst making both the catalyst and its preparation more environmentally friendly.

As mentioned previously, the as-received catalyst must be reduced to activate its catalytic activity. In this reduction, the goal is to partially reduce from hematite (Fe_2O_3) to magnetite (Fe_3O_4) minimizing any additional reduction that would yield FeO or metallic Fe. Typical field reduction procedures use gas composition, temperature, and time to control the extent of reduction. Under more controlled conditions than typically available in the field, the reducing potential of the gas, which is

$$\text{Reducing potential} = ([CO] + [H_2]/ ([CO_2] + [H_2O]),$$

can be managed by controlling gas composition in addition to reactor temperature and time.

Catalyst attrition resistance is controlled through a combination of composition and processing procedures. For a given catalyst composition, the synthesis conditions such as precipitation conditions, washing conditions, cake reslurry conditions, spray drying conditions and the post processing conditions all play important roles in determining the physical properties of the resultant catalyst formulation. Because of their impact on catalyst attrition resistance, the effect of the aforementioned parameters on catalyst performance and physical stability were investigated as part of this catalyst development task.

2.1.1 Catalyst Synthesis

The fluid-bed Fe-based HT-WGS catalyst formulations prepared in this project were made using a co-precipitation procedure shown in Figure 2. In this co-precipitation, a mixed salt solution containing the desired precursors of Fe, support, and promoters such as Cu was precipitated using a precipitating agent, typically a basic solution. After completing the precipitation, the mixture was filtered and rinsed with deionized (DI) water to remove any residual precipitation liquor. The resulting filter cake was reslurried with DI water before being spray dried. The spray-dried green catalyst was then calcined in a furnace. The calcined catalyst formulations were then subjected to performance testing and characterization testing.

Figure 2. Schematic representation of the catalyst synthesis process

2.1.2 Summary of Catalyst Formulations Prepared

In the following section, we describe the different catalyst formulations that were prepared to parametrically test different compositions and preparation procedures with the goal of optimizing the performance and attrition resistance of our baseline Fe-based HT-WGS catalyst formulation. To effectively identify trends which could be used for optimization, our approach involved manipulating one specific parameter at a time while maintaining the other parameters constant.

Preparation of baseline Fe-based HT-WGS catalyst formulation

As previously mentioned, the baseline catalyst for this project was developed for another application under a different project. Furthermore, the specific formulation tested during the selection process was from an optimized pilot plant production batch from DOE/NETL Cooperative Agreement DE-FC26-06NT42758. To ensure the team working on the current project was both familiar and had actual hands-on experience with the preparation procedures for making the baseline Fe-based HT-WGS catalyst formulation, one of the first formulations made was to duplicate the baseline catalyst formulation. Preparation of this baseline formulation also ensured that a fresh baseline catalyst formulation was being used for comparison eliminating the potential that the age of the baseline catalyst formulation was adversely impacting its performance.

Preparation of Fluidized-bed Fe-based HT-WGS catalysts with different iron content

A series of catalysts were prepared to investigate the impact of iron oxide content on catalyst performance and attrition resistance. Our target range for the iron concentration was from 0 to 90 wt% with our upper limit being defined by commercial Fe-based HT-WGS catalysts. During our preparation of these catalyst formulations, we found that the attrition resistance for formulations with iron content ≥ 60 wt% would be unacceptable for ATWGS. Thus, the upper practical limit for the iron content of the catalyst formulations prepared was 60 wt%. Table 2 shows the specific iron content of the catalyst formulations prepared. For these formulations we adjusted the support content to compensate for the large changes being made in the iron content. The content of the promoters was maintained constant.

Table 2. Catalyst Formulations with varying Iron Content

Sample ID	13838-38	13838-9	13838-24	13838-14A	13838-34
Fe_2O_3	0	49.17	54.97	60.56	65.01

Preparation of Fluidized-bed Fe-based HT-WGS catalysts with different promoters

A number of different catalyst formulations were made to evaluate the effects of various promoters on catalyst performance and attrition. Because of the importance of Cu as a promoter in commercial Fe-based HT-WGS catalysts, two series of catalyst formulations were made to investigate the effects of copper. In the first series, three catalyst formulations were made in which only the Cu content was varied. The specific copper content for these catalyst formulations is provided in Table 3. In the second series of catalyst formulations, a high Cu content (10 wt%) was selected and the iron content was varied to evaluate if the relative ratio of Cu to Fe affected catalyst activity. The specific Cu and iron contents for this second series of catalyst formulations is shown in Table 4.

Table 3. Catalyst Formulations with varying Copper Content

Sample ID	13838-9	13838-46	13838-33B
CuO	6.01	0.00	10.01

Table 4. Catalyst Formulations with varying Copper Content

Sample ID	13838-33A	13838-33B
CuO	10.01	10.01
Fe_2O_3	45.17	50.20

In another series of catalyst formulations, three different proprietary promoters were added at concentrations between about 5 and 10 wt%. The identity and concentration of the promoter used in each catalyst formulation is provided in Table 5.

Table 5. Catalyst Formulations with varying Promoter Contents

Sample ID	13838-50	13838-33B	13838-42	13838-58
Promoter	A	B	B	C
Content	4.58	4.58	8	10

Improvement of Fluidized-bed Fe-based HT-WGS catalyst attrition.

During the performance testing, it was discovered that higher iron content positively impacted the catalyst activity. It was also clearly demonstrated that the higher iron content resulted in poorer catalyst attrition resistance than for our original preparation procedure. Through our extensive prior experience in developing attrition resistance materials, we have identified key preparation procedures which can be altered to adjust attrition resistance of prepared catalysts. Because any catalyst formulations we prepared with iron content ≥ 60 wt% iron content had improved activity, but failed to have sufficient attrition resistance, we attempted to use our expertise to prepare catalyst formulations with higher than 60 wt% iron content that also had acceptable attrition resistance. These efforts included attempting to modify two of the key preparation procedures that influence attrition resistance. Table 6 shows the catalyst formulations made at different conditions for proprietary preparation procedure A. The target iron content for these formulation was 60 wt%. Table 7 shows the catalyst formulations made at different conditions for proprietary preparation procedure B. Two sets of catalyst formulations were made, one with an iron content of about 60 wt% and one with an iron content of about 55 wt%.

Table 6. Fe-Based HT-WGS Catalyst Formulations prepared with different conditions for Preparation Procedure A

Sample ID	13838-16A	13838-16B	13838-10
Preparation Procedure A	Baseline	2	3

Table 7. Fe-Based HT-WGS Catalyst Formulations prepared with different conditions for Preparation Procedure B

Sample ID	13838-14A	13838-14B	13838-24	13838-62
Preparation Procedure B	Baseline	2	Baseline	2
Iron content	60.56	60.56	54.97	54.60

As the optimization of the catalyst preparation procedure made to accommodate less expensive replacements for the support precursor and precipitating agent also resulted in an improvement in attrition resistance (see the following section), a final preparation using the optimized new preparation procedure was also made with an iron content of about 60 wt%. The identification for this catalyst formulation was 13838-96.

Modifications for Reducing Production Cost of the ATWGS catalysts

Based on RTI's active materials development program which includes working with commercial catalyst manufacturers, we were aware that several modifications could be made to the original baseline production process which could reduce production cost for our ATWGS catalyst formulations. These modifications included:

- Replacement of the support precursor with a cheaper alternative.
- Use of an alternative precipitating agent.

These modifications also result in a reduction of ancillary process equipment to treat emissions generated during the preparation processing and the amount of chemical necessary per pound of catalyst produced. The net result of these modification has been a demonstrated cost reduction in the commercial production of other catalyst formulations RTI has had made.

By starting with these alternative precursors, the preparation procedure needed multiple adjustments to ensure that the final catalyst formulation would have the same properties as our optimal catalyst formulation. Because our key objectives were to optimize catalyst performance and attrition resistance, we used these criteria to sequentially optimize each adjustment to the preparation procedure. The sequential series of catalyst formulations made to optimize the catalyst performance and attrition resistance is provided in Table 8.

Table 8. Optimization matrix for lower cost route ATWGS Catalyst Samples

Sample ID	13838-75	13838-79	13838-83	13838-87	13838-92	13838-33B
Precursors	New (cheaper)	New	New	New	New	Optimized
Preparation Procedure A	Baseline	4	5	6	6	Baseline
Washing	Baseline	Baseline	Baseline	Baseline	7	Baseline

2.2 Catalyst Characterization and Performance Testing

2.2.1 Catalyst Characterization

The prepared catalyst formulations described in Section 2.1 were analyzed by a series of tools including ICP, XRD, BET surface area, tap density and attrition measurement. The results on these measurements will be discussed in the results section.

2.2.2 Microreactor System and Product Analysis

HT-WGS catalyst performance was evaluated in a packed-bed microreactor system with simulated syngas mixtures. The process flow diagram for the microreactor system is shown in Figure 3. Reactant and purge gases are supplied from high pressure cylinders. Gas flows are controlled and monitored with mass flow controllers (MFCs). The gas supply lines downstream of the MFCs are heat traced for preheating the feed gases. The reactor is a 0.5 inch OD stainless steel tube surrounded by a heating jacket, which is uniformly heated using band heaters. Using a thermowell to maintain the pressure seal, the tip of a thermocouple is located within the catalyst bed. This thermocouple is used to monitor and record the temperature of the catalyst bed, control the power output to the band heaters on the reactor and as a high temperature safety trip for the reactor. Prior to loading in the reactor tube, catalyst particles (~100 microns) are mixed with α-alumina particles (~250 microns) to achieve a 3:1 alumina:catalyst ratio on a volume basis. The dilution helps maintain more isothermal reactor conditions by minimizing the temperature rise caused by the heat generated by the WGS reaction.

All process gas lines from the point after the MFCs to the condensation vessels are maintained around 140 °C. Process relief valve are located upstream and downstream of the reactor system for system safety. Products and unconverted reactants exit the fixed-bed reactor and flow into one of the three condenser vessels. These vessels are cooled below 20 °C using thermoelectric coolers. Two of the collection vessels have an internal volume of 50 cm^3 and the third has an internal volume of 150 cm^3, allowing condensation products to be continuously collected for 24-72 hrs. Liquid products are manually drained at room temperature using the combination of ball and needle valves downstream of the condensers. Only one of the three condensers is used at any time during the run. The other two condensers stay isolated, but can be switched online using the solenoid valves to direct the product flow. This ability to switch to a different active collection vessel is used when draining a collection vessel.

Dry gas samples from the systems are analyzed by an Agilent 3000 gas analyzer (Micro GC). The Micro GC was calibrated for Argon (Ar), H_2, CO, CO_2 and C_1 to C_6 hydrocarbons (namely n-alkanes and 1-alkenes). An Ar tracer was used in the feed gas to quantify product gas flow rates.

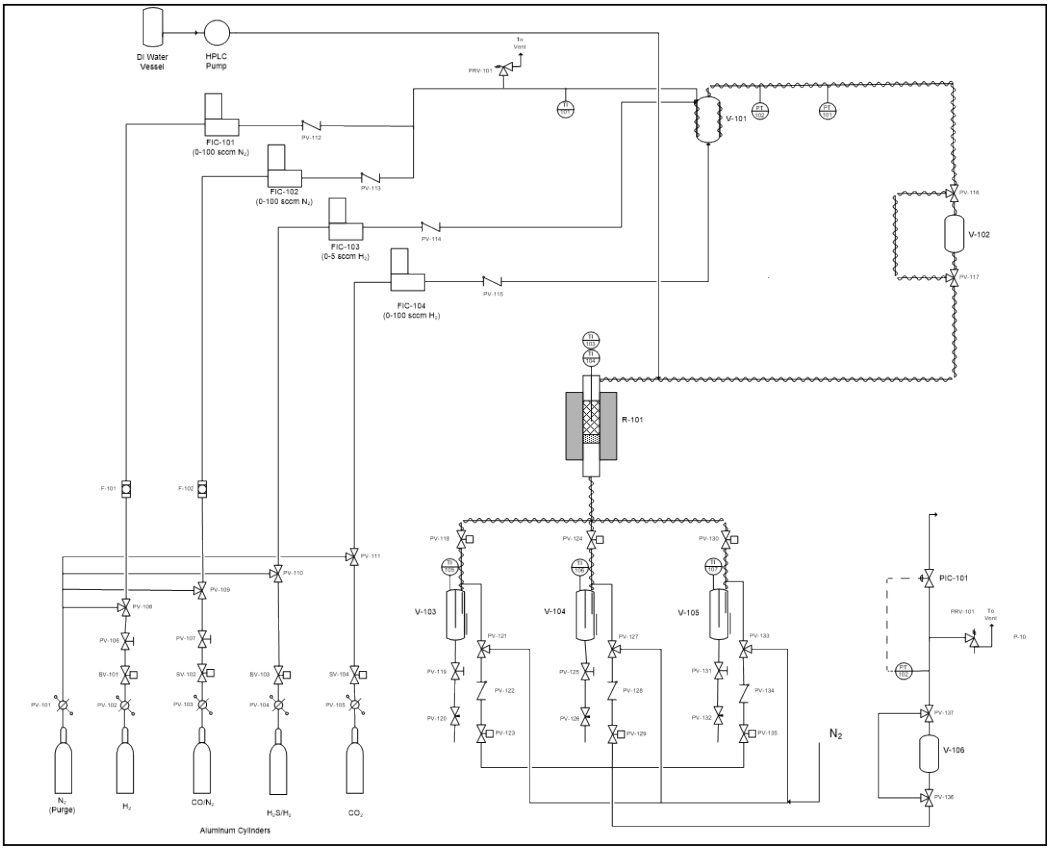

Figure 3. Process Flow Diagram of the Microreactor System

2.2.3 Test Matrix

The active catalyst bed in the reactor tube was comprised of a 3:1 alumina:catalyst ratio on a volume basis that was sandwiched between the two inert layers of alumina. The catalyst loading in the reactor tube was about 3g. The catalyst was reduced in-situ under the syngas environment. Two types of catalyst performance tests were conducted. One was used to evaluate catalyst activity. The other was used to test catalyst stability. In the activity test, the effluent composition was measured at a series of four temperatures between 300ºC and 400°C. For the stability test, all the operating conditions were maintained constant for > 150 hours of operation during which changes in the effluent composition were monitored to identify changes in CO conversion and selectivity for competing reactions, namely methanation. Table 9 lists the specific operation conditions for the catalyst activity and stability tests.

Table 9. Reaction Conditions for Catalyst Performance tests

Reaction Condition	Activity Test	Stability Test
Temperature [°C]	300-450	375
Pressure [psig]	500	500
Space velocity at STP [h^{-1}]	5,000	5,000
Component [vol%]		
H_2	17.7	17.7
CO	23.0	23.0
CO_2	10.6	10.6
CH_4	2.8	2.8
H_2O	45.9	45.9

3. Results and Discussion

3.1 Benchmarking the Catalyst Performance for Commercial and Baseline Catalysts

The catalyst development efforts for this project were clearly defined in that our objective was to develop an optimized catalyst formulation that demonstrated:

- Attrition resistance comparable to catalysts used in commercial fluid catalytic crackers (FCCs),
- Catalyst activity similar to commercial fixed-bed catalysts, and
- Stable conversion performance for about 200 hours.

Shiftmax 120, a commercial HT-WGS catalyst produced by Clariant, was used to establish the numerical targets for representative catalyst activity and stability for conventional commercial catalysts. Figure 4 shows the results from the activity and stability tests completed on Shiftmax 120 at the standard operating conditions.

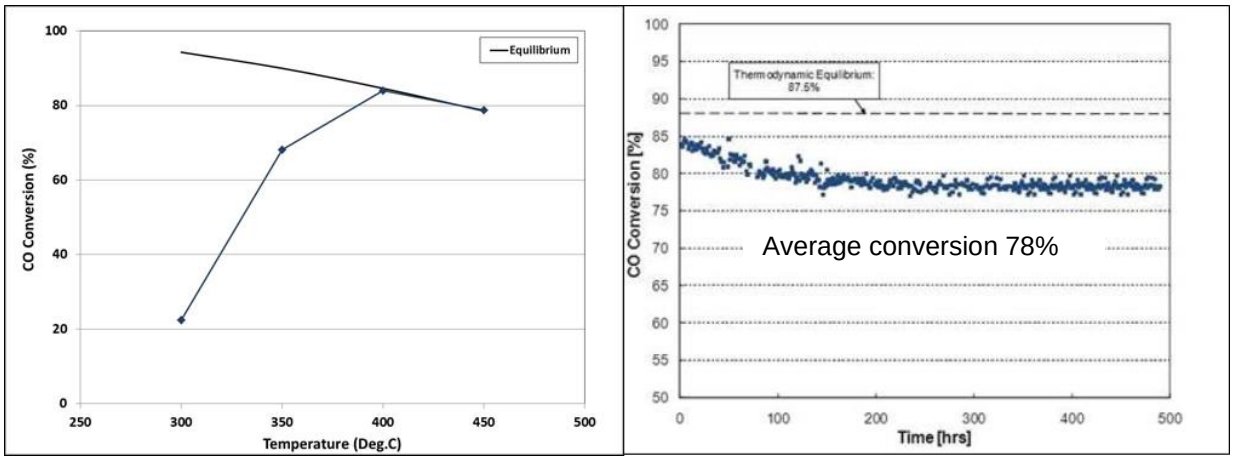

Figure 4. Commercial Catalyst Performance for the HT-WGS reaction

In Figure 4, the left chart shows the results from the standard activity test and the predicted equilibrium conversion based on temperature. These results show that at temperature ≥ 400°C, the reaction rate is fast and the extent of reaction is determined by thermodynamics. At temperatures < 400°C, the rate of reaction is kinetically controlled with the rate dropping off and becoming very slow at temperatures below 300°C.

The results from stability testing, shown in the chart on the right, indicate that after an initial induction period in the actual operating gas, the CO conversion reaches a stable value of around 78% that is maintained for roughly 300 hours.

The results from the standard activity and stability testing for our baseline ATWGS catalyst formulation are provided in Figure 5. The results from the activity test for the baseline catalyst formulation are essentially identical to those obtained for the commercial catalyst. The results from the stability test show that our baseline catalyst formulation achieved a stable CO conversion of about 72 %. Thus, the baseline catalyst formulation achieved a slightly lower stable CO conversion (72% vs. 78%) than the commercial catalyst.

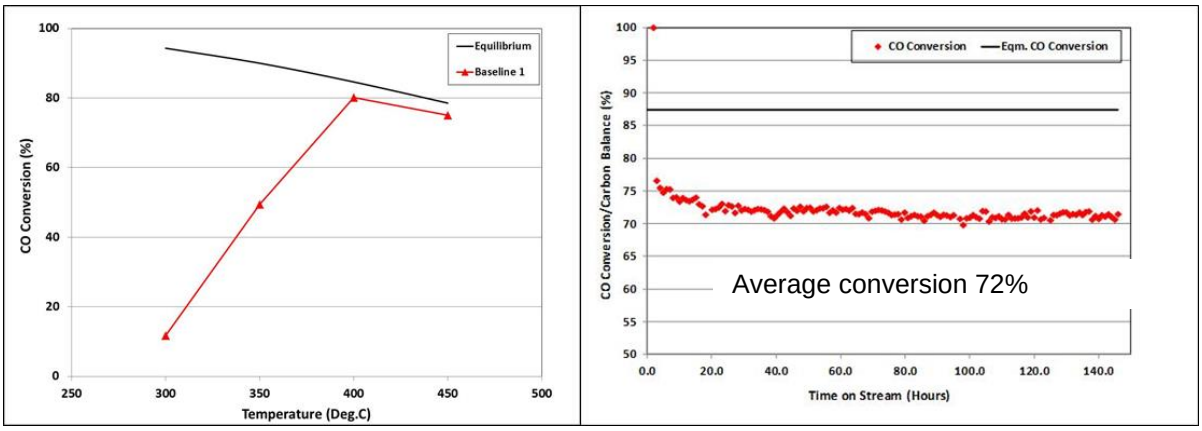

Figure 5. Baseline Catalyst Performance for the HT-WGS reaction

Attrition testing of standard equilibrium fluid catalytic cracking (FCC) catalyst resulted in an attrition loss of about 6.0 wt% and was utilized to establish a comparative performance standard for our ATWGS attrition testing. Attrition testing of our baseline catalyst formulation resulted in an attrition loss of 1.7 wt%. Based on these results, our baseline catalyst formulation has greater attrition resistance than conventional equilibrium FCC catalyst.

To provide better understanding of other physical properties for our baseline catalyst we also measured its BET surface area and compact bulk density. The results from this testing were a BET surface area of 67 m^2/g and density of 1.46g/cm^3.

Figure 6 presents the X-ray diffraction (XRD) patterns of the baseline formulation. XRD patterns show that there are three distinct crystalline phases in the prepared catalyst. Based on the iron content, the predicted concentration of free Fe_2O_3 phase should be about 58%. Thus, the large peak at a two theta value of 33.27, which corresponds to the strongest peak for Fe_2O_3, represents one of the key XRD signatures for our baseline catalyst formulation. The other crystalline phases represent the support material.

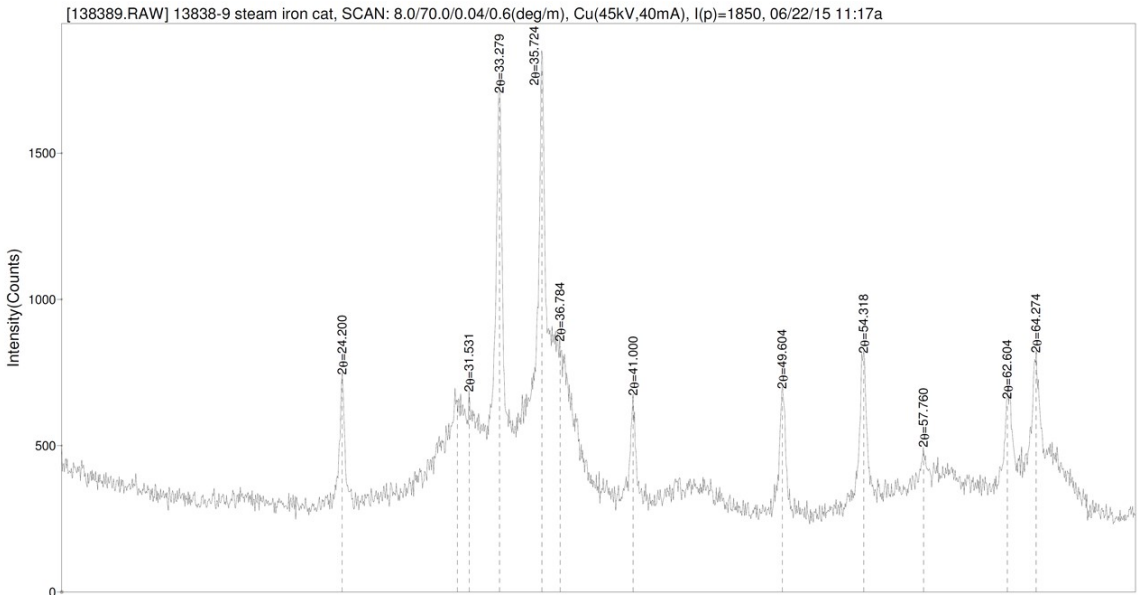

Figure 6. XRD patterns of baseline Fe-based HT-WGS catalyst

Figure 7 presents the results from an activity test showing the results for baseline catalyst formulation used during the original selection process (baseline 1) and the new duplicated laboratory batch prepared by this project's team (baseline 2). The results show that the new duplicated baseline catalyst formulation exhibited relatively comparable catalyst activity to the original baseline formulation. The result for attrition testing for this new duplicated baseline formulation was 1.6%. These results showed that the team could effectively reproduce the baseline catalyst formulation in the laboratory. The next task was to begin optimization of the catalyst formulation to primarily increase stable CO conversion while maintaining catalyst activity and attrition resistance.

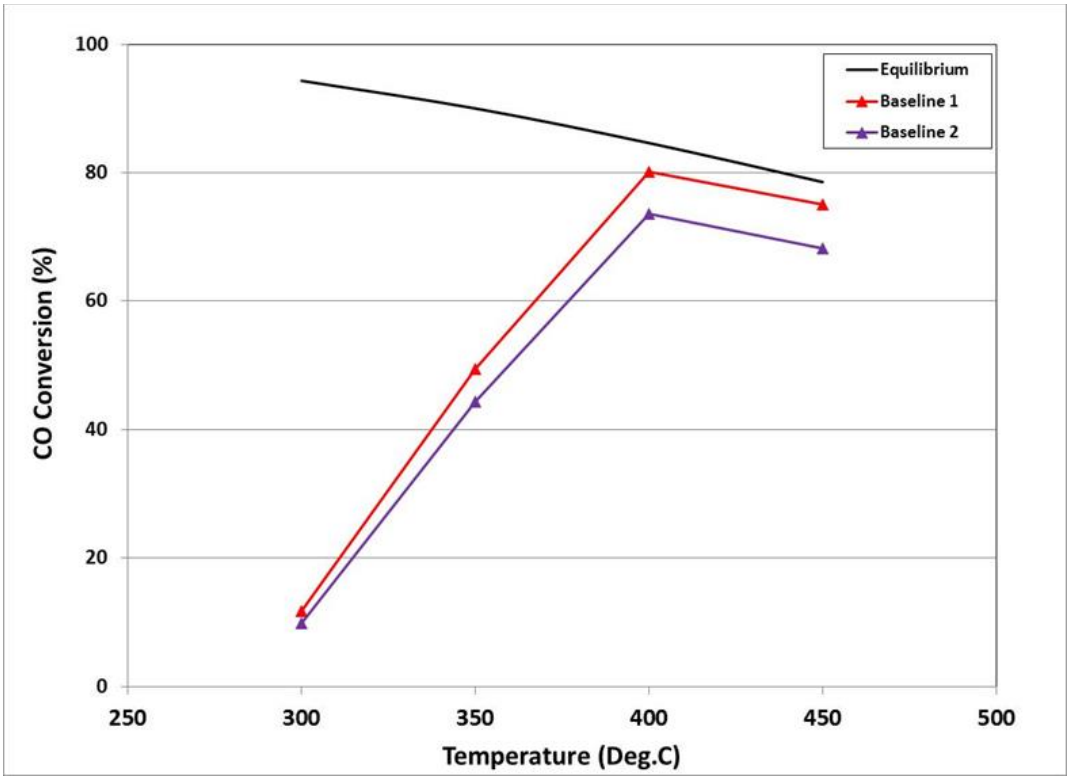

Figure 7. Catalyst Performance of the baseline material

3.2 Effect of iron content on catalyst activity and attrition resistance

Iron oxide is the active component in commercial HT-WGS catalyst. The iron content of the commercial catalyst is as high as 74-89%. In our baseline formulation, iron oxide content is around 46%, which is much lower than the commercial catalyst. An immediate opportunity to increase activity was to increase the iron content of our catalyst formulations. A series of catalyst formulations were made with higher iron content. The results from characterization of the catalyst formulations are provided in Table 10.

Table 10. Characterization results for Catalyst Formulations with varying Iron content

Sample ID	13838-38	13838-9	13838-24	13838-14A	13838-34[2]
Fe_2O_3	0	49.17	54.97	60.56	65.01
Catalyst Characterization Results					
BET SA m^2/g	74.68	66.97	64.47	69.75	--
Attrition (DI% 21/42 μm)[1]	0.97/3.45	1.57/4.42	65/78	72.40/57.00	--
Density (g/cm^3)	1.75	1.46	0.92	0.42	--

[1] RTI has upgraded its attrition test to provide attrition results at two particle sizes to improve information obtained from this test.

[2] As the attrition results for the formulations with 55% and 60% iron content did not meet our target specification, the characterization of this 65% iron formulation was not completed.

Characterization results for catalyst formulations prepared to evaluate the effects of iron content revealed that the formulations with up to 50% iron content exhibited a decent attrition resistance (13838-38 and 13838-9), which was better than FCC catalyst. However, for the catalyst formulations with iron content > 50%, the attrition numbers had increased to >65%, and density dropped significantly. BET surface area, on the other hand, stayed relatively steady (60~70 m^2/g) over all the catalyst formulations across the entire range of iron content.

XRD patterns of catalysts with 50%, 55% and 60% iron oxide content are shown in Figure 8. When the iron content is around 50%, three distinct crystalline phases can be clearly identified with iron oxide as the dominating phase. For catalyst formulations with iron content above 50%, the only clearly crystalline phase is the iron oxide. The crystalline phases associated with the support material are not present. The loss of a strong crystalline support phase would lead to a significant reduction in the mechanical strength of the catalyst formulation. For the XRD peaks associated with iron oxide we also note that this iron oxide phase seems to suggest that even the iron oxide phase is more amorphous and less crystalline than for the baseline formulation.

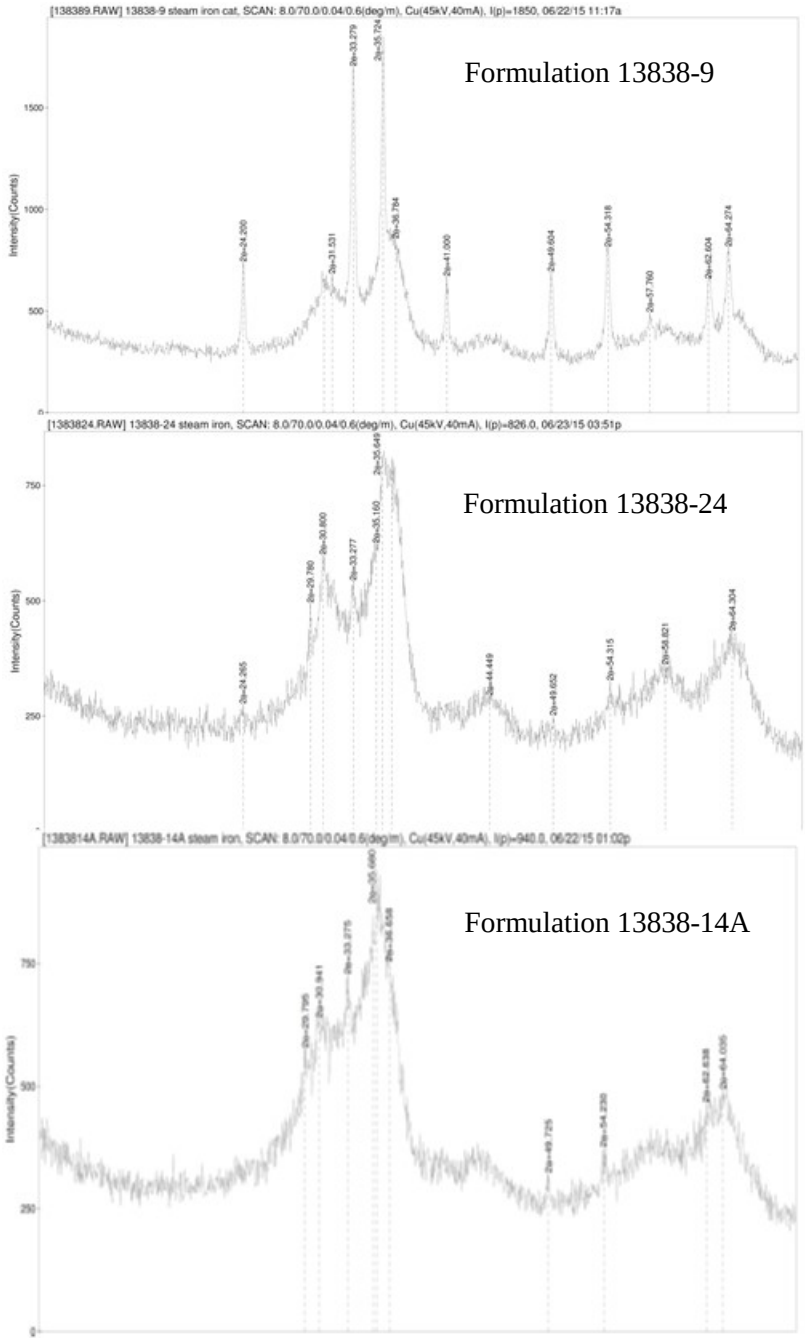

Figure 8. XRD patterns of HT-WGS catalyst with varying Iron contents

Figure 9 presents the results from catalyst activity tests for these different iron content formulations. As can be seen from Figure 9, CO conversion increases with increasing iron content in the catalyst formulation. Catalyst formulations with iron contents of 55 and 60 wt% were able to achieve equilibrium CO conversion values at reaction temperatures ≥ 400°C. It can also be seen that these catalysts with higher iron content also had better activity at lower temperatures

(<350°C). The catalyst formulations demonstrated that iron was essential to increasing catalyst activity at temperatures below 450°C.

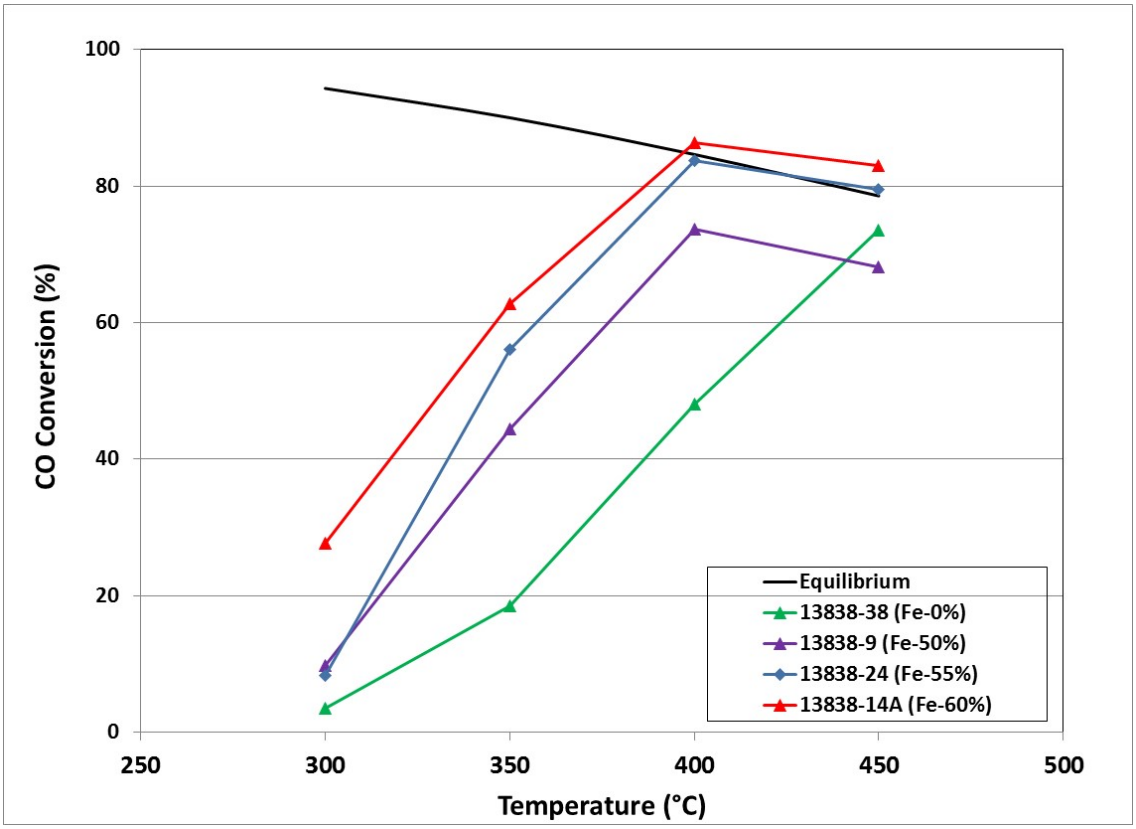

Figure 9. Catalyst Performance as a function of Iron Content

3.3 Efforts on improving attrition for catalysts with higher iron content

Catalyst activity results indicated that there is a trade-off with increasing iron content, which helps boost the catalyst activity, but adversely affects the attrition resistance. When iron content is >50%, the catalyst attrition resistance falls below the accepted target value. Therefore, there is significant potential benefit for improving the attrition resistance of catalyst formulations with iron contents > 50 wt%. Based on our extensive prior experience with preparing attrition resistant materials, we prepared catalyst formulation in which we adjusted conditions for two key preparation procedures that we believed could significantly improve attrition resistance. The results from testing of these catalyst formulations are shown in the following sections.

3.3.1 Preparation Procedure B

Prior to preparation procedure B, a batch of catalyst precursor was divided into two portions. One portion was prepared according to the preparation procedure B conditions used for the original baseline formulation. The other was treated at new conditions for preparation procedure B that we believed could improve attrition resistance. Table 11 shows the characterization results for these two catalyst samples. The catalyst formulation prepared using the same conditions as used for the baseline formulation showed the anticipated high attrition loss. The catalyst formulation using the new preparation procedure B conditions did show some improvement in the attrition resistance, but it was still significantly larger than our target value. The BET surface area and density for this catalyst formulation with an altered preparation procedure B showed significant changes with the surface area decreasing by about 50% and the density increasing by about 50%. Although the modified preparation procedure B did increase the attrition resistance of the catalyst formulation, we could not change preparation procedure B sufficiently to achieve our target attrition test value.

Table 11. Fe-Based HT-WGS Catalyst Formulations prepared with different conditions for Preparation Procedure B

Sample ID	13838-14A	13838-14B
Preparation procedure B	Baseline	2
Catalyst Characterization Results		
BET SA m^2/g	69.75	31.83
Attrition (DI% 21/42 μm)[1]	72.40/57.00	67/49
Density (g/cm^3)	0.42	1.09

[1] RTI has upgraded its attrition test to provide attrition results at two particle sizes to improve information obtained from this test.

XRD patterns for the catalysts for the two formulations prepared with different preparation procedure B conditions are shown in Figure 10. It appears that the change in preparation procedure B had a big impact on the crystallinity of the different catalyst phases. However, the reasons that catalyst formulations with higher iron content have low attrition resistance must have been more complex than just extent of development of the crystalline phases.

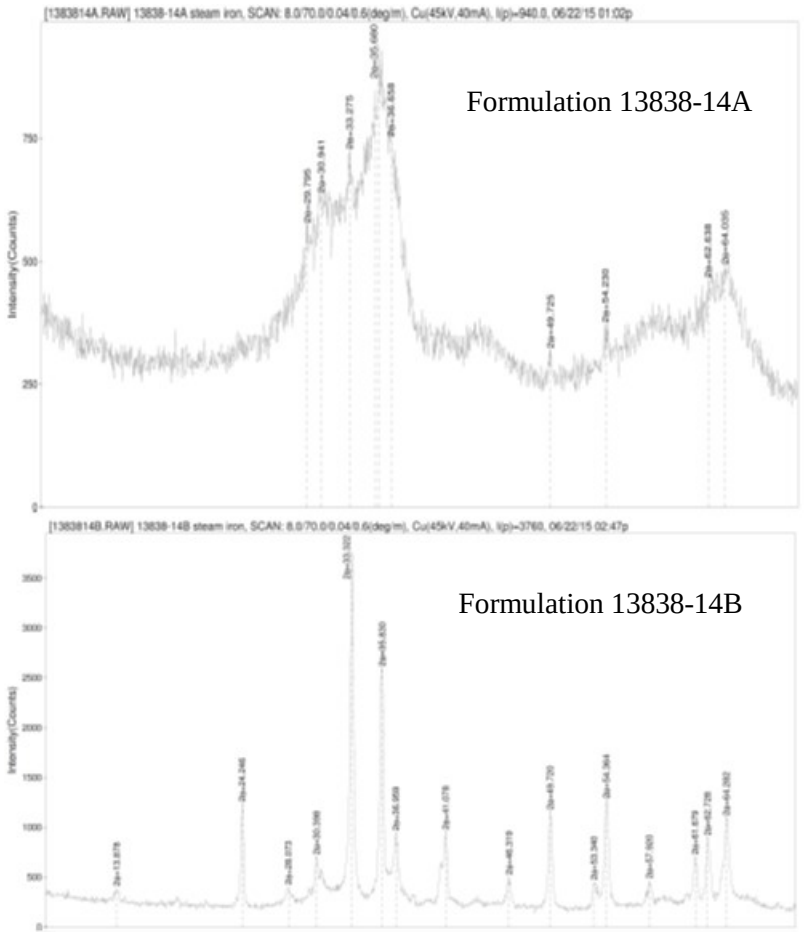

Figure 10. XRD patterns of Fe-based HT-WGS catalyst formulations with different preparation procedure B conditions

The catalyst activity for these two catalyst formulations is shown in Figure 11. The results show the conditions for preparation procedure B selected to achieve higher attrition resistance had an adverse effect on the catalyst activity across the entire range of temperatures tested. Because the XRD patterns for the modified catalyst formulation show better defined crystalline phases, improved catalyst activity, especially at lower temperatures, seems to come from a more amorphous iron phase.

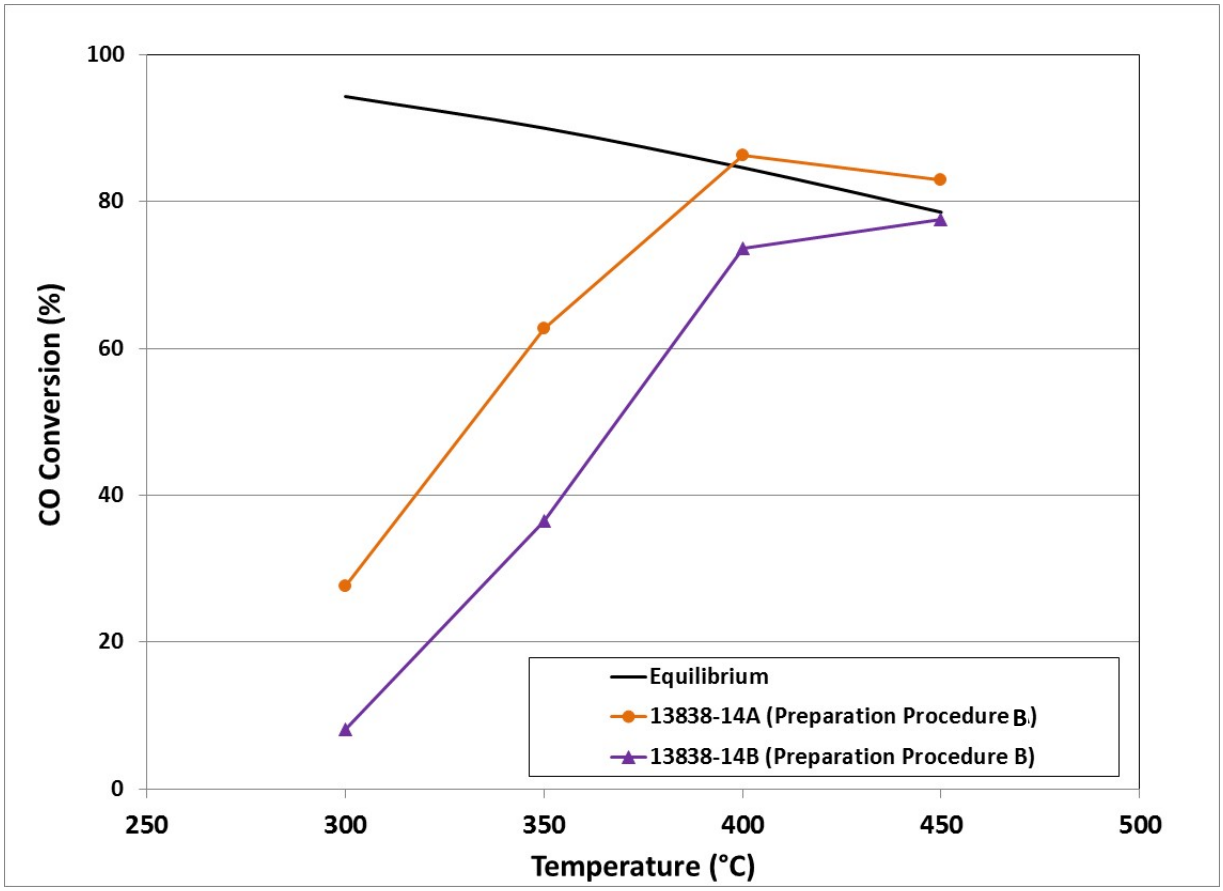

Figure 11. Catalyst Performance for different Preparation Procedure B conditions

3.3.2 Preparation Procedure A

Three catalyst formulations were prepared at different conditions for preparation procedure A at an iron content of 60 wt%. Table 12 presents the catalyst characterization results for these catalyst formulations. It can be seen that new modified conditions for preparation procedure A did result in attrition improvement as results from the attrition test decreased from the value of 65% obtained with the formulation using the baseline procedure A conditions. However, neither of the two new conditions was able to reduce the attrition test result sufficiently to meet our target value.

Table 12. Catalyst Characterization results for Fe-based HT-WGS catalyst formulations with different Preparation Procedure A

Sample ID	13838-16A	13838-16B	13838-10
Preparation procedure A	*Baseline*	*2*	*3*
Catalyst Characterization Results			
BET SA m^2/g	31.83	29.76	30.83
Attrition (DI% 21/42 μm)[1]	65.09/50.45	30.73/43.86	45.38/53.67
Density (g/cm^3)	1.01	1.09	1.03

[1] RTI has upgraded its attrition test to provide attrition results at two particle sizes to improve information obtained from this test

Based on these results, development of a catalyst formulation with iron content ≥ 55 wt% that would have an attrition resistance meeting our target would require significantly more development effort that was originally scoped for this project.

3.4 Improvement of Catalyst Performance through Promoters

In this section, the results from the different catalyst formulation series prepared with different promoters and their amounts are presented. The objective was to improve catalyst activity for the HT-WGS reaction, to depress the hydrocarbon formation especially methane, and to enhance catalyst stability under more constrained operation conditions such as lower steam/carbon ratio and the presence of H_2S.

3.4.1 Effect of Copper Content on Catalyst Activity and Attrition

A series of Fe-based HT-WGS catalyst formulations were prepared with different Cu content. Tables 13 and 14 present the catalyst characterization results for these different formulations. Table 13 shows that for a Cu content of < 5wt%, there is little or no impact on BET surface area, density or attrition resistance. At a Cu content of 10 wt%, the BET surface area and attrition resistance decreased and density increased. Although the attrition resistance decreased, it still meets our target value. Because increasing Cu content does result in lower attrition resistance, we decided that the upper limit for Cu content in our optimized catalyst formulation should not exceed 10 wt%. According to a report in the literature, HT-WGS catalysts prepared with higher than 10 wt% Cu content did not show much additional benefit for catalyst performance.

Table 13. Characterization results for Fe-based Catalyst Formulations with different Cu Content but same Fe content

Sample ID	13838-9	13838-46	13838-33A
CuO	6.01	0.00	10.01
BET SA m^2/g	66.97	67.80	53.49
Attrition (DI% 21/42 μm)[1]	1.57/4.42	1.47/5.32	6.39/10.48
Density (g/cm^3)	1.46	1.42	1.71

[1] RTI has upgraded its attrition test to provide attrition results at two particle sizes to improve information obtained from this test.

Table 14. Characterization results for Fe-based Catalyst Formulations with same Cu Content but different Fe content

Sample ID	13838-33A	13838-33B
CuO	10.01	10.01
Fe_2O_3	45.17	50.20
BET SA m^2/g	65.03	53.49
Attrition (DI% 21/42 μm)[1]	6.06/15.46	6.39/10.48
Density (g/cm^3)	1.61	1.71

[1] RTI has upgraded its attrition test to provide attrition results at two particle sizes to improve information obtained from this test.

XRD patterns for the catalyst formulation with 10 wt% Cu content is shown in Figure 12. As compared to the baseline catalyst, there is no obvious phase changes observed with the introduction of the higher Cu content.

The results from catalyst activity testing for the catalyst formulations with the high Cu content are shown in Figure 13. Figure 13 also provided the results from the baseline catalyst formulation. The catalyst formulations with 10 wt% Cu content exhibited higher CO conversion compared to the baseline catalyst. Thus, the increase of Cu content to 10 wt% results in improved catalyst activity while still meeting our attrition resistance target.

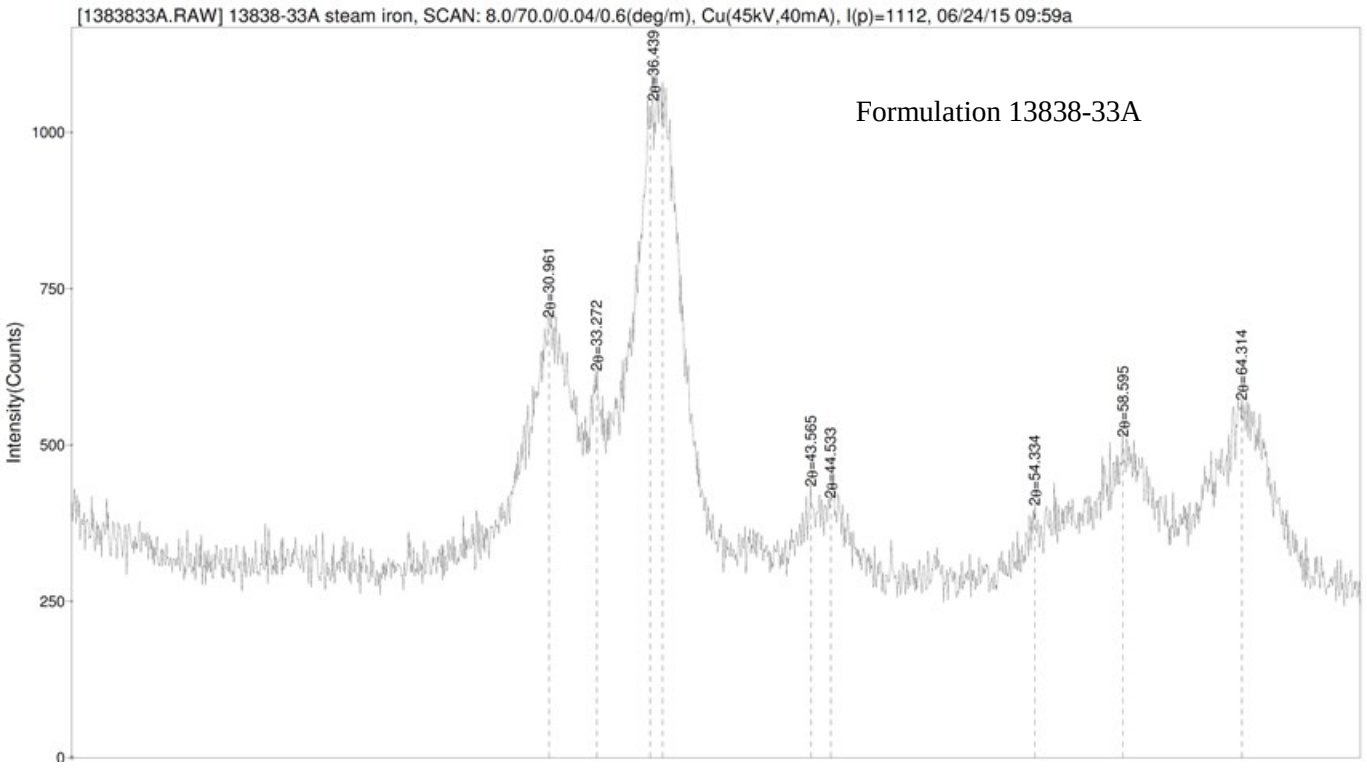

Figure 12. XRD pattern of HT-WGS catalyst with higher copper content (10 wt%)

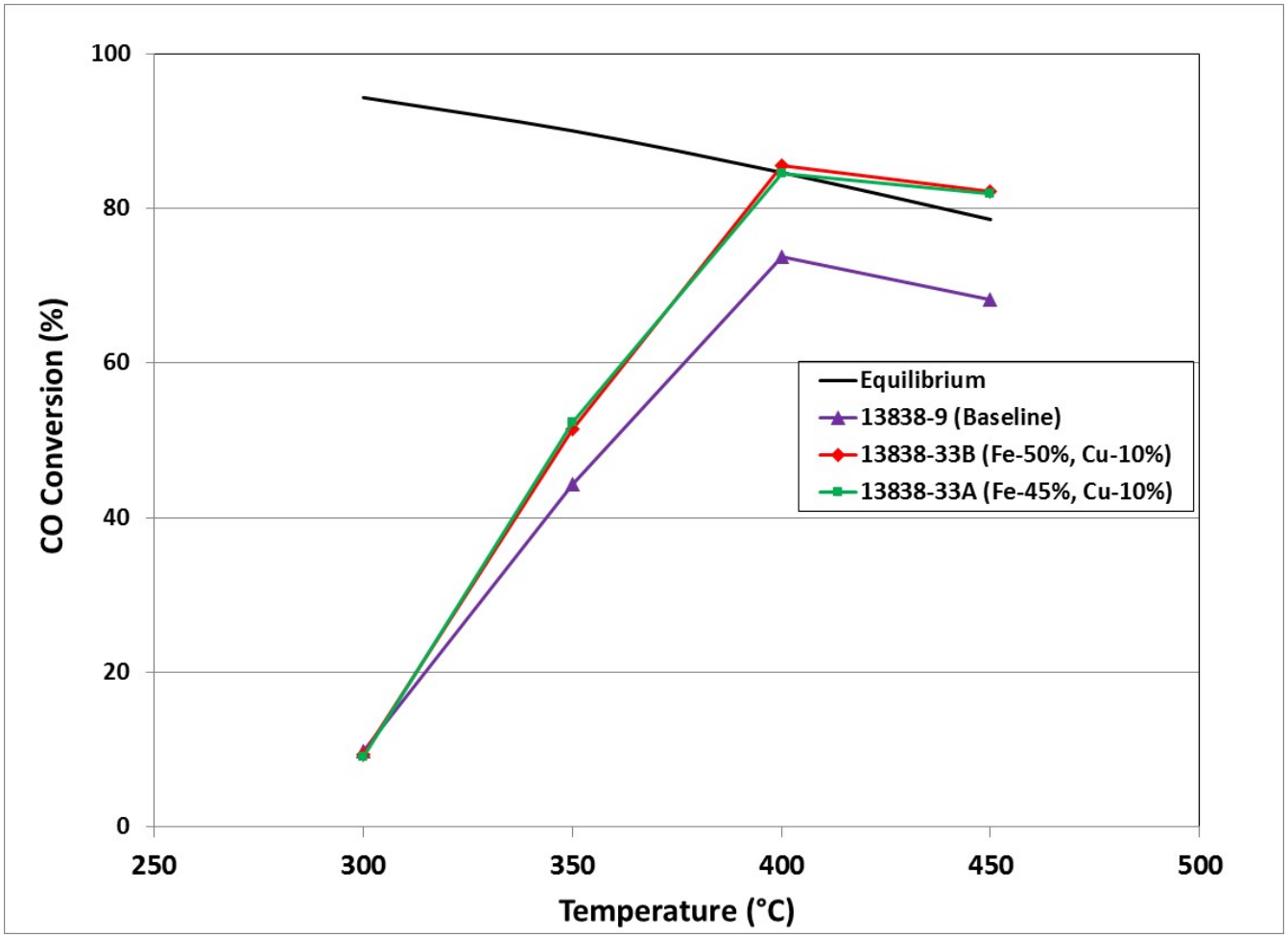

Figure 13. Catalyst Performance as a function of copper content

3.4.2 Effects of Promoter B on Catalyst Performance

The presence of proprietary promoter B was tested as a means of suppressing the formation of hydrocarbons and potentially increasing catalyst life time. The catalyst composition and characterization results are listed in Table 15 and the catalyst activity results are presented in Figure 14.

Table 15. Catalyst Characterization results for Fe-based HT-WGS catalyst Formulations with Different Promoter B Contents

Sample ID	13838-42	13838-9
Promoter B	8	4.58
Catalyst Characterization Results		
BET SA m^2/g	65.98	66.97
Attrition (DI% 21/42 μm)[1]	1.68/4.78	1.57/4.42
Density (g/cm^3)	1.5	1.46

[1] RTI has upgraded its attrition test to provide attrition results at two particle sizes to improve information obtained from this test.

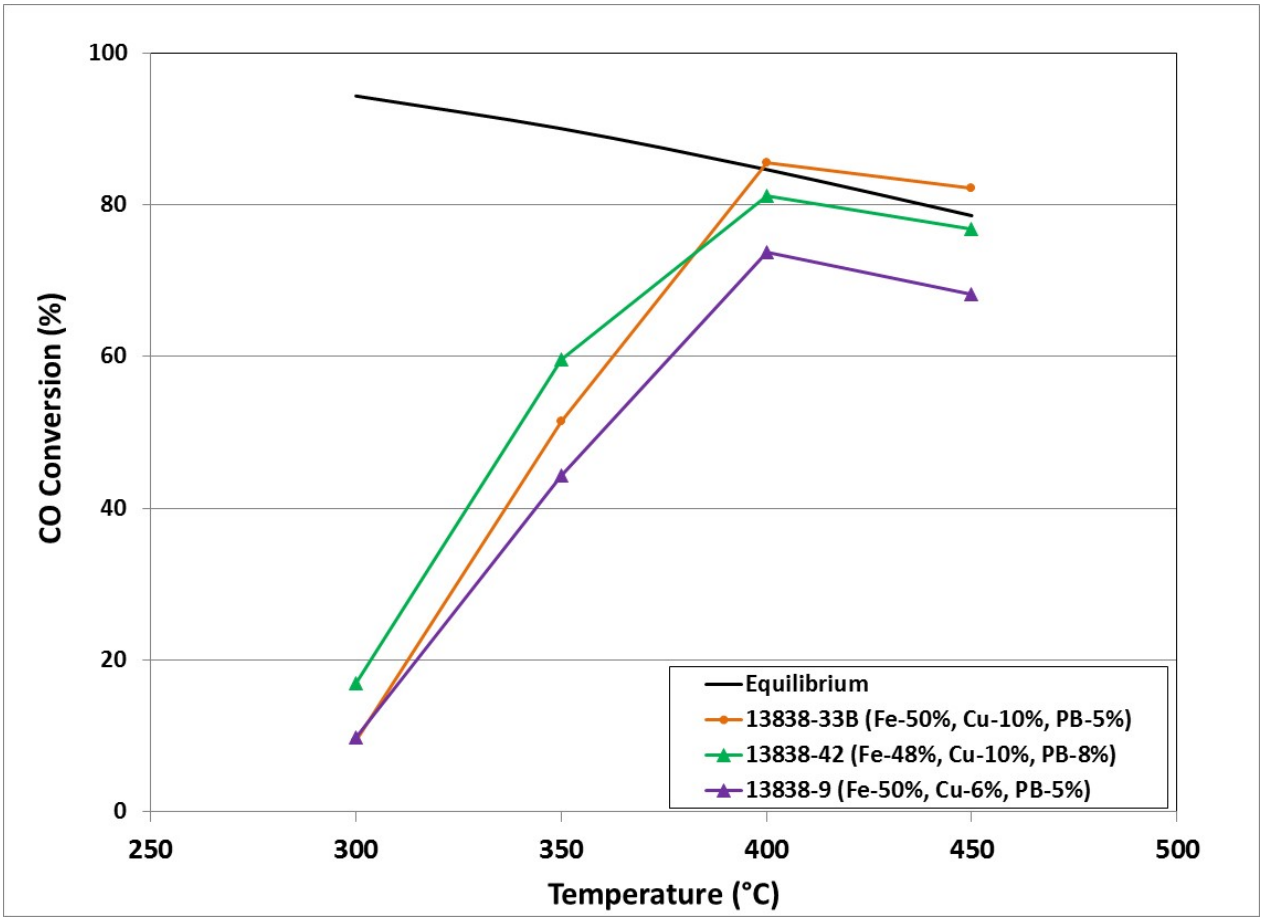

Figure 14. Catalyst Performance for different Contents of Promoter B

Table 15 shows that almost doubling the concentration of promoter B in the catalyst formulation had essentially no significant impact on the BET surface area, density or attrition

resistance. Catalyst activity results, shown in Figure 14, were also essentially identical with a slight increase in CO conversion at temperatures < 400°C. Hydrocarbon formation, which has been expressed as methane selectivity, was very minimal with the selectivity for the competing methanation reaction numbers of ≤1%. No higher hydrocarbon formation (C1+) was detected by GC.

3.4.3 Effect of Promoters A and C on Catalyst Attrition and Activity

Promoters A and C had been reported to have a positive impact on WGS catalyst performance. Table 16 presents the catalyst characterization results for these formulations and Figure 15 presents the catalyst activity results. As with promoter B, Promoters A and C do not seem to have any impact on BET surface area, density or attrition resistance. However, Figure 15 shows that surprisingly both the additives negatively impacted the catalyst performance.

Table 16. Catalyst Characterization results for Fe-based HT-WGS catalyst Formulations with Different Promoter B Contents

Sample ID	13838-50	13838-9	13838-58
Promoter	Baseline	A	C
Content	N/A	4.58	10
Catalyst Characterization Results			
BET SA m^2/g	65.3	66.97	57.8
Attrition (DI% 21/42 μm)[1]	3.1/11.6	1.57/4.42	1.70/5.78
Density (g/cc)	1.87	1.46	1.6

[1] RTI has upgraded its attrition test to provide attrition results at two particle sizes to improve information obtained from this test.

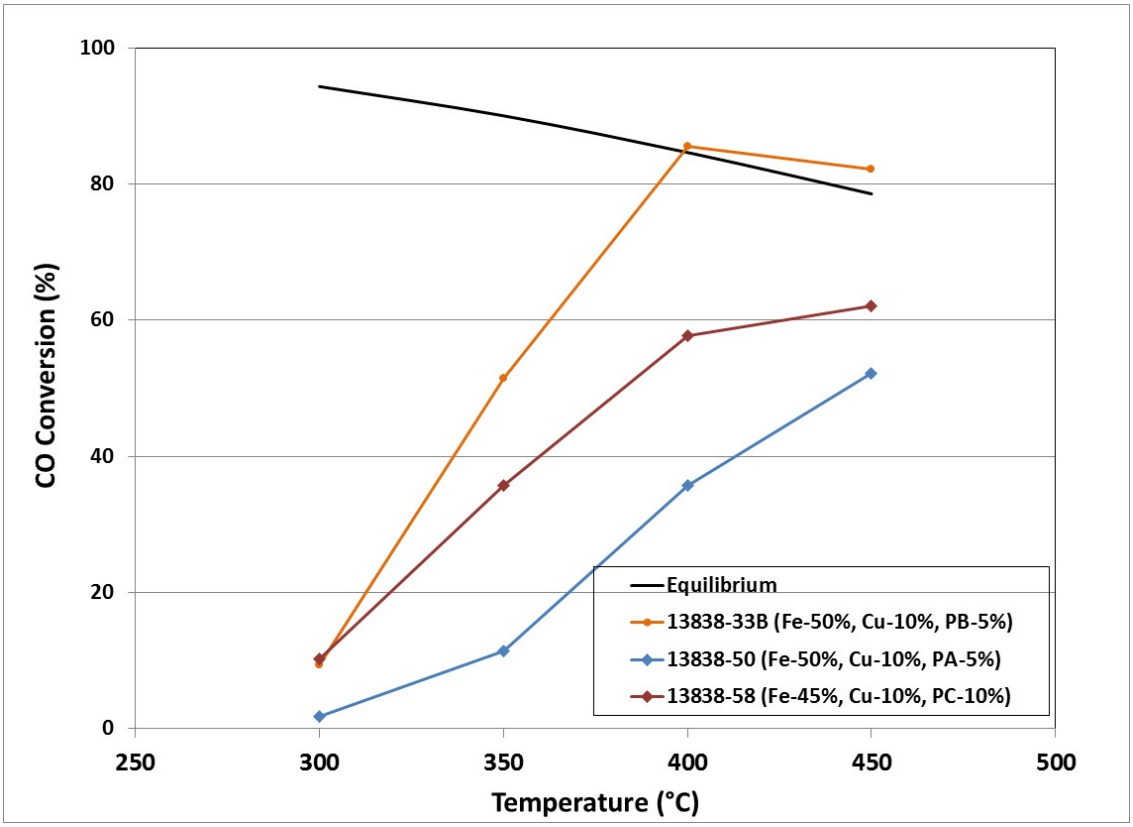

Figure 15. Catalyst Activity with Promoters A and C

3.5 Long-term stability of the optimized Fe-based HT-WGS catalyst

Based on the discussion in the previous sections, the only modification that had resulted in an improvement in catalyst activity that still met our attrition resistance target was increasing the Cu content to 10 wt%. A stability test was conducted for this optimized catalyst formulation (13838-33B). Figure 16 presents the results of this catalyst stability test. It can be seen that the catalyst exhibited a stable CO conversion for a duration of about 200 hours, with negligible selectivity towards methane formation. The stable CO conversion was found to be about 75%, which is more favorably comparable to that exhibited by the commercial HT-WGS catalyst (78%) than our baseline formulation (72%).

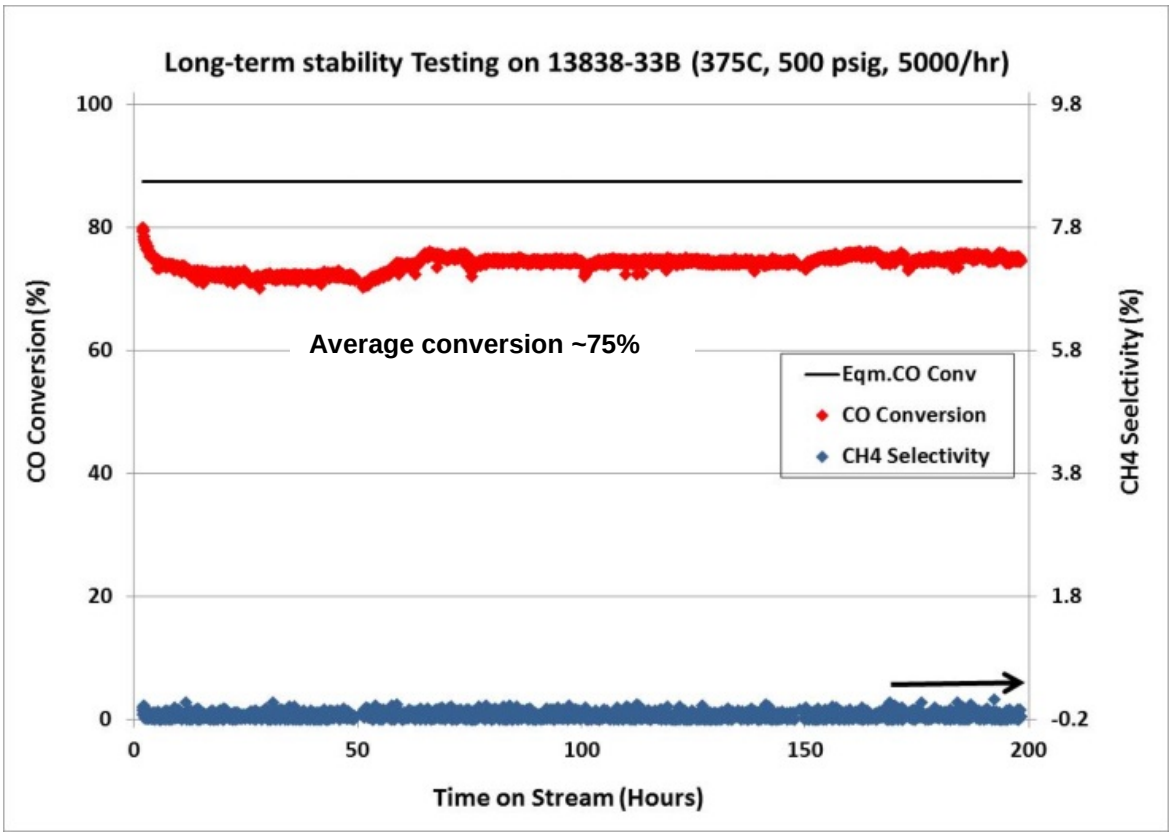

Figure 16. Catalyst Performance of HT-WGS sample (13838-33B) as a function of TOS

3.6 Modifications for Reducing Production Cost

Leveraging RTI's proprietary expertise associated with the commercial production of catalysts, we identified an alternative support precursor and precipitating agent that could significantly reduce the production cost for our fluidized-bed Fe-based HT-WGS catalyst formulation and potentially reduce emissions generated during catalyst production. Because of the potential cost benefits, an effort was made to use the alternative support precursor and precipitating agent along with sequential adjustments to preparation procedure A to optimize the catalyst formulation for this production process. Table 17 summarizes the catalyst characterization results for the formulations prepared in this optimization effort and provides comparison values for the new optimized catalyst formulation. Figure 17 presents a graphical representation of the catalyst characterization results for this series.

Table 17. Optimization Matrix for Reducing Catalyst Production Cost

Sample ID	13838-75	13838-79	13838-83	13838-87	13838-33B
Precursors	New	New	New	New	Optimized
Preparation procedure A	Baseline	4	5	6	Baseline
BET SA m^2/g	79.4	62.7	62.3	57.2	53.5
Attrition (DI% 21/42 μm)[1]	10.9/18.80	8.14/19.70	8.48/19.5	5.75/15.58	6.39/10.48
Density (g/cc)	1.11	1.32	1.42	1.57	1.71

[1] RTI has upgraded its attrition test to provide attrition results at two particle sizes to improve information obtained from this test

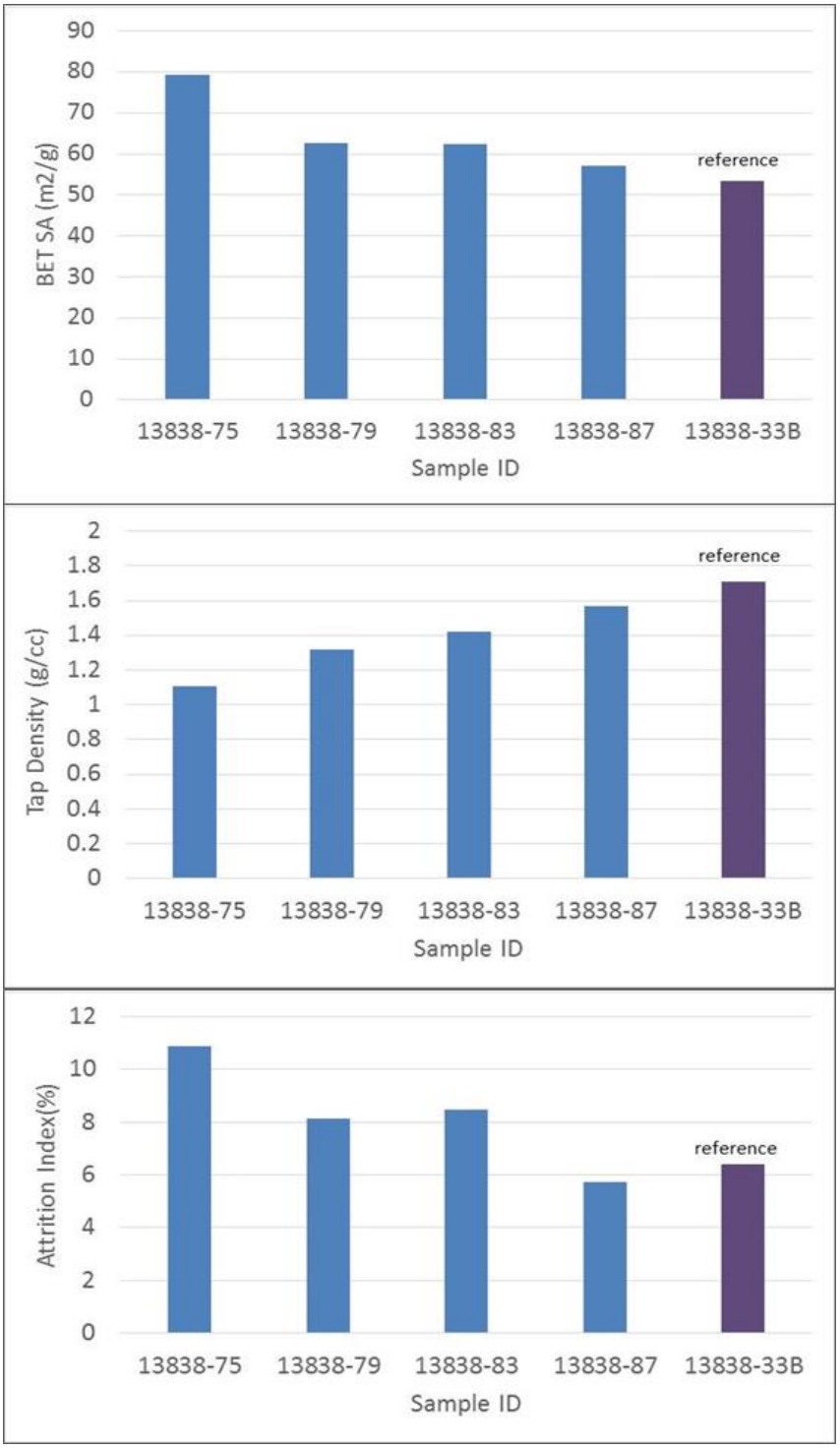

Figure 17. A comparison of BET surface area, tap density and attrition index of the catalysts prepared using the Reduced Cost Production Process

As was anticipated, use of an alternative support precursor and precipitating agent resulted in a catalyst formulation that was similar to our new optimized catalyst formulation but could be optimized further. Through sequential adjustments in preparation procedure A, the attrition resistance of the catalyst formulation from the new reduced cost production process was optimized. For the final optimized catalyst formulation using the reduced cost production process, the attrition test value was about 5.8% which is slightly lower (i.e., better) than for the optimized catalyst formulation made with the baseline production process.

ICP analysis indicated relatively high concentrations of residual ion content in the catalyst formulations with the new precursors and optimization for preparation procedure A. (Formulations 13838-75 to 13838-87). As the presence of this residual ion might have an adverse effect on catalyst performance, in particular catalyst stability, a final optimization formulation was prepared with different washing conditions. This new formulation with improved washing conditions successfully reduced the residual ion concentration by over 90%.

Figure 18 presents the results for activity testing of the catalyst formulations prepared with these new alternative precursors. Catalyst formulation 13838-87, which had an attrition resistance value better than our target value, also demonstrated the highest CO conversion especially for temperatures between 300°C and 400°C.

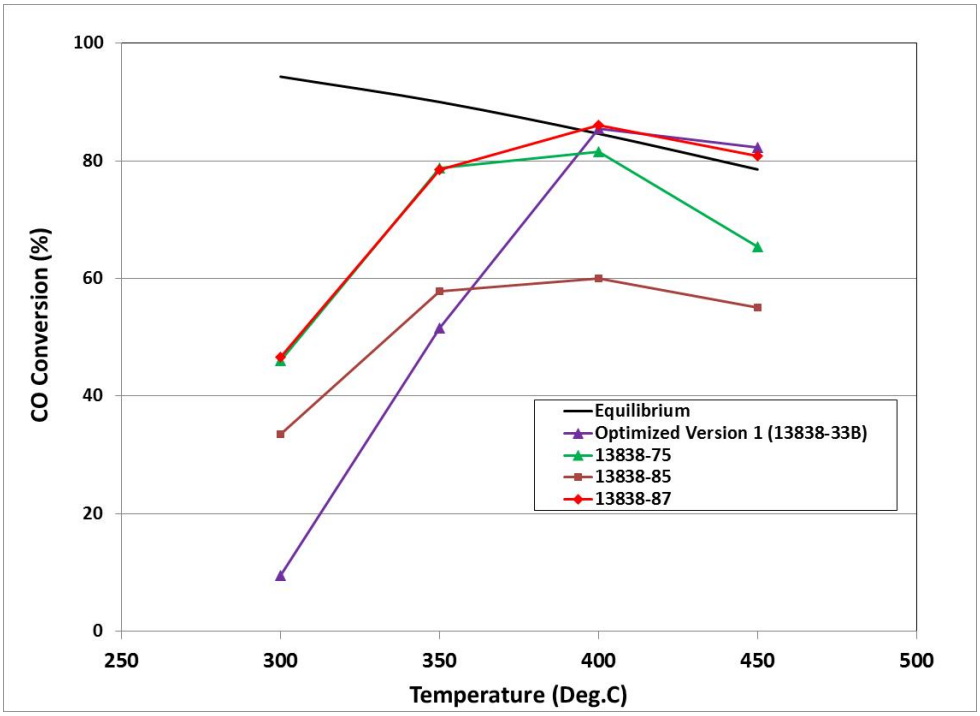

Figure 18. Catalyst Performance of the catalysts with lower cost route

Because this catalyst formulation 13838-87 should have additional benefits from a lower production cost, we conducted a standard catalyst stability test with this formulation. The results of the stability test are shown in Figure 19. Unfortunately, after about 400 hours of testing, our GC broke down and we had to install a replacement GC. This action caused the gap of data in Figure 19 just after 400 hours of operation and the slight shift in CO conversion when this replacement GC was brought online. In spite of this event, this catalyst formulation demonstrated a long term stable CO conversion of about 77%. Because this catalyst formulation 13838-87 best fulfilled our catalyst selection criteria and was made with the lowest cost commercial production process, this catalyst formulation represents our final optimized and recommended ATWGS catalyst formulation for this project.

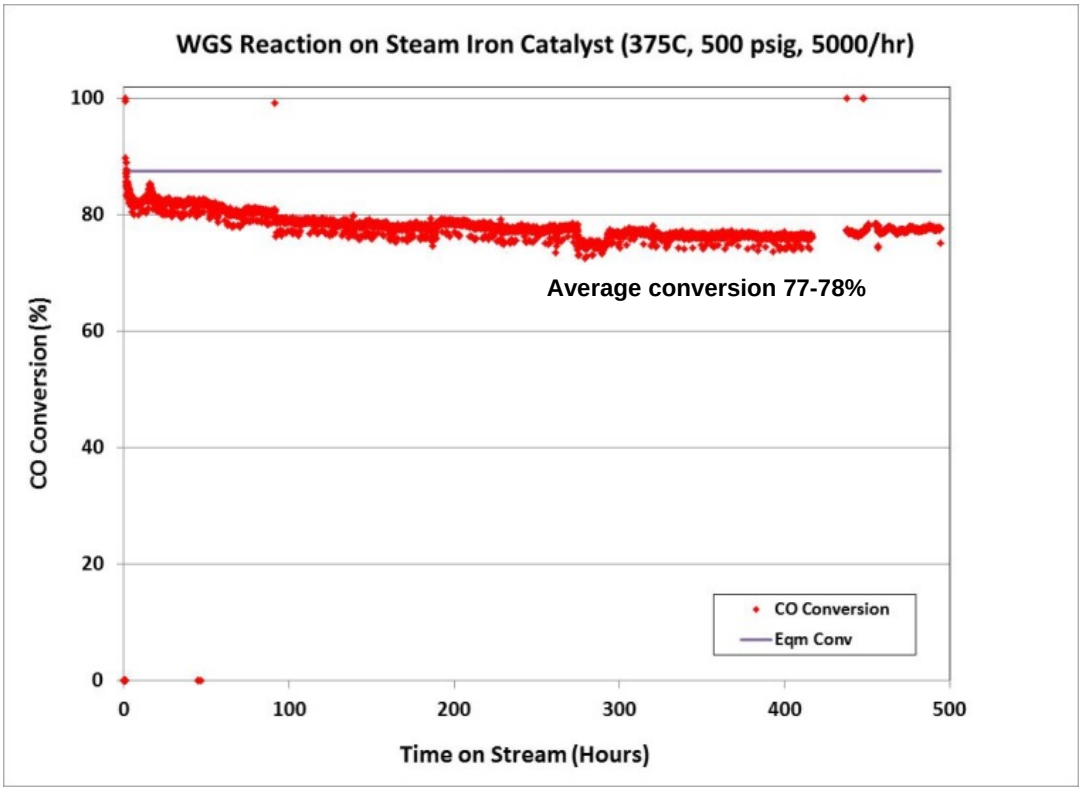

Figure 19. Catalyst Performance of HT-WGS sample (13838-87) as a function of TOS

4. Conclusions

Multiple versions of potential ATWGS catalyst formulations were synthesized and tested under this project task with the objective of optimizing the catalyst performance and attrition resistance of the baseline ATWGS catalyst formulation identified under DOE/NETL Cooperative Agreement DE-FE0012066. Through these catalyst formulations we were able to show that increasing iron content did result in more WGS activity, but at Fe concentrations > 50 wt% the resulting attrition values for these samples did not meet our target value. Several attempts to alter the preparation procedures to improve the attrition resistance of catalyst formulations did improve the attrition value, but they still did not meet our target attrition value. The main activity benefits at the higher Fe concentrations seem to be linked with an amorphous Fe phase which does not easily lend itself to preparing mechanically strong attrition-resistant catalyst formulations.

Evaluation of potential promoter materials did result in the demonstration that increasing Cu content to about 10 wt% did increase WGS activity. However, the catalyst formulations with 10 wt% Cu also had slightly higher attrition values, but these values were still within our target value. Our optimized catalyst formulation (13838-33B) with 10 wt% Cu demonstrated a long term stable CO conversion of about 75%. This became our first version of an optimized ATWGS catalyst.

Based on RTI's previous proprietary experience with commercial catalyst production, we were also able to identify an alternative support precursor and precipitating agent that could lower production cost and potentially eliminate emissions during the production process. Although introduction of these new precursor components did require some additional optimization of the preparation procedures, we did successfully identify a catalyst formulation that had higher WGS activity and acceptable attrition resistance. In long-term stability testing, the stable CO conversion for this catalyst formulation was close to 77% (almost identical to commercial HT-WGS catalyst). Because of its excellent overall performance (WGS activity, attrition resistance, and catalyst stability) that met all of our fundamental criteria and the utilization of a reduced cost production process, we selected this formulation (13838-87) as our final optimized and recommended ATWGS catalyst formulation for this project.

Based on the catalyst development efforts completed on this project, we have thus been able to identify two optimized catalyst formulations (13838-33B and 13838-87) having combined performance (WGS activity, long-term stability, and attrition resistance) that represent an improvement over the original baseline catalyst formulation. The best of these optimized formulations (13838-87) meets all of our key criteria with the added advantage that its production process is commercially viable, employs low cost precursors, and eliminates the need for any special emission control equipment in the production process.

One specific advantage of all the catalyst formulations prepared under this project has been the absence of chromium. This is a key component in commercial HT-WGS catalysts. The presence of hexavalent chromium ion in the production process and in the eventual disposal of the spent catalysts increases the potential for human exposure to this toxic chromium ion. Because none of the catalyst formulations developed in this project contain any chromium, these catalyst formulations are more environmentally friendly than standard commercial HT-WGS catalysts.

5. References

1. K. Kochloefl, in: G. Etrl, H. Knozinger, J. Weitkamp (Eds.), Handbook of Heterogeneous Catalysis, vol. 4, Wiley-VCH, Weinheim, 1997, pp. 1831–1843.
2. D.S. Newsome, Catalysis Reviews: Science and Engineering 21 (2) (1980) 275.
3. L. Lloyd, D.E. Ridler, M.V. Twigg, in: M.V. Twigg (Ed.), Catalyst Handbook, 2nd ed., Wolfe Publishing Ltd., London, 1989, pp. 293–295.
4. L. Zhang, X. Wang, J.M.M. Millet, P.H. Matter, U.S. Ozkan, Applied Catalysis A: General 351 (2008) 1.
5. G.K. Reddy, K. Gunasekera, P. Boolchand, J. Dong, P.G. Smirniotis, Journal of Physical Chemistry C 115 (2011) 7586.
6. T. Popa, G. Xu, T.F. Barton, M.D. Argyle, Applied Catalysis A: General 379 (2010) 15.
7. L. Lloyd, D.E. Ridler, M.V. Twigg, in: M.V. Twigg (Ed.), Catalyst Handbook, 2nd ed., Wolfe Publishing Ltd., London, 1989, pp. 302–304.

September 2016

Subtask 4.4 Topical Report: Basic Engineering Package for the Advanced Transport Water Gas Shift Process

DOE/NETL Cooperative Agreement: DE-FE0023577
Reporting Period Start: February 1, 2015
Reporting Period End: September 30, 2015

Authors: P. Sharma, D. Denton, and B. Turk

Submitted By

RTI International
P.O. Box 12194
Research Triangle Park, NC
27709-2194
http://www.rti.org/

Disclaimer

This report was prepared as an account of work sponsored by an agency of the United States Government. Neither the United States Government nor any agency thereof, nor any of their employees, makes any warranty, express or implied, or assumes any legal liability or responsibility for the accuracy, completeness, or usefulness of any information, apparatus, product, or process disclosed, or represents that its use would not infringe privately owned rights. Reference herein to any specific commercial product, process, or service by trade name, trademark, manufacturer, or otherwise does not necessarily constitute or imply its endorsement, recommendation, or favoring by the United State Government or any agency thereof. The views and opinions of authors expressed therein do not necessarily state or reflect those of the United States Government or any agency thereof.

Abstract

Under DOE Cooperative Agreement DE-FE0023577, a detailed techno-economic analysis prepared by Nexant evaluating the integration of advanced gasification technologies by Gas Technology Institute (GTI) and syngas cleanup and water gas shift (WGS) processes by Research Triangle Institute (RTI) for both integrated gasification combined cycle and coal-to-methanol applications (which included 90% carbon capture) established that the configuration which included RTI's Advanced Transport Water Gas Shift (ATWGS) process coupled with other GTI and RTI advanced technologies for gasification and syngas cleanup had the lowest costs, highest thermal efficiency, and lowest emissions of sulfur and CO_2 of all configurations evaluated. Under this same Cooperative Agreement, RTI also successfully optimized a catalyst formulation suitable for RTI's ATWGS process using catalyst activity, stability, attrition resistance, and commercial production benefits as optimization criteria. These two accomplishments show the potential for accelerating continued research and development leading to commercial deployment of RTI's ATWGS process. A final task under this Cooperative Agreement was the preparation of a preliminary basic engineering package (BEP) for an ATWGS pilot plant supporting future development efforts.

As part of this BEP, RTI developed a process flow diagram, a heat and mass balance, and a preliminary equipment design for a pilot scale ATWGS process. As no specific host site was available, key site specific information necessary for the design was based on reasonable assumptions rather than actual data. As a consequence, this preliminary BEP will have to be tailored somewhat when the actual site specific data does become available. As part of its effort in preparing this preliminary BEP, RTI also calculated a budgetary estimate using APSEN tools for completing the detailed design, construction, and one calendar year of operation for this pilot-scale ATWGS system. The estimated cost for construction and installation of the pilot-scale ATWGS system was approximately $2.0 million with an estimated operating budget of approximately $1.65 million for 4,000 hours of operation over one calendar year.

Table of Contents

List of Tables

List of Figures

Number **Page**

Executive Summary

RTI is developing an advanced transport reactor water gas shift (ATWGS) process that offers cost and thermal efficiency benefits over conventional commercial water gas shift processes. Under DOE/NETL Cooperative Agreement DE-FE0023577, a detailed techno-economic analysis was completed by Nexant for the integration of advanced technologies from the Gas Technology Institute (GTI) and Research Triangle Institute (RTI) into integrated gasification combined cycle (IGCC) and coal-to-methanol (CTM) production applications (with 90% carbon capture) in which the configuration with the best overall performance in terms of cost, thermal efficiency and reduction of sulfur and CO_2 emissions included RTI's ATWGS. Under a different task on this same DOE/NETL Cooperative Agreement, RTI has been able to successfully optimize a fluidized-bed attrition resistant catalyst formulation for this ATWGS process with catalyst activity essentially identical to a commercial fixed-bed catalyst. The next developmental step for RTI's ATWGS process would be a pilot-scale demonstration using a limited commercial production batch of this optimized catalyst formulation.

Preparation of the preliminary basic engineering package (BEP) for this pilot-scale demonstration was one of the subtasks under this DOE/NETL Cooperative Agreement. Because a specific host site has not yet been identified, reasonable assumptions relating to the amount and composition of the syngas as well as the amount and availability of utilities and supporting processes were made. To ensure that all the sizes of the equipment in the transport reactor were > 1 inch in diameter, to avoid issues created by wall effects at smaller sizes, the syngas flow rate for the pilot plant was assumed to be 5,000 standard cubic feet per hour (scfh). The site was also assumed to be capable of supplying electricity, 400 psig steam, cooling water and 400 psig nitrogen. Although it might be possible to use the shifted syngas, the assumption for this pilot-scale demonstration was that the shifted syngas would be flared. The host site was assumed to have a flare system capable of handling this added load and a treatment or disposal process for the process condensate.

With these preliminary assumptions about the host site, we developed a process flow diagram and heat and mass balances for this pilot-scale system. ASPEN Plus V8.8 was used for process simulations to develop the heat and mass balances for the pilot-scale system.

Based on the process simulations, an equipment list for the major pieces of equipment was generated. Leveraging RTI's experience with transport reactor design, a preliminary design for the transport reactor system was developed. The transport reactor design comprised of a mixing zone (10' x 4"), a riser (44' x 1.5"), a standpipe (35' x 1"), a solid cooler (10' x 2") and loop seal transfer lines (5' x 1"). ASPEN Plus V8.8 was used to size the remainder of the major equipment.

Aspen Process Economic Analyzer (APEA) was used to estimate the capital costs of the equipment. The total estimated bare-erected cost of the pilot-scale system was $2,003,530. The transport reactor represents about 75% of the total equipment cost. Based on RTI's experience with the operation of pilot-scale systems at host sites, RTI put together an operation plan for an operation period of one calendar year to complete an estimated 4,000 hours of operation. The operating cost was estimated by accounting for labor, consumables and utilities cost. The labor costs were estimated assuming 24/7 operation provided by four operating teams with two operators per shift with one person providing full time maintenance support. The total estimated cost for the operating plan including labor, consumables, and utilities, was estimated to be about $1.65 million.

1. Introduction

RTI is developing an advanced transport reactor water gas shift (ATWGS) process that has lower costs and higher thermal efficiency than conventional fixed-bed water gas shift (WGS) processes. In a conventional fixed-bed WGS process, the exothermic heat generated by the WGS reaction, $CO + H_2O = CO_2 + H_2$ (ΔH = -41 kJ/mole), results in temperature rise in the reactor and heating of the product gas. At steady state, essentially all of the exothermic reaction heat is carried out of the reactor by the product gas. As a consequence of the limited heat capacity of the product gas, the temperature of the product gas is very high. This has a number of adverse consequences, which are:

- Lower conversion. The WGS reaction is an equilibrium reaction that because of its exothermic nature has lower conversion as the temperature is increased.
- Reduced catalyst life. The primary deactivation mechanism for WGS catalysts is sintering of the active component, which is faster at higher temperatures.
- Reduced thermal efficiency. To keep the reactor temperature below the maximum recommended manufacturer reaction temperature, especially for CO-rich syngas mixtures, significantly more stream must be added in the WGS process.

In RTI's ATWGS process, the catalyst is circulated through a transport reactor system. Thus, both the product gas and catalyst particles carry the exothermic reaction heat out of the reactor. By passing the catalyst particles through a solids cooler, the sensible heat of the solids can be recovered as high-quality steam. Because both the product gas and catalyst, which represents a much larger thermal mass, are responsible for removing the heat of reaction from the reactor, the reactor will operate at a lower temperature with an improved equilibrium conversion. By optimizing the fraction of heat carried out of the reactor between the product gas (steam) and catalyst, it is possible to lower the steam consumption in the WGS process, which will increase thermal efficiency.

In a techno-economic analysis study completed by Nexant as part of the Department of Energy/National Energy Technology Laboratory (DOE/NETL) cooperative agreement DE-FE0023577, RTI's ATWGS process showed reductions in capital and operating costs and an increase in the net power generated by the steam turbine compared to RTI's advanced fixed-bed WGS (AFWGS) process. Although it was outside the scope of Nexant's study, RTI's preliminary estimates indicated that when compared with conventional commercial WGS processes, both RTI's advanced WGS processes (ATWGS and AFWGS) show at least 30% reduction in capital cost and 40% improvement in the net amount of high pressure steam generated.

In DOE/NETL cooperative agreement DE-FE0023577, RTI completed catalyst development in which a catalyst formulation was identified which had catalyst activity nearly identical to a commercial fixed-bed WGS catalyst, demonstrated stability for close to 500 hours of continuous operation, and had an attrition value identical to that of an equilibrium fluid catalyst cracking (FCC) catalyst. These criteria were chosen as the selection criteria for identifying a catalyst that would successfully enable our ATWGS process. This optimal catalyst formulation was also optimized for lowest commercial production cost. Therefore, a viable catalyst formulation is available for preparation of commercial vendor production batches.

As part of RTI's effort under the DOE/NETL cooperative agreement DE-FE0023577, RTI also developed a preliminary basic engineering package (BEP) for a pilot plant scale system of the ATWGS process. This BEP and preparation of a limited commercial production batch are key components needed for the next step of pilot plant demonstration of the ATWGS process. This topical report provides the documentation for this BEP.

2. Process Overview

2.1 Process Description

The process flow diagram (PFD) for the ATWGS process is shown in Figure 1. The primary components of the ATWGS process are the transport reactor, solids cooler and a fluidized-bed WGS catalyst. In the proposed pilot-scale system, some pre-conditioning equipment for the syngas has been included. The three functions to be performed by this pre-conditioning equipment are to heat up the syngas to a suitable inlet temperature, reduce the sulfur concentration of the syngas feed to < 50 parts-per-million by volume (ppmv), and enable adding steam to the syngas feed. The post-conditioning equipment consists of several heat exchangers to remove the sensible heat for the product syngas, a filter to capture catalyst fines entrained out of the reactor, and a knock out pot for collection of condensed water.

In our pilot-scale ATWGS system, we propose to use a transport reactor system that is composed of a mixing zone and a riser. In the mixing zone, the syngas feed is intimately mixed with the catalyst particles returning from the solids cooler. By incorporating a mixing zone, we ensure that the syngas and catalyst are adequately mixed to promote fast heat and mass transfer between the syngas and catalyst particles. Because of the mixing in this zone, the WGS reaction will begin to occur.

At the top of the mixing zone, the diameter of the reactor decreases, which increases the superficial velocity and results in the entrainment of the catalyst particles by the gas. The syngas continues to undergo more WGS as it is entrained through the riser.

After being entrained by the syngas through the riser, the gas-solid mixture enters a cyclone that effectively separates the product gas from the catalyst particles. The product gas with some fines that are too small to be captured by the cyclone are sent on to the post-condition system which cools the product gas, captures the catalyst fines in a filter, and separates any condensate from the syngas prior to sending it on to a flare. The catalyst particles separated by the cyclone fall into the solids cooler, where some of their sensible heat is extracted as steam before being returned to the mixing zone.

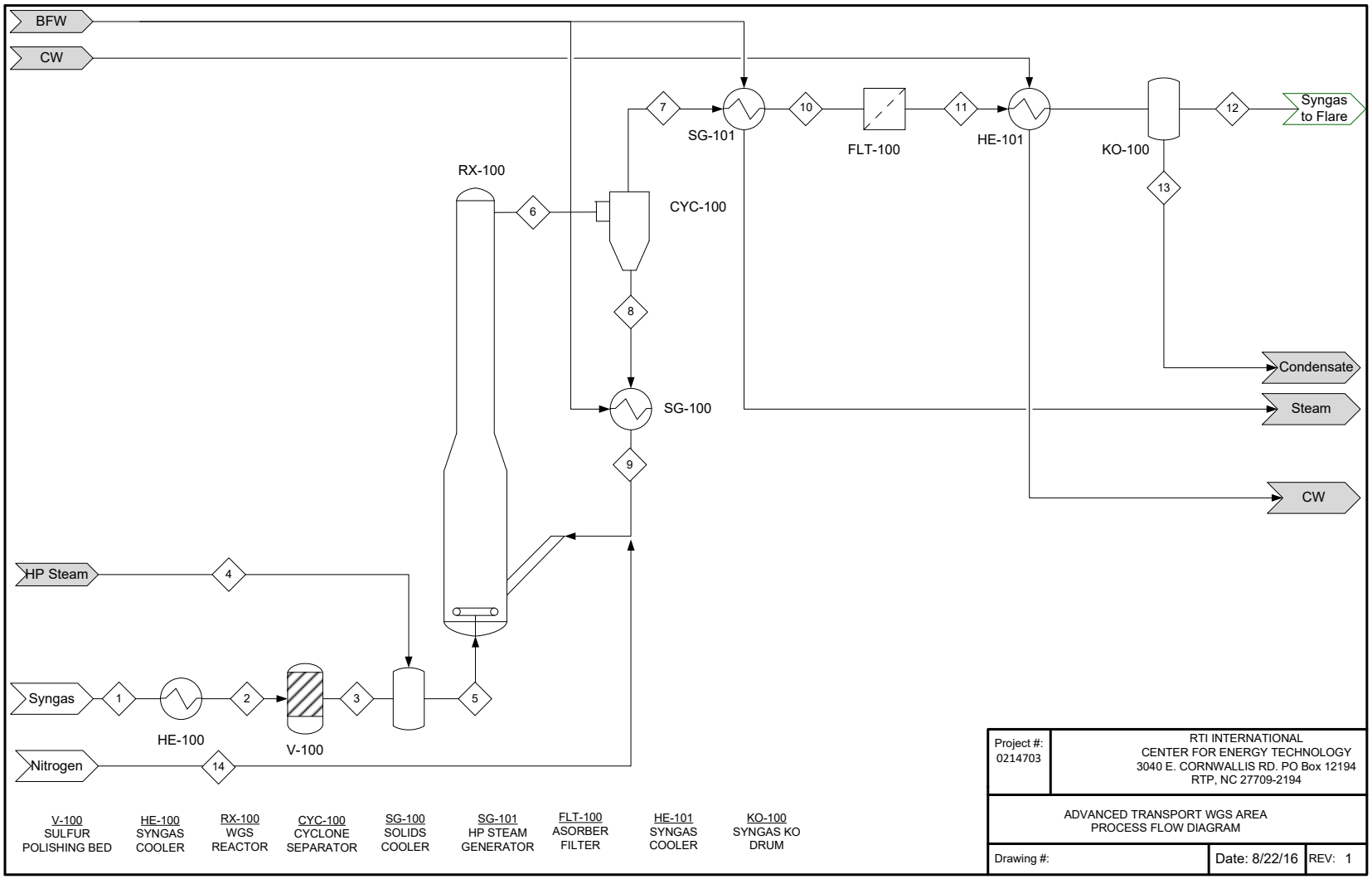

Figure 1. Process Flow Diagram for Advanced Transport Water Gas Shift Process

2.2 Host Site Specifications/Assumptions

One of the first steps in the preparation of the BEP would be selection of a potential host site for this pilot-scale demonstration. The selection of a host site is important, because the host site will provide a large amount of the information that is required to establish a design basis document. Some of this host site information includes the composition and amount of syngas available for pilot plant testing, the amount and availability of the utilities, the existing facilities to treat byproduct streams like shifted syngas and wastewater, available footprint for the pilot-scale system, standard meteorological data, and safety and other process specifications that are site specific.

In the absence of a selected host site, we have made some fundamental assumptions. For the syngas source, we have used the syngas composition and process conditions available from Gas Technology Institute's (GTI"s) R-GAS™ gasifier. The specific syngas conditions assumed are listed in Table 1. We have also assumed an inlet syngas flow of 5,000 standard cubic feet per hour (scfh) to ensure that all the dimensions of the reactor system will be ≥1 inch so as to avoid any wall effect issues that make operation more challenging. We have assumed that the host site will have the available treatment facilities with sufficient extra permitted capacity to flare our syngas product and treat or adequately dispose of any process condensate generated. We have assumed that the catalyst fines generated can be handled as non-hazardous solid waste. The host site is also assumed to have the specific utilities listed in Table 2. Finally, the host site was assumed to have available space near the syngas source for the pilot-scale system.

Table 1. Feed Syngas Composition and Conditions

Composition, vol%	
H_2	16.66
CO	24.05
CO_2	5.88
CH_4	0.18
H_2S	0. 06
N_2	10.34
H_2O	42.82
Conditions	
Temperature, °F	500
Pressure, psia	380
Total Molar Flow lbmol/hr	13.9
Total Mass Flow lb/hr	282.7

Table 2. Assumed Site Utilities

Utility	Conditions
Steam	450°F and 400 psig
Nitrogen	75°F and 400 psig
Cooling Water	48°F
Instrument Air	60-100 psig (dew point <-22 °F)
Electric Power	3 phase 110/240V

2.3 Heat and Mass Balance

The heat and mass balances for the pilot-scale system were developed with ASPEN Plus V8.8. For these heat and mass balances, the target CO conversion for the reactor was 90%. The results from the heat and mass balances are provided in Table 3. The stream numbers in Table 3 correspond to the stream numbers in the PFD in Figure 1.

Table 3. Heat and Mass Balance for the Advanced Transport Water Gas Shift Process

Component Mole Fraction	Syngas In	Syngas In to Polishing Bed	Syngas Exit from Polishing Bed	Shift Steam	Syngas In to WGS Reactor	Syngas Exit from WGS Reactor	Syngas Exit from WGS Reactor	Solids In to the Cooler	Solids Exit from the Cooler	Syngas In to the Filter	Syngas Exit from the Filter	Syngas In to the Condenser	Syngas Exit from the Condenser	Nitrogen for Solids Fluidization
	1	2	3	4	5	6	7	8	9	10	11	12	13	14
H2	0.1666	0.1666	0.1667	0.0000	0.1530	0.3501	0.3434	0.0000	0.0000	0.3434	0.3434	0.4701	0.0000	0.0000
CO	0.2405	0.2405	0.2406	0.0000	0.2208	0.0227	0.0223	0.0000	0.0000	0.0223	0.0223	0.0305	0.0000	0.0000
CO2	0.0588	0.0588	0.0588	0.0000	0.0540	0.2514	0.2465	0.0000	0.0000	0.2465	0.2465	0.3375	0.0000	0.0000
CH4	0.0018	0.0018	0.0018	0.0000	0.0017	0.0017	0.0016	0.0000	0.0000	0.0016	0.0016	0.0023	0.0000	0.0000
H2S	0.0006	0.0006	0.0000	0.0000	0.0000	0.0000	0.0000	0.0000	0.0000	0.0000	0.0000	0.0000	0.0000	0.0000
COS	0.0000	0.0000	0.0000	0.0000	0.0000	0.0000	0.0000	0.0000	0.0000	0.0000	0.0000	0.0000	0.0000	0.0000
NH3	0.0000	0.0000	0.0000	0.0000	0.0000	0.0000	0.0000	0.0000	0.0000	0.0000	0.0000	0.0000	0.0000	0.0000
HCL	0.0000	0.0000	0.0000	0.0000	0.0000	0.0000	0.0000	0.0000	0.0000	0.0000	0.0000	0.0000	0.0000	0.0000
N2	0.1034	0.1034	0.1035	0.0000	0.0950	0.0971	0.1144	0.0000	1.0000	0.1144	0.1144	0.1566	0.0000	1.0000
AR	0.0000	0.0000	0.0000	0.0000	0.0000	0.0000	0.0000	0.0000	0.0000	0.0000	0.0000	0.0000	0.0000	0.0000
H2O	0.4282	0.4282	0.4284	1.0000	0.4756	0.2770	0.2716	0.0000	0.0000	0.2716	0.2716	0.0029	1.0000	0.0000
HCN	0.0000	0.0000	0.0000	0.0000	0.0000	0.0000	0.0000	0.0000	0.0000	0.0000	0.0000	0.0000	0.0000	0.0000
O2	0.0000	0.0000	0.0000	0.0000	0.0000	0.0000	0.0000	0.0000	0.0000	0.0000	0.0000	0.0000	0.0000	0.0000
SO2	0.0000	0.0000	0.0000	0.0000	0.0000	0.0000	0.0000	0.0000	0.0000	0.0000	0.0000	0.0000	0.0000	0.0000
S	0.0000	0.0000	0.0000	0.0000	0.0000	0.0000	0.0000	0.0000	0.0000	0.0000	0.0000	0.0000	0.0000	0.0000
Total Flow lbmol/hr	13.9	13.9	13.9	1.3	15.2	15.2	15.5	0.0	0.0	15.5	15.5	11.3	4.2	0.3
Total Flow lb/hr	282.7	282.7	282.4	22.5	304.9	305.9	314.3	0.0	0.9	314.3	314.3	239.1	75.2	9.3
Total Flow cuft/hr	371.4	438.8	444.5	19.3	477.1	551.9	570.9	0.0	1.1	415.6	423.1	201.4	1.2	4.7
Solid Flow lb/hr	0.0	0.0	0.0	0.0	0.0	1577.0	0.0	1577.0	1577.0	0.0	0.0	0.0	0.0	0.0
Temperature F	500	650	650	450	637	725	725	725	647	400	400	95	95	75
Pressure psia	380	375	370	415	370	350	345	345	345	340	334	330	330	400
Vapor Frac	1.00	1.00	1.00	1.00	1.00	1.00	1.00	0.00	1.00	1.00	1.00	1.00	0.00	1.00
Liquid Frac	0.00	0.00	0.00	0.00	0.00	0.00	0.00	1.00	0.00	0.00	0.00	0.00	1.00	0.00
Enthalpy Btu/lb	-3092	-3031	-3033	-5597	-3223	-3334	-3241	-6899	143	-3379	-3379	-2785	-6802	-4
Enthalpy Btu/hr	-8.74E+05	-8.57E+05	-8.57E+05	-1.26E+05	-9.83E+05	-1.02E+06	-1.02E+06	-1.09E+07	1.33E+02	-1.06E+06	-1.06E+06	-6.66E+05	-5.11E+05	-3.34E+01
Density lb/cuft	0.8	0.6	0.6	1.2	0.6	0.6	0.6	248.6	0.8	0.8	0.7	1.2	62.1	2.0
Average MW	20.3	20.3	20.3	18.0	20.1	20.1	20.3	102.0	28.0	20.3	20.3	21.1	18.0	28.0

3. Equipment List and Design

The specific equipment for which design estimations were completed for the ATWGS pilot-scale system are listed in Table 4. The heat and mass balances from Table 3 provided the basis from which the equipment was sized. ASPEN Plus V8.8 was used for estimating design parameters for all of the ancillary equipment including the Start-up Heater (HE-101), Sulfur Polishing Bed (V-100), Cyclone (CYC-100), Syngas Cooler (SG-101), Syngas Filter (FLT-100), and Syngas Cooler (HE-101). For the key components of the transport reactor system, the specific dimensions were calculated based on our knowledge and expertise in fluidized/transport systems and input from external expert consultants.

Table 4. Equipment List for Pilot –Scale ATWGS System

TAG ID	DESCRIPTION
HE-100	Start-up Heater
V-100	Sulfur Polishing Bed
RX-100	WGS Transport Reactor with Refractory Lining
CYC-100	Cyclone Separator
SG-100	Solids Cooler (Steam Generator)
SG-101	Syngas Cooler (Steam Generator)
FLT-100	Syngas Filter
HE-101	Syngas Cooler

Transport Reactor Design (RX-100)

The results from the catalyst development efforts indicate that at temperatures above 650°F, the CO conversion approaches equilibrium conditions. At temperatures below 650°F, the rate of CO is kinetically controlled. Because of this knowledge, we included a mixing zone and riser in our transport reactor design. For our design of the mixing zone, we attempted to achieve constant stirred tank reaction (CSTR) conditions. With CSTR conditions, not only would we maximize mixing of the syngas feed with the catalyst particles returning from the solids cooler, but also back mixing of the hotter catalyst particles that have been heated by the WGS reaction. With this design approach, the temperature in the mixing zone will be over 650°F and the WGS reaction will rapidly proceed towards equilibrium.

The first step of the design for the mixing zone and riser was to determine the choking velocity. Using the information on the catalyst particles size and density, we estimated the choking velocity and selected a gas superficial gas velocity of approximately half the choking velocity in the mixing zone to achieve our target mixing conditions. For the riser, we selected a gas superficial velocity of over twice the choking velocity to ensure efficient entrainment of the catalyst particles through the riser. To calculate the height of the mixing zone and riser, a residence time of about 4 seconds was selected for each of the mixing zone and riser. Based on temperatures >650°F, the reaction rate should be fast enough to achieve 90% CO conversion in a fraction of the 8 seconds of total residence time in the transport reactor (4 seconds in mixing zone and 4 seconds in the riser). Based on the gas superficial velocities, the diameter of the mixing zone was calculated to be 3.7 inches and the riser to be 1.5 inches.

A detailed pressure balance across the entire transport reactor system was completed by estimating pressure drop across different sections of the reactor system, to ensure stable, consistent and sufficient solid circulation. The dimensions of different sections of the transport reactor are listed in Table 5.

Table 5. Dimensions of Transport Reactor Sections for ATWGS Pilot-Scale System

Section	Height (feet)	Diameter (inches)
Mixing zone	10	4
Riser	44	1.5
Standpipe	35	1
Solids cooler	10	2
Loop seal transfer line	5	1

Solid Cooler Design (SG-100)

The key design goal for the solids cooler was to remove sufficient sensible heat from the catalyst particles to enable reducing the steady state operating temperature in the reactor and reduce the addition of steam to the syngas for controlling reactor temperature. Because the available literature suggests that vertical tubes enable better heat transfer from a moving bed of solids, we chose a shell and tube heat exchanger that is mounted vertically with the catalyst particles flowing from top to bottom on the shell side and the boiler feed water in the tube side.

Although every effort was made to get a commercial vendor of commercial solids coolers to complete the design, we were not successful because of the small size of the specific solids cooler for our pilot-scale system and the fact our goal was just preparation of a preliminary BEP. Because the fundamental function of any heat exchanger is the heat transfer, we realized that with the correct values for the heat transfer on the solids side of the exchanger we could calculate the

dimensions for our solids cooler. Because we would not have the design and operating experience that has allowed commercial solids cooler vendors to optimize the performance of their equipment, we should make a conservative selection of the heat transfer coefficient. After carefully reviewing the available literature for heat transfer we came up with an estimated range for the heat transfer coefficient for our system. Our final selection of the heat transfer coefficient for the solids was 150 Btu/hr-ft^2-°F and a log mean temperature difference (LMTD) of 347°F. Although we were not able to find a vendor that would provide this solids cooler design, we were able to find several external technical experts that were willing to review our design and provide comments. These experts approved our choice of heat transfer coefficient on the solids side and overall design of our solids cooler. Our final vetted design consisted of a double pipe heat exchanger arrangement placing a 1 inch ID x 8 feet long inner tube inside a 2" ID shell to provide the 1.2 ft^2 of estimated required heat transfer area.

Instrumentation and Control System

Our approach to the control for this ATWGS pilot-scale system was to assume that key automated control would include flow rates of the different process streams, temperature control, and system pressure control. In general, we assumed that a field operator would provide significant assistance in the operation of the system particularly with processes like emptying the filter lock hopper system. No actual control system was selected as this selection is typically based on using software, hardware and a graphical interface design that is familiar to the host site personnel.

Another feature for our ATWGS pilot-scale system was to ensure that the transport reactor system would be heavily instrumented with thermocouples and differential pressure taps to facilitate monitoring the hydrodynamic movement of the catalyst particles through the system. In addition, we would need to analyze the syngas composition of the syngas feed and product gas. The main species of interest include carbon monoxide, carbon dioxide, hydrogen, steam, and C1 to C4 hydrocarbons. Although our preferred choice would be continuous online analyzers, this will probably not be possible based on the large number of species that needs to be measured. The next best alternative would be a gas chromatograph with a relatively short run/cycle time.

Safety and Environmental Considerations (Permits)

A detailed PHA or HAZOP will be conducted on the ATWGS pilot-scale system on the system design prior to the release for actual construction and just prior to the start of commissioning. No specific permitting activities were completed as part of this BEP, but these will need to be addressed when a host site is selected and work on detailed design of the pilot-scale ATWGS system begins.

Without a specific host site, a significant number of assumptions had to be made to complete the design of the key equipment for the ATWGS pilot-scale system. When an actual host site is selected these assumptions will need to be altered to match the available conditions at the

host site. The host site will also be able to provide much more specific information about their recommendation of preferred equipment vendors, recommended control systems and strategies, operating philosophies, safety specifications and permitting requirements. More details on the design and specification for each system are provided in Appendix A.

4. Preliminary Operational Plan

Towards the end of construction of the ATWGS pilot-scale system, a PHA or HAZOP will be scheduled to ensure that any recommendations at the review completed at the end of detailed design were implemented and to address any changes that were made as part of the construction effort. A commissioning plan will be prepared to ensure efficient and effective shake down of the equipment. One important feature of this commissioning plan will be to avoid and definitively minimize the use of hydro-testing to minimize the introduction of a fluid in the transport reactor system that might lead to agglomeration of the catalyst particles upon contact with the fluid.

During the commissioning, start up and operating and shut down procedures for the ATWGS pilot-scale system will be developed by the commissioning team. The primary goals of the startup will be to load any required catalyst, pressurize the system, start catalyst circulation and heat up with an inert process gas, like nitrogen. The transition to operating conditions will be initiated by the introduction of steam followed by syngas when there is evidence of a suitable amount of steam in the product stream. The introduction of syngas should initiate the WGS reaction which will result in a temperature rise in the reactor. As this temperature rises, the flow of water will be increased in the solids cooler to begin removing this heat. The syngas flow to the reactor and water flow in the solids cooler will gradually be increased to the target operating conditions. During operation, we will focus on two key objectives. The first will be to vary and/or parametrically test the performance and /or operating conditions to explore the range of suitable, acceptable, and optimal operating conditions and performance. After completing this objective, the next objective will be to select a single set of operating conditions and attempt to complete as much continuous operation as possible to establish availability and recommendations for scheduled maintenance. Our preliminary estimate for the total calendar time for operation is one year with the goal of achieving roughly 4,000 hours of total operation.

A set of shutdown procedures will also need to be prepared. These shutdown procedures will need to include appropriate shutdown sequences for any trip associated with the host site's syngas production system and/or utility, any trip or failure in the pilot-scale system that would require the system to be shut down for operator safety and/or equipment protection or repair, and finally a controlled shutdown of the pilot-scale system. These shutdown procedures will also need to employ the approved lock-out tag-out (LOTO) protocol used by the host site.

5. Cost Estimate

5.1 Capital Cost Estimation Methodology

With the equipment design completed, ASPEN Process Economic Analyzer (APEA) and vendor quotes (where available from historical data) were used to develop the bare erected cost of each piece of major equipment. These bare erected costs (BEC) for the major equipment in the ATWGS pilot-scale system are provided in Table 6 along with information and tag identification numbers.

The Solids Cooler is a proprietary technology thereby making it difficult to obtain cost quotes. This piece of equipment was costed using the closest heat exchanger design listed in ASPEN PROCESS ECONOMIC ANALYZER. The equipment design and cost were then carefully discussed and vetted with external experts for their accuracy.

Table 6. Capital cost of the major equipment in the Advanced Transport Water Gas Shift process

TAG ID	DESCRIPTION	TYPE	BEC ($)
HE-100	Start-up Heater	Furnace	135,600
V-100	Sulfur Polishing Bed	ZnO Bed	126,800
RX-100	WGS Transport Reactor with Refractory Lining	Transport Reactor	1,558,708
CYC-100	Cyclone Separator	Cyclone Separator	10,800
SG-100	Solids Cooler (Steam Generator)	Shell and Tube Heat Exchanger	35,769
SG-101	Syngas Cooler (Steam Generator)	Shell and Tube Heat Exchanger	64,800
FLT-100	Syngas Filter	Sintered Metal Filter	19,605
HE-101	Syngas Cooler	Shell and Tube Heat Exchanger	51,400
Total Capex			**2,003,530**

The total estimated BEC of the plant is $2,003,530, including factored instrumentation and controls costs. The major contributor to the total cost, as expected, is the transport reactor which constitutes about 75% of the total equipment cost. Since facility integration costs are highly specific to a given facility, they were not included in this cost estimate. When an actual host site is identified, this estimated BEC will need to be revised to account for facility integration and for any differences between the assumptions made and the actual conditions that exist at the host site.

5.2 Operation and Maintenance Costs

In addition to the cost of construction of the ATWGS pilot-scale system, there will be costs associated with the operations. The key components of this operating cost will be labor, utilities, and supplies. For the labor, we have estimated that we will have four operating teams consisting of two operators with one monitoring the process control system and the second being a field operator. These operating teams will be used to provide 24/7 operation when the pilot plant is running. Thus, we have assumed the operating team will be required for the entire calendar year. When the pilot plant is down, we have assumed that the operating teams will take on the role of supporting maintenance and repair of the pilot plant to return to operation as rapidly as possible. We have assumed that we will have one full time maintenance person that can lead the repair/modification activities during down times and provide additional support, plan/complete maintenance activities, and/or proactively plan activities for future shut downs.

Without a specific host site, it is very difficult to estimate the amount and cost of the utilities that will be required. As this is an importance cost, we have included an estimated monthly allowance for utilities of about $20 K with a total cost for the year of operation of $250K.

We have also included the cost of preparation of a limited commercial batch of the fluidized-bed WGS catalyst. We have assumed that this limited commercial production batch should be enough to fill the pilot plan system two times.

Our estimated operating costs are shown in Table 7.

Table 7. Operating Costs for the Advanced Transport Water Gas Shift Process

	INITIAL & ANNUAL O&M EXPENSES					
Case:	ATWGS System with Transport Reactor Technology					
Period of Operation	**1 yr**					
Plant Size (scfh of syngas treated)	**5,000**					
OPERATING & MAINTENANCE LABOR						
Skilled Operating Labor rate (base)			$50.00	$/hr		
Operating Labor Rate (base)			$40.00	$/hr		
Maintenance Labor Rate (base)			$40.00	$/hr		
Operating Labor Burden:			30.00	% of base		
Labor Overhead Charge			25.00	% of labor		
Operating Labor Requirements per Shift			**units/mod**			
Skilled Operator			1.0			
Operator			1.0			
TOTAL Operating Jobs			2.0			
						Annual Cost $
Annual Operating Labor Cost						$1,222,020
Maintenance Labor Cost						$129,314
TOTAL FIXED OPERATING COSTS						**$1,351,334**
VARIABLE OPERATING COSTS						
Chemicals	Initial Fill	Annual	Unit Cost			
Water Gas Shift Catalyst (lbs)	300	300	15.00		$4,500	$4,500
ZnO (lbs)	1236	7416	5.00		$6,180	$37,080
Subtotal Chemicals					**$10,680**	**$41,580**
Utilities						**$250,000**
TOTAL OPERATING COSTS						**$1,653,594**

6. Conclusions and Path Forward

A preliminary BEP for a pilot-scale ATWGS system has been prepared to develop a preliminary budgetary estimate with which to seek funding to design, build, and operate a pilot-scale ATWGS system at a host site. Because a specific host site has not yet been identified, assumptions were made about the host site. The key assumptions were that the host site should have the ability to provide a suitable syngas stream at about 400 psig. We have also assumed that the host site will have sufficient space to install the pilot-scale system and the necessary utilities. The specific utilities that have been assumed in the preparation of this BEP include electric power, 400 psig nitrogen, 400 psig steam, cooling water and instrument air. In terms of support equipment/facilities, we have assumed that the product syngas will be flared and water treatment facilities exist for the process condensate.

With these assumptions we developed heat and mass balances, sized equipment and estimated bare erected equipment costs. For operating costs we estimated operator and maintenance personnel needs to support one calendar year of 24/7 operation. Because this is a pilot-scale system, we have assumed that we will be able to complete approximately 4,000 hours of operation during this year. We have also budgeted for the production of two reactor fills for the fluidized-bed WGS catalyst and a reasonable estimate for utilities.

Based on the cost estimation completed, the cost for construction and installation of the pilot-scale ATWGS system would be about $2.0 million with an estimated operating budget of approximately $1.65 million for one calendar year of operation.

The path forward for the current technology would involve the following steps:

- Identification of a funding opportunity that will support this pilot-scale project,
- Identification and negotiation of a host site agreement,
- Completion of a detailed engineering package for the pilot-scale ATWGS system for the specific host site,
- Construction and installation of the ATWGS pilot plant,
- Preparation of a limited commercial production batch for sufficient fluidized-bed WGS catalyst for at least two system fills,
- Development of commissioning, startup, operating and shut down procedures, and
- Implementation of the operational plan.

Appendix A

The following sections provide additional process descriptions for the major equipment and equipment specifications generated during design.

Sulfur Polishing Bed (V-100)

The design conditions for the sulfur polishing bed are listed below:

Design Condition	Value / Specification
Gas Flow	4960 sft^3/hr
Design GHSV	250 /hr
Vessel Diameter	2.6 ft
Bed Height	10.5 ft

Transport Reactor Design (Mixing Column)

After addition of the shift steam, syngas at about 370 psig and 637 °F enters the transport reactor system from the mixing column bottom, using a gas distributor. In the mixing column, syngas comes in contact with the circulated catalyst, entering the reactor at 650 °F, at a catalyst circulation flow rate of 1577 lb/hr. The exothermicity of the WGS reaction increases the temperature in the mixing column to 700 °F. The design and size of the WGS reactor is primarily dictated by the kinetics of the WGS reaction, namely the residence time of the syngas in contact with the catalyst in the mixing column and the riser. The total contact time between the reactant gases and the catalyst for the water gas shift reaction ranges between 4-8 secs. The mixing column is designed for a contact/residence time of about 4 secs and a superficial gas velocity of approximately half the calculated choking velocity. The table below summarizes the mixing column design details.

Design Condition	Value / Specification
Syngas Feed Flow Rate	488.8 ft^3/h
Operating Temperature	700°F
Operating Pressure	370 psia
Design Gas Hourly Space Velocity	30,000 sft^3/h of gas/ft^3 of catalyst
Residence Time	3.8 sec
Diameter	3.7 inch
Height	9.3 ft

Transport Reactor Design (Riser)

To achieve the catalyst transport through the riser column, superficial gas velocity is increased by reducing the dimensions of the column. The design superficial gas velocity and column dimensions were chosen to be significantly above the choking velocity estimate. As discussed above, the total contact time (about 8 secs) between the reactant gases and solid catalyst was evenly split between the mixing column and riser column. Table below summarizes the mixing column design details.

Design Condition	Value / Specification
Syngas Feed Flow Rate	488.8 ft^3/h
Operating Temperature	700°F
Operating Pressure	370 psia
Residence Time	4.0 sec
Diameter	1.5 inch
Height	44.3 ft

Solids Cooler Design (SG-100)

The hot catalyst material drops from the cyclone bottom at a rate of 1577 lb/hr. The catalyst needs to be cooled to extract the exothermic heat associated with the WGS reaction. The heat is extracted and utilized to generate steam. The temperature of the hot catalyst that drops from the cyclone bottom is about 700°F. This catalyst needs to be cooled to 650°F before introducing it back in the mixing column of the WGS reactor to close the heat balance in the reactor system. The amount of sensible heat to be removed is 3.8×10^4 Btu/hr. Catalyst cooling is achieved by dropping the catalyst down on the shell side of a shell-and-tube heat exchanger with steam generation occurring in the tubes. These tubes are placed vertically. Assuming a heat transfer coefficient of 150 Btu/hr-ft^2-F (vetted with experts) and an LMTD of 347 °F, the heat demand can be met using 1.2 ft^2 of heat transfer area. The required heat transfer area can be achieved by a double pipe heat exchanger arrangement placing a 1" ID x 8'long tube inside a 2" ID shell.

The Solids Cooler is a proprietary technology thereby making it difficult to obtain cost quotes. The equipment was costed using the closest heat exchanger design listed in ASPEN PROCESS ECONOMIC ANALYZER. The equipment design and cost were then carefully discussed and vetted with an external expert for their accuracy. The Design conditions for the solid cooler system are listed here:

Design Condition	Value / Specification
Heat duty	3.8×10^4 Btu/hr
Overall heat transfer coefficient	150 Btu/hr-sqft-F
Log-mean temperature difference	347 °F
Heat transfer area	1.2 ft^2

Cyclone Separator Design (CYC-100)

The gas-solid mixture exiting the top of the riser column enters a cyclone separator where the solids drop out and gas exits from the top. Cyclones typically exhibit a solid separation efficiency in excess of 99%. CYC-100 was designed for an inlet gas velocity of 80 ft/s. The table below summarizes the cyclone separator design details.

Design Condition	Value / Specification
Inlet Width	0.25”
Inlet Height	0.75”
Diameter Body	3”
Length of the body	4”
Length of the cone	2”
Gas Exit Diameter	1”
Dust Exit Diameter	0.5”

Filter Design (FLT-100)

The design conditions for the filter are listed below:

Design Condition	Value / Specification
Operation	With pulsed air feed to dislodge solids deposited on the filter
Feed gas flow rate	415.6 ft^3/hr
Solids loading	0.02 lbs/hr
Solids removal efficiency	Meets PM 2.5 standard (15 µg/m^3)

Syngas Cooling (SG-101 and HE-101)

The hot syngas exiting the top of the cyclone is cooled to about 400°F to remain at least 50°F above the syngas dew point. High pressure water is used as the cooling medium to generate steam on the tube-side. The design conditions for SG-101 are listed here:

Design Condition	Value / Specification
Heat duty	4.3 x 10^4 Btu/hr
Overall heat transfer coefficient	50 Btu/hr-sqft-F
Log-mean temperature difference	194 °F
Heat transfer area	7.4 ft^2

The syngas exiting the filter needs to be cooled before sending it to the flare system. Cooling water is used as the cooling medium on the tube side. The design conditions for HE-101 are listed here:

Design Condition	Value / Specification
Heat duty	9.4 x 10^4 Btu/hr

Overall heat transfer coefficient	50 Btu/hr-sqft-F
Log-mean temperature difference	230 °F
Heat transfer area	13.7 ft^2

Combined GTI R-GAS™ and RTI Advanced Syngas Cleanup with RTI Advanced Transport Water-Gas Shift Technologies for IGCC and CTL Applications

Submitted to

GTI and DOE-NETL

By

101 Second Street, Suite 1000, San Francisco, CA 94105-3672 USA

tel: +1 415 369 1100 fax: +1 415 369 0894

September 2016

DISCLAIMER

This report was prepared as an account of work sponsored by an agency of the United States Government. Neither the United States Government nor any agency thereof, nor any of their employees, makes any warranty, express or implied, or assumes any legal liability or responsibility for the accuracy, completeness, or usefulness of any information, apparatus, product, or process disclosed, or represents that its use would not infringe privately owned rights. Reference herein to any specific commercial product, process, or service by trade name, trademark, manufacturer, or otherwise does not necessarily constitute or imply its endorsement, recommendation, or favoring by the United States Government or any agency thereof. The views and opinions of authors expressed herein do not necessarily state or reflect those of the United States Government or any agency thereof.

ABSTRACT

This study evaluated the techno-economic benefits of integrating RTI's novel Advanced Transport Water-Gas Shift (ATWGS) reactor technology into a combined GTI R-GAS™ gasification and RTI advanced syngas desulfurization process for integrated gasification combined cycle (IGCC) and coal-to-liquids (CTL) production applications. These integrated technologies offer significant benefits relative to the best performing state-of-the-art reference case. For IGCC, the combined technologies yield 1.7 percentage points IGCC efficiency improvement with 20% lower capital cost and 18% lower cost of electricity. For Coal To Methanol these technologies yield 3.5 percentage points higher plant thermal efficiency with a 22% reduction in capital cost and 19% lower methanol Required Selling Price.

Contents

Tables

Figures

Acronyms and Abbreviations

°F	Degree Fahrenheit
AACRP	Advanced Amine CO2 Removal Process
AFWGS	Advanced Fixed-Bed Water-Gas Shift Process
AGR	Acid Gas Removal
AOI	Area of Interest
AR	Aerojet Rocketdyne
Ar	Argon
ASU	Air Separation Unit
ATWGS	Advanced Transport Water-Gas Shift Process
B/L	Battery Limit
BACT	Best Available Control Technology
BEC	Bare Erected Cost
BFD	Block Flow Diagram
BFW	Boiler Feed Water
BOP	Balance of Plant
Btu	British Thermal Unit
CAPEX	Capital Expenditure
CCF	Capital Charge Factor
CF	Capacity Factor
CH4	Methane
Circ	Circulating
CMT	Constant Maturity Treasury
CO	Carbon Monoxide
CO_2	Carbon Dioxide
COE	Cost of Electricity
COS	Carbonyl Sulfide
CTG	Combustion Turbine Power Generation
CTL	Coal-to-Liquids
CTM	Coal-to-Methanol
CW	Cooling Water
DBT	Dry Bulb Temperature
DCS	Distributed Control System
DOE	U.S. Department of Energy
DSP	Dry Solids Pump
DSRP	Direct Sulfur Recovery Process
EPC	Engineering, Procurement and Construction

EPRI	Electric Power Research Institute
FCC	Fluid Catalytic Cracking
FO	Fuel Oil
FOA	Funding Opportunity Announcement
FBR	Fixed Bed Reactor
ft	feet
gal	Gallon
GE	General Electric
GTI	Gas Technology Institute
H_2	Hydrogen
H_2O	Water
H_2S	Hydrogen Sulfide
Hg	Mercury
HGCU	Hot Gas Clean Up
HHV	Higher Heating Value
HMB	Heat and Material Balance
HP	High Pressure
Hr	Hour
HRSG	Heat Recovery Steam Generator
I & C	Instrumentation & Control
IGCC	Integrated Gasification Combined Cycle
IOU	Investor Owned Utility
IP	Intermediate Pressure
IPCE	In Plant Cost Estimator
kWe	Kilowatt electric
kWh	kilowatt hour
LAER	Lowest available emissions rate
Lb	Pound Mass
LHV	Lower Heating Value
LIBOR	London Interbank Offered Rates
LNB	Low NOx Burner
LOX	Liquid oxygen
LP	Low Pressure
LTGC	Low temperature gas cooling
max	Maximum
ME	Major Equipment
MEC	Major Equipment Cost
MeOH	Methanol
min	Minimum
Misc	Miscellaneous

MM	million
MU	Makeup
MWe	Megawatt electric
MWh	megawatt hour
N_2	Nitrogen
NETL	National Energy Technology Laboratory
NGCC	Natural Gas Combined Cycle
NOx	Oxides of Nitrogen
NSPS	New Source Performance Standards
NSR	New Source Review
O&M	Operating and Maintenance
O_2	Oxygen
OPEX	Operating Expenditure
OSBL	Outside Battery Limit
PC	Pulverized Coal
PCC	Post-Combustion Capture
PFB	Pressurized Feed Bin
PFD	Process Flow Diagram
PM	Particulate Matter
ppmv	Parts per million by volume
Ppmvd	Parts per million by volume, dry basis
ppmW,	Parts per million by weight
PRB	Powder River Basin
PSFM	Power Systems Financial Model
Psi	Pounds Per Square Inch
psia	Pounds Per Square Inch, absolute
psig	Pounds Per Square Inch, gauge
QGESS	Quality Guidelines for Energy System Studies
RSP	Required Selling Price
RTI	Research Triangle Institute
SC	Supercritical
scfm	Standard Cubic Feet per Minute
SCGP	Shell Coal Gasification Process
SO_2	Sulfur Dioxide
SOPO	Statement of Project Objectives
SRU	Sulfur Recovery Unit
STG	Steam Turbine Power Generation
T&S	Transportation and Storage
TDC	Total Direct Cost
TEA	Techno-Economic Analysis

TFC	Total Field Cost
TG	Turbine Generator
TGTU	Tail Gas Treatment Unit
TIC	Total Installed Cost
TOC	Total Overnight Cost
TPC	Total Plant Cost
Tpd	tons per day
US, USA	United States of America
vol%	Percentage by Volume
WBT	Wet Bulb Temperature
WDP	Warm Gas Desulfurization Process
WGS	Water-Gas Shift
WHR	Waste Heat Recovery
WT	Waste Treatment

Executive Summary

Under DOE funding from Cooperative Agreement DE-FE0023577, Gas Technology Institute (GTI), Research Triangle Institute (RTI), and Nexant are tasked to evaluate the techno-economic benefits of integrating RTI's novel Advanced Transport Water-Gas Shift (ATWGS) reactor technology into a combined GTI R-GAS™ gasification and RTI advanced syngas desulfurization process for integrated gasification combined cycle (IGCC) and coal-to-liquids (CTL) production applications.

The techno-economic benefits of a combined GTI R-GAS™ (previously Aerojet Rocketdyne [AR]) gasification/RTI advanced syngas desulfurization process have been studied under a prior and separate DOE Cooperative Agreement (DE-FE0012066). The study showed that synergistic benefits of efficiency improvement and cost reduction can be obtained from integrating these two advanced technologies, in comparison with using conventional gasification (Shell Coal Gasification Process) and acid gas removal (Selexol™ and Rectisol®) technologies. The current study evaluates the potential benefits of integrating RTI's ATWGS technology into the R-GAS™ /RTI advanced syngas desulfurization process for further improvement, for both IGCC and CTL applications.

The overall objective of this project is to (1) assess how best to integrate the ATWGS technology into the combined R-GAS™ and RTI advanced syngas desulfurization process, and (2) evaluate the techno-economic benefits of such an integrated process.

The specific case studies completed provide a comparison of an integrated plant utilizing GTI's R-GAS™, RTI's advanced syngas desulfurization process and ATWGS technologies with a reference plant using commercially available technologies, and a case from the previous DE-FE0012066 that also utilizes GTI's R-GAS™ gasification and RTI's syngas desulfurization process, RTI's advanced fixed-bed water-gas shift process (AFWGS), and an activated amine CO_2 recovery process (AACRP). All comparison studies conducted for this report capture 90% CO_2 for storage.

As stated in the Technology Analysis Plan (TAP) presented to DOE, one of the goals of this TEA is to characterize separately the impacts of the GTI R-GAS™ gasifier and RTI ATWGS technologies. Table E-1 summarizes the results of all the IGCC cases studied, which includes Case 1a through 1d from the prior DE-FE0012066 study, and Case 1e from this study, and provides some insight into the relative impacts of the GTI and RTI technologies.

Table E-1
Impact of GTI R-GAS™ and RTI ATWGS Technologies on IGCC

Case	Case 1a	Case 1b	Case 1c	Case 1d	Case 1e
IGCC Configuration					
Gasifier	Shell	GTI	GTI	Shell	GTI
Sulfur and CO_2 Removal	Selexol™	RTI WDP	Selexol™	RTI WDP	RTI WDP
Shift Reactors	Sour FBR	AFWGS	Sour FBR	AFWGS	ATWGS
Plant Parameters					
Steam Turbine output (MWe)	224.1	211.3	209.3	226.4	215.5
Efficiency, % HHV	31.32%	32.75%	32.70%	31.53%	33.06%
Capital Cost (TOC), $/kW	5,400	4,428	4,709	5,054	4,316
COE, mills/kWh	145.3	122.0	128.3	137.3	119.2
Relative Impact					
Case comparison basis		**1b vs. 1c**	**1c vs. 1a**	**1d vs. 1a**	**1e vs. 1b**
Steam Turbine output (MWe)		+2.0 (1.0%)	-14.8 (-6.6%)	+2.3 (1.0%)	+4.2 (+2.0%)
Efficiency, % HHV			+1.38% pt		+0.31% pt
Capital Cost (TOC), $/kW			-691 (12.8%)		-112 (2.5%)
COE, mills/kWh			-17.0 (11.7%)		-2.8 (2.3%)

The GTI gasifier technology offers favorable impacts on all plant parameters relative to the DOE Reference design configuration of Case 1a (i.e., comparing Case 1c with 1a): with 1.38 percentage point increase in plant efficiency, a 12.8% reduction in TOC, and an 11.7% reduction in COE. With respect to comparing the two water-gas shift technologies that RTI offers (ATWGS in Case 1e versus AFWGS in Case 1b), the ATWGS in Case 1e has a slight advantage over that of Case 1b, with an incremental increase in efficiency of 0.31 percentage points and an extra 4.2 MWe from the stream turbine while reducing the capital cost and cost of electricity by 2.5% and 2.3% respectively. Table E-1 confirms the improved thermal efficiency of RTI's advanced WGS processes, as seen from the increases in steam turbine output between cases with conventional WGS processes and AFWGS/ATWGS (i.e., Case 1b vs. Case 1c, Case 1a vs. Case 1d, and Case 1e vs. Case 1b).

Table E-2 summarizes the results of all the CTM cases studied, which includes Case 2a through 2d from the prior DE-FE0012066 study, and Case 2e from this study, and provides some insight into the relative impacts of the GTI and RTI technologies on CTM production.

Table E-2
Impact of GTI R-GAS™ and RTI AWGS Technologies on CTM

Case	Case 2a	Case 2b	Case 2c	Case 2d	Case 2e
CTM Configuration					
Gasifier	Shell	GTI	GTI	Shell	GTI
Sulfur and CO_2 Removal	Rectisol®	RTI WDP	Rectisol®	RTI WDP	RTI WDP
Shift Reactors	Sour FBR	AFWGS	Sour FBR	AFWGS	ATWGS
Plant Parameters					
Steam Turbine output (MWe)	264.7	239.2	199.1	292.8	248.7
Thermal Efficiency, % LHV	53.1%	56.3%	56.5%	52.9%	56.6%
Capital Cost (TOC), $1,000/mtpd	577.1	453.1	476.3	549.3	449.0
Loan Guarantee RSP, $/ton	424.1	347.3	359.5	408.9	343.3
Relative Impact					
Case comparison basis		**2b vs. 2c**	**2c vs. 2a**	**2d vs. 2a**	**2e vs. 2b**
Steam Turbine output (MWe)		+40.1 (20.1%)	-65.6 (-24.8%)	+28.1 (10.6%)	+9.5(4.0%)
Thermal Efficiency, % LHV			+3.4% pt		+0.3% pt
Capital Cost (TOC), $1,000/mtpd			-100.8 (17.5%)		-4.1 (0.9%)
Loan Guarantee RSP, $/ton			-64.6 (15.2%)		-4.0 (1.2%)

The GTI gasifier technology offers favorable impacts on all plant parameters relative to the Case 2a DOE Reference CTM plant configuration (i.e., comparing Case 2c with 2a): with a 3.4 percentage point increase in thermal efficiency, a 17.5% reduction in TOC, and a 15.2% reduction in RSP. When comparing the two RTI advanced WGS processes (ATWGS in Case 2e versus AFWGS in Case 2b), ATWGS in Case 2e increases thermal efficiency by 0.3 percentage points and steam turbine output by 9.5 MWe while reducing the capital cost and RSP by 0.9% and 1.2%, respectively.

As with the IGCC scenario, RTI considers both AFWGS (Case 1b and 2b) and ATWGS (Case 1e and 2e) processes as advanced water-gas shift technologies that can offer significant techno-economic advantages over a conventional WGS process. RTI's claim of improved thermal efficiency can be seen in Table E-2 based on increases in steam turbine output between cases with conventional WGS processes and AFWGS/ATWGS (i.e., Case 2b vs. Case 2c, Case 2d vs. Case 2a, and Case 2e vs. Case 2b). It is recommended that a follow-up study to be conducted to investigate it in more detail.

Section 1 Introduction

1.1 BACKGROUND

Under DOE funding from Cooperative Agreement DE-FE0023577, Gas Technology Institute (GTI), Research Triangle Institute (RTI), and Nexant are tasked with evaluating the techno-economic benefits of integrating RTI's novel Advanced Transport Water-Gas Shift (ATWGS) technology into a combined GTI R-GAS™ gasification and RTI advanced syngas desulfurization process for integrated gasification combined cycle (IGCC) and coal-to-liquids (CTL) production applications with 90% carbon capture.

The techno-economic benefits of a combined GTI R-GAS™ (previously Aerojet Rocketdyne [AR]) gasification/RTI advanced syngas desulfurization process have been studied under a prior and separate DOE Cooperative Agreement (DE-FE0012066). The study showed that synergistic benefits of efficiency improvement and cost reduction can be obtained from integrating these two advanced technologies, in comparison with using conventional gasification (Shell Coal Gasification Process) and acid gas removal (Selexol™ and Rectisol®) technologies. The current study evaluates the potential benefits of integrating RTI's ATWGS technology into the R-GAS™ /RTI advanced syngas desulfurization process for further improvement, for both IGCC and CTL applications.

1.2 STUDY OBJECTIVES

The overall objective of this project is to (1) assess how best to integrate the ATWGS technology into the combined R-GAS™ and RTI advanced syngas desulfurization process, and (2) evaluate the techno-economic benefits of such an integrated process.

This report documents the study completed for both IGCC power production and CTL applications, specifically, methanol production from a coal-to-methanol (CTM) plant.

The specific case studies completed provide a comparison of an integrated plant utilizing GTI's R-GAS™, RTI's advanced syngas desulfurization process and ATWGS technologies with a reference plant using commercially available technologies, and a case from the previous DE-FE0012066 study that also utilizes GTI's R-GAS™ gasification and RTI's advanced syngas desulfurization process, which includes RTI's warm gas desulfurization process (WDP), RTI's direct sulfur recovery process (DSRP), RTI's advanced fixed-bed water-gas shift process (AFWGS), and an activated amine CO_2 recovery process (AACRP). All comparison studies conducted for this report capture 90% CO_2 for storage.

The IGCC plant and CTM plant findings are summarized in Section 12 (Conclusions and Recommendations) of this report.

Section 2 IGCC Design and Economic Analysis Basis

2.1 DESIGN REFERENCES

The reference plant design used for this study was selected from "*Cost and Performance Baseline for Fossil Energy Plants, Volume 3a: Low Rank Coal to Electricity*, May 2011, DOE/NETL. 2010/1399" (NETL Report 1399). NETL Report 1399 contains a series of IGCC designs based on various gasifiers. The reference IGCC case used for comparison against the GTI gasification and RTI advanced syngas cleanup and AACRP systems was Case S1B. NETL Report 1399, along with the following DOE/NETL's Series of Quality Guidelines for Energy Systems Studies (QGESS) contain a comprehensive set of IGCC design bases and assumptions, as well as reference costs and economic evaluation guidelines that were used to complete the techno-economic analyses (TEAs) in this report.

- "*Specifications for Selected Feedstocks*, January 2012, DOE/NETL. 341/011812",
- "*Process Modeling Design Parameters*, January 2012, DOE/NETL. 341/081911",
- "*CO_2 Impurity Design Parameters*, January 2012, DOE/NETL. 341/011212",
- "*Detailed Coal Specifications*, January 2012, DOE/NETL-401/01211",
- "*Cost Estimation Methodology for NETL Assessments of Power Plant Performance*, April 2011, DOE/NETL. 2011/1455",
- "*Capital Cost Scaling Methodology*, January 2013, DOE/NETL. 341/013113", and
- "*Fuel Prices for Selected Feedstocks in NETL Studies*, November 2012, DOE/NETL 341/11212"

While the TEA reporting requirements specified that the costs be presented in 2011 dollars, the costs provided in NETL Report 1399 were reported in 2007 dollars. A separate DOE/NETL report, "*Updated Costs (June 2011 Basis) for Selected Bituminous Baseline Cases*, August 2012, DOE/NETL-341/082312" (NETL Report 341/082312), was thus used to develop the escalated capital and operating cost estimates in June 2011 dollars.

2.2 CASE CONFIGURATIONS

To identify and determine any synergistic advantages of integrating the RTI ATWGS technology, an additional design case was developed, on top of the four cases previously completed in the DE-FE0012066 study. These are shown in Table 2-1. One of these cases is the Reference Case, which is Nexant's model of Case S1B selected from NETL Report 1399. The most promising case from the previous study is Case 1b, the IGCC plant with CO_2 capture that integrates GTI's R-GAS™ gasification technology with RTI's advanced syngas cleanup process (WDP + AFWGS + AACRP + DSRP). Case 1e, which adds RTI's ATWGS technology to the two advanced technologies of Case 1b (RTI's ATWGS replaces RTI's AFWGS), is the case of interest for the current study. It is anticipated to provide additional synergistic benefits above and beyond that of Case 1b.

The specific technologies included in each of the five IGCC configurations are identified in the IGCC case study matrix shown in Table 2-1.

Table 2-1
Case Study Matrix for IGCC with CO_2 Capture

Case Name for Current Study	Case 1a[1]	Case 1b	Case 1c	Case 1d	Case 1e
Case Name in Previous Study[2]	Case 2a	Case 2b	Case 2c	Case 2d	N/A
Gasification Technology					
Shell Gasification with Lockhopper-Based Feed System	✓			✓	
GTI R-GAS™ Gasifier with Dry Solids Pump (DSP) Feed System		✓	✓		✓
Gas Cleanup[3]					
Two-Stage Selexol™ for CO_2 and Sulfur Removal	✓		✓		
RTI WDP with AACRP		✓		✓	✓
Water-Gas Shift					
Sour Shift	✓		✓		
RTI AFWGS		✓		✓	
RTI ATWGS					✓
GE 7FB Advanced Gas Turbine	✓	✓	✓	✓	✓
CO_2 Drying and Compression (to 2,200 psig)	✓	✓	✓	✓	✓

[1] Reference Case based on Nexant's benchmark simulation of the NETL Report 1399 Case S1B

[2] Previous study cases used "2" as a prefix e.g Case 2a, 2b, 2c and 2d because these were addressing Task 2 of the study.

[3] Selexol™ removes H_2S and CO_2. Additional trace contaminant cleanup technologies will be included as defined by DOE/NETL baseline studies

Reference case from previous DE-FE0012066 study

Best performing case from previous DE-FE0012066 study

Other DE-FE0012066 study cases

Case of interest in this study

2.2.1 Case 1a: Reference Shell IGCC Power Plant with Selexol™-Based AGR

The Shell gasification-based IGCC case with CO_2 capture utilizing Montana PRB subbituminous coal (Case S1B from NETL Report 1399) was selected as the Reference Case and was previously evaluated in the DE-FE0012066 study.

The reference Shell gasification-based IGCC case is a coal-fired IGCC plant generating enough hydrogen-rich fuel gas to fill two advanced GE 7F-turbines rated nominally at 215 MWe each, for a total of 430 MWe at the Montana site's elevation, while enabling 90% capture of the carbon in the raw syngas. The power plant is equipped with a heat recovery steam generator (HRSG) and steam turbine (ST) to generate additional power from waste heat of the flue gas. Adding in the steam turbine power and subtracting auxiliary loads (including CO_2 capture and compression), the reference IGCC plant's nominal net export capacity is 450 MWe. This reference IGCC plant includes both conventional sour water-gas shift (WGS) and two-stage Selexol™ processes to achieve the required sulfur and CO_2 removal. The Reference Case, together with the rest of the cases under evaluation, has a capacity factor (CF) of 80%. This reflects the maximum availability demonstrated in commercial IGCC plants. A simplified reference Case 1a IGCC plant Block Flow Diagram (BFD) is shown in Figure 2-1.

Figure 2-1
Case 1a: Reference Shell Gasifier with Selexol™ AGR IGCC - Simplified BFD

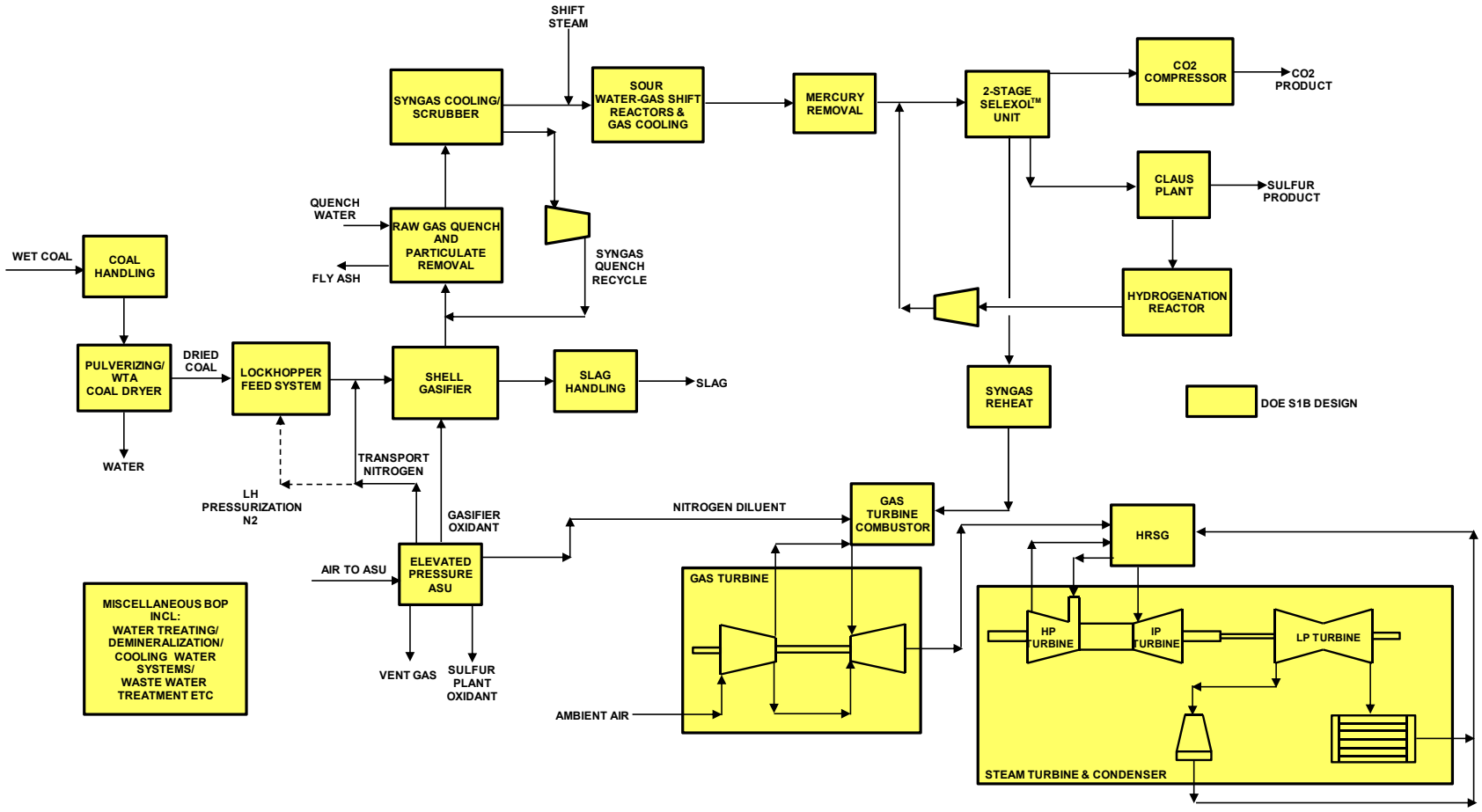

2.2.2 Case 1b: GTI R-GAS™ with RTI WDP IGCC

Case 1b is the design that was evaluated previously in the DE-FE0012066 study. It integrates the GTI's R-GAS™ gasification technology with the RTI advanced syngas cleanup and AACRP systems. Due to the different cold gas efficiency of the R-GAS™ gasifier, the IGCC plant consumes a different amount of coal feed when compared with Case 1a in order to produce nominally, the same amount of hydrogen-rich syngas to fill the two advanced GE 7F-turbines and generate 430 MWe at the Montana site. Like Case 1a, the power plant is equipped with a HRSG and ST to generate additional power from waste heat of the flue gas. Due to the different quality and quantity of steam generated from process heat recovery, as well as differences in process steam consumption, the ST output differs from that of Case 1a.

A combination of RTI's WDP unit and AACRP unit replaces the two-stage Selexol™ unit in Case 1a to remove the sulfur and CO_2 from the syngas. RTI's WDP removes H_2S and COS from the syngas after it leaves the particulate filters, without requiring additional cooling. The treated syngas undergoes sweet shift in RTI's AFWGS before it is cooled and sent to the AACRP unit for CO_2 capture. The AACRP unit captures CO_2 equivalent to >90% of the raw syngas' carbon content in order to meet the CO_2 emissions specifications.

The Case 1b IGCC plant BFD is shown in Figure 2-2. This figure serves to demarcate the battery limits and highlights the interfaces between GTI's and RTI's proprietary systems (colored blue and red respectively) and the rest of the IGCC processes (in yellow) that were Nexant's responsibility for designing. The blue block represents GTI's Dry Solids Pump (DSP) and R-GAS™ gasifier systems, which replaces the lockhopper feed system and Shell gasifier in the Reference Case 1a IGCC plant. The red blocks within the broken-line rectangle represent RTI's advanced syngas cleanup and AACRP processes and comprise the WDP for sulfur removal, DSRP to produce elemental sulfur, AFWGS, low-temperature gas cooling (LTGC), and AACRP.

Case 1b was shown to be the best performing case in the previous DE-FE0012066 TEA study. Hence with the current study, it will be the yardstick for comparison with the new Case 1e. Any incremental improvement in Case 1e's cost and performance over Case 1b can be attributed to the replacement of RTI's AFWGS technology with RTI's ATWGS technology, which integrates the use of an transport reactor, solids cooler and novel fluid-bed high temperature water-gas shift catalyst. It should be noted that since Case 1b incorporated RTI's AFWGS process, the full benefit of RTI's ATWGS compared with conventional WGS technologies is not determinable from just the comparison of these two cases; it should be greater than the incremental improvements indicated by this comparison.

2.2.3 Case 1c and Case 1d

Cases 1c and 1d were previously evaluated in the DE-FE0012066 study to evaluate the benefits of GTI's R-GAS™ technology and RTI advanced syngas cleanup technology individually. These cases bear no further elaboration since they have been studied already.

.

Figure 2-2
Case 1b: GTI R-GAS™ Gasifier with RTI WDP IGCC Plant - Simplified BFD

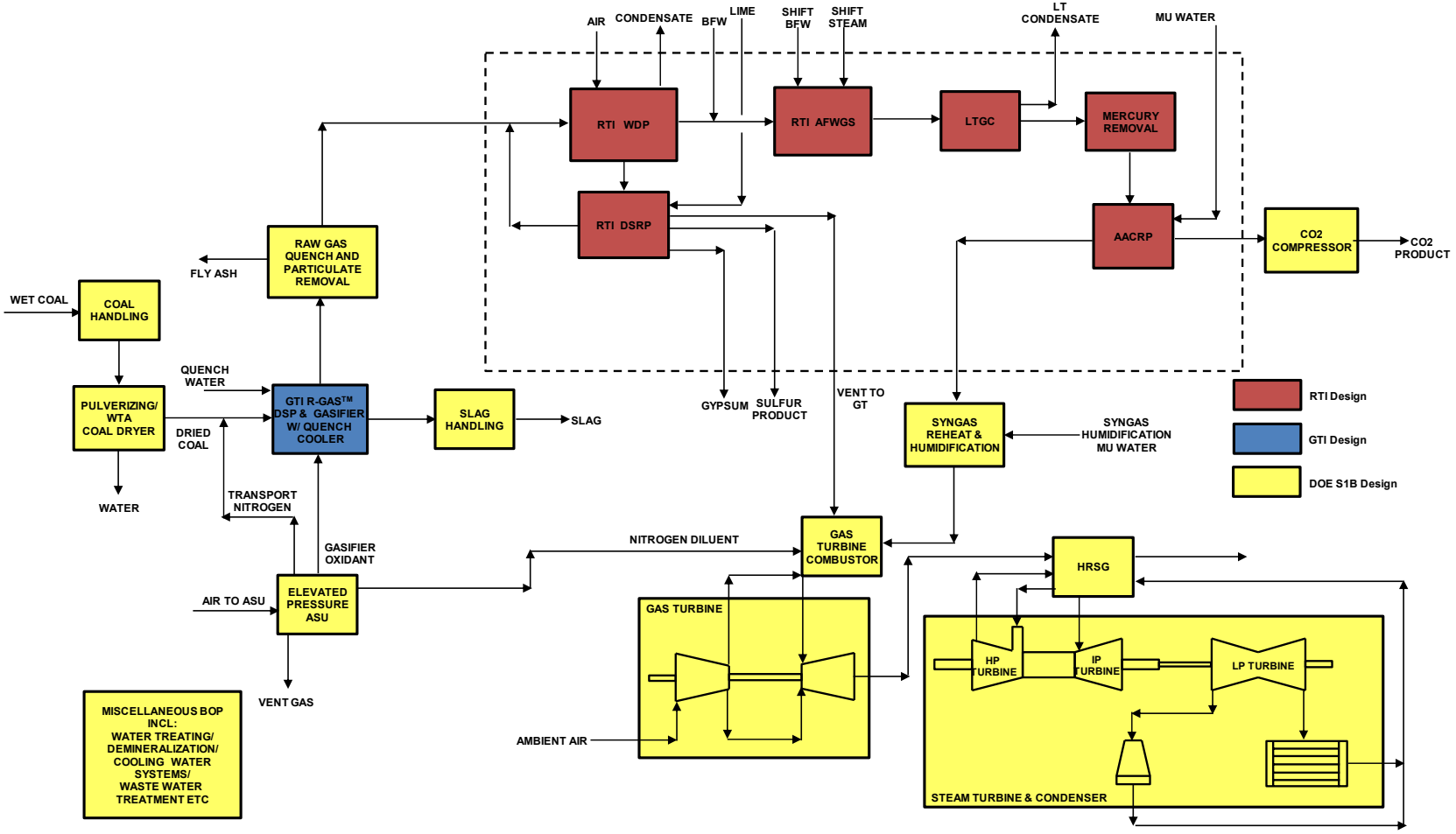

2.2.4 Case 1e: GTI R-GAS™ with RTI WDP and RTI ATWGS IGCC

The IGCC power plant of interest for the current study is the design that integrates the GTI R-GAS™ gasification system, RTI advanced syngas cleanup and AACRP systems with the RTI ATWGS units.

The Case 1e IGCC shall consume the same amount of coal feed as Case 1b, since both use the GTI R-GAS™ gasification system that have the same cold gas efficiency. The same amount of syngas shall be produced to fill two advanced GE 7F-turbines to generate 430 MWe at the Montana site. The power plant will also be equipped with a HRSG and ST to generate additional power from waste heat recovery from the flue gas. Due to possible differences in process waste heat recovery schemes when integrated with ATWGS, the Case 1e ST output may differ from Case 1b.

In Case 1e, RTI's WDP removes H_2S and COS from the hot syngas from GTI's gasifier after it leaves the particulate filters. The treated syngas will then undergo shift in the ATWGS unit (replacing Case 1b's AFWGS unit) before it is cooled and sent to the AACRP unit for CO_2 capture. The AACRP unit will capture CO_2 equivalent to at least 90% of the raw syngas' carbon content in order to meet the CO_2 emissions specifications. RTI's DSRP will be used for sulfur recovery.

The Case 1e IGCC plant BFD is shown in Figure 2-3. This figure serves to demarcate the battery limits and highlights the interfaces between GTI's and RTI's proprietary systems. Like Case 1b, the blue block represents GTI's DSP and gasifier systems, while the red blocks within the broken-line rectangle represent RTI's advanced syngas cleanup and AACRP processes. The difference here is the green block within the broken-line rectangle, which represents RTI's ATWGS unit, which replaces the AFWGS unit in Case 1b. The remaining IGCC processes (in yellow) will be designed by Nexant and based on the NETL Report 1399 Case S1B design

.

.

Figure 2-3
Case 1e: GTI R-GAS™ Gasifier with RTI WDP/RTI ATWGS IGCC Plant - Simplified BFD

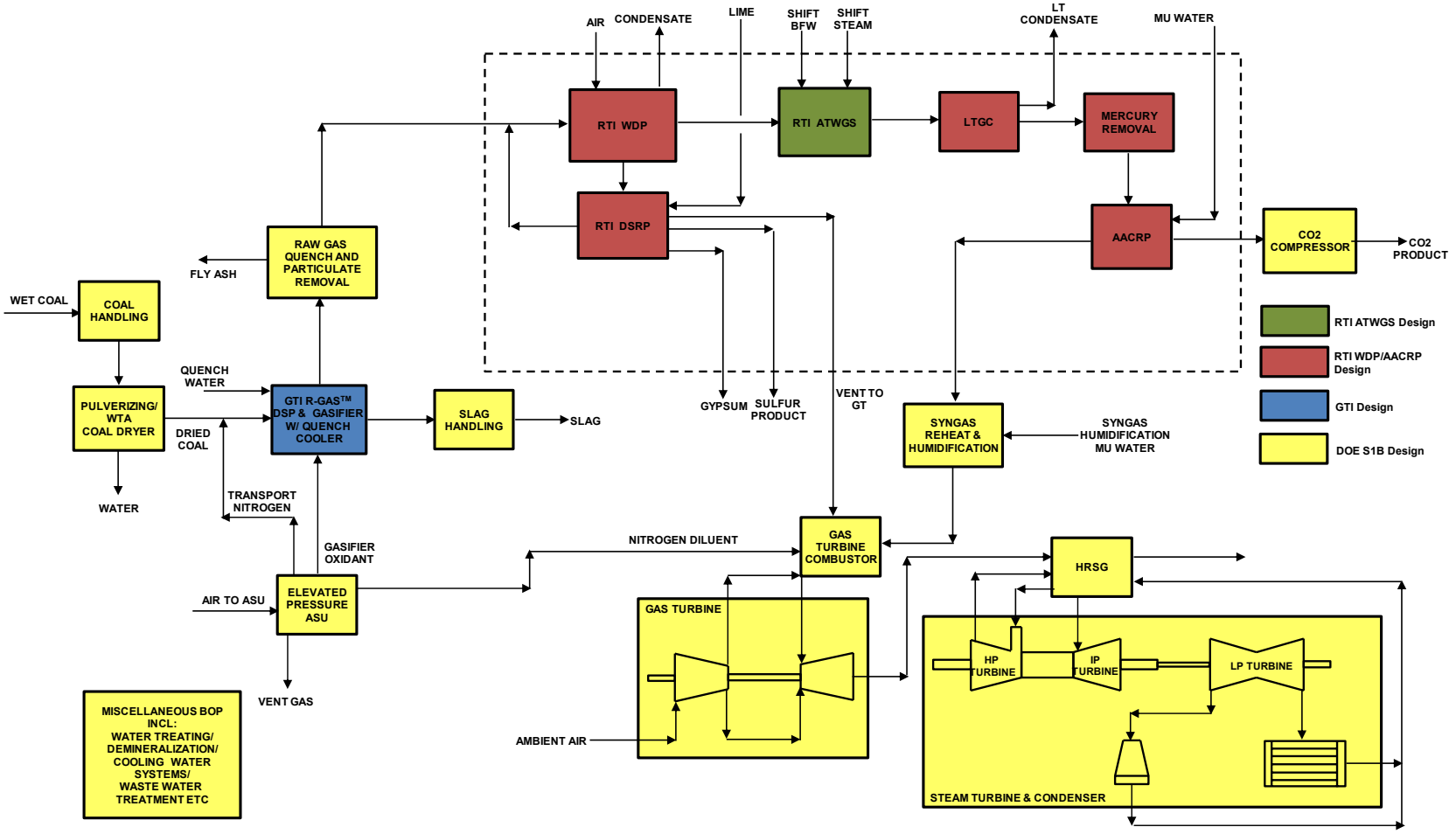

2.3 DESIGN CRITERIA

2.3.1 Heat and Material Balance

Nexant carried out a simulation of the IGCC cases on ASPEN Plus to obtain the process heat and material balances (HMB). This also facilitated a more detailed estimation of the overall plant utility balance, including heat recovery in the HRSG, power generation from the steam cycle, as well as cooling water load breakdown, all of which helped determine the overall IGCC plant performance with more certainty.

In the DE-FE0012066 study, Nexant developed a design of the Case 1a Shell IGCC with Selexol™-based acid gas removal (AGR) process using Case S1B data from the NETL Report 1399 as the reference. The resulting stream flows, heat and material balances, and power generation from the gas and steam turbine were benchmarked and cross-checked against the reference Case S1B and the results were within a reasonable range of accuracy.

For Case 1b from the DE-FE0012066 study, Nexant provided GTI and RTI with the benchmark design's stream conditions and flows to the gasification and syngas cleanup units respectively. Using these as inputs into their models, GTI and RTI determined the HMB, utility consumptions, equipment sizes and costs around their respective process systems. These outputs were then transmitted as inputs into Nexant's IGCC simulation to complete the modeling of Case 1b.

The same methodology was followed for the current TEA study. For Case 1e, since the ATWGS reactor system is within the larger broken-line rectangle from Figure 2-3, the same stream conditions and flows from Nexant's benchmark design to the RTI blocks are still valid. Nexant uses RTI's provided outputs (HMB, utilities consumption, consumables, and equipment costs) for Case 1e in its IGCC model to complete the case's overall techno-economic analysis.

2.3.2 R-GAS™ Gasifier and Feed System

For Case 1e, the specifications of GTI's R-GAS™ gasifier and DSP are the same as Case 1b. The same information from GTI for Case 1b was used in modeling Case 1e

2.3.3 RTI WDP System

RTI provided Nexant with the major stream flows and conditions into, within, and out of their proprietary advanced syngas cleanup process and AACRP, enabling Nexant to integrate these processes into its model. For cost estimations of RTI's advanced syngas cleanup and AACRP, RTI provided estimated turnkey costs that were based on experiences gained from their pilot plant and 50 MW demonstration plant constructions. RTI also provided Nexant with the advanced syngas cleanup and AACRP systems' utilities and consumables. These were used as inputs to establish the overall IGCC performance, TPC and variable operating costs for Cases 1b and 1e.

2.3.4 RTI ATWGS System

For Case 1e, RTI developed a HMB for a system that included both the ATWGS and LTGS processes. For this system RTI designed the ATWGS process such that the composition, temperature and pressure of the inlet and outlet streams were identical to those in Case 1b. RTI provided Nexant with the major stream flows and conditions into, within, and out of their system

that included both the ATWGS and LTGC systems. For cost estimations, RTI provided Nexant with the turnkey costs of the overall ATWGS system. RTI also provided Nexant with a list containing the ATWGS system's utilities and consumables rates, which are used as inputs to establish the overall IGCC performance, TPC and variable operating costs for Case 1e.

2.3.5 Other Systems

The costs for the remaining IGCC systems not directly related to the GTI advanced gasification, RTI advanced syngas cleanup, and RTI ATWGS systems were estimated by Nexant via capacity-factor from the corresponding system costs listed in the reference NETL Report 1399 and escalated to year 2011 costs.

2.4 SITE-RELATED CONDITIONS

As with the reference DOE NETL design, the IGCC plant in this study is assumed to be located in Montana, with site-related conditions extracted from QGESS as shown below:

- Location — Montana, US
- Elevation, ft above sea level — 3,400
- Topography — Level
- Size, acres — 300
- Transportation — Rail
- Ash/slag disposal — Off Site
- Water — Municipal (50%)/Groundwater (50%)
- Access — Landlocked, having access by train and highway
- CO_2 disposition — Compressed to 2,215 psia at battery limit before being transported 50 miles for sequestration in a saline formation at a depth of 4,055 ft. (Study scope limited to delivery at IGCC battery limit only)

2.5 METEOROLOGICAL DATA

Maximum design ambient conditions for material balances, thermal efficiencies, system design and equipment sizing are per QGESS specification as listed below:

- Barometric pressure, psia — 13.0
- Dry bulb temperature (DBT) — 42 °F
- Wet bulb temperature (WBT) — 37 °F
- Ambient relative humidity, % — 62

2.6 COAL PROPERTIES AND FIRING RATE

Design coal feed to the IGCC power plants is Montana PRB subbituminous coal with characteristics presented in Table 2-2. The as-received coal properties shown in Table 2-2 are from the QGESS *Detailed Coal Specifications* document. The as-received coal is dried to 6%

moisture by the WTA coal drying process (German acronym for "fluidized bed dryer with integrated waste heat recovery") and fed to the gasifier. The gasifier will gasify enough dried PRB coal to produce sufficient syngas to fully load two advanced GE 7F turbines (rated nominally at 215 MW each) at the Montana site's elevation.

Table 2-2
Montana PRB Coal Specification

Rank	Subbituminous	
Seam	Montana Rosebud PRB	
Source	Western Energy Co.	
Ultimate Analysis, weight%	As-Received	Dried Coal to Gasifier
Carbon	50.07	63.40
Hydrogen	3.38	4.29
Nitrogen	0.71	0.90
Chlorine	0.01	0.01
Sulfur	0.73	0.92
Oxygen	11.14	14.11
Ash	8.19	10.37
Moisture	25.77	6.00
Total	100.0	100.0
Proximate Analysis, weight%	As-Received	Dried Coal to Gasifier
Volatile Matter	30.34	38.42
Fixed Carbon	35.70	45.20
Ash	8.19	10.38
Moisture	25.77	6.00
Total	100.0	100.0
Higher Heating Value (HHV), Btu/lb	8,564	10,825
Sulfur Analysis*, weight%		Dry
Pyritic		0.63
Sulfate		0.01
Organic		0.34
Mercury, ppmW (moisture-free basis)		0.081
Ash Fusion Temperatures at Reducing Conditions, °F		
Initial Deformation	2,238	
Softening	2,254	
Hemispherical	2,270	
Fluid	2,298	

*In accordance with NETL Report 1399, this study assumes that all sulfur in the coal is converted in the gasifier and leaves with the syngas

2.7 CO_2 PRODUCT TREATING AND PURIFICATION DESIGN CRITERIA

For this study, recovered CO_2 is delivered at the battery limit (B/L), with specifications listed in Table 2-3 for saline reservoir sequestration per the QGESS *CO_2 Impurities Design Parameters* document.

Table 2-3
CO_2 Product Specifications

Compositions:		
CO_2,	vol% (Min)	95
N_2	vol% (Max)	4
Ar	vol% (Max)	
O_2,	vol% (Max)	
H_2	vol% (Max)	
CH_4,	vol% (Max)	
H_2O,	ppmv (Max)	300
H_2S	vol% (Max)	0.01
NH_3	ppmv (Max)	50
SO_2,	ppmv (Max)	100
NOx,	ppmv (Max)	100
CO,	ppmv (Max)	35
B/L pressure, psig		2,200
B/L Temperature, °F		95

2.8 POWER GENERATION & AUXILIARY LOADS

The NETL Report 1399 provided a breakdown of the Case S1B (Shell gasification-based IGCC with CO_2 Capture) power generation by gas and steam turbine power generation. It also provided the auxiliary loads for Case S1B, broken down into its major systems. For this study, Nexant estimated the gas and steam turbines' power outputs using its ASPEN Plus model, based on its interpretation of the Case S1B IGCC plant's design. Auxiliary loads were estimated, wherever applicable, by prorating from the S1B case using relevant scaling parameters obtained from the model's heat and material balance.

Table 2-4 shows the power production and auxiliary load breakdown of the original DOE/NETL Case S1B from the NETL Report 1399, which Case 1a of this study was modeled upon and benchmarked against. For reference purposes, the scaling parameters are also shown in the table.

The GTI R-GAS™ gasification system and RTI advanced syngas cleanup and AACRP systems have different auxiliary loads that are not scalable with some of the loads specified in the reference Case S1B. GTI and RTI have provided the auxiliary loads for their systems and these were used directly as inputs to the auxiliary load calculation.

Table 2-4
DOE S1B IGCC Power Production and Auxiliary Load Summary

Power Generation	Electrical Load, kWe	Scaling Capacity
Gas Turbine Power	430,900	Model Output
Steam Turbine Power	232,500	Model Output
TOTAL POWER, kWe	663,400	
Auxiliary Load Description	**Electrical Load, kWe**	**Scaling Capacity**
Coal Handling	510	As Received Coal
Coal Milling	2,730	As Received Coal
Slag Handling	580	Slag Flow
WTA Coal Dryer Compressor	9,370	Moisture Removed
WTA Coal Dryer Auxiliaries	620	Moisture Removed
Air Separation Unit Auxiliaries	1,000	Oxygen Production
Air Separation Unit Main Air Compressor	63,550	Oxygen Production
Oxygen Compressor	8,830	Oxygen Production
Nitrogen Compressors	33,340	N_2 Diluent + Conveying N_2
CO_2 Compressor	31,560	CO_2 Product Flow
Boiler Feedwater Pumps	3,260	Boiler Feed Water (BFW) Flow
Condensate Pump	230	Condensate Flow
Quench Water Pump	760	Quench Water Flow
Syngas Recycle Compressor	820	Recycle Syngas Flow
Circulating Water Pump	2,730	Circulating Water Flow
Ground Water Pumps	310	Circulating Water Flow
Cooling Tower Fans	1,780	Cooling Water Flow
Air Cooled Condenser Fans	2,960	Condenser Duty
Scrubber Pumps	20	Syngas Flow to Scrubber
Acid Gas Removal	18,400	CO_2 + H_2S Flow
Gas Turbine Auxiliaries	1,000	Gas Turbine Power Output
Steam Turbine Auxiliaries	100	Steam Turbine Power Output
Claus Plant/TGTU Auxiliaries	250	H_2S Flow
Claus Plant TG Recycle Compressor	1,530	H_2S Flow
Miscellaneous Balance of Plant	3,000	As Received Coal
Transformer Losses	2,550	Total Power Output
TOTAL AUXILIARIES, kWe	191,790	
NET POWER, kWe	471,610	

2.9 RAW WATER SUPPLY

Raw water makeup was assumed to be provided 50% by a publicly owned treatment works and 50% from groundwater.

2.10 ENVIRONMENTAL DESIGN TARGETS

The IGCC emission targets were established in the Electric Power Research Institute's (EPRI) design basis for their CoalFleet for Tomorrow Initiative, documented in "*CoalFleet User Design Basis Specifications for Coal-Based IGCC Power Plants*, EPRI, Palo Alto, CA, 2009." The design targets were established specifically for bituminous coal but apply to subbituminous case as well. The emissions requirements and limits for the reference IGCC power plant, as specified in NETL Report 1399, are listed in Table 2-5 below:

Table 2-5
IGCC Environmental Targets

Pollutant	Environmental Target	NSPS Limit
NOx	15 ppmv (dry) @ 15% O_2	1.0 lb/MWh
SO_2	0.0128 lb/MMBtu	1.4 lb/MWh
Particulate Matter (PM)	0.0071 lb/MMBtu	0.015 lb/MMBtu
Hg	>90% capture	20 x 10^{-6} lb/MWh

Total air pollutants in all vents must meet the above specifications even if atmospheric venting is minimal.

2.11 OTHER SITE SPECIFIC REQUIREMENTS

Although the following design parameters are considered site-specific, and are not quantified for this study, allowances for normal conditions and construction are included in the cost estimates.

- Flood plain considerations
- Existing soil/site conditions
- Water discharges and reuse
- Rainfall/snowfall criteria
- Seismic design
- Buildings/enclosures
- Fire protection
- Local code height requirements
- Noise-regulations/impact on site and surrounding area

2.12 IGCC CAPITAL COST ESTIMATION METHODOLOGY

2.12.1 General

For IGCC plants with CO_2 capture, the NETL Report 1399 provided a code of accounts grouped into 14 major systems. Each of these major systems is broken down further into different subsystems. This type of code-of-accounts structure has the advantage of grouping all reasonably allocable components of a system or process into a specific system account.

For the IGCC cases evaluated in this study, capital cost scaling following the guidelines and parameters that are described in the NETL *Capital Cost Scaling Methodology* document was used to perform the cost estimation for systems that are not related to the GTI advanced gasification and RTI advanced syngas cleanup and advanced water-gas shift (AFWGS and ATWGS) systems. In general, this cost estimation methodology involves determining the scaling parameters, exponents and coefficients from the *Capital Cost Scaling Methodology*, as well as the reference cost and baseline capacity from the NETL Report 1399. Once these have been established, the capital cost can be estimated based on the revised capacity from the HMB developed by Nexant's ASPEN models of the IGCC cases.

Most of the costs associated with the proprietary equipment within the GTI R-GAS™ gasification system and RTI advanced syngas cleanup and advanced water-gas shift (AFWGS and ATWGS) systems were provided by GTI and RTI respectively. For non-proprietary equipment within their processes, Nexant performed a bottoms-up, major equipment (ME) factored cost estimation for them. The approaches used for the GTI and RTI systems are described in greater detail in Section 2.12.2 and 2.12.3 respectively. The descriptions of these approaches are provided for the reader's convenience, because most of this work was actually completed in the DE-FE0012066 study. For this study, RTI developed cost estimates for their ATWGS system with the approach described in Section 2.12.3.

2.12.2 GTI R-GAS™ System Capital Cost Estimate Criteria

2.12.2.1 GTI-Licensed Systems Cost Estimates

Costs for equipment in the GTI R-GAS™ gasification system that are proprietary to GTI, such as the DSP and R-GAS™ gasifier were provided by GTI. Nexant used and reported these costs on an as-provided basis. The level of detail provided in these cost estimates was determined by GTI itself.

2.12.2.2 Nexant-Designed System Cost Estimates

For auxiliary equipment within the GTI R-GAS™ gasification section that is not included in the technology licensor's package, such as the gasifier circulating cooling water pumps, cyclones and filters, Nexant performed a bottom-up cost estimate based on equipment sizing. Based on the equipment sizes defined by process HMB, cost for each piece of major equipment was estimated based on either vendor quotes or using commercial estimation software (ASPEN In-Plant Cost Estimator). Installation labor hours for the equipment were factored from Nexant's in-house historical data by equipment type.

As defined in the DOE Report 1399, an average labor wage at $39.7/hr, with an all-in labor cost of $51.6/hr (including wages plus 30% burden to cover fringe benefits, payroll based taxes, and insurance premiums) was assumed for calculating the 2011 installation labor costs. No over-time or other premiums were added. Nexant also assumed that the average labor productivity for the site was 105% of the US Gulf coast productivity.

Bulk material and installation costs are added to complete the major equipment direct installation costs. Bulk material costs, which include instrumentation, piping, structure steel, insulation, electrical, painting, concrete & site preparation works that are needed to complete the major equipment installations, were factored from major equipment cost (MEC) based on Nexant's in-

house historical data for similar services. Installation labor for each bulk commodity was factored from in-house historical data by type. Sum total of MEC plus bulk material cost plus installation labor costs forms the total direct cost (TDC) for the Nexant-Designed systems.

Construction indirect costs were then factored from total direct labor costs based on in-house historical data, and added to the system TDC to give the total field cost (TFC) for the Nexant-Designed systems. Construction indirect cost covers the cost for setup, maintenance and removal of temporary facilities, warehousing, surveying and security services, maintenance of construction tools and equipment, consumables and utilities purchases, and field office payrolls. It should be noted that the term TFC is the equivalent of the Bare Erected Cost (BEC) used in the DOE Report 1399.

2.12.3 RTI Advanced Syngas Cleanup and AACRP System Capital Cost Estimate Criteria

For RTI's advanced syngas cleanup system, RTI's process model incorporates actual data from the pilot plant testing at Eastman Chemical and the 50 MWe pre-commercial demonstration plant at Tampa Electric Company. For AACRP, RTI developed a detailed process model using ProMax with TSWEET kinetics for the CO_2-amine reactions. This process model was reviewed by a recognized expert in the field of acid gas removal technologies. RTI has worked to validate these models against actual pilot and demonstration plant data for RTI's proprietary technology and any publicly available DOE reports for the more commercial technologies.

Using these models, RTI developed HMBs and sized equipment lists. Using process conditions and experience gained from the pilot plant and demonstration plant operation, materials of construction were identified. With the sized equipment list and materials of construction, RTI developed equipment cost estimates from actual vendor quotes or scaled equipment costs from the 50 MWe pre-commercial demonstration unit for a majority of the equipment. For some of the more generic and non-proprietary equipment, the equipment costs were developed using the Aspen In Plant Cost Estimator (IPCE) program. RTI then used the same factored estimates used in NETL Report 1399 to estimate BEC for WDP, DSRP and AACRP. This BEC information from RTI was used by Nexant directly in its calculation of the overall IGCC capital expenditure (CAPEX).

For RTI's ATWGS system, RTI used cost data from the WDP system from the 50 MWe pre-commercial demonstration unit to develop the cost estimate for the transport reactor, which effectively utilized actual vendor cost data. As obtaining a quote from commercial solid cooler vendors was not possible because of proprietary issues, RTI worked with several technical experts that have designed and assisted in troubleshooting actual operating solid coolers to review and validate RTI's estimated solids cooler package and cost. The reviewed costs were provided to Nexant.

In addition to using the actual pilot plant and pre-commercial demonstration plant data for developing equipment costs, RTI used this available data to develop utility and variable costs especially for sorbent, catalysts, and solvent. Estimates of the utilities and variable costs were also provided to Nexant to complete its overall IGCC performance analysis, and to calculate the IGCC plant's overall variable operating costs.

2.12.4 Balance of Plant Capital Cost Estimate Criteria

The capital cost estimates for the rest of the IGCC systems that are unrelated to coal gasification, sulfur and CO_2 removal, were developed based on the Case S1B Shell IGCC plant with CO_2 capture case in the NETL Report 1399. The costs were adjusted for differences in unit or plant capacity according to NETL's Guidelines as described in the NETL *Capital Cost Scaling Methodology* document.

Table 2-6 shows the code of accounts for the IGCC plant. These systems are further broken down to include the various subsystems. The scaling parameters for these Balance of Plant (BOP) subsystems, as laid out by the NETL *Capital Cost Scaling Methodology* document, are also shown in this table.

Table 2-6
Code of Accounts for Report IGCC Plant

Acct No.	Item/Description	Scaling Parameter
1	COAL & SORBENT HANDLING	
1.1	Coal Receive & Unload	Coal Feed Rate
1.2	Coal Stackout & Reclaim	Coal Feed Rate
1.3	Coal Conveyors & Yard Crush	Coal Feed Rate
1.4	Other Coal Handling	Coal Feed Rate
1.9	Coal & Sorbent Handling Foundations	Coal Feed Rate
2	COAL & SORBENT PREP & FEED	
2.1	Coal Crushing & Drying	Coal Feed Rate
2.2	Prepared Coal Storage & Feed	Coal Feed Rate
2.3	Dry Coal Injection System	Calculated
2.4	Misc Coal Prep & Feed	Coal Feed Rate
2.9	Coal & Sorbent Feed Foundation	Coal Feed Rate
3	FEEDWATER & MISC. BOP SYSTEMS	
3.1	Feedwater System	BFW (HP only)
3.2	Water Makeup & Pretreating	Raw Water Makeup
3.3	Other Feedwater Subsystems	BFW (HP only)
3.4	Service Water Systems	Raw Water Makeup
3.5	Other Boiler Plant Systems	Raw Water Makeup
3.6	FO Supply Sys and Nat Gas	Coal Feed Rate
3.7	Waste Treatment Equipment	Raw Water Makeup
3.8	Misc Power Plant Equipment	Coal Feed Rate
4	GASIFIER & ACCESSORIES	
4.1	Gasifier, Syngas Cooler & Auxiliaries	Syngas Throughput
4.3	ASU/Oxidant Compression	O_2 Production
4.4	Scrubber & Low Temperature Cooling	Syngas Flow
4.6	Other Gasification Equipment	Syngas Flow
4.9	Gasification Foundations	Syngas Flow
5A	GAS CLEANUP & PIPING	
5A.1	Double Stage Selexol™	Gas Flow to AGR
5A.2	Elemental Sulfur Plant	Sulfur Production
5A.3	Mercury Removal	Hg Bed Carbon Fill
5A.4	Shift Reactors/COS Hydrolysis	WGS/COS Catalyst
5A.5	Blowback Gas Systems	Candle Filter Flow
5A.6	Fuel Gas Piping	Fuel Gas Flow
5A.9	HGCU Foundations	Sulfur Production
5B	CO_2 REMOVAL & COMPRESSION	
5B.2	CO_2 Compression & Drying	CO_2 Flow
6	COMBUSTION TURBINE/ACCESSORIES	
6.1	Combustion Turbine Generator	Fuel Gas Flow
6.2	Combustion Turbine Foundations	Fuel Gas Flow
7	HRSG, DUCTING & STACK	
7.1	Heat Recovery Steam Generator	HRSG Duty
7.3	Ductwork	Vol Flow to Stack
7.4	Stack	Vol Flow to Stack
7.9	HRSG, Duct & Stack Foundations	Vol Flow to Stack

Acct No.	Item/Description	Scaling Parameter
8	STEAM TURBINE GENERATOR	
8.1	Steam TG & Accessories	Turbine Capacity
8.2	Turbine Plant Auxiliaries	Turbine Capacity
8.3a	Condenser & Auxiliaries	Condenser Duty
8.3b	Air Cooled Condenser	Condenser Duty
8.4	Steam Piping	BFW (HP Only)
8.9	TG Foundations	Turbine Capacity
9	COOLING WATER SYSTEM	
9.1	Cooling Towers	Cooling Tower Duty
9.2	Circulating Water Pumps	Circ H_2O Flow Rate
9.3	Circ. Water System Auxiliaries	Circ H_2O Flow Rate
9.4	Circ Water Piping	Circ H_2O Flow Rate
9.5	Makeup Water System	Raw Water Makeup
9.6	Component Cooling Water System	Circ H_2O Flow Rate
9.9	Circ. Water System Foundations	Circ H_2O Flow Rate
10	ASH/SPENT SORBENT HANDLING SYS	
10.1	Slag Dewatering & Cooling	Slag Production
10.6	Ash Storage Silos	Slag Production
10.7	Ash Transport & Feed Equipment	Slag Production
10.8	Misc. Ash Handling System	Slag Production
10.9	Ash/Spent Sorbent Foundation	Slag Production
11	ACCESSORY ELECTRIC PLANT	
11.1	Generator Equipment	Turbine Capacity
11.2	Station Service Equipment	Auxiliary Load
11.3	Switchgear & Motor Control	Auxiliary Load
11.4	Conduit & Cable Tray	Auxiliary Load
11.5	Wire & Cable	Auxiliary Load
11.6	Protective Equipment	Auxiliary Load
11.7	Standby Equipment	Total Gross Output
11.8	Main Power Transformers	Total Gross Output
11.9	Electrical Foundations	Total Gross Output
12	INSTRUMENTATION & CONTROL	
12.4	Other Major Component Control	Auxiliary Load
12.6	Control Boards, Panels & Racks	Auxiliary Load
12.7	Computer & Accessories	Auxiliary Load
12.8	Instrument Wiring & Tubing	Auxiliary Load
12.9	Other I & C Equipment	Auxiliary Load
13	IMPROVEMENT TO SITE	
13.1	Site Preparation	Accounts 1-12
13.2	Site Improvements	Accounts 1-12
13.3	Site Facilities	Accounts 1-12
14	BUILDING & STRUCTURES	
14.1	Combustion Turbine Area	Gas Turbine Power
14.2	Steam Turbine Building	Accounts 1-12
14.3	Administration Building	Accounts 1-12
14.4	Circulation Water Pumphouse	Circ H_2O Flow Rate
14.5	Water Treatment Buildings	Raw Water Makeup
14.6	Machine Shop	Accounts 1-12
14.7	Warehouse	Accounts 1-12
14.8	Other Buildings & Structures	Accounts 1-12
14.9	Waste Treating Building & Structures	Raw Water Makeup

As Table 2-6 is based on a reference design from DOE/NETL Report 1399, it does not necessarily have an account and/or subaccount number for the advanced technologies being evaluated in this study. To support a more direct comparison of these advanced technologies with the existing commercial technologies, the advanced technologies used the same account and/or subaccount numbers as the existing commercial technologies that they are most analogous to. For technologies without a defined account number, one was created. Because one of the technologies of interest for this TEA is WGS, a special subaccount number was created. The necessity of heat extraction for WGS systems for CO-rich coal-derived syngas demands incorporation of heat exchangers into the overall WGS system. A special subaccount number for WGS (5A.4a) that combines the costs from DOE's sub account numbers 4.4 (LT Heat Recovery and FG Saturation) and 5A.4 (Shift Reactors) was created to provide the best means to effectively capture the overall costs for all the equipment needed to support the WGS process and enable effective comparisons across the cases. Table 2-7 provides a list of the advanced technologies evaluated in this study and their associated account numbers.

Table 2-7
Code of Accounts for Advanced Technologies being Evaluated

Account Number	Title	Advanced Technology
2.3	Dry Coal Injection System	GTI DSP
4.1	Gasifier, Syngas Cooler & Auxiliaries	GTI R-GAS™ Gasifier
5A.1	RTI WDP	RTI WDP
5A.2	RTI DSRP	RTI DSRP
5A.4a	LT Heat Recovery, FG Saturation, & Shift Reactors	AFWGS and ATWGS
5B.1	AACRP	AACRP

2.12.5 Home Office, Engineering Fees and Project/Process Contingencies

Engineering and construction management fees and home office cost, project and process contingencies were factored from each subsystem's TFC. These were then added to the TFC to come up with the total plant cost (TPC) of the system. Factors from Case S1B in the NETL Report 1399 were used.

Process contingency is intended to compensate for uncertainty in cost estimates caused by performance uncertainties associated with the development status of a technology. Process contingency for the advanced technologies of interest in this study were developed according to the criteria recommended by the Association for Advancement of Cost Engineering International (AACE) as specified in DOE/NETL's *Cost Estimation Methodology for NETL Assessment of Power Plant Performance*. Table 2-8 shows the process contingencies applied for the advanced technologies in this study.

Table 2-8
Process Contingencies for Advanced Technologies being Evaluated

Advanced Technology	Process Contingency (% of Associated Process Capital)	Rationale
GTI DSP	20%	The AR DSP and static splitter feed system are currently demonstrated at the small pilot level. The system shares similar types of commercially demonstrated equipment with the conventional lockhopper feed system e.g feed bins, compressors.
GTI R-GAS™ Gasifier	25%	At 25%, this is within range of contingencies applied to technologies demonstrated at the small pilot level
AACRP	20%	This is consistent with the contingency applied for similar processes such as Selexol™ and Rectisol® in the DOE/NETL studies.
RTI DSRP	20%	The DSRP technology has been demonstrated in RTI's pilot testing at Eastman Chemical Company (DE-AC26-99FT40675)
RTI WDP	20%	The WDP technology has been demonstrated in RTI's 50 MWe demonstration plant project (DE-FE0000489)
WGS	0%	Sweet and sour water-gas shift technology is commercially proven
ATWGS	20%	This is within range of contingencies applied to technologies demonstrated at the small pilot level

2.12.6 Owner's Cost

Owner's cost was then added to TPC to come up with the total overnight cost (TOC) for the system. Owner's costs as defined in the NETL Report 1399 include the following:

- Preproduction costs –
  - 6 months of all labor cost
  - 1 month of maintenance materials
  - 1 month of non-fuel consumables
  - 1 month of waste disposal
  - 25% of 1 month fuel cost at 100% capacity factor
  - 2% TPC

- Inventory capital -
  - 60 day supply of fuel and consumable at 100% CF
  - 0.5% TPC

- Initial cost for catalyst, sorbent and chemicals per design
- Land cost = $900,000 (300 acres x $3,000/acre)
- Other owner's costs at 15% TPC
- Financing costs at 2.7% TPC

2.13 OPERATION & MAINTENANCE COSTS

The operation and maintenance (O&M) costs pertain to those charges associated with operating and maintaining the power plants over their expected life. These costs include:

- Operating labor
- Maintenance – material and labor
- Administrative and support labor
- Consumables
- Fuel
- Waste disposal

There are two components of O&M costs; fixed O&M, which is independent of power generation, and variable O&M, which is proportional to power generation. Variable O&M costs were estimated based on 80% CF.

2.13.1 Fixed Costs

Operating labor cost was determined based on the number of operators required to work in the plant. Other assumptions used in calculating the total fixed cost include:

- 2011 base hourly labor rate, $/hr $39.7
- Length of work-week, hrs 50
- Labor burden, % 30
- Administrative/support labor, % O&M labor 25
- Maintenance material + labor, % TPC 2.8
- Maintenance labor only, % maintenance material + labor 35
- Property taxes and insurances, % TPC 2

2.13.2 Variable Costs

The cost of consumables, including fuel, was determined based on the individual rates of consumption, the unit cost of each specific consumable commodity, and the plant annual operating hours. Waste quantities and disposal costs were evaluated similarly to the consumables.

The unit costs for major consumables and waste disposal was selected from NETL Report 1399, QGESS *Updated Costs (June 2011 Basis) for Selected Bituminous Baseline Cases* and from the QGESS *Fuel Prices for Selected Feedstocks in NETL Studies* documents.

The 2011 coal price as delivered to the Montana IGCC plant was $19.63/ton, per the QGESS *Fuel Prices for Selected Feedstocks in NETL Studies* document.

2.13.3 CO_2 Transport and Storage Costs

As specified in NETL Report 1399, CO_2 Transport, Storage and Monitoring (TS&M) costs used for the Montana IGCC plant location is $22/tonne. The COEs are reported both with and without the cost of CO_2 TS&M.

2.14 FINANCIAL MODELING BASIS

2.14.1 Cost of Electricity

The primary metric used to evaluate overall financial performance is the cost of electricity (COE) for the IGCC plant. All costs were expressed in the "first-year-of-construction" year dollars, and the resulting COE was also expressed in "first-year-of-construction" year dollars.

The same financial modeling methodology was used for this study as per the NETL Report 1399 and guidelines in the QGESS *Cost Estimation Methodology for NETL Assessments of Power Plant Performance* document. This is a simplified method that is a function of the plant TPC, capital charge factor (CCF), fixed and variable operating costs, CF and net power generation, as shown in the equation below:

$$COE = \frac{\begin{matrix}first\ year \\ capital\ charge\end{matrix} + \begin{matrix}first\ year \\ fixed\ operating \\ costs\end{matrix} + \begin{matrix}first\ year \\ variable\ operating \\ costs\end{matrix}}{\begin{matrix}annual\ net\ megawatt\ hours \\ of\ power\ generated\end{matrix}}$$

$$COE = \frac{(CCF)(TOC) + OC_{FIX} + (CF)(OC_{VAR})}{(CF)(MWH)}$$

where:

CCF = Capital Charge Factor

TOC = Total Overnight Cost

OC_{FIX} = Fixed Operating Cost

CF = Capacity Factor

OC_{VAR} = Variable Operating Cost

MWH = Megawatt-hours generated

The CCF used in evaluating the COE was pre-calculated using the NETL Power Systems Financial Model (PSFM). This factor is valid for global economic assumptions used for a pre-determined finance structure and capital expenditure period. For the IGCC with CO_2 capture cases, the financial performance evaluations are in accordance with the high-risk, Investor Owned Utility (IOU) finance structure with a 5 year capital expenditure period. The resulting CCF is 0.1243.

2.14.2 Cost of CO_2 Avoided

Per the reporting requirements of the TEA, the cost of CO_2 avoided shall be reported, if a reference non-capture plant is available. Since the scope of work did not specify the modeling of an analogous case without capture, a reference baseline supercritical (SC) pulverized coal (PC) boiler plant firing the same coal at the same design conditions is used instead, as recommended by the NETL Report 1399. The equation for the CO_2 avoided cost is:

The baseline SC PC plant firing PRB coal is a 550 MWe plant with results presented in Table 2-9.

Table 2-9
Baseline SC PC Results for CO_2 Avoided Cost Calculation

	PRB Coal
Net Output, MW	550
*2011 COE, mills/kWh	79.42
Emissions, lb/net-MWh	1,892

*The 2011 COE for 550MW PRB coal-fired SC PC plant was escalated to 2011 by applying an escalation factor to the 2007 COE of 57.80. This factor is obtained by dividing the 2011 550 MW Illinois #6 coal fired SC PC COE by the corresponding 2007 COE (80.95/58.91)*57.8=79.42

2.14.3 CO_2 Sales Price

Sensitivity analysis was used to establish the impact of CO_2 sales on IGCC COE. The CO_2 sales price at the IGCC plant gate was varied between \$0/tonne (baseline case assuming no value to the product CO_2) and \$60/tonne.

The formula used to calculate the revised COE after taking into account CO_2 sales was

$$COE = Baseline\ COE\ - \frac{(CO_2\ Sales\ Price)\ \times annual\ tonnes\ of\ CO_2\ product}{annual\ net\ megawatt\ hours\ of\ power\ generated}$$

2.14.4 Cost of CO_2 Emissions

Sensitivity analysis on cost of CO_2 emissions was also performed using the CO_2 emissions cost as a variable. The emissions cost ranged between \$0/tonne (baseline case assuming no CO_2 emissions cost) and \$60/tonne.

The formula used to calculate the revised COE after taking into cost of CO_2 emissions was

$$COE = Baseline\ COE + \frac{(Cost\ of\ CO_2\ Emissions)\ \times annual\ tonnes\ of\ CO_2\ emitted}{annual\ net\ megawatt\ hours\ of\ power\ generated}$$

Section 3 Case 1a: Shell with Selexol™ AGR IGCC

The Case 1a process descriptions, performance and cost results in this section were previously presented in Nexant's DE-FE0012066 IGCC report. They are reproduced here for the reader's ease of reference.

3.1 PROCESS OVERVIEW

The reference Case 1a IGCC power plant, Nexant's simulation of the NETL Report 1399 Case S1B, is a Montana PRB coal-fired IGCC plant designed to generate enough hydrogen-rich syngas to fill two advanced GE 7F-turbines rated nominally at 215 MWe each for a total of 430 MWe at the Montana site's elevation. The power plant is equipped with a HRSG and steam turbines to maximize power recovery. It is designed to capture CO_2 equivalent to 90% of the raw syngas' carbon content using the two-stage Selexol™ process. The nominal net IGCC power export capacity after accounting for the auxiliary loads which include CO_2 capture and compression is 460 MWe.

In order to achieve the 90% CO_2 removal target, the raw syngas must be converted to hydrogen-rich syngas by the WGS reaction. Steam in the syngas for the WGS reaction is provided partly by the steam generated from quench cooling of the gasifier syngas and partly by water evaporation in the scrubber. Additional steam is injected to the syngas stream to push the equilibrium towards a high conversion of CO. The WGS catalyst also hydrolyzes the COS to H_2S for capture in the AGR process. The recovered H_2S is converted into elemental sulfur in the Claus plant.

The IGCC plant is assumed to operate as a base-loaded unit with annual on-stream CF of 80% or 7,000 hrs/year at full capacity. This capacity factor was selected as it represents the maximum availability demonstrated by commercial IGCC plants.

3.2 IGCC COMMON PROCESS AREAS

As shown in Figure 2-1, the Case 1a IGCC power plant consists of the following major process and/or utility blocks. Some of these blocks, or process areas, are common to the Case 1b and 1e plant configurations. These common process areas are in bold and italicized.

- ***Coal Sizing Handling***
- ***Coal Prep, Drying***
- ***Feed Water & Miscellaneous BOP Systems***
- ***Air Separation Unit (ASU)***
- Dry Coal Feed & Shell SCGP Gasifier System
- Syngas Cooling (Quench, Scrubbing, Steam Generation)
- Gas Cleaning (Filters, WGS & AGR)
- ***Mercury Removal***
- ***CO_2 Compression and Purification Facilities***
- Sulfur Plant

- ***Combustion Turbine Power Generation (CTG)***
- ***HRSG, Ducting and Stack***
- ***Steam Turbine Power Generation (STG)***
- ***Cooling Water Systems***
- ***BFW/Condensate System***
- ***Slag Recovery and Handling***
- ***Accessory Electric Plant***
- ***Instrumentation and Control***

The common areas are presented in brief here for general background information, and to avoid unnecessary repetition in the other cases. Detailed descriptions of these process areas can be found in Section 3.1 of the NETL Report 1399. Where there is case specific performance information, these features are presented in the relevant case sections.

3.2.1 Coal Sizing and Handling

The PRB coal is delivered to the site by 100-ton rail cars. It is unloaded into two receiving hoppers and fed to the vibratory feeder. It is then transferred through intermediate hoppers and silos to the coal crusher where it is reduced to 1-1/4" x 0 size.

3.2.2 Coal Preparation and Drying

A paper presented by Shell in the Gasification Technology Conference was cited in the Reference S1B case. The paper described the drying of subbituminous coal to 6% moisture before feeding it to the Shell entrained-flow gasifier. This moisture content is considered compatible with the storage, transport and feed injection requirements for the Shell entrained flow gasifier.

The coal drying process selected in the NETL Report 1399 is the fine grain WTA (fluidized bed drying technology with built-in waste heat recovery) process, illustrated in Figure 3-1. It was chosen for its ability to recover the coal moisture for use in a closed loop drying process instead of discharging the moisture to the atmosphere and that syngas is not required to provide heat for coal drying. GTI has indicated that its DSP and compact gasifier are compatible with the PRB coal that has been dried to 6% moisture by a WTA dryer.

Figure 3-1
WTA Coal Drying Process Schematic

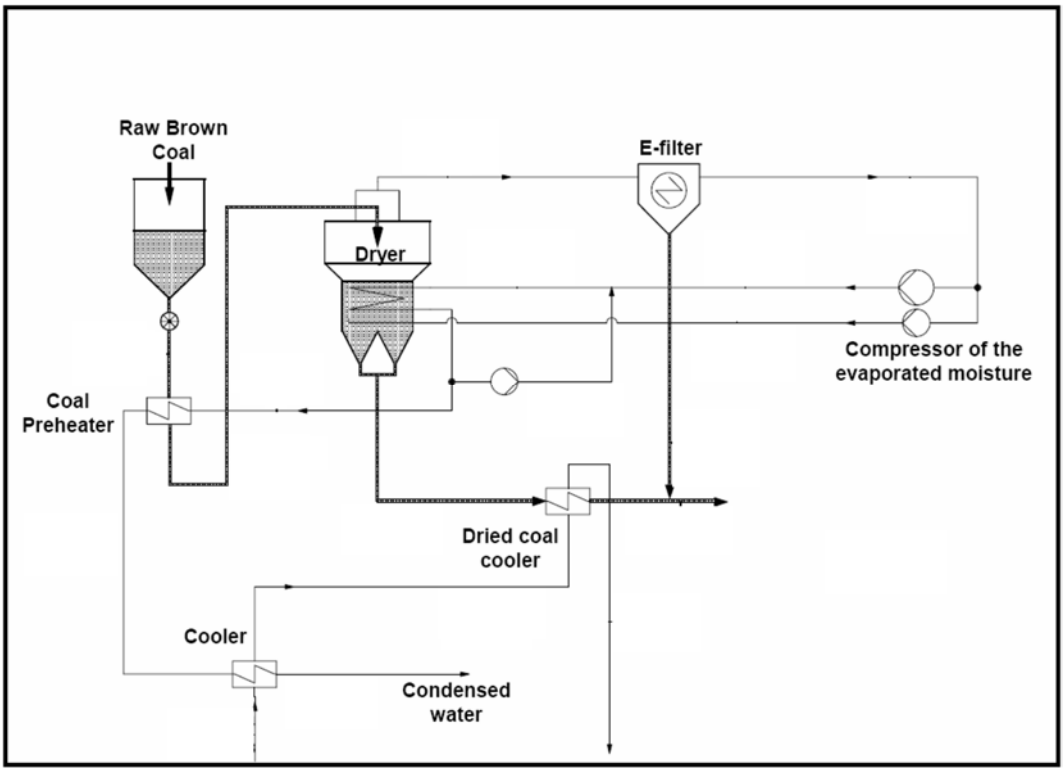

3.2.3 ASU

The reference Case S1B utilizes an "elevated pressure" ASU in which the main air compressor discharge pressure is 190 psia. No air supply integration with the Gas Turbine (GT) compressor is used. In addition to providing 95% oxygen to the gasifiers and the Claus plant, the ASU also provides diluent nitrogen to the GT combustor to increase GT power output, maintaining optimum firing temperatures and minimize the formation of NO_x.

The battery limit conditions for the ASU products are summarized in Table 3-1 below:

Table 3-1
ASU Product Conditions

ASU Product	Pressure, psia	Temperature, °F
95% O_2	125	90
Diluent N_2	384	385
Transport N_2	815	387
ASU Vent	16.4	64

3.2.4 Mercury Removal

Mercury is removed from the syngas at elevated pressure and prior to combustion because syngas volumes are much smaller than flue gas volumes. Mercury removal is achieved via an

activated carbon bed adsorption system as cited in the NETL Report 1399. Data on the performance of carbon bed systems was obtained from the Eastman Chemical Company, which uses carbon beds at its syngas facility in Kingsport, Tennessee.

3.2.5 CO_2 Compression and Dehydration

Raw CO_2 greater than 99% purity leaves the Selexol™ AGR plant at the conditions of 150 psia and 60°F. It is compressed to supercritical condition of 2,215 psia using a multi-stage, intercooled compressor. The CO_2 stream is dehydrated to a dew point of -40 °F at the appropriate inter-stage pressure using a thermal swing adsorptive dryer.

3.2.6 Slag and Ash Handling

Slag material drains from the gasifier into a water bath in the bottom of the gasifier vessel. The slag-water slurry is transferred to a slag crusher where the slag is crushed into pea size fragments. The slurry containing 5 to 10% solids is then transferred to a dewatering bin through a lockhopper for dewatering. The water is clarified and reused as makeup to the water scrubber. The dried slag is stored for disposal.

3.2.7 Combustion Turbine Power Generation

The GT generator selected is an advanced F class turbine. Nitrogen from the ASU is used for dilution to limit NO_x formation and to adjust the syngas LHV to 115-132 Btu/Scf. Inlet air is compressed to a pressure ratio of 16:1 for the GT combustion process. Hot combustion products are expanded in a three stage turbine expander with a last stage exhaust temperature of around 1,050°F. The nominal gross GT output per turbine is 215 MW at the Montana site location.

3.2.8 Steam Turbine and HRSG

The 1,050°F GT exhaust is cooled in the HRSG by generating HP, IP and LP steams for the ST and process users. The cooled GT flue gas exits the HRSG at 270°F and is vented to the atmosphere through a stack. Two HRSG trains (2 x 50%), in tandem with the combustion turbines, are in operation.

The IGCC uses one steam turbine to generate power from the steam generated in the HRSG and process waste heat recovery (WHR) systems. HP steam at 1,800 psig and 1,000 °F and IP steam at 467 psia and 1,000 °F are used in the HP and IP stages of the ST for power generation. LP exhaust steam from the last ST stage is condensed by splitting 50/50 to a surface condenser and an air-cooled condenser to conserve cooling water. The condensers operate at 0.698 psia with a corresponding condensing temperature of 90 °F.

The condensates are collected and sent to a deaerator to remove dissolve gases and treated to provide BFW for the steam generators. Two 50% capacity BFW pumps are provided for each of the three (HP, IP and LP) steam generators.

3.2.9 Cooling Water Systems

Exhaust steam from the ST is split 50/50 to a surface condenser cooled with cooling water and to an air-cooled condenser using ambient air and forced convection. The major impact of utilizing

this parallel cooling method is a significant reduction in water requirement when compared to a wet cooling system.

The circulating water system is a closed-cycle cooling water system that supplies cooling water to the surface condenser to condense one-half of the main turbine exhaust steam. The system also supplies cooling water to the AGR plant as required, and to the auxiliary cooling system. The auxiliary cooling system is a closed loop process that utilizes a higher quality water to remove heat from compressor intercoolers, oil coolers and other ancillary equipment and transfers that heat to the main circulating cooling water system in plate-and-frame heat exchangers. The heat transferred to the circulating water in the surface condenser and other applications is removed by a mechanical draft cooling tower.

The system consists of two 50% capacity vertical circulating water pumps (CWP), a mechanical draft evaporative cooling tower, and CS cement-lined interconnecting piping. The pumps are single-stage vertical pumps. The piping system is equipped with butterfly isolation valves and all required expansion joints. The cooling tower is a multi-cell wood frame counter-flow mechanical draft cooling tower.

3.2.10 BFW/Condensate System

The function of the feedwater (FW) system is to pump the various FW streams from the deaerator storage tank in the HRSG to the respective steam drums. Minimum flow recirculation to prevent overheating and cavitation of the pumps during startup and low loads is provided by an automatic recirculation valve and associated piping that discharges back to the deaerator storage tank. Pneumatic flow control valves control the recirculation flow. The FW pumps are supplied with instrumentation to monitor and alarm on low oil pressure, or high bearing temperature. FW pump suction pressure and temperature are also monitored. In addition, the suction of each FW pump is equipped with a startup strainer.

3.2.11 Accessory Electric Plant

The accessory electric plant consists of switchgear and control equipment, generator equipment, station service equipment, conduit and cable trays, and wire and cable. It also includes the main transformer, all required foundations, and standby equipment.

3.2.12 Instrumentation and Control

An integrated plant-wide distributed control system (DCS) is provided, per the description given in the NETL Report 1399.

3.3 CASE 1a PROCESS DESCRIPTION

Case 1a is modeled upon the process information provided in Case S1B within the NETL Report 1399. The system description follows the BFD in Figure 3-2 and stream numbers reference the same figure. Table 3-1 provides Nexant's model generated process data for the numbered streams in the BFD.

Coal Preparation and Drying

Coal receiving and handling is part of the IGCC common areas and covered in Section 3.2.1. Coal is crushed in the coal mill and then delivered to a surge hopper, which in turn delivers the coal to the coal pre-heater. The WTA coal drying process, described in Section 3.2.2 reduces the PRB coal moisture content from 25.77 wt% to 6 wt%.

Coal Feed System

The dried coal is drawn from the surge hoppers and fed through a pressurization lock hopper system to a dense phase pneumatic conveyor, which uses nitrogen from the ASU to convey the coal to the gasifiers.

Air Separation Unit

The ASU plant is designed with two production trains. The air compressor is powered by an electric motor. Nitrogen is also recovered, compressed, and used as diluent in the GT combustor and as a coal transport fluid.

Shell Gasifier

There are two Shell dry feed, pressurized, up flow, entrained, slagging gasifiers, operating at 615 psia. Coal reacts with oxygen in a reducing environment to produce principally hydrogen and carbon monoxide with some CO_2 formed. High-temperature heat recovery in each gasifier train is accomplished in three steps, including the gasifier membrane wall, which maintains a protective ash layer over the membrane wall. The product gas from the gasifier is cooled using a syngas recycle quench to lower the temperature below the ash melting point. Syngas then goes through a raw gas cooler, which lowers the gas temperature and contributes to the production of HP steam for use in steam cycle.

The solids are removed as both slag and ash. Liquid slag is solidified in a water bath and removed via a lock hopper system. Ash carried over with the syngas is removed in a ceramic candle filter. The collected ash is also removed from the filter via a lock hopper system. The syngas scrubber downstream of the gasifier removes any remaining PM passing the candle filter because of leakage around the filter seals or any undetected candle failure that allows the passage of large particulates.

Syngas Scrubber/Sour Water Stripper

The raw syngas exiting the ceramic particulate filter enters the scrubber for removal of chlorides and any remaining particulates. The quench scrubber washes the syngas in a countercurrent flow in two packed beds, which removes essentially all traces of entrained particles. The bottoms from the scrubber are sent to the slag removal and handling system for processing.

The sour water stripper removes ammonia, sulfur, and other impurities from the waste stream of the scrubber. The sour gas stripper consists of a sour drum that accumulates sour water from the gas scrubber and condensate from low temperature syngas cooling.

Water-Gas Shift and COS Hydrolysis

To enable 90% carbon capture from the syngas, the gasifier syngas product must be converted to hydrogen-rich syngas. This is achieved by converting most of the syngas CO to hydrogen and CO_2 by reacting the CO with water over a bed of catalyst, per the following reaction:

$$CO + H_2O \leftrightarrow CO_2 + H_2$$

Steam for the WGS is provided partly by the vaporization of water during syngas quench cooling and partly by saturation of the overhead gas in the syngas scrubber. Additional steam is injected to the syngas stream to push the equilibrium towards a high conversion of CO. The shift catalyst is sulfur-tolerant and it also hydrolyses the COS to H_2S for removal in the AGR system.

Cooling is provided between reactors to control the exothermic temperature rise. A parallel set of reactors is required due to the high gas mass flow rate. The heat exchanger after the second WGS reactor is a gas-gas exchanger used to preheat the syngas prior to the first WGS reactor.

Mercury Removal and AGR

Mercury removal is achieved via an activated carbon process described in Section 3.2.4. The AGR process is a two-stage Selexol™ process where H_2S is removed in the first stage and CO_2 in the second stage of absorption. The process results in three product streams, the clean syngas, a CO_2-rich stream and an acid gas feed to the Claus plant. The acid gas contains about 17 percent H_2S and 66 percent CO_2 with a balance of primarily H_2.

CO_2 Compression and Dehydration

CO_2 from the AGR process is generated at 17 and 150 psia. The lower pressure CO_2 stream is compressed from 17 psia to 150 psia and then combined with the CO_2 stream at 150 psia. The combined CO_2 stream is further compressed to a supercritical condition at 2,215 psia using a multiple-stage, intercooled compressor. During compression, the CO_2 stream is dehydrated to a dew point of -40°F using a thermal swing adsorptive dryer. The raw CO_2 stream from the Selexol™ process contains over 99 percent CO_2. The dehydrated CO_2 is transported to the plant fence line for sequestration outside the battery limit (OSBL).

Claus Unit

The sulfur recovery unit (SRU) is a Claus bypass type SRU utilizing oxygen instead of air. The Claus plant produces molten sulfur by converting approximately one third of the H_2S in the feed to SO_2, then reacting the H_2S and SO_2 to sulfur and water. The combined Claus technology and tail gas recycle results in an overall sulfur recovery exceeding 99 percent. Utilizing oxygen instead of air in the Claus plant reduces the overall cost of the sulfur recovery plant. The acid gas

feed consists of acid gas from both the AGR and a vent stream from the sour water stripper in the gasifier section.

Power Block

Clean syngas from the two-stage Selexol™ unit is reheated to 385°F. It is then diluted with nitrogen to meet the heating value specifications before it enters the GT combustor. The exhaust gas exits the GT at a nominal 1,050°F and enters the HRSG where additional heat is recovered. The flue gas exits the HRSG at 270°F and is discharged through the plant stack. The steam raised in the HRSG is used to power an advanced commercially available ST using a nominal 1,800 psig/1,000°F/1,000°F steam cycle. There is no air integration between the GT and the ASU.

Balance of Plant

Balance of plant items are covered in Sections 3.2.9 through 3.2.12.

3.4 SPARING PHILOSOPHY

The sparing philosophy for Case 2a is as provided below. Single train designs are utilized throughout with exceptions where equipment has exceeded its maximum capacity limit and thus requires an additional train. The design has:

- Two ASU trains (2 x 50%)
- Two trains of coal drying (2 x 50%)
- Two trains of gasification, including dry feed system, Shell gasifier, syngas cooler, cyclone and candle filter (2 x 50%)
- Two syngas clean-up trains (2 x 50%)
- Two trains of two-stage Selexol™ (2 x 50%)
- One Claus plant for sulfur recovery (1 x 100%)
- Two gas turbines/HRSG tandems (2 x 50%)
- One steam turbine (1 x 100%)

Figure 3-2
Case 1a: Reference Shell Gasifier with Selexol™ AGR IGCC - Simplified BFD

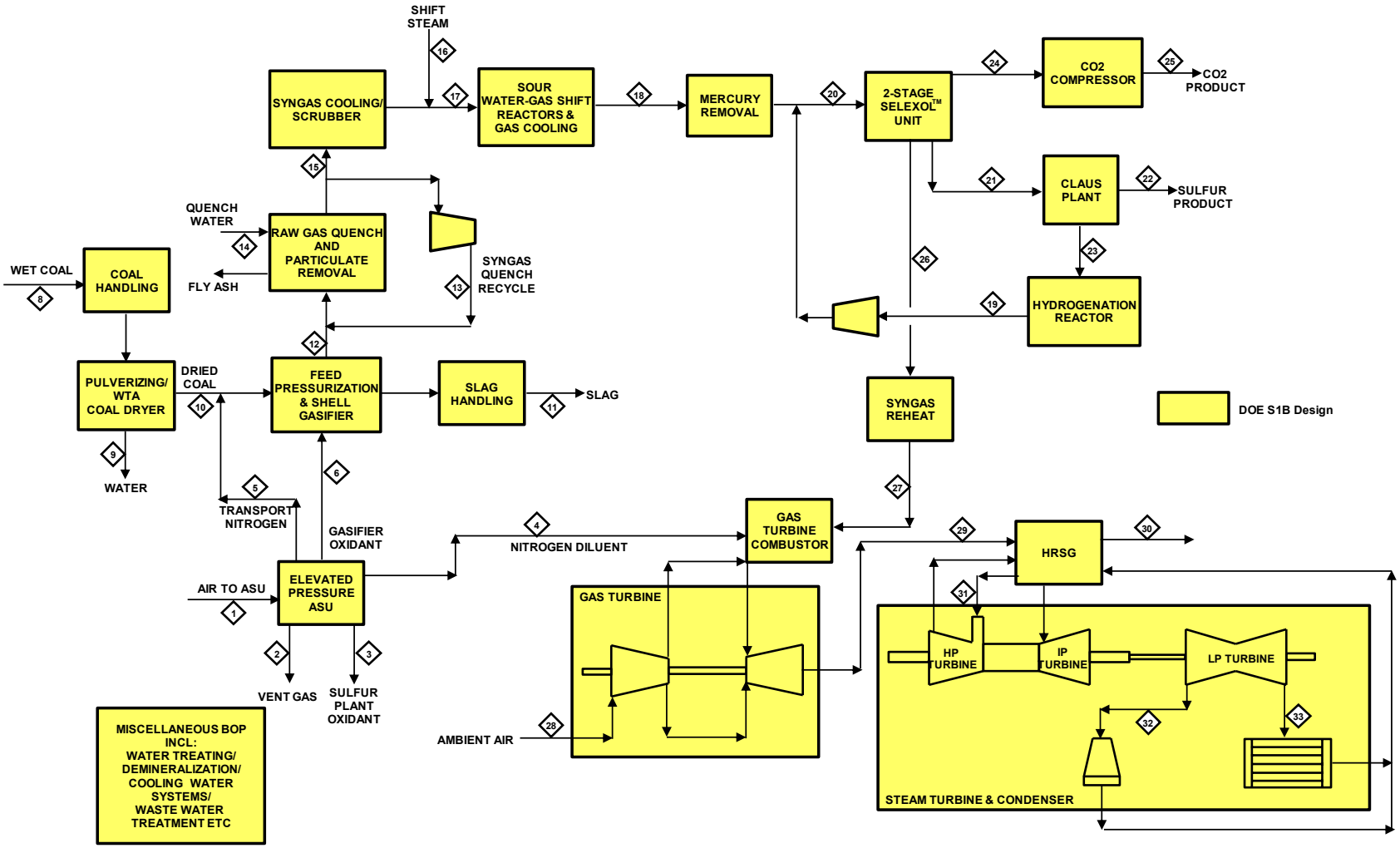

Table 3-2
Case 1a Stream Table

Description	Air to ASU	ASU Vent Gas	Sulfur Plant Oxidant	Nitrogen Diluent	Transport Nitrogen	Gasifier Oxidant	Wet Coal	Coal Moisture	Dried Coal	Slag	Hot Syngas	Syngas Quench Recycle	Quench Water	Cooled Syngas	Shift Steam	Syngas to Shift
Stream No.	1	2	3	4	5	6	8	9	10	11	12	13	14	15	16	17
V-L Mole Fraction																
Ar	0.0093	0.0165	0.0316	0.0023	0.0023	0.0318	0	0	0	0	0.0093	0.0054	0	0.0054	0	0.0046
CH4	0	0	0	0	0	0	0	0	0	0	0	0	0	0	0	0
CO	0	0	0	0	0	0	0	0	0	0	0.6010	0.3466	0	0.3466	0	0.2981
CO2	0.0003	0.0047	0	0	0	0	0	0	0	0	0.0327	0.0188	0	0.0188	0	0.0162
COS	0	0	0	0	0	0	0	0	0	0	0.0005	0.0003	0	0.0003	0	0.0003
H2	0	0	0	0	0	0	0	0	0	0	0.2609	0.1504	0	0.1504	0	0.1294
H2O	0.0064	0.0988	0	0	0	0	0	1.0000	0	0	0.0287	0.4391	0.9980	0.4391	1.0000	0.5198
H2S	0	0	0	0	0	0	0	0	0	0	0.0030	0.0017	0	0.0017	0	0.0015
N2	0.7759	0.7586	0.0177	0.9921	0.9921	0.0178	0	0	0	0	0.0609	0.0351	0	0.0351	0	0.0302
NH3	0	0	0	0	0	0	0	0	0	0	0.0029	0.0025	0.0020	0.0025	0	0
O2	0.2081	0.1213	0.9506	0.0054	0.0054	0.9504	0	0	0	0	0	0	0	0	0	0
SO2	0	0	0	0	0	0	0	0	0	0	0	0	0	0	0	0
S	0	0	0	0	0	0	0	0	0	0	0	0	0	0	0	0
HCl	0	0	0	0	0	0	0	0	0	0	0	0	0	0	0	0
Total	1.0000	1.0000	1.0000	1.0000	1.0000	1.0000	0	1.0000	0	0	1.0000	1.0000	1.0000	1.0000	1.0000	1.0000
V-L Flowrate, lbmol/hr	54448	3446	202	37684	2061	11054	0	6841	0	0	38321	14737	28138	66459	9745	77266
V-L Flowrate, lb/hr	1573240	95747	6499	1057430	57841	355725	0	123241	0	0	826852	295746	506858	1333710	175559	1528540
Solids Flow Rate, lb/hr	0	0	0	0	0	0	585971	0	462730	49444	0	0	0	0	0	0
Temperature, F	42	64	90	385	387	292	42	75	158	2602	2602	474	338	450	550	450
Pressure, psia	13.0	16.4	125.0	384.0	815.0	740.0	13.0	48.0	14.8	615.0	615.0	615.0	115.0	570.0	600.0	555.0
Enthalpy, Btu/lb	-33.3	-463.2	1.8	75.1	74.8	43.8		-6823			-798	-3120	-6549	-3129	-5611	-3457
Density, lb/cuft	0.070	0.089	0.687	1.180	2.473	2.961		62.273			0.401	1.266	56.011	1.206	1.144	1.171

Table 3-2 (cont'd)
Case 1a Stream Table

Description	Syngas to Hg Removal	Tail Gas Recycle	Syngas to Selexol	H2S to Claus	Sulfur Product	Selexol™ CO2 Out	CO2 Product	Treated Syngas	Reheat Syngas	Ambient Air to GT	GT Flue Gas	Stack Gas	HP SH Steam	Air-Cooled LP Cond	Water-Cooled LP Cond	BFW to HRSG
Stream No.	18	19	20	21	22	24	25	26	27	28	29	30	31	32	33	34
V-L Mole Fraction																
Ar	0.0060	0.0095	0.0060	0.0024	0	0.0002	0.0002	0.0095	0.0095	0.0093	0.0089	0.0089	0	0	0	0
CH4	0	0	0	0	0	0	0	0	0	0	0	0	0	0	0	0
CO	0.0099	0.0033	0.0098	0.0044	0	0.0002	0.0002	0.0156	0.0156	0	0	0	0	0	0	0
CO2	0.3974	0.6415	0.4008	0.6579	0	0.9919	0.9948	0.0491	0.0491	0.0003	0.0089	0.0089	0	0	0	0
COS	0	0	0	0	0	0	0	0	0	0	0	0	0	0	0	0
H2	0.5437	0.1156	0.5376	0.1177	0	0.0046	0.0046	0.8618	0.8608	0	0	0	0	0	0	0
H2O	0.0018	0.1393	0.0037	0.0430	0	0.0029	0.0000	0.0001	0.0006	0.0064	0.1207	0.1207	1.0000	1.0000	1.0000	1.0000
H2S	0.0022	0.0058	0.0023	0.1650	0	0	0	0	0	0	0	0	0	0	0	0
N2	0.0391	0.0851	0.0398	0.0096	0	0.0002	0.0002	0.0638	0.0644	0.7759	0.7551	0.7551	0	0	0	0
NH3	0	0	0	0	0	0	0	0	0	0	0	0	0	0	0	0
O2	0	0	0	0	0	0	0	0	0	0.2081	0.1063	0.1063	0	0	0	0
SO2	0	0	0	0	0	0	0	0	0	0	0	0	0	0	0	0
S	0	0	0	0	1.0000	0	0	0	0	0	0	0	0	0	0	0
HCl	0	0	0	0	0	0	0	0	0	0	0	0	0	0	0	0
Total	1.0000	1.0000	1.0000	1.0000	1.0000	1.0000	1.0000	1.0000	1.0000	1.0000	1.0000	1.0000	1.0000	1.0000	1.0000	1.0000
V-L Flowrate, lbmol/hr	59670	852	60522	829	132	22046	21981	37527	37570	221242	280034	280034	48880	43893	43893	83101
V-L Flowrate, lb/hr	1211450	28987	1240440	29927	4231	964151	962980	244215	245240	6392720	7695380	7695380	880585	790735	790735	1497100
Solids Flow Rate, lb/hr	0	0	0	0	0	0	0	0	0	0	0	0	0	0	0	0
Temperature, F	95	102	115	119		60	162	87	385	42	1049	270	999	90	90	240
Pressure, psia	479.7	5.6	479.7	23.7		149.7	2214.7	469.6	460.0	12.9	13.5	13.0	1815.0	0.7	0.7	105.0
Enthalpy, Btu/lb	-3344	-3615	-3342	-3246		-3852		-1383	-1059	-33	-249	-461	-5387	-6808	-6808	-6658
Density, lb/cuft	1.671	0.032	1.622	0.139		1.254	28.796	0.514	0.327	0.069	0.023	0.046	2.282	62.117	62.117	59.099

3.5 PERFORMANCE RESULTS

The Nexant-modeled Case 1a IGCC plant with CO_2 capture consumes 7,032 tpd PRB coal at the Montana site and produces a net output of 461 MWe with a net plant efficiency of 31.32% on a HHV basis. Overall performance for the Case 1a IGCC plant is summarized in Table 3-3, which includes auxiliary power requirements.

Table 3-3
Case 1a Plant Performance Summary

POWER SUMMARY (Gross Power at Generator Terminals, kWe)	Case 1a
Gas Turbine Power	429,973
Steam Turbine Power	224,080
TOTAL POWER, kWe	**654,053**
Auxiliary Load Summary, kWe	
Coal Handling	510
Coal Milling	2,730
Slag Handling	580
WTA Coal Dryer Compressor	9,370
WTA Coal Dryer Auxiliaries	620
Air Separation Unit Auxiliaries	1,003
Air Separation Unit Main Air Compressor	63,719
Oxygen Compressor	8,830
Nitrogen Compressors	33,340
CO_2 Compressor	31,545
Boiler Feedwater Pumps	4,331
Condensate Pump	217
Quench Water Pump	760
Syngas Recycle Compressor	820
Circulating Water Pump	3,090
Ground Water Pumps	335
Cooling Tower Fans	2,015
Air Cooled Condenser Fans	2,847
Scrubber Pumps	20
Acid Gas Removal	18,391
Gas Turbine Auxiliaries	998
Steam Turbine Auxiliaries	96
Claus Plant/TGTU Auxiliaries	249
Claus Plant TG Recycle Compressor	1,517
Miscellaneous Balance of Plant	3,000
Transformer Losses	2,514
TOTAL AUXILIARIES, kWe	**193,448**
NET POWER, kWe	**460,605**
Net Plant Efficiency, % (HHV)	31.32%
Net Plant Heat Rate, Btu/kWh	10,895
CONDENSER COOLING DUTY, MMBtu/hr	**1,202**
CONSUMABLES	
As-Received Coal Feed, lb/hr	585,971
Thermal Input, kWt	1,470,705
Raw Water Withdrawal, gpm	3,683
Raw Water Consumption, gpm	2,844

Table 3-4 shows the carbon balance for the Case 1a IGCC plant. The carbon input to the plant consists of carbon in the air in addition to carbon in the coal. Carbon in the air is not part of the carbon capture equation, but is not neglected in the balance since the model accounts for the air components throughout. Carbon leaves the plant as unburned carbon in the slag, CO_2 in the stack gas, ASU vent gas, and the CO_2 capture product. The carbon capture efficiency is defined as the amount of carbon in the CO_2 product stream relative to the amount of carbon in the coal less carbon contained in the slag. For Case 1a, the carbon capture efficiency is 90%.

Table 3-4
Case 1a Overall Carbon Balance

Overall Carbon Balance, lb/hr	In	Out
Coal Feed	293,384	
ASU Air	196	
Air to Gas Turbine	797	
ASU Vent		196
Carbon in Slag		1,467
Sulfur Product		0
Stack Gas		29,973
CO_2 Product		262,741
Convergence Tolerance		0
Total	**294,377**	**294,377**

Table 3-5 shows the sulfur balance for the plant. Sulfur input comes solely from the sulfur in the coal. Sulfur output includes the sulfur recovered in the Claus plant, sulfur emitted in the stack gas, and sulfur that is sequestered with the CO_2 product. Sulfur in the slag is considered negligible.

Table 3-5
Case 1a Overall Sulfur Balance

Overall Sulfur Balance, lb/hr	In	Out
Coal Feed	4,263	
Sulfur Product		4,253
Stack Gas		2
CO_2 Product		8
Convergence Tolerance		0
Total	**4,263**	**4,263**

Table 3-6 shows the overall water balance for the Case 1a IGCC plant. Raw water is obtained from groundwater (50%) and from municipal sources (50%). Water demand represents the total amount of water required for a particular process. Some water is recovered within the process, primarily from the coal drying process and as syngas condensate, and that water is used as

internal recycle. Net raw water consumption (not shown in Table 3-6) is defined as the difference between the raw water withdrawal and process water discharge.

Table 3-6
Case 1a Overall Water Balance

Water Use, gpm	Raw Water Withdrawal	Process Effluent Production for Internal Consumption	Internal Consumption	Process Water Discharge
WTA Coal Drying	0	(246)	0	0
Slag Handling	0	0	124	(124)
Quench Cooler	258	0	755	0
Scrubber Blowdown	0	(124)	0	0
Syngas Cooling & Sour Stripper Knockout	0	(753)	0	0
Steam Cycle Makeup	534	0	0	0
Steam Cycle Blowdown	0	(13)	0	0
CO_2 Compression Knockout	0	(2)	0	0
Cooling Tower Makeup	2,891	0	259	0
Cooling Tower Blowdown	0	0	0	(714)
Total	3,683	(1,139)	1,139	(838)

3.6 EQUIPMENT LIST

As the Case 1a Shell IGCC is based on Case S1B in NETL Report 1399, the reader should refer to the Case S1B equipment list in NETL Report 1399.

3.7 CAPITAL COST

Table 3-7 shows the cost breakdown of the Case 1a Shell Gasifier with Selexol™-based AGR IGCC, consistent with the code of accounts format as expressed in the NETL Report 1399. The accounts/subaccounts of interest for this study are:

- 2.3 Dry coal injection system,
- 4 Gasifier & accessories,
- 5A Gas cleanup & piping and
- 5B CO_2 removal and compression.

These are shown with more detail to include the various subaccounts and provide more clarity to the major cost differences among the cases.

Table 3-8 shows the calculation and addition of owner's costs to determine the TOC, used to calculate COE.

The estimated TOC of the Case 1a Shell Gasifier with Selexol™ AGR IGCC using PRB coal in 2011 dollars is $5,400/kW.

Table 3-7
Case 1a Total Plant Cost Summary

Case 1a: Shell Gasifier with Selexol™ AGR IGCC		Coal Feed, lb/hr	585,971					Plant Size	460.6 MW, net			
Low Rank Western Coal Baseline Study	PRB	Coal HHV, Btu/lb	8,564					Net Efficiency	31.32%			
Acct		Equipment	Material	Labor		Sales	Bare Erected	Eng'g CM	Contingencies		TOTAL PLANT COST	
No.	Item/Description	Cost	Cost	Direct	Indirect	Tax	Cost $	H.O & Fee	Process	Project	$	$/kW
1	COAL & SORBENT HANDLING	**$19,442**	**$3,409**	**$14,872**	**$0**	**$0**	**$37,723**	**$3,423**	**$0**	**$8,228**	**$49,375**	**$107**
2	COAL & SORBENT PREP & FEED											
2.3	Dry Coal Injection System	$57,741	$0	$39,047	$0	$0	$96,788	$8,337	$0	$21,025	$126,150	$274
2.x	Other Coal & Sorbent Prep & Feed Systems	$62,434	$10,880	$17,044	$0	$0	$90,358	$7,894	$0	$19,649	$117,901	$256
	SUBTOTAL 2.	**$120,176**	**$10,880**	**$56,091**	**$0**	**$0**	**$187,147**	**$16,230**	**$0**	**$40,674**	**$244,051**	**$530**
3	FEEDWATER & MISC BOP SYSTEMS	**$9,280**	**$7,068**	**$9,151**	**$0**	**$0**	**$25,499**	**$2,408**	**$0**	**$6,472**	**$34,379**	**$75**
4	GASIFIER & ACCESSORIES											
4.1	Gasifier, Syngas Cooler & Auxiliaries (Shell)	$189,728	$0	$81,332	$0	$0	$271,060	$24,215	$37,263	$51,121	$383,659	$833
4.3	ASU/Oxidant Compression	$221,843	$0	$0	$0	$0	$221,843	$21,503	$0	$24,335	$267,681	$581
4.6	Flare Stack System	$0	$1,721	$696	$0	$0	$2,417	$232	$0	$529	$3,179	$7
4.9	Gasification Foundations	$0	$10,698	$6,380	$0	$0	$17,078	$1,564	$0	$4,660	$23,302	$51
	SUBTOTAL 4.	**$411,571**	**$12,419**	**$88,408**	**$0**	**$0**	**$512,399**	**$47,514**	**$37,263**	**$80,645**	**$677,821**	**$1,472**
5A	GAS CLEANUP & PIPING											
5A.1	Double Stage Selexol™	$83,479	$0	$70,351	$0	$0	$153,830	$14,877	$30,766	$39,894	$239,368	$520
5A.2	Elemental Sulfur Plant	$5,124	$998	$6,566	$0	$0	$12,688	$1,232	$0	$2,784	$16,705	$36
5A.3	Mercury Removal	$3,489	$0	$2,637	$0	$0	$6,125	$591	$306	$1,404	$8,426	$18
5A.4a	LT Heat Recovery, FG Saturation & Shift Reactors	$39,500	$0	$32,664	$0	$0	$72,164	$7,022	$0	$15,837	$95,022	$206
5A.6	Blow back Gas Systems	$2,680	$451	$254	$0	$0	$3,385	$321	$0	$741	$4,447	$10
5A.7	Fuel Gas Piping	$0	$1,047	$684	$0	$0	$1,731	$161	$0	$379	$2,270	$5
5A.9	HGCU Foundations	$0	$944	$636	$0	$0	$1,581	$145	$0	$518	$2,243	$5
	SUBTOTAL 5.	**$134,271**	**$3,440**	**$113,791**	**$0**	**$0**	**$251,503**	**$24,350**	**$31,072**	**$61,557**	**$368,482**	**$800**
5B	CO2 REMOVAL & COMPRESSION											
5B.1	CO2 Removal System	$0	$0	$0	$0	$0	$0	$0	$0	$0	$0	$0
5B.2	CO2 Compression & Drying	$37,766	$0	$12,616	$0	$0	$50,381	$4,850	$0	$11,046	$66,278	$144
	SUBTOTAL 5B.	**$37,766**	**$0**	**$12,616**	**$0**	**$0**	**$50,381**	**$4,850**	**$0**	**$11,046**	**$66,278**	**$144**
6	COMBUSTION TURBINE/ACCESSORIES	**$111,211**	**$923**	**$8,948**	**$0**	**$0**	**$121,083**	**$11,476**	**$11,909**	**$14,882**	**$159,350**	**$346**
7	HRSG, DUCTING & STACK	**$31,810**	**$2,997**	**$9,301**	**$0**	**$0**	**$44,108**	**$4,168**	**$0**	**$5,590**	**$53,866**	**$117**
8	STEAM TURBINE GENERATOR	**$75,940**	**$985**	**$19,237**	**$0**	**$0**	**$96,162**	**$9,214**	**$0**	**$17,626**	**$123,002**	**$267**
9	COOLING WATER SYSTEM	**$5,916**	**$7,860**	**$7,214**	**$0**	**$0**	**$20,989**	**$1,951**	**$0**	**$4,915**	**$27,856**	**$60**
10	ASH/SPENT SORBENT HANDLING SYS	**$23,279**	**$1,783**	**$11,463**	**$0**	**$0**	**$36,525**	**$3,505**	**$0**	**$4,372**	**$44,402**	**$96**
11	ACCESSORY ELECTRIC PLANT	**$36,081**	**$16,053**	**$29,135**	**$0**	**$0**	**$81,269**	**$6,994**	**$0**	**$16,927**	**$105,189**	**$228**
12	INSTRUMENTATION & CONTROL	**$12,908**	**$2,617**	**$8,487**	**$0**	**$0**	**$24,012**	**$2,175**	**$1,200**	**$4,595**	**$31,981**	**$69**
13	IMPROVEMENTS TO SITE	**$3,743**	**$2,206**	**$9,823**	**$0**	**$0**	**$15,772**	**$1,558**	**$0**	**$5,199**	**$22,529**	**$49**
14	BUILDINGS & STRUCTURES	**$0**	**$7,728**	**$8,781**	**$0**	**$0**	**$16,510**	**$1,502**	**$0**	**$2,959**	**$20,970**	**$46**
	CALCULATED TOTAL COST	**$1,033,395**	**$80,369**	**$407,318**	**$0**	**$0**	**$1,521,081**	**$141,319**	**$81,444**	**$285,688**	**$2,029,531**	**$4,406**

Table 3-8
Case 1a Total Overnight Cost Summary

Owner's Costs	$ x $1,000	$/kW
Preproduction Costs		
6 months All Labor	$16,801	$36
1 Month Maintenance Materials	$3,801	$8
1 Month Non-Fuel Consumables	$483	$1
1 Month Waste Disposal	$456	$1
25% of 1 Months Fuel Cost at 100% CF	$1,050	$2
2% of TPC	$40,591	$88
Total	**$63,181**	**$137**
Inventory Capital		
60 day supply of fuel at 100% CF	$8,282	$18
60 day supply of non-fuel consumables at 100% CF	$721	$2
0.5% of TPC (spare parts)	$10,148	$22
Total	**$19,150**	**$42**
Initial Cost for Catalyst and Chemicals	**$15,343**	**$33**
Land	**$900**	**$2**
Other Owner's Cost	**$304,430**	**$661**
Financing Costs	**$54,797**	**$119**
Total Owner's Costs	**$457,802**	**$994**
Total Overnight Costs (TOC)	**$2,487,333**	**$5,400**

3.8 OPERATING COSTS

Table 3-9 shows the operating cost breakdown for the Case 1a IGCC.

Table 3-9
Case 1a Initial and Annual O&M Costs

	INITIAL & ANNUAL O&M EXPENSES					
Case:	Case 1a Shell Gasifier with Selexol™ AGR IGCC					
Plant Size (MWe)	**461**			**Heat Rate (Btu/kWh):**		10,895
Primary/Secondary Fuel:	**PRB**			**Fuel Cost ($/MMBtu):**		
Design/Construction	5 years			**Book Life (yrs):**		20
TPC (Plant Cost) Year	June 2011			**TPI Year:**		2016
Capacity Factor (%)	80			**CO2 Captured (TPD)**		11548
OPERATING & MAINTENANCE LABOR						
Operating Labor						
Operating Labor Rate (base):	$39.70	$/hr				
Operating Labor Burden:	30.00	% of base				
Labor Overhead Charge	25.00	% of labor				
Operating Labor Requirements per Shift	**units/mod**		**Total Plant**			
Skilled Operator	2.0		2.0			
Operator	10.0		10.0			
Foreman	1.0		1.0			
Lab Tech's etc	3.0		3.0			
TOTAL Operating Jobs	16.0		16.0			
					Annual Cost $	Annual Unit Cost $/kW-net
Annual Operating Labor Cost					$7,233,658	
Maintenance Labor Cost					$19,647,891	
Administration & Support Labor					$6,720,387	
Property Taxes and Insurance					$40,590,623	
TOTAL FIXED OPERATING COSTS					**$74,192,558**	
VARIABLE OPERATING COSTS						$/kWh-net
Maintenance Material Cost					**$36,488,940**	
Consumables	Consumption Initial	/Day	Unit Cost	Initial Fill Cost		
Water(/1000 gallons)	0	2,652	1.67	**$0**	**$1,296,014**	
Chemicals						
MU & WT Chem (lb)	0	15797	0.27	$0	$1,235,509	
Carbon (Hg Removal) (lb)	116627	160	1.63	$190,102	$76,154	
COS Catalyst (m3)	0	0	3751.70	$0	$0	
Water Gas Shift Catalyst (ft3)	6023	4.12	771.99	$4,649,335	$929,220	
Selexol Solution (gal)	285508	90.96	36.79	$10,503,835	$977,132	
SCR Catalyst (m3)	0	0	0.00	$0	$0	
Ammonia (19% NH3) (ton)	0	0	0.00	$0	$0	
Claus Catalyst (ft3)	w/equip	2.00	203.15	$0	$118,670	
Subtotal Chemicals				**$15,343,273**	**$3,336,684**	
Other						
Supplemental Fuel (MMBtu)	0	0	0.00	$0	$0	
Gases, N2 etc.(/100scf)	0	0	0.00	$0	$0	
LP Steam (/1000 lbs)	0	0	0.00	$0	$0	
Subtotal Other				**$0**	**$0**	
Waste Disposal:						
Spent Mercury Catalyst (lb)	0	160	0.65	$0	$30,368	
Flyash (ton)	0	0	0.00	$0	$0	
Slag (ton)	0	593	25.11	$0	$4,350,327	
Subtotal Waste Disposal				**$0**	**$4,380,695**	
By-products & Emissions						
Sulfur (tons)	0	51	0.00	$0	$0	
Subtotal By-Products				**$0**	**$0**	
TOTAL VARIABLE OPERATING COSTS				**$15,343,273**	**$45,502,333**	
Fuel (tons)	**0**	**7032**	**19.63**	**$0**	**$40,305,148**	

3.9 COST OF ELECTRICITY

Table 3-10 shows a summary of the power output, capital expenditure (CAPEX), operating expenditure (OPEX), COE and cost of CO_2 capture for the Case 1a Shell Gasifier with Selexol™ AGR IGCC. The Case 1a IGCC COE is estimated to be 145.3 mills/kWh.

Table 3-10
Plant Performance and Economic Summary

Case	Case 1a
CAPEX, $MM	
Total Installed Cost (TIC)	$1,521
Total Plant Cost (TPC)	$2,030
Total Overnight Cost (TOC)	$2,487
OPEX, $MM/yr (100% Capacity Factor Basis)	
Fixed Operating Cost (OC_{fix})	$74.2
Variable Operating Cost, less Fuel (OC_{var})	$56.9
Fuel (OC_{fuel})	$50.4
Total OPEX	$181.5
Power Production, MWe	
Gas Turbine	430.0
Steam Turbine	224.1
Auxiliary Power Consumption	193.4
Net Power Output	460.6
Power Generated, MWh/yr (MWH)	4,034,901
SO_2 Emissions (lb/MWh_{gross})	0.0063
SO_2 Emissions (lb/$MMBtu_{gross}$)	0.0008
COE, excl CO_2 TS&M, mills/kWh	**145.3**
COE, incl CO_2 TS&M, mills/kWh	**166.2**
Cost of CO_2 Avoided excl CO_2 TS&M, $/ton CO_2	**79.7**
Cost of CO_2 Avoided incl CO_2 TS&M, $/ton CO_2	**105.0**

.

Section 4 Case 1b: GTI R-GAS™ with RTI WDP IGCC

The Case 1b process descriptions, performance and cost results in this section were previously presented in Nexant's DE-FE0012066 IGCC report. They are reproduced here for the reader's ease of reference.

4.1 PROCESS OVERVIEW

The Case 1b IGCC power plant, like the Case 1a plant, is a Montana PRB coal-fired IGCC plant designed to generate enough hydrogen-rich fuel gas to fill two advanced GE 7F-turbines to generate a total of 430 MWe at the Montana site's elevation. To maximize power recovery, the power plant is equipped with HRSGs and ST. It is designed to capture CO_2 equivalent to 90% of the raw syngas' carbon content.

The IGCC plant operates as a base-loaded unit with an annual on-stream CF of 80%.

The Case 1b GTI R-GAS™ with RTI WDP IGCC has the following characteristics that differentiate it from the Case 2a Shell Reference IGCC:

- The GTI dry solids pump (DSP) feed system replaces the reference case's lockhopper system for feeeding dried coal to the gasifier. Nexant had previously evaluated the GTI DSP feed system in comparison to the Shell lockhopper feed system in a separate study (DE-FE0012062). The results from the earlier study were used to establish the performance and cost of the DSP feed system for this case.

- The GTI R-GAS™ gasifier replaces the Shell gasifier from Case 1a.

- Syngas leaving the R-GAS™ gasifier that has been quenched enters RTI's WDP for sulfur removal at above 700°F instead of going through a low temperature scrubber per Case 1a.

- After sulfur removal in the WDP, the treated syngas in Case 1b then enters RTI's AFWGS process. Unlike the Case 1a sour shift reactors, the Case 1b AFWGS process consists of fixed-bed reactors (using commercial high-temperature sweet water-gas shift catalyst) combined in such a manner as to significantly reduce the overall steam requirement and reactor capital cost while still meeting catalyst vendor steam to CO recommendations. These reactors operate at standard temperature for commercial high-temperature sweet water-gas shift processes, but at a higher inlet temperature than commercial sour shift processes. Commercial sweet water-gas shift catalysts cost about half as much as commercial sour water-gas shift catalysts.

- After the hydrogen-rich shifted syngas is cooled, it enters an AACRP unit for CO_2 capture. Unlike Selexol™, which is a physical solvent, activated methyldiethanolamine is a chemical solvent. As ~99.9% of the sulfur compounds have been removed upstream by the WDP process, the AACRP process only has to remove CO_2 and is less complicated than the two-stage Selexol™ process. However, the AACRP unit also captures ~99% of

any residual sulfur left in the syngas following WDP along with the CO_2, resulting in an overall system total sulfur reduction of >99.99% (sub-ppmv total sulfur in the final cleaned syngas).

- The DSRP replaces the Claus process in Case 1a. In the DSRP, sulfur leaving the WDP process in the form of SO_2 is reduced by a slipstream of shifted, hydrogen-rich syngas, forming elemental sulfur, H_2S and COS. The elemental sulfur is condensed while the remaining H_2S and COS are re-oxidized in the presence of air to SO_2. The SO_2 is then removed in a lime scrubber, forming gypsum ($CaSO_4.2H_2O$).

Figure 4-1
Case 1b: GTI R-GAS™ with RTI WDP IGCC - Simplified BFD

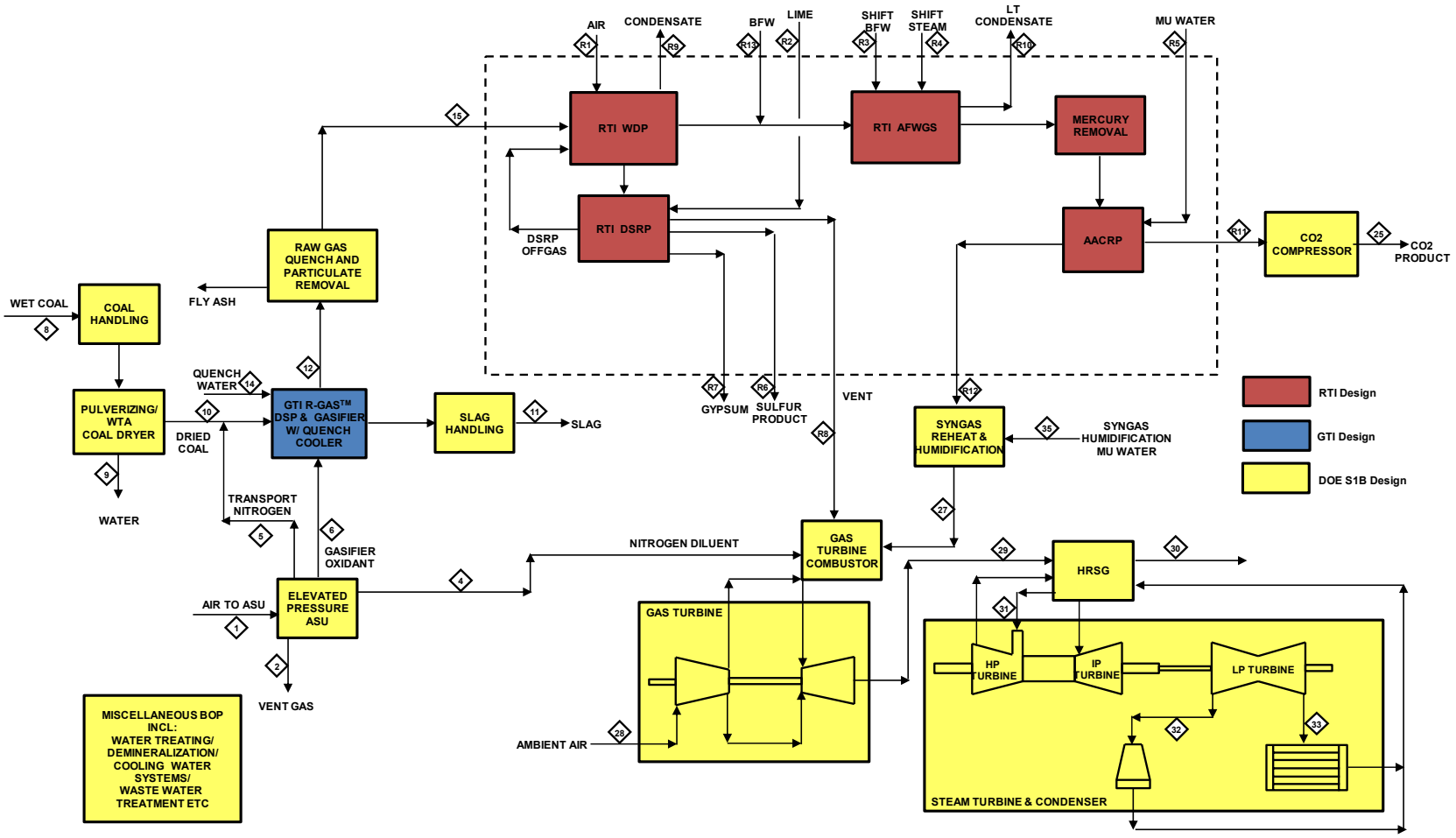

Table 4-1
Case 1b Stream Table

Description	Air to ASU	ASU Vent Gas	Nitrogen Diluent	Transport Nitrogen	Gasifier Oxidant	Wet Coal	Coal Moisture	Dried Coal	Slag	Hot Syngas	Quench Water	Cooled Syngas
Stream No.	1	2	4	5	6	8	9	10	11	12	14	15
V-L Mole Fraction												
Ar	0.0093	0.0165	0.0022	0.0023	0.0318	0	0	0	0	0.0087	0	0.0053
CH4	0	0	0	0	0	0	0	0	0	0.0087	0	0.0053
CO	0	0	0	0	0	0	0	0	0	0.6515	0	0.3954
CO2	0.0003	0.0047	0	0	0	0	0	0	0	0.0054	0	0.0033
COS	0	0	0.0	0	0	0	0	0	0	0.0004	0	0.0002
H2	0	0	0	0	0	0	0	0	0	0.2814	0	0.1708
H2O	0.0064	0.0988	0.0527	0	0	0	1.0000	0	0	0.0068	0.9981	0.3965
H2S	0	0	0	0	0	0	0	0	0	0.0033	0	0.0020
N2	0.7759	0.7586	0.9398	0.9921	0.0178	0	0	0	0	0.0323	0	0.0196
NH3	0	0	0	0	0	0	0	0	0	0.0009	0.0019	0.0013
O2	0.2081	0.1213	0.0051	0.0054	0.9504	0	0	0	0	0	0	0
SO2	0	0	0	0	0	0	0	0	0	0	0	0
S	0	0	0	0	0	0	0	0	0	0	0	0
HCl	0	0	0	0	0	0	0	0	0	0	0	0
Ca(OH)2	0	0	0	0	0	0	0	0	0	0	0	0
CaSO.2H2O	0	0	0	0	0	0	0	0	0	0	0	0
Total	1.0000	1.0000	1.0000	1.0000	1.0000	0	1.0000	0	0	1.0000	1.000	1.0000
V-L Flowrate, lbmol/hr	46199	2924	34692	858	9551	0	6569	0	0	35193	22797	57990
V-L Flowrate, lb/hr	1334910	81243	955052	24076	307353	0	118344	0	0	729703	410652	1140350
Solids Flow Rate, lb/hr	0	0	0	0	0	562689	0	444345	46071	0	0	0
Temperature, F	42	64	386	387	292		75			2347	290	760
Pressure, psia	13.0	16.4	384.0	815.0	740.0	13.0	48.0	14.8	615.0	615.0	115.0	605.0
Enthalpy, Btu/lb	-33.3	-463.2	-121.3	74.8	43.8		-6823			-741	-6599	-2830
Density, lb/cuft	0.070	0.089	1.159	2.473	2.961		62.273			0.420	57.620	0.910

Table 4-1 (cont'd)
Case 1b Stream Table

Description	WDP Air	Lime	Shift Steam	Shift BFW	AACRP MU Water	Sulfur Product	Gypsum	DSRP Vent	WDP Cond	Syngas Cool Cond	AACRP CO2 Out	Treated Syngas	Syngas Cool BFW
Stream No.	R1	R2	R3	R4	R5	R6	R7	R8	R9	R10	R11	R12	R13
V-L Mole Fraction													
Ar	0.0093	0	0	0	0	0	0	0.0141	0	0	0.0000	0.0088	0
CH4	0	0	0	0	0	0	0	0	0	0	0.0001	0.0087	0
CO	0	0	0	0	0	0	0	0	0	0	0.0001	0.0561	0
CO2	0.0003	0	0	0	0	0	0.0039	0.0195	0	0	0.9409	0.0010	0
COS	0	0	0	0	0	0	0	0	0	0	0	0	0
H2	0	0	0	0	0	0	0	0	0	0	0.0020	0.8853	0
H2O	0.0064	0.973695	1.0000	1.0000	1.0000	0	0.9759	0.0005	1.0000	0.9966	0.0569	0.0035	1.0000
H2S	0	0	0	0	0	0.0	0	0	0	0	0	0.0000	0
N2	0.7759	0	0	0	0	0	0.0003	0.9659	0	0	0.0000	0.0366	0
NH3	0	0	0	0	0	0	0	0	0	0	0	0	0
O2	0.2081	0	0	0	0	0	0	0	0	0	0	0	0
SO2	0	0	0	0	0	0	0	0	0	0	0	0	0
S	0	0	0	0	0	1.0000	0	0	0	0	0	0	0
HCl	0	0	0	0	0	0	0	0	0	0	0	0	0
Ca(OH)2	0	0.026305	0	0	0	0	0.0010	0	0	0	0	0	0
CaSO.2H2O	0	0	0	0	0	0	0.0189	0	0	0	0	0	0
Total	1.0000	1.0000	1.0000	1.0000	1.0000	1.0000	1.0000	1.0000	1.0000	1.0000	1.0000	1.0000	1.0000
V-L Flowrate, lbmol/hr	1138	39493	12541	6375	1293	105	1185	784	3	23854	22470	34541	2830
V-L Flowrate, lb/hr	32882	794001	225930	114842	23296	3369	24978	22322	57	429761	953647	172039	50983
Solids Flow Rate, lb/hr	0	0	0	0	0	0	0	0	0	0	0	0	0
Temperature, F	42	75	550	453	122	600	123	100	80	100	122	122	453
Pressure, psia	13.0	13.0	600.0	763.0	511.0	447.0	30	448.0	13.0	515.0	30.7	511.0	763.0
Enthalpy, Btu/lb	-33	-7	-5596	-12872	-6817	2685		-115	-6863	-6824	-3884	-637	-6436
Density, lb/cuft	0.070	0.005	1.135	47.278	60.524	113.093		2.143	61.590	61.182	0.212	0.401	47.278

Table 4-1 (cont'd)
Case 1b Stream Table

Description	CO2 Product	Reheat Syngas	Ambient Air to GT	GT Flue Gas	Stack Gas	HP SH Steam	Air-Cooled LP Cond	Water-Cooled LP Cond	BFW to HRSG	Syngas Humid MU H2O
Stream No.	25	27	28	29	30	31	32	33	34	35
V-L Mole Fraction										
Ar	0.0000	0.0086	0.0093	0.0089	0.0089	0	0	0	0	0
CH4	0.0001	0.0085	0	0	0	0	0	0	0	0
CO	0.0001	0.0549	0	0	0	0	0	0	0	0
CO2	0.9976	0.0010	0.0003	0.0085	0.0085	0	0	0	0	0
COS	0	0	0	0	0	0	0	0	0	0
H2	0.0021	0.8655	0	0	0	0	0	0	0	0
H2O	0	0.0258	0.0064	0.1281	0.1281	1.0000	1.0000	1.0000	1.0000	1.0000
H2S	0	0	0	0	0	0	0	0	0	0
N2	0.0000	0.0358	0.7759	0.7480	0.7480	0	0	0	0	0
NH3	0	0	0	0	0	0	0	0	0	0
O2	0	0	0.2081	0.1065	0.1065	0	0	0	0	0
SO2	0	0	0	0	0	0	0	0	0	0
S	0	0	0	0	0	0	0	0	0	0
HCl	0	0	0	0	0	0	0	0	0	0
Ca(OH)2	0	0	0	0	0	0	0	0	0	0
CaSO.2H2O	0	0	0	0	0	0	0	0	0	0
Total	1.0000	1.0000	1.0000	1.0000	1.0000	1.0000	1.0000	1.0000	1.0000	1.0000
V-L Flowrate, lbmol/hr	21192	35323	221242	275784	275784	56501	47147	47147	93001	2610
V-L Flowrate, lb/hr	930634	186202	6392720	7556290	7556290	1017890	849365	849365	1675430	47024
Solids Flow Rate, lb/hr	0	0	0	0	0	0	0	0	0	0
Temperature, F	162	207	42	1074	270	999	90	90	220	42
Pressure, psia	2214.7	511.0	12.9	13.5	13.0	1815.0	0.7	0.7	105.0	13.0
Enthalpy, Btu/lb		-913	-33	-268	-489	-5387	-6808	-6808	-6678	-6905
Density, lb/cuft	28.796	0.371	0.069	0.022	0.046	2.282	62.117	62.117	59.628	63.210

4.2 CASE 1b PROCESS DESCRIPTION

Case 1b was modeled by adapting the Case 1a model with gasifier and syngas cleanup process information provided by GTI and RTI. The system description below follows the BFD in Figure 4-1 and stream numbers referenced in the same figure. Table 4-1 provides the generated process data for the numbered streams in the BFD.

Coal Preparation and Drying

Same as Case 1a

GTI DSP Coal Feed System

Dried coal from the atmospheric storage silo enters the GTI DSPs via gravity flow. Three DSPs, each with a nominal capacity of 1,000 tons per day (tpd), are required to service each gasification train. The DSPs increase the pressure of the coal from atmospheric to 700 psia and subsequently discharge the coal continuously to a pressurized feed bin. The DSP also uses some nitrogen as an educting gas, which serves to evacuate and clean out the pump of solids during operation.

Coal is continuously withdrawn from the pressurized feed bin and conveyed by HP nitrogen via a single feed line to the gasifier. To maximize conversion efficiency of fuel to syngas in the gasifier, GTI uses its proprietary static splitter system.

Air Separation Unit

Same as Case 1a except no oxygen is routed to the SRU.

GTI R-GAS™ Gasifier

For the Case 1b IGCC, two R-GAS™ gasifier trains operating at 615 psia are needed to generate the required amount of syngas. Fuel feeds from the pressurized feed bin via the dense phase feed line, conveyed by HP nitrogen. To maximize conversion efficiency of fuel to syngas, GTI splits the feedstock from a single feed line into multiple injection ports via its proprietary static splitter system. The injection ports maximize mixing of coal and oxygen to initiate the gasification reaction.

The R-GAS™ gasifier is oriented in a vertical, down-firing position. The gasifier reaction is initiated with a torch burner, which is ignited at full gasifier pressure. The ignition torch runs on natural gas and oxygen.

The gasifier injector faceplate and the gasifier liner are water cooled to maintain the metal components at temperatures conducive to long life. The cooling water shall be clean enough (HP BFW quality) to prevent scale buildup or clogging of internal cooling passages.

The gasifier's raw syngas product is partially quenched from about 2,350°F to 760°F through the introduction of quench water spray. The quench water enters the gasifier through multiple hydraulic atomizing spray nozzles.

The solids are removed as slag and ash. Liquid slag is solidified in a water bath and removed via a lock hopper system. Ash carried over with the syngas is removed in a candle filter. The ash is also removed via a lock hopper system.

Syngas Scrubber

Unlike in Case 1a, the syngas scrubber is eliminated in Case 1b as the hot syngas at around 760°F enters the RTI WDP directly without requiring cooling.

Warm Syngas Cleanup Process

The Case 1b RTI advanced syngas cleanup process consists of the following system components: WDP, DSRP, AFWGS, and LTGC. AACRP is integrated with the RTI advanced syngas cleanup process for CO_2 removal. These are described in greater detail below.

Warm Gas Desulfurization Process

The WDP process, shown in Figure 4-2, uses transport-bed reactors that are similar to commercial FCC reactor designs. It consists of a pair of reactors: an adsorber and a regenerator. Hot syngas leaving the candle filter is routed to the WDP adsorber where it is contacted with a circulating ZnO-based attrition-resistant sorbent (developed and patented by RTI) to remove the sulfur bearing compounds, primarily H_2S and COS, from the syngas. The following reactions take place when the sorbent contacts the raw syngas:

$$H_2S + ZnO \rightarrow ZnS + H_2O$$
$$COS + ZnO \rightarrow ZnS + CO_2$$

Regenerated sorbent from the regenerator, along with recycled sorbent from the adsorber standpipe, contact the raw syngas, which enters the adsorber near the bottom of the unit. The treated, essentially sulfur-free syngas is separated from sorbent via a cyclone. Any remnant attrited or fine particulate solids entrained in the essentially sulfur-free syngas are removed in a filter. A majority of the sorbent separated by the cyclone is recycled to the adsorber via a standpipe, while a portion of the sorbent is fed to the regenerator.

Within the regenerator, oxidation of the ZnS-containing sorbent takes place, producing SO_2 and regenerating ZnO, per the following reaction:

$$ZnS + 3/2\ O_2 \rightarrow ZnO + SO_2$$

The regenerator uses air as the oxidant. Air is compressed in a multi-stage air compressor up to the regenerator operating pressure before it is fed into the regenerator. The oxidation reaction is exothermic, raising the temperature of the resulting mixture to about 1,300°F. The regenerator offgas containing SO_2 is heat exchanged with the compressed air stream before the offgas enters the DSRP. The regenerated sorbent is recycled back to the adsorber, where it adsorbs H_2S and COS again.

Figure 4-2
WDP Process Schematic

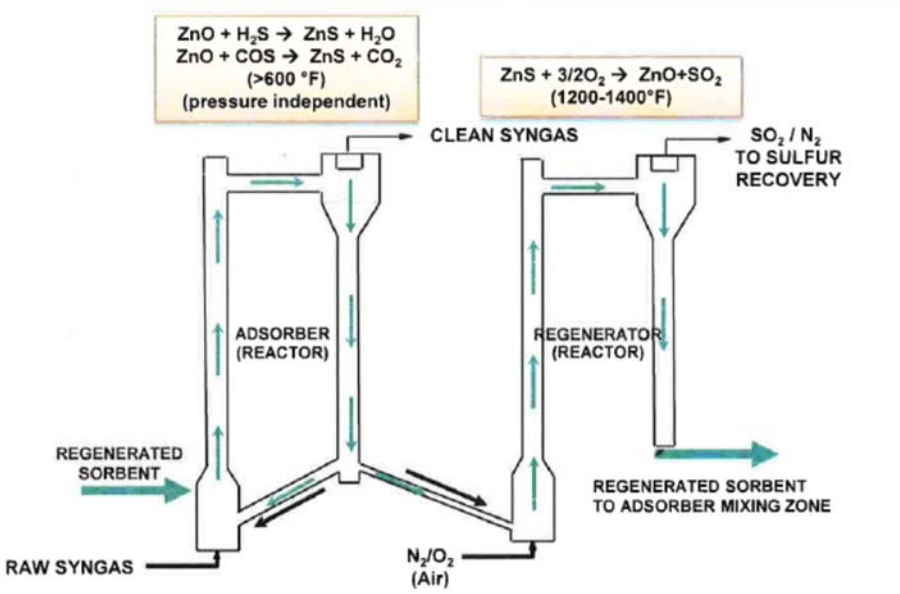

[Similar to Commercial FCC Reactor Designs]

Direct Sulfur Recovery Process

The offgas from the regenerator contains essentially SO_2, and N_2. It goes through a filter to remove any entrained solids and is cooled before it is sent into the fixed-bed DSRP reactor where SO_2 is reduced to elemental sulfur according to the following reactions:

$$SO_2 + 2\ CO \rightarrow 2\ CO_2 + S$$
$$SO_2 + 2\ H_2 \rightarrow 2\ H_2O + S$$

The reducing gas is provided by a hydrogen-rich syngas slip stream from the shift reactors. A slight excess of the reducing gas is used to ensure complete reduction of the SO_2. Some H_2S and COS are formed alongside the elemental sulfur. The product stream from the DSRP reactor is sent onto a sulfur condenser unit where the elemental sulfur is condensed and separated. Heat is recovered in the condenser by making low pressure steam.

The condenser overhead gas still contains some residual H_2S and COS. These are re-oxidized to SO_2 in a fixed-bed oxidation reactor containing a redox catalyst in the presence of compressed air, which functions as the oxidant. The compressed air is a slipstream drawn from the air compressor in the WDP section.

Finally, the SO_2-containing gas leaving the oxidation reactor is cooled and sent to a lime scrubber downstream. Lime, or calcium hydroxide ($Ca(OH)_2$), reacts with the SO_2 in the

presence of oxygen to form gypsum ($CaSO_4.2H_2O$) per the following reactions, which is akin to the Wet Flue Gas Desulfurization (WFGD) process used for scrubbing flue gas.

$$Ca(OH)_2 + SO_2 \rightarrow CaSO_3 + H_2O$$
$$CaSO_3 + 2\ H_2O + ½\ O_2 \rightarrow CaSO_4.2H_2O$$

The gypsum leaves the bottom of the scrubber as a byproduct of the IGCC. The treated, sulfur-free overhead gas is split into three portions. One portion is recycled to the DSRP to help control reactor temperature rise due to the exothermic heat from the DSRP reactions. The second portion is compressed and routed to the WDP process to be utilized as the stripping or fluidizing gas in the WDP adsorber and regenerator. The remainder is routed to the GT to increase its mass flow and produce more power.

Advanced Fixed-Bed Water-Gas Shift

To enable 90% carbon capture from the syngas, the gasifier syngas product must be converted to hydrogen-rich syngas. This is achieved by converting most of the syngas CO to hydrogen and CO_2 by reacting the CO with water over a catalyst bed. As the syngas has already been treated by WDP and contains low parts-per-million sulfur, high-temperature sweet water-gas shift catalyst, which does not need to be sulfur-tolerant is used.

RTI's AFWGS system is used to achieve an overall CO to CO_2 conversion of about 91%. Part of the steam for the WGS reaction is provided by the vaporized quench water in the GTI compact gasifier. In RTI's AFWGS process, a series of fixed-bed reactors using commercial high-temperature sweet shift catalyst are combined in a manner that enables a significant reduction in overall steam consumption and capital cost of the WGS process, while still meeting catalyst manufacturer's steam to CO recommendations and achieving the high CO conversion process requirement. Reducing the steam consumed in the WGS process results in higher overall thermal efficiency of the process making incorporation of carbon capture more attractive. RTI's AFWGS technology was proven as part of the 50-MWe pre-commercial demonstration of their WDP technology.

Low Temperature Gas Cooling and Mercury Removal

The shifted syngas goes through a series of heat exchangers to generate various levels of steam and preheat boiler feed water before it finally undergoes cooling by cooling water. The cooled syngas is sent to a knockout (KO) drum where the condensate is drained. Mercury is removed from the overhead syngas leaving the KO drum via the process described in Section 3.2.4.

Activated Amine CO_2 Removal Process

The AACRP is based on the activated methyldiethanolamine process, which is marketed commercially by companies such as BASF, Shell and UOP for the removal of acid gases like hydrogen sulfide (H_2S) and carbon dioxide (CO_2). The scrubbing agent is an aqueous alkaline amine solution. For this application, the CO_2-containing syngas is passed through a reactor that contains the alkaline amine scrubbing solution, where the bulk of the CO_2 removal takes place.

An acid-base reaction occurs where the CO_2 reacts with alkaline amine and is captured in solution.

To achieve the desired extent of CO_2 capture, and to ensure that the overhead gas meets the volatile organic compound (VOC) specifications, a lean amine absorber is used to treat the syngas leaving the main alkaline amine absorber. Water enters at the top of this absorber where it contacts and scrubs the CO_2-lean syngas. This serves to remove any entrained alkaline amine droplets in the syngas.

The rich, CO_2-loaded solution is sent to a regenerator to release the absorbed CO_2. The solution is first depressurized, flashing off some CO_2 in the process and helping to reduce the overall heat of CO_2 regeneration. The low-pressure solution is then sent to a thermal regenerator, where heat is applied to release the remaining CO_2. Regenerated alkaline amine solution is recycled to the absorber and used again.

It should be noted that as an alternative, hydraulic pressure recovery turbines (HPRTs) could be utilized to recover power from the depressurization of the rich amine. This reduces the total auxiliary power consumption, thus increasing net power output at the expense of greater capital cost. A trade-off study could be performed in the future to determine the effects of installing the HPRTs.

CO_2 Compression and Dehydration

CO_2 from the AACRP is generated at a single pressure of 30.7 psia. The CO_2 stream is compressed to a supercritical condition at 2,215 psia using a multiple-stage, intercooled compressor. During compression, the CO_2 stream is dehydrated to a dew point of -40°F using a thermal swing adsorptive dryer. After compression and dehydration the CO_2 product meets the sequestration specifications for injection into saline aquifers, as stated in the *CO_2 Impurity Design Parameters* QGESS document. This CO_2 product is transported to the plant fence line for sequestration OSBL.

Power Block

Clean syngas from the AACRP unit, at 122°F, is contacted with hot, BFW-grade water (220°F) that was used to cool the R-GAS™ gasifier. This serves to reheat the syngas and add mass to it via vaporization of the water, maximizing power generation from the GT. The fuel gas is then diluted with nitrogen and the SO_2 scrubber overhead gas to meet the heating value specifications before it enters the GT combustor. The exhaust gas exits the GT at a nominal 1,050°F and enters the HRSG where additional heat is recovered. The flue gas exits the HRSG at 270°F and is discharged through the plant stack. The steam raised in the HRSG is used to power an advanced commercially available steam turbine using a nominal 1,800 psig/1,000°F/1,000°F steam cycle. There is no air integration between the gas turbine and the ASU.

Balance of Plant

Balance of plant items are covered in Sections 3.2.9 through 3.2.12.

4.3 SPARING PHILOSOPHY

The sparing philosophy for Case 1b is as provided below. Single train designs were utilized throughout with exceptions where equipment had exceeded its maximum capacity limit or dimensions for acceptable transportation to the site required an additional train. The design has:

- Two ASU trains (2 x 50%)
- Two trains of coal drying (2 x 50%)
- Two trains of gasification, including dry feed system, R-GAS™ gasifier, syngas quench cooler, cyclone and candle filter (2 x 50%)
- One WDP train (1 x 100%)
- One DSRP train (1 x 100%)
- One AFWGS and LTGC train (1 x 100%)
- One AACRP train (3 x 33% for the rich amine absorber and LP flash drum, 1 x 100% for the rest of the process)
- Two gas turbines/HRSG tandems (2 x 50%)
- One steam turbine (1 x 100%)

4.4 PERFORMANCE RESULTS

The Nexant-modeled Case 1b IGCC plant with CO_2 capture consumes 6,752 tpd of PRB coal at the Montana site to produce a net output of 463 MWe at a net plant efficiency of 32.75% on a HHV basis. Overall performance for the Case 1b IGCC plant is summarized in Table 4-2, which includes auxiliary power requirements. Loads that are unique to the GTI and RTI processes are shown in bold and italicized.

Table 4-2
Case 1b Plant Performance Summary

POWER SUMMARY (Gross Power at Generator Terminals, kWe)	**Case 1b**
Gas Turbine Power	429,904
Steam Turbine Power	211,301
TOTAL POWER, kWe	**641,206**
AUXILIARY LOAD SUMMARY, kWe	
Coal Handling	490
Coal Milling	2,622
Slag Handling	540
WTA Coal Dryer Compressor	8,998
WTA Coal Dryer Auxiliaries	595
DSP	***1,803***
Air Separation Unit Auxiliaries	851
Air Separation Unit Main Air Compressor	54,067
Oxygen Compressor	7,630
Nitrogen Compressors	26,624
CO_2 Compressor	32,295
Boiler Feedwater Pumps	4,234
Condensate Pump	233
Quench Water Pump	616
Gasifier Cooling BFW Circulating Pump	***3,723***
Circulating Water Pump	2,752
Ground Water Pumps	322
Cooling Tower Fans	1,794
Air Cooled Condenser Fans	2,715
AACRP	***16,970***
Gas Turbine Auxiliaries	998
Steam Turbine Auxiliaries	91
RTI WDP	***1,983***
DSRP	***283***
Miscellaneous Balance of Plant	3,000
Transformer Losses	2,465
TOTAL AUXILIARIES, kWe	**178,691**
NET POWER, kWe	**462,518**
Net Plant Efficiency, % (HHV)	32.75%
Net Plant Heat Rate, Btu/kWh	10,419
CONDENSER COOLING DUTY, MMBtu/hr	**1,147**
CONSUMABLES	
As-Received Coal Feed, lb/hr	562,689
Thermal Input, kWt	1,412,271
Raw Water Withdrawal, gpm	3,532
Raw Water Consumption, gpm	2,777

Table 4-3 shows the carbon balance for the Case 1b IGCC plant. The carbon capture efficiency is defined as the amount of carbon in the CO_2 product stream relative to the amount of carbon in the coal feed less the carbon contained in the slag. For Case 1b, the carbon capture efficiency is 90.1%.

Table 4-3
Case 1b Overall Carbon Balance

Overall Carbon Balance, lb/hr	In	Out
Coal Feed	281,727	
ASU Air	166	
Air to WDP	4	
Air to Gas Turbine	797	
ASU Vent		166
LTGC Condensate to Cooling Tower		278
Carbon in Slag		0
Stack Gas		28,278
CO_2 Product		253,972
Convergence Tolerance		
Total	**282,694**	**282,694**

Table 4-4 shows the sulfur balance for the plant. Sulfur input comes solely from the sulfur in the coal. Sulfur output includes the elemental sulfur condensed in the DSRP, gypsum from the lime scrubber, sulfur emitted in the stack gas, and the trace amount that is in the CO_2 product. Sulfur in the slag is considered negligible.

Table 4-4
Case 1b Overall Sulfur Balance

Overall Sulfur Balance, lb/hr	In	Out
Coal Feed	4,094	
Gypsum		713
Sulfur Product		3,369
Stack Gas		0
CO_2 Product		12
Convergence Tolerance		0
Total	**4,094**	**4,094**

Table 4-5 shows the overall water balance for the Case 1b IGCC plant.

Table 4-5
Case 1b Overall Water Balance

Water Use, gpm	Raw Water Withdrawal	Process Effluent Production for Internal Consumption	Internal Consumption	Process Water Discharge
WTA Coal Drying	0	(236)	0	0
Slag Handling	0	0	119	(119)
Quench Cooler	38	0	782	0
Syngas Cooling Knockout	0	(856)	0	0
Syngas Humidification	94	0	0	0
Steam Cycle Makeup	842	0	0	0
Steam Cycle Blowdown	0	(11)	0	0
CO_2 Compression Knockout	0	(46)	0	0
Cooling Tower Makeup	2,558	0	248	0
Cooling Tower Blowdown	0	0	0	(636)
Total	3,532	(1,150)	1,150	(755)

4.5 EQUIPMENT LIST

The equipment list for the GTI/RTI processes that differ from the reference Shell Gasifier with Selexol™ AGR IGCC case are shown in Table 4-6 below.

Table 4-6
Case 1b Equipment List

ACCOUNT 2 COAL PREPARATION AND FEED
Subaccount 2.3 Dry Coal Injection System

Equipment No.	Description	Type	Design Condition	Operating Qty	Spares
1	GTI DSP Feed System	GTI Proprietary dry solids pump with coal feed bins	1,000 tpd	6 DSPs	0

ACCOUNT 4 GASIFIER, ASU AND ACCESSORIES
Subaccount 4.1 Gasifier & Auxiliaries

Equipment No.	Description	Type	Design Condition	Operating Qty	Spares
1	R-GAS™ Gasifier	Vertical, down-fired gasifier with multiple fuel injection ports and including water quench	3,000 tpd	2	0
2	Circulating HP BFW Pump	Centrifugal	Proprietary	2	2
3	Makeup HP BFW Pump	Centrifugal	50 gpm @ 470 ft H_2O	2	2
4	Ash Filters	Candle	10,500 acfm	2	0
5	Syngas Cyclone	High efficiency	600,000 lb/hr	2	0

ACCOUNT 5A SYNGAS CLEANUP
Subaccount 5A.1 RTI WDP

Equipment No.	Description	Type	Design Condition	Operating Qty	Spares
1	WDP Adsorption Reactor	Proprietary Transport Reactor	22,300 acfm	1	0
2	WDP Regeneration Reactor	Proprietary Transport Reactor	625 acfm	1	0
3	Adsorption Cyclone Separator	Cyclone Separator	22,300 acfm	1	0
4	Stripper Cyclone Separator	Cyclone Separator	625 acfm	1	0
5	Adsorber Filter	Candle Filter	22,300 acfm	1	0
6	Regenerator Offgas Filter	Candle Filter	625 acfm	1	0
7	Adsorber Filter Lock Hopper + Fines Bin		Proprietary	1	0
8	Regenerator Filter Lock Hopper + Fines Bin		Proprietary	1	0

9	Sorbent Feeder Package (incl Hopper)		Proprietary	1	0
10	Regenerator Air Heat Exchanger	Shell and Tube	27,000 lb/hr	1	0
11	Recycle Syngas Compressor	Centrifugal	43 acfm @ 514 psia	1	0
12	Regenerator Air Compressor	Centrifugal	7,850 acfm @ 13 psia	1	0
13	DSRP Offgas Compressor	Centrifugal	90 acfm @ 511 psia	1	0
14	Syngas Recycle Compressor	Centrifugal	5 acfm @ 591 psia	1	0

ACCOUNT 5A SYNGAS CLEANUP
Subaccount 5A.2 RTI DSRP

Equipment No.	Description	Type	Design Condition	Operating Qty	Spares
1	DSRP Fixed Bed Reactor	Packed Bed Reactor	119,000 lb/hr	1	0
2	Tail Gas Oxidation Reactor	Packed Bed Reactor	120,000 lb/hr	1	0
3	DSRP Feed Gas Preheater	Shell and Tube	4.8 MMBtu/hr	1	0
4	Sulfur Condenser	Shell and Tube	3,400 lb/hr sulfur	1	0
5	Oxidation Reactor Gas Preheater	Shell and Tube	2.8 MMBtu/hr	1	0
6	Liquid Sulfur Separator	Pressure Vessel	3,400 lb/hr sulfur	1	0
7	Recycle Gas Compressor	Centrifugal	850 acfm @ 448 psia	1	0
8	Pulsing Gas Compressor	Centrifugal	Average 10 acfm @ 511 psia	1	0
9	Scrubber Recycle Cooler	Shell and Tube	18.2 MMBtu/hr	1	0
10	SO_2 Scrubber	Tray Column	1,430 lb/hr SO_2	1	0
11	Recycle Pump	Centrifugal	1,500 gpm @ 150 ft H_2O	1	0
12	Lime Slurry Pump	Centrifugal	50 gpm @ 950 ft H_2O	1	0
13	Gypsum Filter	Bag Filter	1,200 acfm	1	0
14	Lime Makeup Drum	Pressure Vessel	17,000 lb/hr	1	0

ACCOUNT 5A SYNGAS CLEANUP
Subaccount 5A.4 Shift Reactors

Equipment No.	Description	Type	Design Condition	Operating Qty	Spares
1	AFWGS Reactor 1	Packed Bed Reactor	Proprietary	1	0
2	AFWGS Reactor 2	Packed Bed Reactor	Proprietary	1	0
3	AFWGS Reactor 3	Packed Bed Reactor	Proprietary	1	0

ACCOUNT 5B CO_2 REMOVAL & COMPRESSION
Subaccount 5B.1 AACRP

Equipment No.	Description	Type	Design Condition	Operating Qty	Spares
1	Rich Amine Absorber	Packed Column	217,000 cuft/hr syngas	3	0
2	Lean Amine Absorber	Packed Column w/ Wash Trays	495,000 cuft/hr syngas	1	0
3	Amine Stripper	Packed Column	1,709,000 cuft/hr gas flow	1	0
4	LP Flash	Packed Column	1,785,000 cuft/hr gas flow	3	0
5	LP Flash Reflux Drum	Reflux Drum	1,513,000 cuft/hr CO_2	3	0
6	Lean/Rich Amine Exchanger	Shell and Tube	520,000 lb/hr	6	0
7	Amine Stripper Reboiler	Shell and Tube	560,000 lb/hr amine	6	0
8	Lean Amine Cooler	Shell and Tube	1,734,000 lb/hr amine	2	0
9	Flash Overhead Condenser	Shell and Tube	114,000 lb/hr CO_2	3	0
10	MP Flash Condenser	Shell and Tube	5,230 lb/hr amine	1	0
11	Lean Amine Pump	Centrifugal	2,050 gpm	3	0
12	Semi-lean Amine Pump	Centrifugal	13,430 gpm	3	1
13	Rich Amine Pump	Centrifugal	13,100 gpm	1	0
14	Flash Reflux Pump	Centrifugal	51 gpm	3	0
15	Amine Stripper Bottoms Pump	Centrifugal	6,035 gpm	1	1
16	Filter Pump	Centrifugal	670 gpm	1	0
17	MP Flash Recycle KO Drum	KO Drum	15,650 cuft/hr	1	0
18	MP Flash Drum	Reflux Drum	126,019 cuft/hr	1	0
19	Recycle Gas Compressor	Centrifugal	261 acfm @ 195 psia	1	0
20	Amine Tank	Vertical Vessel	14,700 gallons	1	0
21	Filter Package	Filter Package	670 gpm	1	1
22	Filter Package Vessel	Vessel	3,350 gallons	1	1

4.6 CAPITAL COST

Table 4-7 shows the cost breakdown of the Case 1b GTI R-GAS™ with RTI WDP IGCC, expressed in a consistent format with the code of accounts in the NETL Report 1399. The accounts/subaccounts of interest for this study are:

- 2.3 Dry Coal Injection System,
- 4 Gasifier & Accessories,
- 5A Gas Cleanup & Piping and
- 5B CO_2 Removal and Compression.

These are shown with more detail to include the various subaccounts and provide more clarity to the major cost differences among the cases.

Table 4-8 shows the calculation and addition of owner's costs to determine the TOC, used to calculate COE.

The estimated TOC, in 2011 dollars, of the Case 1b GTI R-GAS™ with RTI WDP IGCC is $4,428/kW.

Table 4-7
Case 1b Total Plant Cost Summary

Case 1b: GTI R-GAS™ with RTI WDP/AFWGS IGCC		Coal Feed, lb/hr	562,689					Plant Size	462.5 MW, net			
Low Rank Western Coal Baseline Study	PRB	Coal HHV, Btu/lb	8564					Net Efficiency	32.75%			

Acct No.	Item/Description	Equipment Cost	Material Cost	Labor Direct	Labor Indirect	Sales Tax	Bare Erected Cost $	Eng'g CM H.O & Fee	Contingencies Process	Contingencies Project	TOTAL PLANT COST $	TOTAL PLANT COST $/kW
1	COAL & SORBENT HANDLING	**$18,960**	**$3,324**	**$14,503**	**$0**	**$0**	**$36,787**	**$3,338**	**$0**	**$8,024**	**$48,149**	**$104**
2	COAL & SORBENT PREP & FEED											
2.3	Dry Coal Injection System	$53,924	$0	$35,407	$0	$0	$89,331	$7,694	$17,866	$22,978	$137,870	$298
2.x	Other Coal & Sorbent Prep & Feed Systems	$60,786	$10,592	$16,594	$0	$0	$87,972	$7,685	$0	$19,131	$114,788	$248
	SUBTOTAL 2.	**$114,710**	**$10,592**	**$52,001**	**$0**	**$0**	**$177,304**	**$15,380**	**$17,866**	**$42,109**	**$252,659**	**$546**
3	FEEDWATER & MISC BOP SYSTEMS	**$9,563**	**$7,520**	**$9,267**	**$0**	**$0**	**$26,350**	**$2,485**	**$0**	**$6,636**	**$35,472**	**$77**
4	GASIFIER & ACCESSORIES											
4.1	Gasifier, Syngas Cooler & Auxiliaries (GTI)	$37,796	$18,898	$57,067	$0	$0	$113,761	$10,163	$28,440	$22,855	$175,218	$379
4.3	ASU/Oxidant Compression	$197,746	$0	$0	$0	$0	$197,746	$19,167	$0	$21,691	$238,605	$516
4.6	Flare Stack System	$0	$1,620	$655	$0	$0	$2,274	$218	$0	$498	$2,991	$6
4.9	Gasification Foundations	$0	$10,066	$6,003	$0	$0	$16,069	$1,471	$0	$4,385	$21,925	$47
	SUBTOTAL 4.	**$235,542**	**$30,583**	**$63,725**	**$0**	**$0**	**$329,850**	**$31,020**	**$28,440**	**$49,429**	**$438,739**	**$949**
5A	GAS CLEANUP & PIPING											
5A.1	RTI WDP	$23,171	$0	$27,805	$0	$0	$50,977	$4,930	$10,195	$13,220	$79,322	$172
5A.2	RTI DSRP	$6,324	$0	$7,000	$0	$0	$13,324	$1,294	$2,665	$3,457	$20,740	$45
5A.3	Mercury Removal	$3,273	$0	$2,474	$0	$0	$5,747	$555	$287	$1,317	$7,905	$17
5A.4a	LT Heat Recovery, FG Saturation & RTI AFWGS Reactors	$26,731	$0	$23,556	$0	$0	$50,287	$4,899	$0	$11,037	$66,223	$143
5A.6	Blow back Gas Systems	$2,620	$441	$248	$0	$0	$3,309	$314	$0	$724	$4,347	$9
5A.7	Fuel Gas Piping	$0	$858	$561	$0	$0	$1,419	$132	$0	$311	$1,862	$4
5A.9	Gas Clean Up Foundations	incl w / WDP	$0	incl w / WDP	$0	$0	$0	$0	$0	$0	$0	$0
	SUBTOTAL 5.	**$62,119**	**$1,299**	**$61,644**	**$0**	**$0**	**$125,063**	**$12,124**	**$13,147**	**$30,066**	**$180,400**	**$390**
5B	CO2 REMOVAL & COMPRESSION											
5B.1	RTI AACRP	$24,855	$0	$20,878	$0	$0	$45,733	$4,423	$9,147	$11,860	$71,163	$154
5B.2	CO2 Compression & Drying	$38,555	$0	$12,879	$0	$0	$51,434	$4,952	$0	$11,277	$67,663	$146
	SUBTOTAL 5B.	**$63,410**	**$0**	**$33,757**	**$0**	**$0**	**$97,167**	**$9,375**	**$9,147**	**$23,137**	**$138,826**	**$300**
6	COMBUSTION TURBINE/ACCESSORIES	**$111,211**	**$923**	**$8,948**	**$0**	**$0**	**$121,083**	**$11,476**	**$11,909**	**$14,882**	**$159,350**	**$345**
7	HRSG, DUCTING & STACK	**$32,165**	**$2,964**	**$9,336**	**$0**	**$0**	**$44,465**	**$4,202**	**$0**	**$5,621**	**$54,288**	**$117**
8	STEAM TURBINE GENERATOR	**$74,757**	**$944**	**$19,221**	**$0**	**$0**	**$94,923**	**$9,073**	**$0**	**$17,613**	**$121,609**	**$263**
9	COOLING WATER SYSTEM	**$5,467**	**$7,313**	**$6,726**	**$0**	**$0**	**$19,506**	**$1,813**	**$0**	**$4,573**	**$25,892**	**$56**
10	ASH/SPENT SORBENT HANDLING SYS	**$22,268**	**$1,715**	**$10,966**	**$0**	**$0**	**$34,949**	**$3,354**	**$0**	**$4,185**	**$42,488**	**$92**
11	ACCESSORY ELECTRIC PLANT	**$35,230**	**$15,501**	**$28,227**	**$0**	**$0**	**$78,959**	**$6,793**	**$0**	**$16,415**	**$102,168**	**$221**
12	INSTRUMENTATION & CONTROL	**$12,771**	**$2,589**	**$8,397**	**$0**	**$0**	**$23,757**	**$2,152**	**$1,187**	**$4,546**	**$31,641**	**$68**
13	IMPROVEMENTS TO SITE	**$3,682**	**$2,170**	**$9,662**	**$0**	**$0**	**$15,514**	**$1,532**	**$0**	**$5,114**	**$22,160**	**$48**
14	BUILDINGS & STRUCTURES	**$0**	**$7,560**	**$8,588**	**$0**	**$0**	**$16,148**	**$1,469**	**$0**	**$2,897**	**$20,515**	**$44**
	CALCULATED TOTAL COST	**$801,857**	**$94,999**	**$344,968**	**$0**	**$0**	**$1,241,824**	**$115,587**	**$81,696**	**$235,248**	**$1,674,355**	**$3,620**

Table 4-8
Case 1b Total Overnight Cost Summary

Owner's Costs	$ x $1,000	$/kW
Preproduction Costs		
6 months All Labor	$14,652	$32
1 Month Maintenance Materials	$3,136	$7
1 Month Non-Fuel Consumables	$528	$1
1 Month Waste Disposal	$425	$1
25% of 1 Months Fuel Cost at 100% CF	$1,008	$2
2% of TPC	$33,487	$72
Total	**$53,236**	**$115**
Inventory Capital		
60 day supply of fuel at 100% CF	$7,953	$17
60 day supply of non-fuel consumables at 100% CF	$530	$1
0.5% of TPC (spare parts)	$8,372	$18
Total	**$16,855**	**$36**
Initial Cost for Catalyst and Chemicals	**$6,148**	**$13**
Land	**$900**	**$2**
Other Owner's Cost	**$251,153**	**$543**
Financing Costs	**$45,208**	**$98**
Total Owner's Costs	**$373,500**	**$808**
Total Overnight Costs (TOC)	**$2,047,853**	**$4,428**

4.7 OPERATING COSTS

Table 4-9 shows the operating cost breakdown for the Case 1b IGCC.

Table 4-9
Case 1b Initial and Annual O&M Costs

INITIAL & ANNUAL O&M EXPENSES			
Case:	Case 1b - GTI R-GAS™ w/ RTI WDP/AFWGS IGCC		
Plant Size (MWe)	**463**	**Heat Rate (Btu/kWh):**	10,419
Primary/Secondary Fuel:	**PRB**	**Fuel Cost ($/MMBtu):**	
Design/Construction	5 years	**Book Life (yrs):**	20
TPC (Plant Cost) Year	June 2011	**TPI Year:**	2016
Capacity Factor (%)	80	**CO2 Captured (TPD)**	11165

OPERATING & MAINTENANCE LABOR

Operating Labor

Operating Labor Rate (base):	$39.70	$/hr
Operating Labor Burden:	30.00	% of base
Labor Overhead Charge	25.00	% of labor

Operating Labor Requirements per Shift	units/mod	Total Plant
Skilled Operator	2.0	2.0
Operator	10.0	10.0
Foreman	1.0	1.0
Lab Tech's etc	3.0	3.0
TOTAL Operating Jobs	16.0	16.0

	Annual Cost $	Annual Unit Cost $/kW-net
Annual Operating Labor Cost	$7,233,658	
Maintenance Labor Cost	$16,209,414	
Administration & Support Labor	$5,860,768	
Property Taxes and Insurance	$33,487,065	
TOTAL FIXED OPERATING COSTS	**$62,790,904**	

VARIABLE OPERATING COSTS

						$/kWh-net
Maintenance Material Cost					**$30,103,197**	
Consumables	Consumption Initial	Consumption /Day	Unit Cost	Initial Fill Cost		
Water(/1000 gallons)	0	2,543	1.67	**$0**	**$1,243,123**	
Chemicals						
MU & WT Chem (lb)	0	15152	0.27	$0	$1,185,087	
Carbon (Hg Removal) (lb)	111993	154	1.63	$182,549	$73,128	
RTI WDP Sorbent (lb)	Proprietary	Proprietary	Proprietary	$2,459,501	$1,541,514	
RTI DSRP Catalyst (lb)	22000	12.1	11.15	$245,300	$39,248	
DSRP Oxidation/Reduction Catalyst (lb)	22000	12.1	1.56	$34,320	$5,491	
Lime (lb)	0	41904	0.0382	$0	$467,550	
AFWGS Catalyst (lb)	5793	3.2	394.38	$2,284,823	$365,572	
Activated Amine (lb)	336647	184	2.80	$941,894	$150,703	
Subtotal Chemicals				**$6,148,386**	**$3,828,293**	
Other						
Supplemental Fuel (MMBtu)	0	0	0.00	$0	$0	
Gases, N2 etc.(/100scf)	0	0	0.00	$0	$0	
LP Steam (/1000 lbs)	0	0	0.00	$0	$0	
Subtotal Other				**$0**	**$0**	
Waste Disposal:						
Spent Mercury Catalyst (lb)	0	154	0.65	$0	$29,161	
Flyash (ton)	0	0	0.00	$0	$0	
Slag (ton)	0	553	25.11	$0	$4,053,550	
Subtotal Waste Disposal				**$0**	**$4,082,711**	
By-products & Emissions						
Sulfur (tons)	0	40	0	0	0	
Gypsum (tons)	0	300	0	0	0	
Subtotal By-Products				**$0**	**$0**	
TOTAL VARIABLE OPERATING COSTS				**$6,148,386**	**$39,257,324**	
Fuel (tons)	**0**	**6752**	**19.63**	**$0**	**$38,703,730**	

4.8 COST OF ELECTRICITY

Table 4-10 shows a summary of the power output, CAPEX, OPEX, COE and cost of CO_2 capture for the Case 1b GTI R-GAS™ with RTI WDP IGCC. The estimated COE for the Case 1b IGCC is 122.0 mills/kWh

Table 4-10
Plant Performance and Economic Summary

Case	Case 1b
CAPEX, $MM	
Total Installed Cost (TIC)	$1,242
Total Plant Cost (TPC)	$1,674
Total Overnight Cost (TOC)	$2,048
OPEX, $MM/yr (100% Capacity Factor Basis)	
Fixed Operating Cost (OC_{fix})	$62.8
Variable Operating Cost, less Fuel (OC_{var})	$49.1
Fuel (OC_{fuel})	$48.4
Total OPEX	$160.2
Power Production, MWe	
Gas Turbine	429.9
Steam Turbine	211.3
Auxiliary Power Consumption	178.7
Net Power Output	462.5
Power Generated, MWh/yr (MWH)	4,051,626
SO_2 Emissions (lb/MWh_{gross})	0.0013
SO_2 Emissions (lb/MMBtu)	0.0002
COE, excl CO_2 TS&M, mills/kWh	**122.0**
COE, incl CO_2 TS&M, mills/kWh	**142.0**
Cost of CO_2 Avoided excl CO2 TS&M, $/ton CO_2	**51.0**
Cost of CO_2 Avoided incl CO2 TS&M, $/ton CO_2	**75.1**

Section 5 Case 1e: GTI R-GAS™ with RTI WDP and ATWGS IGCC

5.1 PROCESS OVERVIEW

The IGCC case of interest in this study is the Case 1e IGCC power plant. Like the previous two cases, Case 1e is a Montana PRB coal-fired IGCC plant designed to generate hydrogen-rich syngas to fill two advanced GE 7F-turbines for a total gas turbine power generation of 430 MWe at the Montana site's elevation. The IGCC power plant is equipped with HRSGs and ST to maximize power recovery. It is designed to capture CO_2 equivalent to 90% of the raw syngas' carbon content. The IGCC plant operates as a base-loaded unit with an annual on-stream CF of 80%.

The Case 1e IGCC is similar to the Case 1b GTI R-GAS™ with RTI WDP IGCC, with the following differentiating characteristic:

- The RTI ATWGS process replaces RTI's AFWGS process. The ATWGS process is based on a transport reactor, solids cooler, and RTI proprietary fluidized-bed high-temperature sweet water-gas shift catalyst.

The coal feed rate is the same as Case 1b since both utilize the R-GAS™ gasification process operating under the same conditions, hence same cold gas efficiency, to generate enough syngas for firing in the two GE F-turbines.

5.2 CASE 1e PROCESS DESCRIPTION

The system description below for Case 1e follows the BFD in Figure 5-1 and stream numbers reference the same figure. Figure 5-1 provides the Nexant generated process data for the numbered streams in the BFD.

Coal Preparation and Drying

Same as Case 1a

GTI DSP Coal Feed System

Same as Case 1b

Air Separation Unit

Same as Case 1a

GTI R-GAS™ Gasifier

Same as Case 1b

Warm Syngas Cleanup Process

The Case 1e RTI advanced syngas cleanup process consists of the following major system components: WDP, DSRP, ATWGS, and LTGC. AACRP is integrated with the RTI advanced syngas cleanup process for CO_2 removal.

Warm Gas Desulfurization Process

Same as Case 1b

Direct Sulfur Recovery Process

Same as Case 1b

Advanced Transport Water-Gas Shift

Case 1e uses RTI's ATWGS reactor, which replaces RTI's AFWGS process in Case 1b. The transport reactor design used in the ATWGS process leverages commercial expertise associated with commercial fluidized catalytic cracker (FCC) technologies. A proprietary fluidized-bed high-temperature sweet shift catalyst has been developed and optimized leveraging RTI's expertise in developing attrition-resistant fluid bed materials.

In RTI's ATWGS process, additional temperature control for the exothermic WGS reaction is provided by the normal movement of the fluidized-bed catalyst within the system and a solids cooler. Additional process benefits of this novel approach to temperature control are the ability to achieve higher equilibrium conversion at lower operating temperature and additional high quality steam generation from the solids cooler. RTI has completed testing of this proprietary fluidized-bed catalyst in a small pilot plant system with simulated syngas mixtures.

Low Temperature Gas Cooling and Mercury Removal

Same as Case 1b

Activated Amine CO_2 Removal Process

Same as Case 1b

CO_2 Compression and Dehydration

Same as Case 1a

Claus Unit

Same as Case 1a

Power Block

Same as Case 1b

Balance of Plant

Balance of plant items are covered in Sections 3.2.9 through 3.2.12.

Figure 5-1
Case 1e: GTI R-GAS™ with RTI WDP/RTI ATWGS IGCC Plant - Simplified BFD

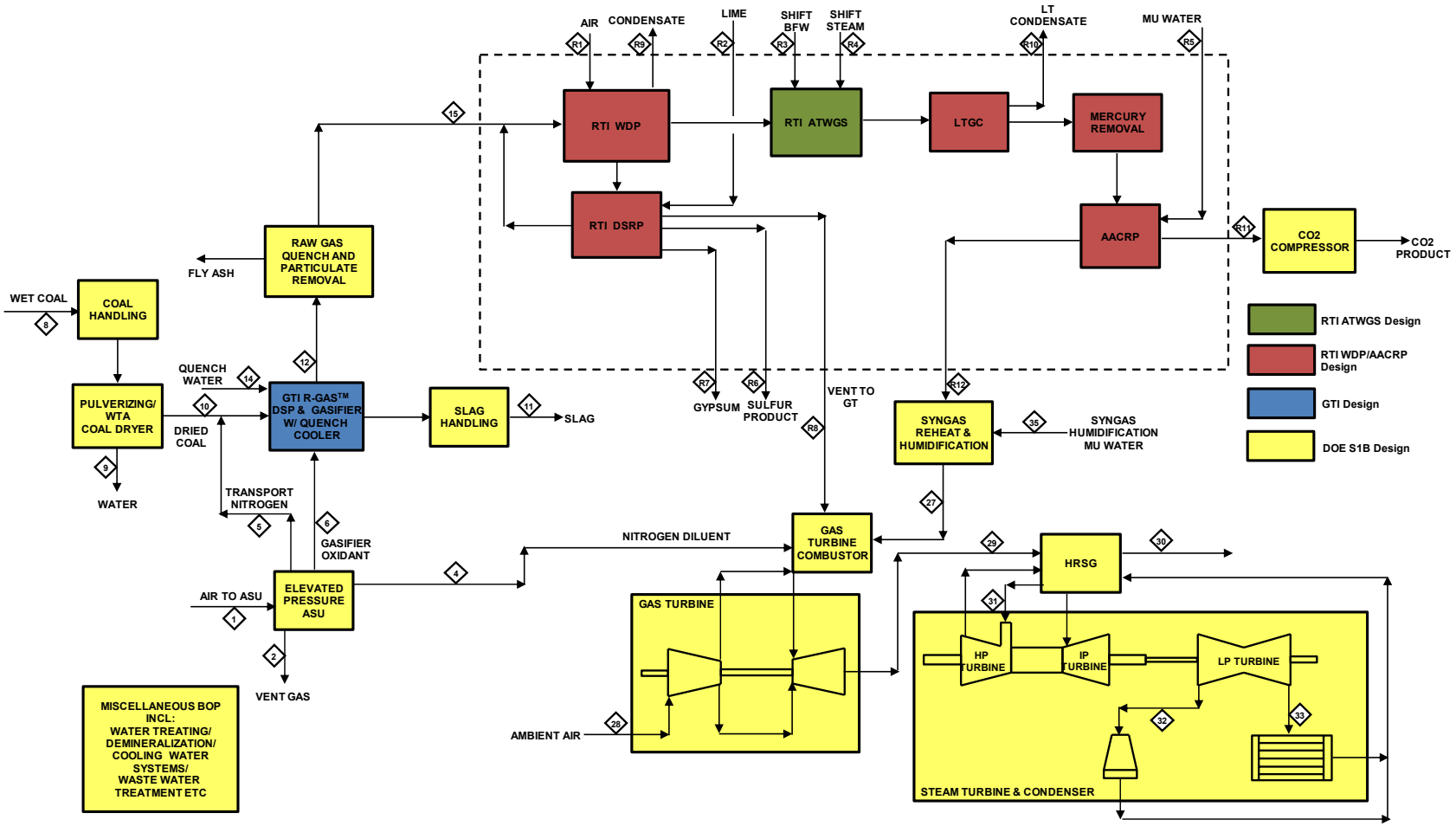

Table 5-1
Case 1e Stream Table

Description	Air to ASU	ASU Vent Gas	Nitrogen Diluent	Transport Nitrogen	Gasifier Oxidant	Wet Coal	Coal Moisture	Dried Coal	Slag	Hot Syngas	Recycle Syngas	Quench Water	Cooled Syngas
Stream No.	1	2	4	5	6	8	9	10	11	12	13	14	15
V-L Mole Fraction													
Ar	0.0093	0.0165	0.0022	0.0023	0.0318	0	0	0	0	0.0087	0.0053	0	0.0053
CH4	0	0	0	0	0	0	0	0	0	0.0087	0.0053	0	0.0053
CO	0	0	0	0	0	0	0	0	0	0.6515	0.3954	0	0.3954
CO2	0.0003	0.0047	0	0	0	0	0	0	0	0.0054	0.0033	0	0.0033
COS	0	0	2.53E-09	0	0	0	0	0	0	0.0004	0.0002	0	0.0002
H2	0	0	0	0	0	0	0	0	0	0.2814	0.1708	0	0.1708
H2O	0.0064	0.0988	0.053	0	0	0	1.0000	0	0	0.0068	0.3965	0.9981	0.3965
H2S	0	0	0	0	0	0	0	0	0	0.0033	0.0020	0	0.0020
N2	0.7759	0.7586	0.9398	0.9921	0.0178	0	0	0	0	0.0323	0.0196	0	0.0196
NH3	0	0	0	0	0	0	0	0	0	0.0009	0.0013	0.0019	0.0013
O2	0.2081	0.1213	0.0051	0.0054	0.9504	0	0	0	0	0	0	0	0
SO2	0	0	0	0	0	0	0	0	0	0	0	0	0
S	0	0	0	0	0	0	0	0	0	0	0	0	0
HCl	0	0	0	0	0	0	0	0	0	0	0	0	0
Ca(OH)2	0	0	0	0	0	0	0	0	0	0	0	0	0
CaSO.2H2O	0	0	0	0	0	0	0	0	0	0	0	0	0
Total	1.0000	1.0000	1.0000	1.0000	1.0000	0.0000	1.0000	0.0000	0.0000	1.0000	1.0000	1.0000	1.0000
V-L Flowrate, lbmol/hr	46199	2924	34692	858	9551	0	6569	0	0	35193	0	22797	57990
V-L Flowrate, lb/hr	1334910	81243	955052	24076	307353	0	118344	0	0	729703	0	410652	1140350
Solids Flow Rate, lb/hr	0	0	0	0	0	562689	0	444345	46071	0	0	0	0
Temperature, F	42	64	386	387	292		75			2347	767	290	760
Pressure, psia	13.0	16.4	384.0	815.0	740.0	13.0	48.0	14.8	615.0	615.0	615.0	115.0	605.0
Enthalpy, Btu/lb	-33.3	-463.2	-121.3	74.8	43.8		-6823			-741	-2828	-6599	-2830
Density, lb/cuft	0.070	0.089	1.159	2.473	2.961		62.273			0.420	0.920	57.620	0.910

Table 5-1 (cont'd)
Case 1e Stream Table

Description	WGD Air	Lime	Shift Steam	Shift BFW	MDEA MU Water	Sulfur Product	Gypsum	DSRP Vent	WDP Cond	Syngas Cool Cond	MDEA CO2 Out	Treated Syngas	Syngas Cool BFW
Stream No.	R1	R2	R3	R4	R5	R6	R7	R8	R9	R10	R11	R12	R13
V-L Mole Fraction													
Ar	0.0093	0	0	0	0	0	0	0.0141	0	0	0.0000	0.0088	0
CH4	0	0	0	0	0	0	0	0	0	0	0.0001	0.0087	0
CO	0	0	0	0	0	0	0	0	0	0	0.0001	0.0559	0
CO2	0.0003	0	0	0	0	0	0.0039	0.0184	0	0	0.9409	0.0010	0
COS	0	0	0	0	0	0	0	0	0	0	0	0	0
H2	0	0	0	0	0	0	0	0	0	0	0.0020	0.8854	0
H2O	0.0064	0.9737	1.0000	1.0000	1.0000	0	0.9759	0.0005	1.0000	0.9961	0.0568	0.0035	1.0000
H2S	0	0	0	0	0	2.66E-07	0	0	0	0	0	0.0000	0
N2	0.7759	0	0	0	0	0	0	0.9670	0	0	0.0000	0.0366	0
NH3	0	0	0	0	0	0	0	0	0	0	0	0	0
O2	0	0	0	0	0	0	0	0	0	0	0	0	0
SO2	0	0	0	0	0	0	0	0	0	0	0	0	0
S	0	0	0	0	0	1.0000	0	0	0	0	0	0	0
HCl	0	0	0	0	0	0	0	0	0	0	0	0	0
Ca(OH)2	0	0.0263	0	0	0	0	0.0010	0	0	0	0	0	0
CaSO.2H2O	0	0	0	0	0	0	0.0189	0	0	0	0	0	0
Total	1.0000	1.0000	1.0000	1.0000	1.0000	1.0000	1.0000	1.0000	1.0000	1.0000	1.0000	1.0000	1.0000
V-L Flowrate, lbmol/hr	1138	39493	7585	10700	1293	105	1185	781	3	20385	22477	34542	0
V-L Flowrate, lb/hr	32882	794001	136642	192764	23296	3369	24978	22238	57	367253	953973	171931	0
Solids Flow Rate, lb/hr	0	0	0	0	0	0	0	0	0	0	0	0	0
Temperature, F	42	75	550	450	122	600	123	100	80	100	122	122	450
Pressure, psia	13.0	13.0	600.0	763.0	511.0	447.0	30	448.0	13.0	515.0	30.7	511.0	763.0
Enthalpy, Btu/lb	-33	-7	-5611	-12872	-6817	2685		-109	-6863	-6822	-3884	-635	-6436
Density, lb/cuft	0.070	0.005	1.143	51.607	60.524	113.093		2.142	61.590	61.165	0.212	0.401	51.607

Table 5-1 (cont'd)
Case 1e Stream Table

Description	CO2 Product	Reheat Syngas	Ambient Air to GT	GT Flue Gas	Stack Gas	HP SH Steam	Air-Cooled LP Cond	Water-Cooled LP Cond	BFW to HRSG	Syngas Humid MU H2O
Stream No.	25	27	28	29	30	31	32	33	34	35
V-L Mole Fraction										
Ar	0.0000	0.0086	0.0093	0.0089	0.0089	0	0	0	0	0
CH4	0.0001	0.0085	0	0	0	0	0	0	0	0
CO	0.0001	0.0547	0	0	0	0	0	0	0	0
CO2	0.9976	0.0010	0.0003	0.0085	0.0085	0	0	0	0	0
COS	0	0	0	0	0	0	0	0	0	0
H2	0.0021	0.8656	0	0	0	0	0	0	0	0
H2O	0	0.0258	0.0064	0.1281	0.1281	1.0000	1.0000	1.0000	1.0000	1.0000
H2S	0	0	0	0	0	0	0	0	0	0
N2	0.0000	0.0358	0.7759	0.7480	0.7480	0	0	0	0	0
NH3	0	0	0	0	0	0	0	0	0	0
O2	0	0	0.2081	0.1065	0.1065	0	0	0	0	0
SO2	0	0	0	0	0	0	0	0	0	0
S	0	0	0	0	0	0	0	0	0	0
HCl	0	0	0	0	0	0	0	0	0	0
Ca(OH)2	0	0	0	0	0	0	0	0	0	0
CaSO.2H2O	0	0	0	0	0	0	0	0	0	0
Total	1.0000	1.0000	1.0000	1.0000	1.0000	1.0000	1.0000	1.0000	1.0000	1.0000
V-L Flowrate, lbmol/hr	21200	35325	221242	275783	275783	46394	45212	45212	89131	2610
V-L Flowrate, lb/hr	930960	186095	6392720	7556100	7556100	835805	814505	814505	1605720	47024
Solids Flow Rate, lb/hr	0	0	0	0	0	0	0	0	0	0
Temperature, F	162	207	42	1074	270	999	90	90	225	42
Pressure, psia	2214.7	511.0	12.9	13.5	13.0	1815.0	0.7	0.7	105.0	13.0
Enthalpy, Btu/lb		-912	-33	-268	-489	-5387	-6808	-6808	-6673	-6905
Density, lb/cuft	28.796	0.371	0.069	0.022	0.046	2.282	62.117	62.117	59.510	63.210

5.3 SPARING PHILOSOPHY

The sparing philosophy for Case 1e is as provided below. Single train designs were utilized throughout with exceptions where equipment had exceeded its maximum capacity limit or dimensions for acceptable transportation to the site required an additional train. The design has:

- Two ASU trains (2 x 50%)
- Two trains of coal drying (2 x 50%)
- Two trains of gasification, including dry feed system, R-GAS™ gasifier, syngas quench cooler, cyclone and candle filter (2 x 50%)
- One WDP train (1 x 100%)
- One DSRP train (1 x 100%)
- One ATWGS and LTGC train (1 x 100%)
- One AACRP train (3 x 33% for the rich amine absorber and LP flash drum, 1 x 100% for the rest of the process)
- Two gas turbines/HRSG tandems (2 x 50%)
- One steam turbine (1 x 100%)

5.4 PERFORMANCE RESULTS

The Nexant-modeled Case 1e IGCC plant with CO_2 capture consumes 6,752 tpd of PRB coal at the Montana site to produce a net output of 467 MWe at a net plant efficiency of 33.06% on a HHV basis. Overall performance for the Case 1e IGCC plant is summarized in Table 5-2, which includes auxiliary power requirements. Loads that are unique to the GTI and RTI processes are shown in bold and italicized.

Table 5-2
Case 1e Plant Performance Summary

POWER SUMMARY (Gross Power at Generator Terminals, kWe)	Case 1e
Gas Turbine Power	429,895
Steam Turbine Power	215,453
TOTAL POWER, kWe	**645,348**
AUXILIARY LOAD SUMMARY, kWe	
Coal Handling	490
Coal Milling	2,622
Slag Handling	540
WTA Coal Dryer Compressor	8,998
WTA Coal Dryer Auxiliaries	595
DSP	***1,803***
Air Separation Unit Auxiliaries	851
Air Separation Unit Main Air Compressor	54,067
Oxygen Compressor	7,630
Nitrogen Compressors	26,624
CO_2 Compressor	32,295
Boiler Feedwater Pumps	4,050
Condensate Pump	224
Quench Water Pump	616
Gasifier Cooling BFW Circulating Pump	***3,723***
Circulating Water Pump	2,715
Ground Water Pumps	318
Cooling Tower Fans	1,770
Air Cooled Condenser Fans	2,710
ATWGS	***0***
AACRP	***16,970***
Gas Turbine Auxiliaries	998
Steam Turbine Auxiliaries	93
RTI WDP	***1,998***
DSRP	***283***
Miscellaneous Balance of Plant	3,000
Transformer Losses	2,481
TOTAL AUXILIARIES, kWe	**178,460**
NET POWER, kWe	**466,887**
Net Plant Efficiency, % (HHV)	33.06%
Net Plant Heat Rate, Btu/kWh	10,321
CONDENSER COOLING DUTY, MMBtu/hr	**1,144**
CONSUMABLES	
As-Received Coal Feed, lb/hr	562,689
Thermal Input, kWt	1,412,271
Raw Water Withdrawal, gpm	3,495
Raw Water Consumption, gpm	2,748

Table 5-3 shows the carbon balance for the Case 1e IGCC plant. The carbon capture efficiency is defined as the amount of carbon in the CO_2 product stream relative to the amount of carbon in the coal feed less the carbon contained in the slag. For Case 1e, the carbon capture efficiency is 90.2%.

Table 5-3
Case 1e Overall Carbon Balance

Overall Carbon Balance, lb/hr	In	Out
Coal Feed	281,727	
ASU Air	166	
Air to WDP	4	
Air to Gas Turbine	797	
ASU Vent		166
LTGC Condensate to Cooling Tower		270
Carbon in Slag		0
Stack Gas		28,196
CO_2 Product		254,061
Convergence Tolerance		1
Total	**282,694**	**282,694**

Table 5-4 shows the sulfur balance for the plant. Sulfur input comes solely from the sulfur in the coal. Sulfur output includes the sulfur recovered in the Claus plant, sulfur emitted in the stack gas, and the trace amount that is in the CO_2 product. Sulfur in the slag is considered negligible.

Table 5-4
Case 1e Overall Sulfur Balance

Overall Sulfur Balance, lb/hr	In	Out
Coal Feed	4,094	
Gypsum		713
Sulfur Product		3,369
Stack Gas		0
CO_2 Product		12
Convergence Tolerance		0
Total	**4,094**	**4,094**

Table 5-5 shows the overall water balance for the Case 1e IGCC plant.

Table 5-5
Case 1e Overall Water Balance

Water Use, gpm	Raw Water Withdrawal	Process Effluent Production for Internal Consumption	Internal Consumption	Process Water Discharge
WTA Coal Drying	0	(236)	0	0
Slag Handling	0	0	119	(119)
Quench Cooler	163	0	658	0
Syngas Cooling Knockout	0	(731)	0	0
Syngas Humidification	94	0	0	0
Steam Cycle Makeup	717	0	0	0
Steam Cycle Blowdown	0	(11)	0	0
CO_2 Compression Knockout	0	(46)	0	0
Cooling Tower Makeup	2,521	0	247	0
Cooling Tower Blowdown	0	0	0	(628)
Total	3,495	(1,024)	1,024	(747)

5.5 EQUIPMENT LIST

The list in Table 5-6 below shows the equipment that differs from the Case 1b.

Table 5-6
Case 1e Equipment List

ACCOUNT 5A SYNGAS CLEANUP
Subaccount 5A.1 RTI WDP

Equipment No.	Description	Type	Design Condition	Operating Qty	Spares
11	Recycle Syngas Compressor	Centrifugal	81 acfm @ 514 psia	1	0

Subaccount 5A.4 Shift Reactors

Equipment No.	Description	Type	Design Condition	Operating Qty	Spares
1	ATWGS Reactor	Transport Reactor	Proprietary	1	0
2	Cyclone Separator	Cyclone	Proprietary	1	0
3	Sorbent Feeder Package (incl Hopper)		Proprietary	1	0
4	Solids Cooler	Shell and Tube Heat Exchanger	Proprietary	1	0

5.6 CAPITAL COST

Table 5-7 shows the cost breakdown of the Case 1e GTI R-GAS™ with RTI WDP/ATWGS IGCC, expressed in a format that is consistent with the code of accounts in the NETL Report 1399. The accounts/subaccounts of interest for this study are:

- 2.3 Dry Coal Injection System,
- 4 Gasifier & Accessories,
- 5A Gas Cleanup & Piping and
- 5B CO_2 Removal and Compression

These are shown with more detail to include the various subaccounts to provide more clarity as to where the major cost differences are when compared to the other cases.

Table 5-8 shows the calculation and addition of owner's costs to determine the TOC, used to calculate COE.

The estimated TOC of the Case 1e GTI R-GAS™ with RTI WDP/ATWGS IGCC using PRB coal in 2011 dollars is $4,316/kW.

Table 5-7
Case 1e Total Plant Cost Summary

Case 1e: GTI R-GAS™ with RTI WDP/ATWGS IGCC		Coal Feed, lb/hr	562,689					Plant Size	466.9 MW, net			
Low Rank Western Coal Baseline Study	PRB	Coal HHV, Btu/lb	8564					Net Efficiency	33.06%			

Acct No.	Item/Description	Equipment Cost	Material Cost	Labor Direct	Labor Indirect	Sales Tax	Bare Erected Cost $	Eng'g CM H.O & Fee	Contingencies Process	Contingencies Project	TOTAL PLANT COST $	TOTAL PLANT COST $/kW
1	COAL & SORBENT HANDLING	**$18,960**	**$3,324**	**$14,503**	**$0**	**$0**	**$36,787**	**$3,338**	**$0**	**$8,024**	**$48,149**	**$103**
2	COAL & SORBENT PREP & FEED											
2.3	Dry Coal Injection System	$53,924	$0	$35,407	$0	$0	$89,331	$7,694	$17,866	$22,978	$137,870	$295
2.x	Other Coal & Sorbent Prep & Feed Systems	$60,786	$10,592	$16,594	$0	$0	$87,972	$7,685	$0	$19,131	$114,788	$246
	SUBTOTAL 2.	**$114,710**	**$10,592**	**$52,001**	**$0**	**$0**	**$177,304**	**$15,380**	**$17,866**	**$42,109**	**$252,659**	**$541**
3	FEEDWATER & MISC BOP SYSTEMS	**$8,983**	**$6,833**	**$8,850**	**$0**	**$0**	**$24,665**	**$2,330**	**$0**	**$6,263**	**$33,258**	**$71**
4	GASIFIER & ACCESSORIES											
4.1	Gasifier, Syngas Cooler & Auxiliaries (GTI)	$37,796	$18,898	$57,067	$0	$0	$113,761	$10,163	$28,440	$22,855	$175,218	$375
4.3	ASU/Oxidant Compression	$197,746	$0	$0	$0	$0	$197,746	$19,167	$0	$21,691	$238,605	$511
4.6	Flare Stack System	$0	$1,620	$655	$0	$0	$2,274	$218	$0	$498	$2,991	$6
4.9	Gasification Foundations	$0	$10,066	$6,003	$0	$0	$16,069	$1,471	$0	$4,385	$21,925	$47
	SUBTOTAL 4.	**$235,542**	**$30,583**	**$63,725**	**$0**	**$0**	**$329,850**	**$31,020**	**$28,440**	**$49,429**	**$438,739**	**$940**
5A	GAS CLEANUP & PIPING											
5A.1	RTI WDP	$23,954	$0	$28,745	$0	$0	$52,699	$5,097	$10,540	$13,667	$82,002	$176
5A.2	RTI DSRP	$6,324	$0	$7,000	$0	$0	$13,324	$1,294	$2,665	$3,457	$20,740	$44
5A.3	Mercury Removal	$3,273	$0	$2,474	$0	$0	$5,747	$555	$287	$1,317	$7,905	$17
5A.4a	LT Heat Recovery, FG Saturation & RTI ATWGS Reacto	$20,384	$0	$15,763	$0	$0	$36,146	$3,513	$1,818	$8,296	$49,772	$107
5A.6	Blow back Gas Systems	$2,620	$441	$248	$0	$0	$3,309	$314	$0	$724	$4,347	$9
5A.7	Fuel Gas Piping	$0	$858	$561	$0	$0	$1,419	$132	$0	$311	$1,862	$4
5A.9	Gas Clean Up Foundations	incl w / WDP	$0	incl w / WDP	$0	$0	$0	$0	$0	$0	$0	$0
	SUBTOTAL 5.	**$56,554**	**$1,299**	**$54,791**	**$0**	**$0**	**$112,644**	**$10,905**	**$15,310**	**$27,772**	**$166,628**	**$358**
5B	CO2 REMOVAL & COMPRESSION											
5B.1	RTI AACRP	$24,855	$0	$20,878	$0	$0	$45,733	$4,423	$9,147	$11,860	$71,163	$152
5B.2	CO2 Compression & Drying	$38,555	$0	$12,879	$0	$0	$51,434	$4,952	$0	$11,277	$67,663	$145
	SUBTOTAL 5B.	**$63,410**	**$0**	**$33,757**	**$0**	**$0**	**$97,167**	**$9,375**	**$9,147**	**$23,137**	**$138,826**	**$297**
6	COMBUSTION TURBINE/ACCESSORIES	**$111,211**	**$923**	**$8,948**	**$0**	**$0**	**$121,083**	**$11,476**	**$11,909**	**$14,882**	**$159,350**	**$341**
7	HRSG, DUCTING & STACK	**$26,625**	**$2,964**	**$8,263**	**$0**	**$0**	**$37,852**	**$3,574**	**$0**	**$4,897**	**$46,323**	**$99**
8	STEAM TURBINE GENERATOR	**$73,557**	**$958**	**$18,619**	**$0**	**$0**	**$93,134**	**$8,924**	**$0**	**$17,050**	**$119,108**	**$255**
9	COOLING WATER SYSTEM	**$5,416**	**$7,253**	**$6,671**	**$0**	**$0**	**$19,339**	**$1,798**	**$0**	**$4,535**	**$25,672**	**$55**
10	ASH/SPENT SORBENT HANDLING SYS	**$22,268**	**$1,715**	**$10,966**	**$0**	**$0**	**$34,949**	**$3,354**	**$0**	**$4,185**	**$42,488**	**$91**
11	ACCESSORY ELECTRIC PLANT	**$35,312**	**$15,494**	**$28,221**	**$0**	**$0**	**$79,027**	**$6,798**	**$0**	**$16,424**	**$102,249**	**$219**
12	INSTRUMENTATION & CONTROL	**$12,769**	**$2,588**	**$8,395**	**$0**	**$0**	**$23,753**	**$2,151**	**$1,187**	**$4,545**	**$31,636**	**$68**
13	IMPROVEMENTS TO SITE	**$3,676**	**$2,167**	**$9,647**	**$0**	**$0**	**$15,490**	**$1,530**	**$0**	**$5,106**	**$22,126**	**$47**
14	BUILDINGS & STRUCTURES	**$0**	**$7,541**	**$8,567**	**$0**	**$0**	**$16,108**	**$1,465**	**$0**	**$2,890**	**$20,464**	**$44**
	CALCULATED TOTAL COST	**$788,995**	**$94,234**	**$335,922**	**$0**	**$0**	**$1,219,151**	**$113,416**	**$83,859**	**$231,248**	**$1,647,674**	**$3,529**

Table 5-8
Case 1e Total Overnight Cost Summary

Owner's Costs	$ x $1,000	$/kW
Preproduction Costs		
6 months All Labor	$14,490	$31
1 Month Maintenance Materials	$3,086	$7
1 Month Non-Fuel Consumables	$558	$1
1 Month Waste Disposal	$425	$1
25% of 1 Months Fuel Cost at 100% CF	$1,008	$2
2% of TPC	$32,953	$71
Total	**$52,520**	**$112**
Inventory Capital		
60 day supply of fuel at 100% CF	$7,953	$17
60 day supply of non-fuel consumables at 100% CF	$525	$1
0.5% of TPC (spare parts)	$8,238	$18
Total	**$16,716**	**$36**
Initial Cost for Catalyst and Chemicals	**$5,677**	**$12**
Land	**$900**	**$2**
Other Owner's Cost	**$247,151**	**$529**
Financing Costs	**$44,487**	**$95**
Total Owner's Costs	**$367,451**	**$787**
Total Overnight Costs (TOC)	**$2,015,125**	**$4,316**

5.7 OPERATING COSTS

Table 5-9 shows the operating cost breakdown for the Case 1e IGCC.

Table 5-9
Case 1e Initial and Annual O&M Costs

INITIAL & ANNUAL O&M EXPENSES					
Case:	Case 1e - GTI R-GAS™ w/ RTI WDP/ATWGS IGCC				
Plant Size (MWe)	**467**		**Heat Rate (Btu/kWh):**		10,321
Primary/Secondary Fuel:	**PRB**		**Fuel Cost ($/MMBtu):**		
Design/Construction	5 years		**Book Life (yrs):**		20
TPC (Plant Cost) Year	June 2011		**TPI Year:**		2016
Capacity Factor (%)	80		**CO2 Captured (TPD)**		11169

OPERATING & MAINTENANCE LABOR				
Operating Labor				
Operating Labor Rate (base):	$39.70	$/hr		
Operating Labor Burden:	30.00	% of base		
Labor Overhead Charge	25.00	% of labor		
Operating Labor Requirements per Shift	**units/mod**	**Total Plant**		
Skilled Operator	2.0	2.0		
Operator	10.0	10.0		
Foreman	1.0	1.0		
Lab Tech's etc	3.0	3.0		
TOTAL Operating Jobs	16.0	16.0		
			Annual Cost $	Annual Unit Cost $/kW-net
Annual Operating Labor Cost			$7,233,658	
Maintenance Labor Cost			$15,951,128	
Administration & Support Labor			$5,796,196	
Property Taxes and Insurance			$32,953,472	
TOTAL FIXED OPERATING COSTS			**$61,934,455**	

VARIABLE OPERATING COSTS						
						$/kWh-net
Maintenance Material Cost					**$29,623,524**	
Consumables	Consumption Initial	Consumption /Day	Unit Cost	Initial Fill Cost		
Water(/1000 gallons)	0	2,516	1.67	**$0**	**$1,229,856**	
Chemicals						
MU & WT Chem (lb)	0	14991	0.27	$0	$1,172,439	
Carbon (Hg Removal) (lb)	111993	154	1.63	$182,549	$73,128	
RTI WDP Sorbent (lb)	Proprietary	Proprietary	Proprietary	$2,459,501	$1,541,514	
RTI DSRP Catalyst (lb)	22000	12.1	11.15	$245,300	$39,248	
DSRP Oxidation/Reduction Catalyst (lb)	22000	12.1	1.56	$34,320	$5,491	
Lime (lb)	0	41904	0.04	$0	$467,550	
ATWGS Catalyst (lb)	Proprietary	Proprietary	Proprietary	$1,813,435	$672,422	
Activated Amine (lb)	336647	184	2.80	$941,894	$150,703	
Subtotal Chemicals				**$5,676,999**	**$4,122,495**	
Other						
Supplemental Fuel (MMBtu)	0	0	0.00	$0	$0	
Gases, N2 etc.(/100scf)	0	0	0.00	$0	$0	
LP Steam (/1000 lbs)	0	0	0.00	$0	$0	
Subtotal Other				**$0**	**$0**	
Waste Disposal:						
Spent Mercury Catalyst (lb)	0	154	0.65	$0	$29,161	
Flyash (ton)	0	0	0.00	$0	$0	
Slag (ton)	0	553	25.11	$0	$4,053,550	
Subtotal Waste Disposal				**$0**	**$4,082,711**	
By-products & Emissions						
Sulfur (tons)	0	40	0	0	0	
Gypsum (tons)	0	300	0	0	0	
Subtotal By-Products				**$0**	**$0**	
TOTAL VARIABLE OPERATING COSTS				**$5,676,999**	**$39,058,586**	
Fuel (tons)	**0**	**6752**	**19.63**	**$0**	**$38,703,730**	

5.8 COST OF ELECTRICITY

Table 5-10 shows a summary of the power output, CAPEX, OPEX, COE and cost of CO_2 capture for the Case 1e GTI R-GAS™ with RTI WDP/ATWGS IGCC. The estimated Case 1e IGCC COE is 119.2 mills/kWh.

Table 5-10
Plant Performance and Economic Summary

Case	Case 1e
CAPEX, $MM	
Total Installed Cost (TIC)	$1,219
Total Plant Cost (TPC)	$1,648
Total Overnight Cost (TOC)	$2,015
OPEX, $MM/yr (100% Capacity Factor Basis)	
Fixed Operating Cost (OC_{fix})	$61.9
Variable Operating Cost, less Fuel (OC_{var})	$48.8
Fuel (OC_{fuel})	$48.4
Total OPEX	$159.1
Power Production, MWe	
Gas Turbine	429.9
Steam Turbine	215.5
Auxiliary Power Consumption	178.5
Net Power Output	466.9
Power Generated, MWh/yr (MWH)	4,089,934
SO_2 Emissions (lb/MWh_{gross})	0.0013
SO_2 Emissions (lb/MMBtu)	0.0002
COE, excl CO_2 TS&M, mills/kWh	**119.2**
COE, incl CO_2 TS&M, mills/kWh	**139.1**
Cost of CO_2 Avoided excl CO2 TS&M, $/ton CO_2	**47.7**
Cost of CO_2 Avoided incl CO2 TS&M, $/ton CO_2	**71.5**

Section 6 IGCC Sensitivity Analysis

Sensitivity analysis was carried out to determine the effects of various parameters of the GTI R-GAS™ system and RTI advanced syngas cleanup, including WDP, DSRP, AFWGS/ATWGS and AACRP on the overall IGCC COE. The parameters investigated include: overall system capital cost, feedstock cost, IGCC plant capacity factor, CO_2 sales price, and cost of CO_2 emissions.

6.1 GTI R-GAS™ SYSTEM COST

Figure 6-1 shows how the Case 1b and 1e IGCC COEs change as the GTI DSP and R-GAS™ gasifier TPC varies from -30% to +30%. Also shown in figure is the reference Case 1a IGCC COE at 145.3 mills/kWh.

Figure 6-1
Sensitivity Analysis – COE vs GTI R-GAS™ TPC

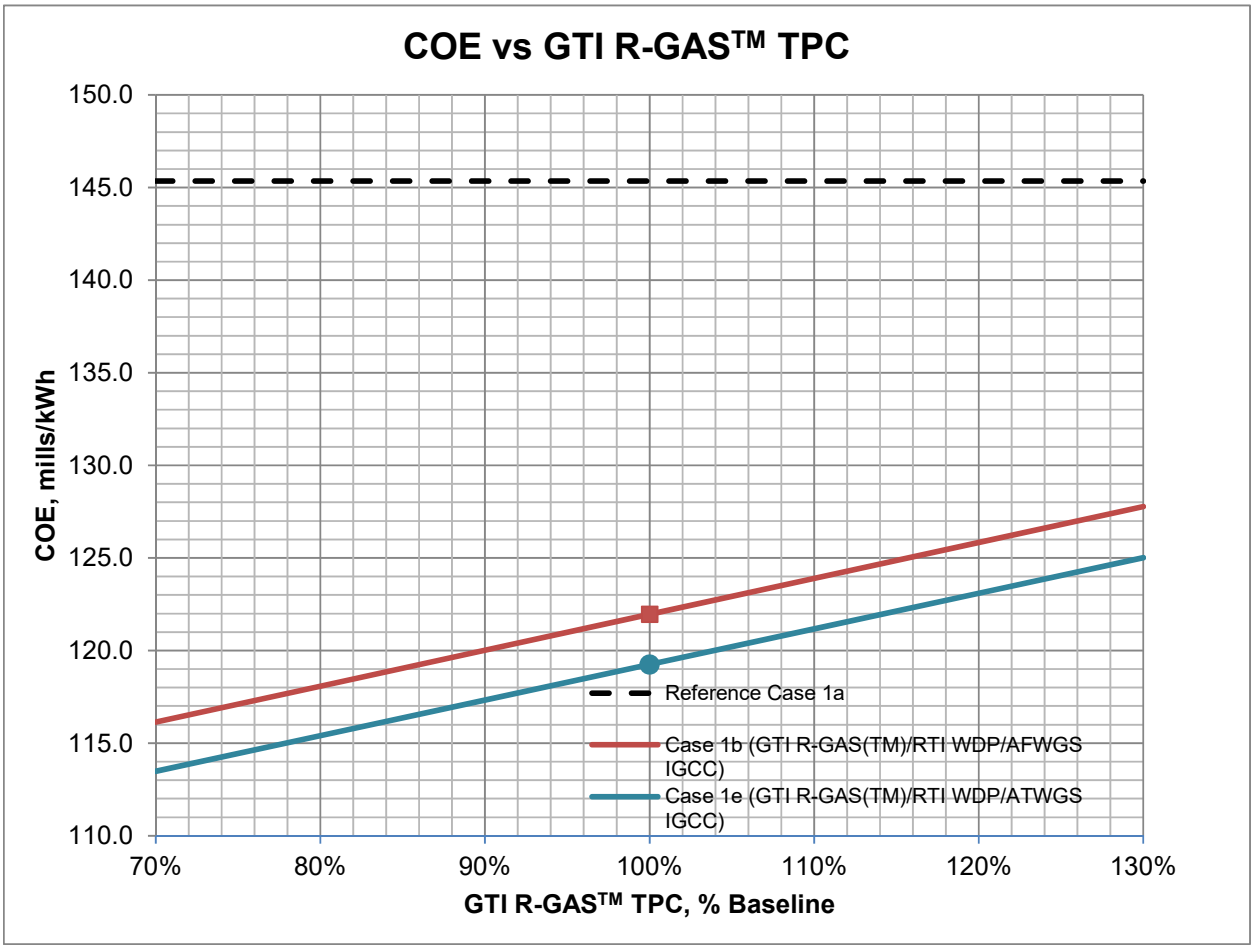

For both the Case 1b and Case 1e IGCC cases, roughly every 5% increase in the R-GAS™ gasification system (including DSP and gasifier) TPC, or the equivalent of $16MM in TPC, increases the IGCC COE by 1 mill/kWh.

6.2 RTI WDP SYSTEM COST

Figure 6-2 shows how the Case 1b and 1e IGCC COEs change as the RTI WDP system TPC varies from -30% to +30%. The RTI WDP system TPC includes the costs for the RTI WDP, DSRP and AACRP processes. It also includes the AFWGS TPC for Case 1b and ATWGS TPC for Case 1e. For reference purposes, the Case 1a IGCC COE of 145.3 mills/kWh is shown in Figure 6-2 as well.

Figure 6-2
Sensitivity Analysis – COE vs RTI WDP System Cost

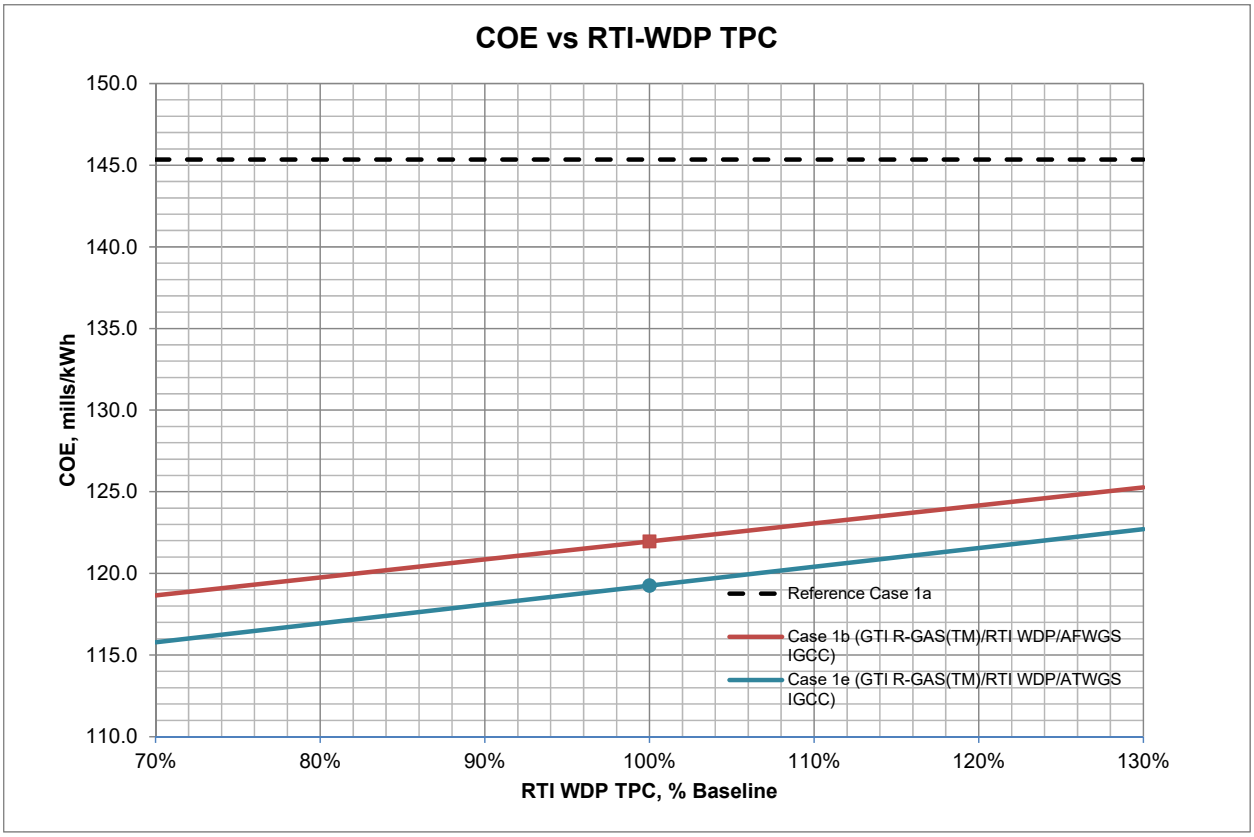

For both cases, roughly every 9% increase in RTI WDP TPC, equivalent to about $16MM, increases the IGCC COE by 1 mill/kWh.

6.3 ATWGS TPC

Figure 6-3 shows how the Case 1e COE changes with respect to just the ATWGS TPC as it varies from -30% to +30%. For reference purposes, the Case 1a IGCC COE of 145.3 mills/kWh and Case 1b IGCC COE of 122.0 mills/kWh are shown in Figure 6-3 as well.

Figure 6-3 shows that at the high-end (+30% of baseline) of the ATWGS TPC, its COE, at 120.6 mills/kWh varies little from the baseline and is still less than the Case 1a and Case 1b IGCC. This is because the ATWGS TPC makes up only a small fraction of the total CAPEX and variation to the TPC does not affect the COE to a large extent.

Figure 6-3
Sensitivity Analysis – COE vs RTI ATWGS System Cost

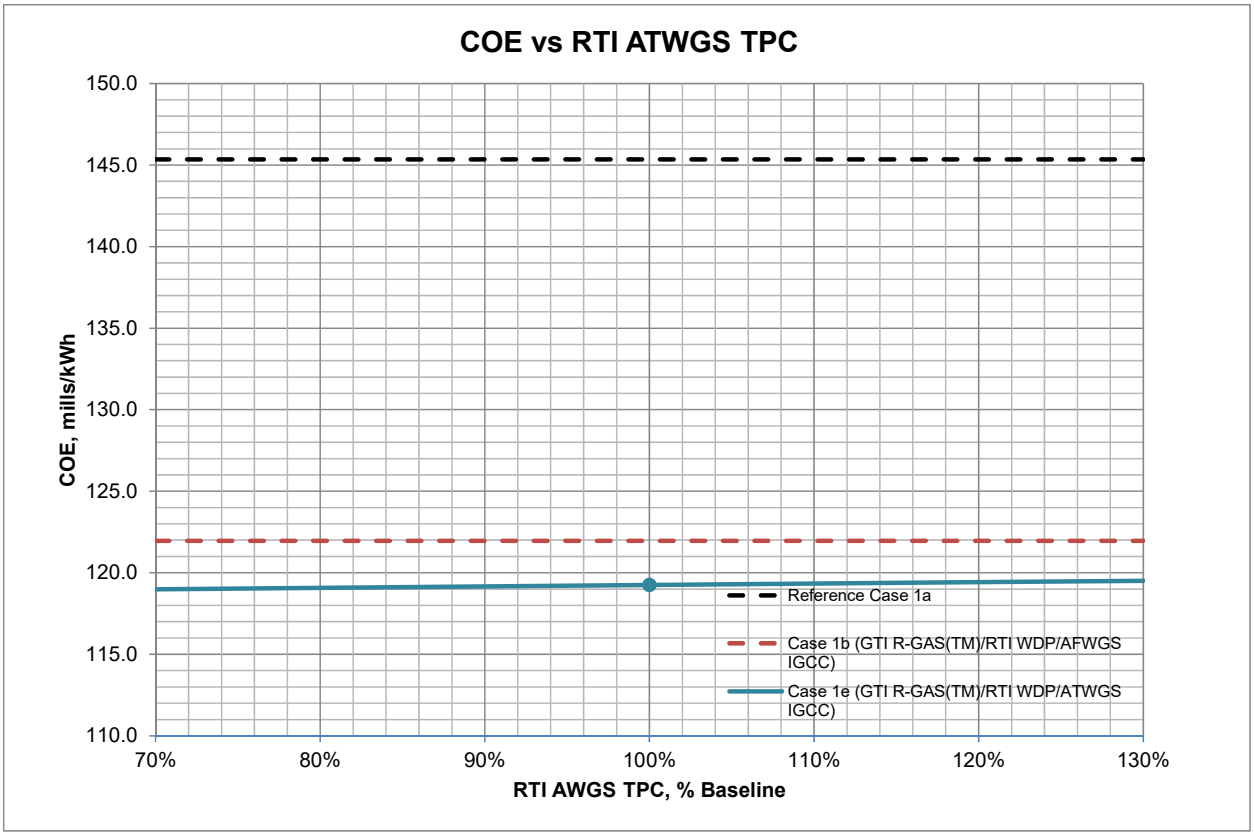

6.4 ATWGS CATALYST COST

Figure 6-4 shows how the Case 1e COE changes with respect to the ATWGS catalyst cost as it varies from -50% to +50%. The Case 1a IGCC COE and Case 1b IGCC COE of 145.3 mills/kWh and 122.0 mills/kWh respectively are shown in Figure 6-4 as well.

Figure 6-4 shows that at the high-end (+50% of baseline) of the ATWGS catalyst cost, its COE, at 120.5 mills/kWh, varies little from the baseline and is still lower than the Case 1a and Case 1b IGCC.

Figure 6-4
Sensitivity Analysis – COE vs RTI ATWGS Catalyst Cost

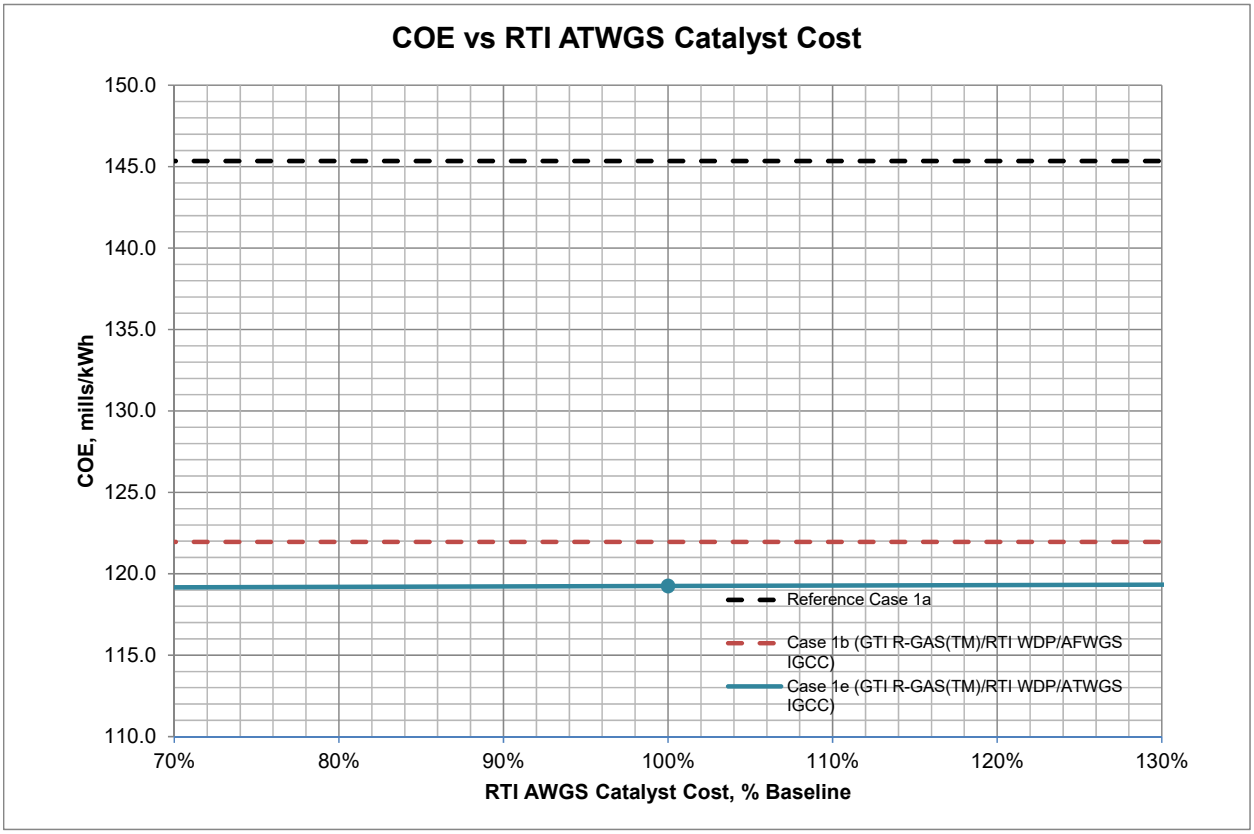

6.5 CAPACITY FACTOR

The baseline IGCC plant capacity factor used in this study is 80%. Figure 6-5 shows how the IGCC COE varies with plant CF as it varies from 75% to 85%.

Figure 6-5
Sensitivity Analysis – COE vs IGCC Plant Capacity Factor

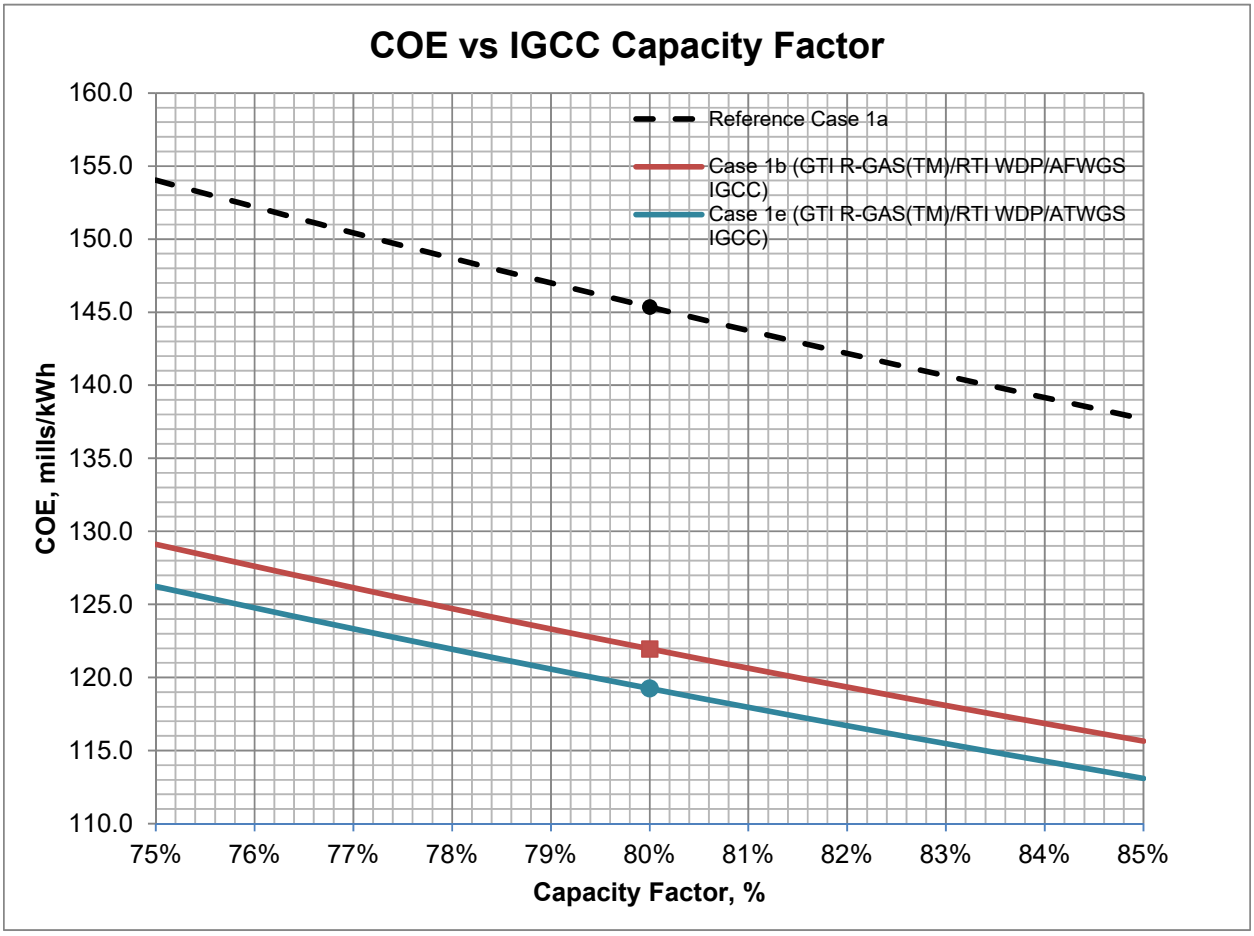

6.6 FEEDSTOCK PRICE

The baseline IGCC plant PRB coal feedstock price used in this study is $19.63/ton. Figure 6-6 shows how the IGCC COE varies with coal price as it varies from $10/ton to $60/ton.

Figure 6-6
Sensitivity Analysis – COE vs Feedstock Price

6.7 CO_2 SALES PRICE

Sensitivity to CO_2 sales at plant gate prices is shown in Figure 6-7. The baseline case assumes that the CO_2 product carries no value ($0/tonne). The sales price is subsequently varied to a maximum of $60/tonne to determine its effect on the IGCC plant's COE.

Figure 6-7
Sensitivity Analysis – COE vs CO_2 Sales Price

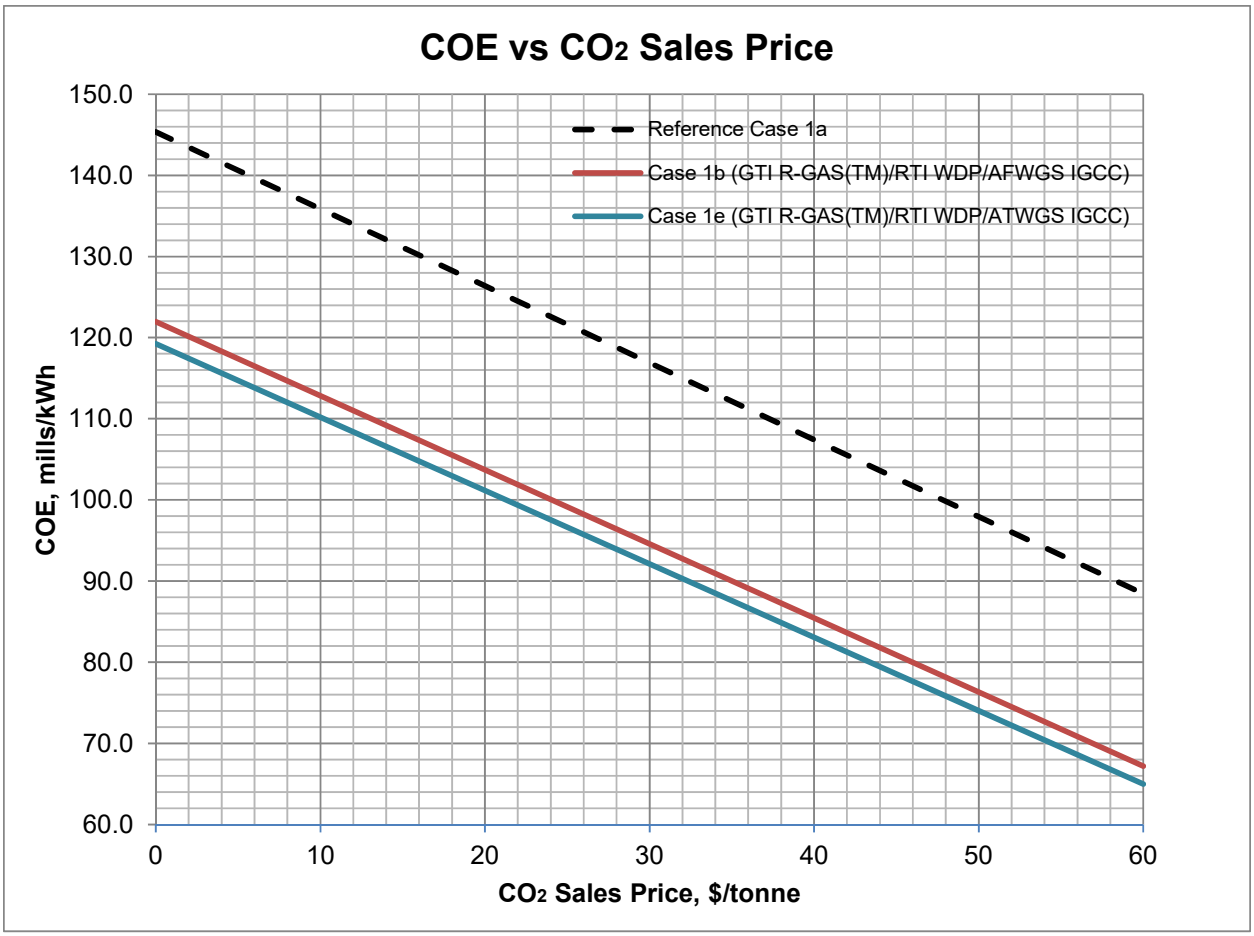

6.8 COST OF CO_2 EMISSIONS

The sensitivity to CO_2 emissions costs is shown in Figure 6-8. The baseline case assumes that there are no costs associated with venting CO_2 to the atmosphere ($0/tonne). The cost of CO_2 emissions is subsequently varied to a maximum of $60/tonne to determine its effect on the IGCC plant's COE.

Figure 6-8
Sensitivity Analysis – COE vs Cost of CO_2 Emissions

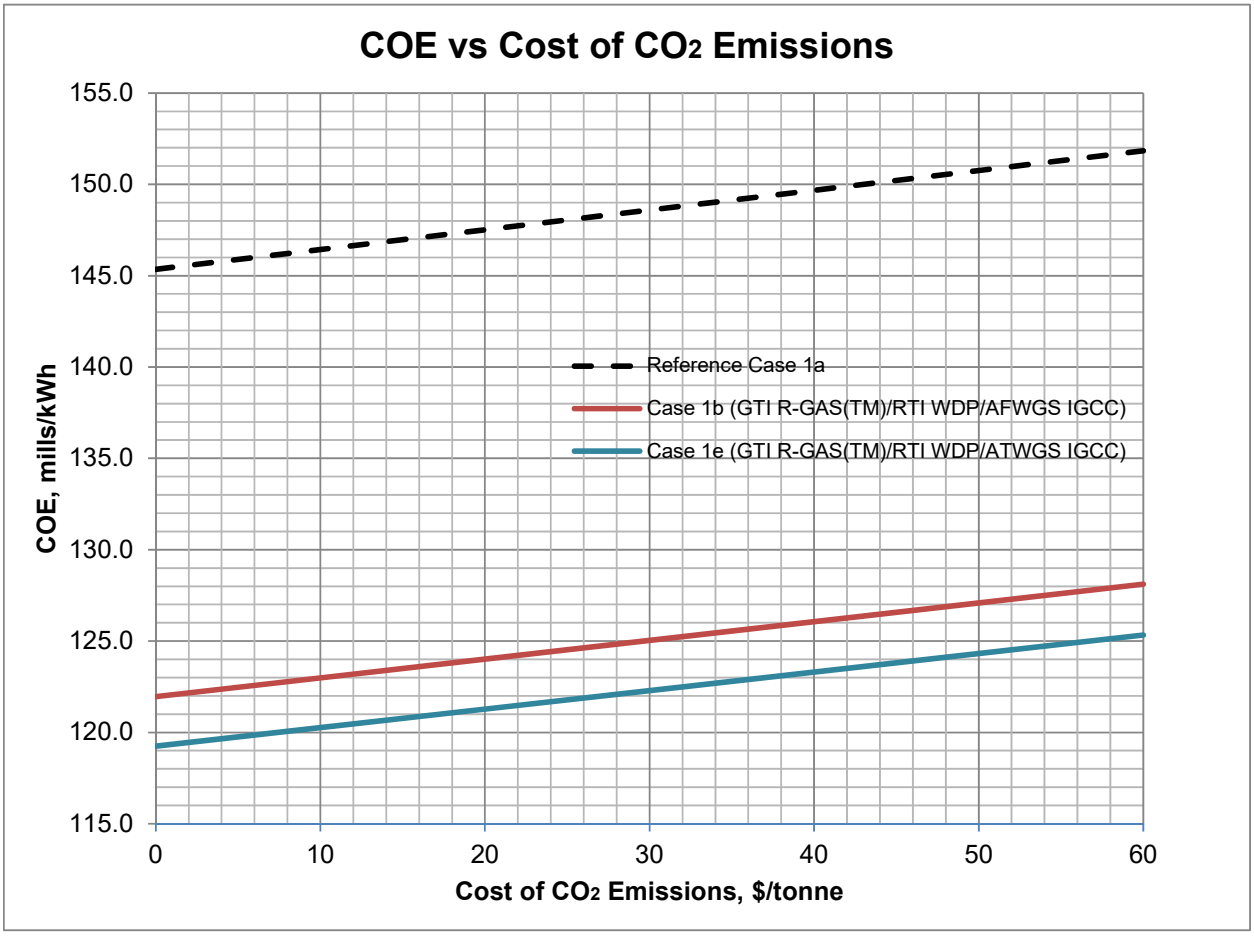

The COE are less sensitive to emissions cost than to CO_2 sales price because much more CO_2 is captured by the IGCC plant than is vented (90% vs 10%), hence the magnitude of the COE sensitivity is about 9 times greater to CO_2 sales price than to cost of CO_2 emissions.

Section 7 CTL - Crude Methanol Production Design Basis

7.1 DESIGN REFERENCES

The reference plant design to be used in this TEA is selected from "*Baseline Analysis of Crude Methanol Production from Coal and Natural Gas*, Revised July 29, 2014, DOE/NETL. 341/020514" (DOE Crude Methanol Study). The reference CTM case used for comparison in the previous DE-FE0012066 study against the GTI R-GAS™ and RTI advanced syngas cleanup/ AACRP systems was the DOE Crude Methanol Study's Case 2 CTM plant with CO_2 capture and sequestration. As this TEA is a continuation of the previous DE-FE0012066 study, but with the addition of RTI's ATWGS reactor technology, Case 2 will be continued to serve as the reference case for comparison.

The DOE Crude Methanol Study is used as the main reference for the CTM plant design, along with the same series of QGESS documents specified earlier in Section 2.1.

Additionally, "*Cost and Performance Baseline for Fossil Energy Plants Volume 1: Bituminous Coal and Natural Gas to Electricity*, Revision 2, November 2010, DOE/NETL. 2010/1397" (NETL Report 1397) contains a natural gas combined cycle (NGCC) design with CO_2 capture using Fluor's Econamine FG Plus℠ process. Its performance provided the basis for the design of the methanol synthesis plant's power cycle and post-combustion CO_2 capture.

While the TEA reporting requirements specified that the costs be presented in 2011 dollars, the costs provided for the NGCC design in NETL Report 1397 were reported in 2007 dollars. A separate DOE/NETL's report, "*Updated Costs (June 2011 Basis) for Selected Bituminous Baseline Cases*, August 2012, DOE/NETL-341/082312" (NETL Report 341/082312), was used as the reference to develop the escalated NGCC capital and operating cost estimates in June 2011 dollars.

7.2 CASE CONFIGURATIONS

To identify and determine any synergistic advantages of integrating the RTI ATWGS reactor technology, an additional design case is developed, on top of the four CTM cases previously completed in the DE-FE0012066 study. These are shown in Table 7-1. One of these cases is the Reference Case, which is Nexant's model of the reference Case 2 selected from the DOE Crude Methanol Study. The most promising case from the previous study is Case 2b, the CTM plant with CO_2 capture that integrates GTI's R-GAS™ gasification technology with RTI's advanced syngas cleanup process. Case 2e, which adds RTI's ATWGS technology to the two advanced technologies in Case 2b, is the case of interest for the current study. It is anticipated to provide additional synergistic benefits above and beyond that of Case 2b.

The specific technologies included in each of the five CTM plant configurations are identified in the CTM case study matrix shown in Table 7-1.

Table 7-1
Case Study Matrix for CTM Plants with CO_2 Capture

Case Name for Current Study	Case 2a[1]	Case 2b	Case 2c	Case 2d	Case 2e
Case Name in Previous Study[2]	Case 3a	Case 3b	Case 3c	Case 3d	N/A
Gasification Technology					
Shell Gasification with Lockhopper-Based Feed System	✓			✓	
GTI R-GAS™ Gasifier with DSP Feed System		✓	✓		✓
Gas Cleanup[3]					
Rectisol® for CO_2 and Sulfur Removal	✓		✓		
RTI WDP with AACRP		✓		✓	✓
Water-Gas Shift					
Sour Shift	✓		✓		
RTI AFWGS		✓		✓	
RTI ATWGS					✓
Methanol Production	✓	✓	✓	✓	✓
NGCC Power Generation with Fluor Econamine CO_2 Capture	✓	✓	✓	✓	✓
CO_2 Drying and Compression (to 2,200 psig)	✓	✓	✓	✓	✓

[1] Reference Case based on Nexant's benchmark simulation of the DOE Crude Methanol Study Case 2
[2] Previous study cases used "3" as a prefix e.g Case 3a, 3b, 3c and 3d because these were addressing Task 3 of the study.
[3] Rectisol® removes H_2S and CO_2. Additional trace contaminant cleanup technologies will be included as defined by DOE/NETL baseline studies

Reference case from previous DE-FE0012066 study
Best performing case from previous DE-FE0012066 study
Other DE-FE0012066 study cases
Case of interest in this study

7.2.1 Case 2a: Reference Shell Gasifier with Rectisol® AGR CTM Plant

The Shell gasification with Rectisol® AGR CTM plant utilizing Montana PRB subbituminous coal (Case 2 from the DOE Crude Methanol Study) was selected as the Reference Case and was previously evaluated in the DE-FE0012066 study. The choice of this case from the DOE Crude Methanol Study was straightforward since it is the only CTM case that includes CO_2 capture for sequestration. Table 7-2 provides a more detailed description of Case 2 of the DOE Crude Methanol Study.

Table 7-2
DOE Crude Methanol Study Case 2 Description

Case	Feedstock	Steam Cycle, psig/°F/°F	Combustion Turbine	Gasifier Technology	Oxidant	Sulfur Removal/ Recovery	CO_2 Separa-tion	Products
2	Coal/Syngas	1800/1050 /1050	SGT6-2000E	Shell	95mol% O_2	Rectisol®/ Claus	Rectisol® & Amine[1]	Methanol

[1] Amine process is added to NGCC system only

The reference Shell-gasification based methanol production case is a coal-based plant generating enough syngas to produce approximately 10,000 metric tons of methanol per day (3,326,000 gal/day based on 332.6 gal/metric ton). This plant size is considered large scale but typical for the current design of new plants.

The two-stage Rectisol® process is designed for 90% CO_2 removal. The post-combustion amine capture process for the natural gas-fired flue gas is also designed for 90% CO_2 removal. The 90% design for both CO_2 point sources results in a total carbon capture rate of >90% for the overall plant.

Both the gasification and methanol synthesis processes generate a large amount of heat that is recovered, in the form of steam for process requirements and power generation. Additional power is generated for in-plant use, via a combined cycle operation utilizing natural gas as fuel. In combination with the associated steam turbines, the total power generated from the methanol plant's power cycle is equal to its total estimated auxiliary loads (i.e. the DOE Crude Methanol Study Case 2 plant's operations is power neutral), with near-zero export/import power.

Nexant developed a conceptual design of the Case 2a Shell CTM plant with two-stage Rectisol®-based AGR process using data from Case 2 of the DOE Crude Methanol Study as the reference. The resulting stream flows, heat and material balances, methanol production and power generation from the NGCC were benchmarked and cross-checked against the DOE Crude Methanol Study Case 2 to ensure that the results are within a reasonable range of accuracy

A BFD of the Case 2a CTM plant is shown in Figure 7-1. The Reference Case, together with the rest of the cases under evaluation, is assumed to operate with an annual CF of 90% or 7,884 hrs/year at full capacity.

Figure 7-1
Case 2a: Shell Gasifier with Rectisol® AGR CTM Plant - Simplified BFD

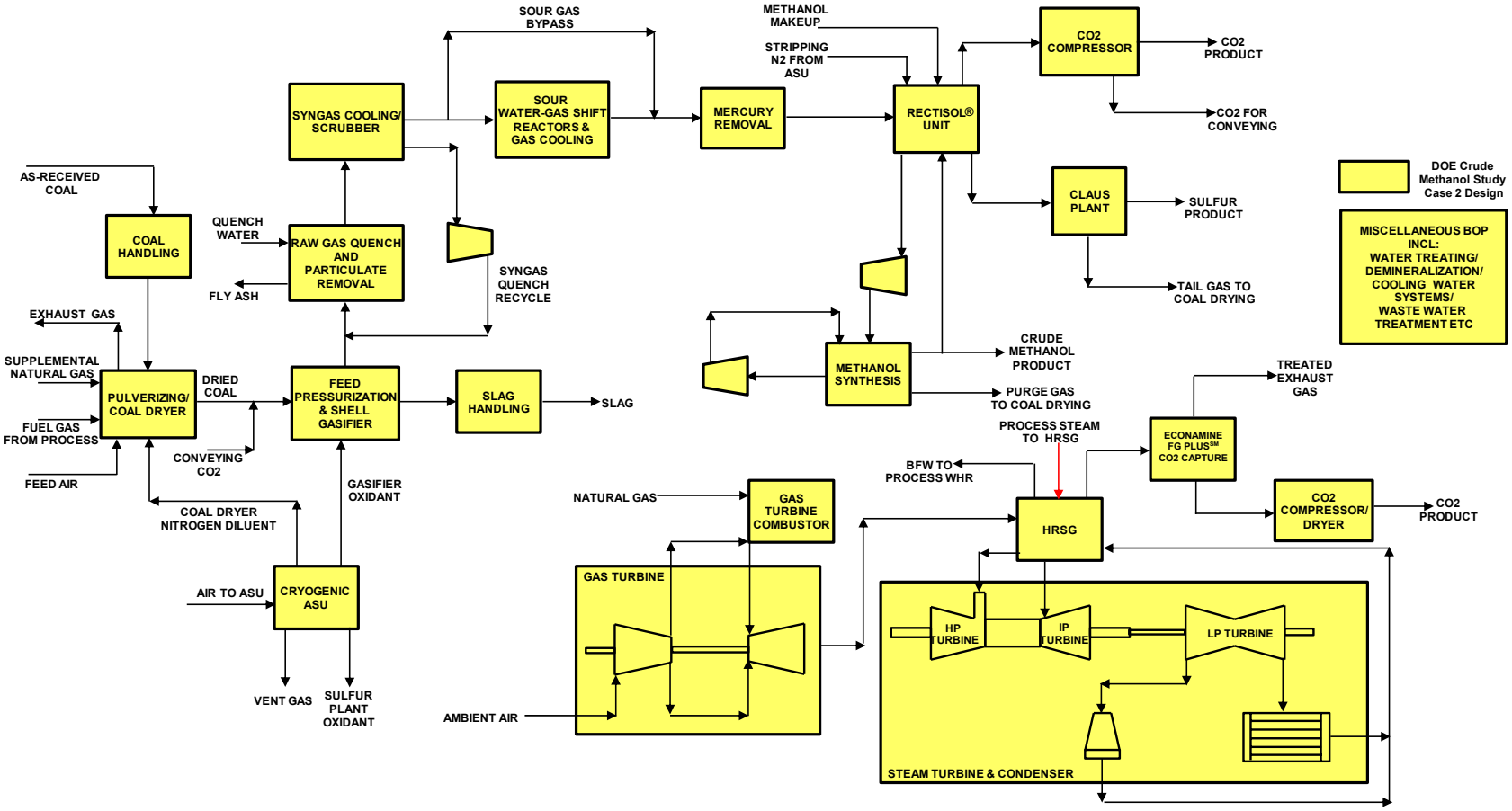

7.2.2 Case 2b: GTI R-GAS™ with RTI WDP CTM Plant

Case 2b is the design that was evaluated previously in the DE-FE0012066 study. It integrates GTI's R-GAS™ gasification technology with the RTI advanced syngas cleanup and AACRP systems. Due to the different cold gas efficiency of the R-GAS™ gasifier, the CTM plant consumes a different amount of coal feed when compared with Case 2a in order to produce nominally, the same amount of syngas required to produce 10,000 metric tons of methanol per day. For the NGCC plant, three GE MS6001B turbines were required to meet the plant's demands such that no power import is required. However, due to differences between the Case 2b plant's auxiliary power consumption, as well as differences in process waste heat recovery and associated steam generation from the reference Case 2a, a small amount of excess power is produced and exported to the grid for extra revenue.

A combination of RTI's WDP unit and AACRP unit replaces the Rectisol® unit in Case 2a to remove the sulfur and CO_2 from the syngas. RTI's WDP removes H_2S and COS from the syngas after it leaves the particulate filters, without requiring additional cooling. The treated syngas undergoes sweet shift in RTI's AFWGS process before it is cooled and sent to AACRP unit for CO_2 capture. The AACRP captures >90% of the CO_2 in the raw syngas in order to meet the CO_2 emissions specifications. RTI's DSRP technology is used for sulfur recovery.

The Case 2b CTM plant BFD is shown in Figure 7-2. This figure serves to demarcate the battery limits and highlights the interfaces between GTI's and RTI's proprietary systems (colored blue and red respectively) and the rest of the CTM processes (in yellow) that are derived from Case 2 of the DOE Crude Methanol Study. The blue block represents GTI's DSP and R-GAS™ gasifier system, which replaces the lockhopper feed system and Shell gasifier in the reference Case 2a CTM plant. The red blocks within the broken-line rectangle represent RTI's advanced syngas cleanup and AACRP processes and comprise the WDP for sulfur removal, DSRP to produce elemental sulfur, AFWGS for WGS, LTGC, and AACRP for CO_2 removal.

Case 2b was shown to be the best performing case in the previous TEA study.

Hence with the current study, it is the yardstick for comparison with the new Case 2e. Any incremental improvement in Case 2e's cost and performance over Case 2b can be attributed to the integration of RTI's ATWGS technology. It should be noted that since Case 2b incorporated RTI's AFWGS process, the full benefit of RTI's ATWGS compared with conventional WGS technologies is not determinable from just the comparison of these two cases but it should be greater than the incremental improvements indicated by this comparison.

7.2.3 Case 2c and Case 2d

Cases 2c and 2d were previously evaluated in the DE-FE0012066 study to evaluate the benefits of GTI's R-GAS™ gasification technology and RTI's advanced syngas cleanup technology individually. These cases bear no further elaboration since they have been studied already. They are included in Table 7-1 for completeness only and are not relevant to the current TEA study.

Figure 7-2
Case 2b: GTI R-GAS™ Gasifier with RTI WDP CTM Plant - Simplified BFD

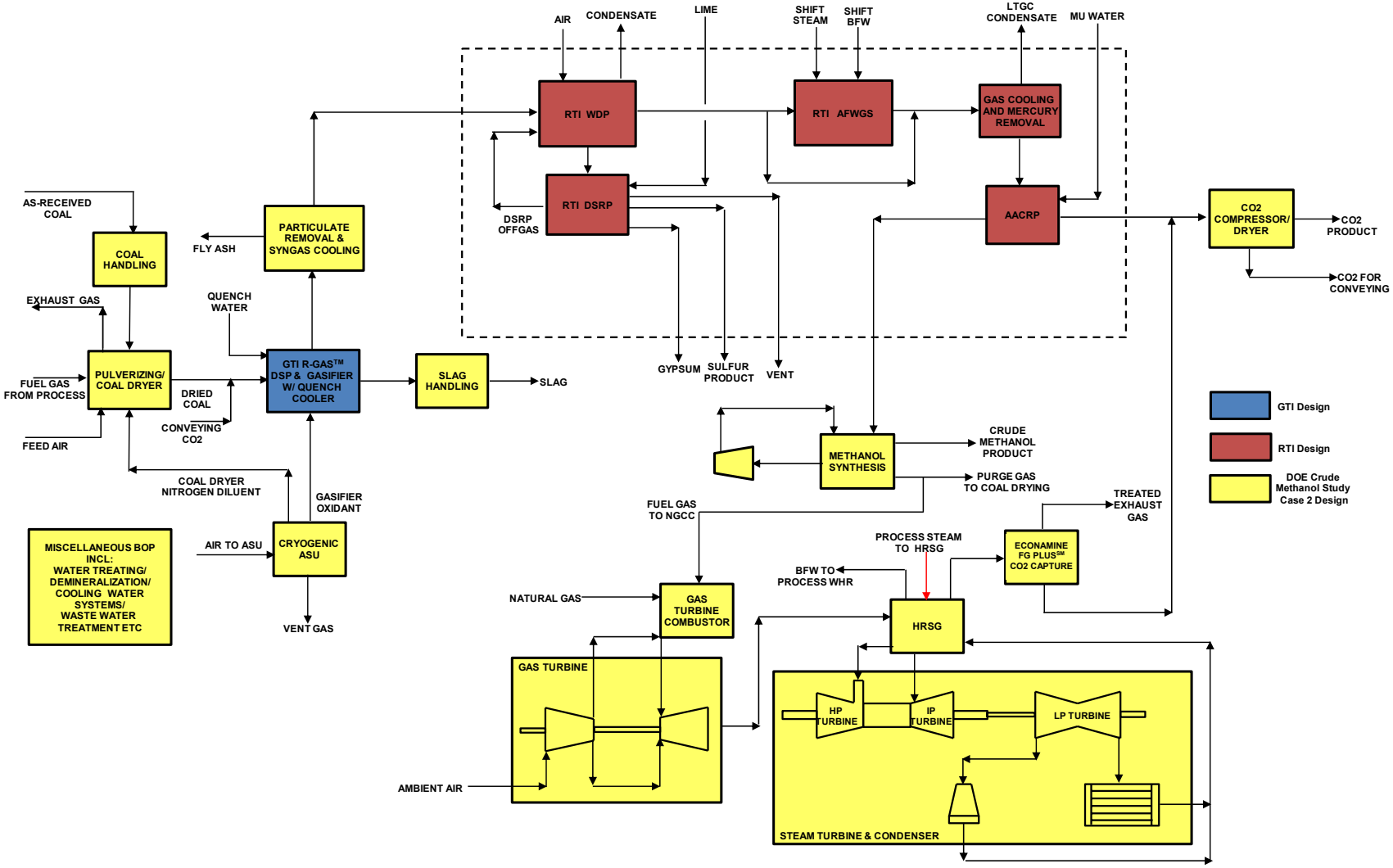

7.2.4 Case 2e: GTI R-GAS™ with RTI WDP and RTI ATWGS CTM Plant

The CTM plant of interest for the current study is the design that integrates the GTI R-GAS™ gasification technology, RTI advanced syngas cleanup and AACRP systems with the RTI ATWGS units.

The Case 2e CTM plant consumes the same amount of coal feed as Case 2b, since both use the R-GAS™ gasification system with the same cold gas efficiency. The same amount of syngas is produced to make 10,000 metric tons of methanol per day. The Case 2e CTM plant is also equipped with an NGCC plant to meet the auxiliary power demands such that no power import is required. However, due to potential differences in process waste heat recovery schemes when integrated with the ATWGS unit, the small amount of excess power produced and exported to the grid for extra revenue may differ from that of Case 2b.

In Case 2e, RTI's WDP and AACRP units are used to remove sulfur and CO_2 from the syngas that is produced in the AR gasification system. RTI's WDP removes H_2S and COS from the hot syngas after it leaves the particulate filters. A portion of the treated syngas will then undergo shift in the ATWGS unit (replacing Case 2b's AFWGS unit), while the remaining syngas bypasses the reactors. The shifted syngas is then mixed with the bypass syngas such that the H_2/CO ratio is 2:1, suitable for methanol synthesis. The mixed syngas is then cooled and sent to the AACRP unit for CO_2 capture. The AACRP unit captures > 90% of the CO_2 in the raw syngas in order to meet the CO_2 emissions specifications.

The Case 2e CTM plant BFD is shown in Figure 7-3. This figure serves to demarcate the battery limits and highlights the interfaces between GTI's and RTI's proprietary systems. Like Case 2b, the blue block represents GTI's DSP and R-GAS™ gasifier systems, while the red blocks within the broken-line rectangle represent RTI's advanced syngas cleanup and AACRP processes and comprise the WDP, DSRP, LTGC, and AACRP. The difference here is the green block inside the broken-line rectangle, representing RTI's ATWGS reactor units, which replaces the AFWGS unit in Case 2b. The remaining IGCC processes (in yellow) are designed by Nexant and are based on the DOE Crude Methanol Study Case 2 design.

Figure 7-3
Case 2e: GTI R-GAS™ with RTI WDP/RTI ATWGS CTM Plant - Simplified BFD

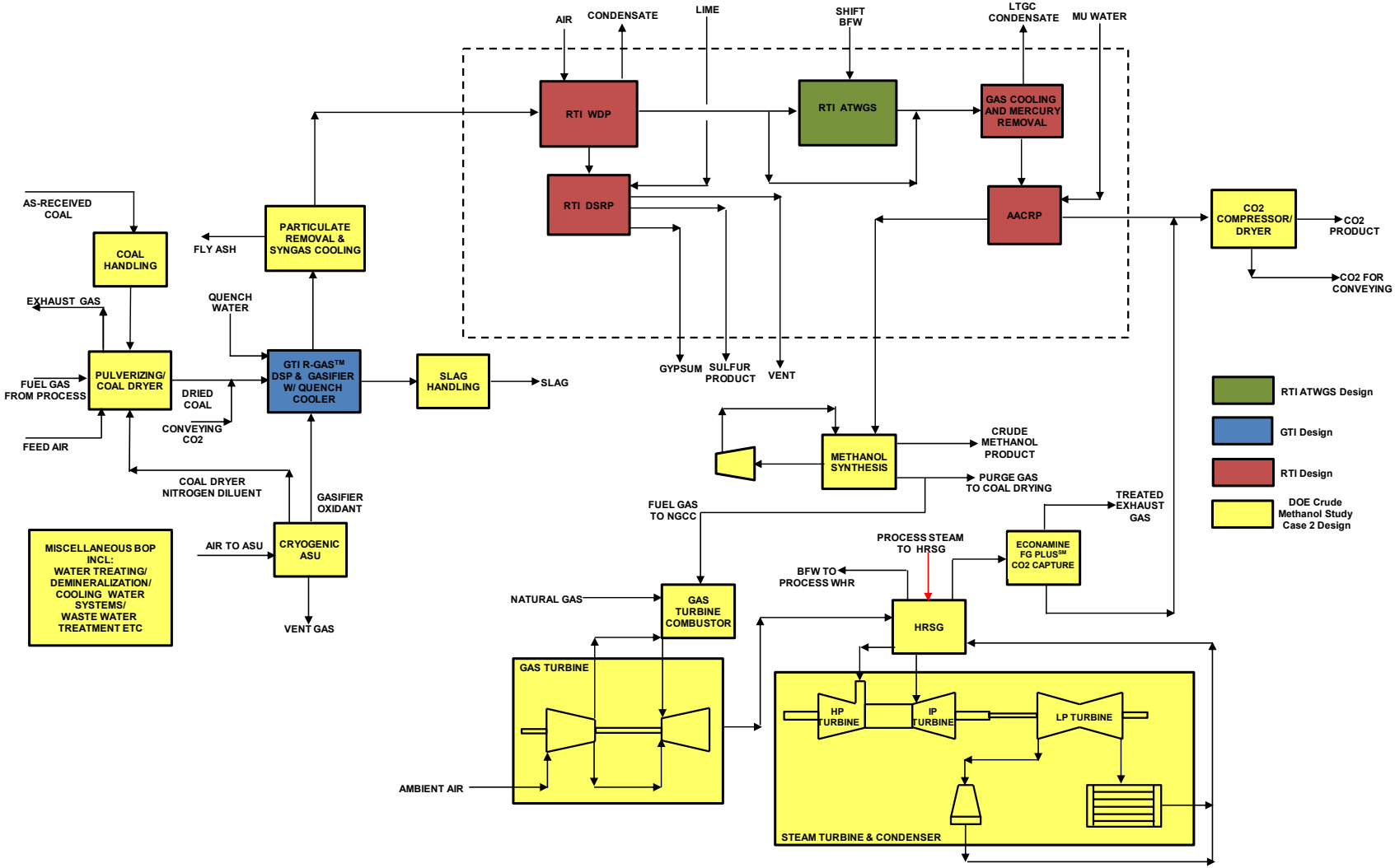

7.3 NOVEL TECHNOLOGY BASIS

7.3.1 Heat and Material Balance

Nexant carried out a simulation of the CTM cases on ASPEN Plus to obtain the HMB. The detailed sets of HMB helped to establish a better estimation of the overall plant utility balance, including process waste heat recovery, generation from the power cycle, as well as cooling water load breakdown, all of which lead to determine the overall CTM plant performance with more consistency among the various schemes.

In the DE-FE0012066 study, Nexant provided GTI and RTI with the benchmark design's stream conditions and flows to the gasification and syngas cleanup units respectively in the previous study. Using these as inputs into their models, GTI and RTI determined the HMB around their respective process systems, overall utilities consumption, and equipment sizes. These outputs were then transmitted as inputs into Nexant's CTM simulation to complete the modeling of Case 2b.

7.3.2 GTI R-GAS™ Gasifier and Feed System

For the Case 2e CTM plant, the specifications of the GTI R-GAS™ gasifier and DSP are the same as Case 2b. The same information from AR for Case 2b was used in modeling Case 2e.

7.3.3 RTI WDP System

RTI provided Nexant with the major stream flows and conditions into, within, and out of their proprietary advanced syngas cleanup process and AACRP, enabling Nexant to integrate these processes into its model. For cost estimations of RTI's advanced syngas cleanup and AACRP, RTI provided Nexant with their turnkey costs that are based on actual cost data from the pilot plant and 50 MW pre-commercial demonstration plant constructions. RTI also provided Nexant with a list containing the advanced syngas cleanup and AACRP systems' utilities and consumables rates. These were used as inputs to establish the overall CTM plant performance, TPC and variable operating costs for Case 2b. The same information from RTI for these systems was used in modeling Case 2e.

7.3.4 RTI ATWGS System

For Case 2e, RTI developed a HMB for a system that included both the ATWGS and LTGC processes. For this system, RTI designed the ATWGS process such that the composition, temperature and pressure of the inlet and outlet streams were identical to those in Case 2b. RTI provided Nexant with the major stream flows and conditions into, within, and out of their system that included both the ATWGS and LTGC systems. For cost estimations of the ATWGS system, RTI provided Nexant with the costs of the overall ATWGS system. RTI also provided Nexant with a list containing the ATWGS system's utilities and consumables rates, which were used as inputs to establish the overall CTM plant performance, TPC and variable operating costs for Case 2e.

7.3.5 Other Systems

The costs for the remaining CTM plant systems that are not directly related to the GTI R-GAS™, RTI advanced syngas cleanup, ATWGS and AACRP systems are developed by Nexant, as done in the previous study.

7.4 SITE-RELATED CONDITIONS

The CTM plant in this study is assumed to be located in a generic, Midwestern USA site, with site-related conditions as shown below:

- Location — Greenfield, Midwestern USA
- Elevation, ft above sea level — 0
- Topography — Level
- Size, acres — 300
- Transportation — Rail
- Ash/slag disposal — Off Site
- Water — Municipal (50%)/Groundwater (50%)
- Access — Landlocked, having access by train and highway
- CO_2 disposition — Compressed to 2,215 psia at battery limit before being transported 50 miles for sequestered in a saline formation at a depth of 4,055 ft (Study scope limited to delivery at battery limit only)

7.5 METEOROLOGICAL DATA

Maximum design ambient conditions for material balances, thermal efficiencies, system design and equipment sizing are:

- Barometric pressure, psia — 14.696
- Dry bulb temperature (DBT) — 59 °F
- Wet bulb temperature (WBT) — 51.5 °F
- Ambient relative humidity, % — 60

7.6 FUEL PROPERTIES

7.6.1 Coal Characteristics

Design coal feed to the CTM power plants is Montana PRB subbituminous coal with the same characteristics as those presented earlier in Table 2-2. The as-received coal is dried to 6% moisture with heat provided by burning the purge gas from the methanol synthesis process and other process generated fuel gas in an incinerator using air as the oxidant. The hot incinerator flue gas is mixed with N_2 from the ASU and recycle exhaust gas to maintain a drying gas to dry the coal.

7.6.2 Natural Gas Characteristics

The natural gas composition used in this analysis, representative of natural gas after going through standard midstream processing, is presented in Table 7-3.

Table 7-3
Natural Gas Composition

Compositions:		Volume Percentage
Methane	CH_4	93.1
Ethane	C_2H_6	3.2
Propane	C_3H_8	0.7
n-Butane	C_4H_{10}	0.4
Carbon Dioxide	CO_2	1.0
Nitrogen	N_2	1.6
	Total	100.0
LHV, Btu/lb		20,410
LHV, Btu/scf		932
HHV, Btu/lb		22,600
HHV, Btu/scf		1,032

7.7 CO_2 PRODUCT TREATING AND PURIFICATION DESIGN CRITERIA

Similar to the IGCC cases, recovered CO_2 is delivered at the B/L, with specifications listed earlier in Table 2-3 for saline reservoir sequestration per the QGESS *CO_2 Impurities Design Parameters* document.

7.8 POWER GENERATION & AUXILIARY LOADS

The DOE Crude Methanol Study provided a breakdown of the Case 2 (Shell Gasification-based CTM Plant with CO_2 Capture) auxiliary loads, as well as power generation by the NGCC plant. For the power generation portion of the cases studied in the current TEA, Nexant provided a revision using its natural gas combined cycle model, which takes into account the power requirement of the entire plant, process steam generated in the CTM island, as well as steam consumptions in both the CTM and power islands. Auxiliary loads are estimated, wherever applicable, by pro-rating from the DOE Crude Methanol Study Case 2 using relevant scaling parameters obtained from the model's heat and material balance.

Table 7-4 shows the power production and auxiliary load breakdown of the original DOE Crude Methanol Study Case 2, which Case 2a of this study is modeled upon and benchmarked against. For reference purposes, the scaling parameters are also shown in the table.

The GTI R-GAS™ gasification system and RTI advanced syngas cleanup and AACRP systems have different auxiliary loads that are not scalable with some of the loads specified in the DOE Methanol Study Case 2. GTI and RTI provided the auxiliary loads for these systems and these were used directly as inputs to the auxiliary load calculation.

Table 7-4
DOE Crude Methanol Study Case 2 Auxiliary Load and Power Production Summary

Power Cycle Power Generation	Electrical Load, kWe	Scaling Capacity
Gas Turbine Power	113,700	*Calculated from Model*
Steam Turbine Power	276,400	*Calculated from Model*
Total	390,100	
CTM Auxiliary Load Description	**Electrical Load, kWe**	**Scaling Capacity**
Coal Handling & Milling	9,090	As Received Coal
Slag Handling	1,940	Slag Flow
Air Separation Unit	179,940	Oxygen Production
Syngas Recycle Compressor	6,600	Recycle Syngas Flow
Incinerator Air Blower	2,680	Incinerator Air Flow
Direct-Fired Boiler Air Blower	310	Direct Fired Boiler Air Flow
Flash Bottoms Pump	720	Flash Bottoms Flow
Scrubber Pumps	1,070	Scrubber Flow
Rectisol® Auxiliary	51,270	*Calculated from Vendor Data*
Claus Plant Auxiliary	250	Sulfur Flow
CO_2 Compressor Auxiliary	68,820	CTM CO_2 Product Flow
Syngas Compressor	20,760	Syngas Flow to Methanol Unit
Recycle Gas Compressor	3,370	Recycle Gas Flow
Water Treatment	3,530	Total Wastewater + MU Water Flow
Air Cooler Fans	1,800	Gas Cooling Duty
Circulating Water Pump	9,430	CTM Circulating Water Flow
Boiler Feed Water Pump	1,500	CTM BFW Flow
Cooling Tower Fans	510	CTM Cooling Duty
Steam Turbine Auxiliaries	100	CTM Steam Turbine Production
Miscellaneous BOP	5,000	Fixed
TOTAL CTM AUXILIARIES, kWe	368,690	
Power Cycle Auxiliary Load Description	**Electrical Load, kWe**	**Scaling Capacity**
Condensate Pumps	210	*Calculated from Model*
Boiler Feedwater Pumps	3,910	*Calculated from Model*
Amine System Auxiliaries	3,000	CO_2 Product Flow
NGCC CO_2 Compression	4,800	CO_2 Product Flow
Circulating Water Pump	3,730	*Calculated from Model*
Ground Water Pumps	350	Ground Water Flow
Cooling Tower Fans	2,030	Power Cycle Cooling Duty
SCR	10	Fixed
Gas Turbine Auxiliaries	700	Gas Turbine Output
Steam Turbine Auxiliaries	100	Steam Turbine Output
Miscellaneous BOP	500	Fixed
Transformer Losses	2,140	Power Cycle Gross Output
POWER CYCLE AUXILIARIES, kWe	21,480	
NET PLANT POWER, kWe	-70	

7.9 RAW WATER SUPPLY

Raw water makeup is assumed to be provided 50% by a publicly owned treatment works and 50% from groundwater.

7.10 ENVIRONMENTAL DESIGN TARGETS

The environmental limits presented in this section refer to the gasification/power cycle only, because the environmental requirements for the methanol plant are considered beyond the scope of the study.

The environmental targets for the study were considered on a technology- and fuel-specific basis. Since all the cases are located at a greenfield site, permitting a new plant would involve the New Source Review (NSR) permitting process. The NSR process requires installation of emission control technology, meeting either the best available control technology (BACT) determinations for new sources located in areas meeting ambient air quality standards, or the lowest achievable emission rate (LAER) technology for sources located in areas that do not meet ambient air quality standards. This CTM TEA uses the BACT guidelines, summarized in Table 7-5.

Table 7-5
BACT Environmental Design Basis

Pollutant	**Control Technology**	**Limit**
Sulfur Oxides (SO_2)	Rectisol® + Claus Plant/ Econamine Plus FG Plus^{SM}	≤ 0.050 lb/MMBtu
Nitrogen Oxides (NOx)	Low NOx Burner (LNB) and N_2 Dilution primarily with humidification as needed	15 ppmvd (@ 15% O_2)
Particulate Matter (PM)	Cyclone/Barrier Filter/Wet Scrubber/AGR Absorber	0.006 lb/MMBtu
Mercury (Hg)	Activated Carbon Bed	95% removal

Total air pollutants in all vents must meet the above specifications even if atmospheric venting is minimal.

7.11 OTHER SITE SPECIFIC REQUIREMENTS

These follow the requirements specified previously in Section 2.11.

7.12 CTM PLANT CAPITAL COST ESTIMATION METHODOLOGY

7.12.1 General

For the CTM plants with CO_2 capture, the DOE Crude Methanol Study provided the code of accounts and grouped into 14 major systems. The cost methodology here is the same as the IGCC cases except for the different reference used.

Table 7-6 shows the code of accounts for the CTM plant, as derived from the DOE Crude Methanol Study. These systems are further broken down to include the various subsystems. The scaling parameters for the subsystems are also shown in this table.

Table 7-6
Code of Accounts for Report CTM Plant

Acct No.	Item/Description	Scaling Parameter
1	COAL & SORBENT HANDLING	
1.1	Coal Receive & Unload	Coal Feed Rate
1.2	Coal Stackout & Reclaim	Coal Feed Rate
1.3	Coal Conveyors & Yard Crush	Coal Feed Rate
1.4	Other Coal Handling	Coal Feed Rate
1.9	Coal & Sorbent Handling Foundations	Coal Feed Rate
2	COAL & SORBENT PREP & FEED	
2.1	Coal Crushing & Drying	Coal Feed Rate
2.2	Prepared Coal Storage & Feed	Coal Feed Rate
2.3	Dry Coal Injection System	Calculated
2.4	Misc Coal Prep & Feed	Coal Feed Rate
2.9	Coal & Sorbent Feed Foundation	Coal Feed Rate
3	FEEDWATER & MISC. BOP SYSTEMS	
3.1	Feedwater System	BFW (HP only)
3.2	Water Makeup & Pretreating	Raw Water Makeup
3.3	Other Feedwater Subsystems	BFW (HP only)
3.4	Service Water Systems	Raw Water Makeup
3.5	Other Boiler Plant Systems	Raw Water Makeup
3.6	FO Supply Sys and Nat Gas, incl Pipeline	Coal Feed Rate
3.7	Waste Treatment Equipment	Raw Water Makeup
3.8	Misc Power Plant Equipment	Gross Power Output
4	GASIFIER & ACCESSORIES	
4.1	Gasifier, Syngas Cooler & Auxiliaries	Syngas Throughput
4.3	ASU/Oxidant Compression	O_2 Production
4.4	LT Heat Recovery & FG Saturation	Syngas Flow
4.6	Flare Stack System	Syngas Flow
4.9	Gasification Foundations	Syngas Flow
5A	GAS CLEANUP & PIPING	
5A.1	Rectisol® System	Gas Flow to AGR
5A.2	Elemental Sulfur Plant	Sulfur Production
5A.3	Mercury Removal	Hg Bed Carbon Fill
5A.4a	COS Hydrolysis	COS Catalyst
5A.4b	Shift Reactors	WGS Catalyst
5A.5	Pressure Swing Adsorption System	Syngas Flow
5A.6	Blowback Gas System	Syngas Flow
5A.7	Fuel Gas Piping	Fuel Gas Flow
5A.9	HGCU Foundations	Sulfur Production
5B	CO_2 REMOVAL & COMPRESSION	
5B.1	NGCC CO_2 Removal System	NGCC CO_2 Flow
5B.2	CO_2 Compression & Drying	Total CO_2 Product
5C	METHANOL PRODUCTION	
5C.1	Methanol Synthesis	Methanol Product

Acct No.	Item/Description	Scaling Parameter
6	COMBUSTION TURBINE/ACCESSORIES	
6.1	Combustion Turbine Generator	Natural Gas Flow
6.9	Combustion Turbine Foundations	Natural Gas Flow
7	HRSG, DUCTING & STACK	
7.1	Heat Recovery Steam Generator	HRSG Area
7.2	HRSG Accessories	HRSG Area
7.9	HRSG, Duct & Stack Foundations	Vol Flow to Stack
8	STEAM TURBINE GENERATOR	
8.1	Steam TG & Accessories	Turbine Capacity
8.2	Turbine Plant Auxiliaries	Turbine Capacity
8.3a	Condenser & Auxiliaries	Condenser Duty
8.3b	Air Cooled Condenser	Condenser Duty
8.4	Steam Piping	BFW (HP Only)
8.9	TG Foundations	Turbine Capacity
9	COOLING WATER SYSTEM	
9.1	Cooling Towers	Cooling Tower Duty
9.2	Circulating Water Pumps	Circ H_2O Flow Rate
9.3	Circ. Water System Auxiliaries	Circ H_2O Flow Rate
9.4	Circ Water Piping	Circ H_2O Flow Rate
9.5	Makeup Water System	Raw Water Makeup
9.6	Component Cooling Water System	Circ H_2O Flow Rate
9.9	Circ. Water System Foundations	Circ H_2O Flow Rate
10	ASH/SPENT SORBENT HANDLING SYS	
10.1	Slag Dewatering & Cooling	Slag Production
10.6	Ash Storage Silos	Slag Production
10.7	Ash Transport & Feed Equipment	Slag Production
10.8	Misc. Ash Handling System	Slag Production
10.9	Ash/Spent Sorbent Foundation	Slag Production
11	ACCESSORY ELECTRIC PLANT	
11.1	Generator Equipment	Turbine Capacity
11.2	Station Service Equipment	Auxiliary Load
11.3	Switchgear & Motor Control	Auxiliary Load
11.4	Conduit & Cable Tray	Auxiliary Load
11.5	Wire & Cable	Auxiliary Load
11.6	Protective Equipment	Auxiliary Load
11.7	Standby Equipment	Total Gross Output
11.8	Main Power Transformers	Total Gross Output
11.9	Electrical Foundations	Total Gross Output
12	INSTRUMENTATION & CONTROL	
12.4	Other Major Component Control	Auxiliary Load
12.6	Control Boards, Panels & Racks	Auxiliary Load
12.7	Computer & Accessories	Auxiliary Load
12.8	Instrument Wiring & Tubing	Auxiliary Load
12.9	Other I & C Equipment	Auxiliary Load
13	IMPROVEMENT TO SITE	
13.1	Site Preparation	Accounts 1-12
13.2	Site Improvements	Accounts 1-12
13.3	Site Facilities	Accounts 1-12

Acct No.	Item/Description	Scaling Parameter
14	BUILDING & STRUCTURES	
14.1	Combustion Turbine Area	Gas Turbine Power
14.2	Steam Turbine Building	Accounts 1-12
14.3	Administration Building	Accounts 1-12
14.4	Circulation Water Pumphouse	Circ H_2O Flow Rate
14.5	Water Treatment Buildings	Raw Water Makeup
14.6	Machine Shop	Accounts 1-12
14.7	Warehouse	Accounts 1-12
14.8	Other Buildings & Structures	Accounts 1-12
14.9	Waste Treating Building & Structures	Raw Water Makeup

As Table 7-6 is based on Case 2 of the DOE Crude Methanol Study, it does not necessarily have account and/or subaccount numbers for the advanced technologies being evaluated in this study. To support a more direct comparison of these advanced technologies with the existing commercial technologies, the advanced technologies were assigned the same account and/or subaccount numbers as the existing commercial technologies that they are most analogous to. For technologies without a defined account number, one was created. Because one of the technologies of interest for this TEA is WGS, a special subaccount number was created. The necessity of heat extraction for WGS systems for CO-rich coal-derived syngas demands incorporation of heat exchangers into the overall WGS system. A special subaccount number for WGS (5A.4c) that combines the costs from DOE's sub account numbers 4.4 (LT Heat Recovery and FG Saturation) and 5A.4b (Shift Reactors) was created to provide the best means to effectively capture the overall costs for all the equipment needed to support the WGS process and enable effective comparisons across the cases. Table 7-7 provides a list of the advanced technologies evaluated in this study and their associated account numbers.

Table 7-7
Code of Accounts for Advanced Technologies being Evaluated

Account Number	Title	Advanced Technology
2.3	Dry Coal Injection System	GTI DSP
4.1	Gasifier, Syngas Cooler & Auxiliaries	GTI R-GAS™ Gasifier
5A.1	AACRP	AACRP
5A.2	RTI DSRP	RTI DSRP
5A.4a	RTI WDP System	RTI WDP
5A.4c	LT Heat Recovery, FG Saturation & Shift Reactors	AFWGS/ATWGS

7.12.2 Home Office, Engineering Fees and Project/Process Contingencies

The estimation of these costs for the CTM plants follow the same methodology as outlined in Section 2.12.5 except that factors from the DOE Crude Methanol Study Case 2 are used.

7.12.3 Owner's Cost

The calculation of the CTM plant's owner's cost follow the same guidelines specified in Section 2.12.6.

7.13 OPERATION & MAINTENANCE COSTS

The CTM plant O&M costs pertain to those charges associated with operating and maintaining these plants over their expected life. These costs include:

- Operating labor
- Maintenance – material and labor
- Administrative and support labor
- Consumables
- Fuel
- Waste disposal

There are two components of O&M costs; fixed O&M, which is independent of methanol production, and variable O&M, which is proportional to methanol production. Variable O&M costs were estimated based on 90% CF.

7.13.1 Fixed Costs

Operating labor cost was determined based on the number of operators required to work in the plant. Other assumptions used in calculating the total fixed cost include:

- 2011 base hourly labor rate, $/hr $39.7
- Length of work-week, hrs 50
- Labor burden, % 30
- Administrative/support labor, % O&M labor 25
- Maintenance material + labor, % TPC 2.4
- Maintenance labor only, % maintenance material + labor 40
- Property taxes and insurances, % TPC 2

7.13.2 Variable Costs

The cost of consumables, including fuel, was determined based on the individual rates of consumption, the unit cost of each specific consumable commodity, and the plant annual operating hours. Waste quantities and disposal costs were evaluated similarly to the consumables.

The unit costs for major consumables and waste disposal was selected from DOE Crude Methanol Study Case 2, QGESS *Updated Costs (June 2011 Basis) for Selected Bituminous Baseline Cases* and from the QGESS *Fuel Prices for Selected Feedstocks in NETL Studies* document.

The 2011 as-delivered coal price for the Midwestern, USA CTM plant is $36.57/ton, per the QGESS *Fuel Prices for Selected Feedstocks in NETL Studies* document. The 2011 natural gas price delivered to the same plant is $6.13/MMBtu (HHV).

7.13.3 CO_2 Transport and Storage Costs

As specified in the DOE Crude Methanol Report, the CO_2 T&S cost used for the Midwestern CTM plant is $11/tonne. Per the TEA reporting requirements, the methanol required selling price (RSP) for the CTM plants are reported both with and without CO_2 T&S costs.

7.14 FINANCIAL MODELING BASIS

7.14.1 Required Selling Price (RSP)

The figure-of-merit used to evaluate the CTM plant's overall financial performance is the methanol RSP, expressed in $/gal of crude methanol. All costs are expressed in "first-year-of-construction" year dollars, and the resulting RSP is also expressed in "first-year-of-construction" year (2011) dollars.

RSPs for each case are calculated assuming: (i) a financial structure representative of a commercial fuels project, and (ii) a financial structure with loan guarantees or other government subsidies. The financial assumptions and structures used to estimate the RSPs are shown in Table 7-8.

Table 7-8
Financial Assumptions for Methanol RSP Calculation

Parameter	Value	
TAXES		
Income Tax Rate	38% (Effective, 34% Federal , 6% State)	
Capital Depreciation	20 years, 150% declining balance	
Investment Tax Credit	None	
Tax Holiday	None	
FINANCING TERMS		
Repayment Term of Debt	30 years	
Grace Period on Debt Repayment	None	
Debt Reserve Fund	None	
TREATMENT OF CAPITAL COSTS		
Capital Cost Escalation During Construction (nominal annual rate)	3.6%	
Distribution of Total Overnight Capital over the Capital Expenditure Period (before escalation)	5 Year Period: 10%, 30%, 25%, 20%, 15%	
Working Capital	Zero for all parameters	
% of Total Overnight Capital that is Depreciated	100%	
INFLATION		
RSP, O&M, Fuel Escalation (nominal annual rate)	3.0% RSP, O&M, COE, Fuel	
FINANCIAL STRUCTURE (COMMERCIAL FUELS PROJECTS)		
Type of Security	**Percent of Total**	**Current (Nominal Dollar Cost)**
Debt	50	8% (LIBOR = 3.5% + 4.5%)
Equity	50	20%
FINANCIAL STRUCTURE (LOAN GUARANTEE PROJECTS)		
Type of Security	**Percent of Total**	**Current (Nominal Dollar Cost)**
Debt	60	4.56% (CMT = 4.34% + 0.22%)
Equity	40	20%

The simplified, capital charge factor (CCF)-based financial modeling methodology is used in the CTM cases to calculate methanol product RSP. The CCFs used in evaluating the COE were pre-calculated using the NETL PSFM and are 0.218 and 0.170 for the commercial fuels and loan guarantee finance structures respectively. These are valid only for the global economic assumptions listed in Table 7-8, the stated finance structures (commercial fuels and loan guarantees), and the stated capital expenditure period (5 years).

The simplified equation used to calculate methanol product RSP is shown in the equation below:

$$RSP = \frac{\text{first year capital charge} + \text{first year fixed operating costs} + \text{first year variable operating costs}}{\text{annual gallons of crude methanol produced}}$$

$$RSP = \frac{(CCF)(TOC) + OC_{fix} + (CF)(OC_{var})}{(CF)(gal/yr\ MeOH)}$$

where:

CCF = Capital Charge Factor

TOC = Total Overnight Cost

OC_{fix} = Fixed Operating Cost

CF = Capacity Factor

OC_{var} = Variable Operating Cost

7.14.2 CO_2 Sales Price

Sensitivity analysis is done to determine the impact of CO_2 sales on CTM plant's RSP. The varying parameter is the CO_2 sales price at the CTM plant gate and ranges between \$0/tonne (baseline case assuming no value to the product CO_2) and \$60/tonne.

The formula used to calculate the revised RSP after taking into account CO_2 sales is shown below:

$$RSP_{CO_2Sales} = Baseline\ RSP - \frac{(CO_2\ Sales\ Price) \times annual\ tonnes\ of\ CO2\ product}{annual\ gallons\ of\ crude\ methanol\ produced}$$

7.14.3 Cost of CO_2 Emissions

The TEA also requires sensitivity analysis on cost of CO_2 emissions to be performed. The varying parameter is the CO_2 emissions cost. The range of the emissions cost is between \$0/tonne (baseline case assuming no CO_2 emissions cost) and \$60/tonne.

The formula used to calculate the revised RSP after taking into account the cost of CO_2 emissions is shown below:

$$RSP_{CO_2Emissions} = Baseline\ RSP + \frac{(Cost\ of\ CO_2\ Emissions)\ x\ annual\ tonnes\ of\ CO_2\ emitted}{annual\ gallons\ of\ crude\ methanol\ produced}$$

7.14.1 Cost of CO_2 Captured/Avoided

As the CO_2 sales price increases, the methanol RSP values decrease and approach the without-capture RSP values. The cost of CO_2 captured can be interpreted as the breakeven plant gate sale price where the cost of capture equals the revenue generated by selling the recovered CO_2.

As the task of modeling the corresponding non-capture CTM plants is out of this study's scope, a simplified calculation is used to estimate each non-capture plant's methanol product RSP. In this calculation, it is assumed that the only differences between the non-capture and capture plants are the elimination of the CO_2 compression and the NGCC post-combustion CO_2 capture (PCC) systems. The resulting non-capture CTM plant still uses the same amount of coal and natural gas fuel but directly vents the NGCC flue gas and captured CO_2 from the process AGR unit.

The capital costs associated with these systems are eliminated, reducing the overall plant CAPEX. Additionally, the auxiliary power demands of these systems are also eliminated, resulting in a CTM plant with more power export to the grid. Both of these factors yield a lower methanol RSP for the non-capture CTM plant.

The cost of CO_2 captured is defined as the plant gate CO_2 sale price where each capture case equals its corresponding without-capture RSP, ***excluding CO_2 TS&M costs.*** The cost of CO_2 avoided has the same definition, except that it ***includes CO_2 TS&M costs***. Based on this definition, the cost of CO_2 avoided is always greater than the cost of CO_2 captured.

Section 8 Case 2a: Shell with Rectisol® AGR CTM Plant

The Case 2a process descriptions, performance and cost results in this section were previously presented in Nexant's DE-FE0012066 CTM report. They are reproduced here for the reader's ease of reference.

8.1 PROCESS OVERVIEW

The conversion of coal-to-methanol is a two-step process: first conversion of the coal to the appropriate quality syngas via gasification and applying the water-gas shift reaction, and second, converting the syngas to methanol by catalytic conversion.

Syngas is generated in the Case 2a reference plant from the gasification of PRB coal in a high-pressure, oxygen-blown Shell quench-type gasifier. The high temperature entrained-bed gasifier uses a partial water quench and syngas cooler to cool the hot syngas stream and generate steam for the water-gas shift reactors and power generation. Crude raw syngas (post-quench) from the gasification unit is scrubbed and split into two streams. The first stream is fed to a sour water-gas shift reactor to increase the hydrogen content so that a hydrogen/carbon monoxide (H_2/CO) molar ratio of 2:1 in the feed stream to the methanol synthesis reactor can be achieved, while the second stream bypasses the shift reactors. The streams are combined downstream to achieve the desired composition. The partial bypass mode of operation allows the shift reactor to operate at a higher conversion ratio resulting in a smaller size. The syngas is cooled in a low-temperature heat recovery system and then cleaned of mercury in a fixed-bed reactor. Sulfur and CO_2 are removed from the syngas via the two-stage Rectisol® process in preparation for methanol synthesis. The treated syngas is fed into fixed-bed methanol synthesis reactors to generate methanol.

As with Case 2 in the DOE Crude Methanol Study, the Case 2a reference plant uses an NGCC to generate sufficient power to meet the auxiliary loads and make the plant power neutral. Consequently, the Case 2a reference plant uses both coal and natural gas in the production of methanol and has the necessary processes to capture more than 90% of the carbon in the coal and natural gas.

The Case 2a reference plant is assumed to operate with an annual on-stream CF of 90% or 7,884 hr/year at full capacity.

8.2 CTM PLANT COMMON PROCESS AREAS

As shown in Figure 7-1 in Section 7.2.1, the Case 2a reference plant consists of the following major process and/or utility blocks. Some of these blocks, or process areas, are common to the Case 2b and 2e plant configurations. These common process areas are in bold and italicized.

- ***Coal Sizing Handling***
- ***Coal Prep, Drying***
- ***Feed Water & Miscellaneous BOP Systems***
- ***Air Separation Unit (ASU)***

- Dry Coal Feed & Shell SCGP Gasifier System
- Syngas Cooling (Quench, Scrubbing, Steam Generation)
- Gas Cleaning (Filters, WGS & AGR)
- ***Mercury Removal***
- CO_2 Compression and Purification Facilities
- Sulfur Plant
- ***Methanol Reactor and Synthesis Loop***
- ***Natural Gas Combined Cycle (NGCC)***
- ***HRSG, Ducting and Stack***
- ***Cooling Water Systems***
- ***BFW/Condensate System***
- ***Slag Recovery and Handling***
- ***Accessory Electric Plant***
- ***Instrumentation and Control***

The common areas are presented in brief here for general background information, and to avoid unnecessary repetition in the other cases. Detailed descriptions of these process areas can be found in Section 3.3 of the DOE Crude Methanol Study. Where there is case specific performance information, these features are presented in the relevant case sections.

8.2.1 Coal Milling, Grinding and Drying

The Shell process uses a dry feed system that is sensitive to the coal moisture content. For coal to flow smoothly through the lockhoppers that pressurize coal to the gasifier, the coal's surface moisture must be removed. The PRB coal used in this study contains 25.77% total moisture on an as-received basis. It is dried to 6% moisture for smooth flow through the dry feed system. The coal is simultaneously crushed and dried in the coal mill, then delivered to a surge hopper.

PRB coal is delivered to the site by 100-ton rail cars. It is unloaded into two receiving hoppers and fed to the vibratory feeder. It is then transferred through intermediate hoppers and silos to the coal crusher where it is reduced to 1-1/4" x 0 size.

8.2.2 Coal Preparation and Drying

The Shell process uses a dry feed system that is sensitive to coal moisture content. It was assumed that the coal must be dried to 6% moisture to allow for smooth flow through the dry feed system before feeding into the Shell entrained-flow gasifier. This moisture content is considered compatible with the storage, transport and feed injection requirements for the Shell entrained-flow gasifier.

The drying heat is provided by burning tail-gas from the Claus plant, flash gas and purge gas from the methanol synthesis process in an incinerator with air as the oxidant. In Nexant's simulation of the coal drying process, it was noted that after combining these fuel streams, there was still insufficient heat in Case 2a to dry the PRB coal from 25.77% to 6% moisture. Supplemental natural gas therefore had to be fired to provide the remaining heat to dry the coal sufficiently.

The hot incinerator flue gas mixes with nitrogen from the ASU and a portion of the dryer exhaust gas in order to maintain a drying gas temperature of less than 500ºF with oxygen content lower than 8%.

8.2.3 Air Separation Unit

All cases include an ASU for generating oxygen. The ASU is a conventional, cryogenic, pumped liquid oxygen (LOX) unit that provides oxygen for the gasification process, as well as nitrogen for ancillary equipment. The ASU is designed to produce 95 mol% oxygen (O_2) for use in the gasifier and Claus plant. The air compressor is powered by an electric motor. Nitrogen is recovered and used as a diluent for coal drying, as described earlier in 8.2.2.

The battery limit conditions for the ASU products are summarized below:

Table 8-1
ASU Product Conditions

ASU Product	Pressure, psia	Temperature, ºF
95% O_2	23.2	55
Diluent N_2	14.7	63
ASU Vent	16.4	64

8.2.4 Mercury Removal

Mercury removal is achieved by a packed bed of sulfur-impregnated activated carbon operating at 105ºF. This packed-bed vessel is located upstream of the sulfur recovery unit with 20-second superficial gas residence time to achieve more than 90% removal of mercury in addition to removal of some portion of other volatile heavy metals such as arsenic. Mercury-removal systems using sulfur-impregnated activated carbon downstream of a coal gasifier have a reported bed life of 18 to 24 months, and usually replacement is required due to fouling of the bed rather than mercury saturation.

8.2.5 Slag and Ash Handling

Slag material drains from the gasifier into a water bath at the bottom of the gasifier vessel. The slag-water slurry is transferred to a slag crusher where the slag is crushed into pea size fragments. The slurry containing 5 to 10% solids is then transferred to a dewatering bin through a lockhopper. The separated water is clarified and reused as makeup to the water scrubber. The dried slag is stored for disposal.

8.2.6 Methanol Reactor and Synthesis Loop

The methanol synthesis route chosen for this study is the vapor-phase methanol process based on the breadth of operating experience with vapor-phase production units. The methanol reactor converts H_2 and CO to methanol in a packed-bed of catalyst. The primary side reactions produce ethanol, propanol and formaldehyde.

CO_2-lean syngas containing 2-3% CO_2 with a H_2/CO ratio of 2:1 from the AGR process is compressed to the synthesis loop operating pressure of 755 psia in a syngas compressor. The compressed syngas is mixed with recycled gas, heated to 400ºF, and routed to the methanol reactor. The reactor is steam cooled to facilitate near isothermal operation at 475ºF and 735 psia. In-line blowers, coolers and knock-out drums are used within the synthesis loop to maintain pressure and remove crude methanol.

In order to promote continuous production, the methanol reactor effluent is cooled to condense out the crude methanol that is removed in a phase separator. About 96% of the separated gas is compressed to reactor pressure and recycled along with fresh syngas to the methanol reactor. This recycling elevates the overall conversion of carbon, overcoming the low per-pass conversion of CO. A small purge gas stream (approximately 4%) is removed from the synthesis loop to limit the build-up of inert gas species. The purge gas is routed to the incinerator to be used as fuel for coal-drying.

8.2.7 Heat Recovery and Power Generation

Both the gasification and methanol synthesis processes generate a large amount of heat that can be recovered in the form of saturated steam, which is then used for either process requirements or power generation. The process steam is generated at three different pressure levels: high pressure (HP) steam at 2,415 psia, intermediate pressure (IP) steam at 360 psia and low pressure (LP) steam at 75 psia.

In the DOE Crude Methanol Study, auxiliary power demand for the Case 2 CTM plant with CO_2 sequestration is met by two Rolls-Royce Trent 60 natural gas-fired turbines, each generating about 60 MWe of power. An additional 276 MWe is produced from the steam cycle, which uses a single reheat (2,400 psig/1,050°F/1,050°F) cycle. However, in Nexant's simulation of the power cycle, it was determined that the gas turbine flue gas outlet temperature was not high enough to superheat/reheat all the steam raised in the gasification and methanol synthesis section for power generation in the steam turbine.

Nexant's model of the power cycle uses three GE MS6001B gas turbines, each producing a nominal 45 MWe, and is more similar in operation to the cases from the DOE/NETL-2011/1477 Report (*Cost and Performance Baseline for Fossil Energy Plants Volume 4: Coal-to-Liquids via Fischer-Tropsch Synthesis*).

A steam turbine was used to generate power from the steam generated in the HRSG and WHR systems. HP steam at 2,415 psia and 900 °F and IP steam at 360 psia and 750 °F are used in the HP and IP stages of the steam turbine for power generation. There is no IP reheat in the HRSG as the gas turbine flue gas exhaust temperature is not high enough. LP exhaust steam from the last steam turbine stage is condensed by splitting 50/50 to a surface condenser and an air-cooled condenser to conserve cooling water. The condensers operate at 0.698 psia with a corresponding condensing temperature of 90 °F.

The condensates are collected and sent to a deaerator to remove dissolved gases and treated to provide BFW for the steam generators.

In order to achieve an overall CO_2 capture rate greater than 90%, the NGCC exhaust gas leaving the HRSG, which contains CO_2 from the combustion of natural gas, has to be cooled before undergoing post-combustion capture. Fluor's Econamine FG Plus^{SM} process was used to capture 90% of the NGCC exhaust CO_2. The DOE/NETL 1397 report provides a more detailed description of this process.

8.2.8 Cooling Water Systems

Exhaust steam from the steam turbine is split 50/50 to a surface condenser cooled with cooling water and to an air-cooled condenser using ambient air and forced convection. The major impact of utilizing this parallel cooling method is a significant reduction in water requirement when compared to a wet cooling system.

The circulating water system is a closed-cycle cooling water system that supplies cooling water to the surface condenser to condense one-half of the main turbine exhaust steam. The system also supplies cooling water to the AGR plant as required, and to the auxiliary cooling system. The auxiliary cooling system is a closed-loop process that utilizes a higher quality water to remove heat from compressor intercoolers, oil coolers and other ancillary equipment and transfers that heat to the main circulating cooling water system in plate-and-frame heat exchangers. The heat transferred to the circulating water in the surface condenser and other applications is removed by a mechanical draft cooling tower.

The system consists of two 50% capacity vertical circulating water pumps, a mechanical draft evaporative cooling tower, and CS cement-lined interconnecting piping. The pumps are single-stage vertical pumps. The piping system is equipped with butterfly isolation valves and all required expansion joints. The cooling tower is a multi-cell wood frame counter-flow mechanical draft cooling tower.

8.2.9 BFW/Condensate System

The function of the boiler feed water (BFW) system is to pump the various BFW streams from the deaerator storage tank in the HRSG to the respective steam drums. Minimum flow recirculation to prevent overheating and cavitation of the pumps during startup and low loads is provided by an automatic recirculation valve and associated piping that discharges back to the deaerator storage tank. Pneumatic flow control valves control the recirculation flow. The BFW pumps are supplied with instrumentation to monitor and alarm on low oil pressure, or high bearing temperature. BFW pump suction pressure and temperature are also monitored. In addition, the suction of each pump is equipped with a startup strainer.

8.2.10 Water Balance

Water required for the operation of the facility is obtained from a source such as a lake, river, or well. If the quality of the water is adequate, raw water is used directly as makeup to the cooling tower and the gasifier quench. To meet the rest of the plant's water needs, makeup must be treated first by filtration to create service-quality water. This quality of water serves as makeup to the plant's potable water, demineralized water, fire water, and service water systems. Higher quality boiler feedwater is treated by a typical reverse osmosis and electrodeionization package.

Water rejected by the system is of an acceptable quality to be used as makeup to the cooling tower.

In addition to meeting the makeup water needs of the facility, water treatment systems must be capable of capturing and treating on-site waste streams. Wastewater created by the gasification process must pass through a number of pretreatment steps before being combined with other wastewater streams. Metals, ammonia, and suspended solids are removed from the stream through the use of a clarifier and a biological treatment unit. Once processed, the wastewater can be combined with the cooling tower blowdown as well as other plant waste streams in a final clarifier. Dechlorination and pH adjustment are performed as needed at this step of the process in order to meet all local discharge regulations. Solids separated out in this process are dried by means of a filter press and taken away for offsite disposal.

8.3 CASE 2a PROCESS DESCRIPTION

Case 2a is modeled upon process information provided in Case 2 of the Crude Methanol Report. The overall block flow diagram of the Case 2a reference plant is shown in Figure 8-1, with the accompanying stream flows shown in Table 8-2. Additional descriptions of the Case 2a plant's various processes are provided below. To better visualize the different unit operations in the CTM plant, simplified process flow diagrams (PFDs) of the various plant processes are depicted in Figure 8-2 through Figure 8-9. Table 8-3 through Table 8-10 provide the model-generated process data for the numbered streams referenced in the PFDs.

Coal Preparation and Drying

Coal receiving and handling is part of the Case 1a plant common areas and covered in Section 8.2.1. Coal is crushed in the coal mill and delivered to a surge hopper, which in turn delivers the coal to the coal pre-heater. The coal drying process, depicted in Figure 8-2 and described earlier in Section 8.2.2, reduces the PRB coal moisture content from 25.77 wt% to 6 wt%. The mass balances of the coal drying process are presented in Table 8-3.

Coal Feed System

The dried coal is drawn from the surge hoppers and fed through a pressurization lock hopper system to a dense phase pneumatic conveyor, which uses a stream of high pressure CO_2 (~800 psia) withdrawn from the CO_2 compressors to convey the coal to the gasifiers.

Air Separation Unit

The ASU process for the Case 2a reference plant is shown in Figure 8-3 with the gasification, quench and dry solid removal processes. The mass balance of this process is presented in Table 8-4.

The ASU's main air compressor is powered by an electric motor. Nitrogen is recovered and mainly used as a diluent in the coal drying process. A small, separate stream of nitrogen is compressed to be used as a stripping gas in the Rectisol® process.

Shell Gasifier

The gasification and quench processes are shown in Figure 8-3 and the mass balances are presented in Table 8-4. The stream numbers on the PFD correspond to the stream numbers in the mass balance tables.

Syngas is generated from the gasification of PRB coal in a high-pressure, oxygen-blown Shell quench-type gasifier. The high-temperature entrained-bed gasifier uses a partial water quench and syngas cooler to cool the hot syngas stream and generate steam for the water-gas shift reactors and power generation.

In the gasifier, the coal feedstock reacts with O_2 in a reducing environment to produce principally H_2 and CO with a small amount of CO_2. High-temperature heat recovery in each gasifier train is accomplished in three steps, including the gasifier membrane wall, which maintains a protective ash layer over the membrane wall. The product gas from the gasifier is cooled using a syngas recycle quench to lower the temperature below the ash melting point. Syngas then goes through a raw gas cooler, which lowers the gas temperature and contributes to the production of HP steam for use in the steam cycle.

The solids are removed as both slag and ash. Liquid slag is solidified in a water bath and removed via a lock hopper system. Ash carried over with the syngas is removed in a ceramic candle filter. The collected ash is also removed via a lock hopper system. The syngas scrubber downstream of the gasifier removes any possibility of remaining PM passing the candle filter further downstream, by protecting against leakage from the filter seals or any undetected candle breakage that would allow large particulates into the scrubber.

The design size used in this study requires the use of eight operating trains with one spare train for a total of nine gasifiers. The facility contains one spare gasifier train to allow operation at 90% CF and to generally improve availability. The spare gasifier train feeds into the same gas clean-up trains as the other gasifier trains so that start-up/operation is transparent to the downstream processes.

Dry Solids Removal and Wet Scrubbing

The raw syngas exiting the ceramic particulate filter enters the scrubber for removal of chlorides and any remaining particulates. The quench scrubber washes the syngas in a countercurrent flow in two packed beds, which removes essentially all traces of entrained particles. The bottoms from the scrubber are sent to the slag removal and handling system for processing.

The dry solid removal processes are shown in Figure 8-3 with the ASU, gasification and quench processes. The mass balance for this process is shown in Table 8-4. The wet scrubber is shown in Figure 8-4, along with the water-gas shift process and its mass balance is shown in Table 8-5.

Water-Gas Shift

The water-gas shift process is shown in Figure 8-4 and its material balance is shown Table 8-5. The stream numbers on the PFD correspond to the stream numbers in the mass balance table.

Coal-derived syngas from the wet scrubber enters the sour shift and cooling section. In order to achieve a 2:1 ratio of H_2 to CO in the final syngas to the methanol synthesis reactors, approximately 55 to 60 percent of the coal-derived syngas is shifted, with the remainder bypassing the shift reactors. Two shift reactors in series are used to achieve the desired H_2/CO composition in the syngas. Cooling is provided between the series of reactors to control the exothermic temperature rise. A gas-gas heat exchanger after the first WGS reactor is used to preheat the syngas prior to entering it, while also cooling the outlet gas before entering the second WGS reactor.

After the second-stage shift and subsequent cooling, the shifted syngas from the second-stage shift reactor outlet mixes with the bypass syngas and is further cooled before being sent to the downstream Rectisol® unit for sulfur and CO_2 removal.

Like the reference case in the DOE Crude Methanol Study, the Case 2a syngas leaving the first WGS reactor exceeds 900°F. It should be noted that this condition potentially leads to side reactions may deactivate the catalyst prematurely and change the product slate. Though not shown in this case, it may be necessary to inject additional steam, which will function as a heat carrier, to decrease the syngas temperature at the first WGS reactor outlet.

Low Temperature Gas Cooling and Mercury Removal

The low temperature gas cooling process, together with the mercury removal process, is shown in Figure 8-5 and its material balance is shown Table 8-6. The stream numbers on the PFD correspond to the stream numbers in the mass balance table.

Syngas is cooled in a number of steps to effectively recover heat to maximize efficiency. As the shifted syngas is cooled, IP and LP steam, process condensate and feed water are being heated.

Low pressure steam is used to strip NH_3 and other absorbed gases from the condensate in a sour water stripper. These stripped gases are sent to the Claus sulfur recovery unit to be treated with other sour gas streams. The stripped condensate mixes with process condensate separated from the syngas. The mixture is pumped and heated to about 390ºF before being fed into the wet scrubbers.

Mercury removal is achieved via an activated carbon process described earlier in Section 8.2.4.

Acid Gas Removal

The AGR and CO_2 compression processes are shown in Figure 8-6, while the material balance is shown in Table 8-7. The stream numbers labeled on the PFD correspond to the stream numbers in the material balance table.

The CTM plant removes both H_2S and CO_2 within the same process via the Rectisol® unit. The Rectisol® AGR process was specified primarily because the methanol synthesis catalyst requires an H_2S level below 100 parts per billion by volume (ppbv) in order to maintain an adequate catalyst lifetime.

The Rectisol® process uses chilled methanol as a solvent. For reasons mentioned in the previous DE-FE0012066 report, Nexant contacted Linde, licensor of the Rectisol® process, who agreed to provide the process' HMB for Case 2a.

In the Rectisol® process data provided by Linde, the CO_2 product stream has half the CO concentration or 3,000 ppmv compared with the CO_2 product in the Case 2 of the DOE Crude Methanol Study. This is still two orders of magnitude higher than the CO limit (35 ppmv) for saline reservoir CO_2 sequestration shown in Table 2-3, derived from the QGESS CO_2 Impurity Design Parameters document. However, from the same table, the CO concentration is within range stated in literature (10-5,000 ppmv) and is thus considered acceptable.

Linde also indicated that while the Rectisol® process' cost as reported in the DOE Crude Methanol Study is lower than its quotes, the estimate is still within range, after accounting for the cost being reported in 2011 dollars. For Case 2a, the Rectisol® unit's cost estimate uses the DOE Crude Methanol Study's Rectisol® cost.

CO_2 Compression

The CO_2 stream recovered from the Rectisol® unit is compressed to 2,215 psia in a multiple-stage, intercooled compressor to supercritical conditions. No drying is required since the CO_2 regenerated by the Rectisol® unit is free of water. Some CO_2 is withdrawn from this stream to be used for transporting the coal to the gasifier.

Sulfur Recovery Unit

The sulfur recovery unit (SRU) is shown in Figure 8-7, while the material balance is shown in Table 8-8. The stream numbers labeled on the PFD correspond to the stream numbers in the material balance table.

The purpose of the SRU is to treat the acid gas from the Rectisol® unit and sour gas streams from the sour water strippers to make an effluent gas acceptable for venting to the atmosphere or burning.

For this study, the SRU is a Claus bypass type SRU utilizing O_2 instead of air. The Claus plant produces molten sulfur by converting approximately one third of the H_2S in the feed to SO_2, then reacting the H_2S and SO_2 to sulfur and water. The combined Claus technology and tail gas recycle results in an overall sulfur recovery exceeding 99 percent. The liquid sulfur recovered goes to the sulfur pit, while the tail gas proceeds to the incinerator for coal drying.

Methanol Reactor and Synthesis Loop

The methanol synthesis process is shown in Figure 8-8, while the material balance is shown in Table 8-9. The stream numbers labeled on the PFD correspond to the stream numbers in the material balance table. The process follows the description stated earlier in Section 8.2.6.

In its correspondence with Nexant, Linde specified that a certain amount of makeup methanol is required for continued operation of the Rectisol® AGR process. To account for this, the makeup methanol quantity to the Rectisol® unit was debited against the gross crude methanol production from the methanol synthesis unit. The net methanol production from the plant is therefore the methanol synthesis unit's gross production rate less the Rectisol® makeup quantity.

NGCC

Nexant's model of the power cycle uses three GE MS6001B gas turbines, each producing a nominal 45MW, and is more similar in operation to the cases from the DOE/NETL-2011/1477 Report (*Cost and Performance Baseline for Fossil Energy Plants Volume 4: Coal-to-Liquids via Fischer-Tropsch Synthesis*).

A steam turbine was used to generate power from the steam generated in the HRSG and WHR systems. HP steam at 2,415 psia and 900 °F and IP steam at 360 psia and 750 °F are used in the HP and IP stages of the steam turbine for power generation. There is no IP reheat in the HRSG as the gas turbine flue gas is hot enough. LP exhaust steam from the last steam turbine stage is condensed by splitting 50/50 to a surface condenser and an air-cooled condenser to conserve cooling water. The condensers operate at 0.698 psia with a corresponding condensing temperature of 90 °F.

The PFD for the NGCC section is shown in Figure 8-9, while the material balance is shown in Table 8-10. The stream numbers labeled on the PFD correspond to the stream numbers in the material balance table.

Power Cycle Flue Gas Post Combustion CO_2 Capture and Compression

As mentioned in Section 8.2.7, Fluor's Econamine FG Plus^{SM} process was used to capture CO_2 from the flue gas leaving the NGCC HRSG. Unlike the Rectisol® unit's regenerated CO_2, the CO_2 leaving the Econamine FG Plus^{SM} capture process still contains moisture. It is thus compressed separately to 2,215 psia by a multi-stage, intercooled centrifugal compressor that is equipped with a thermal swing adsorptive dryer, which dehydrates the CO_2 stream to a dew point of -40ºF. The virtually moisture-free supercritical CO_2 stream is delivered to the plant B/L as sequestration ready.

Figure 8-1
Case 2a Reference Plant – Overall BFD

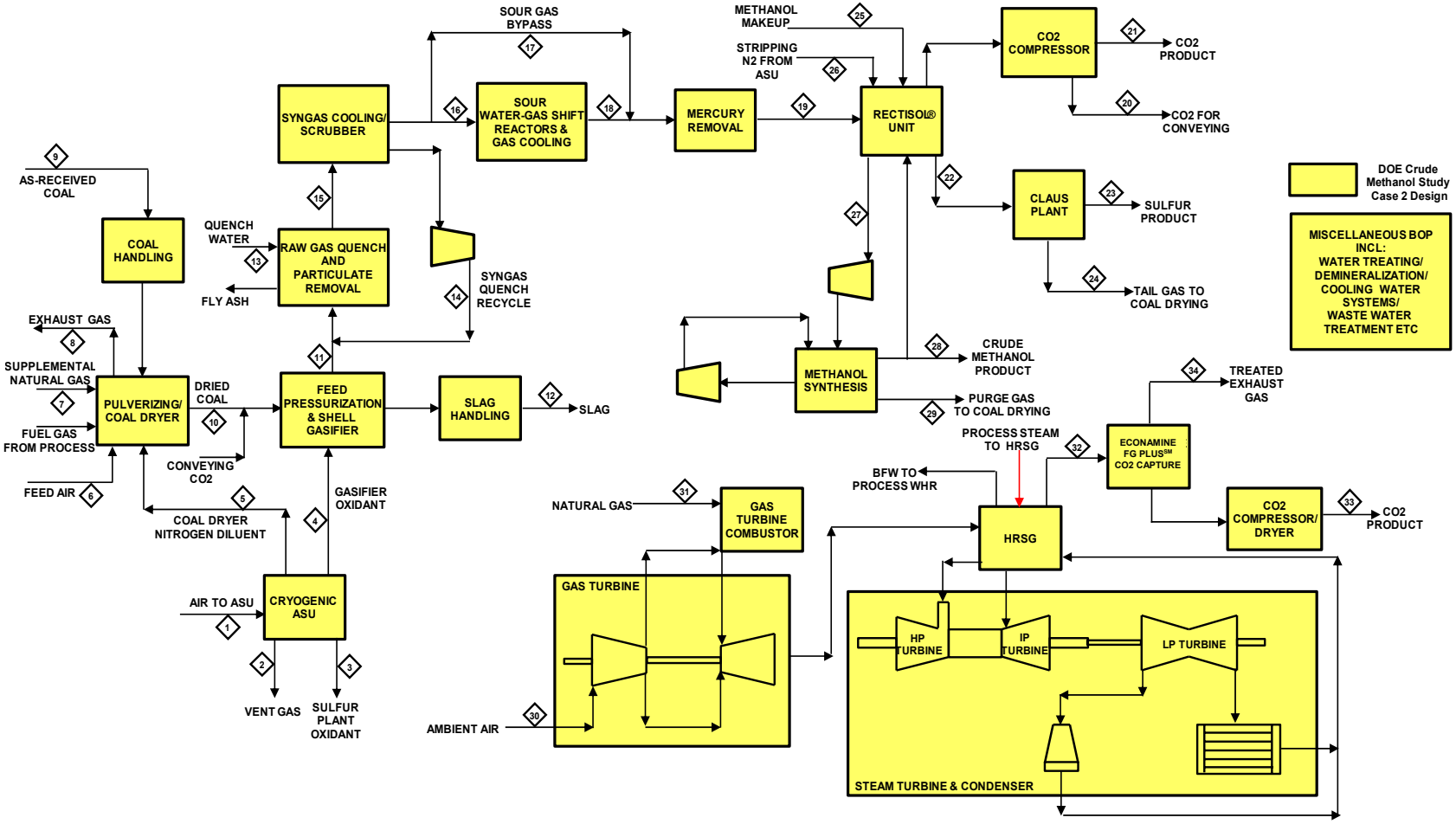

Table 8-2
Case 2a Reference Plant – Overall Stream Table

Description	Air to ASU	ASU Vent Gas	Sulfur Plant Oxidant	Gasifier Oxidant	Nitrogen Diluent to Dryer	Air Feed to Coal Dryer	Supple-mental NG Feed	Coal Dryer Exhaust	As-Received Coal	Dried Coal	Raw Syngas	Slag	Quench Water	Cool Syngas Recycle	Syngas to Scrubber	Syngas to Shift	Bypass Syngas
Stream No.	1	2	3	4	5	6	7	8	9	10	11	12	13	14	15	16	17
V-L Mole Fraction																	
Ar	0.0092	0.0219	0.0300	0.0300	0.0023	0.0092	0	0.0087	0	0	0.0088	0	0	0.0047	0.0052	0.0047	0.0047
CH4	0	0	0	0	0	0	0.9310	0	0	0	0.0001	0	0	0.0000	0.0000	0.0000	0.0000
CO	0	0	0	0	0	0	0	0	0	0	0.6197	0	0	0.3319	0.3654	0.3319	0.3319
CO2	0.0003	0.0052	0	0	0	0.0003	0	0	0	0	0.0639	0	0	0.0343	0.0377	0.0343	0.0343
COS	0	0	0	0	0	0	0	0	0	0	0.0005	0	0	0.0003	0.0003	0.0003	0.0003
H2	0	0	0	0	0	0	0	0	0	0	0.2313	0	0	0.1239	0.1364	0.1239	0.1239
H2O	0.0099	0.1535	0	0	0	0	0	0.1452	0	0	0.0616	0	1.0000	0.4973	0.4467	0.4973	0.4973
H2S	0	0	0	0	0	0	0	0	0	0	0.0030	0	0	0.0016	0.0018	0.0016	0.0016
N2	0.7732	0.6989	0.0200	0.0200	0.9921	0.7732	0.0160	0.8008	0	0	0.0111	0	0	0.0059	0.0065	0.0059	0.0059
NH3	0	0	0	0	0	0	0	0	0	0	0.0000	0	0	0	0	0	0
O2	0.2074	0.1206	0.9500	0.9500	0.0054	0.2074	0	0	0	0	0	0	0	0	0	0	0
SO2	0	0	0	0	0	0	0	0.0000	0	0	0	0	0	0	0	0	0
S	0	0	0	0	0	0	0	0	0	0	0	0	0	0	0	0	0
HCN	0	0	0	0	0	0	0	0	0	0	0	0	0	0	0	0	0
HCl	0	0	0	0	0	0	0	0	0	0	0	0	0	0	0	0	0
Ca(OH)2	0	0	0	0	0	0	0	0	0	0	0	0	0	0	0	0	0
CaSO.2H2O	0	0	0	0	0	0	0	0	0	0	0	0	0	0	0	0	0
Methanol	0	0	0	0	0	0	0	0	0	0	0	0	0	0	0	0	0
Ethanol	0	0	0	0	0	0	0	0	0	0	0	0	0	0	0	0	0
Propanol	0	0	0	0	0	0	0	0	0	0	0	0	0	0	0	0	0
Ethane	0	0	0	0	0	0	0.0320	0	0	0	0	0	0	0	0	0	0
Propane	0	0	0	0	0	0	0.0070	0	0	0	0	0	0	0	0	0	0
n-Butane	0	0	0	0	0	0	0.0040	0	0	0	0	0	0	0	0	0	0
Total	1.0000	1.0000	1.0000	1.0000	1.0000	1.0000	1.0000	1.0000	0	0	1.0000	0	1.0000	1.0000	1.0000	1.0000	1.0000
V-L Flowrate, lbmol/hr	152690	9675	195	31278	110619	17089	130	154945	0	0	106160	0	61508	135448	303115	123016	75152
V-L Flowrate, lb/hr	4406168	264163	6273	1005820	3104006	493137	2252	4222847	0	0	2393030	0	1108084	2768779	6269875	2514637	1536237
Solids Flow Rate, lb/hr	0	0	0	0	0	0	0	0	1618190	1277850	0	136541	0	0	0	0	0
Temperature, F	59	64	72	292	70	59	80	156	59	156	2646		392	432	820	411	411
Pressure, psia	14.7	16.4	23.2	711.0	18.0	14.7	20.0	14.3	14.7	14.3	650.0	650.0	685.0	650.0	650.0	605.3	605.3

Table 8-2 (cont'd)
Case 2a Reference Plant – Overall Stream Table

Description	Shifted Syngas	Syngas to Rectisol	Convey'g CO2	CO2 Product	Rectisol® Tail Gas to Claus	Sulfur Product	Tail Gas to Coal Drying	Methanol Makeup	Stripping N2 from ASU	Treated Syngas to MeOH	Crude Methanol Product	MeOH Synthesis Purge Gas	Air to Gas Turbine	Natural Gas Feed	NGCC Flue Gas Exhaust	CO2 Product	Treated NGCC Exhaust
Stream No.	18	19	20	21	22	23	24	25	26	27	28	29	30	31	32	33	34
V-L Mole Fraction																	
Ar	0.0047	0.0069	0.0002	0.0002	0	0	0.0046	0	0.0023	0.0098	0.0001	0.1408	0.0092	0	0.0089	0	0.0097
CH4	0.0000	0.0000	0	0	0	0	0	0	0	0.0001	0	0.0008	0	0.9310	0	0	0
CO	0.0420	0.2220	0.0040	0.0040	0.0019	0	0.0085	0	0	0.3135	0	0.1798	0	0	0	0	0
CO2	0.3245	0.3131	0.9701	0.9701	0.6645	0	0.5659	0	0	0.0349	0.0114	0.2207	0.0003	0.0100	0.0349	1.0000	0.0038
COS	0.0000	0.0001	0	0	0	0	0.0012	0	0	0.0000	0	0	0	0	0	0	0
H2	0.4139	0.4439	0.0006	0.0006	0.0019	0	0.0037	0	0	0.6302	0	0.2655	0	0	0	0	0
H2O	0.2071	0.0027	0	0	0	0	0.3954	0	0	0	0.0119	0.0001	0.0099	0	0.0761	0	0.0332
H2S	0.0018	0.0025	0	0	0.2997	0	0.0028	0	0	0	0	0	0	0	0	0	0
N2	0.0059	0.0087	0.0246	0.0246	0.0142	0	0.0147	0	0.9921	0.0115	0.0001	0.1723	0.7732	0.0160	0.7473	0	0.8096
NH3	0	0	0	0	0	0	0	0	0	0	0	0	0	0	0	0	0
O2	0	0	0.0001	0.0001	0	0	0.0017	0	0.0054	0	0	0	0.2074	0	0.1328	0	0.1438
SO2	0	0	0	0	0	0	0.0014	0	0	0	0	0	0	0	0	0	0
S	0	0	0	0	0	1.0000	0	0	0	0	0	0	0	0	0	0	0
HCN	0	0	0	0	0.0002	0	0.0002	0	0	0	0	0	0	0	0	0	0
HCl	0	0	0	0	0	0	0	0	0	0	0	0	0	0	0	0	0
Ca(OH)2	0	0	0	0	0	0	0	0	0	0	0	0	0	0	0	0	0
CaSO.2H2O	0	0	0	0	0	0	0	0	0	0	0	0	0	0	0	0	0
Methanol	0	0	0.0004	0.0004	0	0	0	1.0000	0	0.0001	0.9751	0.0200	0	0	0	0	0
Ethanol	0	0	0	0	0	0	0	0	0	0	0.0014	0	0	0	0	0	0
Propanol	0	0	0	0	0	0	0	0	0	0	0.0001	0	0	0	0	0	0
Ethane	0	0	0	0	0	0	0	0	0	0	0	0	0	0.032	0	0	0
Propane	0	0	0	0	0	0	0	0	0	0	0	0	0	0.007	0	0	0
n-Butane	0	0	0	0	0	0	0	0	0	0	0	0	0	0.004	0	0	0
Total	1.0000	1.0000	1.0000	1.0000	1.0000	1.0000	1.0000	1.0000	1.0000	1.0000	1.0000	1.0000	1.0000	1.0000	1.0000	1.0000	1.0000
V-L Flowrate, lbmol/hr	123016	135645	5651	33904	1150	360	1402	22	923	95521	29303	5744	114330	3930	118374	3719	109265
V-L Flowrate, lb/hr	2514659	2923802	245924	1475527	47123	11529	46531	719	25907	1175263	938622	151588	3299204	68087	3367302	163687	3106521
Solids Flow Rate, lb/hr	0	0	0	0	0	0	0	0	0	0	0	0	0	0	0	0	0
Temperature, F	606	111	257	162	59	320	320	123	86	82	118	130	59	60	297	124	85
Pressure, psia	567.0	515.7	770.0	2215	28	20	20	40	75.0	485	40	717	14.5	474.7	14.9	2215	15.0

Figure 8-2
Case 2a Reference Plant – Coal Drying PFD

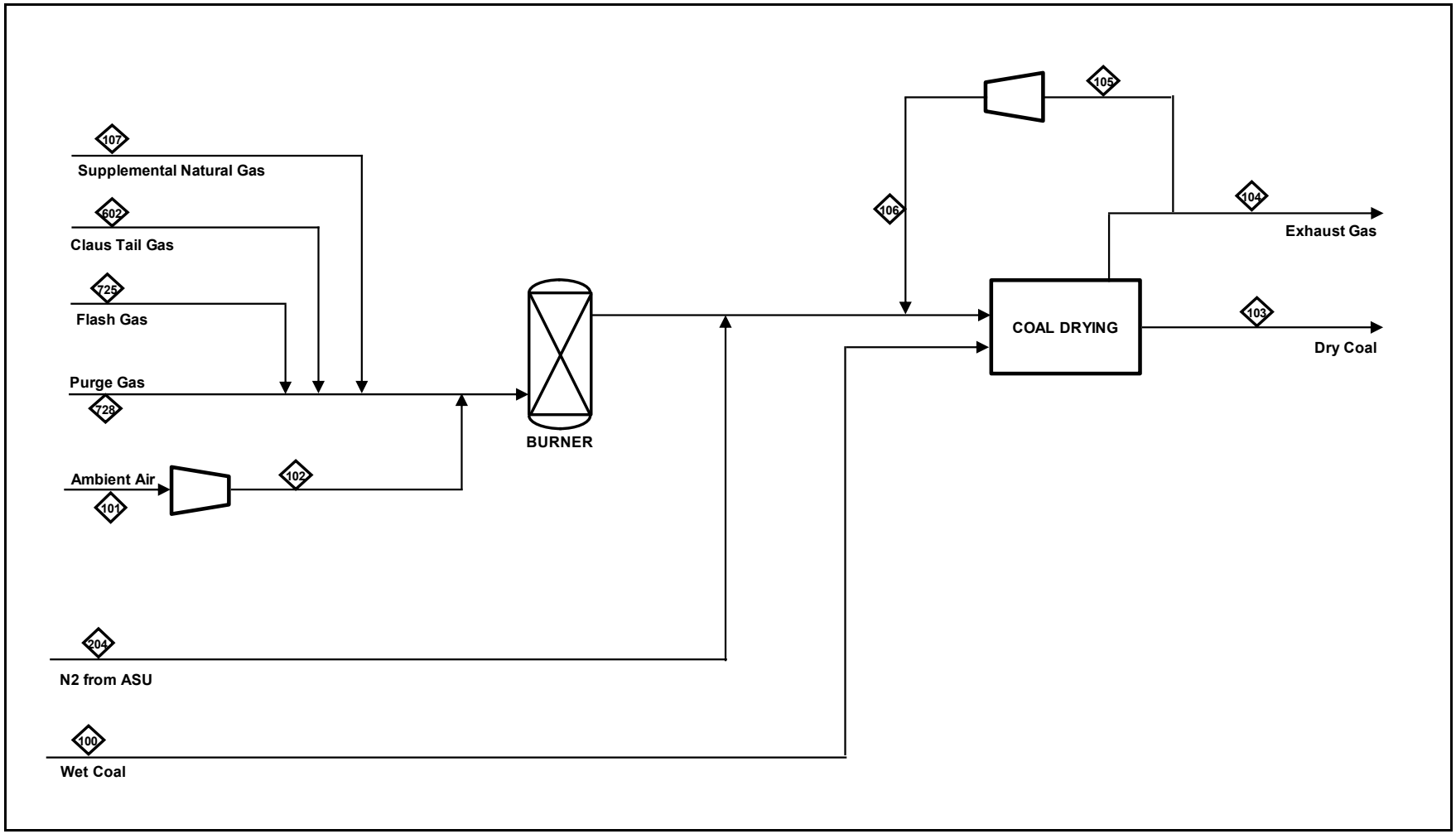

Table 8-3
Case 2a Reference Plant – Coal Drying Stream Table

STREAM	100	101	102	103	104	105	106	107	204	602	725	728
Description	Wet Coal	Ambient Air	Feed Air	Dry Coal	Exhaust Gas	LP Recycle Gas	HP Recycle Gas	Supplemental Nat Gas	Dilution Nitrogen	Claus Tail Gas	MeOH Flash Gas	MeOH Purge Gas
Mole Flow (Vapor/Liquid)/lbmol/hr												
AR	0	158	158	0	1350	727	727	0	254	6	122	809
CH4	0	0	0	0	0	0	0	121	0	0	1	4
CO	0	0	0	0	0	0	0	0	0	12	54	1033
CO2	0	6	6	0	5247	2825	2825	1	0	793	1425	1267
COS	0	0	0	0	0	0	0	0	0	2	0	0
H2	0	0	0	0	0	0	0	0	0	5	33	1525
H2O	0	169	169	0	22505	12118	12118	0	22	554	2	0
H2S	0	0	0	0	0	0	0	0	0	4	0	0
N2	0	13212	13212	0	124077	66811	66811	2	109745	21	108	990
NH3	0	0	0	0	0	0	0	0	0	0	0	0
O2	0	3544	3544	0	1758	947	947	0	597	2	0	0
SO2	0	0	0	0	8	4	4	0	0	2	0	0
S	0	0	0	0	0	0	0	0	0	0	0	0
HCN	0	0	0	0	0	0	0	0	0	0	0	0
HCL	0	0	0	0	0	0	0	0	0	0	0	0
Methanol -- CH3OH	0	0	0	0	0	0	0	0	0	0	398	115
Ethanol -- C2H5OH	0	0	0	0	0	0	0	0	0	0	0.4	0.1
Propanol -- C3H8O	0	0	0	0	0	0	0	0	0	0	0	0
Ethane -- C2H6	0	0	0	0	0	0	0	4	0	0	0	0
Propane -- C3H8	0	0	0	0	0	0	0	1	0	0	0	0
n-Butane -- C4H10	0	0	0	0	0	0	0	1	0	0	0	0
Total V/L Flow, lbmol/hr	0	17089	17089	0	154945	83432	83432	130	110619	1402	2143	5744
Total V/L Flow, lb/hr	0	493137	493137	0	4222847	2273841	2273841	2252	3104006	46531	85001	151587
Solids Mass Flow, lb/hr	1618190	0	0	1277850	0	0	0	0	0	0	0	0
Coal	1618190	0	0	1277850	0	0	0	0	0	0	0	0
Ash	0	0	0	0	0	0	0	0	0	0	0	0
Carbon	0	0	0	0	0	0	0	0	0	0	0	0
Total Flow (Solids + V/L), lb/hr	1618190	493137	493137	1277850	4222847	2273841	2273841	2252	3104006	46531	85001	151587
Pressure, psia	14.7	14.7	17	14.3	14.3	14.3	16	20	18	20	40	717
Temperature, F		59	90		156	156	183	80	70	320	118	130

Figure 8-3
Case 2a Reference Plant – ASU/Coal Gasification PFD

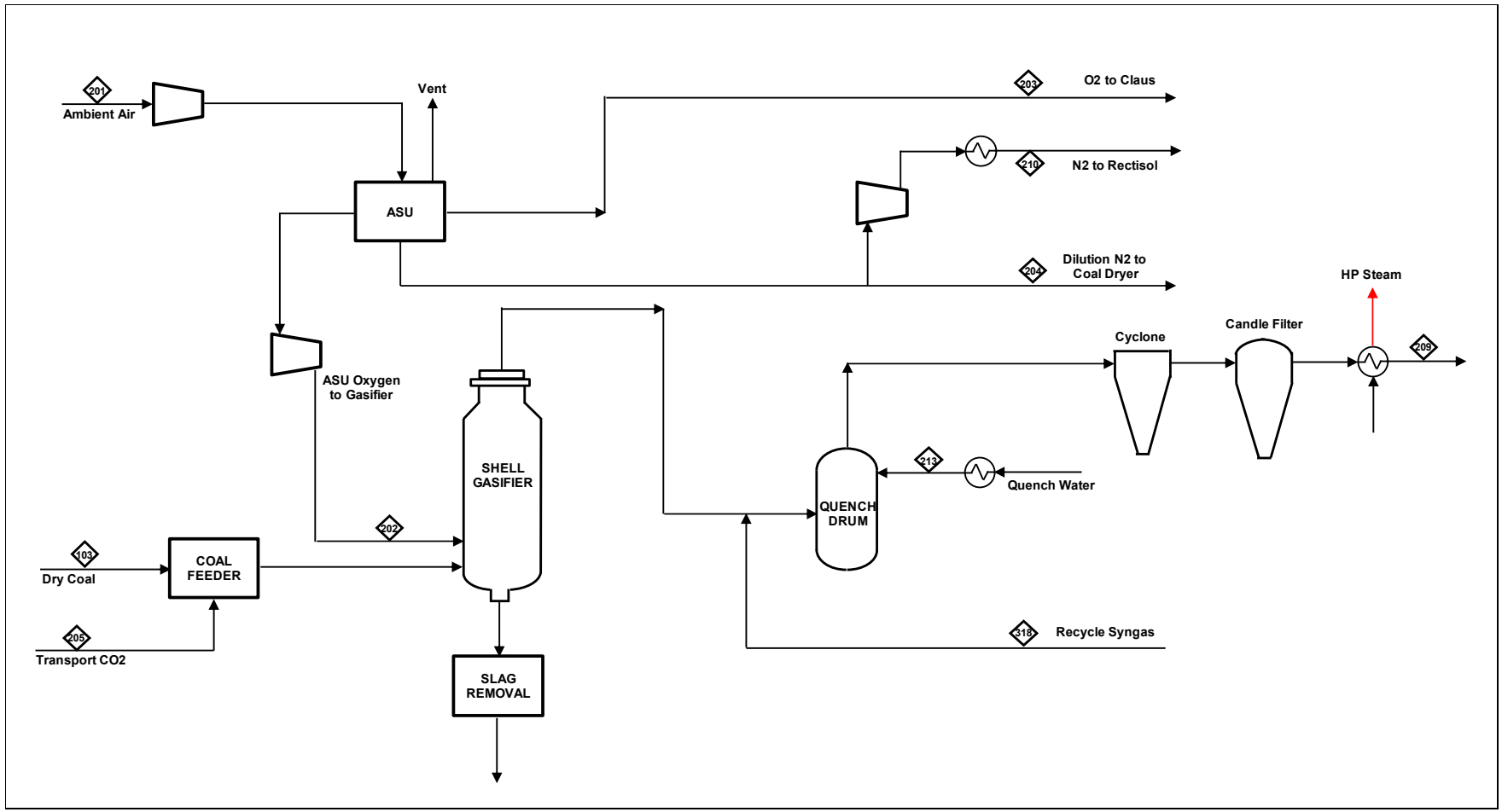

Table 8-4
Case 2a Reference Plant – ASU/Coal Gasification Stream Table

STREAM	201	202	203	204	205	103	318	213	214	209	210
Description	Ambient Air	Oxygen to Gasifier	Oxygen to Claus	N2 to Coal Dryer	Conveying CO2	Dry Coal	Recycle Syngas	Quench Water	Slag Out	Raw Cooled Syngas	Stripping N2 to Rectisol
Mole Flow (Vapor/Liquid)/lbmol/hr											
AR	1412	938	6	254	1	0	642	0	0	1581	2
CH4	0	0	0	0	0	0	4	0	0	9	0
CO	0	0	0	0	23	0	44960	0	0	110745	0
CO2	50	0	0	0	5482	0	4646	0	0	11427	0
COS	0	0	0	0	0	0	35	0	0	86	0
H2	0	0	0	0	3	0	16783	0	0	41338	0
H2O	1507	0	0	22	0	0	67361	61508	0	135412	0
H2S	0	0	0	0	0	0	216	0	0	532	0
N2	118053	626	4	109745	139	0	802	0	0	1976	916
NH3	0	0	0	0	0	0	0	0	0	5	0
O2	31668	29714	185	597	1	0	0	0	0	0	5
SO2	0	0	0	0	0	0	0	0	0	0	0
S	0	0	0	0	0	0	0	0	0	0	0
HCN	0	0	0	0	0	0	0	0	0	1	0
HCL	0	0	0	0	0	0	0	0	0	3	0
Methanol -- CH3OH	0	0	0	0	2	0	0	0	0	0	0
Ethanol -- C2H5OH	0	0	0	0	0	0	0	0	0	0	0
Propanol -- C3H8O	0	0	0	0	0	0	0	0	0	0	0
Ethane -- C2H6	0	0	0	0	0	0	0	0	0	0	0
Propane -- C3H8	0	0	0	0	0	0	0	0	0	0	0
n-Butane -- C4H10	0	0	0	0	0	0	0	0	0	0	0
Total V/L Flow, lbmol/hr	152690	31278	195	110618.9	5651	0	135448	61508	0	303115	923
Total V/L Flow, lb/hr	4406168	1005820	6273	3104006	245924	0	2768779	1108084	0	6269875	25907
Solids Mass Flow, lb/hr	0	0	0	0	0	1277850	0	0	136541	0	0
Coal	0	0	0	0	0	1277850	0	0	0	0	0
Ash	0	0	0	0	0	0	0	0	132490	0	0
Carbon	0	0	0	0	0	0	0	0	4051	0	0
Total Flow (Solids + V/L), lb/hr	4406168	1005820	6273	3104006	245924	1277850	2768779	1108084	136541	6269875	25907
Pressure, psia	14.7	711	23.2	18.0	770.0	14.3	650	685	650	605.3	75
Temperature, F	59	292	72	70	257		432	392		603	86

Figure 8-4
Case 2a Reference Plant – Wet Scrubber/Water-Gas Shift PFD

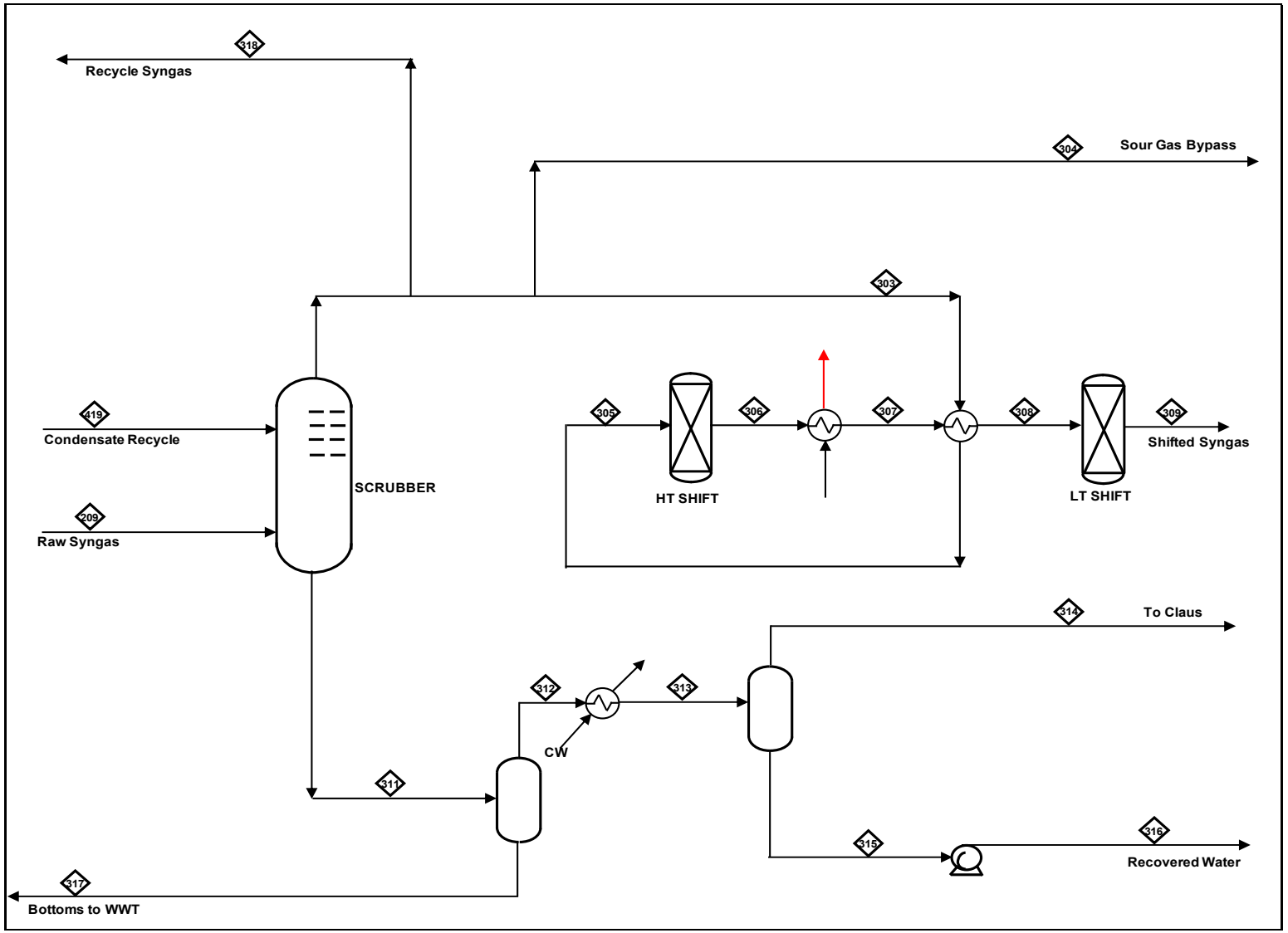

Table 8-5
Case 2a Reference Plant – Wet Scrubber/Water-Gas Shift Stream Table

STREAM	209	419	303	304	305	306	307	308	309	311	312	313	314	315	317	318
Description	Raw Syngas	Condensate Recycle	Syngas to Shift	Bypass Syngas	Hot Syngas	Hot 1st Shift Syngas	Warm 1st Shift Syngas	Cold 1st Shift Syngas	Hot 2nd Shift Syngas	Scrubber Bottoms	Scrubber Hot Vapor	Scrubber Cold Vapor	Scrubber Sour Gas	LP Recycle Water	Bottoms to WWT	Recycle Syngas
Mole Flow (Vapor/Liquid)/lbmol/hr																
AR	1581	0	583	356	583	583	583	583	583	1	1	1	1	0	0	642
CH4	9	0	3	2	3	3	3	3	3	0	0	0	0	0	0	4
CO	110745	1	40833	24945	40833	13206	13206	13206	5165	9	9	9	9	0	0	44960
CO2	11427	24	4219	2578	4219	31875	31875	31875	39918	8	8	8	8	0	0	4646
COS	86	0	32	19	32	3	3	3	1	0	0	0	0	0	0	35
H2	41338	3	15242	9312	15242	42869	42869	42869	50910	4	4	4	4	0	0	16783
H2O	135412	80532	61178	37375	61178	33521	33521	33521	25479	50031	7865	7865	1	7864	42166	67361
H2S	532	3	197	120	197	226	226	226	227	2	2	2	2	1	0	216
N2	1976	0	729	445	729	729	729	729	729	0	0	0	0	0	0	802
NH3	5	3	0	0	0	0	0	0	0	4	3	3	0	3	2	0
O2	0	0	0	0	0	0	0	0	0	0	0	0	0	0	0	0
SO2	0	0	0	0	0	0	0	0	0	0	0	0	0	0	0	0
S	0	0	0	0	0	0	0	0	0	0	0	0	0	0	0	0
HCN	1	0	0	0	0	0	0	0	0	0	0	0	0	0	0	0
HCL	3	0	0	0	0	0	0	0	0	0	0	0	0	0	0	0
Methanol -- CH3OH	0	0	0	0	0	0	0	0	0	0	0	0	0	0	0	0
Ethanol -- C2H5OH	0	0	0	0	0	0	0	0	0	0	0	0	0	0	0	0
Propanol -- C3H8O	0	0	0	0	0	0	0	0	0	0	0	0	0	0	0	0
Ethane -- C2H6	0	0	0	0	0	0	0	0	0	0	0	0	0	0	0	0
Propane -- C3H8	0	0	0	0	0	0	0	0	0	0	0	0	0	0	0	0
n-Butane -- C4H10	0	0	0	0	0	0	0	0	0	0	0	0	0	0	0	0
Total V/L Flow, lbmol/hr	303115	80566	123016	75152	123016	123016	123016	123016	123016	50059	7892	7892	24	7868	42168	135448
Total V/L Flow, lb/hr	6269875	1452070	2514637	1536237	2514637	2514654	2514654	2514654	2514659	902127.8	142467	142467	709.809	141758	759660	2768779
Solids Mass Flow, lb/hr	0	0	0	0	0	0	0	0	0	0	0	0	0	0	0	0
Coal	0	0	0	0	0	0	0	0	0	0	0	0	0	0	0	0
Ash	0	0	0	0	0	0	0	0	0	0	0	0	0	0	0	0
Carbon	0	0	0	0	0	0	0	0	0	0	0	0	0	0	0	0
Total Flow (Solids + V/L), lb/hr	6269875	1452070	2514637	1536237	2514637	2514654	2514654	2514654	2514659	902128	142467	142467	710	141758	759660	2768779
Pressure, psia	605	762	605.3	605.3	600.3	593	584	575	567	600	51	46	46	46	51	605
Temperature, F	603	392	411	411	530	942	600	484	606	411	284	130	130	130	284	411

Figure 8-5
Case 2a Reference Plant – Low Temperature Gas Cooling PFD

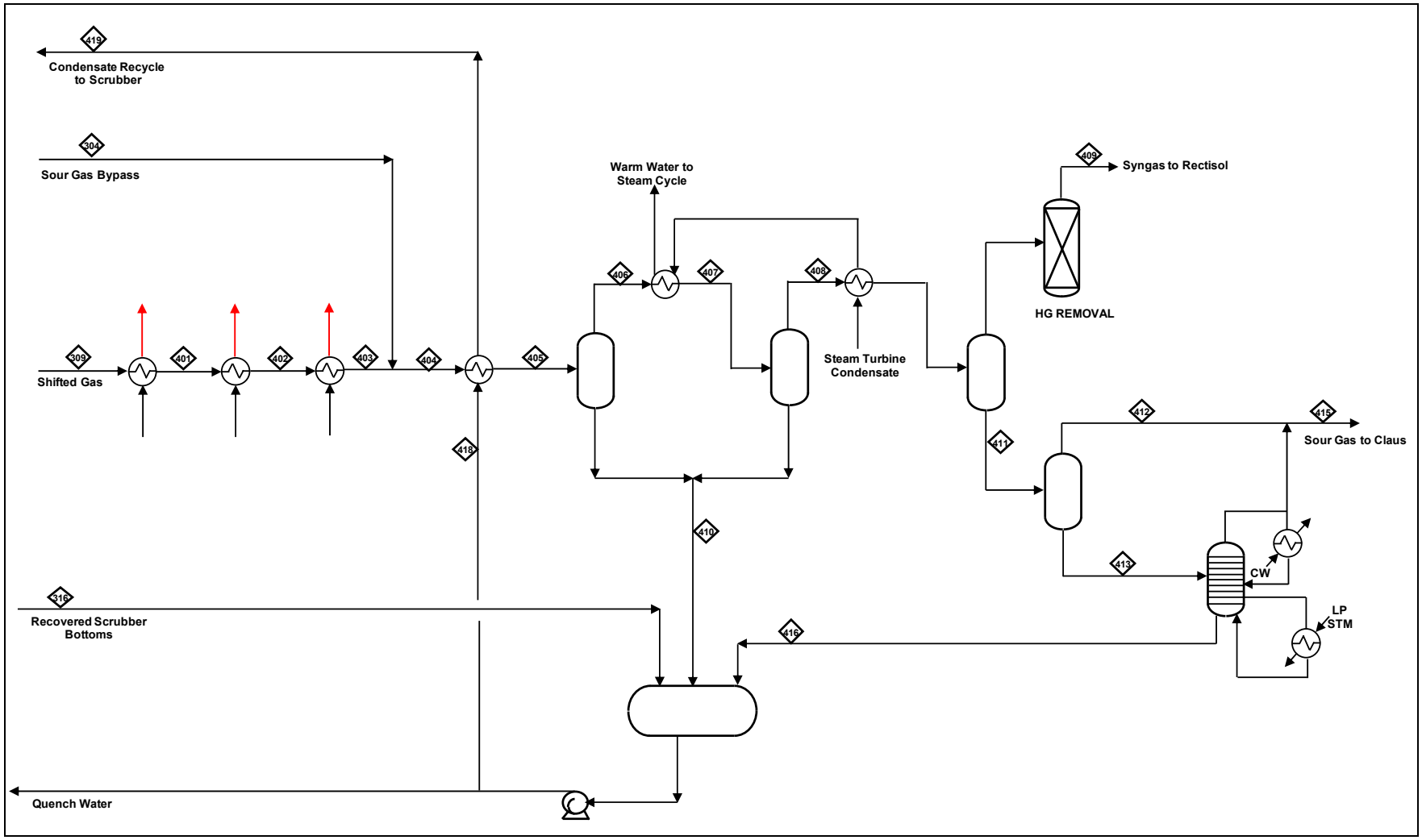

Table 8-6
Case 2a Reference Plant – Low Temperature Gas Cooling Stream Table

STREAM	309	403	304	404	405	406	407	408	409	415	416	316	419	213
Description	Hot 2nd Shift Syngas	Cooled Shift Syngas	Bypass Syngas	Mixed Syngas	Mixed Syngas Shift	1st KO Drum Vapor	Cool 1st KO Drum Vapor	2nd KO KO Drum Vapor	Syngas to Rectisol	Sour Gas	Sour Stripper Bottoms	HP Recycle Water	Condensate Recycle	Quench Water
Mole Flow (Vapor/Liquid)/lbmol/hr														
AR	583	583	356	939	939	939	939	938	938	0	0	0	0	0
CH4	3	3	2	5	5	5	5	5	5	0	0	0	0	0
CO	5165	5165	24945	30111	30111	30110	30110	30109	30109	0	0	0	1	0
CO2	39918	39918	2578	42496	42496	42487	42487	42472	42468	4	0	0	24	0
COS	1	1	19	20	20	20	20	20	20	0	0	0	0	0
H2	50910	50910	9312	60222	60222	60221	60221	60219	60219	0	0	0	3	0
H2O	25479	25479	37375	62853	62853	49716	49716	23394	366	210	22819	7864	80532	61508
H2S	227	227	120	347	347	347	347	345	345	0	0	1	3	0
N2	729	729	445	1174	1174	1174	1174	1174	1174	0	0	0	0	0
NH3	0	0	0	0	0	0	0	0	0	0	0	3	3	0
O2	0	0	0	0	0	0	0	0	0	0	0	0	0	0
SO2	0	0	0	0	0	0	0	0	0	0	0	0	0	0
S	0	0	0	0	0	0	0	0	0	0	0	0	0	0
HCN	0	0	0	0	0	0	0	0	0	0	0	0	0	0
HCL	0	0	0	0	0	0	0	0	0	0	0	0	0	0
Methanol -- CH3OH	0	0	0	0	0	0	0	0	0	0	0	0	0	0
Ethanol -- C2H5OH	0	0	0	0	0	0	0	0	0	0	0	0	0	0
Propanol -- C3H8O	0	0	0	0	0	0	0	0	0	0	0	0	0	0
Ethane -- C2H6	0	0	0	0	0	0	0	0	0	0	0	0	0	0
Propane -- C3H8	0	0	0	0	0	0	0	0	0	0	0	0	0	0
n-Butane -- C4H10	0	0	0	0	0	0	0	0	0	0	0	0	0	0
Total V/L Flow, lbmol/hr	123016	123016	75152	198168	198168	185020	185020	158678	135645	214	22819	7868	80566	61508
Total V/L Flow, lb/hr	2514659	2514659	1536237	4050895	4050895	3813804	3813804	3338853	2923802	3954.688	411096	141758	1452070	1108084
Solids Mass Flow, lb/hr	0	0	0	0	0	0	0	0	0	0	0	0	0	0
Coal	0	0	0	0	0	0	0	0	0	0	0	0	0	0
Ash	0	0	0	0	0	0	0	0	0	0	0	0	0	0
Carbon	0	0	0	0	0	0	0	0	0	0	0	0	0	0
Total Flow (Solids + V/L), lb/hr	2514659	2514659	1536237	4050895	4050895	3813804	3813804	3338853	2923802	3955	411096	141758	1452070	1108084
Pressure, psia	567	552.69	605.3	552.7	549.7	544	540.69	540.69	515.69	61	74.16	46	762	685
Temperature, F	606	409	411	407	356	350	306	306	111	277	307	550	392	392

Figure 8-6
Case 2a Reference Plant – Rectisol® AGR and CO_2 Compression PFD

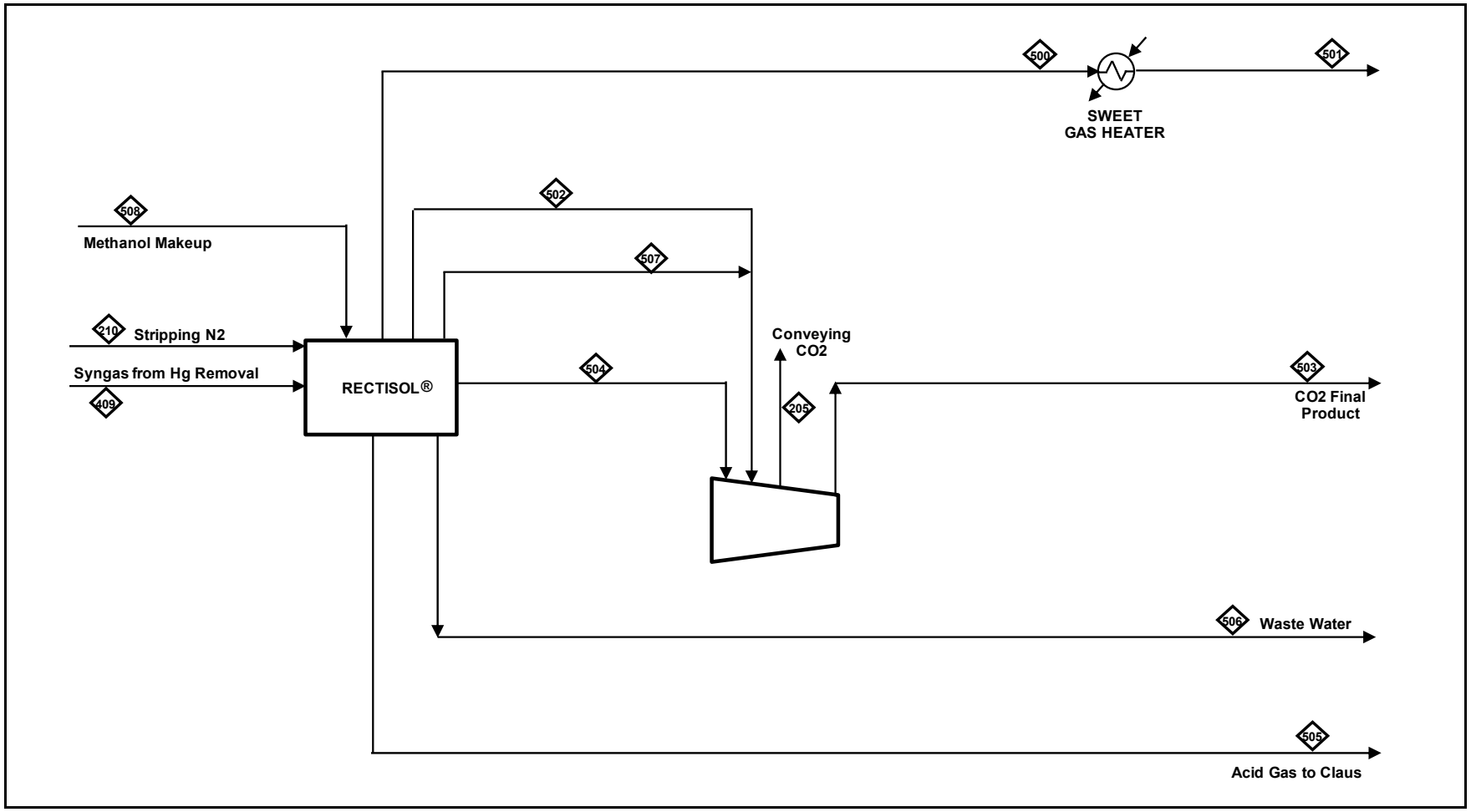

Table 8-7
Case 2a Reference Plant – Rectisol® AGR and CO_2 Compression Stream Table

STREAM	409	210	500	504	502	503	205	505	506	507	508
Description	Syngas to Rectisol®	Stripping N2 to Rectisol®	Treated Gas to MeOH	LP CO2 Product Stream	MP CO2 Product Stream	CO2 Final Product	Convey CO2	Acid Gas to Claus	Water to Waste	Fuel Gas to CO2 Product	Makeup Rectisol®
Mole Flow (Vapor/Liquid)/lbmol/hr											
AR	938	2	934	0	2	6	1	0	0	5	0
CH4	5	0	5	0	0	0	0	0	0	0	0
CO	30109	0	29948	2	76	137	23	2	0	81	0
CO2	42468	0	3333	30352	6418	32890	5482	764	0	1600	0
COS	20	0	0	0	0	0	0	20	0	0	0
H2	60219	0	60195	0	9	19	3	2	0	13	0
H2O	366	0	0	0	0	0	0	0	366	0	0
H2S	345	0	0	0	0	0	0	345	0	0	0
N2	1174	916	1099	970	2	835	139	16	0	2	0
NH3	0	0	0	0	0	0	0	0	0	0	0
O2	0	5	0	0	0	4	1	0	0	5	0
SO2	0	0	0	0	0	0	0	0	0	0	0
S	0	0	0	0	0	0	0	0	0	0	0
HCN	0	0	0	0	0	0	0	0	0	0	0
HCL	0	0	0	0	0	0	0	0	0	0	0
Methanol -- CH3OH	0	0	7	10	2	13	2	0	0	3	22
Ethanol -- C2H5OH	0	0	0	0	0	0	0	0	0	0	0
Propanol -- C3H8O	0	0	0	0	0	0	0	0	0	0	0
Ethane -- C2H6	0	0	0	0	0	0	0	0	0	0	0
Propane -- C3H8	0	0	0	0	0	0	0	0	0	0	0
n-Butane -- C4H10	0	0	0	0	0	0	0	0	0	0	0
Total V/L Flow, lbmol/hr	135645	923	95521	31334	6511	33904	5651	1150	366	1709	22
Total V/L Flow, lb/hr	2923802	25907	1175263	1363355	284865	1475527	245923.8	47123	6591	73231	719
Solids Mass Flow, lb/hr	0	0	0	0	0	0	0	0	0	0	0
Coal	0	0	0	0	0	0	0	0	0	0	0
Ash	0	0	0	0	0	0	0	0	0	0	0
Carbon	0	0	0	0	0	0	0	0	0	0	0
Total Flow (Solids + V/L), lb/hr	2923802	25907	1175263	1363355	284865	1475527	245924	47123	6591	73231	719
Pressure, psia	516	75	485	19	42	2215	770	28	36	64	40
Temperature, F	111	86	82	81	81	162	257	59	261	81	123

Figure 8-7
Case 2a Reference Plant – Claus Plant PFD

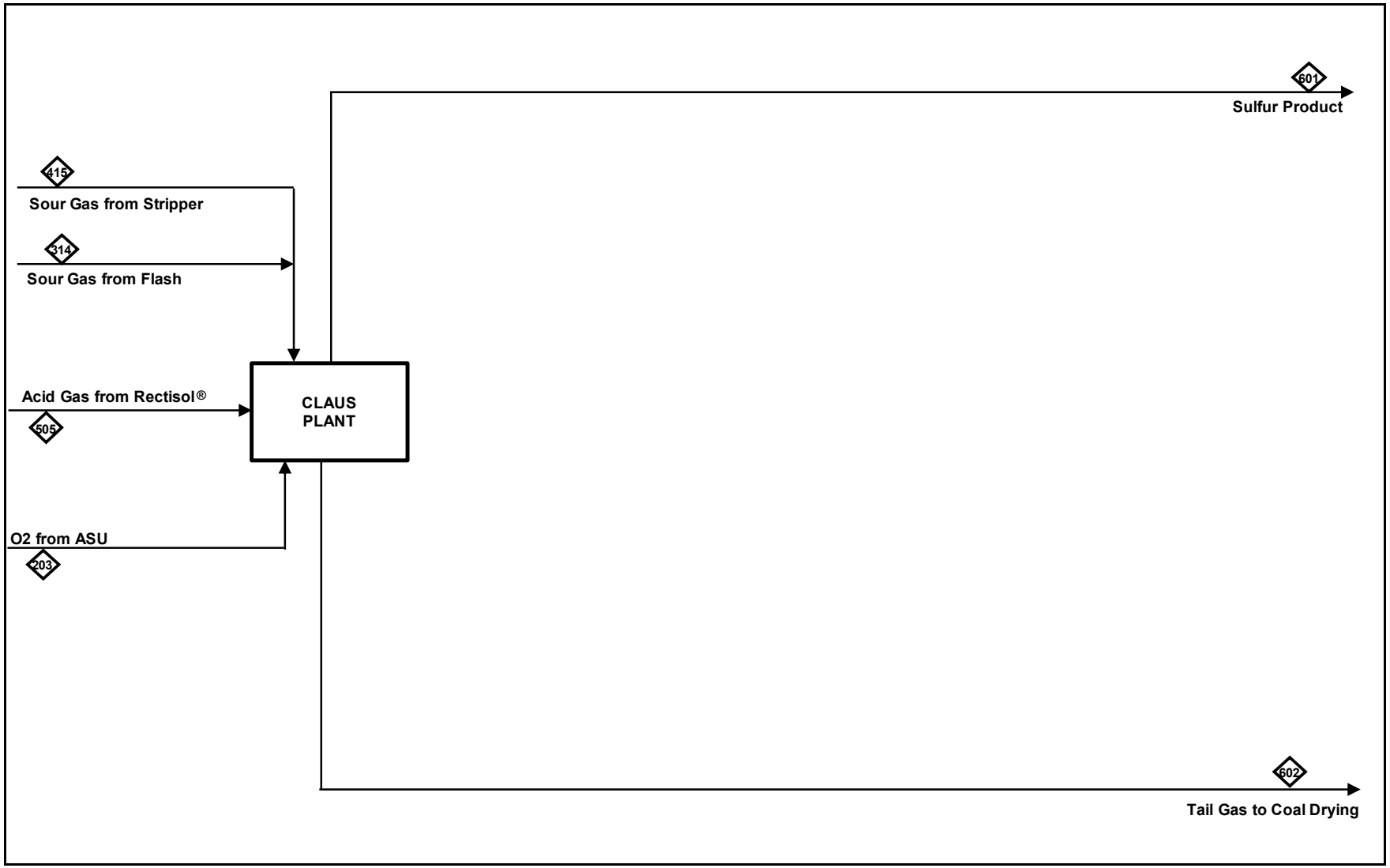

Table 8-8
Case 2a Reference Plant – Claus Plant Stream Table

STREAM	505	415	314	203	601	602
Description	Acid Gas from Rectisol®	Sour Gas from Stripper	Sour Gas from Flash	Claus O2 from ASU	Sulfur Product	Tail Gas to Coal Drying
Mole Flow (Vapor/Liquid)/lbmol/hr						
AR	0	0	1	6	0	6
CH4	0	0	0	0	0	0
CO	2	0	9	0	0	12
CO2	764	4	8	0	0	793
COS	20	0	0	0	0	2
H2	2	0	4	0	0	5
H2O	0	210	1	0	0	554
H2S	345	0	2	0	0	4
N2	16	0	0	4	0	21
NH3	0	0	0	0	0	0
O2	0	0	0	185	0	2
SO2	0	0	0	0	0	2
S	0	0	0	0	360	0
HCN	0	0	0	0	0	0
HCL	0	0	0	0	0	0
Methanol -- CH3OH	0	0	0	0	0	0
Ethanol -- C2H5OH	0	0	0	0	0	0
Propanol -- C3H8O	0	0	0	0	0	0
Ethane -- C2H6	0	0	0	0	0	0
Propane -- C3H8	0	0	0	0	0	0
n-Butane -- C4H10	0	0	0	0	0	0
Total V/L Flow, lbmol/hr	1150	214	24	195	360	1402
Total V/L Flow, lb/hr	47123	3955	710	6273	11529	46531
Solids Mass Flow, lb/hr	0	0	0	0	0	0
Coal	0	0	0	0	0	0
Ash	0	0	0	0	0	0
Carbon	0	0	0	0	0	0
Total Flow (Solids + V/L), lb/hr	47123	3955	710	6273	11529	46531
Pressure, psia	28	61	46	23	20	20
Temperature, F	59	277	130	72	320	320

Figure 8-8
Case 2a Reference Plant – Methanol Synthesis Plant PFD

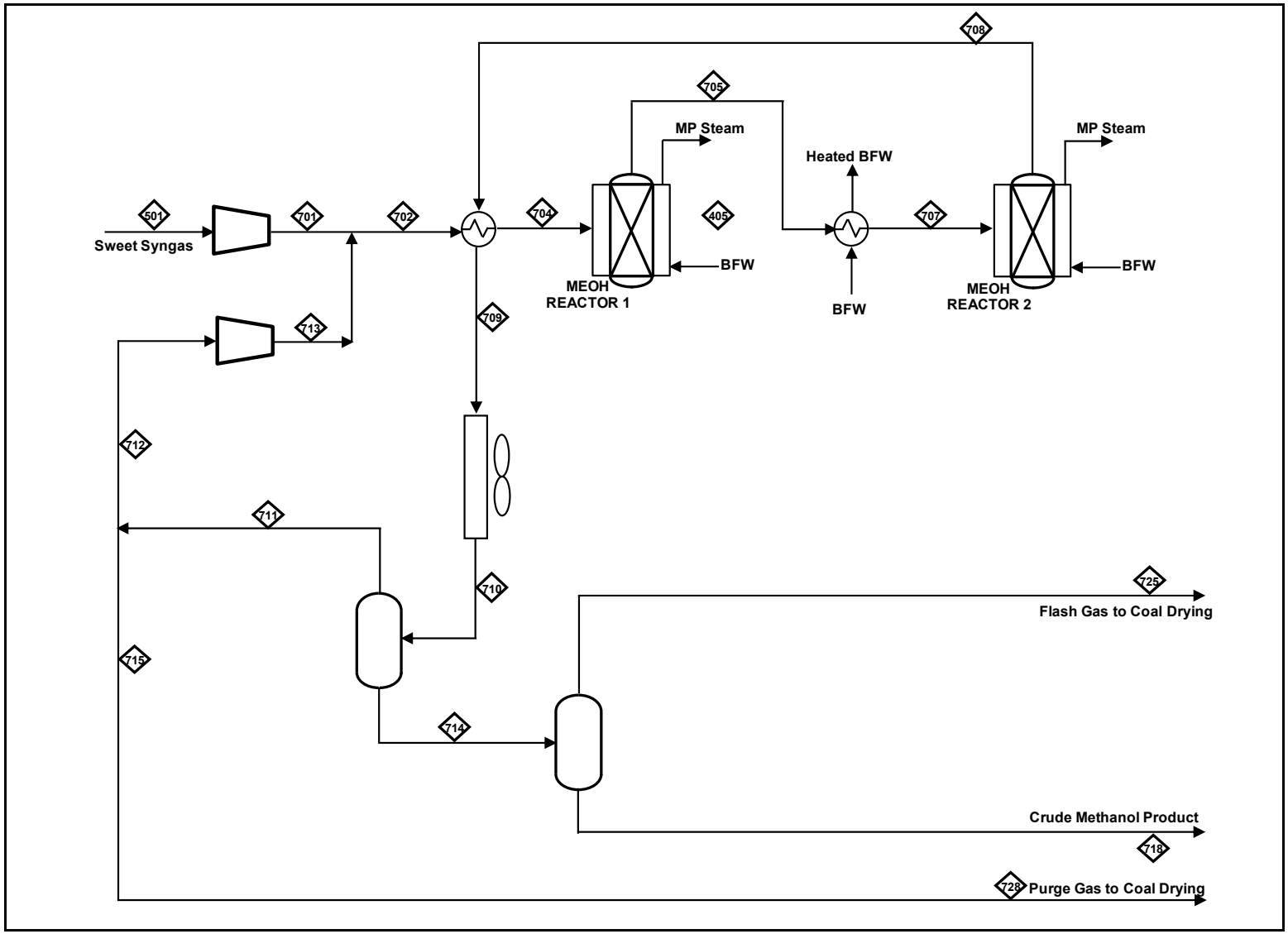

Table 8-9
Case 2a Reference Plant – Methanol Synthesis Plant Stream Table

STREAM	501	701	702	704	705	707	708	709	710	711	712	713	714	718	725	728
Description	Reheated Syngas	HP Sweet Syngas	Mixed Syngas	MEOH Reactor 1 Feed	MEOH Reactor 1 Outlet	MEOH Reactor 2 Feed	MEOH Reactor 2 Outlet	Cooled Raw MeOH	AC Cool Raw MeOH	Flash Gas Ovhd	Recycle Syngas	HP Recycle Syngas	KO Drum Bottoms	Crude MeOH Product	MeOH Flash Gas	MeOH Purge Gas
Mole Flow (Vapor/Liquid)/lbmol/hr																
AR	934	934	20344	20344	20344	20344	20344	20344	20344	20219	19410	19410	125	3	122	809
CH4	5	5	109	109	109	109	109	109	109	108	104	104	1	0	1	4
CO	29948	29948	54739	54739	35143	35143	25878	25878	25878	25824	24791	24791	54	0	54	1033
CO2	3333	3333	33753	33753	33214	33214	33448	33448	33448	31687	30420	30420	1761	335	1425	1267
COS	0	0	0	0	0	0	0	0	0	0	0	0	0	0	0	0
H2	60195	60195	96796	96796	55987	55987	38159	38159	38159	38126	36601	36601	33	0	33	1525
H2O	0	0	11	11	595	595	362	362	362	12	11	11	350	348	2	0
H2S	0	0	0	0	0	0	0	0	0	0	0	0	0	0	0	0
N2	1099	1099	24851	24851	24851	24851	24851	24851	24851	24742	23752	23752	109	2	108	990
NH3	0	0	0	0	0	0	0	0	0	0	0	0	0	0	0	0
O2	0	0	0	0	0	0	0	0	0	0	0	0	0	0	0	0
SO2	0	0	0	0	0	0	0	0	0	0	0	0	0	0	0	0
S	0	0	0	0	0	0	0	0	0	0	0	0	0	0	0	0
HCN	0	0	0	0	0	0	0	0	0	0	0	0	0	0	0	0
HCL	0	0	0	0	0	0	0	0	0	0	0	0	0	0	0	0
Methanol -- CH3OH	7	7	2766	2766	22814	22814	31844	31844	31844	2874	2759	2759	28970	28572	398	115
Ethanol -- C2H5OH	0	0	3	3	43	43	44	44	44	3	3	3	41	41	0	0
Propanol -- C3H8O	0	0	0	0	2	2	2	2	2	0	0	0	2	2	0	0
Ethane -- C2H6	0	0	0	0	0	0	0	0	0	0	0	0	0	0	0	0
Propane -- C3H8	0	0	0	0	0	0	0	0	0	0	0	0	0	0	0	0
n-Butane -- C4H10	0	0	0	0	0	0	0	0	0	0	0	0	0	0	0	0
Total V/L Flow, lbmol/hr	95520.94	95521	233371	233371	193101	193101	175040	175040	175040	143595	137850	137850	31445	29303	2143	5744
Total V/L Flow, lb/hr	1175263	1175263	4813379	4813379	4813343	4813343	4813327	4813327	4813327	3789704	3638116	3638116	1023623	938622	85001.3	151588
Solids Mass Flow, lb/hr	0	0	0	0	0	0	0	0	0	0	0	0	0	0	0	0
Coal	0	0	0	0	0	0	0	0	0	0	0	0	0	0	0	0
Ash	0	0	0	0	0	0	0	0	0	0	0	0	0	0	0	0
Carbon	0	0	0	0	0	0	0	0	0	0	0	0	0	0	0	0
Total Flow (Solids + V/L), lb/hr	1175263	1175263	4813379	4813379	4813343	4813343	4813327	4813327	4813327	3789704	3638116	3638116	1023623	938622	85001	151588
Pressure, psia	483	755	755	747.0	737.0	732.0	727	722	720	717	717	755	717	40	40	717
Temperature, F	125	234	175	400	475	400	430	239	130	130	130	141	130	118	118	130

Figure 8-9
Case 2a Reference Plant -- NGCC PFD

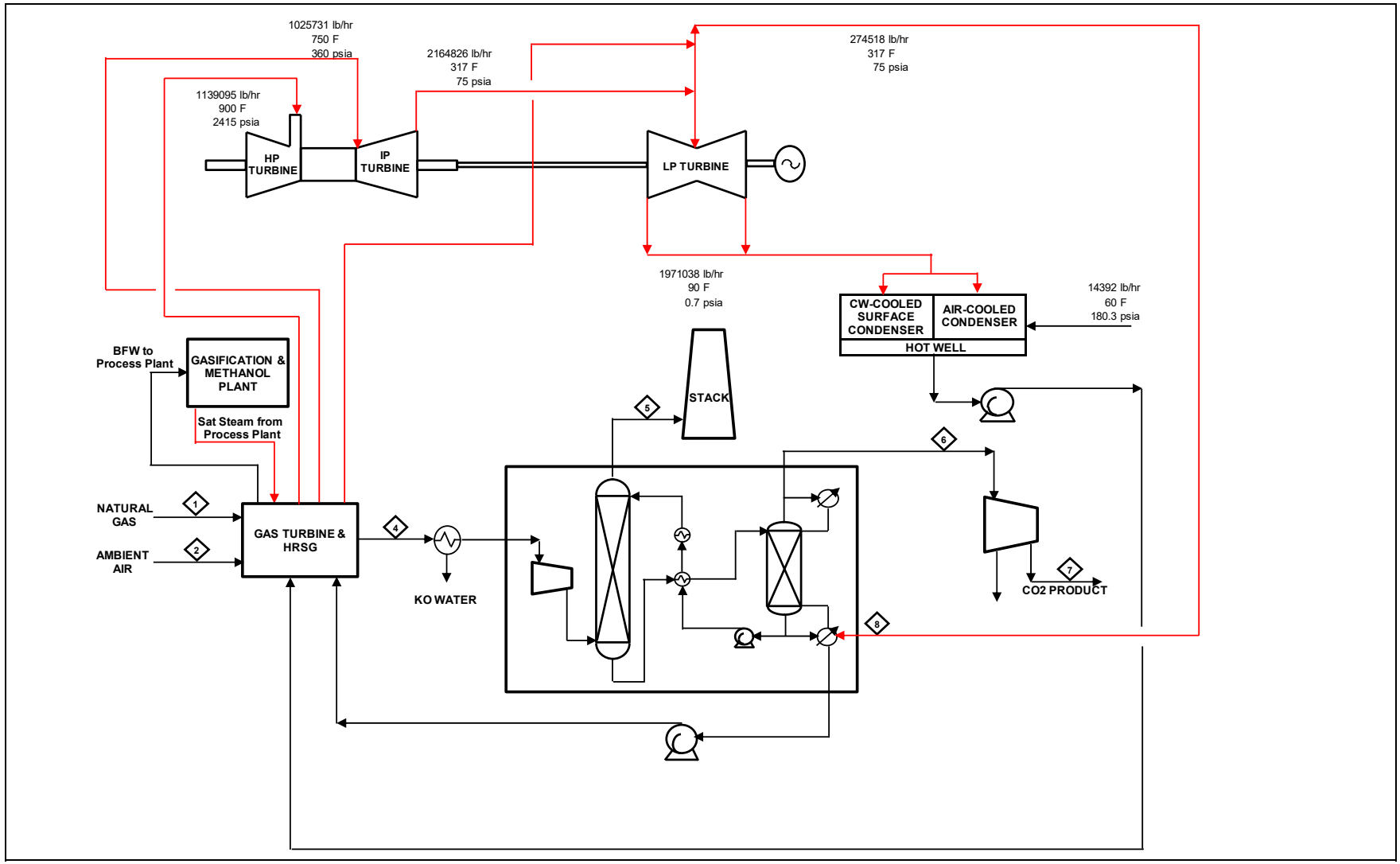

Table 8-10
Case 2a Reference Plant – NGCC Stream Table

STREAM	1	2	4	5	6	7	8
Description	Ambient Air	Natural Gas	Flue Gas to MEA	Treated Gas	CO2 Out	CO2 Product	LP Steam
Mole Flow (Vapor/Liquid)/lbmol/hr							
AR	1053	0	1053	1053	0	0	0
CH4	0	3659	0	0	0	0	0
CO	0	0	0	0	0	0	0
CO2	57	39	4152	415	3736	3736	0
COS	0	0	0	0	0	0	0
H2	0	0	0	0	0	0	0
H2O	1132	0	9016	3626	45	0	15261
H2S	0	0	0	0	0	0	0
N2	88373	63	88436	88436	0	0	0
NH3	0	0	0	0	0	0	0
O2	23715	0	15717	15717	0	0	0
SO2	0	0	0	0	0	0	0
S	0	0	0	0	0	0	0
HCN	0	0	0	0	0	0	0
HCL	0	0	0	0	0	0	0
Methanol -- CH3OH	0	0	0	0	0	0	0
Ethanol -- C2H5OH	0	0	0	0	0	0	0
Propanol -- C3H8O	0	0	0	0	0	0	0
Ethane -- C2H6	0	126	0	0	0	0	0
Propane -- C3H8	0	28	0	0	0	0	0
n-Butane -- C4H10	0	16	0	0	0	0	0
Total V/L Flow, lbmol/hr	114330	3930	118374	109248	3782	3736	15261
Total V/L Flow, lb/hr	3299430	68087.15	3367528	3105993	165255.9	164443.1	274940.1
Total Flow (Solids + V/L), lb/hr	3299430	68087	3367528	3105993	165256	164443	274940
Pressure, psia	14.5	474.7	15	15	24	2215	260
Temperature, F	59	60	297	85	69	124	35

8.4 SPARING PHILOSOPHY

The design size requires eight gasifier trains with one spare train for a total of nine gasifiers (9 x 12.5%). No further sparing information was provided in the DOE Crude Methanol Study for the rest of the CTM plant's systems.

8.5 PERFORMANCE RESULTS

The Nexant-modeled Case 2a reference plant with CO_2 capture consumes 19,418 tpd of PRB coal and 37.0 million standard cubic feet per day (MMSCFD) of natural gas at the Midwestern site and produces 937,909 lb/hr (10,210 mtpd) of crude methanol on a net basis. Overall performance for the Case 2a reference plant is summarized in Table 8-11, which includes auxiliary power requirements.

Table 8-11
Case 2a Reference Plant Performance Summary

POWER SUMMARY (Gross Power at Generator Terminals, kWe)	Case 2a
Gas Turbine Power	127,087
Steam Turbine Power	264,700
TOTAL POWER, kWe	**391,787**
CTM Plant Auxiliary Load Summary, kWe	
Coal Handling	9,090
Slag Handling	2,377
Incinerator Air Blower	4,875
Incinerator Recycle Blower	1,090
Air Separation Unit	175,570
Quench Water Pump	1,661
Syngas Recycle Compressor	6,418
Scrubber Pumps	1,068
Flash Bottoms Pump	570
Rectisol® AGR Auxiliaries	42,263
Claus Plant Auxiliaries	249
CO_2 Compressor Auxiliaries	65,213
Methanol Synthesis Syngas Feed Compressor	22,257
Recycle Gas Compressor	3,289
Air Cooler Fans	1,786
Water Treatment	3,046
Miscellaneous BOP	5,000
Circulating Water Pumps	8,195
Ground Water Pumps	873
Cooling Tower Fans	5,343
SUBTOTAL CTM PLANT AUXILIARIES, kWe	**360,233**
NGCC Plant Auxiliary Load Summary, kWe	
Gas Turbine Auxiliaries	782
Steam Turbine Auxiliaries	100
Transformer Losses	2,149
Miscellaneous BOP	500
Air Cooled Condenser Fans	4,135
Condensate Pumps	748
Boiler Feed Water Pumps	13,967
Amine System Auxiliaries	3,893
NGCC CO_2 Compression	6,033
SCR	16
SUBTOTAL POWER PLANT AUXILIARIES, kWe	**32,324**
TOTAL AUXILIARIES, kWe	**392,558**
NET PLANT POWER, kWe	**-771**
CONSUMABLES	
As-Received Coal Feed, tpd	19,418
Natural Gas Feed Rate, MMBtu/day	38,152
Raw Water Withdrawal, gpm	9,586
Raw Water Consumption, gpm	7,325

Table 8-12 shows the carbon balance for the Case 2a reference plant. The carbon input to the plant consists of carbon in the air in addition to carbon in the coal and natural gas feedstock. Carbon in the air is not part of the carbon capture equation, but is not neglected in the balance since the model accounts for the air components throughout. Carbon leaves the CTM process plant as unburned carbon in the slag, CO_2 in the dryer exhaust gas, ASU vent gas, crude methanol product, and the Rectisol® AGR CO_2 capture product. Additionally, carbon also leaves the power cycle as CO_2 in the stack and Econamine FG Plus^{SM} CO_2 capture product. Carbon in the crude methanol is considered as product, not emissions. The carbon capture efficiency is defined as the amount of carbon in the product streams, which include the crude methanol and the dried and compressed CO_2 products from the Rectisol® AGR and Econamine FG Plus^{SM} CO_2 capture processes, relative to the amount of carbon in the coal and natural gas feedstock less carbon contained in the slag. For Case 2a, the carbon capture efficiency is 92.1%.

Table 8-12
Case 2a Reference Plant – Overall Carbon Balance

Overall Carbon Balance, lb/hr	In	Out
Coal Feed	810,195	
ASU Air	602	
Coal Dryer Air	67	
Coal Dryer Supplemental Natural Gas	1,627	
Power Cycle Natural Gas	49,186	
Power Cycle Combustion Air	450	
ASU Vent		602
Coal Dryer Exhaust Gas		63,020
Carbon in Slag		4,051
Sulfur Product		0
Crude Methanol Product		347,987
Rectisol® AGR CO_2 Product		396,831
NGCC CO_2 Product		44,672
NGCC Exhaust Gas		4,964
Total	**862,127**	**862,127**

Table 8-13 shows the sulfur balance for the plant. Sulfur input comes solely from the sulfur in the coal. Sulfur output includes the sulfur recovered in the Claus plant, sulfur emitted in the coal dryer exhaust gas, and sulfur that is sequestered with the CO_2 product. Sulfur in the slag is considered negligible. The net sulfur emissions include only the sulfur emitted in the coal dryer exhaust gas. Based on this, the net sulfur emissions for the plant are 0.035 lb of SO_2/MMBtu, which meet the sulfur emission limit in the BACT environmental design basis in Table 7-5. However, this sulfur emission exceeds the environmental target used in the companion IGCC studies performed on the advanced technologies. Actual permitting for the plant will also include the methanol process in addition to the gasification and power generation, which generally targets lower sulfur emissions. If the permit for this plant requires lower sulfur emissions, additional sulfur removal would be required for this plant.

Table 8-13
Case 2a Reference Plant – Overall Sulfur Balance

Overall Sulfur Balance, lb/hr	In	Out
Coal Feed	11,772	
Sulfur Product		11,530
Coal Dryer Exhaust Gas		241
CO_2 Product		0
Convergence Tolerance		1
Total	**11,772**	**11,772**

Table 8-14 shows the overall water balance for the Case 2a plant. Raw water withdrawal is the amount of raw water consumed by the plant. The raw water is obtained from groundwater (50%) and from municipal sources (50%). Some water is discharged by the processes as effluent suitable for internal consumption. This effluent is internally recycled and consumed by the slag handling process, as make up to the syngas scrubber, and as makeup to the cooling tower. Some water is discharged from the process to a permitted outfall. Waste water is discharged by the slag handling process, the Rectisol® unit, and as cooling tower blowdown. Raw water consumption (not shown in Table 8-14) is defined as the difference between the raw water withdrawal and process water discharge.

Table 8-14
Case 2a Reference Plant – Overall Water Balance

Water Use, gpm	Raw Water Withdrawal	Process Effluent Production for Internal Consumption	Internal Consumption	Process Water Discharge
Slag Handling	**0**	**0**	**353**	**(353)**
Quench Cooler	**2,214**	**0**	**0**	**0**
Syngas Scrubber Consumption	**374**	**0**	**2,525**	**0**
Syngas Scrubber Effluent	**0**	**(1,801)**	**0**	**0**
Syngas Cooling Knockout	**0**	**(1,420)**	**0**	**0**
Sour Water Stripper Effluent	**0**	**(821)**	**0**	**0**
Rectisol® Unit	**0**	**0**	**0**	**(13)**
Steam Cycle Makeup	**29**	**0**	**0**	**0**
Steam Cycle Blowdown	**0**	**(29)**	**0**	**0**
Flue Gas Cooling Knockout	**0**	**(192)**	**0**	**0**
CO_2 Compression Knockout	**0**	**(2)**	**0**	**0**
Cooling Tower Makeup	**6,969**	**0**	**1,387**	**0**
Cooling Tower Blowdown	**0**	**0**	**0**	**(1,895)**
Total	**9,586**	**(4,265)**	**4,265**	**(2,261)**

Positive values represent consumption while negative values represent production

8.6 EQUIPMENT LIST

No equipment list was provided for the reference case in the DOE Crude Methanol Study. However, the reference case systems that warrant consideration in this study (gasification, syngas cleanup and CO_2 capture systems) are similar to the ones listed in Case S1B in the *Cost and Performance Baseline for Fossil Energy Plants, Volume 3a: Low Rank Coal to Electricity: IGCC Cases, DOE/NETL-2010/1399* report (NETL Report 1399). The reader should hence refer to the Case S1B equipment list in NETL Report 1399.

8.7 CAPITAL COST

Table 8-15 shows the cost breakdown of the Case 2a reference plant, consistent with the code of accounts format as expressed in the DOE Crude Methanol Study. The accounts/subaccounts of interest for this study are:

- 2.3 Dry Coal Injection System,
- 4 Gasifier & Accessories,
- 5A Gas Cleanup & Piping and
- 5B CO_2 Removal and Compression

These are shown with more detail to include the various subaccounts and provide more clarity to the major cost differences among the cases.

Table 8-16 shows the calculation and addition of owner's costs to determine the TOC, which is used to calculate the product methanol RSP.

The estimated TOC of the Case 2a reference plant in 2011 dollars is $5,892MM.

Table 8-15
Case 2a Reference Plant – Total Plant Cost Summary

Case 2a: Shell with Rectisol® AGR CTM Plant		Coal Feed, lb/hr	1,618,190			Plant Size	10210 metric tons per day		
Low Rank Western Coal Baseline Study	PRB	Coal HHV, Btu/lb	8,564						

Acct No.	Item/Description	Equipment Cost	Material Cost	Labor Direct	Labor Indirect	Bare Erected Cost $	Eng'g CM H.O & Fee	Contingencies Process	Contingencies Project	TOTAL PLANT COST $
1	COAL & SORBENT HANDLING	**$36,523**	**$6,549**	**$28,311**	**$0**	**$71,383**	**$6,479**	**$0**	**$15,572**	**$93,434**
2	COAL & SORBENT PREP & FEED									
2.3	Dry Coal Injection System	$203,470	$0	$137,594	$0	$341,064	$29,375	$0	$74,088	$444,527
2.x	Other Coal & Sorbent Prep & Feed Systems	$151,813	$28,795	$43,835	$0	$224,443	$19,633	$0	$48,816	$292,892
	SUBTOTAL2.	**$355,283**	**$28,795**	**$181,429**	**$0**	**$565,507**	**$49,008**	**$0**	**$122,904**	**$737,419**
3	FEEDWATER & MISC BOP SYSTEMS	**$29,758**	**$8,475**	**$18,183**	**$0**	**$56,416**	**$5,299**	**$0**	**$14,019**	**$75,734**
4	GASIFIER & ACCESSORIES									
4.1	Gasifier, Syngas Cooler & Auxiliaries (Shell)	$429,138	$0	$194,177	$0	$623,315	$55,887	$89,766	$118,739	$887,707
4.3	ASU/Oxidant Compression	$602,252	$0	$0	$0	$602,252	$58,376	$0	$66,062	$726,690
4.6	Flare Stack System	$0	$1,462	$666	$0	$2,128	$204	$0	$466	$2,798
4.9	Gasification Foundations	$0	$31,373	$18,710	$0	$50,083	$4,585	$0	$13,667	$68,335
	SUBTOTAL 4.	**$1,031,390**	**$32,835**	**$213,553**	**$0**	**$1,277,778**	**$119,052**	**$89,766**	**$198,934**	**$1,685,530**
5A	GAS CLEANUP & PIPING									
5A.1	Rectisol® System	$353,257	$0	$0	$0	$353,257	$33,374	$70,651	$91,457	$548,738
5A.2	Elemental Sulfur Plant	$10,010	$1,951	$12,826	$0	$24,787	$2,407	$0	$5,439	$32,633
5A.3	Mercury Removal	$7,601	$0	$5,745	$0	$13,346	$1,289	$667	$3,060	$18,362
5A.4c	LT Heat Recovery, FG Saturation & Shift Reactors	$101,746	$0	$45,334	$0	$147,080	$14,322	$0	$32,280	$193,682
5A.5	Syngas Compressor	$6,426	$0	$4,864	$0	$11,290	$1,075	$0	$1,237	$13,603
5A.6	Blow back Gas Systems	$6,751	$1,136	$640	$0	$8,527	$809	$0	$1,867	$11,203
5A.7	Fuel Gas Piping	$0	$2,917	$1,908	$0	$4,825	$447	$0	$1,054	$6,326
5A.9	HGCU Foundations	$0	$2,644	$1,782	$0	$4,426	$407	$0	$1,450	$6,283
	SUBTOTAL 5.	**$485,790**	**$8,648**	**$73,099**	**$0**	**$567,537**	**$54,130**	**$71,318**	**$137,845**	**$830,830**
5B	CO2 REMOVAL & COMPRESSION									
5B.1	NGCC CO2 Removal System	$22,922	$0	$6,907	$0	$29,829	$2,489	$5,966	$7,658	$45,942
5B.2	CO2 Compression & Drying (Rectisol®)	$67,218	$0	$25,340	$0	$92,558	$8,868	$0	$20,285	$121,711
5B.3	CO2 Compression & Drying (NGCC)	$10,028	$0	$3,839	$0	$13,867	$1,160	$0	$3,005	$18,032
	SUBTOTAL 5B.	**$100,168**	**$0**	**$36,086**	**$0**	**$136,254**	**$12,517**	**$5,966**	**$30,948**	**$185,685**
5C	METHANOL PRODUCTION	**$132,878**	**$55,904**	**$111,809**	**$0**	**$300,591**	**$30,060**	**$0**	**$66,130**	**$396,781**
6	COMBUSTION TURBINE/ACCESSORIES	**$47,397**	**$394**	**$3,814**	**$0**	**$51,605**	**$11,171**	**$11,909**	**$14,852**	**$89,537**
7	HRSG, DUCTING & STACK	**$29,304**	**$819**	**$6,961**	**$0**	**$37,083**	**$3,079**	**$0**	**$4,038**	**$44,201**
8	STEAM TURBINE GENERATOR	**$101,175**	**$1,098**	**$25,478**	**$0**	**$127,752**	**$11,474**	**$0**	**$27,159**	**$166,385**
9	COOLING WATER SYSTEM	**$18,209**	**$19,919**	**$14,802**	**$0**	**$52,930**	**$4,897**	**$0**	**$11,755**	**$69,582**
10	ASH/SPENT SORBENT HANDLING SYS	**$82,188**	**$3,649**	**$77,402**	**$0**	**$163,239**	**$15,794**	**$0**	**$18,685**	**$197,719**
11	ACCESSORY ELECTRIC PLANT	**$39,477**	**$23,169**	**$40,631**	**$0**	**$103,277**	**$8,979**	**$0**	**$22,375**	**$134,631**
12	INSTRUMENTATION & CONTROL	**$12,562**	**$3,797**	**$10,536**	**$0**	**$26,894**	**$2,414**	**$1,345**	**$5,493**	**$36,146**
13	IMPROVEMENTS TO SITE	**$5,886**	**$2,892**	**$15,404**	**$0**	**$24,182**	**$2,388**	**$0**	**$7,971**	**$34,541**
14	BUILDINGS & STRUCTURES	**$0**	**$7,904**	**$10,958**	**$0**	**$18,862**	**$1,705**	**$0**	**$3,335**	**$23,902**
	CALCULATED TOTAL COST	**$2,507,988**	**$204,847**	**$868,455**	**$0**	**$3,581,291**	**$338,447**	**$180,304**	**$702,016**	**$4,802,057**

Table 8-16
Case 2a Reference Plant – Total Overnight Cost Breakdown

Owner's Costs	$ x $1,000
Preproduction Costs	
6 months All Labor	$33,441
1 Month Maintenance Materials	$6,427
1 Month Non-Fuel Consumables	$1,007
1 Month Waste Disposal	$1,259
25% of 1 Months Fuel Cost at 100% CF	$7,178
2% of TPC	$96,041
Total	**$145,354**
Inventory Capital	
60 day supply of fuel at 100% CF	$56,640
60 day supply of non-fuel consumables at 100% CF	$1,401
0.5% of TPC (spare parts)	$24,010
Total	**$82,051**
Initial Cost for Catalyst and Chemicals	**$11,284**
Land	**$900**
Other Owner's Cost	**$720,308**
Financing Costs	**$129,656**
Total Owner's Costs	**$1,089,553**
Total Overnight Costs (TOC)	**$5,891,609**

8.8 OPERATING COSTS

Table 8-17 shows the operating expenditure (OPEX) breakdown for the Case 2a reference plant.

Table 8-17
Case 2a Reference Plant – Initial and Annual O&M Costs

INITIAL & ANNUAL O&M EXPENSES					
Case:	Case 2a - Shell CTM w/Rectisol®-based AGR and CO2 Capture				
Plant Size (mtpd Methanol)	**10,210**				
Primary/Secondary Fuel:	**PRB/Natural Gas**				
Design/Construction	5 years			**Book Life (yrs):**	20
TPC (Plant Cost) Year	June 2011			**TPI Year:**	2016
Capacity Factor (%)	90			**CO2 Captured (TPD)**	19380

OPERATING & MAINTENANCE LABOR

Operating Labor

Operating Labor Rate (base):	$39.70	$/hr
Operating Labor Burden:	30.00	% of base
Labor Overhead Charge	25.00	% of labor

Operating Labor Requirements per Shift	**units/mod**	**Total Plant**
Skilled Operator	2.0	2.0
Operator	10.0	10.0
Foreman	1.0	1.0
Lab Tech's etc	3.0	3.0
TOTAL Operating Jobs	16.0	16.0

	Annual Cost $
Annual Operating Labor Cost	$7,233,658
Maintenance Labor Cost	$46,271,978
Administration & Support Labor	$13,376,409
Property Taxes and Insurance	$96,041,131
TOTAL FIXED OPERATING COSTS	**$162,923,176**

VARIABLE OPERATING COSTS

Maintenance Material Cost **$69,407,968**

Consumables	Consumption Initial	Consumption /Day	Unit Cost	Initial Fill Cost	
Water(/1000 gallons)	0	6,902	1.67	**$0**	**$3,795,083**
Chemicals					
MU & WT Chem (lb)	0	41122	0.27	$0	$3,618,240
Carbon (Hg Removal) (lb)	263903	402	1.63	$430,162	$215,253
COS Catalyst (m3)	N/A	N/A	N/A	$0	$0
Water Gas Shift Catalyst (ft3)	10514	7.20	771.99	$8,116,617	$1,826,896
MEA Solvent (ton)	152	0.21	3751.70	$569,647	$255,903
SCR Catalyst (m3)	N/A	N/A	N/A	$0	$0
Ammonia (ton)	N/A	N/A	N/A	$0	$0
Methanol Synthesis Catalyst (ft3)	4054	3.70	534.68	$2,167,532	$649,538
Claus Catalyst (ft3)	w/equip	2.05	203.15	$0	$136,916
Subtotal Chemicals				**$11,283,957**	**$6,702,747**
Other					
Supplemental Electricity (MWh consumed)	0	18.5	62.33	$0	$378,778
Gases, N2 etc.(/100scf)	0	0	0.00	$0	$0
LP Steam (/1000 lbs)	0	0	0.00	$0	$0
Subtotal Other				**$0**	**$378,778**
Waste Disposal:					
Spent Mercury Catalyst (lb)	0	402	0.65	$0	$85,837
Flyash (ton)	0	0	0.00	$0	$0
Slag (ton)	0	1638	25.11	$0	$13,515,321
Subtotal Waste Disposal				**$0**	**$13,601,158**
By-products & Emissions					
Sulfur (tons)	0	138.3	0.00	$0	$0
Supplemental Electricity (MWh generated)	0	0	-59.59	$0	$0
Subtotal By-Products				**$0**	**$0**
TOTAL VARIABLE OPERATING COSTS				**$11,283,957**	**$93,885,734**
Coal (tons)	**0**	**19,418**	**36.57**	**$0**	**$233,276,555**
Natural Gas (MMBtu)	**0**	**38,152**	**6.13**	**$0**	**$76,827,051**

8.9 METHANOL PRODUCT REQUIRED SELLING PRICE

Table 8-18 shows a summary of the power output, CAPEX, OPEX, and methanol product RSP for the Case 2a reference plant. The Case 2a reference plant methanol RSP is estimated to be $1.46/gal under the loan guarantee finance structure and $1.72/gal under the commercial fuels finance structure.

Table 8-18
Case 2a Reference Plant – Overall Performance and Economic Summary

Case	Case 2a	
CAPEX, $MM		
Total Installed Cost (TIC)	$3,581	
Total Plant Cost (TPC)	$4,802	
Total Overnight Cost (TOC)	$5,892	
OPEX, $MM/yr (100% Capacity Factor Basis)		
Fixed Operating Cost (OC_{fix})	$162.9	
Variable Operating Cost, less Fuel (OC_{var})	$103.9	
Coal Feedstock (OC_{coal})	$259.2	
Natural Gas Feedstock (OC_{NG})	$85.4	
Import/(Export) Power (OC_{Power})	$0.4	
Total OPEX	$611.8	
Plant Output		
Crude Methanol Product, tons per year	4,108,017	
Net Power Output, MWe	-0.77	
Required Selling Price[A]		
Excluding CO_2 TS&M[BE], $/short ton	**424.1**	**500.6**
Including CO_2 TS&M[BE], $/short ton	**441.3**	**517.8**
RSP Component Details ($/gal)		
Capital[B]	0.90	1.15
Fixed O&M	0.15	
Variable O&M	0.08	
Coal	0.21	
Natural Gas	0.07	
Power	0.00	
CO_2 TS&M	0.06	
RSP[B] Total ($/gal)	**1.46**	**1.72**
Costs of CO_2 Captured[B,C] ($/tonne)	**17.2**	**19.2**
Costs of CO_2 Avoided[B,D] ($/tonne)	**28.2**	**30.2**

[A] Capacity factor assumed to be 90 percent
[B] Values shown are for two financial structures
The first (lower value) is based on the loan guarantee finance structure
The second (higher value) is based on the commercial fuels finance structure
[C] Excludes CO_2 TS&M
[D] Includes CO_2 TS&M
[E] Based on 301.73 gallons/short ton (332.6 gallons/metric ton)

Section 9 Case 2b: GTI R-GAS™ with RTI WDP CTM Plant

The Case 2b process descriptions, performance and cost results in this section were previously presented in Nexant's DE-FE0012066 CTM report. They are reproduced here for the reader's ease of reference.

9.1 PROCESS OVERVIEW

The Case 2b GTI R-GAS™ with RTI WDP CTM plant, like the Case 2a reference plant, uses Montana PRB coal and is designed to generate enough syngas to produce a nominal 10,000 mtpd of methanol. The Case 2b plant is equipped with gas and steam turbines to generate power via NGCC to meet the plant's auxiliary power demands. No power import is required, and excess power is exported to the grid as byproduct for additional revenue. The Case 2b plant is designed to capture CO_2 with a carbon capture efficiency of more than 90% of the carbon in the coal and natural gas.

The Case 2b plant is assumed to operate with an annual on-stream CF of 90% or 7,884 hr/year at full capacity and has the following characteristics that differentiate it from the Case 2a reference plant:

- The GTI DSP feed system replaces the reference case's lockhopper system used to feed dried coal to the gasifier. Nexant had previously evaluated the GTI DSP feed system in comparison to the Shell lockhopper feed system in a separate study (DE-FE0012062) for DOE on behalf of Aerojet Rocketdyne. The results from this earlier study have been used to establish the performance and cost of the DSP feed system for this case.

- The GTI R-GAS™ gasifier replaces the Shell gasifier from Case 2a.

- Syngas leaving the gasifier that has been quenched enters RTI's WDP for sulfur removal at above 760°F instead of going through a low temperature scrubber as in Case 2a.

- After sulfur removal in RTI's WDP, the treated syngas in Case 2b then enters RTI's AFWGS process. Instead of a sour shift WGS process used in Case 2a, the Case 2b AFWGS process consists of fixed–bed reactors (using commercial high-temperature sweet shift catalyst) combined in such a manner as to significantly reduce the overall steam consumption and reactor capital cost while still meeting the catalyst vendor's steam to CO recommendations. These reactors are operated at standard temperatures for commercial high-temperature sweet water-gas shift processes, but at a higher inlet temperature than commercial sour shift processes.

- After the hydrogen-rich shifted syngas is cooled, it enters an AACRP unit for CO_2 capture. Unlike Rectisol® that uses a physical solvent, AACRP uses activated methyldiethanolamine, which is a chemical solvent. As ~99.9% of the sulfur compounds have been removed upstream by the WDP process, the AACRP process only has to remove CO_2 and is less complicated than the two-stage Rectisol® process. The AACRP unit also captures ~99% of any residual sulfur left in the syngas following WDP along

with the CO_2, resulting in an overall system total sulfur reduction of >99.99% (sub-ppmv total sulfur in the final cleaned syngas).

- The DSRP replaces the Claus process used in Case 2a. In the DSRP, sulfur leaving the WDP process in the form of SO_2 is reduced by a slipstream of shifted, hydrogen-rich syngas, forming elemental sulfur, H_2S and COS. The elemental sulfur is condensed while the remaining H_2S and COS are re-oxidized in the presence of air to SO_2. The SO_2 is then removed in a lime scrubber, forming gypsum ($CaSO_4.2H_2O$). This combined approach for sulfur capture results in very low net SO_2 emissions.

Due to the different cold gas efficiency of the GTI R-GAS™ gasification process, the R-GAS™ gasifier consumes a different amount of coal feed compared to the Shell gasifier in Case 2a in order to produce the same amount of syngas to produce nominally 10,000 mtpd of methanol.

9.2 CASE 2b PROCESS DESCRIPTION

Case 2b is modeled by adapting the Case 2a reference model with gasifier and syngas cleanup process information provided by GTI and RTI. The system description below follows the BFD in Figure 9-2 and stream numbers referenced in the same figure. The overall BFD for the Case 2b plant is shown in Figure 9-2, with the accompanying stream flows shown in Table 9-1. Additional descriptions of the Case 2b plant's various processes are provided below. To better visualize the different unit operations in the Case 2b plant, simplified PFDs of the various plant processes are depicted in Figure 9-2 through Figure 9-9. Table 9-2 through Table 9-8 provide the model-generated process data for the numbered streams referenced in the PFDs.

Coal Preparation and Drying

Same as Case 2a except no supplemental natural gas firing is required in the dryer. For Case 2b, the methanol synthesis purge gas has enough heating value that it can be used as fuel for coal drying without the need of natural gas as supplementary fuel.Figure 9-3 depicts the coal drying process while Table 9-2 presents the mass balances.

GTI DSP Coal Feed System

Dried coal from the atmospheric storage silo enters the GTI DSPs via gravity flow. Three DSPs, each with a nominal capacity of 1,000 tons per day (tpd), are required to service each of the gasification trains. The DSPs increase the pressure of the coal from atmospheric to 1,100 psia and subsequently discharge the coal continuously to a pressurized feed bin.

Coal is continuously withdrawn from the pressurized feed bin and conveyed by HP CO_2 via a single feed line to each gasifier. To maximize conversion efficiency of fuel to syngas in the gasifier, GTI uses its proprietary static splitter system.

Air Separation Unit

Same as Case 2a except no oxygen is routed to the Claus plant.

GTI R-GAS™ Gasifier

For the Case 2b plant, five GTI R-GAS™ gasifier trains operating at 915 psia are needed to generate the required amount of syngas. Each gasification train includes a single gasifier with a nominal capacity of 3,000 tpd sized for a bituminous (Illinois #6) coal feed. Based on recent pilot plant gasifier testing under DE-FE0023577 with PRB coal, demonstrating >98% conversion in less than 1/3 the residence time associated with the nominal design gasifier capacity, each of these gasifiers is estimated to provide a minimum of 3,600 tpd capacity operating on the reference sub-bituminous coal feedstock. This allows four out of five gasifiers to gasify 14,400 tpd of coal out of the 14,500 required for Case 2b, providing 99% capacity factor without an installed spare.

Fuel feeds from the pressurized feed bin via the dense phase feed line, conveyed by HP CO_2. To maximize conversion efficiency of fuel to syngas, GTI splits the feedstock from a single feed line into multiple injection ports via its proprietary static splitter system. The injection ports maximize mixing of coal and oxygen to initiate the gasification reaction.

The GTI R-GAS™ gasifier is oriented in a vertical, down-firing position. The gasifier reaction is initiated with a torch burner, which is ignited at full gasifier pressure. The ignition torch runs on natural gas and oxygen.

The gasifier injector faceplate and the gasifier liner are water cooled to maintain the metal components at temperatures conducive to long life. The cooling water needs to be clean enough (HP BFW quality) to prevent scale buildup or clogging of internal cooling passages.

The gasifier's raw syngas product is partially quenched from about 2,350°F to around 800°F through the introduction of quench water spray. The quench water enters the gasifier through multiple hydraulic atomizing spray nozzles.

The solids are removed as slag and ash. Liquid slag is solidified in a water bath and removed via a lock hopper system. Ash carried over with the syngas is removed in a candle filter. The ash is also removed via a lock hopper system.

The GTI DSP, ASU, gasification and quench processes are shown in Figure 9-4 and their mass balances are presented in Table 9-3.

Dry Solids Removal

Same process description as Case 2a but it operates at a higher pressure. The solids removal process is shown in Figure 9-4.

After solids removal, the syngas then goes through a raw gas cooler, which lowers the gas temperature and contributes to the production of HP steam for use in steam cycle. The syngas then enters the RTI WDP unit immediately downstream for sulfur removal.

Unlike Case 2a, the syngas scrubber is eliminated in Case 2b as the hot syngas at around 760°F enters the RTI WDP directly without quench cooling.

Warm Syngas Cleanup Process

RTI's advanced warm syngas cleanup process consists of five major system components: RTI WDP, RTI DSRP, RTI AFWGS reactors, Low Temperature Gas Cooling (LTGC) and the AACRP unit. These are described in greater detail below.

Warm Desulfurization Process

The WDP process, shown in Figure 9-1, uses transport-bed reactors that are similar to commercial Fluid Catalytic Cracking (FCC) reactor designs. It consists of a pair of these reactors: an adsorber and a regenerator. Hot syngas leaving the candle filter is routed to the WDP adsorber where it is contacted with circulating Zn-containing attrition-resistant sorbent (developed and patented by RTI) to remove the sulfur-bearing compounds, in the form of H_2S and COS, from the syngas. The following reactions take place when the sorbent contacts the raw syngas:

$$H_2S + ZnO \rightarrow ZnS + H_2O$$
$$COS + ZnO \rightarrow ZnS + CO_2$$

Regenerated sorbent from the regenerator, along with recycled sorbent from the adsorber standpipe, contact the raw syngas, which enters the adsorber near the bottom of the unit. The treated, essentially sulfur-free syngas is separated from sorbent via a cyclone. Any remnant attrited or fine particulate solids entrained in the essentially sulfur-free syngas are removed in a filter. A majority of the sorbent separated by the cyclone is recycled to the adsorber via a standpipe, while a portion of the sorbent is fed to the regenerator.

Within the regenerator, oxidation of the ZnS containing sorbent takes place, producing SO_2 and regenerating ZnO, per the following reaction:

$$ZnS + 3/2\ O_2 \rightarrow ZnO + SO_2$$

The regenerator uses air as the oxidant. Air is compressed in a multi-stage air compressor up to the regenerator operating pressure before it is fed into the regenerator. The oxidation reaction is exothermic, raising the temperature of the resulting mixture. The regenerator offgas containing SO_2 is heat exchanged with the compressed air before the offgas enters the DSRP. The regenerated sorbent is recycled back to the adsorber, where it adsorbs H_2S and COS again.

Figure 9-1
WDP Process Schematic

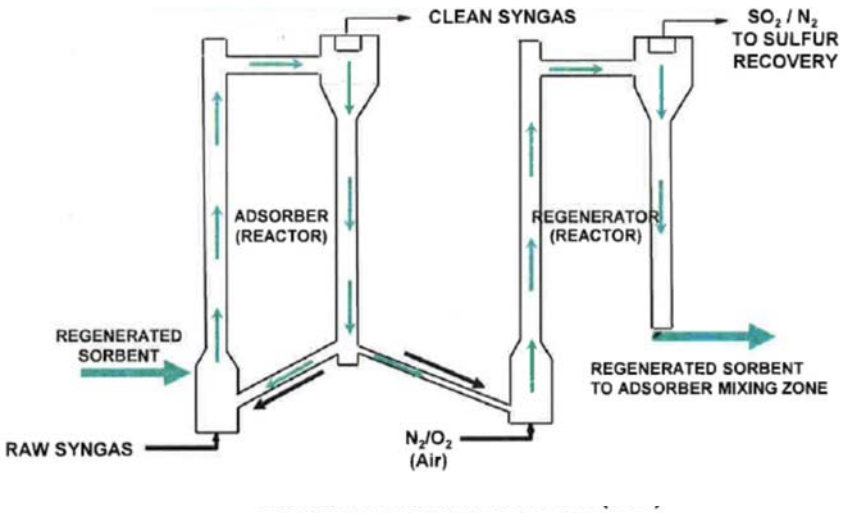

[Similar to Commercial FCC Reactor Designs]

Direct Sulfur Reduction Process

The offgas from the regenerator contains essentially SO_2 and N_2. It goes through a filter to remove any entrained solids and is cooled before it is sent into the fixed-bed DSRP reactor where SO_2 is reduced to elemental sulfur according to the following reactions:

$$SO_2 + 2\ CO \rightarrow CO_2 + S$$
$$SO_2 + H_2 \rightarrow 2\ H_2O + S$$

The reducing gas is provided by a hydrogen-rich syngas slip stream from downstream of the shift reactors. A slight excess of the reducing gas is used to ensure complete reduction of the SO_2. Some H_2S and COS are formed alongside the elemental sulfur. The product stream from the DSRP reactor is sent on to a sulfur condenser unit where the elemental sulfur is condensed and separated. Heat is recovered in the condenser by making low pressure steam.

The condenser overhead gas still contains some residual H_2S and COS. These are re-oxidized to SO_2 in a fixed-bed oxidation reactor containing a redox catalyst in the presence of compressed air, which functions as the oxidant. The compressed air is a slipstream drawn from the air compressor in the WDP section.

Finally, the SO_2-containing gas leaving the oxidation reactor is cooled and sent to a lime scrubber downstream. Lime, or calcium hydroxide ($Ca(OH)_2$), reacts with the SO_2 in the presence of oxygen to form gypsum ($CaSO_4.2H_2O$) per the following reaction, which is akin to the Wet Flue Gas Desulfurization (WFGD) process used for scrubbing flue gas.

$$Ca(OH)_2 + SO_2 \rightarrow CaSO_3 + H_2O$$

$$CaSO_3 + 2\ H_2O + ½\ O_2 \rightarrow CaSO_4.2H_2O$$

The gypsum leaves the bottom of the scrubber as a byproduct of the CTM plant. The treated, sulfur-free overhead gas is split into three portions. One portion is recycled to the DSRP to help control reactor temperature rise due to the exothermic heat from the DSRP reactions. The second portion is compressed and routed to the WDP process to be utilized as stripping or fluidizing gas in the WDP adsorber and regenerator. The remaining portion is vented to the atmosphere.

Advanced Fixed-Bed Water-Gas Shift

The treated syngas from the WDP enters the AFWGS process. In order to achieve a 2:1 ratio of H_2 to CO in the final syngas to the methanol synthesis reactors, approximately 64 percent of the coal-derived syngas is shifted, with the remainder bypassing the shift reactors. Part of the sTwo fixed-bed shift reactors in series are used to achieve the desired H_2/CO composition in the syngas. team for the WGS reaction is provided by vaporized quench water in the R-GAS™ gasifier. In RTI's AFWGS process a series of fixed-bed reactors using high-temperature shift catalyst are combined in a manner that enables a significant reduction in overall steam consumption and capital cost of the WGS process while still meeting the catalyst manufacturer's steam to CO recommendations and achieving the high CO conversion required by the process.

The RTI WDP, DSRP and WGS processes are shown in Figure 9-5 and the mass balances are presented in Table 9-4.

Low Temperature Gas Cooling and Mercury Removal

The shifted syngas goes through a series of heat exchangers to generate various levels of steam and preheat BFW before it finally undergoes cooling by cooling water. The cooled syngas is sent to a knockout (KO) drum where the condensate is drained. Mercury is removed from the overhead syngas leaving the KO drum via the process described in Section 8.2.4. RTI has also developed a warm-gas mercury capture process that operates at ~350°F-390°F, though it was not used here. The LTGC and mercury removal processes are shown in Figure 9-6 and the mass balances presented in Table 9-5.

Activated Amine CO_2 Removal Process

The AACRP is based on the activated methyldiethanolamine process, which is marketed commercially by companies such as BASF, Shell and UOP for the removal of acid gases like H_2S and CO_2. The scrubbing agent is an aqueous alkaline amine solution. For this application, the CO_2-containing syngas is passed through an absorber that contains a circulating alkaline amine scrubbing solution, where the bulk of the CO_2 removal takes place. An acid-base reaction occurs where the CO_2 reacts with alkaline amine and is captured in solution.

To achieve the desired extent of CO_2 capture, and to ensure that the product gas meets the volatile organic compound (VOC) specifications, a lean amine wash column is used to treat the syngas leaving the main alkaline amine absorber. Water enters at the top of this column where it contacts and scrubs the CO_2-lean syngas. This serves to remove any entrained alkaline amine

The rich, CO_2-loaded solution is sent to a regenerator to release the absorbed CO_2. The solution is first depressurized, flashing off some CO_2 in the process and helping to reduce the overall heat of CO_2 regeneration. The low-pressure solution is then sent to a thermal regenerator, where heat is applied to release the remaining CO_2. Regenerated alkaline amine solution is recycled to the absorber and used again.

For the AACRP, the CO concentration in the CO_2 product is about 700 ppmv. Although this is higher than the CO limit (35 ppmv) for saline reservoir CO_2 sequestration as shown in Table 2-3, it is still within the range stated in literature (10-5,000 ppmv). It should also be noted that the CO concentration of the AACRP CO_2 product is one order of magnitude lower than in Case 2a as AACRP is more selective towards absorbing CO_2 when compared with the Rectisol® process.

CO_2 Compression and Dehydration

CO_2 from the AACRP is generated at a single pressure of 20.7 psia. The CO_2 stream is compressed to a supercritical condition at 2,215 psia using a multiple-stage, intercooled compressor. During compression, the CO_2 stream is dehydrated to a dew point of -40°F using a thermal swing adsorptive dryer. The dehydrated CO_2 is transported to the plant fence line for sequestration outside the battery limit (OSBL).

The AACRP and CO_2 compression process are shown in Figure 9-7, while the material balance is shown in Table 9-6. The stream numbers labeled on the PFD correspond to the stream numbers in the material balance table.

Methanol Reactor and Synthesis Loop

The methanol synthesis process is shown in Figure 9-8, while the material balance is shown in Table 9-7. The stream numbers labeled on the PFD correspond to the stream numbers in the material balance table. The process follows the description stated earlier in Section 8.2.4.

For the Case 2b plant, the syngas feed compressor to the methanol synthesis reactors has been eliminated due to the higher system pressure upstream. Also, there is excess purge gas after taking into account the fuel requirements for coal drying. This excess gas is routed to the NGCC to produce power, thus cutting back on the natural gas firing rate for power generation.

NGCC

Same as Case 2a. The PFD for the NGCC section is shown in Figure 9-9, while the material balance is shown in Table 9-8. The stream numbers labeled on the PFD correspond to the stream numbers in the material balance table.

Power Cycle Flue Gas Post Combustion CO_2 Capture and Compression

Like in Case 2a, Fluor's Econamine FG Plus^{SM} process was used to capture CO_2 from the flue gas leaving the NGCC HRSG. The CO_2 leaving the Econamine FG Plus^{SM} capture process, like the AACRP CO_2 product, still contains moisture. The two moisture-bearing CO_2 streams are thus

combined and compressed to 2,215 psia by a multi-stage, intercooled centrifugal compressor that is equipped with a thermal swing adsorptive dryer, which dehydrates the CO_2 stream to a dew point of -40ºF. The virtually moisture-free supercritical CO_2 stream is delivered to the plant B/L as sequestration ready.

Figure 9-2
Case 2b Plant – Overall BFD

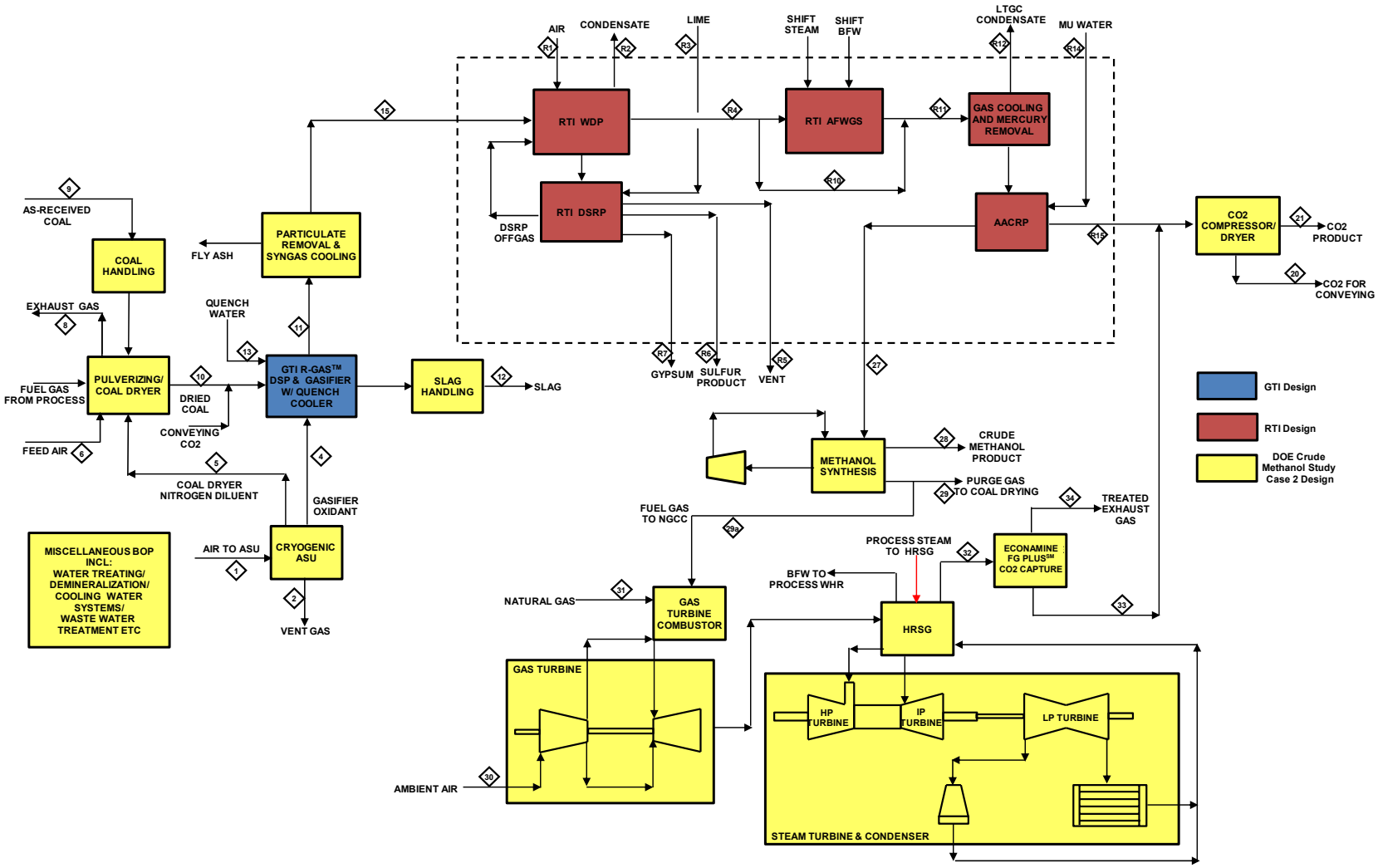

Table 9-1
Case 2b Plant – Overall Stream Table

Description	Air to ASU	ASU Vent Gas	Gasifier Oxidant	Nitrogen Diluent to Dryer	Air Feed to Coal Dryer	Coal Dryer Exhaust	As-Received Coal	Dried Coal	Quenched Syngas	Slag	Quench Water	Syngas to RTI WDP
Stream No.	1	2	4	5	6	8	9	10	11	12	13	15
V-L Mole Fraction												
Ar	0.0092	0.0219	0.0300	0.0023	0.0092	0.0077	0	0	0.0053	0	0	0.0053
CH4	0	0	0	0	0	0	0	0	0.0023	0	0	0.0023
CO	0	0	0	0	0	0	0	0	0.4251	0	0	0.4251
CO2	0.0003	0.0052	0	0	0.0003	0	0	0	0.0134	0	0	0.0134
COS	0	0	0	0	0	0	0	0	0.0002	0	0	0.0002
H2	0	0	0	0	0	0	0	0	0.1719	0	0	0.1719
H2O	0.0099	0.1535	0	0	0.0099	0.1567	0	0	0.3732	0	1.0000	0.3732
H2S	0	0	0	0	0	0	0	0	0.0021	0	0	0.0021
N2	0.7732	0.6989	0.0200	0.9921	0.7732	0.7947	0	0	0.0057	0	0	0.0057
NH3	0	0	0	0	0	0	0	0	0.0007	0	0	0
O2	0.2074	0.1206	0.9500	0.0054	0.2074	0	0	0	0	0	0	0
SO2	0	0	0	0	0	0.0000	0	0	0	0	0	0
S	0	0	0	0	0	0	0	0	0	0	0	0
HCN	0	0	0	0	0	0	0	0	0	0	0	0
HCl	0	0	0	0	0	0	0	0	0	0	0	0
Ca(OH)2	0	0	0	0	0	0	0	0	0	0	0	0
CaSO.2H2O	0	0	0	0	0	0	0	0	0	0	0	0
Methanol	0	0	0	0	0	0	0	0	0	0	0	0
Ethanol	0	0	0	0	0	0	0	0	0	0	0	0
Propanol	0	0	0	0	0	0	0	0	0	0	0	0
Ethane	0	0	0	0	0	0	0	0	0	0	0	0
Propane	0	0	0	0	0	0	0	0	0	0	0	0
n-Butane	0	0	0	0	0	0	0	0	0	0	0	0
Total	1.0000	1.0000	1.0000	1.0000	1.0000	1.0000	0	0	1.0000	0	1.0000	1.0000
V-L Flowrate, lbmol/hr	128485	8141	26484	93860	18222	136198	0	0	151097	0	53860	151097
V-L Flowrate, lb/hr	3707669	222286	851648	2633735	525820	3682889	0	0	3032729	0	970303	3032728
Solids Flow Rate, lb/hr	0	0	0	0	0	0	1528260	1206840	0	125127.4	0	0
Temperature, F	59	64	292	70	59	190	59	190	826		250	755
Pressure, psia	14.7	16.4	1000.0	18.0	14.7	14.3	14.7	14.3	915.0	915.0	980.0	905.0

Table 9-1 (cont'd)
Case 2b Plant – Overall Stream Table

Description	Air to RTI WDP	Comp Air KO Water	Lime	Sweet Syngas	DSRP Vent Gas	Sulfur Product	Gypsum	Bypass Syngas	Syngas to Cooling	Cooled Syngas KO Water	Syngas to aMDEA Unit	Makeup Wash Water	aMDEA CO2 Out
Stream No.	R1	R2	R3	R4	R5	R6	R7	R10	R11	R12	R13	R14	R15
V-L Mole Fraction													
Ar	0.0092	0	0	0.0053	0.0131	0	0	0.0053	0.0041	0	0.0062	0	0
CH4	0	0	0	0.0023	0	0	0	0.0023	0.0018	0	0.0027	0	0
CO	0	0	0	0.4214	0	0	0	0.4214	0.1535	0	0.2321	0	0.0007
CO2	0.0003	0	0	0.0173	0.0627	0	0.0105	0.0173	0.1863	0.0002	0.2815	0	0.9093
COS	0	0	0	0.0000	0	0	0	0.0000	0.0000	0	0	0	0
H2	0	0	0	0.1754	0	0	0	0.1754	0.3088	0	0.4667	0	0.0020
H2O	0.0099	1.0000	0.9737	0.3693	0.0001	0	0.9649	0.3693	0.3386	0.9981	0.0012	1.0000	0.0879
H2S	0	0	0	0.0000	0	0	0	0.0000	0.0000	0	0	0	0
N2	0.7732	0	0	0.0083	0.9240	0	0.0005	0.0083	0.0064	0	0.0097	0	0
NH3	0	0	0	0	0	0	0	0	0	0.0017	0	0	0
O2	0.2074	0	0	0	0	0	0	0	0	0	0	0	0
SO2	0	0	0	0	0	0	0	0	0	0	0	0	0
S	0	0	0	0	0	1.0000	0	0	0	0	0	0	0
HCN	0	0	0	0	0	0	0	0	0	0	0	0	0
HCl	0	0	0	0	0	0	0	0	0	0	0	0	0
Ca(OH)2	0	0	0.0263	0	0	0	0.0010	0	0	0	0	0	0
CaSO.2H2O	0	0	0	0	0	0	0.0227	0	0	0	0	0	0
Methanol	0	0	0	0	0	0	0	0	0	0	0	0	0
Ethanol	0	0	0	0	0	0	0	0	0	0	0	0	0
Propanol	0	0	0	0	0	0	0	0	0	0	0	0	0
Ethane	0	0	0	0	0	0	0	0	0	0	0	0	0
Propane	0	0	0	0	0	0	0	0	0	0	0	0	0
n-Butane	0	0	0	0	0	0	0	0	0	0	0	0	0
Total	1.0000	1.0000	1.0000	1.0000	1.000	1.000	1.000	1.0000	1.0000	1.0000	1.0000	1.0000	1.0000
V-L Flowrate, lbmol/hr	4679	33	8571	153559	3499	130	9514	55604	198242	67089	129107	3556	36778
V-L Flowrate, lb/hr	135022	603	167062	3081007	102062	4167	207924	1115633	3886005	1208828	2635413	64062	1531019
Solids Flow Rate, lb/hr	0	0	0	0	0	0	0	0	0	0	0	0	0
Temperature, F	59	80	75	685	105	305	172	685	844	95	95	122	122
Pressure, psia	14.7	13.0	13.0	894.0	750.8	14.7	14.7	894.0	869.0	844.0	829.0	814.0	20.7

Table 9-1 (cont'd)
Case 2b Plant – Overall Stream Table

Description	Convey'g CO2	CO2 Product	Treated Syngas to MeOH	Crude Methanol Product	MeOH Synthesis Purge Gas	Excess Purge to NGCC	Air to Gas Turbine	Natural Gas Feed	NGCC Flue Gas Exhaust	CO2 to Comp-ression	Treated NGCC Exhaust
Stream No.	20	21	27	28	29	29a	30	31	32	33	34
V-L Mole Fraction											
Ar	0	0	0.0083	0.0001	0.1064	0.1064	0.0092	0	0.0100	0	0.0108
CH4	0	0	0.0036	0	0.0435	0.0435	0	0.9310	0	0	0
CO	0.0008	0.0007	0.3122	0	0.1328	0.1328	0	0	0	0	0
CO2	0.9969	0.9973	0.0302	0.0108	0.2011	0.2011	0.0003	0.0100	0.0367	0.9885	0.0040
COS	0	0	0	0	0	0	0	0	0	0	0
H2	0.0022	0.0019	0.6276	0	0.3235	0.3235	0	0	0	0	0
H2O	0	0	0.0050	0.0167	0.0001	0.0001	0.0099	0	0.0762	0.0115	0.0333
H2S	0	0	0	0	0	0	0	0	0	0	0
N2	0	0	0.0131	0.0001	0.1728	0.1728	0.7732	0.0160	0.7447	0	0.8081
NH3	0	0	0	0	0	0	0	0	0	0	0
O2	0	0	0	0	0	0	0.2074	0	0.1325	0	0.1438
SO2	0	0	0	0	0	0	0	0	0	0	0
S	0	0	0	0	0	0	0	0	0	0	0
HCN	0	0	0	0	0	0	0	0	0	0	0
HCl	0	0	0	0	0	0	0	0	0	0	0
Ca(OH)2	0	0	0	0	0	0	0	0	0	0	0
CaSO.2H2O	0	0	0	0	0	0	0	0	0	0	0
Methanol	0	0	0	0.9713	0.0197	0.0197	0	0	0	0	0
Ethanol	0	0	0	0.0010	0	0	0	0	0	0	0
Propanol	0	0	0	0	0	0	0	0	0	0	0
Ethane	0	0	0	0	0	0	0	0.032	0	0	0
Propane	0	0	0	0	0	0	0	0.007	0	0	0
n-Butane	0	0	0	0	0	0	0	0.004	0	0	0
Total	1.0000	1.0000	1.0000	1.0000	1.0000	1.0000	1.0000	1.0000	1.0000	1.0000	1.0000
V-L Flowrate, lbmol/hr	2940	34551	94905	28979	6571	1216	114330	3690	119065	3974	109716
V-L Flowrate, lb/hr	129095	1517330	1156519	925862	155384	28746	3299204	63929	3391495	173711	3120951
Solids Flow Rate, lb/hr	0	0	0	0	0	0	0	0	0	0	0
Temperature, F	270	162	148	119	130	130	59	60	272	69	85
Pressure, psia	1100.0	2215	814	40	717	717	14.5	474.7	14.9	24	15.0

Figure 9-3
Case 2b Plant – Coal Drying BFD

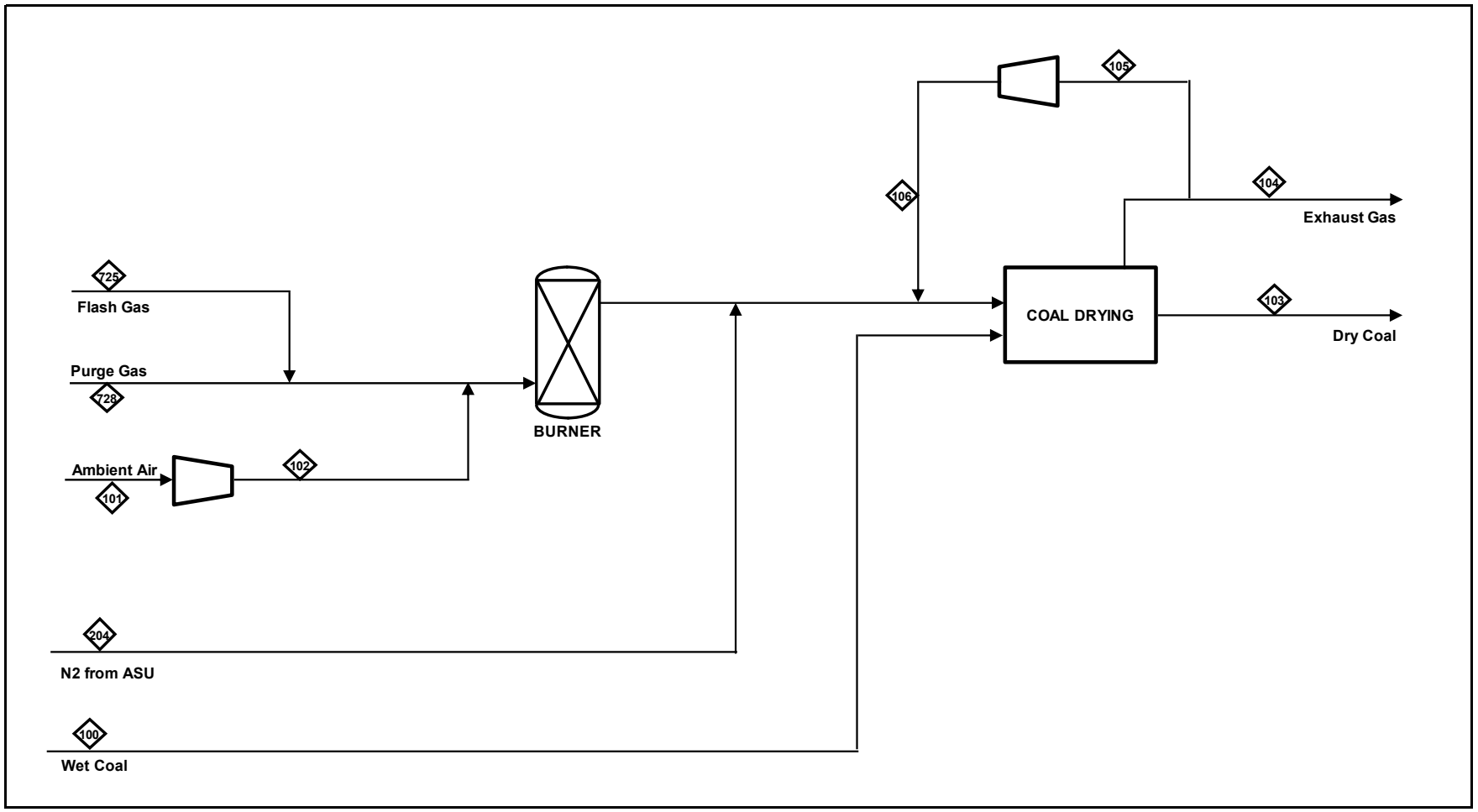

Table 9-2
Case 2b Plant – Coal Drying Stream Table

STREAM	100	101	102	103	104	105	106	204	725	728
Description	Wet Coal	Ambient Air	Feed Air	Dry Coal	Exhaust Gas	LP Recycle Gas	HP Recycle Gas	Dilution Nitrogen	MeOH Flash Gas	MeOH Purge Gas
Mole Flow (Vapor/Liquid)/lbmol/hr										
AR	0	169	169	0	1044	562	562	216	89	570
CH4	0	0	0	0	0	0	0	0	52	233
CO	0	0	0	0	0	0	0	0	38	711
CO2	0	9	9	0	3845	2070	2070	0	1247	1077
COS	0	0	0	0	0	0	0	0	0	0.00268
H2	0	0	0	0	0	0	0	0	39	1733
H2O	0	0	0	0	21156	11392	11392	19	2	1
H2S	0	0	0	0	0	0	0	0	0	0.00114
N2	0	14226	14226	0	108373	58355	58355	93118.15	104	926
NH3	0	0	0	0	0	0	0	0	0	0
O2	0	3817	3817	0	1780	958	958	507	0	0
SO2	0	0	0	0	0	0	0	0	0	0
S	0	0	0	0	0	0	0	0	0	0
HCN	0	0	0	0	0	0	0	0	0	0
HCL	0	0	0	0	0	0	0	0	0	0
Methanol -- CH3OH	0	0	0	0	0	0	0	0	370	105
Ethanol -- C2H5OH	0	0	0	0	0	0	0	0	0.2	0.1
Propanol -- C3H8O	0	0	0	0	0	0	0	0	0	0
Ethane -- C2H6	0	0	0	0	0	0	0	0	0	0
Propane -- C3H8	0	0	0	0	0	0	0	0	0	0
n-Butane -- C4H10	0	0	0	0	0	0	0	0	0	0
Total V/L Flow, lbmol/hr	0	18222	18222	0	136198	73337	73337	93860	1942	5355
Total V/L Flow, lb/hr	0	527831	527831	0	3684901	1984176	1984176	2633735	75258	126638
Solids Mass Flow, lb/hr	1528260	0	0	1206840	0	0	0	0	0	0
Coal	1528260	0	0	1206840	0	0	0	0	0	0
Ash	0	0	0	0	0	0	0	0	0	0
Carbon	0	0	0	0	0	0	0	0	0	0
Total Flow (Solids + V/L), lb/hr	1528260	527831	527831	1206840	3684901	1984176	1984176	2633735	75258	126638
Pressure, psia	14.7	14.7	17	14.3	14.3	14.3	16	18	40	717
Temperature, F		59	90		190	190	219	70	119	130

Figure 9-4
Case 2b Plant – ASU/Coal Gasification PFD

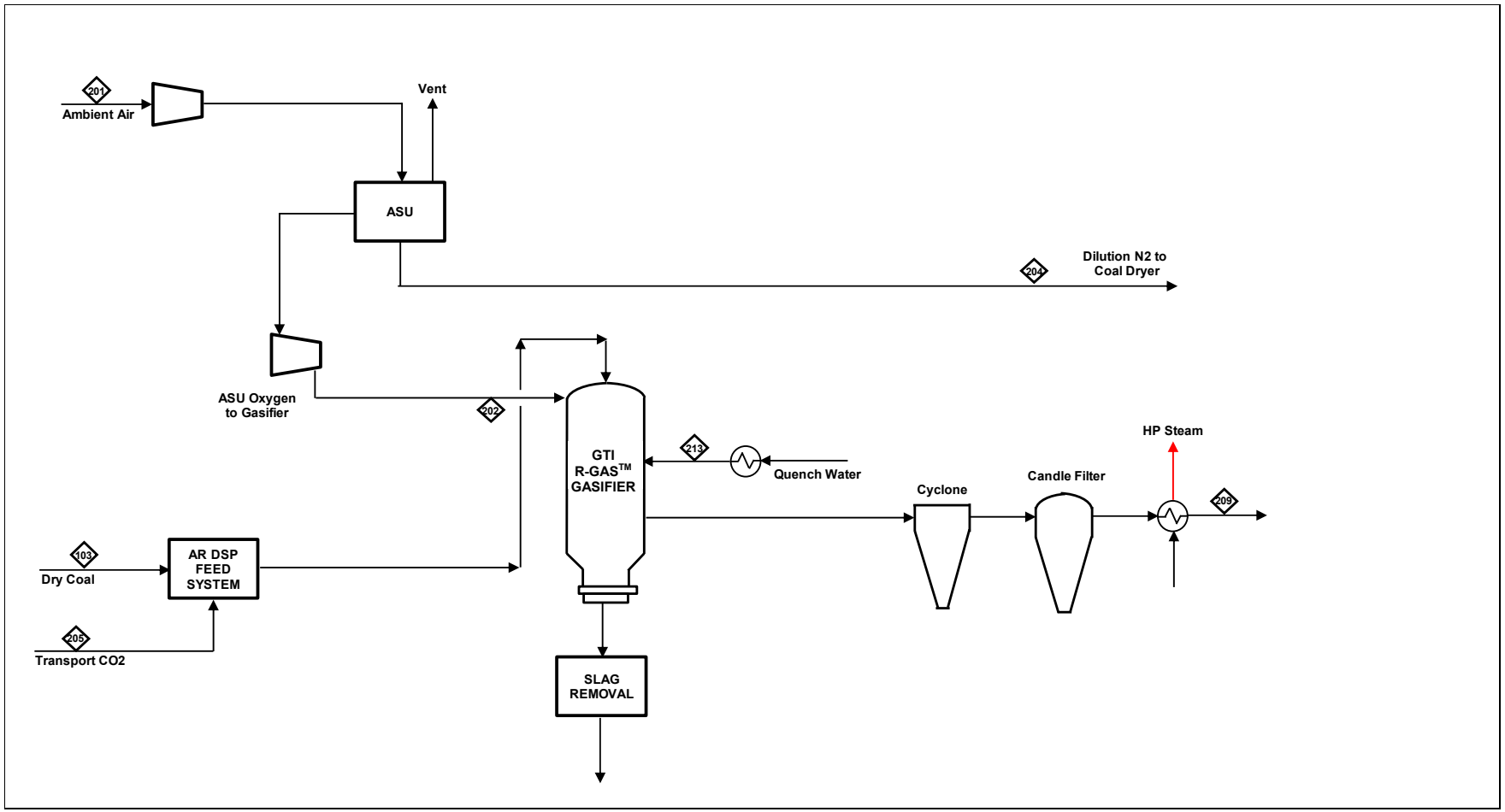

Table 9-3
Case 2b Plant – ASU/Coal Gasification Stream Table

STREAM	201	202	204	205	103	213	214	209
Description	Ambient Air	Oxygen to Gasifier	N2 to Coal Dryer	Conveying CO2	Dry Coal	Quench Water	Slag Out	Raw Cooled Syngas
Mole Flow (Vapor/Liquid)/lbmol/hr								
AR	1188	794	216	0	0	0	0	794
CH4	0	0	0	0	0	0	0	345
CO	0	0	0	2	0	0	0	64237
CO2	42	0	0	2931	0	0	0	2019
COS	0	0	0	0	0	0	0	36
H2	0	0	0	6	0	0	0	25980
H2O	1268	0	19	0	0	53860	0	56396
H2S	0	0	0	0	0	0	0	311
N2	99338	530	93118.15	0	0	0	0	861
NH3	0	0	0	0	0	0	0	111
O2	26648	25159	507	0	0	0	0	0
SO2	0	0	0	0	0	0	0	0
S	0	0	0	0	0	0	0	0
HCN	0	0	0	0	0	0	0	3
HCL	0	0	0	0	0	0	0	3
Methanol -- CH3OH	0	0	0	0	0	0	0	0
Ethanol -- C2H5OH	0	0	0	0	0	0	0	0
Propanol -- C3H8O	0	0	0	0	0	0	0	0
Ethane -- C2H6	0	0	0	0	0	0	0	0
Propane -- C3H8	0	0	0	0	0	0	0	0
n-Butane -- C4H10	0	0	0	0	0	0	0	0
Total V/L Flow, lbmol/hr	128485	26484	93860	2940	0	53860	0	151097
Total V/L Flow, lb/hr	3707669	851647.9	2633735	129095	0	970303	0	3032728
Solids Mass Flow, lb/hr	0	0	0	0	1206840	0	125127.4	0
Coal	0	0	0	0	1206840	0	0	0
Ash	0	0	0	0	0	0	125127	0
Carbon	0	0	0	0	0	0	0	0
Total Flow (Solids + V/L), lb/hr	3707669	851648	2633735	129095	1206840	970303	125127	3032728
Pressure, psia	14.7	1000	18.0	1100.0	14.3	980	915	905.0
Temperature, F	59	292	70	270		250		755

Figure 9-5
Case 2b Plant – RTI WDP/DSRP/AFWGS PFD

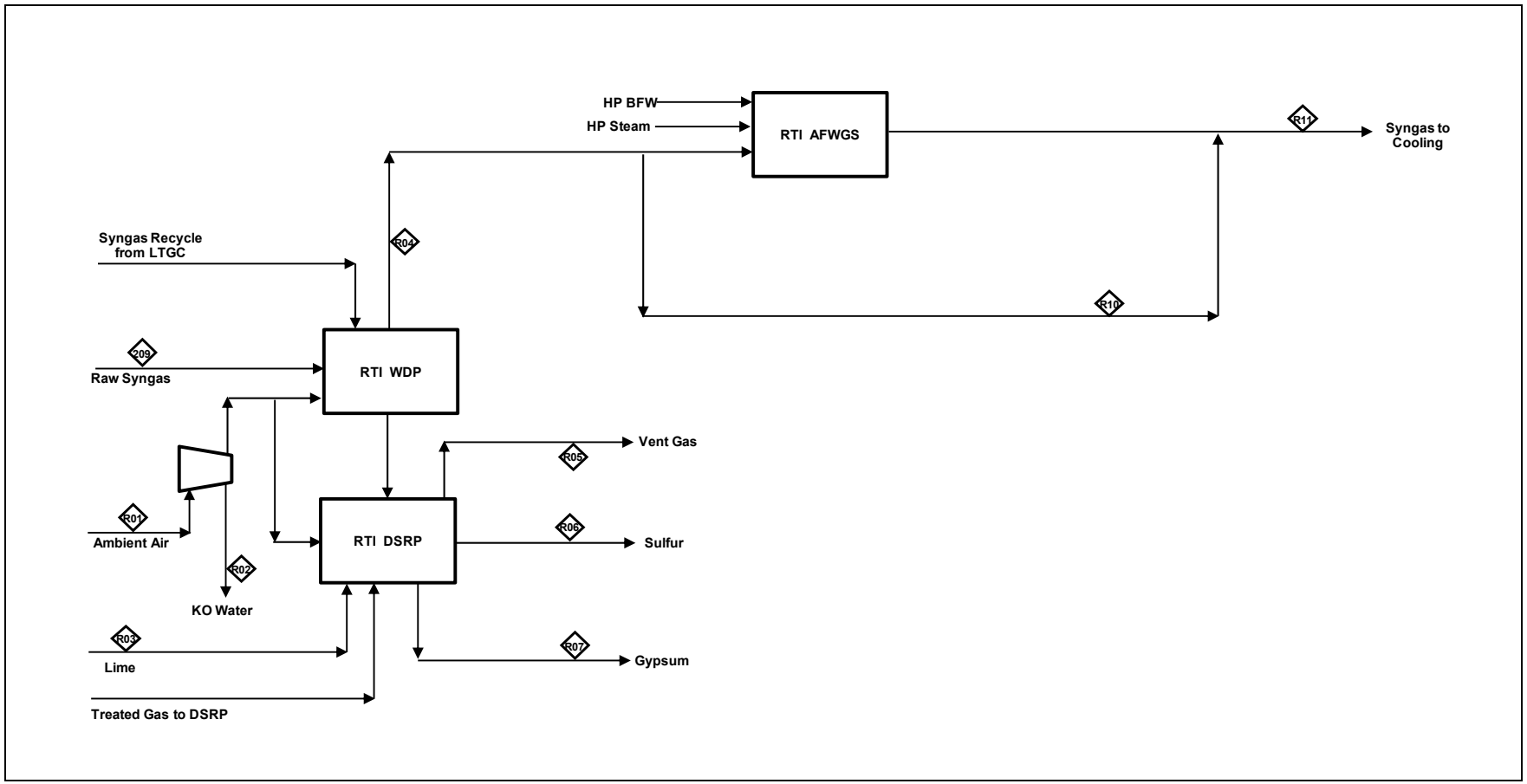

Table 9-4
Case 2b Plant – RTI WDP/DSRP/AFWGS Stream Table

STREAM	209	R01	R02	R03	R04	R05	R06	R07	R10	R11
Description	Raw Syngas	Ambient Air	Comp KO Water	Lime	Treated Gas to Shift	DSRP Vent Gas	Sulfur Product	Gypsum Product	Bypass Syngas	Syngas to LT Cooling
Mole Flow (Vapor/Liquid)/lbmol/hr										
AR	794	43	0	0	812	46	0	0	294	812
CH4	345	0	0	0	351	0	0	0	127	351
CO	64237	0	0	0	64711	0	0	0	23432	30438
CO2	2019	2	0	0	2655	220	0	100	961	36928
COS	36	0	0	0	0	0	0	0	0	0
H2	25980	0	0	0	26935	0	0	0	9753	61208
H2O	56396	46	33	8346	56709	0	0	9179	20534	67119
H2S	311	0	0	0	1	0	0	0	0	1
N2	861	3618	0	0	1274	3233	0	5	461	1274
NH3	111	0	0	0	111	0	0	0	40	111
O2	0	970	0	0	0	0	0	0	0	0
SO2	0	0	0	0	0	0	0	0	0	0
S	0	0	0	0	0	0	130	0	0	0
HCN	3	0	0	0	0	0	0	0	0	0
HCL	3	0	0	0	0	0	0	0	0	0
Methanol -- CH3OH	0	0	0	0	0	0	0	0	0	0
Ethanol -- C2H5OH	0	0	0	0	0	0	0	0	0	0
Propanol -- C3H8O	0	0	0	0	0	0	0	0	0	0
Ethane -- C2H6	0	0	0	0	0	0	0	0	0	0
Propane -- C3H8	0	0	0	0	0	0	0	0	0	0
n-Butane -- C4H10	0	0	0	0	0	0	0	0	0	0
Lime	0	0	0	225	0	0	0	9	0	0
Gypsum	0	0	0	0	0	0	0	216	0	0
Total V/L Flow, lbmol/hr	151097	4679	33	8571	153559	3499	130	9514	55604	198242
Total V/L Flow, lb/hr	3032728	135022	603	167062	3081007	102062	4167	207924	1115633	3886005
Solids Mass Flow, lb/hr	0	0	0	0	0	0	0	0	0	0
Coal	0	0	0	0	0	0	0	0	0	0
Ash	0	0	0	0	0	0	0	0	0	0
Carbon	0	0	0	0	0	0	0	0	0	0
Total Flow (Solids + V/L), lb/hr	3032728	135022	603	167062	3081007	102062	4167	207924	1115633	3886005
Pressure, psia	905	14.7	13.0	13.0	894.0	751	14.7	14.7	894	869
Temperature, F	755	59	80	75	685	105	305	172	685	844

Figure 9-6
Case 2b Plant – LTGC PFD

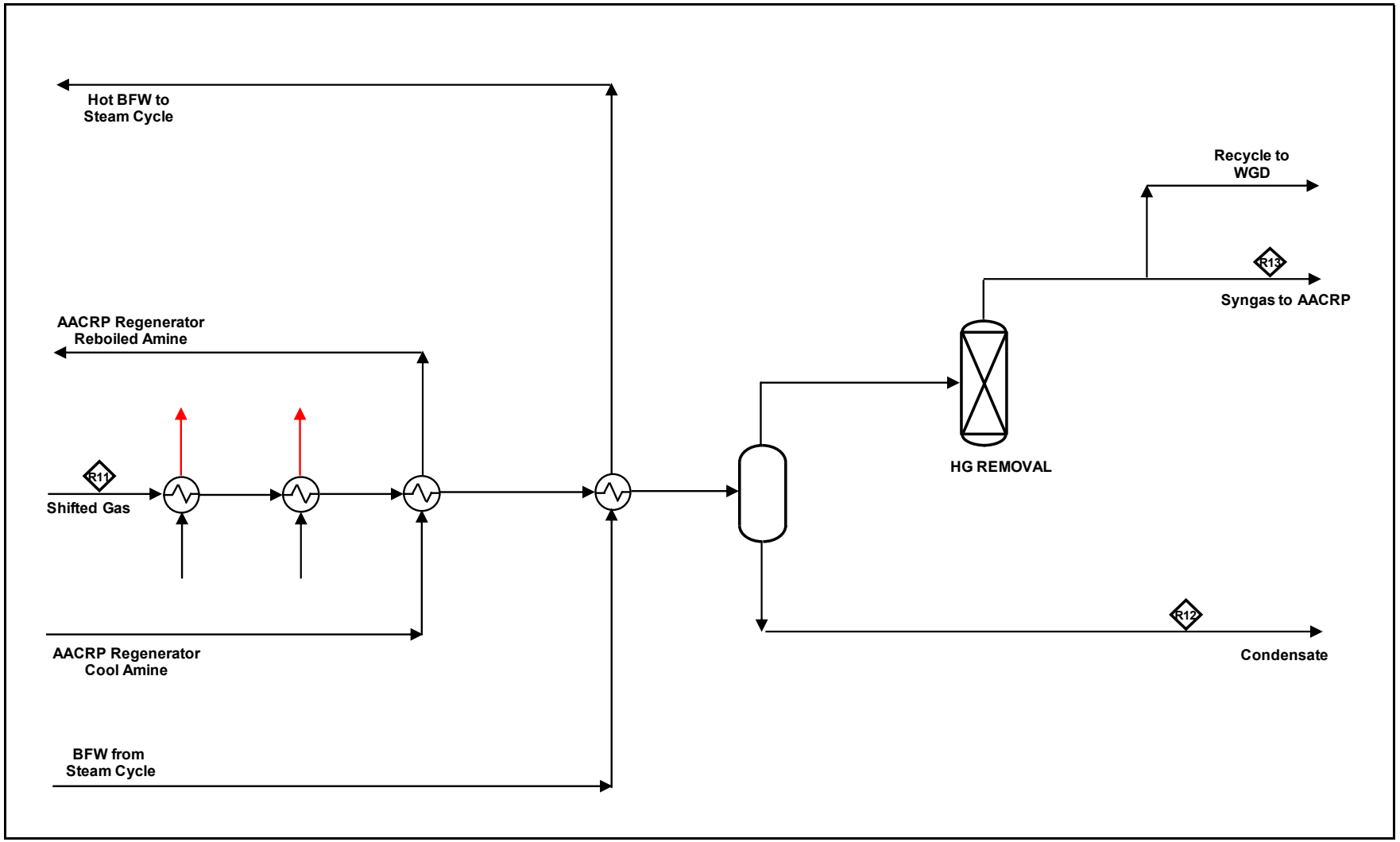

Table 9-5
Case 2b Plant – LTGC Stream Table

STREAM	R11	R12	R13
Description	Shifted Syngas	KO Water	Cooled Syngas
Mole Flow (Vapor/Liquid)/lbmol/hr			
AR	812	0	800
CH4	351	0	345
CO	30438	0	29963
CO2	36928	12	36339
COS	0	0	0
H2	61208	0	60253
H2O	67119	66964	152
H2S	1	0	1
N2	1274	0	1254
NH3	111	111	0
O2	0	0	0
SO2	0	0	0
S	0	0	0
HCN	0	0	0
HCL	0	0	0
Methanol -- CH3OH	0	0	0
Ethanol -- C2H5OH	0	0	0
Propanol -- C3H8O	0	0	0
Ethane -- C2H6	0	0	0
Propane -- C3H8	0	0	0
n-Butane -- C4H10	0	0	0
Total V/L Flow, lbmol/hr	198242	67089	129107
Total V/L Flow, lb/hr	3886005	1208828	2635413
Solids Mass Flow, lb/hr	0	0	0
Coal	0	0	0
Ash	0	0	0
Carbon	0	0	0
Total Flow (Solids + V/L), lb/hr	3886005	1208828	2635413
Pressure, psia	869	844	829
Temperature, F	844	95	95

Figure 9-7
Case 2b Plant – AACRP and CO_2 Compression PFD

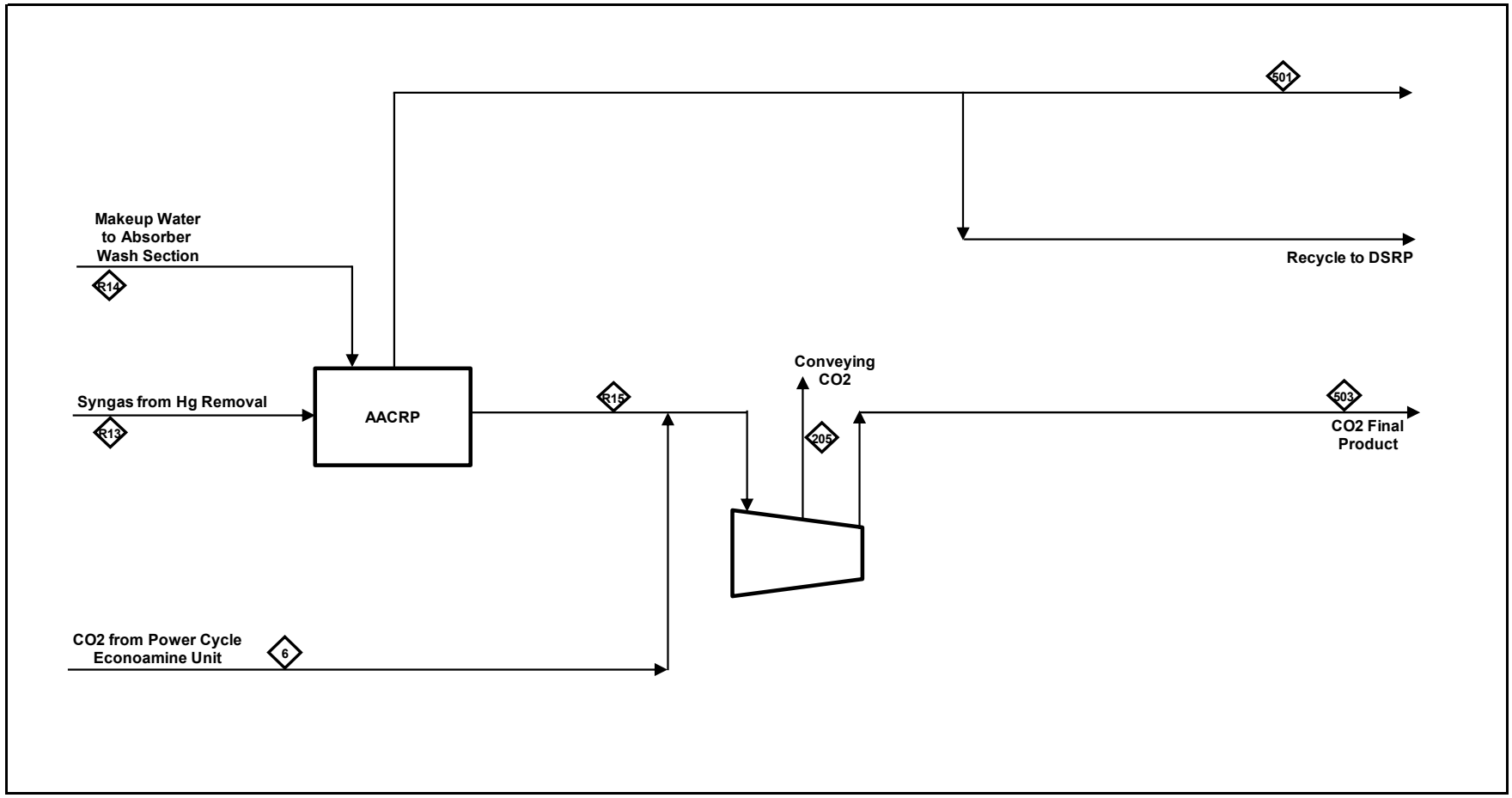

Table 9-6
Case 2b Plant – AACRP and CO_2 Compression Stream Table

STREAM	R13	R14	R15	501	6	205	503
Description	Syngas to AACRP	Makeup Wash Water	AACRP CO2 Product	Syngas to MeOH Synthesis	CO2 from MEA Unit	Convey CO2	CO2 Final Product
Mole Flow (Vapor/Liquid)/lbmol/hr							
AR	812	0	1	790	0	0	1
CH4	351	0	2	340	0	0	2
CO	30438	0	26	29632	0	2	23
CO2	36915	0	33442	2867	3946	2931	34457
COS	0	0	0	0	0	0	0
H2	61208	0	73	59565	0	6	67
H2O	154	3556	3233	471	46	0	0
H2S	1	0	1	0	0	0	1
N2	1274	0	1	1241	0	0	1
NH3	0	0	0	0	0	0	0
O2	0	0	0	0	0	0	0
SO2	0	0	0	0	0	0	0
S	0	0	0	0	0	0	0
HCN	0	0	0	0	0	0	0
HCL	0	0	0	0	0	0	0
Methanol -- CH3OH	0	0	0	0	0	0	0
Ethanol -- C2H5OH	0	0	0	0	0	0	0
Propanol -- C3H8O	0	0	0	0	0	0	0
Ethane -- C2H6	0	0	0	0	0	0	0
Propane -- C3H8	0	0	0	0	0	0	0
n-Butane -- C4H10	0	0	0	0	0	0	0
Total V/L Flow, lbmol/hr	131153	3556	36778	94905	3991	2940	34551
Total V/L Flow, lb/hr	2677177	64062	1531019	1156519	174468	129095	1517330
Solids Mass Flow, lb/hr	0	0	0	0	0	0	0
Coal	0	0	0	0	0	0	0
Ash	0	0	0	0	0	0	0
Carbon	0	0	0	0	0	0	0
Total Flow (Solids + V/L), lb/hr	2677177	64062	1531019	1156519	174468	129095	1517330
Pressure, psia	829	814	20.7	814	24	1100	2215
Temperature, F	95	122	122	148	69	270	162

Figure 9-8
Case 2b Plant – Methanol Synthesis Plant PFD

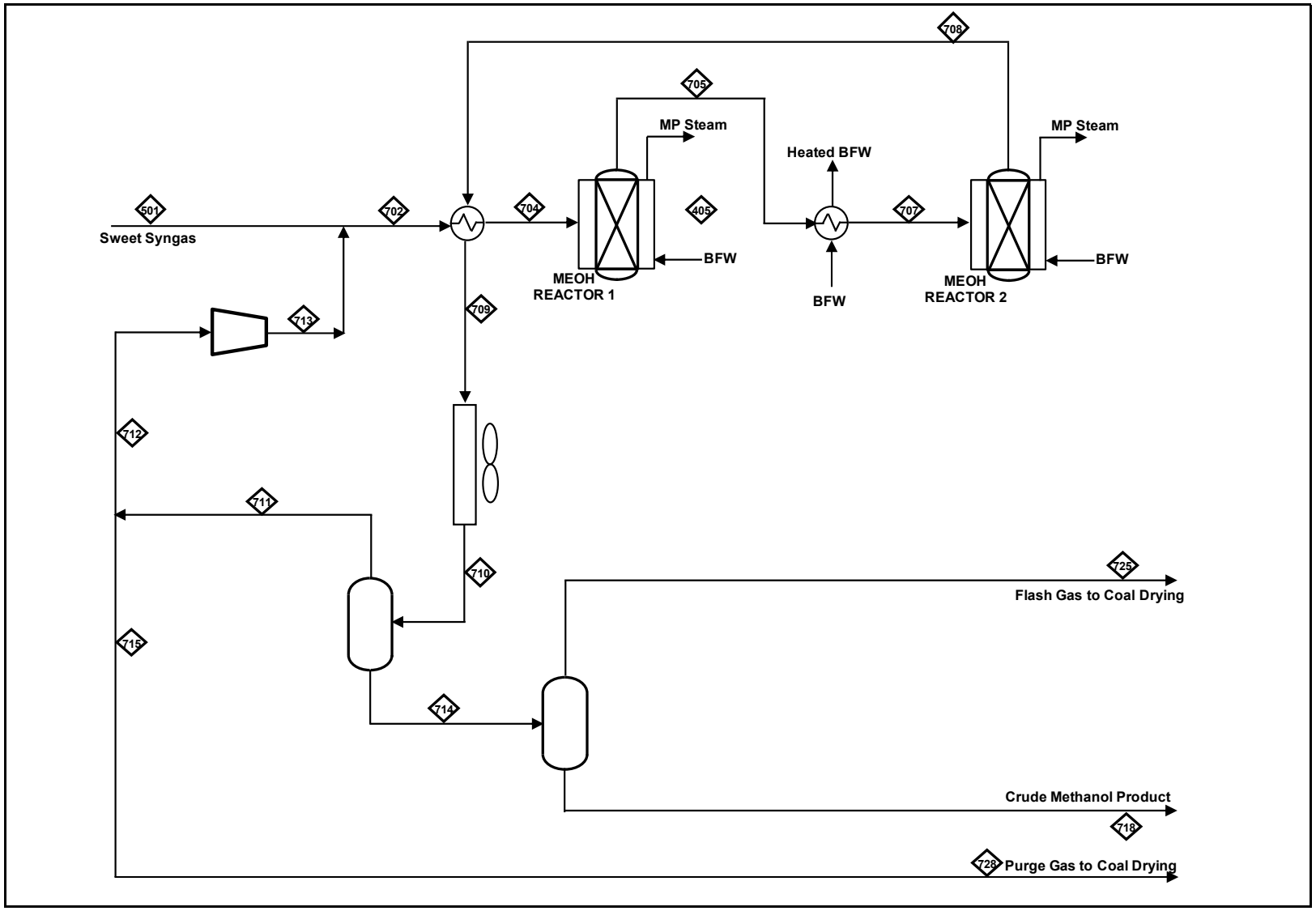

Table 9-7
Case 2b Plant – Methanol Synthesis Plant Stream Table

STREAM	501	704	705	707	708	709	710	711	712	713	714	718	725	728
Description	Reheated Syngas	MEOH Reactor 1 Feed	MEOH Reactor 1 Outlet	MEOH Reactor 2 Feed	MEOH Reactor 2 Outlet	Cooled Raw MeOH	AC Cool Raw MeOH	Flash Gas Ovhd	Recycle Syngas	HP Recycle Syngas	KO Drum Bottoms	Crude MeOH Product	MeOH Flash Gas	MeOH Purge Gas
Mole Flow (Vapor/Liquid)/lbmol/hr														
AR	790	14076	14076	14076	14076	14076	14076	13985	13286	13286	91	2	89	699
CH4	340	5770	5770	5770	5770	5770	5770	5716	5430	5430	54	2	52	286
CO	29632	46213	26363	26363	17492	17492	17492	17453	16582	16582	38	0	38	873
CO2	2867	27980	27793	27793	27995	27995	27995	26434	25112	25112	1561	314	1247	1322
COS	0	0	0	0	0	0	0	0	0	0	0	0	0	0
H2	59565	99956	59694	59694	42558	42558	42558	42520	40391	40391	39	0	39	2126
H2O	471	485	708	708	500	500	500	15	14	14	485	483	2	1
H2S	0	0	0	0	0	0	0	0	0	0	0	0	0	0
N2	1241	22817	22817	22817	22817	22817	22817	22712	21576	21576	105	2	104	1136
NH3	0	0	0	0	0	0	0	0	0	0	0	0	0	0
O2	0	0	0	0	0	0	0	0	0	0	0	0	0	0
SO2	0	0	0	0	0	0	0	0	0	0	0	0	0	0
S	0	0	0	0	0	0	0	0	0	0	0	0	0	0
HCN	0	0	0	0	0	0	0	0	0	0	0	0	0	0
HCL	0	0	0	0	0	0	0	0	0	0	0	0	0	0
Methanol -- CH3OH	0	2455	22422	22422	31101	31101	31101	2584	2455	2455	28517	28147	370	129
Ethanol -- C2H5OH	0	2	35	35	30	30	30	2	2	2	29	28	0	0
Propanol -- C3H8O	0	0	1	1	1	1	1	0	0	0	1	1	0	0
Ethane -- C2H6	0	0	0	0	0	0	0	0	0	0	0	0	0	0
Propane -- C3H8	0	0	0	0	0	0	0	0	0	0	0	0	0	0
n-Butane -- C4H10	0	0	0	0	0	0	0	0	0	0	0	0	0	0
Total V/L Flow, lbmol/hr	94905.3	219753	179679	179679	162341	162341	162341	131420	124848	124848	30920	28979	1942	6571
Total V/L Flow, lb/hr	1156519	4108841	4108806	4108806	4108791	4108791	4108791	3107671	2952322	2952322	1001119	925862	75257.7	155384
Solids Mass Flow, lb/hr	0	0	0	0	0	0	0	0	0	0	0	0	0	0
Coal	0	0	0	0	0	0	0	0	0	0	0	0	0	0
Ash	0	0	0	0	0	0	0	0	0	0	0	0	0	0
Carbon	0	0	0	0	0	0	0	0	0	0	0	0	0	0
Total Flow (Solids + V/L), lb/hr	1156519	4108841	4108806	4108806	4108791	4108791	4108791	3107671	2952322	2952322	1001119	925862	75258	155384
Pressure, psia	814	747	737	732.0	727	722	720	717	717	755	717	40	40	717
Temperature, F	147.8604	400	475	400	430	235	130	130	130	141	130	119	119	130

Figure 9-9
Case 2b Plant -- NGCC PFD

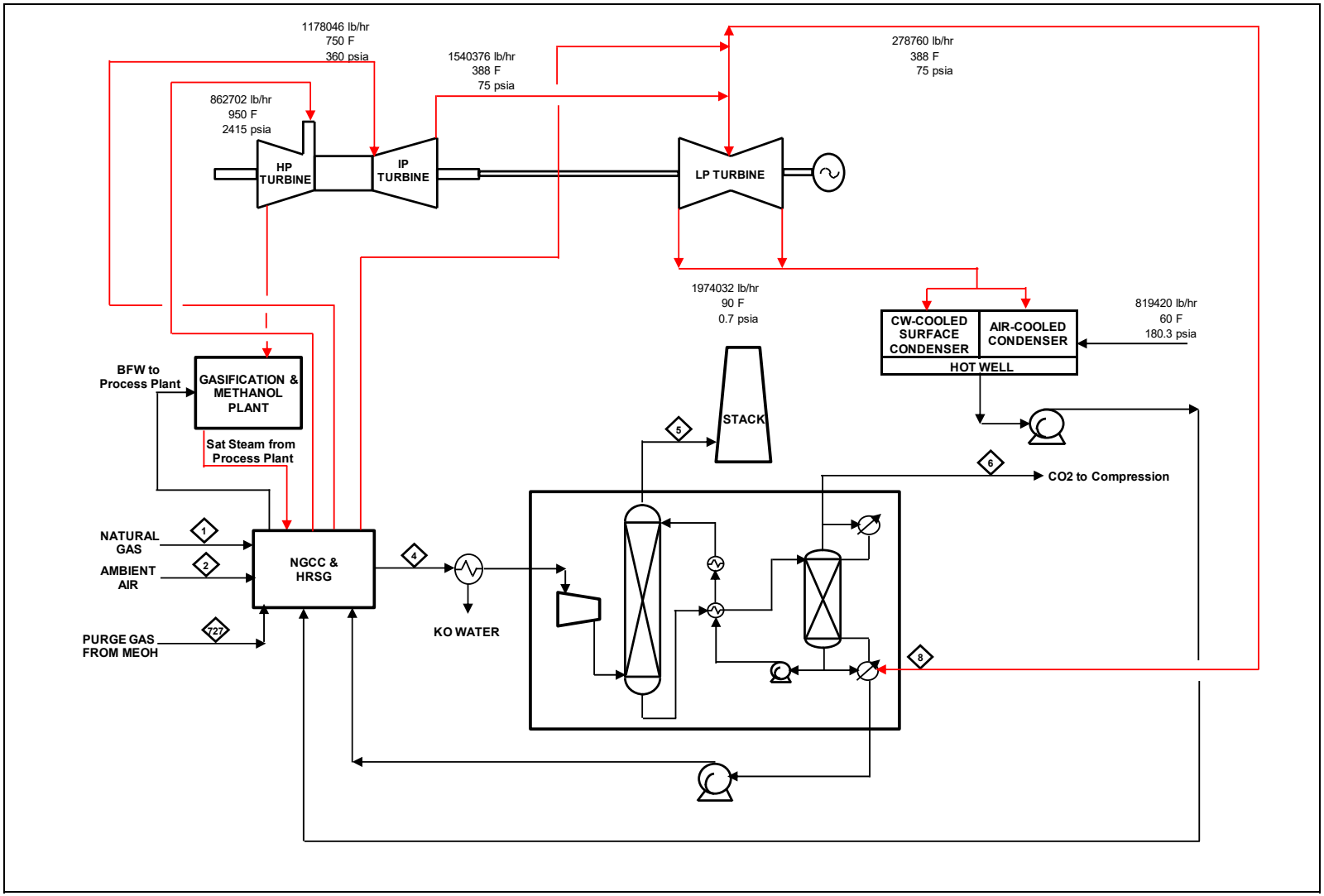

Table 9-8
Case 2b Plant – NGCC Stream Table

STREAM	1	2	4	5	6	8	727
Description	Ambient Air	Natural Gas	Flue Gas to MEA	Treated Gas	CO2 Out	LP Steam	MeOH Purge Gas
Mole Flow (Vapor/Liquid)/lbmol/hr							
AR	1053	0	1182	1182	0	0	129
CH4	0	3435	0	0	0	0	77
CO	0	0	0	0	0	0	161
CO2	57	37	4384	438	3946	0	244
COS	0	0	0	0	0	0	0
H2	0	0	0	0	0	0	393
H2O	1132	0	9081	3661	46	15474	0
H2S	0	0	0	0	0	0	0
N2	88373	59	88643	88643	0	0	210
NH3	0	0	0	0	0	0	0
O2	23715	0	15775	15775	0	0	0
SO2	0	0	0	0	0	0	0
S	0	0	0	0	0	0	0
HCN	0	0	0	0	0	0	0
HCL	0	0	0	0	0	0	0
Methanol -- CH3OH	0	0	0	0	0	0	0
Ethanol -- C2H5OH	0	0	0	0	0	0	0
Propanol -- C3H8O	0	0	0	0	0	0	0
Ethane -- C2H6	0	118	0	0	0	0	0
Propane -- C3H8	0	26	0	0	0	0	0
n-Butane -- C4H10	0	15	0	0	0	0	0
Total V/L Flow, lbmol/hr	114330	3690	119065	109699	3991	15474	1215
Total V/L Flow, lb/hr	3299430	63929	3391721	3120423	174468	278760	28351
Total Flow (Solids + V/L), lb/hr	3299430	63929	3391721	3120423	174468	278760	28351
Pressure, psia	15	475	15	15	24	260	176
Temperature, F	59	60	272	85	69	35	365

9.3 SPARING PHILOSOPHY

The sparing philosophy for the GTI and RTI-provided equipment for the Case 2b CTM plant is provided below. The design has:

- Five trains of gasification, including dry feed system, R-GAS™ gasifier, cyclone and candle filter (5 x 25%)
- One WDP train (1 x 100%)
- One DSRP train (1 x 100%)
- Two AFWGS trains (2 x 50%)
- Two AACRP trains (2 x 50%)

9.4 PERFORMANCE RESULTS

The Nexant-modeled Case 2b plant with CO_2 capture consumes 18,339 tpd of PRB coal and 33.6 MMSCFD of natural gas at the Midwestern site and produces 925,862 lb/hr (10,079 mtpd) of crude methanol. Overall performance for the Case 2b plant is summarized in Table 9-9, which includes auxiliary power requirements. Loads that are unique to the GTI R-GAS™ gasification system, RTI WDP, DSRP, and AACRP are shown in bold and italicized.

Table 9-9
Case 2b Plant Performance Summary

POWER SUMMARY (Gross Power at Generator Terminals, kWe)	Case 2b
Gas Turbine Power	127,856
Steam Turbine Power	239,204
TOTAL POWER, kWe	**367,060**
CTM Plant Auxiliary Load Summary, kWe	
Coal Handling	8,585
Slag Handling	2,178
Incinerator Air Blower	4,521
Incinerator Recycle Blower	1,162
Air Separation Unit	152,581
AR DSP	***8,483***
Quench Water Pump	2,494
RTI WDP	***9,946***
RTI DSRP	***633***
AACRP	***31,991***
AACRP and NGCC CO_2 Compressor Auxiliaries	64,795
Recycle Gas Compressor	2,994
Air Cooler Fans	1,657
Water Treatment	2,749
Miscellaneous BOP	5,000
Circulating Water Pumps	7,232
Ground Water Pumps	788
Cooling Tower Fans	4,715
SUBTOTAL CTM PLANT AUXILIARIES, kWe	**312,504**
NGCC Plant Auxiliary Load Summary, kWe	
Gas Turbine Auxiliaries	787
Steam Turbine Auxiliaries	87
Transformer Losses	2,014
Miscellaneous BOP	500
Air Cooled Condenser Fans	4,273
Condensate Pumps	651
Boiler Feed Water Pumps	15,169
Amine System Auxiliaries	4,112
SCR	16
SUBTOTAL POWER PLANT AUXILIARIES, kWe	**27,608**
TOTAL AUXILIARIES, kWe	**340,113**
NET PLANT POWER, kWe	**26,948**
CONSUMABLES	
As-Received Coal Feed, tpd	18,339
Natural Gas Feed Rate, MMBtu/day	34,675
Raw Water Withdrawal, gpm	8,650
Raw Water Consumption, gpm	6,655

Table 9-10 shows the carbon balance for the Case 2b plant. The carbon input to the plant consists of carbon in the air in addition to carbon in the coal and natural gas feedstock. Carbon in the air is not part of the carbon capture equation, but is not neglected in the balance since the model accounts for the air components throughout. Carbon leaves the CTM plant as unburned carbon (minimal for Case 2b) in the slag, CO_2 in the dryer exhaust gas, ASU vent gas, crude methanol product, and the AACRP CO_2 capture product. Additionally, carbon also leaves the NGCC as CO_2 in the stack and Econamine FG Plus^{SM} CO_2 capture product. Carbon in the crude methanol is considered as product, not emissions. The carbon capture efficiency is defined as the amount of carbon in the product streams, which include the crude methanol, the dried and compressed CO_2 products from the AACRP and Econamine FG Plus^{SM} CO_2 capture processes and gypsum, relative to the amount of carbon in the coal and natural gas feedstock less carbon contained in the slag. For Case 2b, the carbon capture efficiency is 93.4%.

Table 9-10
Case 2b Plant – Overall Carbon Balance

Overall Carbon Balance, lb/hr	In	Out
Coal Feed	765,169	
ASU Air	506	
Coal Dryer Air	72	
Power Cycle Natural Gas	46,182	
Power Cycle Combustion Air	450	
DSRP Air In	18	
ASU Vent		506
Coal Dryer Exhaust Gas		46,140
Carbon in Slag		0
Sulfur Product		0
DSRP Vent		2,636
Gypsum		1,205
Crude Methanol Product		342,579
AACRP CO_2 Product		366,767
NGCC CO_2 Product		47, 184
NGCC Exhaust Gas		5,243
CO_2 in LTGC Condensate (Vented)		151
Convergence Tolerance		-13
Total	**812,398**	**812,398**

Table 9-11 shows the sulfur balance for the plant. Sulfur input comes solely from the sulfur in the coal. Sulfur output includes the elemental sulfur recovered in the DSRP, sulfur recovered in the form of gypsum leaving the lime scrubber, sulfur emitted in the coal dryer exhaust gas, and sulfur that is sequestered with the CO_2 product. Sulfur in the slag is considered negligible. The net sulfur emissions include only the sulfur emitted in the coal dryer exhaust gas. Based on this, the net sulfur emissions for the plant are < 0.0001 lb of SO_2/MMBtu.

Table 9-11
Case 2b Plant – Overall Sulfur Balance

Overall Sulfur Balance, lb/hr	In	Out
Coal Feed	11,118	
Sulfur Product		4,167
Gypsum		6,928
Coal Dryer Exhaust Gas		0
AACRP CO_2 Product		21
Convergence Tolerance		1
Total	**11,118**	**11,118**

Table 9-12 shows the overall water balance for the Case 2b plant. Raw water withdrawal is the amount of raw water consumed by the plant. The raw water is obtained from groundwater (5%) and from municipal sources (50%). Some water is discharged by the processes as effluent suitable for internal consumption. This effluent is internally recycled and consumed by the slag handling process, as wash water to the AACRP, and as makeup to the cooling tower. Some water is discharged from the process to a permitted outfall. Waste water is discharged by the slag handling process and as cooling tower blowdown.

Table 9-12
Case 2b Plant – Overall Water Balance

Water Use, gpm	Raw Water Withdrawal	Process Effluent Produced for Internal Consumption	Internal Consumption	Process Water Discharge
Slag Handling	**0**	**0**	**324**	**(324)**
Quench Cooler	**1,939**	**0**	**0**	**0**
DSRP Air Compressor Knockout	**0**	**(1)**	**0**	**0**
Syngas Cooling Knockout	**0**	**(2,410)**	**0**	**0**
AACRP Wash Water	**0**	**0**	**128**	**0**
CO_2 Compression Knockout	**0**	**(118)**	**0**	**0**
Steam Cycle Makeup	**1,637**	**0**	**0**	**0**
Steam Cycle Blowdown	**0**	**(29)**	**0**	**0**
Flue Gas Cooling Knockout	**0**	**(193)**	**0**	**0**
Cooling Tower Makeup	**5,074**	**0**	**2,300**	**0**
Cooling Tower Blowdown	**0**	**0**	**0**	**(1,671)**
Total	**8,650**	**(2,752)**	**2,752**	**(1,995)**

Positive values represent consumption while negative values represent production

9.5 EQUIPMENT LIST

An equipment list for the Case 2b CTM is shown in Table 9-13 below.

Table 9-13
Case 2b Equipment List

ACCOUNT 2 COAL PREPARATION AND FEED
Subaccount 2.3 Dry Coal Injection System

Equipment No.	Description	Type	Design Condition	Operating Qty	Spares
1	GTI DSP Feed System	GTI Proprietary dry solids pump with coal feed bins	1,000 tpd	15	0

ACCOUNT 4 GASIFIER, ASU AND ACCESSORIES
Subaccount 4.1 Gasifier & Auxiliaries

Equipment No.	Description	Type	Design Condition	Operating Qty	Spares
1	R-GAS™ Gasifier	Vertical, down-fired gasifier with multiple fuel injection ports and including water quench	3,000 tpd	5	0
2	Candle Filters	Ceramic	10,500 acfm	5	0
3	Syngas Cyclone	High efficiency	600,000 lb/hr	5	0

ACCOUNT 5A GAS CLEANUP & PIPING
Subaccount 5A.1 AACRP CO_2 Removal System

Equipment No.	Description	Type	Design Condition	Operating Qty	Spares
1	Rich Amine Absorber	Packed Column	228,500 cuft/hr syngas	4	0
2	Lean Amine Absorber	Packed Column w/ Wash Trays	411,000 cuft/hr syngas	2	0
3	Amine Stripper	Packed Column	965,000 cuft/hr gas flow	2	0
4	LP Flash	Packed Column	2,788,700 cuft/hr gas flow	4	0
5	LP Flash Reflux Drum	Reflux Drum	2,753,000 cuft/hr CO_2	4	0
6	Lean/Rich Amine Exchanger	Shell and Tube	80.7 MMBtu/hr	2	0
7	Amine Stripper Reboiler	Kettle Reboiler	91.9 MMBtu/hr	2	0
8	Lean Amine Cooler	Shell and Tube	46.6 MMBtu/hr	2	0
9	Flash Overhead Condenser	Shell and Tube	20.0 MMBtu/hr	4	0
10	Lean Amine Pump	Centrifugal	1.,380 gpm	4	0
11	Semi-lean Amine Pump	Centrifugal	12,000 gpm	4	1
12	Rich Amine Pump	Centrifugal	2,700 gpm	2	0

13	Flash Reflux Pump	Centrifugal	34 gpm	4	0
14	Amine Stripper Bottoms Pump	Centrifugal	2,620 gpm	2	1
15	Filter Pump	Centrifugal	290 gpm	2	0
16	MP Flash Drum	Reflux Drum	111,200 cuft/hr	2	0
17	Recycle Gas Compressor	Centrifugal	122 acfm @ 456 psia	2	0
18	Amine Tank	Vertical Vessel	7,500 gallons	2	0
19	Filter Package	Filter Package	291 gpm	2	0
18	Filter Package Vessel	Vessel	1,500 gallons	3	0

ACCOUNT 5A GAS CLEANUP & PIPING
Subaccount 5A.2 RTI DSRP System

Equipment No.	Description	Type	Design Condition	Operating Qty	Spares
1	DSRP Fixed Bed Reactor	Packed Bed Reactor	338,000 lb/hr	1	0
2	Tail Gas Oxidation Reactor	Packed Bed Reactor	380,100 lb/hr	1	0
3	DSRP Feed Gas Preheater	Shell and Tube	17 MMBtu/hr	1	0
4	Sulfur Condenser	Shell and Tube	4,100 lb/hr sulfur	1	0
5	Oxidation Reactor Gas Preheater	Shell and Tube	7.9 MMBtu/hr	1	0
6	Liquid Sulfur Separator	Pressure Vessel	4,100 lb/hr sulfur	1	0
7	Recycle Gas Compressor	Centrifugal	1,200 acfm @ 750 psia	1	0
8	Pulsing Gas Compressor	Centrifugal	Average 15 acfm @ 815 psia	1	0
9	Scrubber Recycle Cooler	Shell and Tube	76 MMBtu/hr	1	0
10	SO_2 Scrubber	Tray Column	396,000 lb/hr	1	0
11	Recycle Pump	Centrifugal	1,915 gpm @ 288 ft H_2O	1	0
12	Lime Slurry Pump	Centrifugal	350 gpm @ 1,617 ft H_2O	1	0
13	Gypsum Filter	Bag Filter	1,000 gpm	2	0
14	Lime Makeup Drum	Pressure Vessel	175,000 lb/hr	1	0

ACCOUNT 5A GAS CLEANUP & PIPING
Subaccount 5A.4a RTI WDP System

Equipment No.	Description	Type	Design Condition	Operating Qty	Spares
1	WDP Adsorption Reactor	Proprietary Transport Reactor	38,340 acfm	1	0
2	WDP Regeneration Reactor	Proprietary Transport Reactor	1,140 acfm	1	0
3	Adsorber Cyclone Separator	Cyclone Separator	38,340	1	0

4	Stripper Cyclone Separator	Cyclone Separator	1,140 acfm	1	0
5	Adsorber Filter	Candle Filter	38,340 acfm	1	0
6	Regenerator Offgas Filter	Candle Filter	1,140 acfm	1	0
7	Adsorber Filter Lock Hopper + Fines Bin		Proprietary	1	0
8	Regenerator Filter Lock Hopper + Fines Bin		Proprietary	1	0
9	Sorbent Feeder Package (incl Hopper)		Proprietary	1	0
10	Regenerator Air Heat Exchanger	Shell and Tube	73,300 lb/hr	1	0
11	Recycle Syngas Compressor	Centrifugal	240 acfm @ 829 psia	1	0
12	Regenerator Air Compressor	Centrifugal	30,000 acfm @ 15 psia	1	0
13	DSRP Offgas Compressor	Centrifugal	160 acfm @ 810 psia	1	0
14	Syngas Recycle Compressor	Centrifugal	168 acfm @ 898 psia	1	0

ACCOUNT 5A SYNGAS CLEANUP
Subaccount 5A.4b Shift Reactors

Equipment No.	Description	Type	Design Condition	Operating Qty	Spares
1	AFWGS Reactor 1	Packed Bed Reactor	Proprietary	2	0
2	AFWGS Reactor 2	Packed Bed Reactor	Proprietary	2	0

9.6 CAPITAL COST

Table 9-14 shows the cost breakdown of the Case 2b plant, consistent with the code of accounts format as expressed in the DOE Crude Methanol Study. The accounts/subaccounts of interest for this study are:

- 2.3 Dry Coal Injection System,
- 4 Gasifier & Accessories,
- 5A Gas Cleanup & Piping and
- 5B CO_2 Removal and Compression

These are shown with more detail to include the various subaccounts and provide more clarity to the major cost differences among the cases.

Table 9-15 shows the calculation and addition of owner's costs to determine the TOC, which is used to calculate the product methanol RSP.

The estimated TOC of the Case 2b CTM plant in 2011 dollars is $4,567MM.

Table 9-14
Case 2b Plant – Total Plant Cost Summary

Case 2b: GTI R-GAS™ with RTI WDP/AFWGS CTM Plant		Coal Feed, lb/hr	1,528,260					Plant Size	10079 metric tons per day	
Low Rank Western Coal Baseline Study	PRB	Coal HHV, Btu/lb	8,564							

Acct No.	Item/Description	Equipment Cost	Material Cost	Labor		Sales Tax	Bare Erected Cost $	Eng'g CM H.O & Fee	Contingencies		TOTAL PLANT COST
				Direct	Indirect				Process	Project	$
1	COAL & SORBENT HANDLING	**$35,251**	**$6,321**	**$27,325**	**$0**	**$0**	**$68,897**	**$6,253**	**$0**	**$15,030**	**$90,180**
2	COAL & SORBENT PREP & FEED										
2.3	Dry Coal Injection System	$134,811	$0	$88,517	$0	$0	$223,328	$19,235	$44,666	$57,446	$344,674
2.x	Other Coal & Sorbent Prep & Feed Systems	$146,191	$27,729	$42,212	$0	$0	$216,131	$18,906	$0	$47,008	$282,045
	SUBTOTAL 2.	**$281,001**	**$27,729**	**$130,729**	**$0**	**$0**	**$439,459**	**$38,141**	**$44,666**	**$104,454**	**$626,719**
3	FEEDWATER & MISC BOP SYSTEMS	**$28,134**	**$7,918**	**$16,967**	**$0**	**$0**	**$53,019**	**$4,981**	**$0**	**$13,176**	**$71,176**
4	GASIFIER & ACCESSORIES										
4.1	Gasifier, Syngas Cooler & Auxiliaries (GTI)	$88,269	$44,134	$133,274	$0	$0	$265,677	$23,821	$66,419	$53,388	$409,304
4.3	ASU/Oxidant Compression	$539,576	$0	$0	$0	$0	$539,576	$52,301	$0	$59,187	$651,064
4.6	Flare Stack System	$0	$1,421	$647	$0	$0	$2,068	$198	$0	$453	$2,719
4.9	Gasification Foundations	$0	$30,489	$18,183	$0	$0	$48,671	$4,456	$0	$13,282	$66,409
	SUBTOTAL 4.	**$627,845**	**$76,044**	**$152,104**	**$0**	**$0**	**$855,992**	**$80,776**	**$66,419**	**$126,310**	**$1,129,497**
5A	GAS CLEANUP & PIPING										
5A.1	AACRP	$38,471	$0	$32,316	$0	$0	$70,787	$6,688	$14,157	$18,326	$109,959
5A.2	RTI DSRP System	$16,676	$0	$18,461	$0	$0	$35,137	$3,413	$7,027	$9,115	$54,692
5A.3	Mercury Removal	$7,303	$0	$5,520	$0	$0	$12,822	$1,238	$641	$2,940	$17,641
5A.4a	RTI WDP System	$45,217	$0	$54,260	$0	$0	$99,476	$9,672	$19,895	$25,809	$154,853
5A.4c	LT Heat Recovery, FG Saturation & RTI AFWGS Reactor	$85,391	$0	$27,806	$0	$0	$113,197	$11,027	$0	$24,845	$149,069
5A.5	Syngas Compressor	$0	$0	$0	$0	$0	$0	$0	$0	$0	$0
5A.6	Blow back Gas Systems	$6,453	$1,086	$612	$0	$0	$8,150	$773	$0	$1,785	$10,708
5A.7	Fuel Gas Piping	$0	$2,884	$1,887	$0	$0	$4,771	$442	$0	$1,042	$6,255
5A.9	HGCU Foundations	$0	$0	$0	$0	$0	$0	$0	$0	$0	$0
	SUBTOTAL 5.	**$199,511**	**$3,970**	**$140,861**	**$0**	**$0**	**$344,341**	**$33,253**	**$41,721**	**$83,863**	**$503,178**
5B	CO2 REMOVAL & COMPRESSION										
5B.1	NGCC CO2 Removal System	$23,700	$0	$7,142	$0	$0	$30,843	$2,573	$6,168	$7,917	$47,501
5B.2	CO2 Compression & Drying (AACRP & NGCC)	$68,653	$0	$25,881	$0	$0	$94,534	$9,057	$0	$20,718	$124,309
5B.3	CO2 Compression & Drying (NGCC)	$0	$0	$0	$0	$0	$0	$0	$0	$0	$0
	SUBTOTAL 5B.	**$92,353**	**$0**	**$33,023**	**$0**	**$0**	**$125,377**	**$11,630**	**$6,168**	**$28,635**	**$171,810**
5C	METHANOL PRODUCTION	**$131,611**	**$55,371**	**$110,743**	**$0**	**$0**	**$297,725**	**$29,773**	**$0**	**$65,500**	**$392,998**
6	COMBUSTION TURBINE/ACCESSORIES	**$47,397**	**$394**	**$3,814**	**$0**	**$0**	**$51,605**	**$11,171**	**$11,909**	**$14,852**	**$89,537**
7	HRSG, DUCTING & STACK	**$21,496**	**$601**	**$5,106**	**$0**	**$0**	**$27,203**	**$2,259**	**$0**	**$2,962**	**$32,424**
8	STEAM TURBINE GENERATOR	**$78,650**	**$1,021**	**$16,025**	**$0**	**$0**	**$95,697**	**$8,692**	**$0**	**$18,869**	**$123,258**
9	COOLING WATER SYSTEM	**$18,105**	**$19,849**	**$14,701**	**$0**	**$0**	**$52,655**	**$4,871**	**$0**	**$11,695**	**$69,221**
10	ASH/SPENT SORBENT HANDLING SYS	**$77,771**	**$3,478**	**$73,220**	**$0**	**$0**	**$154,469**	**$14,945**	**$0**	**$17,687**	**$187,101**
11	ACCESSORY ELECTRIC PLANT	**$37,308**	**$21,790**	**$38,364**	**$0**	**$0**	**$97,462**	**$8,474**	**$0**	**$21,084**	**$127,020**
12	INSTRUMENTATION & CONTROL	**$12,333**	**$3,728**	**$10,344**	**$0**	**$0**	**$26,404**	**$2,371**	**$1,320**	**$5,393**	**$35,488**
13	IMPROVEMENTS TO SITE	**$5,758**	**$2,829**	**$15,070**	**$0**	**$0**	**$23,657**	**$2,336**	**$0**	**$7,798**	**$33,791**
14	BUILDINGS & STRUCTURES	**$0**	**$7,644**	**$10,595**	**$0**	**$0**	**$18,239**	**$1,648**	**$0**	**$3,228**	**$23,116**
	CALCULATED TOTAL COST	**$1,694,525**	**$238,686**	**$798,990**	**$0**	**$0**	**$2,732,201**	**$261,573**	**$172,203**	**$540,535**	**$3,706,513**

Table 9-15
Case 2b Plant – Total Overnight Cost Breakdown

Owner's Costs	$ x $1,000
Preproduction Costs	
6 months All Labor	$26,843
1 Month Maintenance Materials	$4,960
1 Month Non-Fuel Consumables	$1,823
1 Month Waste Disposal	$1,154
25% of 1 Months Fuel Cost at 100% CF	$6,716
2% of TPC	$74,130
Total	**$115,627**
Inventory Capital	
60 day supply of fuel at 100% CF	$52,993
60 day supply of non-fuel consumables at 100% CF	$2,262
0.5% of TPC (spare parts)	$18,533
Total	**$73,788**
Initial Cost for Catalyst and Chemicals	**$13,978**
Land	**$900**
Other Owner's Cost	**$555,977**
Financing Costs	**$100,076**
Total Owner's Costs	**$860,345**
Total Overnight Costs (TOC)	**$4,566,859**

9.7 OPERATING COSTS

Table 9-16 shows the OPEX breakdown for the Case 2b plant.

Table 9-16
Case 2b Plant – Initial and Annual O&M Costs

INITIAL & ANNUAL O&M EXPENSES					
Case:	Case 2b: GTI R-GAS™ with RTI WDP/AFWGS CTM Plant				
Plant Size (mtpd Methanol)	**10,079**				
Primary/Secondary Fuel:	**PRB/Natural Gas**				
Design/Construction	5 years			**Book Life (yrs):**	20
TPC (Plant Cost) Year	June 2011			**TPI Year:**	2016
Capacity Factor (%)	90			**CO2 Captured (TPD)**	16121

OPERATING & MAINTENANCE LABOR			
Operating Labor			
Operating Labor Rate (base):	$39.70	$/hr	
Operating Labor Burden:	30.00	% of base	
Labor Overhead Charge	25.00	% of labor	
Operating Labor Requirements per Shift	**units/mod**	**Total Plant**	
Skilled Operator	2.0	2.0	
Operator	10.0	10.0	
Foreman	1.0	1.0	
Lab Tech's etc	3.0	3.0	
TOTAL Operating Jobs	16.0	16.0	
			Annual Cost $
Annual Operating Labor Cost			$7,233,658
Maintenance Labor Cost			$35,715,470
Administration & Support Labor			$10,737,282
Property Taxes and Insurance			$74,130,268
TOTAL FIXED OPERATING COSTS			**$127,816,678**

VARIABLE OPERATING COSTS						
Maintenance Material Cost						**$53,573,206**
Consumables	Consumption Initial	Consumption /Day	Unit Cost	Initial Fill Cost		
Water(/1000 gallons)	0	6,228	1.67	**$0**		**$3,424,561**
Chemicals						
MU & WT Chem (lb)	0	37107	0.27	$0		$3,264,984
Carbon (Hg Removal) (lb)	249237	380	1.63	$406,256		$203,290
WDP Sorbent (lb)	Proprietary	Proprietary	Proprietary	$6,601,715		$5,859,411
AFWGS Catalyst (ft3)	6606	3.62	394.60	$2,606,896		$469,241
MEA Solvent (ton)	160	0.22	3751.70	$601,679		$270,293
AACRP Solvent (lb)	327949	179.70	2.80	$917,558		$165,160
SCR Catalyst (m3)	N/A	N/A	N/A	$0		$0
Ammonia (ton)	N/A	N/A	N/A	$0		$0
Methanol Synthesis Catalyst (ft3)	4011	3.66	534.68	$2,144,768		$642,717
DSRP Catalyst (lb)	54120	29.65	11.15	$603,438		$108,619
Oxidation/Reduction Catalyst (lb)	60940	33.39	1.56	$95,066		$17,112
Calcium Hydroxide (lb)	5200	419040	0.04	$199		$5,259,942
Subtotal Chemicals				**$13,977,576**		**$16,260,769**
Other						
Supplemental Electricity (MWh consumed)	0	0	62.33	$0		$0
Gases, N2 etc.(/100scf)	0	0	0.00	$0		$0
LP Steam (/1000 lbs)	0	0	0.00	$0		$0
Subtotal Other				**$0**		**$0**
Waste Disposal:						
Spent Mercury Catalyst (lb)	0	380	0.65	$0		$81,067
Flyash (ton)	0	0	0.00	$0		$0
Slag (ton)	0	1502	25.11	$0		$12,385,561
Subtotal Waste Disposal				**$0**		**$12,466,628**
By-products & Emissions						
Sulfur (tons)	0	0.0	0.00	$0		$0
Supplemental Electricity (MWh generated)	0	647	-59.59	$0		-$12,660,368
Subtotal By-Products				**$0**		**-$12,660,368**
TOTAL VARIABLE OPERATING COSTS				**$13,977,576**		**$73,064,796**
Coal (tons)	**0**	**18,339**	**36.57**	**$0**		**$220,312,342**
Natural Gas (MMBtu)	**0**	**34,675**	**6.13**	**$0**		**$69,825,571**

9.8 METHANOL PRODUCT REQUIRED SELLING PRICE

Table 9-17 shows a summary of the power output, CAPEX, OPEX, and methanol product RSP for the Case 2b plant. The Case 2b plant methanol RSP is estimated to be $1.21/gal under the loan guarantee finance structure and $1.40/gal under the commercial fuels finance structure.

Table 9-17
Case 2b Plant – Overall Performance and Economic Summary

Case	Case 2b	
CAPEX, $MM		
Total Installed Cost (TIC)		$2,732
Total Plant Cost (TPC)		$3,707
Total Overnight Cost (TOC)		$4,567
OPEX, $MM/yr (100% Capacity Factor Basis)		
Fixed Operating Cost (OC_{fix})		$127.8
Variable Operating Cost, less Fuel (OC_{var})		$95.3
Coal Feedstock (OC_{coal})		$244.8
Natural Gas Feedstock (OC_{NG})		$77.6
Import/(Export) Power (OC_{Power})		($14.1)
Total OPEX		$531.4
Plant Output		
Crude Methanol Product, tons per year		4,055,274
Net Power Output, MWe		26.95
Required Selling Price[A]		
Excluding CO_2 TS&M[BE], $/short ton	**347.3**	**407.3**
Including CO_2 TS&M[BE], $/short ton	**363.6**	**423.7**
RSP Component Details ($/gal)		
Capital[B]	0.70	0.90
Fixed O&M	0.12	
Variable O&M	0.08	
Coal	0.20	
Natural Gas	0.06	
Power	(0.01)	
CO_2 TS&M	0.05	
RSP[B] Total ($/gal)	**1.21**	**1.40**
Costs of CO_2 Captured[B,C] ($/tonne)	**17.3**	**19.4**
Costs of CO_2 Avoided[B,D] ($/tonne)	**28.3**	**30.4**

[A] Capacity factor assumed to be 90 percent
[B] Values shown are for two financial structures
The first (lower value) is based on the loan guarantee finance structure
The second (higher value) is based on the commercial fuels finance structure
[C] Excludes CO_2 TS&M
[D] Includes CO_2 TS&M
[E] Based on 301.73 gallons/short ton (332.6 gallons/metric ton)

Section 10 Case 2e: GTI R-GAS™ with RTI WDP and ATWGS CTM Plant

10.1 PROCESS OVERVIEW

The CTM case of interest for this study is the Case 2e GTI R-GAS™ with RTI WDP and ATWGS CTM plant. This case is identical to the Case 2b CTM plant, with the following differentiating characteristic:

- The RTI ATWGS process replaces RTI's AFWGS process. The ATWGS process is based on a transport reactor, solids cooler, and RTI proprietary fluidized-bed high-temperature sweet water-gas shift catalyst.

The coal feed rate is the same as Case 1b since both utilize the R-GAS™ gasification process operating under the same conditions, hence same cold gas efficiency, to generate the same amount of syngas for firing to nominally produce 10,000 mtpd of methanol.

10.2 CASE 2e PROCESS DESCRIPTION

The system description below for Case 2e follows the BFD in Figure 10-1 and stream numbers referenced in the same figure. The accompanying stream flows are shown in Table 10-1. Additional descriptions of the Case 2e plant's various processes are provided below. Simplified PFDs of the various plant processes are depicted in Figure 10-2 through Figure 10-8. Table 10-2 through Table 10-8 provide the model-generated process data for the numbered streams referenced in the PFDs.

Coal Preparation and Drying

Same as Case 2b. Figure 10-2 depicts the coal drying process while Table 10-2 presents the mass balances.

GTI DSP Coal Feed System

Same as Case 2b

Air Separation Unit

Same as Case 2b.

GTI R-GAS™ Gasifier

Same as Case 2b. The GTI DSP, ASU, gasification and quench processes are shown in Figure 10-3 and their mass balances are presented in Table 10-3.

Dry Solids Removal

Same as Case 2b. The solids removal process is shown in Figure 10-3.

Warm Syngas Cleanup Process

RTI's advanced warm syngas cleanup process for Case 2e consists of five major system components: RTI WDP, RTI DSRP, ATWGS, Low Temperature Gas Cooling (LTGC) and the AACRP unit.

Warm Desulfurization Process

Same as Case 2b.

Direct Sulfur Reduction Process

Same as Case 2b.

ATWGS

Case 2e uses RTI's ATWGS process, which replaces RTI's AFWGS process reactorsused in Case 2b. The ATWGS is a fluidized-bed transport-type reactor with a solids cooler/steam generator and follows the same description as that in the IGCC Case 1e.

In order to achieve a 2:1 ratio of H_2 to CO in the final syngas to the methanol synthesis reactors, approximately 65 percent of the syngas leaving the WDP is sent to the ATWGS reactor, with the remaining syngas bypassing it. A single ATWGS reactor is able to process all the syngas flowing through it in Case 2e, compared to two parallel trains of AFWGS for Case 2b.

A partial quench of the syngas leaving the WDP adsorber with boiler feed water provides all the necessary steam for the WGS reaction in the ATWGS process. Therefore, .no steam injection is required for the syngas stream entering the ATWGS process.

The RTI WDP, DSRP and ATWGS processes are shown in Figure 10-4 and the mass balances are presented in Table 10-4.

Low Temperature Gas Cooling and Mercury Removal

Same as Case 2b. The LTGC and mercury removal processes are shown in Figure 10-5 and the mass balances presented in Table 10-5.

Activated Amine CO_2 Removal Process

Same as Case 2b.

CO_2 Compression and Dehydration

Same as Case 2b. The AACRP and CO_2 compression process are shown in Figure 10-6, while the material balance is shown in Table 10-6. The stream numbers labeled on the PFD correspond to the stream numbers in the material balance table.

Methanol Reactor and Synthesis Loop

Same as Case 2b. The methanol synthesis process is shown in Figure 10-7, while the material balance is shown in Table 10-7. The stream numbers labeled on the PFD correspond to the stream numbers in the material balance table.

NGCC

Same as Case 2b. The PFD for the NGCC section is shown in Figure 10-8, while the material balance is shown in Table 10-8. The stream numbers labeled on the PFD correspond to the stream numbers in the material balance table.

Power Cycle Flue Gas Post Combustion CO_2 Capture and Compression

Same as Case 2b.

Figure 10-1
Case 2e Plant – Overall BFD

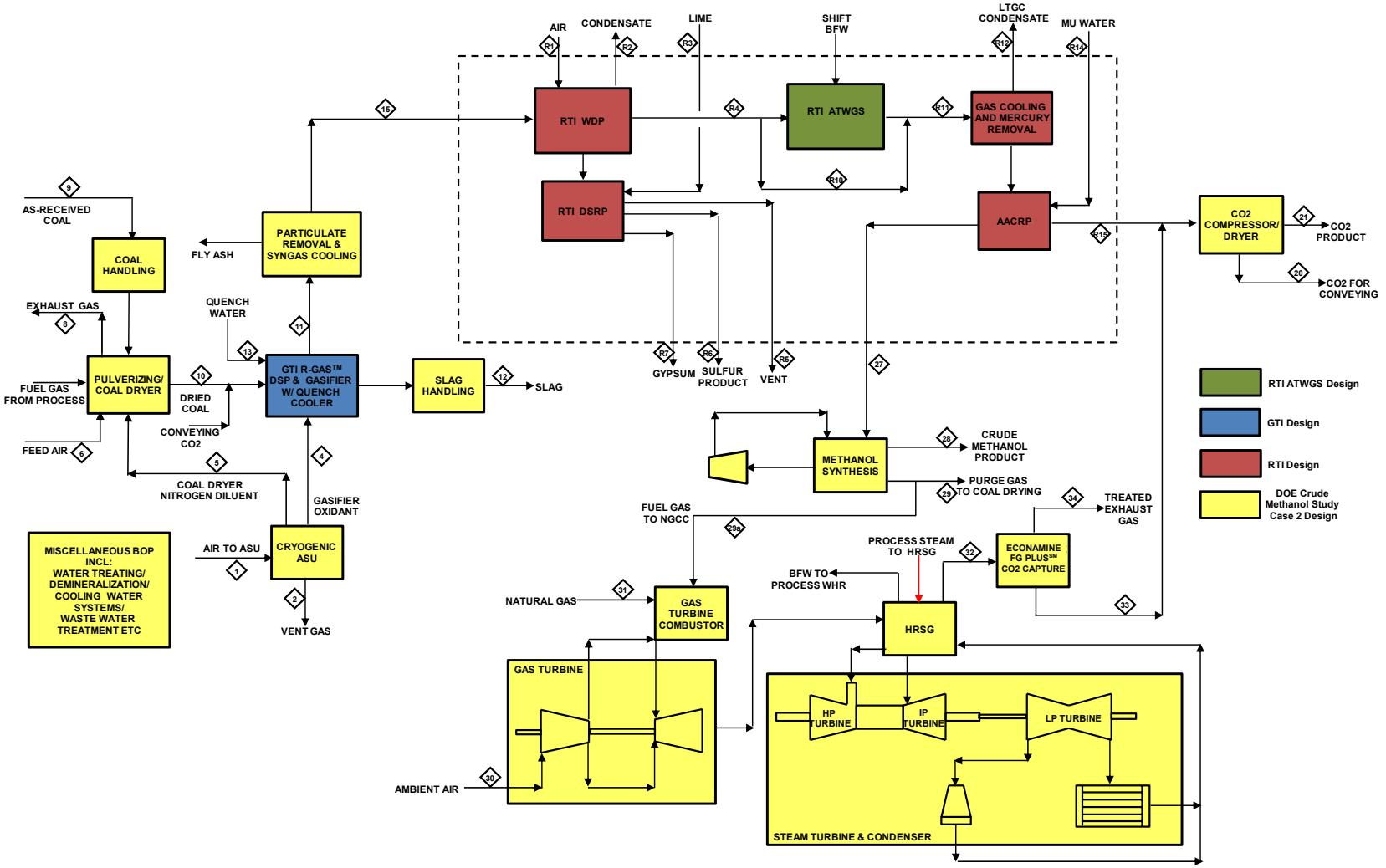

Table 10-1
Case 2e Plant – Overall Stream Table

Description	Air to ASU	ASU Vent Gas	Gasifier Oxidant	Nitrogen Diluent to Dryer	Air Feed to Coal Dryer	Coal Dryer Exhaust	As-Received Coal	Dried Coal	Quenched Syngas	Slag	Quench Water	Syngas to RTI WDP
Stream No.	1	2	4	5	6	8	9	10	11	12	13	15
V-L Mole Fraction												
Ar	0.0092	0.0219	0.0300	0.0023	0.0092	0.0077	0	0	0.0053	0	0	0.0053
CH4	0	0	0	0	0	0	0	0	0.0023	0	0	0.0023
CO	0	0	0	0	0	0	0	0	0.4251	0	0	0.4251
CO2	0.0003	0.0052	0	0	0.0003	0	0	0	0.0134	0	0	0.0134
COS	0	0	0	0	0	0	0	0	0.0002	0	0	0.0002
H2	0	0	0	0	0	0	0	0	0.1719	0	0	0.1719
H2O	0.0099	0.1535	0	0	0.0099	0.1567	0	0	0.3732	0	1.0000	0.3732
H2S	0	0	0	0	0	0	0	0	0.0021	0	0	0.0021
N2	0.7732	0.6989	0.0200	0.9921	0.7732	0.7947	0	0	0.0057	0	0	0.0057
NH3	0	0	0	0	0	0	0	0	0.0007	0	0	0
O2	0.2074	0.1206	0.9500	0.0054	0.2074	0	0	0	0	0	0	0
SO2	0	0	0	0	0	0.0000	0	0	0	0	0	0
S	0	0	0	0	0	0	0	0	0	0	0	0
HCN	0	0	0	0	0	0	0	0	0	0	0	0
HCl	0	0	0	0	0	0	0	0	0	0	0	0
Ca(OH)2	0	0	0	0	0	0	0	0	0	0	0	0
CaSO.2H2O	0	0	0	0	0	0	0	0	0	0	0	0
Methanol	0	0	0	0	0	0	0	0	0	0	0	0
Ethanol	0	0	0	0	0	0	0	0	0	0	0	0
Propanol	0	0	0	0	0	0	0	0	0	0	0	0
Ethane	0	0	0	0	0	0	0	0	0	0	0	0
Propane	0	0	0	0	0	0	0	0	0	0	0	0
n-Butane	0	0	0	0	0	0	0	0	0	0	0	0
Total	1.0000	1.0000	1.0000	1.0000	1.0000	1.0000	0	0	1.0000	0	1.0000	1.0000
V-L Flowrate, lbmol/hr	128485	8141	26484	93860	18222	136198	0	0	151097	0	53860	151097
V-L Flowrate, lb/hr	3707669	222286	851648	2633735	525820	3682889	0	0	3032729	0	970303	3032728
Solids Flow Rate, lb/hr	0	0	0	0	0	0	1528260	1206840	0	125127.4	0	0
Temperature, F	59	64	292	70	59	190	59	190	826		250	755
Pressure, psia	14.7	16.4	1000.0	18.0	14.7	14.3	14.7	14.3	915.0	915.0	980.0	905.0

Table 10-1 (cont'd)
Case 2e Plant – Overall Stream Table

Description	Air to RTI WDP	Comp Air KO Water	Lime	Sweet Syngas	DSRP Vent Gas	Sulfur Product	Gypsum	Bypass Syngas	Syngas to Cooling	Cooled Syngas KO Water	Syngas to aMDEA Unit	Makeup Wash Water	aMDEA CO2 Out
Stream No.	R1	R2	R3	R4	R5	R6	R7	R10	R11	R12	R13	R14	R15
V-L Mole Fraction													
Ar	0.0092	0	0	0.0053	0.0131	0	0	0.0053	0.0041	0	0.0062	0	0
CH4	0	0	0	0.0023	0	0	0	0.0023	0.0018	0	0.0027	0	0
CO	0	0	0	0.4214	0	0	0	0.4214	0.1535	0	0.2321	0	0.0007
CO2	0.0003	0	0	0.0173	0.0627	0	0.0105	0.0173	0.1863	0.0002	0.2815	0	0.9093
COS	0	0	0	0.0000	0	0	0	0.0000	0.0000	0	0	0	0
H2	0	0	0	0.1754	0	0	0	0.1754	0.3088	0	0.4667	0	0.0020
H2O	0.0099	1.0000	0.9737	0.3693	0.0001	0	0.9649	0.3693	0.3386	0.9981	0.0012	1.0000	0.0879
H2S	0	0	0	0.0000	0	0	0	0.0000	0.0000	0	0	0	0
N2	0.7732	0	0	0.0083	0.9240	0	0.0005	0.0083	0.0064	0	0.0097	0	0
NH3	0	0	0	0	0	0	0	0	0	0.0017	0	0	0
O2	0.2074	0	0	0	0	0	0	0	0	0	0	0	0
SO2	0	0	0	0	0	0	0	0	0	0	0	0	0
S	0	0	0	0	0	1.0000	0	0	0	0	0	0	0
HCN	0	0	0	0	0	0	0	0	0	0	0	0	0
HCl	0	0	0	0	0	0	0	0	0	0	0	0	0
Ca(OH)2	0	0	0.0263	0	0	0	0.0010	0	0	0	0	0	0
CaSO.2H2O	0	0	0	0	0	0	0.0227	0	0	0	0	0	0
Methanol	0	0	0	0	0	0	0	0	0	0	0	0	0
Ethanol	0	0	0	0	0	0	0	0	0	0	0	0	0
Propanol	0	0	0	0	0	0	0	0	0	0	0	0	0
Ethane	0	0	0	0	0	0	0	0	0	0	0	0	0
Propane	0	0	0	0	0	0	0	0	0	0	0	0	0
n-Butane	0	0	0	0	0	0	0	0	0	0	0	0	0
Total	1.0000	1.0000	1.0000	1.0000	1.000	1.000	1.000	1.0000	1.0000	1.0000	1.0000	1.0000	1.0000
V-L Flowrate, lbmol/hr	4679	33	8571	153559	3499	130	9514	55604	198242	67089	129107	3556	36778
V-L Flowrate, lb/hr	135022	603	167062	3081007	102062	4167	207924	1115633	3886005	1208828	2635413	64062	1531019
Solids Flow Rate, lb/hr	0	0	0	0	0	0	0	0	0	0	0	0	0
Temperature, F	59	80	75	685	105	305	172	685	844	95	95	122	122
Pressure, psia	14.7	13.0	13.0	894.0	750.8	14.7	14.7	894.0	869.0	844.0	829.0	814.0	20.7

Table 10-1 (cont'd)
Case 2e Plant – Overall Stream Table

Description	Convey'g CO2	CO2 Product	Treated Syngas to MeOH	Crude Methanol Product	MeOH Synthesis Purge Gas	Excess Purge to NGCC	Air to Gas Turbine	Natural Gas Feed	NGCC Flue Gas Exhaust	CO2 to Comp-ression	Treated NGCC Exhaust
Stream No.	20	21	27	28	29	29a	30	31	32	33	34
V-L Mole Fraction											
Ar	0	0	0.0083	0.0001	0.1064	0.1064	0.0092	0	0.0100	0	0.0108
CH4	0	0	0.0036	0	0.0435	0.0435	0	0.9310	0	0	0
CO	0.0008	0.0007	0.3122	0	0.1328	0.1328	0	0	0	0	0
CO2	0.9969	0.9973	0.0302	0.0108	0.2011	0.2011	0.0003	0.0100	0.0367	0.9885	0.0040
COS	0	0	0	0	0	0	0	0	0	0	0
H2	0.0022	0.0019	0.6276	0	0.3235	0.3235	0	0	0	0	0
H2O	0	0	0.0050	0.0167	0.0001	0.0001	0.0099	0	0.0762	0.0115	0.0333
H2S	0	0	0	0	0	0	0	0	0	0	0
N2	0	0	0.0131	0.0001	0.1728	0.1728	0.7732	0.0160	0.7447	0	0.8081
NH3	0	0	0	0	0	0	0	0	0	0	0
O2	0	0	0	0	0	0	0.2074	0	0.1325	0	0.1438
SO2	0	0	0	0	0	0	0	0	0	0	0
S	0	0	0	0	0	0	0	0	0	0	0
HCN	0	0	0	0	0	0	0	0	0	0	0
HCl	0	0	0	0	0	0	0	0	0	0	0
Ca(OH)2	0	0	0	0	0	0	0	0	0	0	0
CaSO.2H2O	0	0	0	0	0	0	0	0	0	0	0
Methanol	0	0	0	0.9713	0.0197	0.0197	0	0	0	0	0
Ethanol	0	0	0	0.0010	0	0	0	0	0	0	0
Propanol	0	0	0	0	0	0	0	0	0	0	0
Ethane	0	0	0	0	0	0	0	0.032	0	0	0
Propane	0	0	0	0	0	0	0	0.007	0	0	0
n-Butane	0	0	0	0	0	0	0	0.004	0	0	0
Total	1.0000	1.0000	1.0000	1.0000	1.0000	1.0000	1.0000	1.0000	1.0000	1.0000	1.0000
V-L Flowrate, lbmol/hr	2940	34551	94905	28979	6571	1216	114330	3690	119065	3974	109716
V-L Flowrate, lb/hr	129095	1517330	1156519	925862	155384	28746	3299204	63929	3391495	173711	3120951
Solids Flow Rate, lb/hr	0	0	0	0	0	0	0	0	0	0	0
Temperature, F	270	162	148	119	130	130	59	60	272	69	85
Pressure, psia	1100.0	2215	814	40	717	717	14.5	474.7	14.9	24	15.0

Figure 10-2
Case 2e Plant – Coal Drying BFD

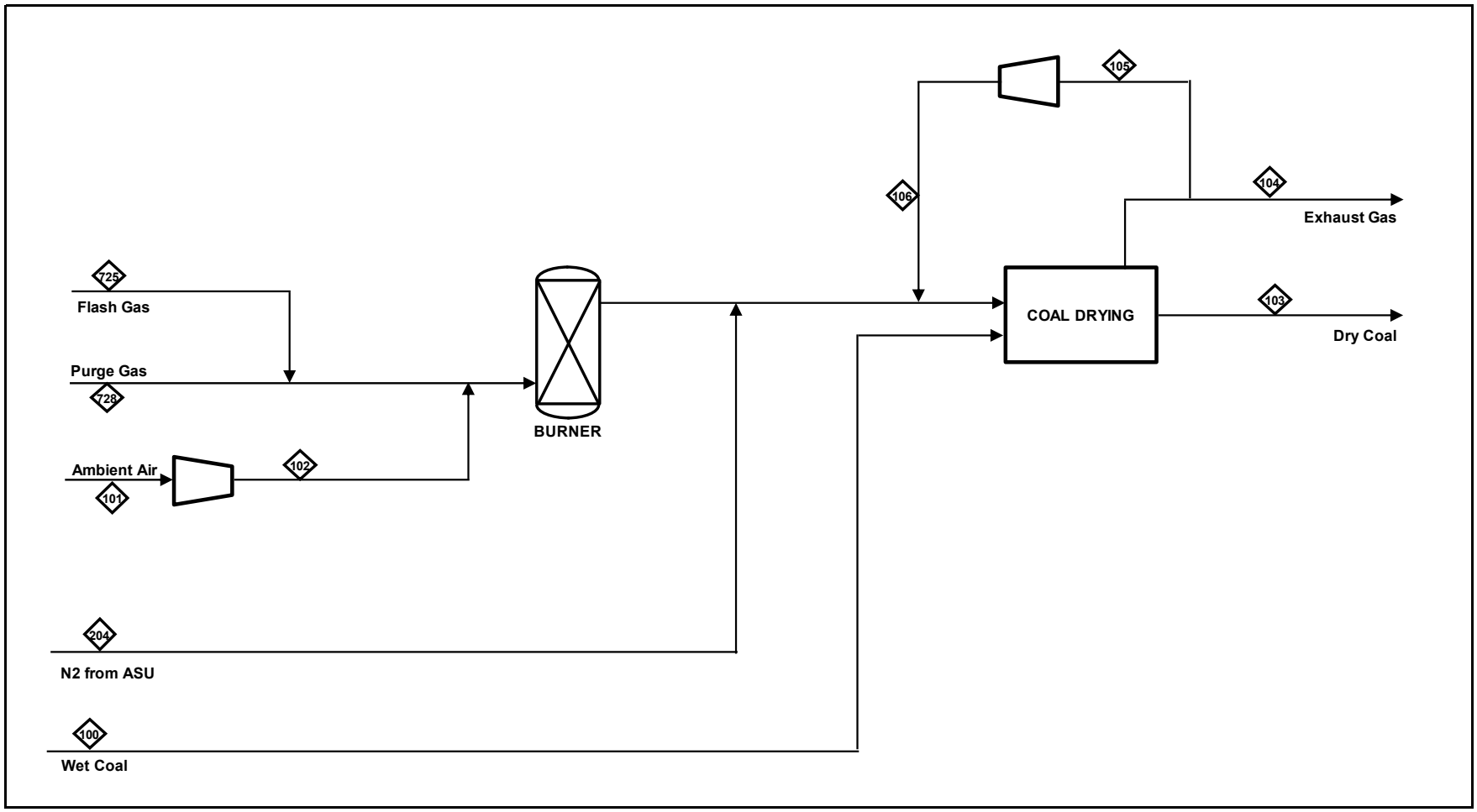

Table 10-2
Case 2e Plant – Coal Drying Stream Table

STREAM	100	101	102	103	104	105	106	204	725	728
Description	Wet Coal	Ambient Air	Feed Air	Dry Coal	Exhaust Gas	LP Recycle Gas	HP Recycle Gas	Dilution Nitrogen	MeOH Flash Gas	MeOH Purge Gas
Mole Flow (Vapor/Liquid)/lbmol/hr										
AR	0	173	173	0	1048	564	564	216	89	570
CH4	0	0	0	0	0	0	0	0	52	233
CO	0	0	0	0	0	0	0	0	36	677
CO2	0	6	6	0	3776	2033	2033	0	1230	1069
COS	0	0	0	0	0	0	0	0	0	0
H2	0	0	0	0	0	0	0	0	39	1781
H2O	0	184	184	0	21384	11514	11514	19	2	1
H2S	0	0	0	0	0	0	0	0	0	0
N2	0	14445	14445	0	108597	58475	58475	93118	104	930
NH3	0	0	0	0	0	0	0	0	0	0
O2	0	3875	3875	0	1835	988	988	507	0	0
SO2	0	0	0	0	0	0	0	0	0	0
S	0	0	0	0	0	0	0	0	0	0
HCN	0	0	0	0	0	0	0	0	0	0
HCL	0	0	0	0	0	0	0	0	0	0
Methanol -- CH3OH	0	0	0	0	0	0	0	0	367	105
Ethanol -- C2H5OH	0	0	0	0	0	0	0	0	0.2	0.1
Propanol -- C3H8O	0	0	0	0	0	0	0	0	0	0
Ethane -- C2H6	0	0	0	0	0	0	0	0	0	0
Propane -- C3H8	0	0	0	0	0	0	0	0	0	0
n-Butane -- C4H10	0	0	0	0	0	0	0	0	0	0
Total V/L Flow, lbmol/hr	0	18683	18683	0	136640	73576	73576	93860	1919	5366
Total V/L Flow, lb/hr	0	539143	539143	0	3694185	1989182	1989182	2633735	74325	125544
Solids Mass Flow, lb/hr	1528260	0	0	1206840	0	0	0	0	0	0
Coal	1528260	0	0	1206840	0	0	0	0	0	0
Ash	0	0	0	0	0	0	0	0	0	0
Carbon	0	0	0	0	0	0	0	0	0	0
Total Flow (Solids + V/L), lb/hr	1528260	539143	539143	1206840	3694185	1989182	1989182	2633735	74325	125544
Pressure, psia	14.7	14.7	17	14.3	14.3	14.3	16	18	40	717
Temperature, F		59	90		190	190	218	70	120	130

Figure 10-3
Case 2e Plant – ASU/Coal Gasification PFD

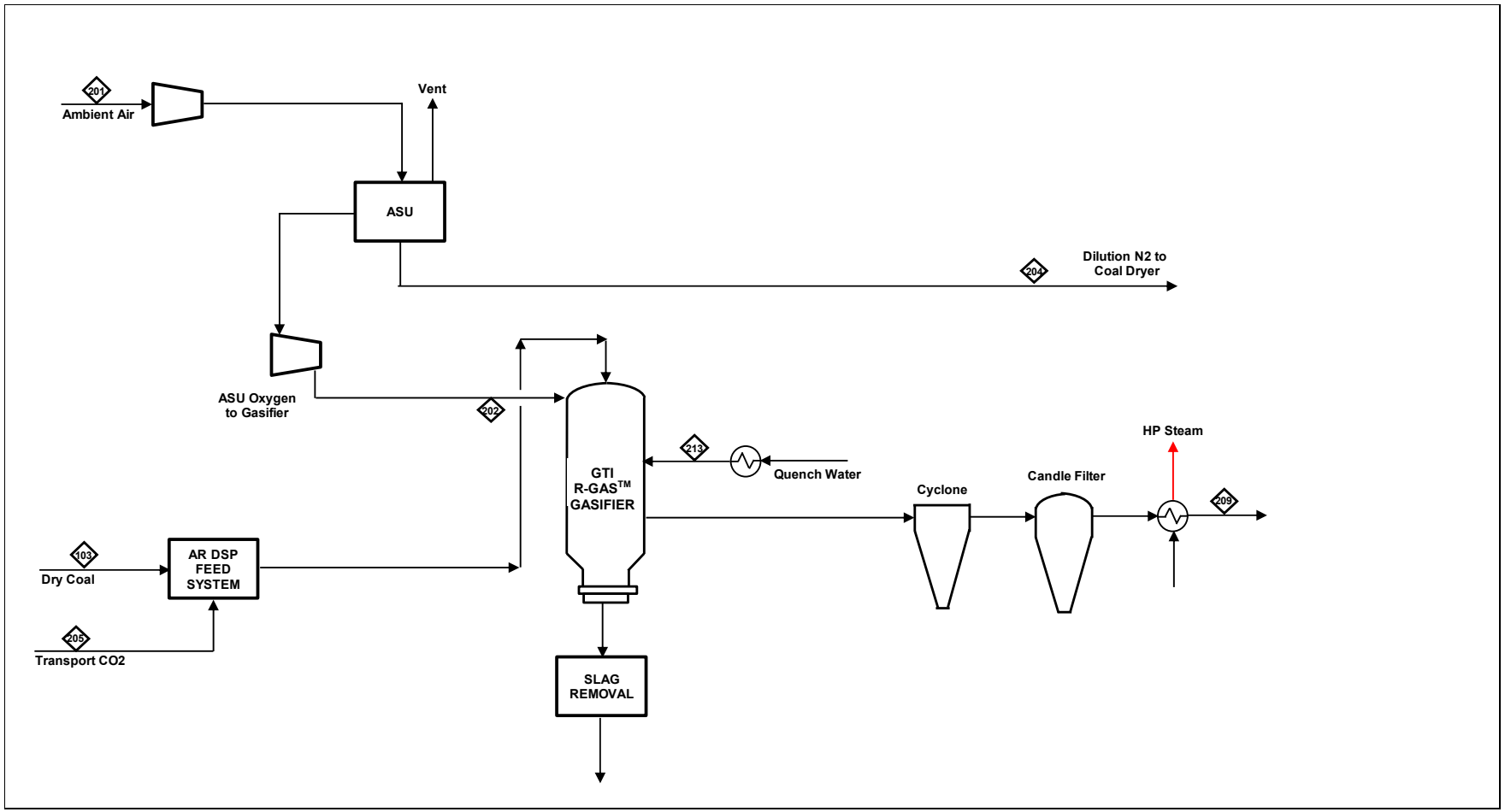

Table 10-3
Case 2e Plant – ASU/Coal Gasification Stream Table

STREAM	201	202	204	205	103	213	214	209
Description	Ambient Air	Oxygen to Gasifier	N2 to Coal Dryer	Conveying CO2	Dry Coal	Quench Water	Slag Out	Raw Cooled Syngas
Mole Flow (Vapor/Liquid)/lbmol/hr								
AR	1188	794	216	0	0	0	0	794
CH4	0	0	0	0	0	0	0	346
CO	0	0	0	2	0	0	0	64236
CO2	42	0	0	2931	0	0	0	2019
COS	0	0	0	0	0	0	0	36
H2	0	0	0	6	0	0	0	25979
H2O	1268	0	19	0	0	53860	0	56396
H2S	0	0	0	0	0	0	0	311
N2	99338	530	93118	0	0	0	0	861
NH3	0	0	0	0	0	0	0	111
O2	26648	25159	507	0	0	0	0	0
SO2	0	0	0	0	0	0	0	0
S	0	0	0	0	0	0	0	0
HCN	0	0	0	0	0	0	0	3
HCL	0	0	0	0	0	0	0	3
Methanol -- CH3OH	0	0	0	0	0	0	0	0
Ethanol -- C2H5OH	0	0	0	0	0	0	0	0
Propanol -- C3H8O	0	0	0	0	0	0	0	0
Ethane -- C2H6	0	0	0	0	0	0	0	0
Propane -- C3H8	0	0	0	0	0	0	0	0
n-Butane -- C4H10	0	0	0	0	0	0	0	0
Total V/L Flow, lbmol/hr	128485	26484	93860	2940	0	53860	0	151096
Total V/L Flow, lb/hr	3707669	851647.9	2633735	129095	0	970303	0	3032729
Solids Mass Flow, lb/hr	0	0	0	0	1206840	0	125127.4	0
Coal	0	0	0	0	1206840	0	0	0
Ash	0	0	0	0	0	0	125127	0
Carbon	0	0	0	0	0	0	0	0
Total Flow (Solids + V/L), lb/hr	3707669	851648	2633735	129095	1206840	970303	125127	3032729
Pressure, psia	14.7	1000	18.0	1100.0	14.3	980	915	905.0
Temperature, F	59	292	70	270		250		755

Figure 10-4
Case 2e Plant – RTI WDP/DSRP/ATWGS PFD

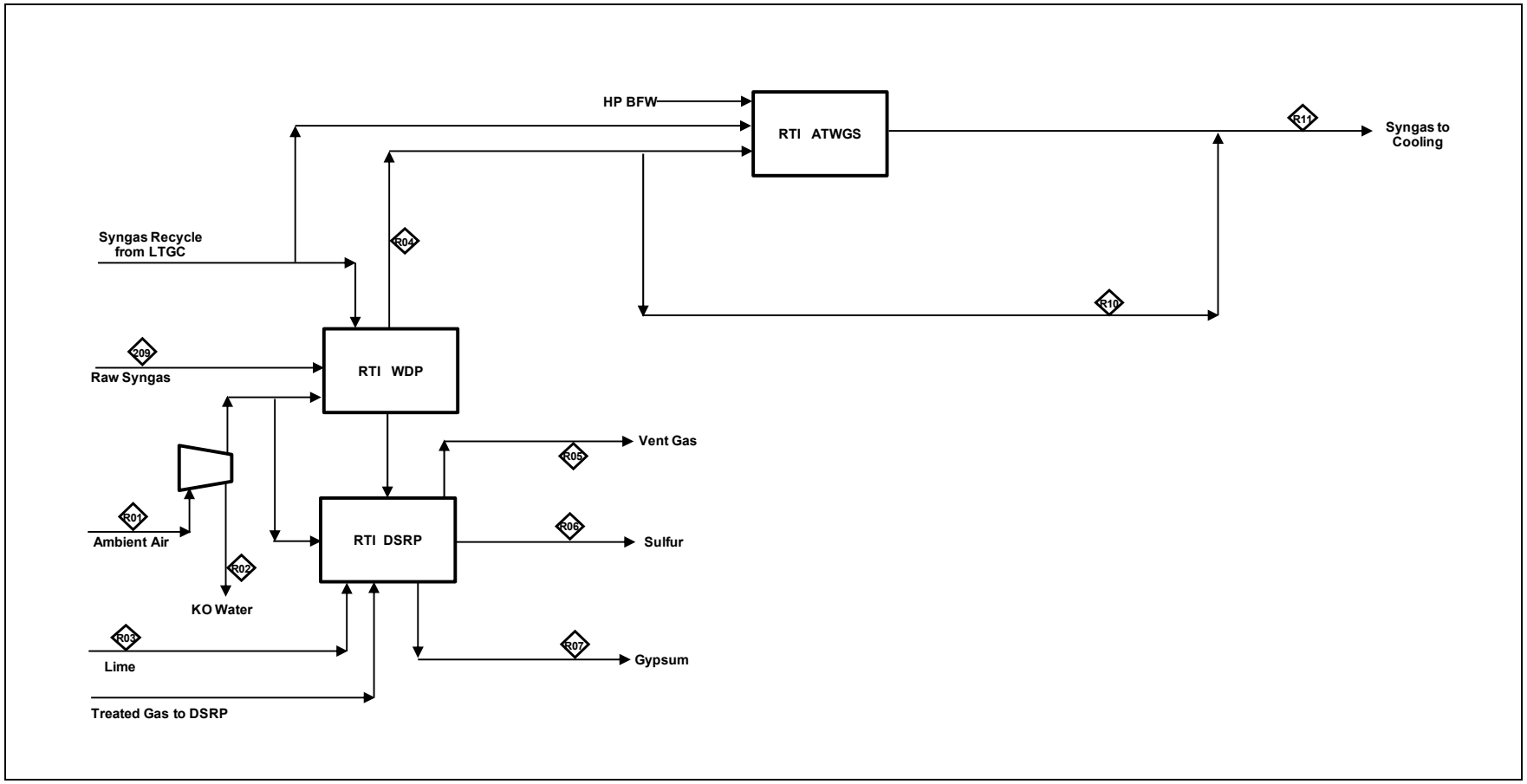

Table 10-4
Case 2e Plant – RTI WDP/DSRP/ATWGS Stream Table

STREAM	209	R01	R02	R03	R04	R05	R06	R07	R10	R11
Description	Raw Syngas	Ambient Air	Comp KO Water	Lime	Treated Gas to Shift	DSRP Vent Gas	Sulfur Product	Gypsum Product	Bypass Syngas	Syngas to LT Cooling
Mole Flow (Vapor/Liquid)/lbmol/hr										
AR	794	43	0	0	806	46	0	0	282	816
CH4	346	0	0	0	348	0	0	0	122	352
CO	64236	0	0	0	64480	0	0	0	22568	30471
CO2	2019	2	0	0	2381	216	0	99	833	37170
COS	36	0	0	0	0	0	0	0	0	0
H2	25979	0	0	0	26472	0	0	0	9265	61541
H2O	56396	46	33	8346	56708	0	0	9179	19848	40719
H2S	311	0	0	0	1	0	0	0	0	1
N2	861	3618	0	0	1270	3227	0	5	445	1285
NH3	111	0	0	0	111	0	0	0	39	111
O2	0	970	0	0	0	0	0	0	0	0
SO2	0	0	0	0	0	0	0	0	0	0
S	0	0	0	0	0	0	130	0	0	0
HCN	3	0	0	0	0	0	0	0	0	0
HCL	3	0	0	0	0	0	0	0	0	0
Methanol -- CH3OH	0	0	0	0	0	0	0	0	0	0
Ethanol -- C2H5OH	0	0	0	0	0	0	0	0	0	0
Propanol -- C3H8O	0	0	0	0	0	0	0	0	0	0
Ethane -- C2H6	0	0	0	0	0	0	0	0	0	0
Propane -- C3H8	0	0	0	0	0	0	0	0	0	0
n-Butane -- C4H10	0	0	0	0	0	0	0	0	0	0
Lime	0	0	0	225	0	0	0	9	0	0
Gypsum	0	0	0	0	0	0	0	216	0	0
Total V/L Flow, lbmol/hr	151096	4679	33	8571	152579	3489	130	9512	53403	172466
Total V/L Flow, lb/hr	3032729	135022	603	167059	3061174	101732	4167	207847	1071411	3423112
Solids Mass Flow, lb/hr	0	0	0	0	0	0	0	0	0	0
Coal	0	0	0	0	0	0	0	0	0	0
Ash	0	0	0	0	0	0	0	0	0	0
Carbon	0	0	0	0	0	0	0	0	0	0
Total Flow (Solids + V/L), lb/hr	3032729	135022	603	167059	3061174	101732	4167	207847	1071411	3423112
Pressure, psia	905	14.7	13.0	13.0	898.0	751	14.7	14.7	898	864
Temperature, F	755	59	80	75	802	105	305	173	802	760

Figure 10-5
Case 2e Plant – LTGC PFD

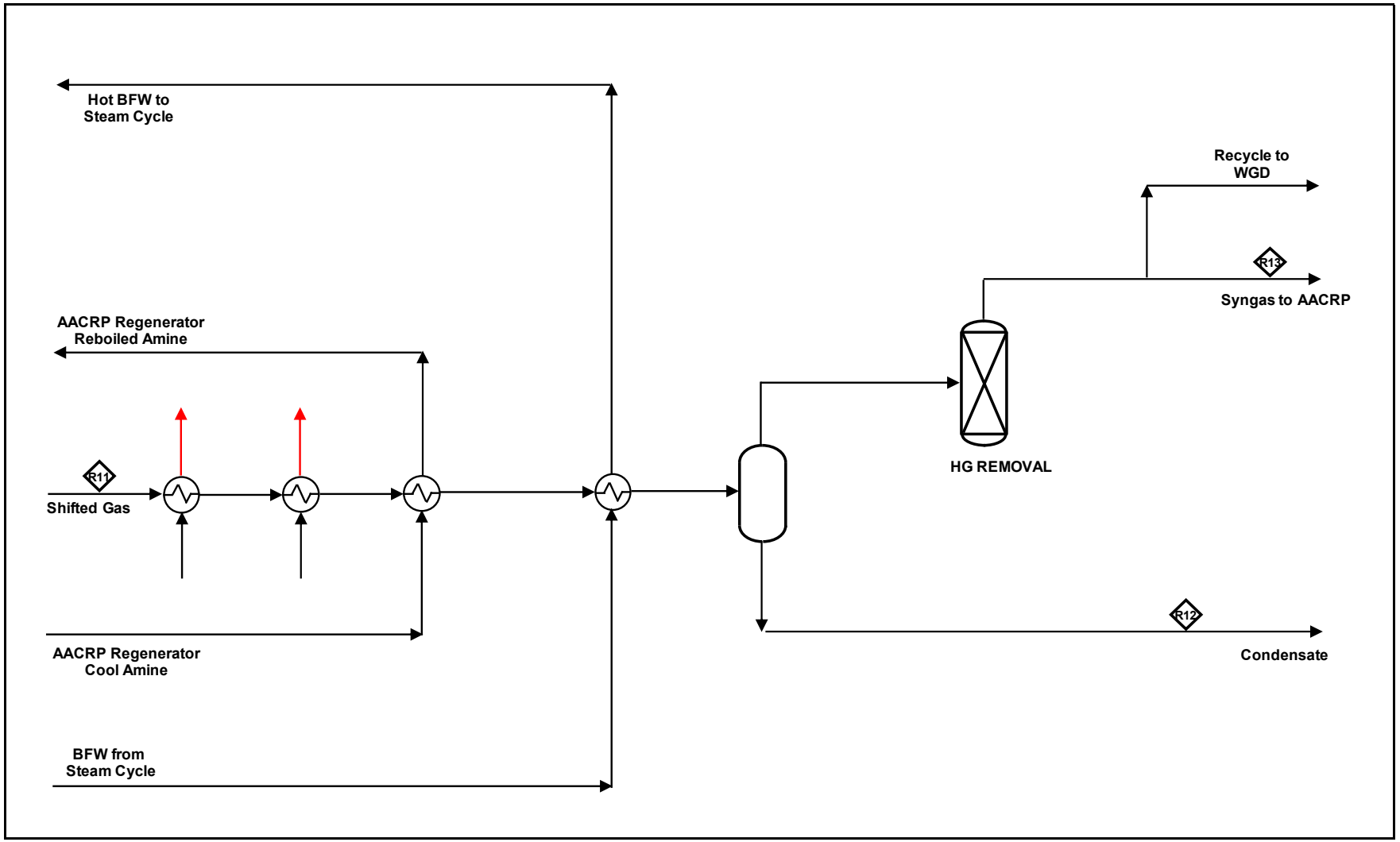

Table 10-5
Case 2e Plant – LTGC Stream Table

STREAM	R11	R12	R13
Description	Shifted Syngas	KO Water	Cooled Syngas
Mole Flow (Vapor/Liquid)/lbmol/hr			
AR	816	0	800
CH4	352	0	346
CO	30471	0	29875
CO2	37170	8	36436
COS	0	0	0
H2	61541	0	60339
H2O	40719	40563	153
H2S	1	0	1
N2	1285	0	1260
NH3	111	111	0
O2	0	0	0
SO2	0	0	0
S	0	0	0
HCN	0	0	0
HCL	0	0	0
Methanol -- CH3OH	0	0	0
Ethanol -- C2H5OH	0	0	0
Propanol -- C3H8O	0	0	0
Ethane -- C2H6	0	0	0
Propane -- C3H8	0	0	0
n-Butane -- C4H10	0	0	0
Total V/L Flow, lbmol/hr	172466	40683	129210
Total V/L Flow, lb/hr	3423112	732995.2	2637579
Solids Mass Flow, lb/hr	0	0	0
Coal	0	0	0
Ash	0	0	0
Carbon	0	0	0
Total Flow (Solids + V/L), lb/hr	3423112	732995	2637579
Pressure, psia	864	839	824
Temperature, F	760	95	95

Figure 10-6
Case 2e Plant – AACRP and CO_2 Compression PFD

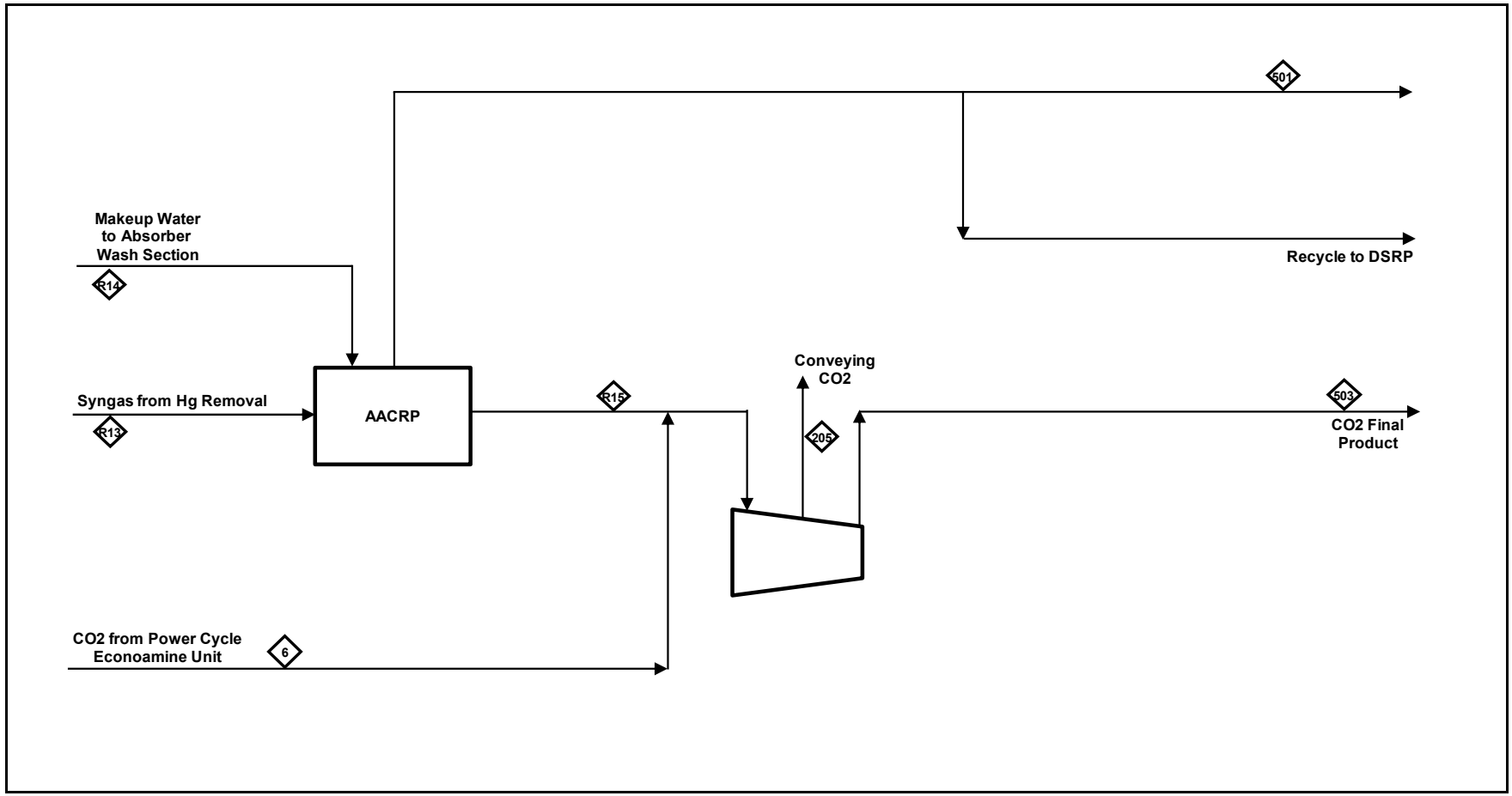

Table 10-6
Case 2e Plant – AACRP and CO_2 Compression Stream Table

STREAM	R13	R14	R15	501	6	205	503
Description	Syngas to AACRP	Makeup Wash Water	AACRP CO2 Product	Syngas to MeOH Synthesis	CO2 from MEA Unit	Convey CO2	CO2 Final Product
Mole Flow (Vapor/Liquid)/lbmol/hr							
AR	816	0	1	791	0	0	1
CH4	352	0	2	340	0	0	2
CO	30470	0	26	29545	0	2	23
CO2	37162	0	33532	2875	3901	2931	34501
COS	0	0	0	0	0	0	0
H2	61541	0	73	59650	0	6	67
H2O	156	3556	3233	471	46	0	0
H2S	1	0	1	0	0	0	1
N2	1285	0	1	1247	0	0	1
NH3	0	0	0	0	0	0	0
O2	0	0	0	0	0	0	0
SO2	0	0	0	0	0	0	0
S	0	0	0	0	0	0	0
HCN	0	0	0	0	0	0	0
HCL	0	0	0	0	0	0	0
Methanol -- CH3OH	0	0	0	0	0	0	0
Ethanol -- C2H5OH	0	0	0	0	0	0	0
Propanol -- C3H8O	0	0	0	0	0	0	0
Ethane -- C2H6	0	0	0	0	0	0	0
Propane -- C3H8	0	0	0	0	0	0	0
n-Butane -- C4H10	0	0	0	0	0	0	0
Total V/L Flow, lbmol/hr	131783	3556	36868	94918	3947	2940	34596
Total V/L Flow, lb/hr	2690117	64062	1534951	1154771	172519	129095	1519296
Solids Mass Flow, lb/hr	0	0	0	0	0	0	0
Coal	0	0	0	0	0	0	0
Ash	0	0	0	0	0	0	0
Carbon	0	0	0	0	0	0	0
Total Flow (Solids + V/L), lb/hr	2690117	64062	1534951	1154771	172519	129095	1519296
Pressure, psia	824	814	20.7	814	24	1100	2215
Temperature, F	95	122	122	148	69	270	162

Figure 10-7
Case 2e Plant – Methanol Synthesis Plant PFD

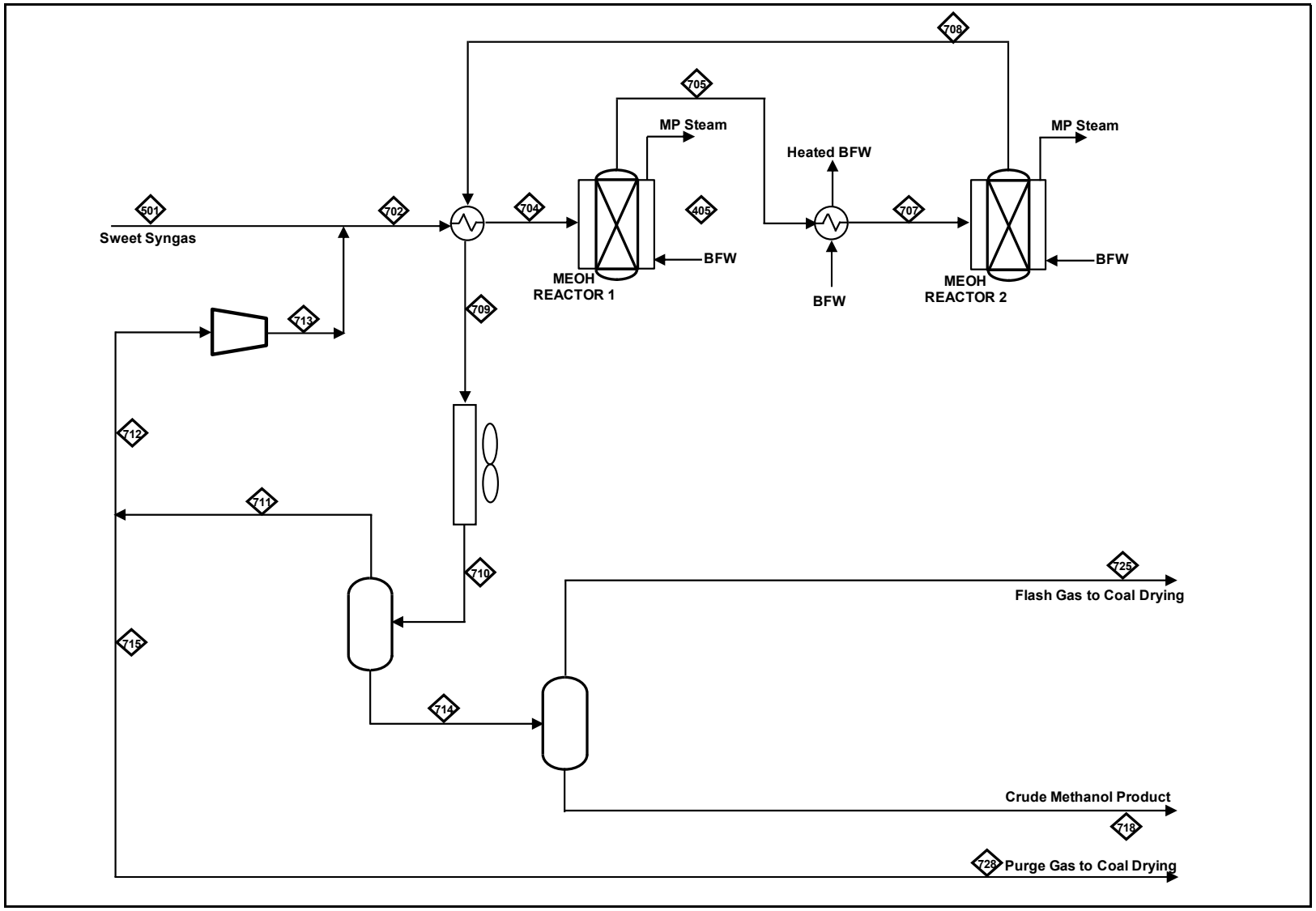

Table 10-7
Case 2e Plant – Methanol Synthesis Plant Stream Table

STREAM	501	704	705	707	708	709	710	711	712	713	714	718	725	728
Description	Reheated Syngas	MEOH Reactor 1 Feed	MEOH Reactor 1 Outlet	MEOH Reactor 2 Feed	MEOH Reactor 2 Outlet	Cooled Raw MeOH	AC Cool Raw MeOH	Flash Gas Ovhd	Recycle Syngas	HP Recycle Syngas	KO Drum Bottoms	Crude MeOH Product	MeOH Flash Gas	MeOH Purge Gas
Mole Flow (Vapor/Liquid)/lbmol/hr														
AR	791	14087	14087	14087	14087	14087	14087	13997	13297	13297	91	2	89	700
CH4	340	5782	5782	5782	5782	5782	5782	5728	5442	5442	54	2	52	286
CO	29545	45318	25485	25485	16638	16638	16638	16602	15773	15773	36	0	36	830
CO2	2875	27788	27569	27569	27767	27767	27767	26224	24913	24913	1543	312	1230	1311
COS	0	0	0	0	0	0	0	0	0	0	0	0	0	0
H2	59650	101167	60842	60842	43744	43744	43744	43704	41517	41517	39	0	39	2185
H2O	471	486	740	740	535	535	535	16	15	15	519	517	2	1
H2S	0	0	0	0	0	0	0	0	0	0	0	0	0	0
N2	1247	22935	22935	22935	22935	22935	22935	22830	21688	21688	105	2	104	1141
NH3	0	0	0	0	0	0	0	0	0	0	0	0	0	0
O2	0	0	0	0	0	0	0	0	0	0	0	0	0	0
SO2	0	0	0	0	0	0	0	0	0	0	0	0	0	0
S	0	0	0	0	0	0	0	0	0	0	0	0	0	0
HCN	0	0	0	0	0	0	0	0	0	0	0	0	0	0
HCL	0	0	0	0	0	0	0	0	0	0	0	0	0	0
Methanol -- CH3OH	0	2451	22436	22436	31096	31096	31096	2580	2451	2451	28516	28149	367	129
Ethanol -- C2H5OH	0	2	34	34	28	28	28	2	2	2	27	26	0	0
Propanol -- C3H8O	0	0	1	1	1	1	1	0	0	0	1	1	0	0
Ethane -- C2H6	0	0	0	0	0	0	0	0	0	0	0	0	0	0
Propane -- C3H8	0	0	0	0	0	0	0	0	0	0	0	0	0	0
n-Butane -- C4H10	0	0	0	0	0	0	0	0	0	0	0	0	0	0
Total V/L Flow, lbmol/hr	94917.85	220016	179910	179910	162614	162614	162614	131683	125098	125098	30931	29012	1919	6584
Total V/L Flow, lb/hr	1154771	4081605	4081570	4081570	4081554	4081554	4081554	3080842	2926833	2926833	1000712	926387	74325.4	154042
Solids Mass Flow, lb/hr	0	0	0	0	0	0	0	0	0	0	0	0	0	0
Coal	0	0	0	0	0	0	0	0	0	0	0	0	0	0
Ash	0	0	0	0	0	0	0	0	0	0	0	0	0	0
Carbon	0	0	0	0	0	0	0	0	0	0	0	0	0	0
Total Flow (Solids + V/L), lb/hr	1154771	4081605	4081570	4081570	4081554	4081554	4081554	3080842	2926833	2926833	1000712	926387	74325	154042
Pressure, psia	814	747	737	732.0	727	722	720	717	717	755	717	40	40	717
Temperature, F	147.8623	400	475	400	430	236	130	130	130	141	130	120	120	130

Figure 10-8
Case 2e Plant -- NGCC PFD

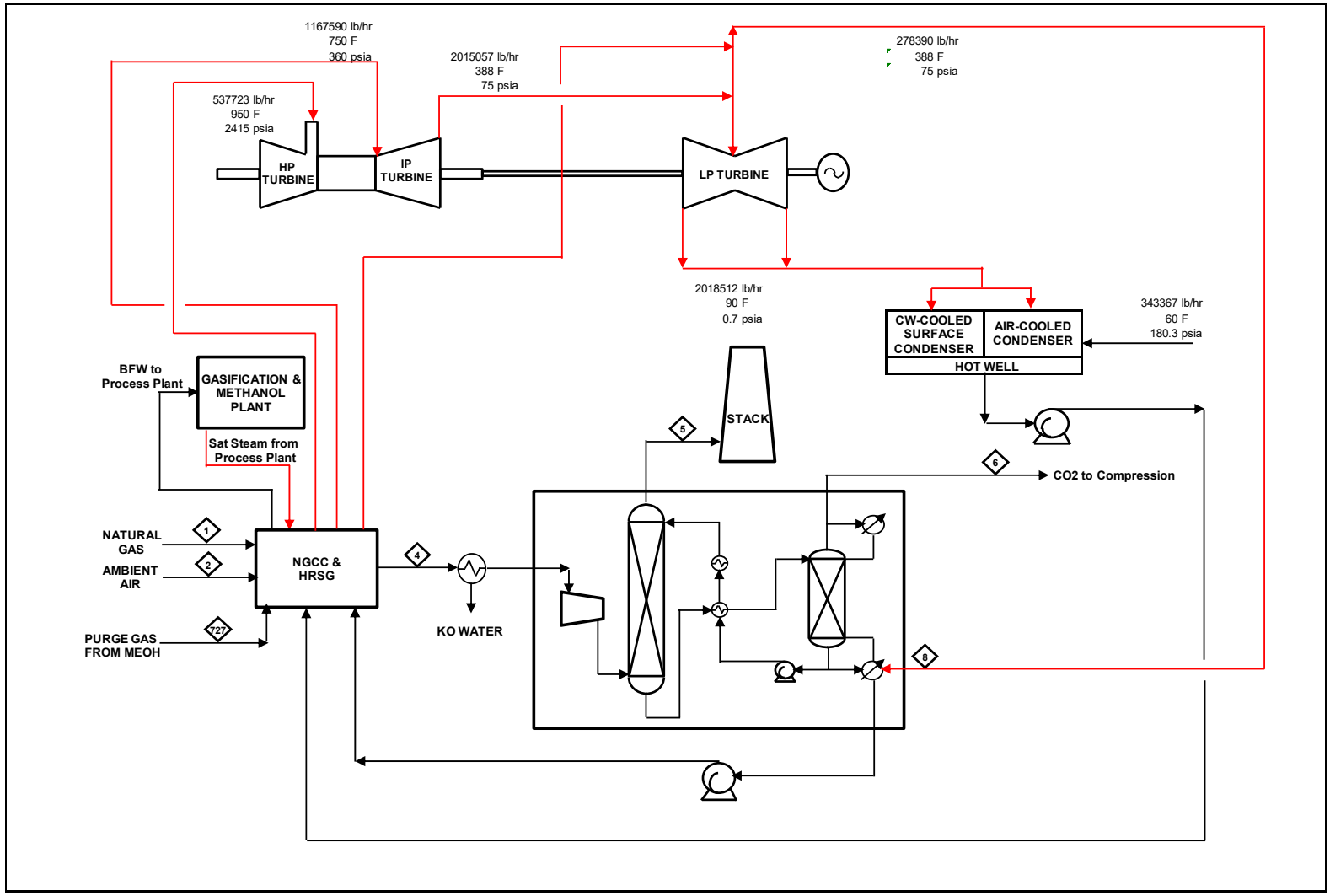

Table 10-8
Case 2e Plant – NGCC Stream Table

STREAM	1	2	4	5	6	8	727
Description	Ambient Air	Natural Gas	Flue Gas to MEA	Treated Gas	CO2 Out	LP Steam	MeOH Purge Gas
Mole Flow (Vapor/Liquid)/lbmol/hr							
AR	1057	0	1187	1187	0	0	130
CH4	0	3435	0	0	0	0	77
CO	0	0	0	0	0	0	138
CO2	38	37	4356	436	3920	0	237
COS	0	0	0	0	0	0	0
H2	0	0	0	0	0	0	428
H2O	1128	0	9089	3668	46	15453	0
H2S	0	0	0	0	0	0	0
N2	88394	59	88665	88665	0	0	210
NH3	0	0	0	0	0	0	0
O2	23712	0	15782	15782	0	0	0
SO2	0	0	0	0	0	0	0
S	0	0	0	0	0	0	0
HCN	0	0	0	0	0	0	0
HCL	0	0	0	0	0	0	0
Methanol -- CH3OH	0	0	0	0	0	0	0
Ethanol -- C2H5OH	0	0	0	0	0	0	0
Propanol -- C3H8O	0	0	0	0	0	0	0
Ethane -- C2H6	0	118	0	0	0	0	0
Propane -- C3H8	0	26	0	0	0	0	0
n-Butane -- C4H10	0	15	0	0	0	0	0
Total V/L Flow, lbmol/hr	114330	3690	119078	109737	3966	15453	1219
Total V/L Flow, lb/hr	3299204	63929	3391639	3121464	173339	278390	27463
Total Flow (Solids + V/L), lb/hr	3299204	63929	3391639	3121464	173339	278390	27463
Pressure, psia	15	475	15	15	24	260	176
Temperature, F	59	60	281	85	69	35	365

10.3 SPARING PHILOSOPHY

The sparing philosophy for the GTI and RTI-provided equipment for the Case 2e CTM plant is provided below. The design has:

- Five trains of gasification, including dry feed system, R-GAS™ gasifier, cyclone and candle filter (5 x 25%)
- One WDP train (1 x 100%)
- One DSRP train (1 x 100%)
- One ATWGS train (1 x 100%)
- Two AACRP trains (2 x 50%)

10.4 PERFORMANCE RESULTS

The Nexant-modeled Case 2e plant with CO_2 capture consumes 18,339 tpd of PRB coal and 33.6 MMSCFD of natural gas at the Midwestern site and produces 926,387 lb/hr (10,085 mtpd) of crude methanol. Overall performance for the Case 2e plant is summarized in Table 10-9, which includes auxiliary power requirements. Loads that are unique to the GTI R-GAS™ gasification system, RTI WDP, DSRP, ATWGS and AACRP are shown in bold and italicized.

Table 10-9
Case 2e Plant Performance Summary

POWER SUMMARY (Gross Power at Generator Terminals, kWe)	Case 2e
Gas Turbine Power	127,940
Steam Turbine Power	248,731
TOTAL POWER, kWe	**376,671**
CTM Plant Auxiliary Load Summary, kWe	
Coal Handling	8,585
Slag Handling	2,178
Incinerator Air Blower	4,534
Incinerator Recycle Blower	1,192
Air Separation Unit	152,581
AR DSP	***8,483***
Quench Water Pump	2,494
RTI WDP	***9,965***
RTI DSRP	***633***
ATWGS	***0***
AACRP	***31,991***
AACRP and NGCC CO_2 Compressor Auxiliaries	64,924
Recycle Gas Compressor	2,994
Air Cooler Fans	1,660
Water Treatment	2,669
Miscellaneous BOP	5,000
Circulating Water Pumps	6,984
Ground Water Pumps	765
Cooling Tower Fans	4,554
SUBTOTAL CTM PLANT AUXILIARIES, kWe	**312,193**
NGCC Plant Auxiliary Load Summary, kWe	
Gas Turbine Auxiliaries	788
Steam Turbine Auxiliaries	90
Transformer Losses	2,066
Miscellaneous BOP	500
Air Cooled Condenser Fans	4,367
Condensate Pumps	663
Boiler Feed Water Pumps	13,177
Amine System Auxiliaries	4,103
SCR	16
SUBTOTAL POWER PLANT AUXILIARIES, kWe	**25,770**
TOTAL AUXILIARIES, kWe	**337,963**
NET PLANT POWER, kWe	**38,707**
CONSUMABLES	
As-Received Coal Feed, tpd	18,339
Natural Gas Feed Rate, MMBtu/day	34,675
Raw Water Withdrawal, gpm	8,401
Raw Water Consumption, gpm	6,463

Table 10-10 shows the carbon balance for the Case 2e plant, per the same description provided for Case 2b in Section 9.4. For Case 2e, the carbon capture efficiency is 93.5%.

Table 10-10
Case 2e Plant – Overall Carbon Balance

Overall Carbon Balance, lb/hr	In	Out
Coal Feed	765,169	
ASU Air	506	
Coal Dryer Air	74	
Power Cycle Natural Gas	46,182	
Power Cycle Combustion Air	450	
DSRP Air In	18	
ASU Vent		506
Coal Dryer Exhaust Gas		45,355
Carbon in Slag		0
Sulfur Product		0
DSRP Vent		2,593
Gypsum		1,185
Crude Methanol Product		342,536
AACRP CO_2 Product		367,837
NGCC CO_2 Product		47, 082
NGCC Exhaust Gas		5,231
CO_2 in LTGC Condensate (Vented)		92
Convergence Tolerance		-17
Total	**812,400**	**812,400**

Table 10-11 shows the sulfur balance for the CTM plant based on the same description for Case 2b given in Section 9.4. The net sulfur emissions for the Case 2e CTM plant is < 0.0001 lb of SO_2/MMBtu.

Table 10-11
Case 2e Plant – Overall Sulfur Balance

Overall Sulfur Balance, lb/hr	In	Out
Coal Feed	11,118	
Sulfur Product		4,167
Gypsum		6,928
Coal Dryer Exhaust Gas		0
AACRP CO_2 Product		21
Convergence Tolerance		2
Total	**11,118**	**11,118**

Table 10-12 shows the overall water balance for the Case 2e plant.

Table 10-12
Case 2e Plant – Overall Water Balance

Water Use, gpm	Raw Water Withdrawal	Process Effluent Produced for Internal Consumption	Internal Consumption	Process Water Discharge
Slag Handling	0	0	324	(324)
Quench Cooler	1,939	0	0	0
DSRP Air Compressor Knockout	0	(1)	0	0
Syngas Cooling Knockout	0	(1,460)	0	0
AACRP Wash Water	0	0	128	0
CO_2 Compression Knockout	0	(118)	0	0
Steam Cycle Makeup	686	0	0	0
Steam Cycle Blowdown	0	(25)	0	0
Flue Gas Cooling Knockout	0	(193)	0	0
Cooling Tower Makeup	5,776	0	1,346	0
Cooling Tower Blowdown	0	0	0	(1,614)
Total	8,401	(1,798)	1,798	(1,938)

Positive values represent consumption while negative values represent production

10.5 EQUIPMENT LIST

The equipment list for the GTI/RTI processes that differ from the reference Case 2b CTM plant are shown in Table 10-13 below.

Table 10-13
Case 2e Equipment List

ACCOUNT 5A GAS CLEANUP & PIPING
Subaccount 5A.4a RTI WDP System

Equipment No.	Description	Type	Design Condition	Operating Qty	Spares
11	Recycle Syngas Compressor	Centrifugal	305 acfm @ 824 psia	1	0

ACCOUNT 5A SYNGAS CLEANUP
Subaccount 5A.4b Shift Reactors

Equipment No.	Description	Type	Design Condition	Operating Qty	Spares
1	ATWGS Reactor	Transport Reactor	Proprietary	1	0
2	Cyclone Separator	Cyclone	Proprietary	1	0
3	Sorbent Feeder Package (incl Hopper)		Proprietary	1	0
4	Solids Cooler	Shell and Tube Heat Exchanger	Proprietary	1	0

10.6 CAPITAL COST

Table 10-14 shows the cost breakdown of the Case 2e plant. The accounts/subaccounts of interest for this study that are shown with more detail are:

- 2.3 Dry Coal Injection System,
- 4 Gasifier & Accessories,
- 5A Gas Cleanup & Piping and
- 5B CO_2 Removal and Compression

Table 10-15 shows the calculation and addition of owner's costs to determine the TOC, which is used to calculate the product methanol RSP.

The estimated TOC of the Case 2e plant in 2011 dollars is $4,527MM.

Table 10-14
Case 2e Plant – Total Plant Cost Summary

Case 2e: GTI R-GAS™ with RTI WDP/ATWGS CTM Plant		Coal Feed, lb/hr	1,528,260					Plant Size	10085 metric tons per day	
Low Rank Western Coal Baseline Study	PRB	Coal HHV, Btu/lb	8,564							

Acct No.	Item/Description	Equipment Cost	Material Cost	Labor Direct	Labor Indirect	Sales Tax	Bare Erected Cost $	Eng'g CM H.O & Fee	Contingencies Process	Contingencies Project	TOTAL PLANT COST $
1	COAL & SORBENT HANDLING	**$35,251**	**$6,321**	**$27,325**	**$0**	**$0**	**$68,897**	**$6,253**	**$0**	**$15,030**	**$90,180**
2	COAL & SORBENT PREP & FEED										
2.3	Dry Coal Injection System	$134,811	$0	$88,517	$0	$0	$223,328	$19,235	$44,666	$57,446	$344,674
2.x	Other Coal & Sorbent Prep & Feed Systems	$146,191	$27,729	$42,212	$0	$0	$216,131	$18,906	$0	$47,008	$282,045
	SUBTOTAL2.	**$281,001**	**$27,729**	**$130,729**	**$0**	**$0**	**$439,459**	**$38,141**	**$44,666**	**$104,454**	**$626,719**
3	FEEDWATER & MISC BOP SYSTEMS	**$27,771**	**$7,773**	**$16,656**	**$0**	**$0**	**$52,200**	**$4,905**	**$0**	**$12,974**	**$70,079**
4	GASIFIER & ACCESSORIES										
4.1	Gasifier, Syngas Cooler & Auxiliaries (GTI)	$88,269	$44,134	$133,274	$0	$0	$265,677	$23,821	$66,419	$53,388	$409,304
4.3	ASU/Oxidant Compression	$539,576	$0	$0	$0	$0	$539,576	$52,301	$0	$59,187	$651,064
4.6	Flare Stack System	$0	$1,421	$647	$0	$0	$2,068	$198	$0	$453	$2,719
4.9	Gasification Foundations	$0	$30,489	$18,183	$0	$0	$48,671	$4,456	$0	$13,282	$66,409
	SUBTOTAL 4.	**$627,845**	**$76,044**	**$152,104**	**$0**	**$0**	**$855,992**	**$80,776**	**$66,419**	**$126,310**	**$1,129,497**
5A	GAS CLEANUP & PIPING										
5A.1	AACRP	$38,471	$0	$32,316	$0	$0	$70,787	$6,688	$14,157	$18,326	$109,959
5A.2	RTI DSRP System	$16,676	$0	$18,461	$0	$0	$35,137	$3,413	$7,027	$9,115	$54,692
5A.3	Mercury Removal	$7,303	$0	$5,520	$0	$0	$12,822	$1,238	$641	$2,940	$17,641
5A.4a	RTI WDP System	$46,096	$0	$54,612	$0	$0	$100,708	$9,792	$20,142	$26,128	$156,770
5A.4c	LT Heat Recovery, FG Saturation & RTI ATWGS Reactor	$68,216	$0	$22,730	$0	$0	$90,946	$8,844	$3,643	$20,687	$124,120
5A.5	Syngas Compressor	$0	$0	$0	$0	$0	$0	$0	$0	$0	$0
5A.6	Blow back Gas Systems	$6,453	$1,086	$612	$0	$0	$8,150	$773	$0	$1,785	$10,708
5A.7	Fuel Gas Piping	$0	$2,881	$1,885	$0	$0	$4,766	$441	$0	$1,041	$6,248
5A.9	HGCU Foundations	$0	$0	$0	$0	$0	$0	$0	$0	$0	$0
	SUBTOTAL 5.	**$183,215**	**$3,967**	**$136,135**	**$0**	**$0**	**$323,317**	**$31,188**	**$45,610**	**$80,023**	**$480,139**
5B	CO2 REMOVAL & COMPRESSION										
5B.1	NGCC CO2 Removal System	$23,669	$0	$7,132	$0	$0	$30,801	$2,570	$6,160	$7,907	$47,438
5B.2	CO2 Compression & Drying (AACRP & NGCC)	$68,777	$0	$25,928	$0	$0	$94,705	$9,073	$0	$20,756	$124,534
5B.3	CO2 Compression & Drying (NGCC)	$0	$0	$0	$0	$0	$0	$0	$0	$0	$0
	SUBTOTAL 5B.	**$92,446**	**$0**	**$33,060**	**$0**	**$0**	**$125,506**	**$11,643**	**$6,160**	**$28,663**	**$171,972**
5C	METHANOL PRODUCTION	**$131,663**	**$55,393**	**$110,787**	**$0**	**$0**	**$297,843**	**$29,785**	**$0**	**$65,526**	**$393,154**
6	COMBUSTION TURBINE/ACCESSORIES	**$47,397**	**$394**	**$3,814**	**$0**	**$0**	**$51,605**	**$11,171**	**$11,909**	**$14,852**	**$89,537**
7	HRSG, DUCTING & STACK	**$14,259**	**$398**	**$3,387**	**$0**	**$0**	**$18,044**	**$1,498**	**$0**	**$1,965**	**$21,507**
8	STEAM TURBINE GENERATOR	**$80,264**	**$1,050**	**$16,356**	**$0**	**$0**	**$97,670**	**$8,874**	**$0**	**$19,222**	**$125,766**
9	COOLING WATER SYSTEM	**$18,205**	**$19,971**	**$14,766**	**$0**	**$0**	**$52,942**	**$4,898**	**$0**	**$11,758**	**$69,598**
10	ASH/SPENT SORBENT HANDLING SYS	**$77,771**	**$3,478**	**$73,220**	**$0**	**$0**	**$154,469**	**$14,945**	**$0**	**$17,687**	**$187,101**
11	ACCESSORY ELECTRIC PLANT	**$37,543**	**$21,737**	**$38,296**	**$0**	**$0**	**$97,576**	**$8,480**	**$0**	**$21,091**	**$127,147**
12	INSTRUMENTATION & CONTROL	**$12,323**	**$3,725**	**$10,335**	**$0**	**$0**	**$26,383**	**$2,368**	**$1,320**	**$5,388**	**$35,459**
13	IMPROVEMENTS TO SITE	**$5,753**	**$2,827**	**$15,057**	**$0**	**$0**	**$23,637**	**$2,334**	**$0**	**$7,791**	**$33,762**
14	BUILDINGS & STRUCTURES	**$0**	**$7,617**	**$10,557**	**$0**	**$0**	**$18,174**	**$1,642**	**$0**	**$3,217**	**$23,033**
	CALCULATED TOTAL COST	**$1,672,707**	**$238,424**	**$792,583**	**$0**	**$0**	**$2,703,714**	**$258,901**	**$176,084**	**$535,950**	**$3,674,650**

Table 10-15
Case 2e Plant – Total Overnight Cost Breakdown

Owner's Costs	$ x $1,000
Preproduction Costs	
6 months All Labor	$26,651
1 Month Maintenance Materials	$4,918
1 Month Non-Fuel Consumables	$1,831
1 Month Waste Disposal	$1,154
25% of 1 Months Fuel Cost at 100% CF	$6,716
2% of TPC	$73,493
Total	**$114,764**
Inventory Capital	
60 day supply of fuel at 100% CF	$52,993
60 day supply of non-fuel consumables at 100% CF	$2,227
0.5% of TPC (spare parts)	$18,373
Total	**$73,593**
Initial Cost for Catalyst and Chemicals	**$13,183**
Land	**$900**
Other Owner's Cost	**$551,198**
Financing Costs	**$99,216**
Total Owner's Costs	**$852,853**
Total Overnight Costs (TOC)	**$4,527,504**

10.7 OPERATING COSTS

Table 10-16 shows the OPEX breakdown for the Case 2e plant.

Table 10-16
Case 2e Plant – Initial and Annual O&M Costs

INITIAL & ANNUAL O&M EXPENSES					
Case:	Case 2e - GTI R-GAS™ with RTI WDP and ATWGS CTM Plant				
Plant Size (mtpd Methanol)	**10,085**				
Primary/Secondary Fuel:	**PRB/Natural Gas**				
Design/Construction	5 years			**Book Life (yrs):**	20
TPC (Plant Cost) Year	June 2011			**TPI Year:**	2016
Capacity Factor (%)	90			**CO2 Captured (TPD)**	16168

OPERATING & MAINTENANCE LABOR				
Operating Labor				
Operating Labor Rate (base):	$39.70	$/hr		
Operating Labor Burden:	30.00	% of base		
Labor Overhead Charge	25.00	% of labor		
Operating Labor Requirements per Shift	**units/mod**		**Total Plant**	
Skilled Operator	2.0		2.0	
Operator	10.0		10.0	
Foreman	1.0		1.0	
Lab Tech's etc	3.0		3.0	
TOTAL Operating Jobs	16.0		16.0	
				Annual Cost $
Annual Operating Labor Cost				$7,233,658
Maintenance Labor Cost				$35,408,448
Administration & Support Labor				$10,660,526
Property Taxes and Insurance				$73,493,020
TOTAL FIXED OPERATING COSTS				**$126,795,652**

VARIABLE OPERATING COSTS					
Maintenance Material Cost					**$53,112,673**
Consumables	Consumption Initial	Consumption /Day	Unit Cost	Initial Fill Cost	
Water(/1000 gallons)	0	6,048	1.67	**$0**	**$3,325,833**
Chemicals					
MU & WT Chem (lb)	0	36038	0.27	$0	$3,170,857
Carbon (Hg Removal) (lb)	249237	380	1.63	$406,256	$203,290
WDP Sorbent (lb)	Proprietary	Proprietary	Proprietary	$6,601,715	$5,859,411
ATWGS Catalyst (ft3)	Proprietary	Proprietary	Proprietary	$1,813,435	$756,474
MEA Solvent (ton)	160	0.22	3751.70	$600,378	$269,708
AACRP Solvent (lb)	327949	179.70	2.80	$917,558	$165,160
SCR Catalyst (m3)	N/A	N/A	N/A	$0	$0
Ammonia (ton)	N/A	N/A	N/A	$0	$0
Methanol Synthesis Catalyst (ft3)	4011	3.66	534.68	$2,144,730	$642,705
DSRP Catalyst (lb)	54120	29.65	11.15	$603,438	$108,619
Oxidation/Reduction Catalyst (lb)	60940	33.39	1.56	$95,066	$17,112
Calcium Hydroxide (lb)	5200	419040	0.04	$199	$5,259,942
Subtotal Chemicals				**$13,182,774**	**$16,453,278**
Other					
Supplemental Electricity (MWh consumed)	0	0	62.33	$0	$0
Gases, N2 etc.(/100scf)	0	0	0.00	$0	$0
LP Steam (/1000 lbs)	0	0	0.00	$0	$0
Subtotal Other				**$0**	**$0**
Waste Disposal:					
Spent Mercury Catalyst (lb)	0	380	0.65	$0	$81,067
Flyash (ton)	0	0	0.00	$0	$0
Slag (ton)	0	1502	25.11	$0	$12,385,561
Subtotal Waste Disposal				**$0**	**$12,466,628**
By-products & Emissions					
Sulfur (tons)	0	0.0	0.00	$0	$0
Supplemental Electricity (MWh generated)	0	929	-59.59	$0	-$18,184,991
Subtotal By-Products				**$0**	**-$18,184,991**
TOTAL VARIABLE OPERATING COSTS				**$13,182,774**	**$67,173,422**
Coal (tons)	**0**	**18,339**	**36.57**	**$0**	**$220,312,342**
Natural Gas (MMBtu)	**0**	**34,675**	**6.13**	**$0**	**$69,825,571**

10.8 METHANOL PRODUCT REQUIRED SELLING PRICE

Table 10-17 shows a summary of the power output, CAPEX, OPEX, and methanol product RSP for the Case 2e plant. The Case 2e plant methanol RSP is estimated to be $1.21/gal under the loan guarantee finance structure and $1.40/gal under the commercial fuels finance structure.

Table 10-17
Case 2e Plant – Overall Performance and Economic Summary

Case	Case 2e	
CAPEX, $MM		
Total Installed Cost (TIC)	$2,704	
Total Plant Cost (TPC)	$3,675	
Total Overnight Cost (TOC)	$4,528	
OPEX, $MM/yr (100% Capacity Factor Basis)		
Fixed Operating Cost (OC_{fix})	$126.8	
Variable Operating Cost, less Fuel (OC_{var})	$94.8	
Coal Feedstock (OC_{coal})	$244.8	
Natural Gas Feedstock (OC_{NG})	$77.6	
Import/(Export) Power (OC_{Power})	($20.2)	
Total OPEX	$523.8	
Plant Output		
Crude Methanol Product, tons per year	4,057,573	
Net Power Output, MWe	38.71	
Required Selling Price[A]		
Excluding CO_2 TS&M[BE], $/short ton	**343.3**	**402.8**
Including CO_2 TS&M[BE], $/short ton	**359.7**	**419.2**
RSP Component Details ($/gal)		
Capital[B]	0.70	0.90
Fixed O&M	0.12	
Variable O&M	0.08	
Coal	0.20	
Natural Gas	0.06	
Power	(0.02)	
CO_2 TS&M	0.05	
RSP[B] Total ($/gal)	**1.19**	**1.39**
Costs of CO_2 Captured[B,C] ($/tonne)	**17.3**	**19.4**
Costs of CO_2 Avoided[B,D] ($/tonne)	**28.3**	**30.4**

[A] Capacity factor assumed to be 90 percent
[B] Values shown are for two financial structures
The first (lower value) is based on the loan guarantee finance structure
The second (higher value) is based on the commercial fuels finance structure
[C] Excludes CO_2 TS&M
[D] Includes CO_2 TS&M
[E] Based on 301.73 gallons/short ton (332.6 gallons/metric ton)

Section 11 CTM Plant Sensitivity Analysis

Sensitivity analysis was carried out to determine the effects of various parameters of the GTI R-GAS™ system, RTI WDP and fixed-bed WGS/ATWGS systems on the overall methanol product RSP. The parameters investigated include: overall system capital cost, ATWGS catalyst cost, CTM plant CF, feedstock (coal and natural gas) cost, electric selling price, CO_2 sales price, cost of CO_2 emissions and CCF.

11.1 GTI R-GAS™ SYSTEM COST

Figure 11-1 shows how the methanol RSPs for Case 2a and 2e change as the GTI DSP and R-GAS™ gasifier TPC vary from -30% to +30%. Also shown in Figure 11-1 are the methanol RSPs for the reference Case 2a at $517.8/ton and $441.3/ton for the commercial fuels and loan guarantee finance structures respectively.

Figure 11-1
Sensitivity Analysis – RSP vs GTI R-GAS™ TPC

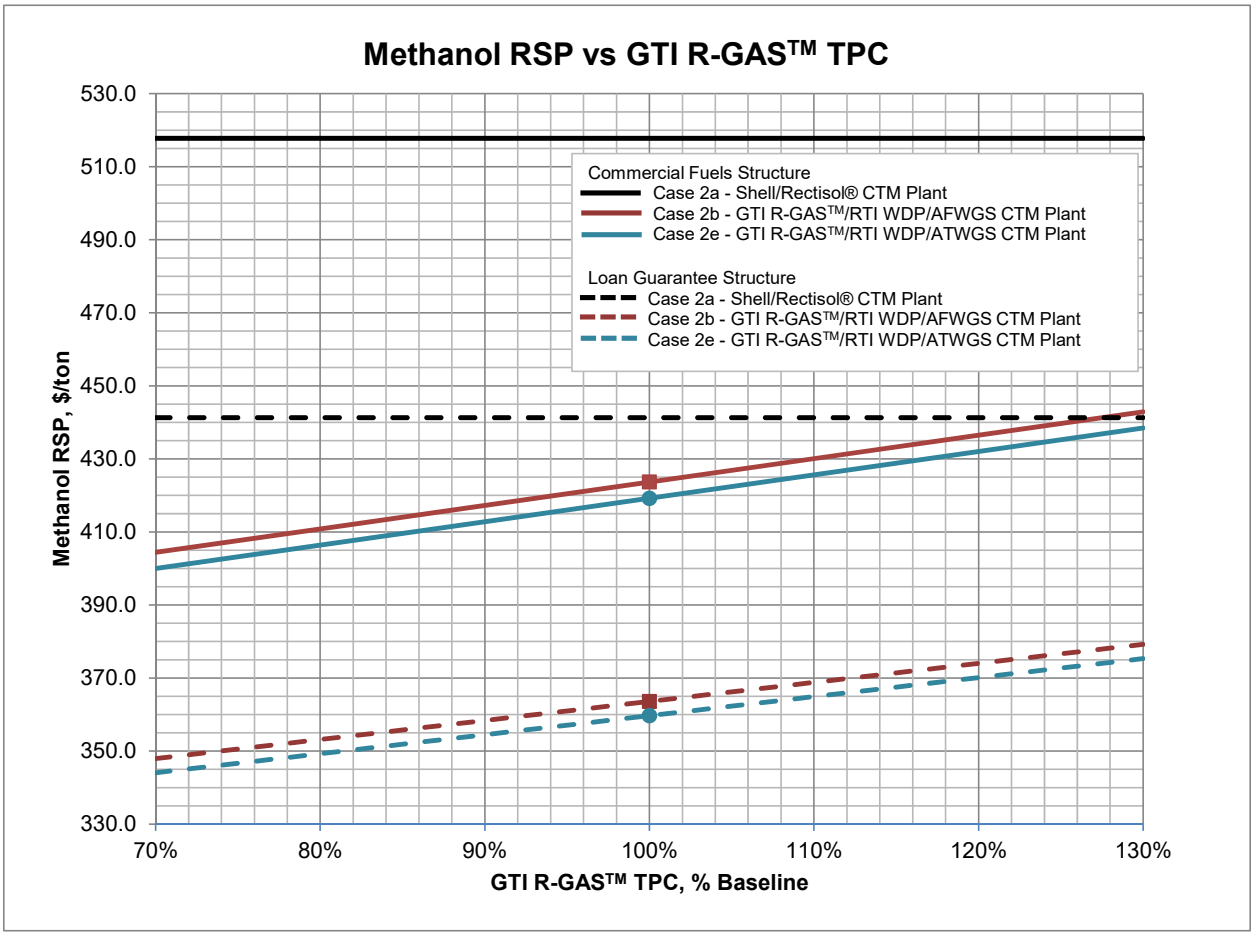

From Figure 11-1, it is shown that at the high end of the GTI R-GAS™ TPC (+30%), the methanol RSPs for Cases 2b and 2e are still less than the methanol RSP for the Case 2a reference plant.

Under the commercial fuels financing structure, every 1.6% increase in DSP and gasifier TPC, equivalent to about $12MM, increases the methanol RSP by $1/ton. Under the loan guarantee financing structure, every 1.9% increase in DSP and gasifier TPC, equivalent to about $14.5MM, increases the methanol RSP by $1/ton.

11.2 RTI WDP SYSTEM COST

Figure 11-2 shows how methanol RSPs for Case 2b and 2e change as the RTI WDP system TPC varies from -30% to +30%. The RTI WDP system TPC includes the costs for the RTI WDP process, DSRP, AFWGS/ATWGS and AACRP process. For reference purposes, the Case 2a reference plant methanol RSPs at $517.8/ton for the commercial fuels and $441.3/ton for the loan guarantee finance structures are shown in Figure 11-2 as well.

Figure 11-2
Sensitivity Analysis – RSP vs RTI WDP TPC

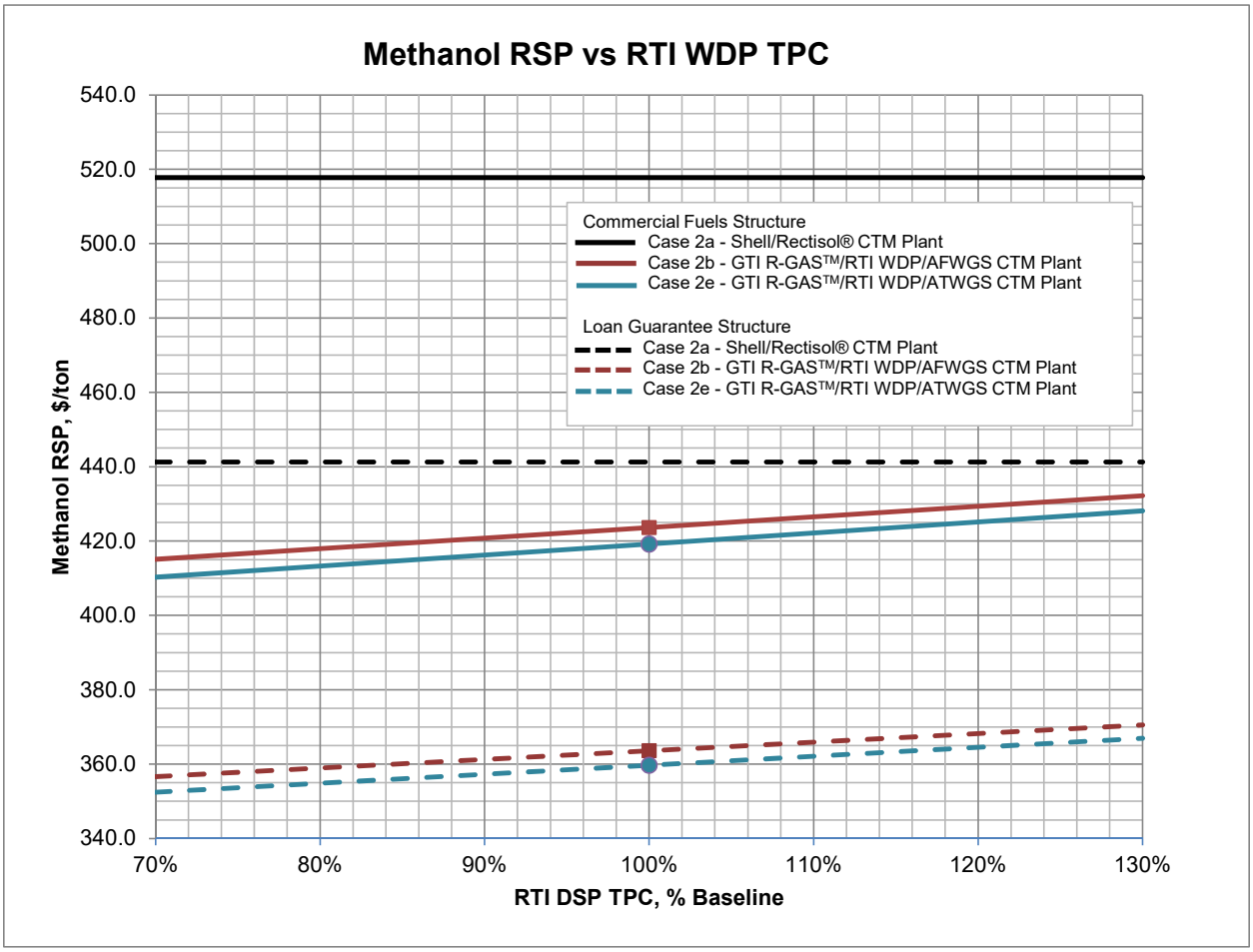

From Figure 11-2, it can be seen that at the high end of the RTI WDP TPC (+30%), the methanol RSPs for Cases 2b and 2e are still less than the RSP for the reference Case 2a CTM plant.

Under the commercial fuels financing structure, every 3.5% increase in RTI WDP TPC, equivalent to about $12MM, increases the methanol RSP by $1/ton. Under the loan guarantee financing structure, every 4.3% increase in RTI WDP TPC, equivalent to about $14.5MM, increases the methanol RSP by $1/ton.

11.3 ATWGSAWGS TPC

Figure 11-3 shows how the Case 2e methanol RSP changes with respect to just the ATWGS TPC as it varies from -30% to +30%. For reference purposes, the Case 2a and 2b methanol RSPs at ($517.8/ton and $423.7/ton respectively) for the commercial fuels and ($441.3/ton and $363.6 respectively) for the loan guarantee finance structures are shown in Figure 11-3.

Figure 11-3
Sensitivity Analysis – COE vs RTI ATWGS System Cost

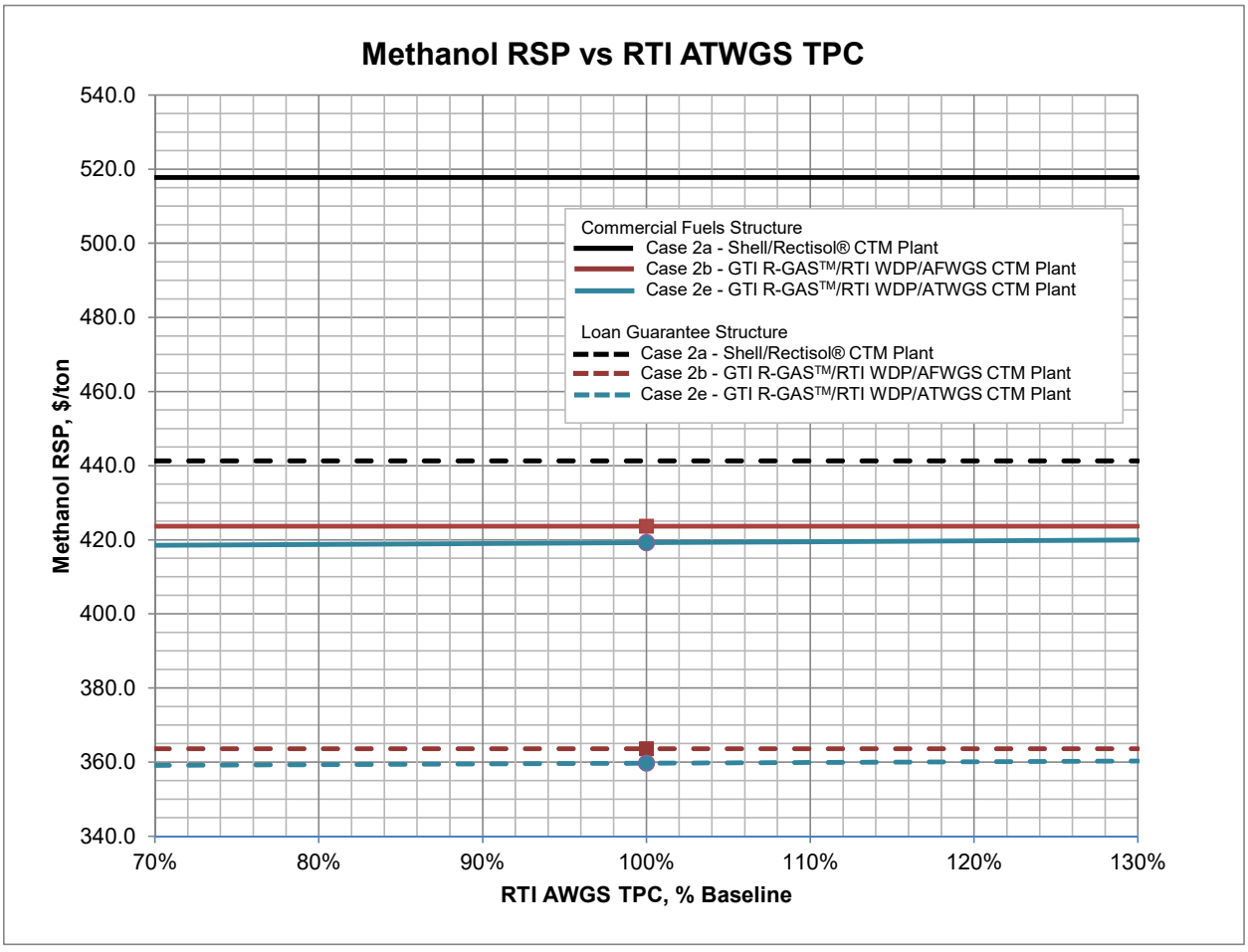

Figure 11-3 shows that at the high-end (+30% of baseline) of the ATWGS TPC, its RSP ($419.9/ton and $360.3/ton for the commercial fuels and loan guarantee finance structures respectively) varies little from the baseline and is still less than the Case 2a and Case 2b

methanol RSPs. This is because the ATWGS TPC makes up only a small fraction of the total CAPEX and variation to its cost does not affect the RSP to a large extent.

11.4 ATWGS CATALYST COST

Figure 11-4 shows how the Case 2e methanol RSP changes with respect to the ATWGS catalyst cost as it varies from -50% to +50%. Also shown in Figure 11-4 are the Case 2a and 2b methanol RSPs for reference.

Like the ATWGS TPC, Figure 11-4 shows that at the high-end (+50% of baseline) of the ATWGS catalyst cost, its methanol RSP is little changed from the baseline and still lower than the Case 2a and Case 2b RSPs.

Figure 11-4
Sensitivity Analysis – COE vs RTI ATWGS Catalyst Cost

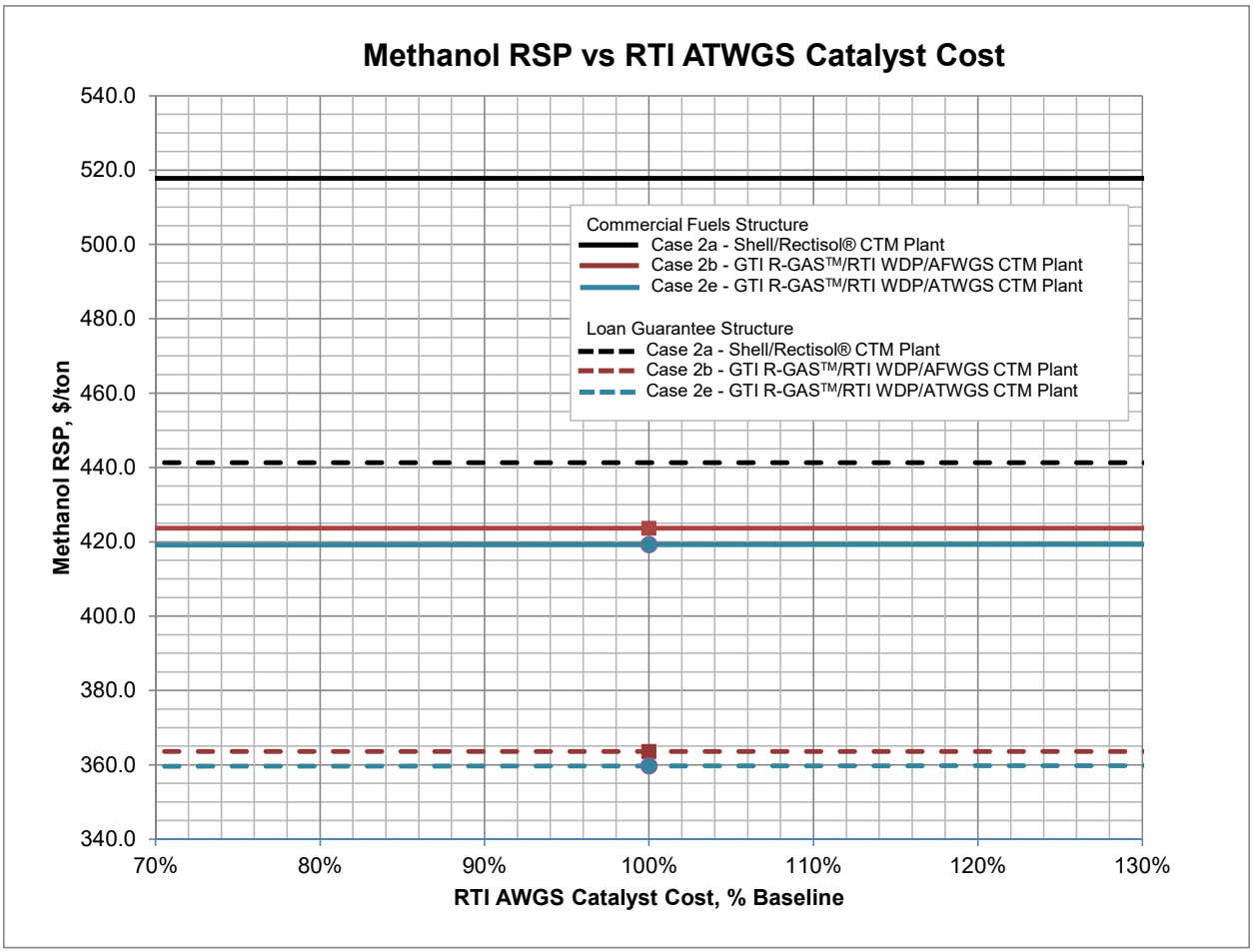

11.5 CAPACITY FACTOR

The baseline CTM plant CF used in this study is 90%. Figure 11-5 shows how the methanol product RSP varies with plant CF as it varies from 70% to 100%.

Figure 11-5
Sensitivity Analysis – RSP vs CTM Plant Capacity Factor

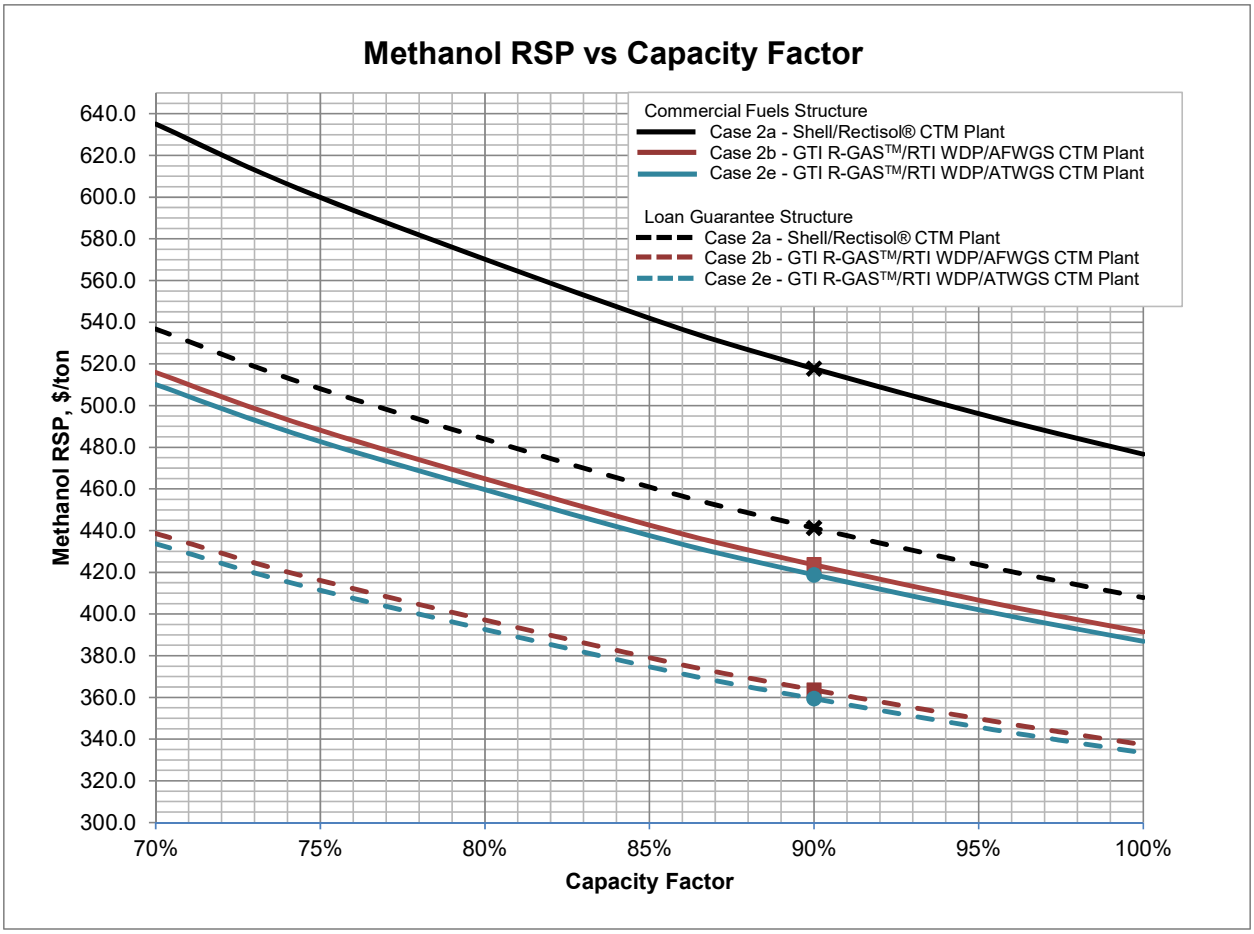

11.6 COAL PRICE

The PRB coal feedstock price used in this study was $36.57/ton, which was specified in the *QGESS Fuel Prices for Selected Feedstocks in NETL Studies* document. Figure 11-6 shows how the methanol RSP varies as the coal price is varied from $10/ton to $60/ton.

For Case 2a, the methanol RSP increases by $1/ton for every $0.56/ton increase in coal price under both the commercial fuels and loan guarantee financing structures.

For the GTI R-GAS™ cases (2b and 2e), the methanol RSPs also increase at about the same rate with increases in coal prices. However, the RSPs are less sensitive to coal pricing than the Shell gasifier cases since the R-GAS™ gasifier has a higher cold gas efficiency and uses less coal to produce the same amount of methanol. In both the commercial fuels and loan guarantee financing structures, the methanol RSP for the Cases 2b and 2e increase by $1/ton for every $0.59/ton increase in coal price.

Figure 11-6
Sensitivity Analysis – RSP vs Coal Feedstock Price

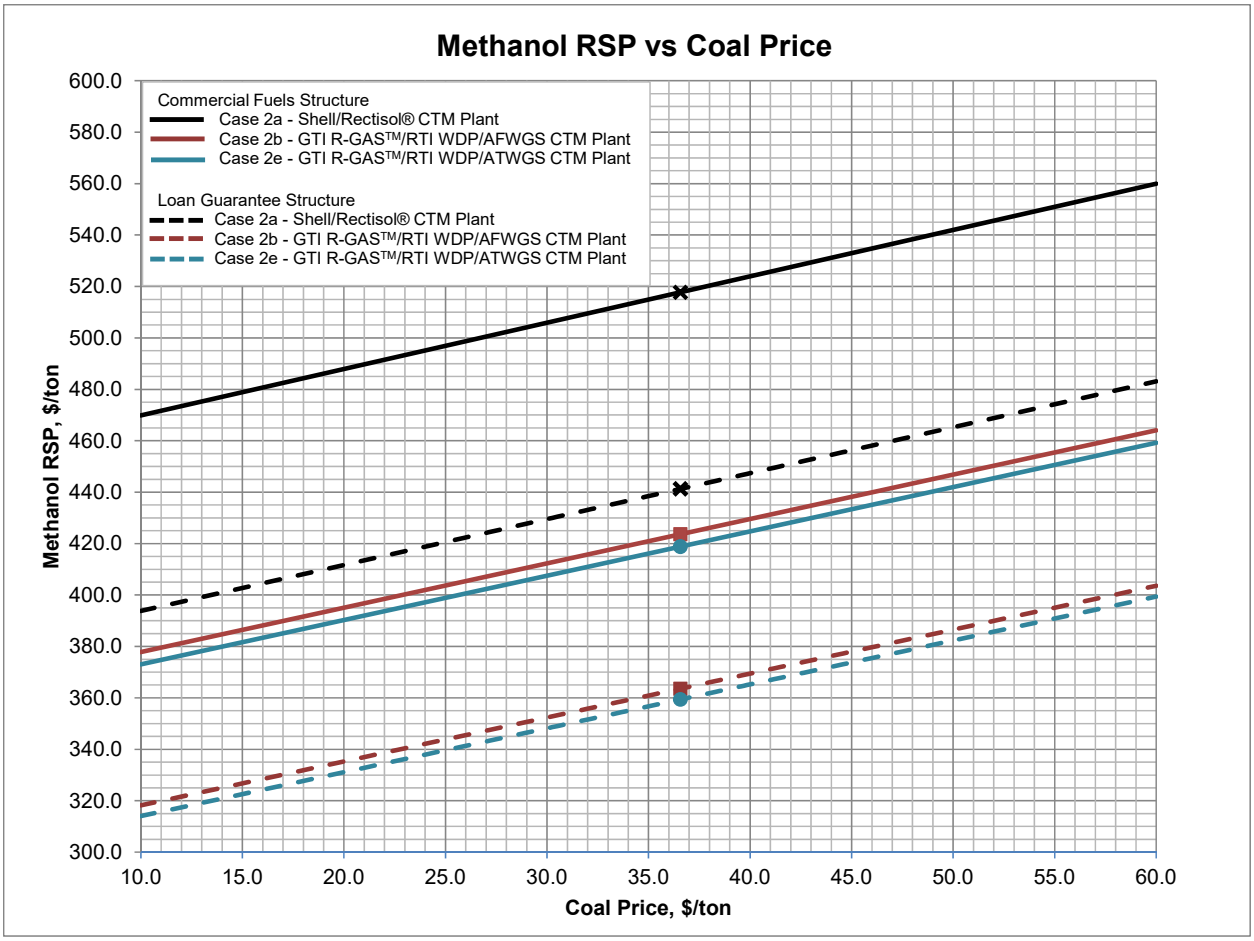

11.7 NATURAL GAS PRICE

Natural gas is used in all cases as fuel to produce power via combined cycle to meet the CTM plant's auxiliary demands. For Case 2a, it is also used as supplemental fuel to be fired in the coal dryer to dry the as-received coal down to 6% moisture. The natural gas feedstock price used in this study was $6.13/MMBtu, which was specified in the *QGESS Fuel Prices for Selected Feedstocks in NETL Studi*es document. Figure 11-7 shows how the methanol RSP varies with natural gas price as it varies from $1/MMBtu to $14/MMBtu.

For Case 2a, under both commercial fuels and loan guarantee financing structures, the methanol RSP increases by $1/ton for every $0.28/MMBtu increase in natural gas price.

Cases 2b and 2e generate 99% of the methanol generated by Case 2a, but consume about 9% less natural gas. This reduction in natural gas consumption comes from the fact that the R-GAS™ gasifier syngas has a higher methane content, which increases the heat content of the purge gas from the methanol process. With a higher heat content, this purge gas eliminates the need for supplemental natural gas for the coal drying process and reduces natural gas consumption in the NGCC.

Under both the commercial fuels and loan guarantee financing structures, the methanol RSP for Cases 2b and 2e increase by $1/ton for every $0.31/MMBtu increase in natural gas price.

Figure 11-7
Sensitivity Analysis – RSP vs Natural Gas Feedstock Price

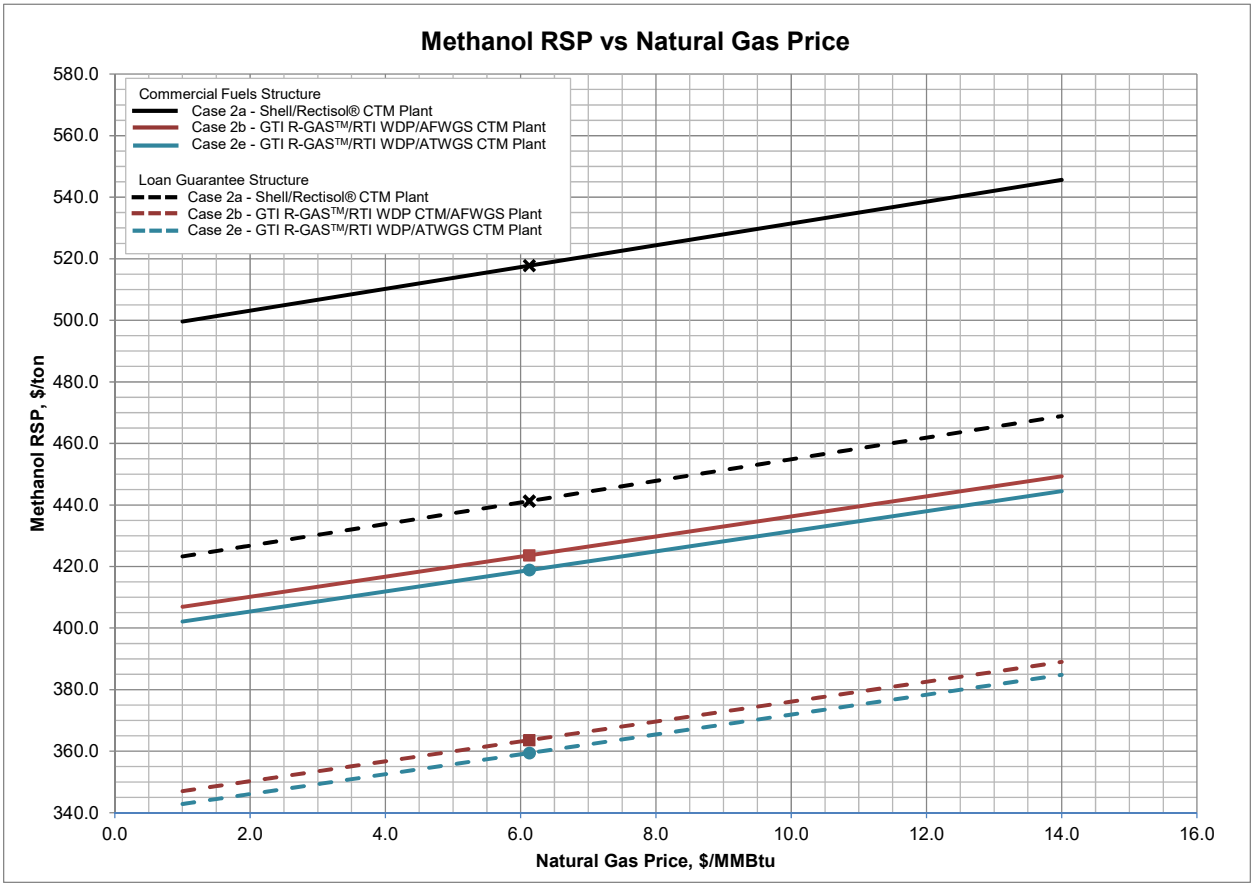

11.8 ELECTRICITY PRICE

The combustion of natural gas in the combustion turbine, combined with heat recovery in the HRSG and WHR in the CTM plant from the exothermic methanol synthesis reaction and other processes, result in a substantial amount of excess electricity being generated in Cases 2b and 2e. The revenue derived from the sale of this excess electricity is applied to the cash flow and results in a lower RSP. The sensitivity of the RSP to the selling price of electricity is shown in Figure 11-8.

The electricity selling price used in this study was $59.59/MWh. While the excess power can be sold to the grid, the sale may be at a steep discount as entities that are negotiating a power purchase agreement will know the power production is an inherent by-product of core methanol production operations. Consequently, the actual achieved transfer price for excess power would be highly project-dependent. A range of $0 - $120/MWh is used in this sensitivity analysis.

Figure 11-8
Sensitivity Analysis – RSP vs Electricity Price

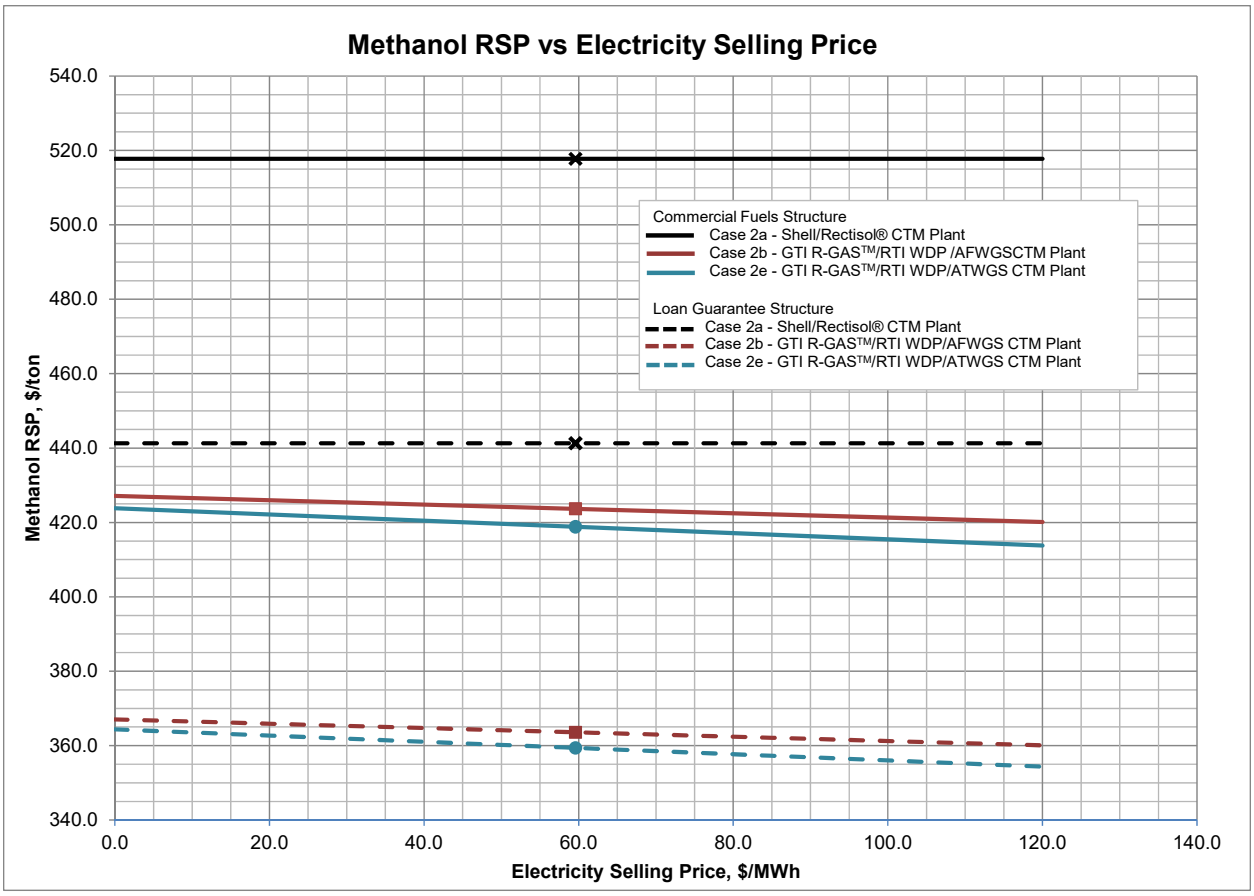

For the Case 2a reference plant, there is a net import power of just 0.8 MW. This plant effectively operates as a power-neutral plant and is considered to have no dependency on electricity prices.

For the Case 2b CTM plant exporting 26.9 MW, every $17/MWh increment in electricity selling price decreases the RSP by $1/ton.

Due to the ATWGS' lower shift steam consumption rate and better utilization of process heat, the Case 2e plant has the highest net power export (38.7 MW). Its methanol RSP also has the greatest dependency on electricity selling price. For both the commercial fuels and loan guarantee financing structures, every $11/MWh increment in electricity selling price decreases the RSP by $1/ton

It should be noted that in the least advantageous scenario where the electricity selling price is $0/MWh i.e. no revenue is derived from power export to the grid, the methanol RSPs for Case 2e is still lower than the Case 2b. In other words, the CTM plant utilizing RTI's ATWGS system still performs better than the case with fixed-bed sweet shift reactors even when the excess power generated has no value.

11.9 CO_2 SALES PRICE

Options for carbon sequestration include both storage in a saline reservoir and usage in enhanced oil recovery (EOR). The impact of selling the captured CO_2 for EOR or other uses at various plant gate sales price, ranging from $0-$60/tonne, is shown in Figure 11-9.

Figure 11-9
Sensitivity Analysis – RSP vs CO_2 Sales Price

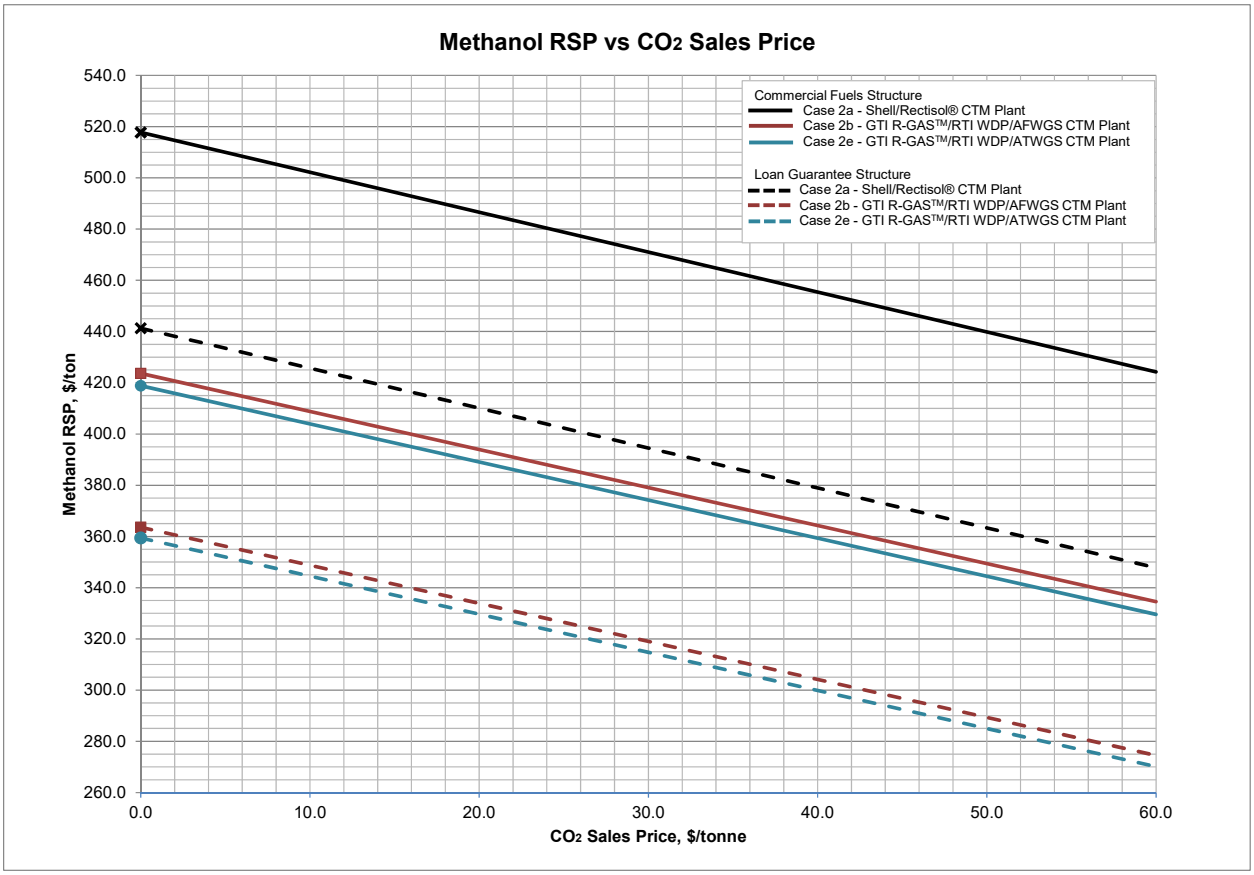

Due to the different rate of CO_2 capture between the Case 2a Rectisol® AGR CTM plants (92.2%) and RTI WDP (93.4% CO_2 capture for Case 2b and 93.5% CO_2 capture for Case 2e), the slopes are slightly different for the three cases. The cases with more CO_2 capture (Cases 2b and 2e) have a greater decrease in methanol RSP as CO_2 sales price increases.

11.10 COST OF CO_2 EMISSIONS

The sensitivity to CO_2 emissions costs is shown in Figure 11-10. The baseline case assumes that there are no costs associated with venting CO_2 to the atmosphere ($0/tonne). The cost of CO_2 emissions is subsequently varied to a maximum of $60/tonne to determine its effect on methanol RSP.

Figure 11-10
Sensitivity Analysis – RSP vs Cost of CO_2 Emissions

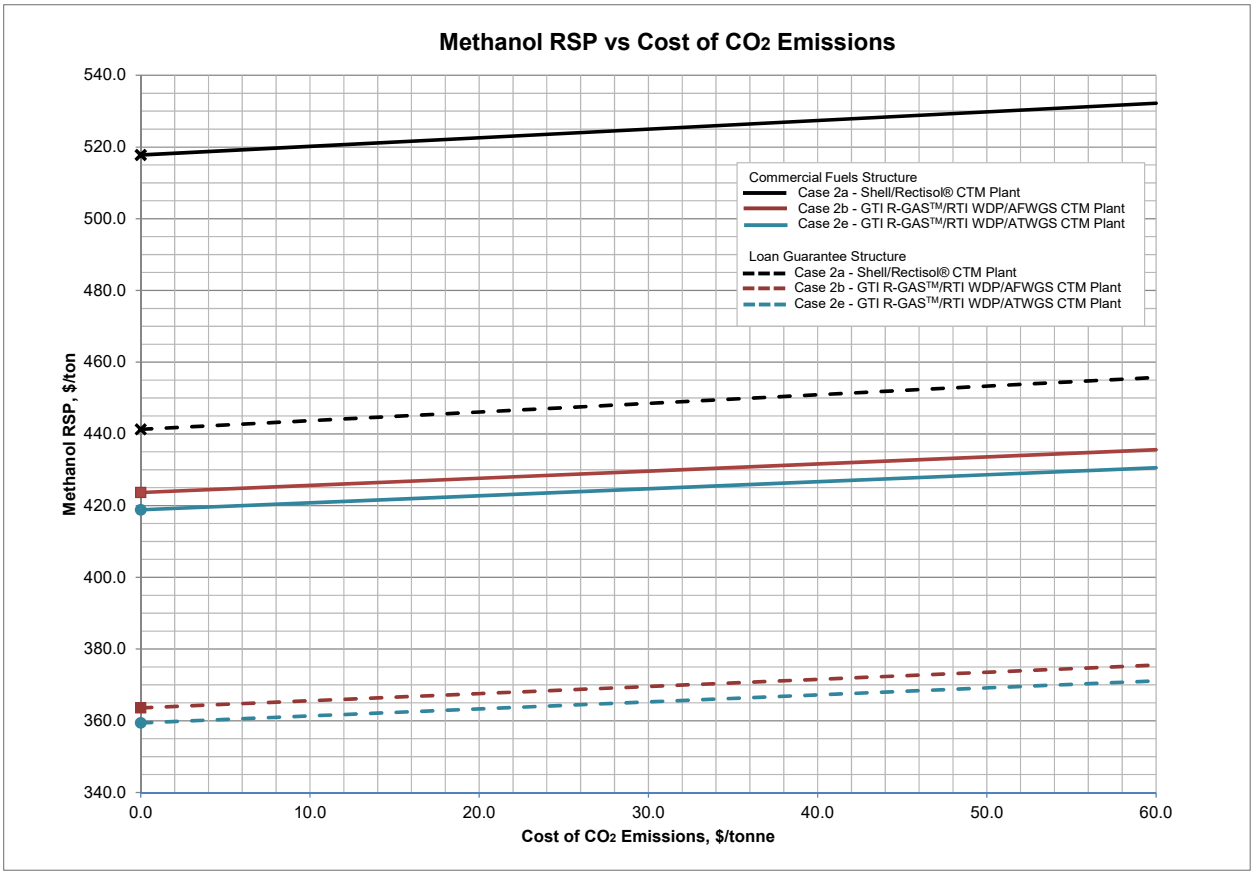

Per the same explanation in Section 11.9, the slopes are slightly different for the three cases due to the different rate of CO_2 capture, hence different CO_2 emissions rate. The cases with more CO_2 capture vent less CO_2 to the atmosphere, so they have a smaller increase in methanol RSP as cost of CO_2 emissions increases.

11.11 CAPITAL CHARGE FACTOR

Two financial structures were assumed for calculating methanol RSPs in this study as described in Section 7.14.1. These structures are based on typical values for fuel projects with and without loan guarantees or government subsidies. The assumed values were used in the PSFM to establish the CCF, which is the portion of the TOC to include in the annual cost of producing a product, for each financial structure. The sensitivity of the methanol RSP to the CCF is illustrated in Figure 11-11. The methanol RSP values were calculated for CCFs ranging from 0.10 to 0.35. The lines denoting CCFs of 0.124 (the value estimated for a high risk investor-owned utility (IOU) project assuming 45 percent debt at 5.5% interest and 55 percent equity and 12% internal rate of return on equity (IRROE)) and 0.35 (the value estimated for 100% equity and 20% IRROE) are also included in the chart.

Figure 11-11
Sensitivity Analysis – RSP vs CCF

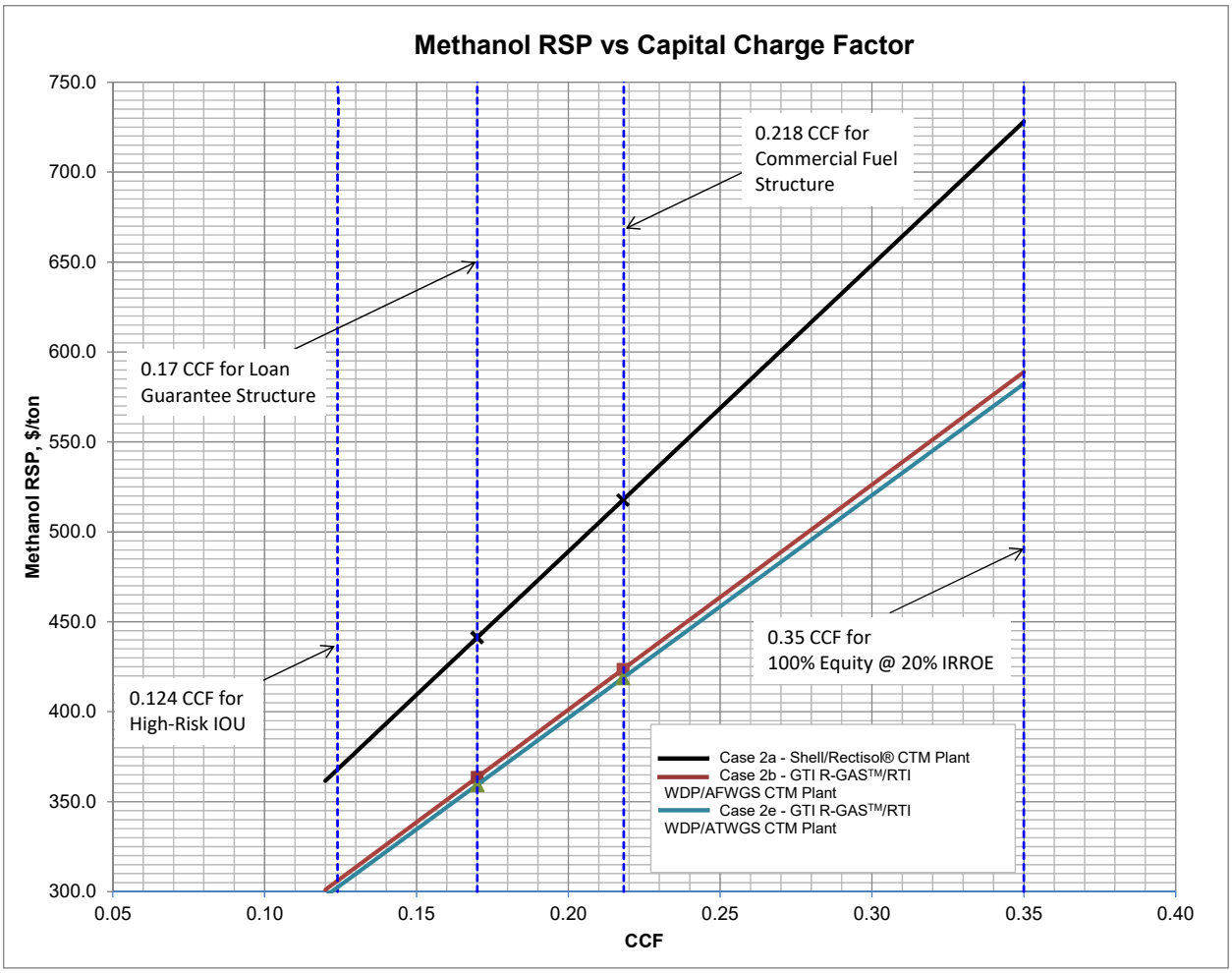

Section 12 Conclusions and Recommendations

12.1 STUDY OBJECTIVE

The objective of this study was to assess the benefits of integrating RTI's ATWGS technology into the combined GTI R-GAS™ and RTI advanced syngas cleanup process, and evaluate the techno-economic benefits of such an integrated process for (1) power production via IGCC and (2) coal-to-liquids (i.e., coal-to-methanol, or CTM) production.

12.1.1 IGCC Cases

The completed IGCC case studies provide a direct comparison of an integrated plant utilizing GTI's R-GAS™, RTI's advanced syngas desulfurization process and ATWGS technologies (Case 1e) with a reference plant using commercially available technologies (Case 1a), and a case from the previous DE-FE0012066 that also utilizes GTI's R-GAS™ gasification and RTI's advanced syngas cleanup process, but with RTI's AFWGS process (Case 1b). All comparison studies conducted for this report capture 90% CO_2 for storage. It should be noted that Case 1e and Case 1b offer a direct comparison of RTI's two different advanced water-gas shift processes (AFWGS and ATWGS). RTI's ATWGS process (Case 1e) consists of a transport reactor, solids cooler and RTI's proprietary fluidized-bed high-temperature water-gas shift catalyst. RTI's AFWGS process uses fixed-bed reactors with commercial high-temperature shift catalyst in a combination that minimizes steam consumption and capital cost for the water-gas shift reaction, while meeting catalyst manufacturer's steam to CO recommendations. Both RTI's advanced water-gas shift processes result in a reduction of steam consumption for the WGS process, which increases the overall process thermal efficiency. It should also be noted that since Case 1b incorporated RTI's AFWGS process, the full benefit of RTI's ATWGS compared with conventional WGS technologies is not determinable from just the comparison of these two cases but it should be greater than the incremental improvements indicated by this comparison. A follow-up study to compare the full benefits of RTI's ATWGS compared with conventional WGS technologies is recommended.

The specific technologies included in each of the three IGCC configurations are identified in the IGCC case study matrix shown in Table 12-1.

Table 12-1
IGCC Case Studies

Case Name for Current Study	Case 1a	Case 1b	Case 1e
Gasification Technology			
Shell Gasification with Lockhopper-Based Feed System	✓		
GTI R-GAS™ Gasifier with Dry Solids Pump (DSP) Feed System		✓	✓
Gas Cleanup[2]			
Two-Stage Selexol™ for CO_2 and Sulfur Removal	✓		
RTI WDP with AACRP		✓	✓
Water-Gas Shift			
Sour Shift	✓		
RTI AFWGS		✓	
RTI ATWGS			✓
GE 7FB Advanced Gas Turbine	✓	✓	✓
CO_2 Drying and Compression (to 2,200 psig)	✓	✓	✓

[1] Reference Case (Case 1a) is Nexant's benchmark simulation of the NETL Report 1399 Case S1B

[2] Selexol™ removes H_2S and CO_2. Additional trace contaminant cleanup technologies will be included as defined by DOE/NETL baseline studies

Reference case from previous DE-FE0012066 study

Best performing case from previous DE-FE0012066 study

Case of interest in this study

12.1.2 CTM Plant Cases

Similar to the IGCC case studies, the CTM cases compare an integrated plant utilizing GTI's R-GAS™, RTI's advanced syngas cleanup process and ATWGS technologies (Case 2e) with a reference plant using commercially available technologies (Case 2a), and a case from DE-FE0012066 that also utilizes GTI's R-GAS™ gasification and RTI's advanced syngas cleanup process, but with RTI's AFWGS process. As with the IGCC case studies, it should be noted that Case 2e and Case 2b offer a direct comparison of RTI's two different advanced water-gas shift processes (AFWGS and ATWGS) for CTM. RTI's ATWGS process (Case 1e) consists of a transport reactor, solids cooler and RTI's proprietary fluidized-bed high-temperature water-gas shift catalyst. RTI's AFWGS process uses fixed-bed reactors with commercial high-temperature shift catalyst in a combination that minimizes steam consumption and capital cost for the water-gas shift reaction, while meeting catalyst manufacturer's steam to CO recommendations. Both RTI's advanced water-gas shift processes result in a reduction of steam consumption for the WGS process, which increases the overall process thermal efficiency. It should also be noted that since Case 2b incorporated RTI's AFWGS process, the full benefit of RTI's ATWGS compared with conventional WGS technologies is not determinable from just the comparison of these two cases, but it should be greater than the incremental improvements indicated by this comparison. A follow-up study to compare the full benefits of RTI's ATWGS compared with conventional WGS technologies is recommended.

The specific technologies included in each of the three CTM plant configurations are identified in the case study matrix shown in Table 12-2.

Table 12-2
CTM Plant Case Studies

Case Name for Current Study	Case 2a	Case 2b	Case 2e
Gasification Technology			
Shell Gasification with Lockhopper-Based Feed System	✓		
GTI R-GAS™ Gasifier with DSP Feed System		✓	✓
Gas Cleanup[2]			
Rectisol® for CO_2 and Sulfur Removal	✓		
RTI WDP with AACRP		✓	✓
Water-Gas Shift			
Sour Shift	✓		
RTI AFWGS		✓	
RTI ATWGS			✓
Methanol Production	✓	✓	✓
NGCC Power Generation with Fluor Econamine CO_2 Capture	✓	✓	✓
CO_2 Drying and Compression (to 2,200 psig)	✓	✓	✓

[1] Reference Case (Case 2a) is Nexant's benchmark simulation of the DOE Crude Methanol Study Case 2

[2] Rectisol® removes H_2S and CO_2. Additional trace contaminant cleanup technologies will be included as defined by DOE/NETL baseline studies

Reference case from previous DE-FE0012066 study

Best performing case from previous DE-FE0012066 study

Case of interest in this study

12.2 IGCC RESULTS SUMMARY

Table 12-3 shows a summary comparison of the CAPEX, OPEX, power production, COE and cost of CO_2 avoided for the three cases.

Table 12-3
IGCC Results Summary

Case	Case 1a	Case 1b	Case 1e
IGCC Configuration			
Gasifier	Shell	GTI R-GAS™	GTI R-GAS™
Sulfur and CO_2 Removal	Selexol™	RTI WDP	RTI WDP
Water-Gas Shift	Sour Shift	AFWGS	ATWGS
CAPEX, $MM			
Total Installed Cost (TIC)	$1,521	$1,242	$1,219
Total Plant Cost (TPC)	$2,030	$1,675	$1,648
Total Overnight Cost (TOC)	$2,487	$2,048	$2,015
OPEX, $MM/yr (100% Capacity Factor Basis)			
Fixed Operating Cost (OC_{fix})	$74.2	$62.8	$61.9
Variable Operating Cost, less Fuel (OC_{var})	$56.9	$49.1	$48.8
Fuel (OC_{fuel})	$50.4	$48.4	$48.4
Total OPEX	$181.5	$160.2	$159.1
Power Production, MWe			
Gas Turbine	430.0	429.9	429.9
Steam Turbine	224.1	211.3	215.5
Auxiliary Power Consumption	193.4	178.7	178.5
Net Power Output	460.6	462.5	466.9
Emissions			
SO_2 Emissions (lb/MWh_{gross})	0.0063	0.0013	0.0013
SO_2 Emissions (lb/MMBtu)	0.0008	0.0002	0.0002
Fuel Rate and Efficiency			
Coal Feed Rate, tpd AR Coal	7,032	6,752	6,752
Net Efficiency, %	31.32%	32.75%	33.06%
Power Generated, MWh/yr (MWH)	4,034,901	4,051,626	4,089,934
TOC CAPEX, $/kW	**5,400**	**4,428**	**4,316**
Total OPEX, $/MWh	**44.97**	**39.55**	**38.91**
COE, excl CO_2 TS&M, mills/kWh	**145.3**	**122.0**	**119.2**
COE, incl CO_2 TS&M, mills/kWh	**166.2**	**142.0**	**139.1**
Cost of CO_2 Avoided excl CO_2 TS&M, $/ton CO_2	**79.7**	**51.0**	**47.7**
Cost of CO_2 Avoided incl CO_2 TS&M, $/ton CO_2	**105.0**	**75.1**	**71.5**

The primary conclusion is that the GTI R-GAS™ with RTI WDP and ATWGS IGCC case (Case 1e), which includes GTI R-GAS™ with RTI's WDP and ATWGS and AACRP, offers the best overall performance in cost, thermal efficiency, and emissions of sulfur and CO_2 for all IGCC cases in this study as well as the previous DE-FE0012066 study. With the best overall performance, the GTI R-GAS™ with RTI WDP and ATWGS IGCC case (Case 1e) offers the lowest values for:

- CAPEX: $2,015 MM [TOC]
- OPEX: $159.1 MM
- COE: 119.2 mills/kWh
- Auxiliary load: 178.5 MWe
- Sulfur emission: 0.0013 lb/MWh (gross)
- Cost of CO_2 avoided: $47.7/ ton CO_2 ,

and the highest values for:

- Net power: 466.9 MWe
- Thermal efficiency 33.06%.

One of the objectives of this study was to evaluate the impact of integrating RTI's ATWGS process with the other advanced technologies. Because of the steam requirements for the water-gas shift reaction as well as the requirement to recover as much of the reaction heat from the WGS reaction as possible to maximize thermal efficiency, an effective evaluation of the WGS process must include both the WGS reactors and the low temperature heat recovery and syngas saturation systems. It was for this reason that the two subaccounts 4.4 and 5A.4 were incorporated into a single subaccount 5A.4a for this study.

An examination of subaccount 5A.4a reveals that the overall WGS process for ATWGS (Case 1e) has a TPC of $49.7 MM compared with $66.2 MM for GTI R-GAS™ with RTI WDP and AFWGS IGCC case (Case 1b). This is a difference of $16.5 MM, which represents a 25% further reduction in TPC. The TPC for the overall WGS process for the reference conventional case (Case 1a) was $95.0 MM. This higher value reflects an overall increase in the amount of equipment for the reference case compared to RTI's two advanced WGS processes. This extra equipment includes more reactors, heat exchangers and a more complex quench system.

One of the additional benefits of RTI's ATWGS process is lower steam consumption for the WGS reaction, due to its lower operating temperature. This results in a higher overall process thermal efficiency as demonstrated by the 4 MWe (1.96%) increase in steam turbine output compared to Case 1b. A similar comparison with the reference case is more challenging as steam generated by the gasification system is relatively large and a consequence of the difference in cold gas efficiencies of the Shell and GTI R-GAS™ systems.

Sensitivity analysis shows that the COE benefit for RTI's ATWGS technology still exists for a 30% increase in the TPC of the technology and cost of the fluidized-bed catalyst for the ATWGS process.

From conversations with various water-gas shift catalyst manufacturers, RTI has found that the steam to CO ratio used for the WGS reactors in the DOE reference cases are lower than those suggested by the manufacturers. A consequence of this is higher outlet temperatures from the shift reactors. The higher the outlet temperature, the faster the catalyst will deactivate.

Although this study does allow a direct comparison between RTI's AFWGS and ATWGS processes, a direct comparison between these two advanced WGS processes and a commercial WGS process cannot be completed because of the significant differences in the overall IGCC system outside of the WGS process. Based on some internal work that RTI has done to quantify the differences between their advanced WGS processes and commercial WGS processes, RTI has found that their advanced WGS processes can reduce TPC by about 30% and increase net high pressure steam generation by over 40% (40% for AFWGS and 100% by ATWGS). As completing the entire TEA for a suitable comparison case with commercial WGS processes was

outside Nexant's current scope of work, it is recommended that a follow-up study be carried out to build this reference case for IGCC and examine it in more detail.

Additionally, as stated in the Technology Analysis Plan (TAP) presented to DOE, one of the goals of this TEA is to characterize separately the impacts of the GTI R-GAS™ gasifier and RTI ATWGS technologies. Table 12-4 summarizes the results of all the IGCC cases studied, which includes Case 1a through 1d from the prior DE-FE0012066 study, and Case 1e from this study, and provides some insight into the relative impacts of the GTI and RTI technologies.

Table 12-4
Impact of GTI R-GAS™ and RTI ATWGS Technologies on IGCC

Case	Case 1a	Case 1b	Case 1c	Case 1d	Case 1e
IGCC Configuration					
Gasifier	Shell	GTI	GTI	Shell	GTI
Sulfur and CO_2 Removal	Selexol™	RTI WDP	Selexol™	RTI WDP	RTI WDP
Shift Reactors	Sour FBR	AFWGS	Sour FBR	AFWGS	ATWGS
Plant Parameters					
Steam Turbine output (MWe)	224.1	211.3	209.3	226.4	215.5
Efficiency, % HHV	31.32%	32.75%	32.70%	31.53%	33.06%
Capital Cost (TOC), $/kW	5,400	4,428	4,709	5,054	4,316
COE, mills/kWh	145.3	122.0	128.3	137.3	119.2
Relative Impact					
Case comparison basis		**1b vs. 1c**	**1c vs. 1a**	**1d vs. 1a**	**1e vs. 1b**
Steam Turbine output (MWe)		+2.0 (1.0%)	-14.8 (-6.6%)	+2.3 (1.0%)	+4.2 (+2.0%)
Efficiency, % HHV			+1.38% pt		+0.31% pt
Capital Cost (TOC), $/kW			-691 (12.8%)		-112 (2.5%)
COE, mills/kWh			-17.0 (11.7%)		-2.8 (2.3%)

The GTI gasifier technology offers favorable impacts on all plant parameters relative to the DOE Reference design configuration of Case 1a (i.e., comparing Case 1c with 1a): with 1.38 percentage point increase in plant efficiency, a 12.8% reduction in TOC, and an 11.7% reduction in COE. With respect to comparing the two water-gas shift technologies that RTI offers (ATWGS in Case 1e versus AFWGS in Case 1b), the ATWGS in Case 1e has a slight advantage over that of Case 1b, with an incremental increase in efficiency of 0.31 percentage points and an extra 4.2 MWe from the stream turbine while reducing the capital cost and cost of electricity by 2.5% and 2.3% respectively. RTI's claim of improved thermal efficiency can be seen in Table 12-4 based on increases in steam turbine output between cases with conventional WGS processes and AFWGS/ATWGS (i.e., Case 1b vs. Case 1c, Case 1d vs. Case 1a, and Case 1e vs. Case 1b). It is recommended that a follow-up study to be conducted to investigate it in more detail.

12.3 CTM PLANT RESULTS SUMMARY

Table 12-5 shows a summary comparison of the CAPEX, OPEX, methanol production, plant power import/export, auxiliary power consumption, RSP and cost of CO_2 captured/avoided.

Table 12-5
CTM Results Summary

Case	Case 2a	Case 2b	Case 2e
CTM Configuration			
Gasifier	Shell	GTI	GTI
Sulfur and CO_2 Removal	Rectisol®	RTI WDP	RTI WDP
Shift Reactors	Sour FBR	AFWGS	ATWGS
CAPEX, $MM			
Total Installed Cost (TIC)	$3,581	$2,732	$2,704
Total Plant Cost (TPC)	$4,802	$3,707	$3,675
Total Overnight Cost (TOC)	**$5,892**	**$4,567**	**$4,528**
OPEX, $MM/yr (100% CF Basis)			
Fixed Operating Cost (OC_{fix})	$162.9	$128.0	$126.8
Variable Operating Cost, less Fuel (OC_{var})	$103.9	$95.3	$94.8
Coal Feedstock (OC_{Coal})	$259.2	$244.8	$244.8
Natural Gas Feedstock (OC_{NG})	$85.4	$77.6	$77.6
Power Import/(Export)	$0.4	($14.1)	($20.2)
Total OPEX	**$611.8**	**$531.4**	**$523.8**
Methanol Production, mtpd (100% CF Basis)			
Gross Methanol Production	10,218	10,079	10,085
Rectisol® Methanol Makeup	8	0	0
Net Methanol Production	**10,210**	**10,079**	**10,085**
NGCC Plant Power Generation, MWe			
Gas Turbine	127.1	127.9	127.9
Steam Turbine	264.7	239.2	248.7
Total Power Generation	**391.8**	**367.1**	**376.7**
Auxiliary Consumption, MWe			
Process Plant			
Coal Handling and Drying	17.4	16.4	16.5
Gasification and ASU	185.3	163.6	163.6
Process AGR	42.5	42.6	42.6
Process CO_2 Compression	65.2	64.8	64.9
Methanol Synthesis	27.3	4.7	4.7
Process Plant BOP	22.5	20.5	20.0
Total Process Plant Auxiliary Consumption	*360.2*	*312.5*	*312.2*
NGCC Plant			
NGCC Auxiliary Consumption	22.4	23.5	21.7
NGCC PCC	3.9	4.1	4.1
NGCC PCC CO_2 Compression	6.0	w/Process	w/Process
Total NGCC Auxiliary Consumption	*32.3*	*27.6*	*25.8*
Total Auxiliary Consumption	**392.6**	**340.1**	**338.0**
Net Power Generation/(Consumption)	**(0.8)**	**26.9**	**38.7**
Fuel Rate and Efficiency			
Coal Feed Rate, tpd AR Coal	19,418	18,339	18,339
Natural Gas Feed Rate, MMBtu/day	38,152	34,675	34,675
Total Thermal Input In (LHV), MMBtu/day	354,934	333,984	333,984
Methanol Fuel Thermal Output (LHV), MMBtu/day	188,547	185,730	185,717
Power Output, MMBtu/day	(63)	2,207	3,170
Thermal Efficiency (LHV), %	**53.1%**	**56.3%**	**56.6%**
CO_2 Capture			
CO_2 Capture Product, tpd	19,413	18,201	18,244
CO_2 Vented, tpd	2,966	2,359	2,319
Carbon Emitted as CO_2, % Carbon in Fuel	7.9%	6.6%	6.5%

Table 12-5 (cont'd)
CTM Results Summary

Case	Case 2a	Case 2b	Case 2e
Methanol RSP			
Methanol RSP, excl CO_2 TS&M, $/short ton[BE]	**424.1 500.6**	**347.3 407.3**	**343.3 402.8**
, incl CO_2 TS&M, $/short ton[BE]	**441.3 517.8**	**363.6 423.7**	**359.9 419.2**
RSP Components Details, $/gal			
Capital[B]	0.90 1.15	0.70 0.91	0.70 0.90
Fixed O&M	0.15	0.12	0.12
Variable O&M	0.08	0.08	0.08
Coal	0.21	0.20	0.20
Natural Gas	0.07	0.06	0.06
Power	0.00	(0.01)	(0.02)
CO_2 TS&M	0.06	0.05	0.05
Total[B]	**1.46 1.72**	**1.21 1.40**	**1.19 1.39**
Cost of CO_2 Captured, $/tonne CO_2[BC]	**17.2 19.2**	**17.3 19.4**	**17.3 19.4**
Cost of CO_2 Avoided, $/tonne CO_2 [BD]	**28.9 30.2**	**28.3 30.4**	**28.3 30.4**

[A] Capacity factor assumed to be 90 percent
[B] Values shown are for two financial structures
The first (lower value) is based on the loan guarantee finance structure
The second (higher value) is based on the commercial fuels finance structure
[C] Excludes CO_2 TS&M
[D] Includes CO_2 TS&M
[E] Based on 301.73 gallons/short ton (332.6 gallons/metric ton)

Figure 12-1 illustrates the breakdown of the methanol RSP.

Figure 12-1
Components of Methanol RSP

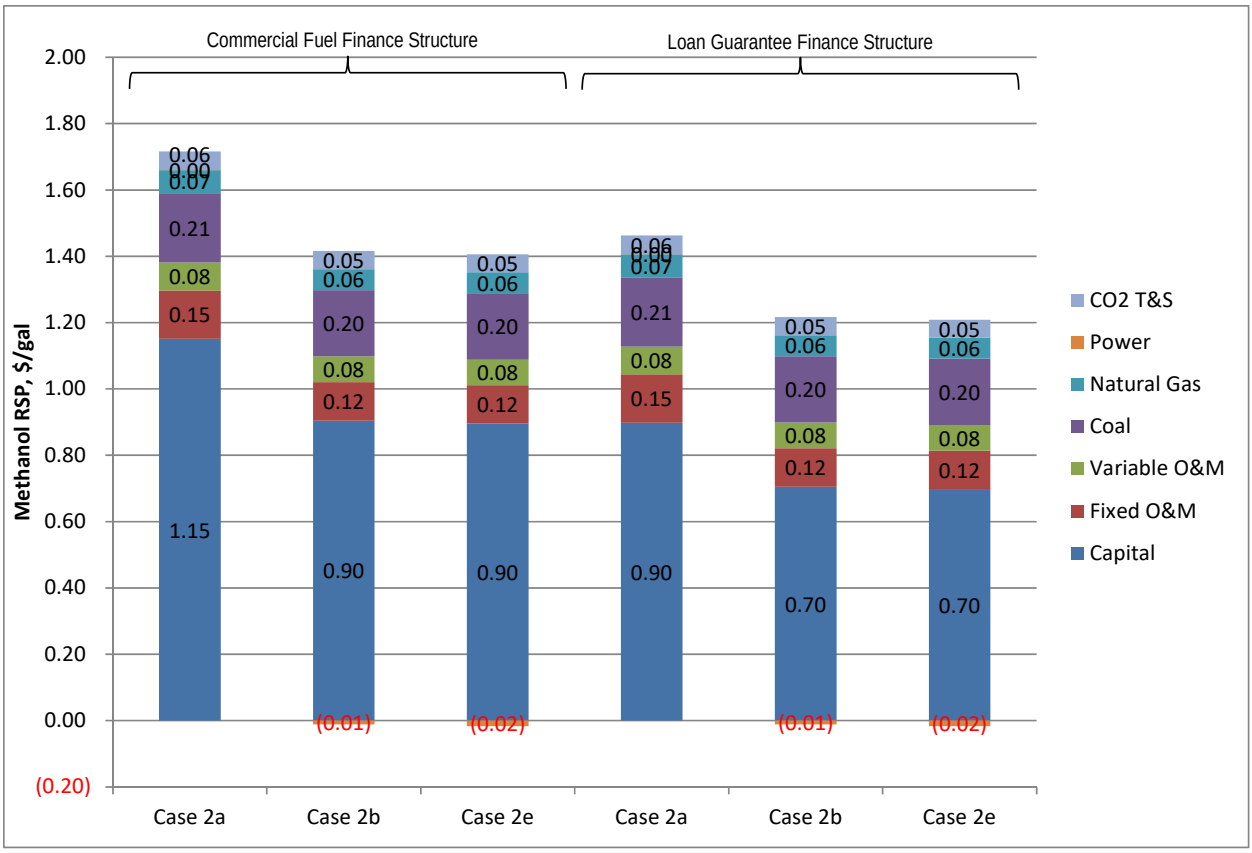

The primary conclusion from this CTM study is similar to that of the IGCC study in that the GTI R-GAS™ with RTI WDP and ATWGS CTM case (Case 2e), which includes GTI R-GAS™ with RTI's WDP and ATWGS and AACRP, offers the best overall performance in cost, thermal efficiency, and emissions of sulfur and CO_2 for all the CTM cases in this study as well as the previous DE-FE0012066 study. With the best overall performance, the GTI R-GAS™ with RTI WDP and ATWGS CTM case (Case 2e) offers the lowest values for:

- CAPEX: $4,528 MM [TOC]
- OPEX: $523.8 MM
- Methanol RSP: $343.3/ton (Loan Guarantee Financial Structure)
- $402.8/ton (Commercial Fuels Finance Structure)
- Auxiliary load: 338.0 MWe
- Sulfur emission: <0.0001 lb SO_2/MMBtu
- CO_2 vented: 2,319 tpd (6.5% of carbon in feedstock)

and the highest values for:

- Net power: 38.7 MWe
- Thermal efficiency 56.6%.

One of the objectives of this study was to evaluate the impact of integrating RTI's ATWGS process with the other advanced technologies. Because of the steam requirements for the water-gas shift reaction as well as the requirement to recover as much as possible the reaction heat from the WGS reaction in order to maximize thermal efficiency, an effective evaluation of the WGS process must include both the WGS reactors and the low temperature heat recovery and syngas saturation systems. It was for this reason that the two subaccounts 4.4 and 5A.4b were incorporated into a single new subaccount 5A.4c for this study.

An examination of subaccount 5A.4c reveals that the overall WGS process for ATWGS (Case 2e) has a TPC of $124.1 MM compared with $149.1 MM for GTI R-GAS™ with RTI WDP and AFWGS CTM case (Case 2b). This is a difference of $25 MM, which represents a 17% reduction in TPC. The TPC for the overall WGS process for the reference CTM case (Case 2a) was $193.7 MM.

One of the additional benefits of RTI's ATWGS process is the lower steam consumption for the WGS reaction since it operates at a lower temperature. All the steam required for the process was supplied by a partial quench of the product syngas from WDP, resulting in a higher process thermal efficiency as demonstrated by the 9.5 MWe (3.97%) increase in steam turbine output higher compared to Case 2b. As with the IGCC study, a similar comparison with the reference case is more challenging as steam generated by the gasification system is relatively large and a consequence of the difference in cold gas efficiencies of the Shell and GTI R-GAS™ systems.

Sensitivity analysis shows that the COE benefit for RTI's ATWGS technology still exists for a 30% increase in the TPC of the technology and cost of the fluidized-bed catalyst for the ATWGS.

As with the IGCC study, while the CMT study also allows a direct comparison between RTI's AFWGS and ATWGS processes, a direct comparison between these two advanced WGS processes and a commercial WGS process cannot be completed because of the significant differences in the overall CTM system outside of the WGS process. It is recommended that a follow-up study be carried out to build this reference case for CTM and examine it in more detail.

Table 12-6 summarizes the results of all the CTM cases studied, including Case 2a through 2d from the prior DE-FE0012066 study, and Case 2e from this study, in order to provide some insight into the relative impacts of the GTI and RTI technologies separately.

Table 12-6
Impact of GTI R-GAS™ and RTI ATWGS Technologies on CTM

Case	Case 2a	Case 2b	Case 2c	Case 2d	Case 2e
CTM Configuration					
Gasifier	Shell	GTI	GTI	Shell	GTI
Sulfur and CO_2 Removal	Rectisol®	RTI WDP	Rectisol®	RTI WDP	RTI WDP
Shift Reactors	Sour FBR	AFWGS	Sour FBR	AFWGS	ATWGS
Plant Parameters					
Steam Turbine output (MWe)	264.7	239.2	199.1	292.8	248.7
Thermal Efficiency, % LHV	53.1%	56.3%	56.5%	52.9%	56.6%
Capital Cost (TOC), $1,000/mtpd	577.1	453.1	476.3	549.3	449.0
Loan Guarantee RSP, $/ton	424.1	347.3	359.5	408.9	343.3
Relative Impact					
Case comparison basis		**2b vs. 2c**	**2c vs. 2a**	**2d vs. 2a**	**2e vs. 2b**
Steam Turbine output (MWe)		+40.1 (20,1%)	-65.6 (-24.8%)	+28.1 (10.6%)	+9.5(4.0%)
Thermal Efficiency, % LHV			+3.4% pt		+0.3% pt
Capital Cost (TOC), $1,000/mtpd			-100.8 (17.5%)		-4.1 (0.9%)
Loan Guarantee RSP, $/ton			-64.6 (15.2%)		-4.0 (1.2%)

As with IGCC, GTI gasifier technology offers favorable impacts on all plant parameters relative to the Case 2a DOE Reference CTM plant configuration (i.e., comparing Case 2c with 2a): with a 3.4 percentage point increase in thermal efficiency, a 17.5% reduction in TOC, and a 15.2% reduction in RSP. When comparing the two RTI advanced WGS processes (ATWGS in Case 2e versus AFWGS in Case 2b), ATWGS in Case 2e increases thermal efficiency by 0.3 percentage points and steam turbine output by 9.5 MWe while reducing the capital cost and RSP by 0.9% and 1.2%, respectively.

As with the IGCC scenario, RTI considers both AFWGS (Case 1b and 2b) and ATWGS (Case 1e and 2e) processes as advanced water-gas shift technologies that can offer significant techno-economic advantages over a conventional WGS process. RTI's claim of improved thermal efficiency can be seen in Table 12-6 based on increases in steam turbine output between cases with conventional WGS processes and AFWGS/ATWGS (i.e., Case 2b vs. Case 2c, Case 2d vs. Case 2a, and Case 2e vs. Case 2b). It is recommended that a follow-up study to be conducted to investigate it in more detail.

TASK 6: QUENCH ZONE SIMULATION FOLLOW-ON WORK

TOPICAL REPORT

Reporting Period

Start Date: July 1, 2016

End Date: September 30, 2016

Principal Author

Andrew Kramer Principal Investigator/Program Manager

September 30, 2016

DOE Award Number

DE-FE0023577 (DOE NETL)

Gas Technology Institute
1700 South Mount Prospect Road
Des Plaines, IL 60018

DISCLAIMER

ABSTRACT

The Gas Technology Institute (GTI) has developed an innovative gasifier concept incorporating advanced technologies in ultra-dense phase dry feed system, rapid mix injector, and advanced component cooling to significantly improve gasifier performance, life, and cost compared to commercially available state-of-the-art systems. A key feature of the GTI gasifier design is the transition from the gasifier outlet into the quench zone, where the raw syngas is cooled to ~ 400°C by injection and vaporization of atomized water. Task 2 of the current project established that suitable similitude could be attained to provide design guidance for the gasifier outlet to avoid build-up of slag, and indicated the follow-on work should be done to better understand jet-jet interaction impacts on quench zone hydrodynamics and overall mixing. Task 6, the current work, offers a detailed assessment of jet-jet interaction between the quench spray and syngas product, of droplet characteristics within the quench spray jets, and of individual droplet interactions within the syngas jet. Analysis determined that the system could best be modelled through scaling of Stokes number for droplet penetration and momentum ratio for jet-jet interactions. Assessment of cold flow model options concluded that a pressurized (~2.5bar) version of the current apparatus provided superior similitude for the study of jet-jet interaction hydrodynamics and overall quench water – syngas mixing than a full scale apparatus, and at lower cost.

TABLE OF CONTENTS

LIST OF FIGURES

LIST OF TABLES

EXECUTIVE SUMMARY

The Gas Technology Institute (GTI) has developed an innovative gasifier concept incorporating advanced technologies in ultra-dense phase dry feed system, rapid mix injector, and advanced component cooling to significantly improve gasifier performance, life, and cost compared to commercially available state-of-the-art systems. A key feature of the GTI gasifier design is the transition from the gasifier outlet into the quench zone, where the raw syngas is cooled to ~ 400°C by injection and vaporization of atomized water. Earlier pilot plant testing revealed a propensity for the original outlet design to accumulate slag in the outlet, leading to erratic syngas flow from the outlet. Subsequent design modifications resolved this issue in the pilot plant gasifier. In order to gain greater insight into the physical phenomena occurring within this zone, GTI developed a cold flow simulation apparatus with Coanda Research & Development with a high degree of similitude to hot fire conditions in the pilot scale gasifier design, and capable of accommodating a scaled-down quench zone for a demonstration-scale gasifier.

A test program assessing hydrodynamics at the gasifier outlet and upper quench zone for both pilot plant designs and a scaled demonstration plant outlet was accomplished under Task 2 of the current project, DE-FE0023577. Task 2 objectives were successfully accomplished, verifying the ability to establish acceptable similitude and providing design guidance for the gasifier outlet to avoid build-up of slag. The test program also indicated other considerations for quench system design that should be considered for a follow-on study, specifically as follows:

- A detailed assessment of jet-jet interactions relevant to an atomized liquid jet and down-flowing gas column. The purpose is to clearly define the physics governing the scale-up of this specific type of jet-jet interaction.
- Using the results from the above assessment, design and fabricate a full scale demonstration gasifier quench zone that is also full length. The purpose of this is twofold – (1) Verify jet-jet interaction dependencies on operating parameters and (2) assess mixing of quench spray within the gas stream to ensure adequate cooling of the syngas before it exits the quench vessel.

A detailed assessment was performed to characterize jet-jet interaction between the quench spray and syngas product, of droplet characteristics within the quench spray jets, and of individual droplet interactions within the syngas jet. Testing of a range of hydraulic spray nozzles established that the droplets behave independently of each other and that they have a range of Stokes numbers, with most of the droplets not instantaneously entrained into the gas stream, and that individual droplet behavior is best modelled on the basis of Stokes number. Analysis of jet-jet interactions led to the conclusion that quench spray jet penetration into the syngas stream is best scaled as a function of quench water/syngas stream momentum ratios.

Given these findings, a number of cold flow simulation apparatus options were evaluated, including a full scale model of a demonstration-scale gasifier quench zone as well as a pressurized system at the scale of the current apparatus. Similitude analysis showed that the pressurized system at current scale gave comparable similitude on momentum ratio to the demonstration scale apparatus, with superior Stokes number similitude, at lower cost. Therefore, it was concluded that a follow-on test program should be performed in a pressurized (~2.5bar) version of the current apparatus to study jet-jet interaction hydrodynamics and overall quench water – syngas mixing.

1.0 INTRODUCTION

1.1 DOCUMENT SCOPE

The purpose of this document is to describe key findings from the quench zone simulation follow-on effort, with emphasis on establishing physically relevant scaling relationships for quench zone hydrodynamics and mixing.

This Topical Report summarizes the effort performed under Task 6: Quench Zone Simulation Follow-on Work as part of contract DE-FE0023577 awarded to Aerojet Rocketdyne, and subsequently novated to the Gas Technology Institute (GTI) by the United States Department of Energy (DOE) – National Energy Technology Laboratory (NETL).

1.2 OBJECTIVES

The Gas Technology Institute is developing an innovative entrained flow gasifier incorporating advanced technology in the dry-feed system, rapid-mix injectors, and component cooling to significantly improve gasifier performance, life, and cost compared to commercially-available state-of-the-art systems. A key feature of the GTI gasifier design is the transition from the gasifier outlet into the quench zone, where the raw syngas is cooled to approximately 400°C by injection and vaporization of atomized water. Early pilot-plant testing revealed a propensity for the original outlet design to accumulate slag in the outlet, leading to asymmetric syngas flow from the outlet. This original design had a cylindrical outlet with water spray nozzles directly underneath the cylinder. Analysis of the test results led to a conical outlet design, with the slag drip-lip recessed back into the gasifier to thermally and hydrodynamically isolate the slag discharge point from the flow and cooling of the quench zone. This conical design was successfully tested in late 2010, and has been incorporated into subsequent pilot plant component designs and is planned for the demonstration-scale gasifier.

Although the current design has been successfully demonstrated over hundreds of hours and multiple feedstocks, there remained uncertainty as to how to scale the design from 18 TPD to approximately 800 TPD. Coanda Research & Development Corporation (CRDC) developed a cold-flow simulation apparatus capable of fully simulating the hydrodynamics and partially simulating the thermodynamics of the pilot plant at full-scale, and the demonstration unit at reduced scale.

The significantly different results from the two different outlet designs in pilot operation provided a unique opportunity to validate the cold flow model for the pilot scale design. The initial testing in 2013 showed clear differences between these two configurations with the cold flow model. On that basis, a program was defined to assess quench zone hydrodynamics over a range of operating parameters and geometries for both pilot plant outlet configurations and a scaled 800 TPD gasifier outlet configuration using the existing facility at Coanda and gasifier designs. The test program was proposed to the United States Department of Energy National Energy Technology Laboratory as Task 2 under DE-FE0023577. Pilot scale testing was performed over a range of geometries and operating variables, using an air/water system, with and without a slag simulant (glycerin).

Results for the pilot scale model, described in the Task 2 Topical Report, demonstrated consistency with observable pilot plant gasifier results. Most notably, the shapes of frozen slag aggregates collected from the bottom of the quench zone were an excellent match to those of the slag simulant drops at the point of detachment from the gasifier exit. The high-speed video recordings provided visualization of interactions between the slag and quench spray, and their effect on slag morphology, and confirmed that excellent hydrodynamic similitude exists between the model and plant. Although the extent of thermodynamic similitude between the model and plant was less satisfactory, the experiments using HA134a as the quench liquid did not show significant differences in gas flow patterns that would imply drastically different behavior with respect to interactions between the slag and quench spray in evaporating flow.

For the scaled demonstration gasifier outlet, the gasifier and outlet components were sized to be installed in the existing pilot-scale quench vessel and provide geometric similitude with the demonstration plant. Demonstration model testing focused on the conical outlet, assessing the impact of key parameters on hydrodynamics. The conditions in the demonstration model were more favorable to liquid ingress into the gasifier outlet. This was deemed to be due to a combination of the larger ratio between the diameter of the reactor and that of the quench vessel, and is also affected by the ratio of gas-to-liquid aggregate momentum. The liquid/gas momentum ratio was varied, and it was determined that, for this geometry, a momentum ratio less than 1.0 avoided quench spray recirculation into the outlet cone. Despite the incursion of liquid into the gasifier outlet cone, experiments did not show contact between the quench spray and simulated slag prior to the latter's disengagement from the drip-lip. Nonetheless, liquid back-flow into the exit cone remains an area of concern for the commercial unit, as the ratio of reactor to quench vessel diameter further increases.

The current study was motivated by concerns regarding the ability to adequately model quench zone hydrodynamics in the demonstration unit at reduced scale. In particular, the parameters governing similitude with respect to penetration of the spray into the syngas jet, mixing behavior, and liquid and syngas kinematics in the demonstration unit are difficult to simultaneously match in the current apparatus. The current work was therefore requested by GTI to improve understanding of momentum exchange between raw syngas and quench spray, prior to proceeding with further cold-flow testing with the demonstration gasifier geometry. The purpose of the study is to assess our current ability to model quench zone hydrodynamic behavior of a demonstration gasifier, evaluate estimated cost and efficacy of alternative options for scaling in cold flow, and recommend a strategy for future testing using the recommended option.

The goal of the current phase of study is to determine an approach for improving similitude of quench zone hydrodynamics of the demonstration gasifier in a cold-flow apparatus, for implementation in a future phase of study. This is achieved through satisfying the following objectives:

1. Re-evaluate quench-zone hydraulic similitude with focus on spray penetration and mixing behavior.
2. Evaluate alternative options for modelling the demonstration gasifier hydrodynamics in cold-flow.
3. Provide an engineering cost estimate of the recommended option from (2).

The options in (2) are evaluated based primarily on their scientific merit. However, a preliminary cost estimate of each option is also provided to inform future decisions.

The effort defined under the contractual Statement of Project Objectives (SOPO) is as follows:

TASK 6 – Quench Zone Simulation Follow-On Work: Coanda Research and Development Corporation will build upon results and conclusions reached under Task 2 by study of slag similitude and the scale up to a commercial unit. This Task 6 work is a follow-on enhancement of subtask 2.2, "Demonstration Scale Model". Task 6 includes considerations for quench system design as specified in the following subtasks:

- Subtask 6.1 – Assessment of Jet-Jet Interactions: A detailed assessment of jet-jet interactions relevant to an atomized liquid jet and down-flowing gas column. The purpose is to clearly define the physics governing the scale-up of this specific type of jet-jet interaction.
- Subtask 6.2 – Design/Estimate Costs of Full Scale Demonstration Gasifier Quench Zone Model: Using the results from the above assessment, design and estimate the costs of fabricating a full scale demonstration gasifier quench zone that is also full length to, (1) Verify jet-jet interaction dependencies on operating parameters and, (2) assess the mixing of quench spray within the gas stream to ensure adequate cooling of the syngas before it exits the quench vessel.

This Topical Report discusses the results accomplished under Task 6 of DE-FE0023577.

1.3 ABBREVIATIONS & ACRONYMS

AGWGST	Advanced Gasifier & Water Gas Shift Technologies
CRDC	Coanda Research & Development Corporation
C_d	Drag Coefficient
DOE	Department of Energy
GTI	Gas Technology Institute
NETL	National Energy Technology Laboratory
TPD	Tons Per Day
PDI	Phased Doppler Interferometry
Re	Reynolds Number
SOPO	Statement of Project Objectives
Sk	Stokes Number

2.0 EXPERIMENTAL METHODS

2.1 SIMILITUDE ANALYSIS

Physical modeling is a means to simulate a given system using another system exhibiting similar flow characteristics. The degree to which the model reflects reality is determined by similitude, the degree to which the two systems are equivalent. There are three types of similitude:

(1) Geometric – where the model and actual systems have the same shape

(2) Kinematic – where the model and actual systems have the same flow patterns

(3) Dynamic – where the model and actual systems have the same ratio of forces

In many instances, a high degree of similitude can be established for specific phenomena of interest. For example, Figure 1 shows good similitude is established between a simple inclined flat plate measuring a few inches in length and the plume of oil dispersing from a grounded tanker several hundred feet long.

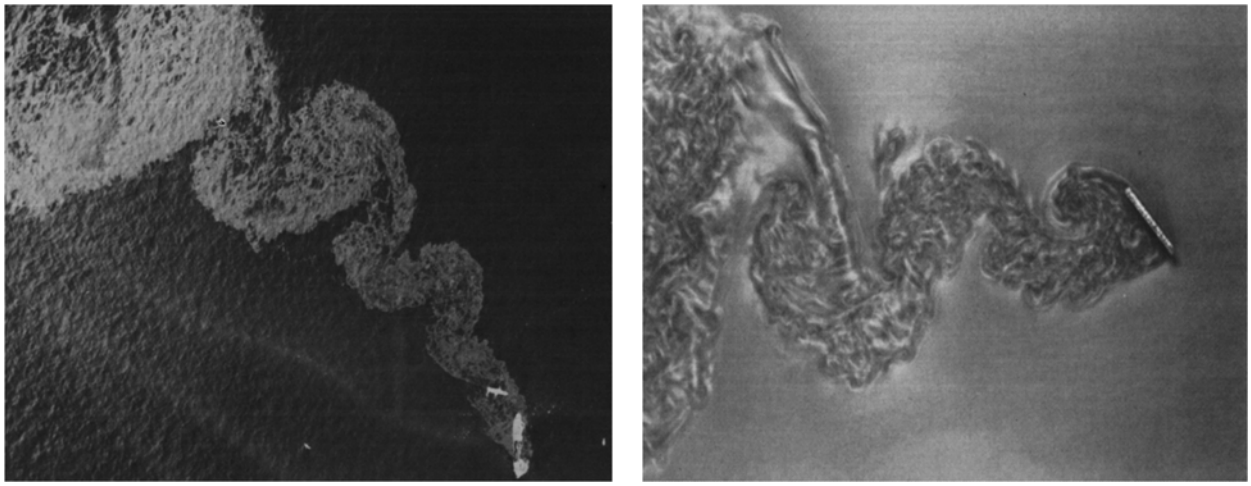

Figure 1: An example of similitude achieved between oil dispersal plume characteristics for a grounded tanker (left) and a model using an inclined flat plate (right)

A detailed discussion of dimensional analysis and similitude is presented in the Task 2 Topical Report. The focus of this Topical Report is specific to analysis of quench zone hydraulic behavior.

2.2 QUENCH ZONE HYDRAULIC BEHAVIOR

The focus of this analysis is on the potential for modelling spray penetration and mixing hydrodynamics in cold-flow, with the results serving as the basis for guiding scale-up decisions to a demonstration scale (approximately 800 TPD capacity) gasifier design. In particular, GTI is interested in focusing the effort on studying factors affecting i) mixing behavior, ii) spray penetration, and iii) disruption of syngas flow. Research into these factors is based on a survey of the literature, theoretical analysis, and a review of data from previous phases of the current study.

Syngas Jet Mixing:

Cooling of the hot syngas from the reactor depends on contact between the hot gas phase and coolant. Thus, in addition to atomization performance of the nozzles, the quench process is also dependent on mixing performance. Satisfactory heat transfer performance can be demonstrated in cold-flow through i) droplet size measurement, and ii) verification of adequate uniformity of the liquid distribution in a plane that is safely upstream of the syngas take-off[1].

The flow of syngas through the quench zone resembles that of a jet discharging axially into a pipe. It therefore shares similarities with jet flows and pipe flows. As has been demonstrated, for example by Dimotakis [1], profiles of mean concentration (and mean velocity) in jet mixing and pipe flows are self-similar for fully-turbulent flows. However, concentration fluctuations decrease with increasing Reynolds number of the jet or pipe flow, as the fluctuating component of velocity increases. We may conclude that the large-scale mixing behavior is similar across a wide range of Reynolds numbers, while the smaller-scale mixing is dependent on Re. For the gasifier quench zone, operating at a lower syngas Reynolds number in the model than in the plant therefore captures the largest scales of mixing, in terms of mean concentration, while providing conservative estimates of concentration fluctuations.

Mixing of Gas Jets and Liquid Sprays:

The flow in the gasifier is further complicated by the quench spray, which mixes with the gas and evaporates. In addition to requiring approximate similitude of the syngas Reynolds number to capture large-scale mixing behavior, we also require adequate similitude in terms of the jet-spray interaction. This means, as a first criterion, the ratio of velocity between the liquid and gas phases should be maintained as closely as is reasonably possible. In addition, however, there are other characteristics of the spray to consider, as described in the following sections.

Penetration of a Single Droplet Into a Gas:

We first consider the simplest type of interaction between an atomized liquid and a gas phase– namely the penetration depth of a single drop in a gas. This is a problem that can be solved using analytical methods based on an initial relative velocity, which decays to zero due to the effects of drag[2].

We begin with a statement of conservation of momentum for an arbitrary drop:

$$F_d = m \cdot \frac{du}{dt} \tag{1}$$

F_d is the drag force, m is the mass of the droplet, and u is its velocity relative to the gas. Substituting $F_d = -C_d \cdot \frac{1}{2}\rho_g u^2$, and $\rho_l \times V_d$ (C_d is the drag coefficient and V_d is the droplet volume):

[1] This is a result of Reynolds analogy, which states that momentum and heat transfer are equivalent for fluids having Prandtl numbers close to 1 (i.e. gases).
[2] In this analysis, we are ignoring effects of gravity, which, in the context of the gasifier quench zone, are negligible.

$$-C_d \cdot \frac{1}{2}\rho_g u^2 \cdot \frac{\pi}{4}d^2 = \rho_l \frac{\pi}{6}d^3 \cdot \frac{du}{dt} \tag{2}$$

This expression simplifies to:

$$\frac{du}{C_d u^2} = -\frac{3\rho_g}{4\rho_l d} \cdot dt \tag{3}$$

The drag coefficient is a function of droplet Reynolds number (see Figure 2):

$$Re_d = \frac{\rho_g u d}{\mu_g} \tag{4}$$

The form of solution obtained for the stopping distance will depend on the drag coefficient model used. It is possible to substitute a curve-fit to Figure 2 into Eq. 3 and solve for the velocity directly. However, it is much easier to simply integrate Eq. 3 numerically for a range of fluid properties and initial Reynolds numbers. For the range of initial Reynolds number of interest (roughly $Re_d < 1{,}000$), and a wide range of the density ratio ρ_l/ρ_g the data are reasonably well-represented by the following equation (see also Figure 3):

$$\frac{x}{d} = \frac{10}{3} \times \frac{\rho_l}{\rho_g} \times \frac{1}{C_d(0.4Re_{d0})} \tag{5}$$

where $C_d(0.4Re_{d0})$ indicates a drag coefficient evaluated at a value of 0.4 of the initial Reynolds number.

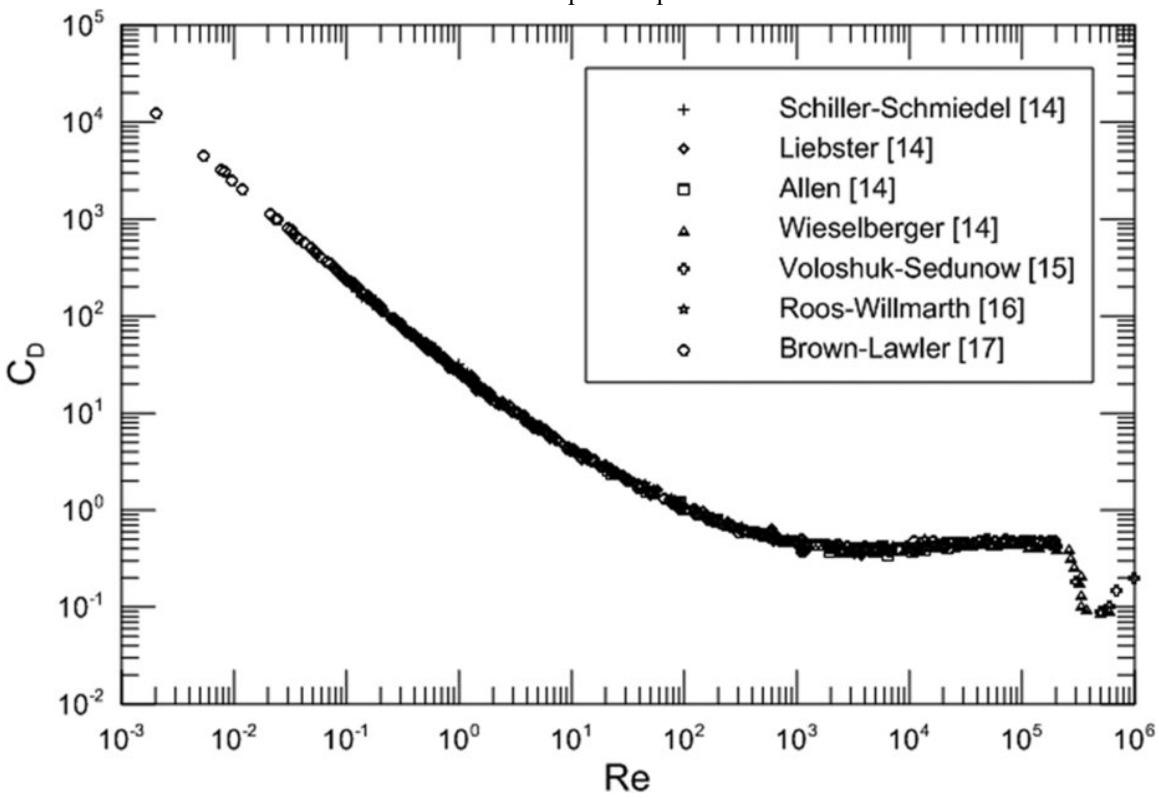

Figure 2: Variation of drag coefficient of spherical particles with Reynolds number. Image by Duan et al. [2] based on data from various sources.

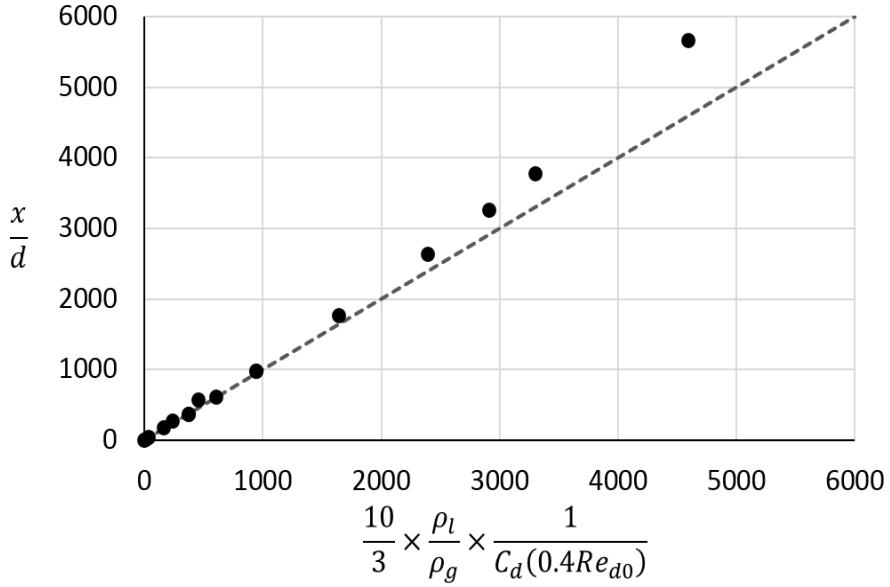

Figure 3: Single drop penetration correlation. The dashed line indicates perfect correlation between the calculated penetration distance and Eq. 5.

Eq. 5 provides the penetration depth of a drop x normalized by the drop diameter d. In the context of the gasifier, however, we are primarily concerned with the penetration of drops in terms of a scale of the syngas flow, such as the reactor diameter D. Thus:

$$\frac{x}{D} = \frac{x}{d} \times \frac{d}{D} = \frac{10}{3} \times \frac{\rho_l}{\rho_g} \times \frac{d}{D} \times \frac{1}{C_d(0.4Re_{d0})} \tag{6}$$

It is noted that in most of the range of interest of Re, the ratio between $C_d(0.4Re_{d0})$ and $C_d(Re_{do})$ is in the range of 1.5 to 2.5. We may therefore approximate Eq. 6 as follows:

$$\frac{x}{D} \simeq \frac{5}{3} \times \left(\frac{\rho_l}{\rho_g} \times \frac{d}{D} \times \frac{1}{C_d} \right) = \frac{5}{3} \times Sk \tag{7}$$

Thus, penetration of individual droplets is governed by similitude of Stokes number.[3]

Jets and Sprays in Cross-Flow:

Having confirmed that the criterion of similarity for penetration of a single droplet in a gas (stationary or flowing) is a Stokes number, we turn our focus now to the problem of interactions between sprays and gas jets. The problem is similar to that of the single droplet, described in the previous section, in that we still expect larger drops (more precisely, drops having larger Stokes number) may penetrate more deeply than smaller drops (having lower Stokes numbers). However, while a single droplet is not expected to have much impact on the gas flow, we might expect that the collective momentum of droplets comprising a dense spray could result in deeper penetration, and changes in the gas flow field.

The subject of jets and sprays in cross-flow has been the focus of many studies in the open literature. In a typical experimental set-up, a nozzle is mounted to be flush with the wall of a wind-tunnel, and interactions between the resulting spray or jet and the cross-flow are examined. It is noted that high Weber number jets disintegrate rapidly into dispersed droplets, and therefore included in the literature survey. The flow structures of jets in cross-flow are also noted to be similar to those of sprays in cross-flow. In particular, both result in deflection of the primary flow, and the presence of a counter-rotating vortex pair (compare e.g., Ghosh & Hunt [3] to Smith & Mungal [4]) as the cross-flow element is entrained in the flow direction.

Zhang and co-workers [5] [6] [7], studied mixing of hollow-cone sprays, similar to those used in the gasifier, and wall-bounded cross-flow. The studies are mainly relevant to the current work in that the authors varied the spray angle and compared results from single nozzle injections to a configuration having dual opposed nozzles. The authors describe the vortical flow-structures of the spray as it is deflected by the gas, and measured liquid distribution (i.e. mixing) downstream of the injection, through particle imaging. They observed that mixing of the liquid phase was enhanced in the dual nozzle configuration, and that mixing was also dependent on spray angle, with more upstream angles promoting faster liquid distribution. Increasing the liquid-to-gas flow ratio was also observed to result in more uniform liquid distribution within a shorter distance downstream of the injection point.

[3] It is noted that in the Stokes flow limit ($Re \to 0$), it can be proven analytically that the criterion of similarity for penetration depth of a single drop is the Stokes number.

Gas Flow Deflection:

Deshpande *et al*. [8] performed a numerical study of a spray in cross flow having very high liquid injection velocity (116 m/s), with what they described as low (6 m/s) and high (16 m/s) cross-flow velocity. As shown in Figure 4, the effect of the spray on the gas flow is significant, with the mean gas streamlines originating near the nozzle position deflecting by approximately half of the liquid penetration distance. The flow structures described for the spray corresponded well to those described in the experiments of Zhang *et al*., referenced above. In addition, experimental work by Phillips *et al.* [9] Bade *et al*. [10], and Nouri & Whitelaw [11], also indicates that sprays can significantly deflect a gas flow.

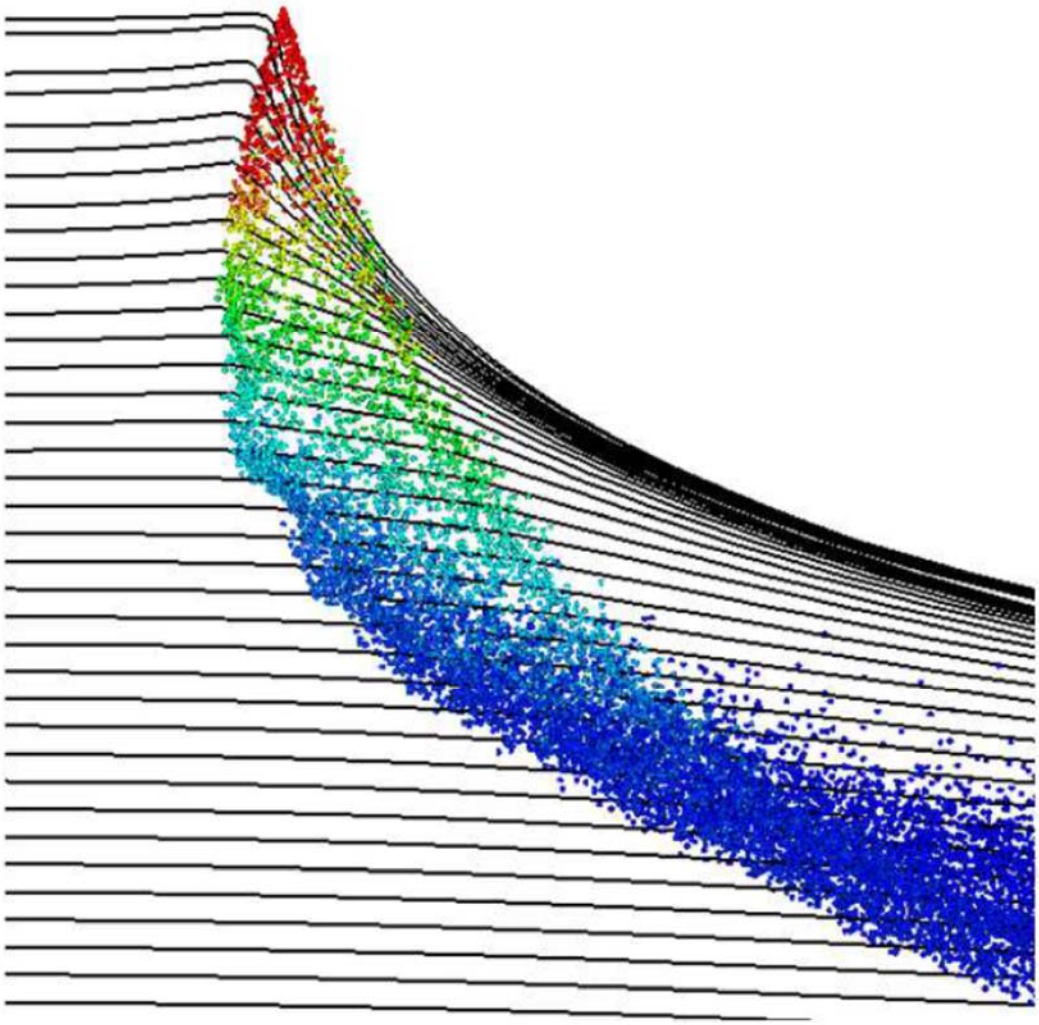

Figure 4: Deflection of gas streamlines by a spray, obtained by numerical simulation (Deshpande et al., 2011). Results are shown for the case of "strong" cross flow ($\boldsymbol{u_l = 116\ m/s}$, $\boldsymbol{u_g = 16\ m/s}$, air & water).

Deflection of gas streamlines similar to that seen in the works cited above could cause issues with quench performance, as the syngas jet may accelerate as it is deflected toward the quench pipe axis

by the array of nozzles. Such deflection toward the axis does apparently occur in some of the pilot results. Evidence of this phenomenon is especially noticeable in testing using HA134a[4]. Figure 5 is a frame from the high-speed video recording of test 3015. The gas (and entrained coolant) appears to flow only along the quench pipe axis, and the much larger area adjacent to the walls, where no liquid is seen, consists of largely stagnant fluid. The velocity of liquid drops along the centerline is estimated (from the time-stamp on the video recording) to be between 5 and 6 m/s, which is less than the gas velocity in the reactor tube (7.5 m/s), though not by a very significant margin.

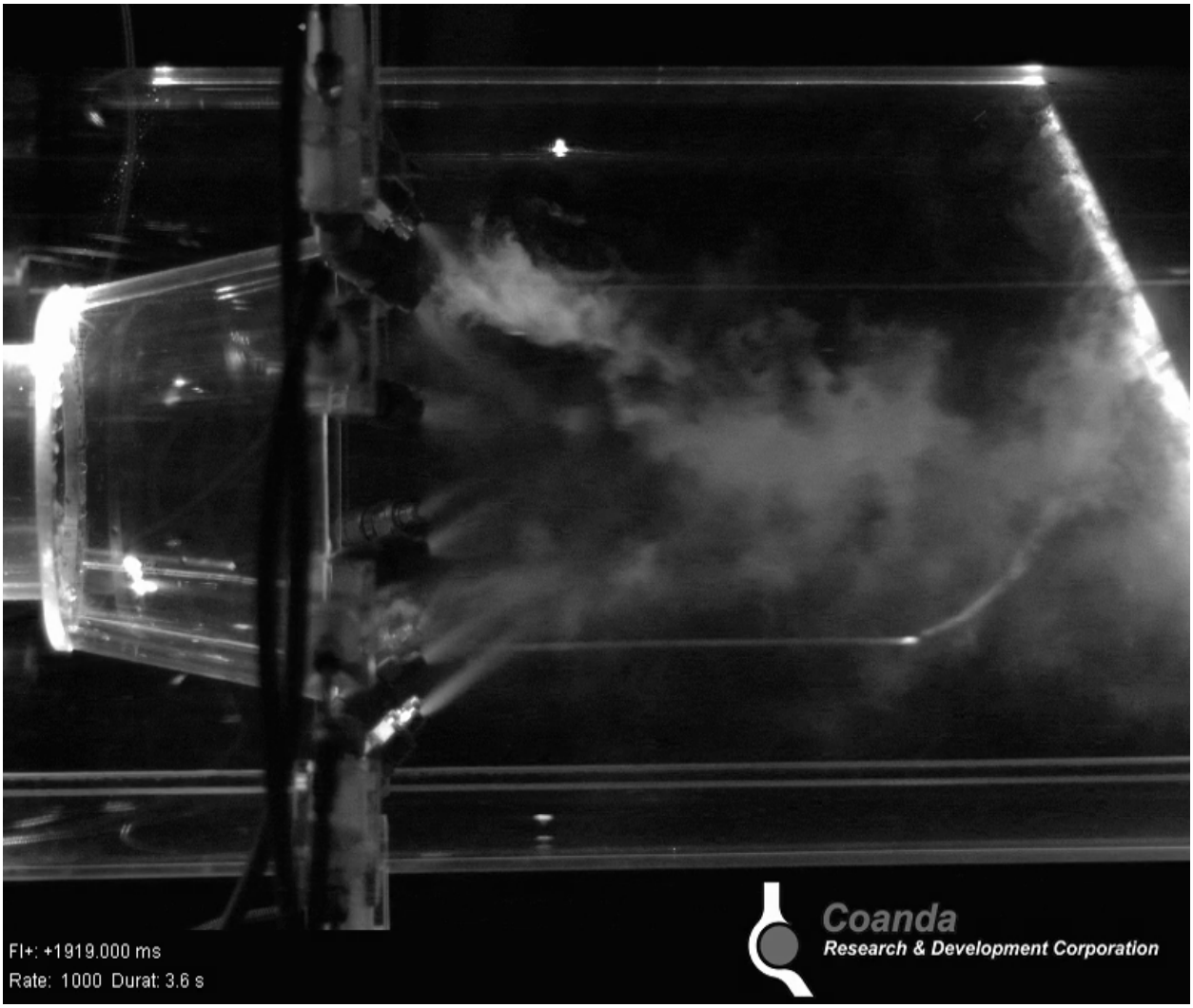

Figure 5: Still image from test 3015 (pilot geometry with conical reactor discharge), showing apparent constriction of the gas flow along the quench pipe axis due to the influence of the circular array of spray nozzles.

[4] This is likely due to better visualization of the central region of the quench pipe with the liquid near the walls having evaporated, rather than any difference in flow patterns when using halocarbon.

Spray and Jet Penetration:

In studies of sprays and jets in cross-flow (e.g. [4] [12] [13]) the spray penetration has been measured as a function of axial distance from the nozzle tip. Similitude is often correlated using expressions of the form:

$$\frac{y}{d} = Aq^n \left(\frac{z}{d}\right)^m \tag{8}$$

where y is the penetration depth, z is distance downstream of the injection point, d is the jet or orifice diameter, and A and n are empirical constants. q is the momentum flux ratio:

$$q = \frac{\rho_l u_l^2}{\rho_g u_g^2} \tag{9}$$

In most such correlations ([13] [14] [15]), the exponents are in the range $0.36 < n < 0.5$ and $0.25 < m < 0.5$. For example, Pratte & Baines [15] suggested values of $A = 2.05$, $n = 0.36$, and $m = 0.28$. The correlation of Freitag & Hassa [13] is based on similar values ($A = 3.0$; $n = 0.4$; $m = 0.27$). The range of these correlations is $3 < q < 1{,}225$, lower than the range of gasifier values. However, Hasselbrink & Mungal [12] present an argument based on similitude that suggests there should be no upper limit for q in Eq. 8.

Thus, for single spray nozzles, penetration is seen to be governed by the momentum flux ratio $\rho_l u_l^2 / \rho_g u_g^2$ and jet or drop diameter d. It can be shown that for the constants in correlations similar to those of Pratte & Baines and Freitag & Hassa, this is nearly identically equivalent to using momentum ratio used in previous phases of the current study:

$$\Pi_5 = \frac{\dot{m}_l u_l}{\dot{m}_g u_g} \tag{10}$$

The derivation is shown below.

Penetration depth, expressed in terms of the gasifier diameter, is given by:

$$\frac{y}{D} = \frac{y}{d} \times \frac{d}{D} = Aq^n \left(\frac{z}{D}\right)^m \left(\frac{d}{D}\right)^{1-m} \tag{11}$$

From continuity:

$$\dot{m}_l = \rho_l u_l \frac{\pi}{4} d^2 \tag{12}$$

$$\dot{m}_g = \rho_g u_g \frac{\pi}{4} D^2 \tag{13}$$

Therefore:

$$\frac{\dot{m}_l u_l}{\dot{m}_g u_g} = \frac{\rho_l u_l^2}{\rho_g u_g^2} \times \frac{d^2}{D^2} = q \times \left(\frac{d}{D}\right)^2 \tag{14}$$

Combining Eqs. 8 and 14:

$$\frac{y}{D} = A\left(\frac{\dot{m}_l u_l}{\dot{m}_g u_g}\right)^n \left(\frac{d}{D}\right)^{-2n} \left(\frac{z}{D}\right)^m \left(\frac{d}{D}\right)^{1-m} \tag{15}$$

$$\frac{y}{D} = A\left(\frac{\dot{m}_l u_l}{\dot{m}_g u_g}\right)^n \left(\frac{z}{D}\right)^m \left(\frac{d}{D}\right)^{1-m-2n} \tag{16}$$

For $n = 0.4 \simeq 3/8$ and $m = 0.27 \simeq 1/4$:

$$\frac{y}{D} = A\left(\frac{\dot{m}_l u_l}{\dot{m}_g u_g}\right)^{\frac{3}{8}} \left(\frac{z}{D}\right)^{\frac{1}{4}} \left(\frac{d}{D}\right)^{1-\frac{1}{4}-\frac{3}{4}} \tag{17}$$

$$\frac{y}{D} = A\left(\frac{\dot{m}_l u_l}{\dot{m}_g u_g}\right)^{\frac{3}{8}} \left(\frac{z}{D}\right)^{\frac{1}{4}} \tag{18}$$

Thus, similitude of spray penetration with downstream distance from the nozzles is primarily a function of the momentum ratio.

Spray Data Analysis:

An understanding of spray nozzle performance is required to properly prescribe the design and operating conditions of a physical cold-flow model. The spray characteristics are first determined for the commercial nozzle, and using this information, a nozzle may be selected for cold-flow testing providing optimum similitude with the plant behavior. Droplet size and velocity are equally important, as they affect both Stokes number and the liquid-to-gas momentum flux ratio, which have been identified as important criteria of similarity with respect to the quench zone hydrodynamics.

Gas Entrainment in Hydraulic Nozzles:

In the numerical simulations of Deshpande *et al*., a large initial relative velocity between the phases led to very rapid droplet deceleration, and a corresponding entrainment of the gas into the jet core. The mathematical and physical basis for this phenomenon is also described by Ghosh & Hunt [3] (see also schematic representation in Figure 6). At a sufficient distance from the spray source, the slip velocity between the gas and droplets will be negligible. This raises the question of whether, at the scales of the gasifier diameter, the spray produced by the quench nozzles behaves largely as droplets suspended in a gas jet, or as droplets moving through a gas flow. This is an important question to answer for a cold-flow model, as the former could possibly be more appropriately modelled using gas jets instead of a liquid spray.

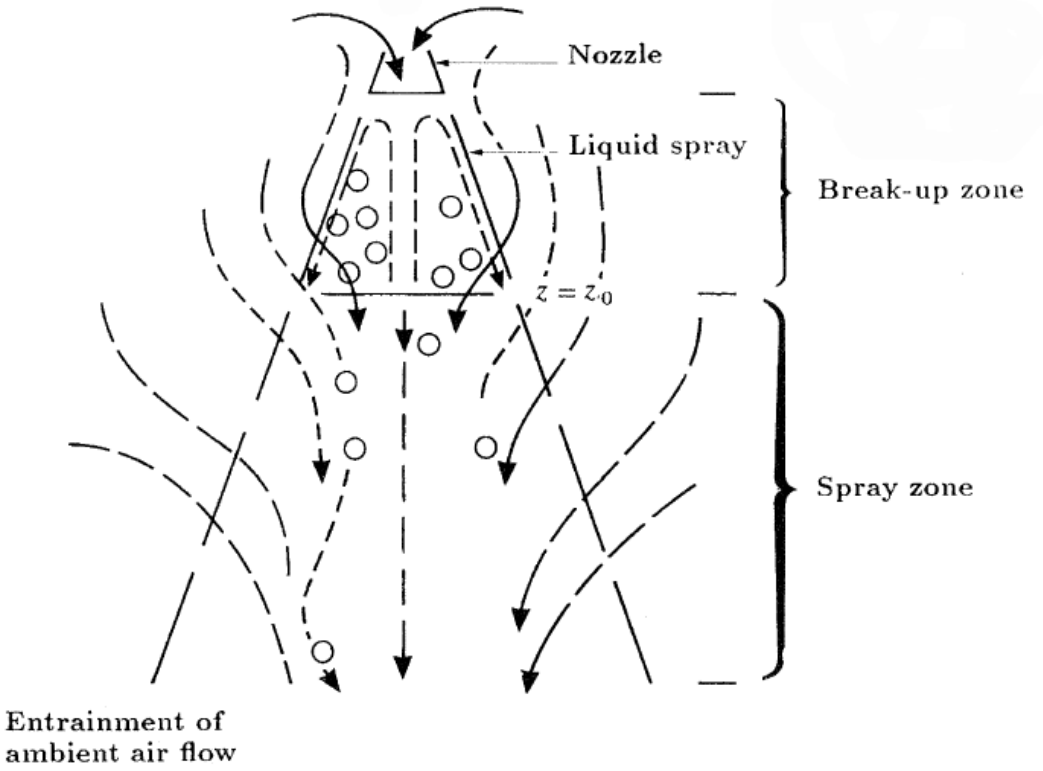

Figure 6: Schematic of a typical spray showing the break-up and spray zones, and air entrained into the spray (Fig. 1-a of Ghosh & Hunt, 1994).

Spray Characterization:

The performance of a set of hydraulic spray nozzles was characterized with phase-Doppler interferometry (PDI), as well as photographs of spray patterns. These nozzles are identified by a number between 1 and 26 which corresponds to the flow rate through the nozzle at a standard injection pressure. Generally, flow capacity is increased by increasing the orifice diameter, and therefore nozzles with a larger capacity number also correspond to larger orifice and droplet diameter.

Spray Pattern:

PDI measurements in still air indicate that the liquid volume fraction farther than 1 inch from the spray is consistently less than 1%. This confirms the hypothesis that we may consider the spray to be well-dispersed, and that droplet interactions are rare. However, when nozzles are arranged in close proximity, the increase in relative velocity between droplets produced by adjacent nozzles increases the probability of collision and coalescence significantly.

Liquid Distribution:

The majority of liquid is to be found near the edge of the spray. The proportion is estimated at roughly 85-90%, however there is no clear demarcation between the inner and outer regions of the spray. This characteristic is shown by Figure 7, which plots the droplet flux profiles as a function of radial position for two distinct nozzles. For both nozzles, the measured droplet flux continuously increases with radial position (away from the centerline) until a maximum is reached near the edge of the spray. When the radial position is further increased past the edge of the spray, the droplet flux drops off significantly.

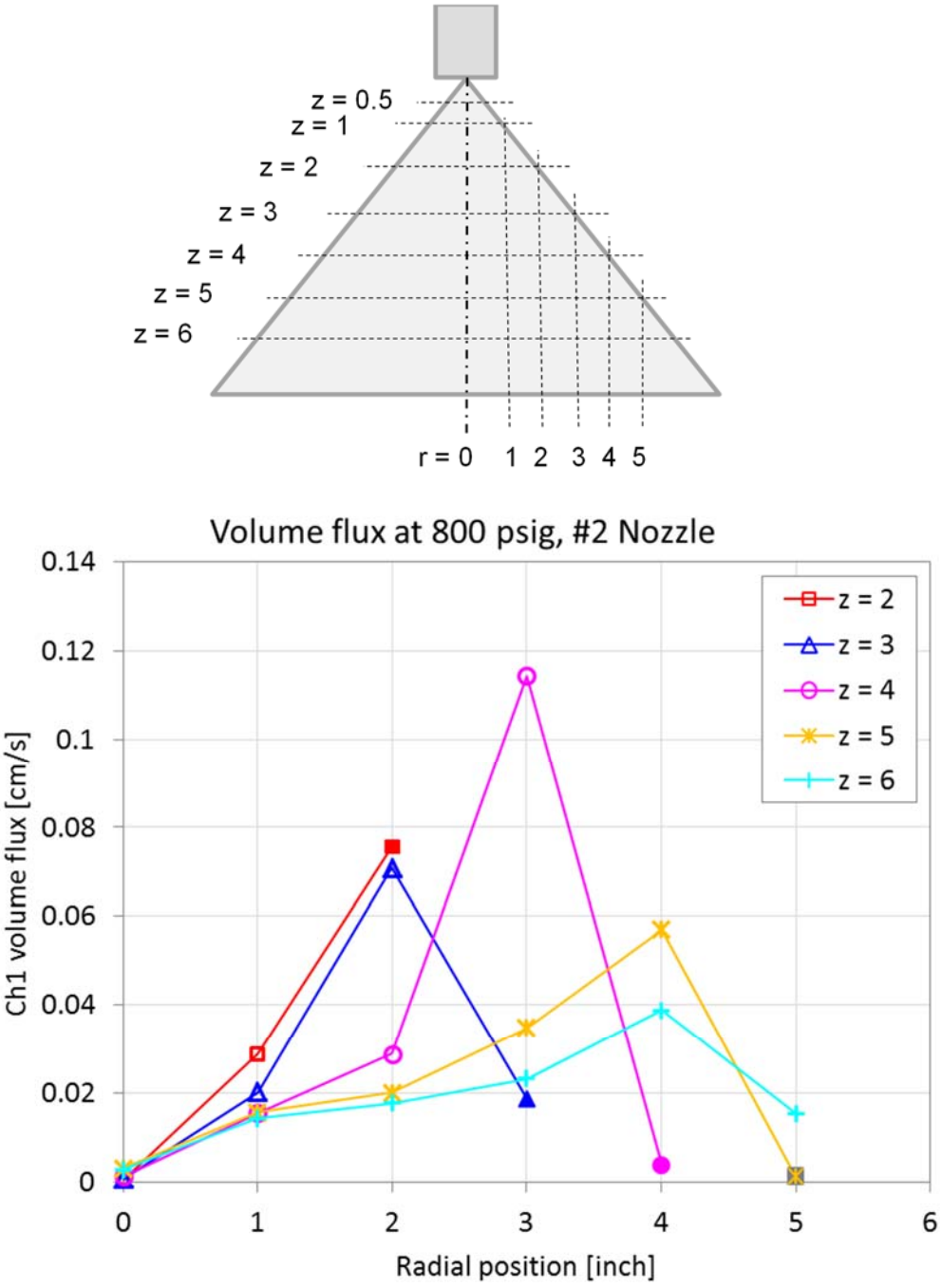

Figure 7: Droplet flux profiles in the radial direction for the #2 nozzle at 800 psig. The flux decays exponentially with distance from the nozzle tip for both nozzles, as shown by the close agreement between the data points and exponential curve-fits.

Velocity and Size Distribution:

Droplet velocities were highest close to the nozzle tip, where agreement with theoretical superficial velocities in the orifice was generally good. For the smaller of the two nozzles tested, the droplet velocities were generally higher along the nozzle centerline, with the exception of the two measurement locations closest to the nozzle tip, where the highest velocities were observed in the densest part of the spray (i.e. the diagonal). For the larger nozzle, the same trends were observed close to the nozzle tip (i.e. highest velocities along the diagonal at 1 inch and 2 inches along the nozzle axis), but at vertical locations of 3 inches or more from the tip, the droplet velocities did not vary significantly with radial location.

The variation of droplet diameter with position along the spray radius and distance from the nozzle axis was measured for two nozzle sizes. For both nozzles tested, droplet diameters remained relatively constant at 20-40 μm along the nozzle axis, and both had strong increasing trends in droplet size with radial position. Both nozzles also showed increasing trends in droplet size with distance away from the nozzle tip along the nozzle axis, however these trends were significantly weaker than the trends observed with radial position. For example, for the larger nozzle, a droplet diameter increase from 30 μm along the centerline to 90 μm along the spray edge was typical, whereas within the edge of the spray, the droplets only varied by less than 20 μm, i.e. 80 μm close to the nozzle tip, to as much as 100 μm at 6 inches away from the tip.

Close to the nozzle tip (distances of 3 inches or less), droplet velocities exhibited strong increasing trends with nozzle pressure. Additionally, the measured liquid droplet velocities were highest in this region, with values close to the theoretical nozzle orifice liquid velocities calculated using continuity.

Droplet sizes decreased with increasing nozzle pressure. However, the decreases were modest at pressures above 500 psig. For example, at 2-3 inches away from the tip, the smaller nozzle exhibited a decrease of only 15 μm in droplet size over a pressure range 500 psig $< \Delta P <$ 1500 psig.

The liquid near the spray axis consists primarily of droplets less than 50 microns in diameter. Average downward velocities are generally less than 10 m/s, and the droplet size and velocity appear randomly distributed. It appears that droplets produced in this size range are preferentially entrained into the core along with gas, due to their low Stokes number.

Larger droplets, which form the bulk of the size distribution ($D_{V_{50}} \approx d_{32} \approx 100$ μm), are rarely found in the core area of the spray. However, they make up the majority of the liquid at the edge of the spray. There is a strong correlation between size and velocity, with velocity increasing with drop size. The largest drops typically have axial velocity of about 20 m/s or more, which increases with injection pressure.

Many of the size distributions at the edge of the spray are bi-modal. However, the position of the spray was often unsteady, especially as axial distance from the nozzle orifice increased. This is due to room air currents, as the tests were conducted in a semi-open environment.

Additionally, relatively stagnant fine mist was observed in the room air outside the spray. The small droplets in distributions near the edge of the spray therefore represent recirculating fine mist in the atmosphere. Such droplets would undoubtedly evaporate nearly instantly in the gasifier. However, their contribution to the total liquid mass is negligible, and we do not feel it is necessary

to filter them from PDI measurements, provided we concentrate our analysis on mass-averaged quantities.

2.3 ANALYTICAL CONCLUSIONS

Spray momentum and penetration are key factors in the gasifier quench performance. However, the optimum condition is not clearly evident: shallow or weak penetration of coolant into the syngas jet leaves a jet of unquenched syngas along the centerline. Although entrained liquid will eventually reach the core through turbulent mixing, this may require use of an excessively long quench tube. Conversely, excessive penetration may overly disrupt the syngas flow, causing unquenched gas to either be accelerated along the centerline, or deflected radially. A major focus of future testing should be to further examine effects of momentum ratio in the demonstration model.

Analysis in previous phases had been based primarily on velocity along the centerline. We should, however, focus greater attention to analysis of the edge of the spray in future phases. The trends in spray characterization data generally remain consistent with prior dimensional analysis. However, because understanding of the spray distribution and pattern is crucial to the scaling process, further nozzle characterization of the spray nozzle selected for the demonstration unit, both as a single nozzle and in proximity with others, is recommended.

The PDI analysis supports a conclusion that the majority of the spray in the quench zone has significant slip velocity relative to the gas in the immediate vicinity of the quench zone, rather than consisting of a gas jet with suspended droplets. It therefore appears that hydraulic nozzles are appropriate for continued testing.

3.0 RESULTS AND DISCUSSIONS

3.1 SCALING EVALUATION

In previous phases of the present investigation, our evaluation of similitude centered on matching the momentum flux ratio of the liquid and gas streams, with the best possible similitude of Stokes number distributions. This was accomplished by adjusting the gas flow rate until the desired momentum ratio was achieved, resulting in kinematic mismatch (i.e. the ratio of liquid and gas velocities was different than in the plant). The analysis conducted in the current phase indicates that the momentum and velocity ratios are the most important criteria of similarity, and that if necessary, similitude of the Stokes number may be relaxed somewhat.

The original scope of the current phase of study was to examine whether improved similitude could be accomplished by increasing the apparatus scale to match that of the demonstration gasifier. Calculations for a full-scale demonstration cold-flow apparatus indicate that there is not a substantial advantage in terms of similitude by increasing the size of apparatus to the demonstration scale. This is primarily because scaling the experiment at atmospheric pressure while maintaining kinematic similitude affects Stokes number and momentum ratio in a similar way. This is because of the mathematical forms of Π_5 and Sk:

$$\Pi_5 = \frac{\dot{m}_l u_l}{\dot{m}_g u_g} = \frac{\rho_l N u_l^2 d_0^2}{\rho_g u_g D^2} \tag{19}$$

$$Sk = \frac{\rho_l}{\rho_g}\frac{d_{V50}}{D}\frac{1}{C_d} \approx \frac{\rho_l}{\rho_g}\frac{d_{V50}}{D}\frac{\rho_g u d_{V50}}{\mu_g} \approx \frac{\rho_l u d_{V50}^2}{\mu_g D} \tag{20}$$

In Eq. 19, N is the total number of nozzles installed in the apparatus, and Eq. 20 is obtained from the approximation that $C_d \propto 1/Re_d$ for relatively small Reynolds numbers.

We now consider Eqs. 19 & 20 in the context of the dimensional parameters which we can control with relative ease:

1. Nozzle size: this is the parameter modified using our current scaling strategy.
2. Apparatus scale: this strategy was the original focus of the present work.
3. Gas density: Pressurized gas is already supplied to the apparatus.
4. Number of nozzles: Increasing the number of nozzles increases liquid mass flow and momentum ratio without affecting velocity or Stokes number.

Table 1 shows a comparison of first-order effects of modifying each of these parameters independently. It is noted that increasing the scale of the apparatus has a similar effect as the current strategy, which is to decrease Stokes number and momentum ratio by selecting a smaller-orifice nozzle. In the actual case, decreasing momentum ratio by selecting a smaller nozzle or

increasing the apparatus scale until the momentum ratio is matched results in larger values of Stokes number in the cold-flow apparatus than in the demonstration gasifier, though the results are clearly better at the larger scale. The mis-match of Stokes number could lead to over-penetration of droplets into the gas jet in the model results, compared to the gasifier flow.

Table 1: First-order effects of modifying operating parameters in a cold-flow model. $\boldsymbol{d}$ = nozzle or droplet diameter, $\boldsymbol{D}$ = scale; $\boldsymbol{\rho_g}$ = gas density (operating pressure); $\boldsymbol{N}$ = number of nozzles; $\boldsymbol{\Delta P}$ = nozzle injection pressure.

Parameter	$\frac{\rho_l N u_l^2 d_0^2}{\rho_g u_g^2 D^2}$	$Sk \approx \frac{\rho_l u d^2}{\mu_g D}$	Notes
$d \downarrow$	$\downarrow\downarrow$	$\downarrow\downarrow$	Current strategy
$D \uparrow$	$\downarrow\downarrow$	$\downarrow$	Similar effects as current strategy
$\rho_g \uparrow$	$\downarrow$	-	Weak effect on Sk
$N \uparrow$	$\uparrow$	-	Possible coalescence for closely-spaced nozzles?

An alternative to increasing the geometric scale that provides slightly more of an advantage in terms of similitude is to increase the pressure (and therefore gas density) at the existing scale. As shown in Table 2, pressurizing the vessel to approximately 2.5 bar[5] (abs) results in further reduction of Stokes number, with approximately the same quality of similitude of the momentum ratio.

In earlier testing, increased internal pressure was shown to affect nozzle performance, most notably producing a narrower spray, even at modest pressure increases. Use of a pressure vessel could therefore result in improved similitude with respect to nozzle spray angle.

As discussed previously, the other method for varying momentum ratio and Stokes number independently is by changing the number of nozzles. There are, however, practical limitations to the number of nozzles that can be physically mounted inside the vessel.

Estimated Cost:

A preliminary cost estimate of implementing each of the apparatus options discussed in the previous study is presented in Table 2. The following is noted about the table:

- These estimates are preliminary only, and do not include any contingency. They are meant only to convey an approximate level of cost commitment required, and are not intended for detailed budget planning.

[5] Further increasing pressure is not feasible, as the flow rate at 2.5 bar is already at the compressor's maximum capacity.

- Continuing to use the current apparatus in its present state entails only the minimum recommissioning costs.
- Because a larger-diameter vessel does not fit within the current apparatus frame this option involves constructing an entirely new apparatus.
- Increasing the pressure in the existing apparatus requires some components, including the test section, to be replaced.

Recommendation:

Based on the similitude evaluation, above, the result of increasing apparatus scale and pressurizing the vessel to approximately 2.5 bar is a closer match of Stokes number. If the ability to vary Stokes number in the range $0.15 < Sk < 0.3$ is desired, then our recommendation is to proceed with planning a test program around an environment pressurized to approximately 2.5 bar.

Table 2: Comparison of scaling options. In each scenario, the nozzle offering optimum similitude is selected.

Apparatus	Momentum	Drag	Cost
Demo Gasifier (reference)	1.0	1.0	
Current Scale	1.12	6.4	$20,000
Full Scale	1.19	2.6	$250,000
Pressurized Current Scale	0.88	2.0	$150,000

4.0 CONCLUSIONS

A review of the literature on jet-jet interactions leads to the conclusion that momentum ratio is the key scaling parameter for establishing hydrodynamic similitude. PDI characterization of a range of hydraulic spray nozzles indicates that movement of individual droplets can be characterized by Stokes number. Therefore, momentum ratio and Stokes number were taken as the key scaling parameters for assessing cold flow apparatus options.

Assessment of cold flow model options for the demonstration-scale (800 TPD) gasifier concluded that a pressurized (~2.5bar) version of the current apparatus provided superior similitude for the study of jet-jet interaction hydrodynamics and overall quench water – syngas mixing than a full scale apparatus, and at lower cost.

REFERENCES

[1] P. E. Dimotakis, "The Mixing Transition in Turbulent Flows," *J. Fluid Mech.,* vol. 409, p. 69–98, 2000.

[2] Z. Duan, H. B. and Y. Duan, "Sphere Drag and Heat Transfer," *Scientific Reports,* vol. 5, 2015.

[3] S. Ghosh and J. Hunt, "Induced Air Velocity within Droplet Driven Sprays," *Proc. Math. Phys. Sci.,* vol. 444, no. 1920, pp. 105-127, 1994.

[4] S. Smith and M. Mungal, "Mixing, structure and scaling of the jet," *J. Fluid Mech.,* vol. 357, pp. 83-122, 1998.

[5] H. Zhang, B. Bai, L. L. H. Sun and J. Yan, "Mixing of Hollow-Cone Spray with a Confined Crossflow in Rectangular Duct," *AIAA J.,* vol. 51, no. 3, pp. 615-622, 2013.

[6] H. Zhang, B. Bai, L. L. H. Sun and J. Yan, "Experimental Study of the Mixing of Two Impinging Pressure-swirl Sprays in Crossflow," *Exp. Therm. Fluid Sci.,* vol. 49, pp. 67-74, 2013.

[7] H. Zhang, B. Bai, L. L. H. Sun and J. Yan, "Droplet Dispersion Characteristics of the Hollow Cone Sprays in Crossflow," *Exp. Therm. Fluid Sci.,* vol. 45, pp. 25-33, 2013.

[8] S. S. Deshpande, J. Gao and M. F. Trujillo, "Characteristics of Hollow Cone Sprays in Crossflow," *Atomization & Sprays,* vol. 21, no. 4, pp. 349-361, 2011.

[9] J. Phillips, P. Miller and N. Thomas, "Air Flow and Droplet Motions Produced by the Interaction of Flat-Fan Sprays and Cross Flows," *Atomization and Sprays,* vol. 10, pp. 83-103, 2000.

[10] K. Bade, W. Kalata and R. J. Schick, "Spray Plume Characteristics at Multiple Cross-Flow Angles, Experimental and Computational Assessments," in *ICLASS 2009, 11th Triennial International Conference on Liquid Atomization and Spray Systems*, Vail, CO, 2009.

[11] J. Nouri and J. Whitelaw, "Gasoline Sprays in Uniform Crossflow," *Atomization and Sprays,* vol. 17, pp. 621-640, 2007.

[12] E. F. Hasselbrink and M. Mungal, "Transverse jets and jet flames. Part 1.," *J. Fluid Mech.,* vol. 443, pp. 1-25, 2001.

[13] S. Freitag and C. Hassa, "Spray Characteristics of a Kerosene Jet in Cross Flow of Air at Elevated Pressure," in *ILASS08-12-1*, Como Lake, Italy, 2008.

[14] P. Wu, K. Kirkendall and R. Fuller, "Spray Structures of Liquid Jets Atomized in Subsonic Flows," *J. Propuls. Power,* vol. 14, pp. 173-182, 1998.

[15] B. Pratte and W. Baines, "Profiles of the Round Turbulent Jet in a Cross Flow," *J Hydronaut. Div. ASCE,* vol. 92, pp. 53-64, 1967.